



COAST GUARD

OFFICE OF RESEARCH & DEVELOPMENT

CONTRACT NO. DOT-CC-60,490-A

HEAVY-DUTY OIL CONTAINMENT SYSTEM

PNEUMATIC BARRIER SYSTEM

AD719278

OIL CONTAINMENT
DIVISION OF WILSON INDUSTRIES, INC.
1301 CONTI STREET, P.O. BOX 1452
HOUSTON, TEXAS 77002

DDC
RECEIVED
JAN 8 1971
REGISTERED
B

JANUARY 1971

FINAL REPORT

Prepared for: COMMANDANT (DAT)
U.S. COAST GUARD HEADQUARTERS
WASHINGTON, D.C., 20591

Reproduced by
NATIONAL TECHNICAL
INFORMATION SERVICE
Springfield, Va. 22151

DISTRIBUTION STATEMENT A
Approved for public release;
Distribution Unlimited

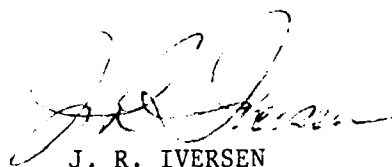
576

DATE: JAN 18 1971

This report has been submitted in fulfillment of contract DOT-CG- 00,490-A and is promulgated subject to the following qualifications:

The contents of this report reflect the views of Wilson Industries, Inc.

which is responsible for the facts and the accuracy of the data presented herein. The contents do not necessarily reflect the official views or policy of the Coast Guard. This report does not constitute a standard, specification or regulation.



J. R. IVERSEN
Captain, U. S. Coast Guard
Chief, Applied Technology Division
Office of Research and Development
U. S. Coast Guard Headquarters
Washington, D. C. 20591

1-8030-10

CFBT	WHITE SECTION	<input checked="" type="checkbox"/>
DOC	BUFF SECTION	<input type="checkbox"/>
UNANNOUNCED		<input type="checkbox"/>
JUSTIFICATION		
BY		
DISTRIBUTION/AVAILABILITY CODES		
DIST.	AVAIL.	and OF SPECIAL

A

**Best
Available
Copy**

PART I FINAL REPORT

HEAVY-DUTY OIL CONTAINMENT SYSTEM

PNEUMATIC BARRIER SYSTEM

FOR

UNITED STATES COAST GUARD

WASHINGTON, D.C.

DEPARTMENT OF TRANSPORTATION



OIL CONTAINMENT

Division of Wilson Industries, Inc.

1301 CONTI STREET • P. O. BOX 1492 • HOUSTON, TEXAS

Copyright October, 1970, Wilson Industries, Inc.

PREFACE

This report contains a description for the concept development of a pneumatic barrier system for a heavy duty oil containment system. The study was conducted at the Hydromechanics Laboratories of Texas A&M University under a sub-contract with Texas A&M Research Foundation.

A great number of personnel participated in the study of this complexity. The following staff members were supervising the tasks mentioned herein:

Dr. L. Bagnall - Pneumatic Supply

Dr. E. I. Bailey - Design of the Barrier

Dr. D. R. Basco - Hydromechanics of Pneumatics and Model Study

Dr. C. J. Garrison - Oil Set-Up by Current

Dr. C. A. Rodenberger - Systems Studies and Plans

Dr. R. M. Sorensen - Oil Set-Up by Wind

Dr. D. Webb - Materials Studies

In addition, other staff members participated in the study: Dr. W. Burton, Dr. N. Hale, Dr. A. Meyer, Dr. T. Ichiye, and several graduate students: J. Machemehl, E. Spencer, W. Song, M. McClenen, E. Rudder, D. van Reenen, as well as several cooperative students: M. van Bavel, Miss R. Duke, D. Stockard and many other undergraduate students whose names cannot all be mentioned here. Ira J. Young assisted in laboratory testing.

The study was under the general supervision of Dr. John B. Herbich. The liaison between Wilson Industries and Texas A&M University was provided by John Hudson and Joe Nelson. Lt. Douglas Teeson was technical representative of the United States Coast Guard for Stage I of the heavy duty oil containment system.

The information found in the following report is not necessarily the sole product of the individual with primary responsibility on each respective task. It would be an almost insurmountable task to separate each contributed piece of information from a compiled and finished writing. Thus, data produced in these pages reflects effort by all personnel involved in this contract, whether or not their names are attached to each report.

Final report edited by
John R. Houser

TABLE OF CONTENTS

	<u>page no.</u>
PREFACE	i
FIGURES	vi
Section I-I	vi
Section I-II	vii
Section II	ix
Section III	xii
FINAL REPORT	
Section I Introduction and General Description	1
I. Description of Proposed System	2
1. Concept Identification	2
2. Field Installations	10
3. Large Scale Model Tests	11
4. Need for Study	12
5. Previous Engineering Studies to Evaluate Basic Concepts	12
6. Environmental Conditions Imposed by the Sponsor	13
7. Proposed System	18
8. Adaptability of the System	21
9. Emphasis on Unique and Significant Features of Design Procedure	23
10. Summary	24
II. Research Conducted	25
1. Oil Set-Up by Wind	26
2. Oil Set-Up by Current	30
3. Hydrodynamics of the Pneumatic System	47
4. General Comment	70
5. Study of Suitable Materials	85
6. Major Decisions	86
Section II Experimental Apparatus and Procedures	91
I. Wind-Wave Channel	92
II. Water-Wave Channel (Recirculating Flume)	95
III. Current Channel (Recirculating Floor Channel)	97
IV. Three-Dimensional Wave Basin	99
V. Research Instrumentation	101
VI. Experimental Procedure and Analysis of Data	102
1. Oil Set-Up by Wind	102
2. Oil Set-Up Due to Current	130

3. Hydrodynamics of Pneumatics	154
4. Model Tests Pneumatic Barrier	196
Section III Design of Major System	221
I. Bubble Generator	222
1. Bubble Screen Generator	222
2. Packaging	239
II. Study of Suitable Materials	242
III. System Characteristics	259
1. Barrier's Oil Retention Capability	259
2. System Strength	264
3. Deployment Capability	270
4. Reliability Standards	271
5. Biological Effects	273
6. Maintenance	296
7. Suitability	300
8. Physical Characteristics	301
9. Deployment and Pick-Up	302
Section IV Prototype Design	305
I. Technical Problems	306
II. Future Studies	307
III. System Performance	311
IV. Optimization of System	312
Section V Plan for Detailed Design for Construction of the Full-Scale Prototype	313
REFERENCES	315
APPENDIX	1a
I. Oil Set-Up Due to Current	2a
II. Oil Set-Up by Wind	42a
III. Hydromechanics of Pneumatics	73a
IV. Model Tests of Pneumatic Barrier	173a
V. Miscellaneous	209a

SLIDES

MOVIES

SECTION I - I

FIGURES

Page

I-I-1	Qualitative pattern of surface currents produced by air bubbles. Pneumatic barrier.	3
I-I-2	Crude oil spill at sea	5
I-I-3	Crude oil spill at sea	6
I-I-4	Pneumatic barrier deployed at sea	7
I-I-5	Pneumatic barrier deployed at sea	8
I-I-6	A ship passes freely over a pneumatic barrier	9
I-I-7	Pneumatic barrier containment system	22

SECTION I-I FIGURES

		Page
I-II-1	Oil set-up due to current	31
I-II-2	Head wave thickness	34
I-II-3	Head wave profile	35
I-II-4	Interfacial shear stress coefficient versus current velocity (corrected for depth effect)	38
I-II-5	Oil layer configuration for 0.5 knot current	39
I-II-6	Oil layer configuration for 1.0 knot current	40
I-II-7	Oil layer configuration for 1.5 knot current	41
I-II-8	Oil layer configuration for 2.0 knot current	42
I-II-9	Oil layer configuration for 2.5 knot current	43
I-II-10	Definitions of geometric, fluid and flow variables	49
I-II-11	Graph of air discharge as a function of maximum surface velocity.	50
I-II-12	Flume comparisons of U_{max} versus unit discharge, q	53
I-II-13	Orifice size comparisons	55
I-II-14	Open channel velocity profiles in 18-in. flume	57
I-II-15	Estimated U_{max} and b' for prototype design	59
I-II-16	U_{max} versus $\sqrt{gh(1-SGo)}$ under modeled design waves.	63
I-II-17	Recommended prototype design chart Pneumatic barrier - 2 knot current	66
I-II-18	Recommended prototype design chart Pneumatic barrier - 1 knot current	68
I-II-19	Pneumatic barrier operating in waves and currents	69
I-II-20	Required pipe diameter versus airflow rate in the pipe	73
I-II-21	Required pipe diameter per foot of manifold length versus surface current generated	75

		<u>Page</u>
I-II-22	Air supply HP required per foot of manifold length versus manifold depth	78
I-II-23	Air supply HP required per foot of manifold length versus overpressure	79
I-II-24	Airflow velocity through manifold holes versus hole size	80
I-II-25	Number of manifold holes per foot of manifold length versus overpressure	82
I-II-26	Number of manifold holes per foot of manifold length versus airflow rate in the pipe at a 25 foot depth	83
I-II-27	Number of manifold holes versus air supply HP required	84

SECTION II FIGURES

	<u>Page</u>
II-I-1	2 ft. by 3 ft. by 120 ft. wave channel 93
II-II-1	Diagrammatic sketch of the small recirculatory flume 96
II-III-1	Sketch of recirculatory floor channel 98
II-IV-1	32 ft. wide 86 ft. long and 2 ft. 6 in. deep wave basin 100
II-VI-1	Schematic two-dimensional wedge of floating oil 103
II-VI-2	Intermediate size, glass-walled wave channel 107
II-VI-3	Measurements taken of oil set-up by wind 108
II-VI-4	Oil set-up by wind 110
II-VI-5	Oil set-up by wind 111
II-VI-6	Oil set-up by wind 112
II-VI-7	Tests on oil set-up by wind 113
II-VI-8	Typical centerline velocity profile 115
II-VI-9	Given design wind profiles 118
II-VI-10	Wind set-up of oil no. 1 119
II-VI-11	Wind set-up of oil no. 2 120
II-VI-12	Wind set-up of oil no. 3 121
II-VI-13	Wind set-up of all three oils 122
II-VI-14	Additional set-up due to waves, oil no. 2 126
II-VI-15	Wind set-up constants 127
II-VI-16	Wind set-up of oil, depth vs fetch 128
II-VI-17	Wind set-up of oil, depth vs fetch 129
II-VI-18	Oil set-up due to current 133
II-VI-19	Photograph of typical head wave profile 136

		<u>Page</u>
II-VI-20	Head wave thickness correlation	140
II-VI-21	Head wave thickness for oils of var. sp. gr.	141
II-VI-22	Head wave profile	142
II-VI-23	Control volume of movement equation	144
II-VI-24	Interfacial shear stress	150
II-VI-25	Definitions of geometric, fluid out flow variables	157
II-VI-26	Air discharge versus maximum surface velocity	160
II-VI-27	Intermediate-size, glass wall flume (tests of pneumatic barrier in stagnant water)	162
II-VI-28	Small, plexiglass wall flume (tests of pneumatic barrier in waves)	163
II-VI-29	Pressure, temperature and flow rate measurement equipment	165
II-VI-30	U_{\max} versus q in 8-inch wide flume	166
II-VI-31	U_{\max} versus q in 2-foot wide channel	167
II-VI-32	U_{\max} versus q in 5-foot wide concrete flume	168
II-VI-33	Measurement of surface current produced by a pneumatic barrier in 5 ft. wide flume	169
II-VI-34	Pneumatic barrier in operation in 5 ft. wide flume	170
II-VI-35	U_{\max} versus q in 18-inch temporary flume	171
II-VI-36	Flume comparisons of U_{\max} versus q	173
II-VI-37	Orifice size comparisons	174
II-VI-38	U_{\max} versus q with $H = T/2$	175
II-VI-39	U_{\max} versus q .	176
II-VI-40	Velocity versus depth profile - two foot flume	179
II-VI-41	Velocity versus depth profile - 18-inch flume	180
II-VI-42	Dimensionless depth profile	181
II-VI-43	Typical decay of U_{\max} with distance x	182
II-VI-44	Dimensionless surface velocity ratios versus location	183

		<u>Page</u>
II-VI-45	Effect of steady current on pneumatic bubble curtain	185
II-VI-46	Effect of steady current on pneumatic bubble curtain measurements of velocities	186
II-VI-47	5-foot wide, 10 foot deep, 150 ft. long concrete flume	187
II-VI-48	Open channel velocity profiles in 18-inch flume	189
II-VI-49	Experimental net effective surface velocity	190
II-VI-50	18-inch flume velocity profiles at various locations. Current plus bubble velocities. Theory versus experiment.	191
II-VI-51	Estimated U'_{\max} and b' for prototype design	193
II-VI-52	U_{\max} versus $\sqrt{gh(1-SGo)}$ for stagnant water	205
II-VI-53	Scale effects in two-foot wave channel	206
II-VI-54	Modeled shallow water wave	209
II-VI-55	Pneumatic barrier operating in waves - small wave tank (oil retained on the right)	210
II-VI-56	Pneumatic barrier operating in waves - intermediate size wave tank	211
II-VI-57	Results of Unna ^b reproduced from Dick and Brebner ^c	212
II-VI-58	U_{\max} versus $\sqrt{gh-(1-SGo)}$ under modeled design waves	213
II-VI-59	U'_{\max} versus $\sqrt{gh(1-SGo)}$ with current	216
II-VI-60	Recommended prototype design chart - 2 knot current	217
II-VI-61	Recommended prototype design chart - 1 knot current	218

SECTION III
FIGURES

	<u>Page</u>
III-I-1 Drag force versus pipe diameter	223
III-I-2 Pipe weight	225
III-I-3 Sonic velocity versus temperature	227
III-I-4 Air density versus pressure	229
III-I-5 Pipe diameter versus pressure	230
III-I-6 Fluidic depth controller	233
III-I-7 Fluidic switch	234
III-I-8 200 Pressure difference	235
III-I-9 400 MTG block	236
III-I-10 300 Float	237
III-I-11 Materials for depth controller	238
III-I-12 Aircraft cargo truck	241
III-III-1 Two knot current containment	260
III-III-2 One knot current containment	261
III-III-3 Pneumatic barrier operating in current	263
III-III-4 Stress plot for 800 foot pipe	266
III-III-5 Stress plot for 1,000 foot pipe	267
III-III-6 Stress plot for 1,200 foot pipe	268
III-III-7 Stress plot of pipe to length	269
III-III-8 Anchor system	272

CONCEPT DEVELOPMENT OF A
PROTOTYPE HEAVY DUTY OIL CONTAINMENT SYSTEM

Section I

Introduction and General
Description of
Proposed System

I-I. Description of a Proposed System

The pneumatic barrier was conceived about sixty years ago as a device which would attenuate ocean waves by a curtain of air rather than by reflection or absorption of energy by the massive structures customarily used. It consists of a perforated pipe through which compressed air is forced. As the air bubbles rise they impart a drag to adjacent water particles resulting in an upward motion of the air/water mixture. When this mixture reaches the surface, the air escapes, while the flow of water branches into two horizontal currents, as shown in Fig. I-I-1. While the turbulence induced by this system produces some attenuation of the waves, it is usually considered that one of the horizontal currents, opposing the incoming wave, results in breaking of the wave and consequent turbulent diffusion of the incident wave energy^{1,2,3}. It is through this wave attenuation and horizontal current that the pneumatic barrier could be used as an oil spillage containment system.

1. Concept Identification

A pneumatic barrier is a bubble screen formed by passing compressed air through a submerged, perforated pipe. While rising to the surface the air bubbles induce a vertical current. The vertical current produces a circulation of the water, the horizontal currents move away from the barrier near

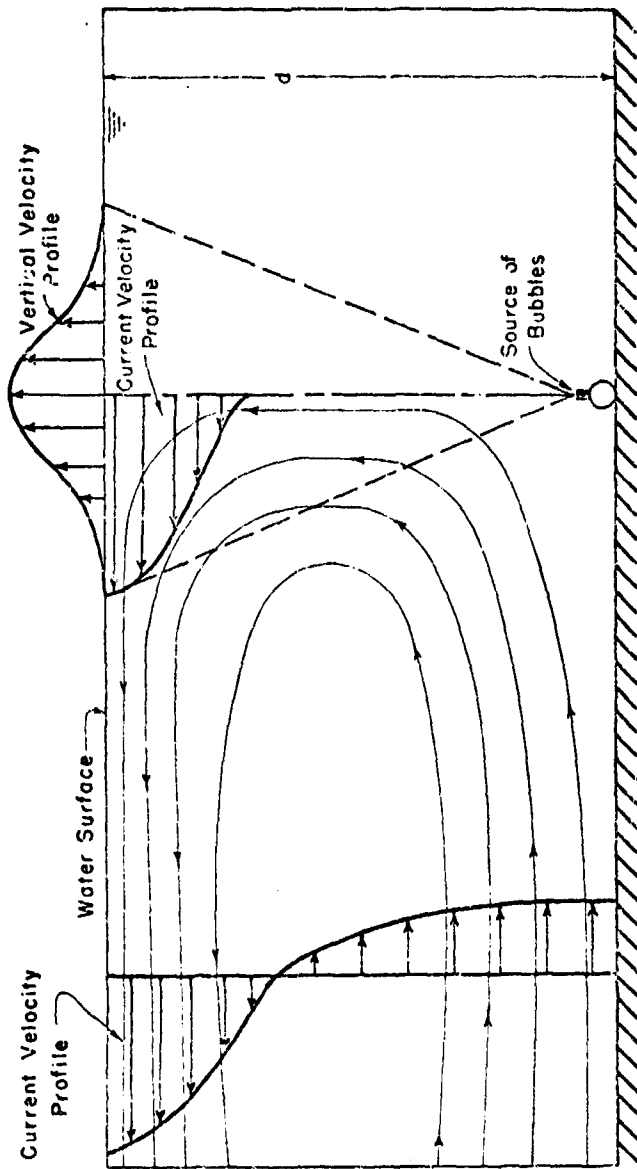


FIGURE I-I-1

QUALITATIVE PATTERN OF SURFACE CURRENTS PRODUCED
BY AIR BUBBLES. PNEUMATIC BARRIER.

the surface. Two symmetrical branches of the horizontal surface current are formed, one moving against the oil spill to contain it and another in the opposite direction, which may (if of sufficient strength) produce some attenuation of incident waves.

By designing the pneumatic barrier in such a way that the number, place and depth of submergence of the pipes, size and number of perforations, volume and pressure of compressed air meet the requirements set for the purpose, the barrier can be applied as an oil containment system. (Fig. I-I-4).

The barrier will consist of a pipe or pipes made of steel submerged at the required depth. The compressors could be located aboard a ship or a floating platform above the barrier. (Fig. I-I-5).

There are two main advantages of the pneumatic barrier:

- (i) It can be located below the air-water interface, thus reducing the magnitude of forces due to waves;
 - (ii) It will allow ships or other craft to cross the barrier without removal, or shut-down of the barrier
- (Fig. I-I-6).

The pneumatic barrier may also be installed permanently around the offshore oil platforms and operated only when needed.

For temporary installation the pneumatic barrier may easily be deployed and retrieved.

In estuaries, the pneumatic barrier may be turned on during flood tide to prevent oil from penetrating into the



FIGURE I-I-2
CRUDE OIL SPILL AT SEA

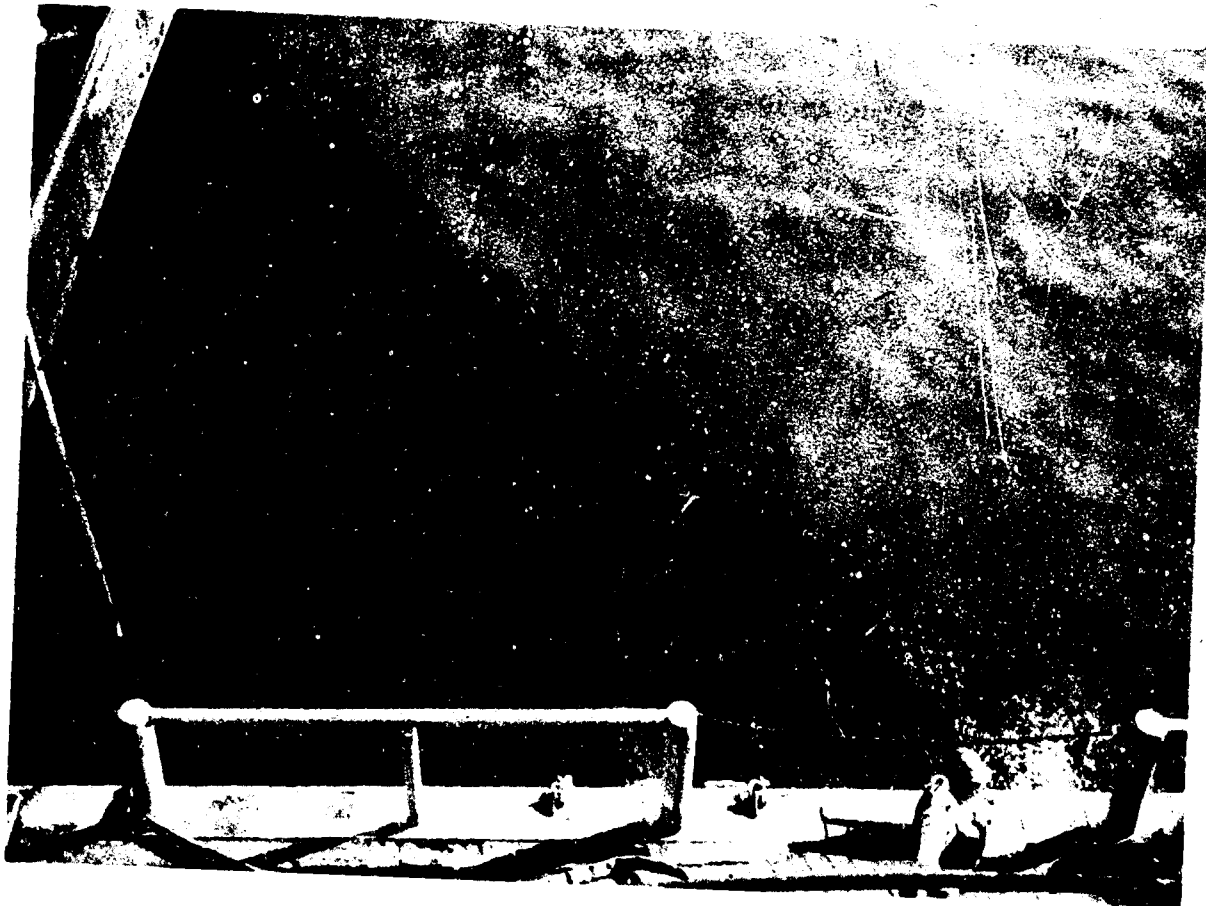


FIGURE I-I-3
CRUDE OIL SPILL AT SEA

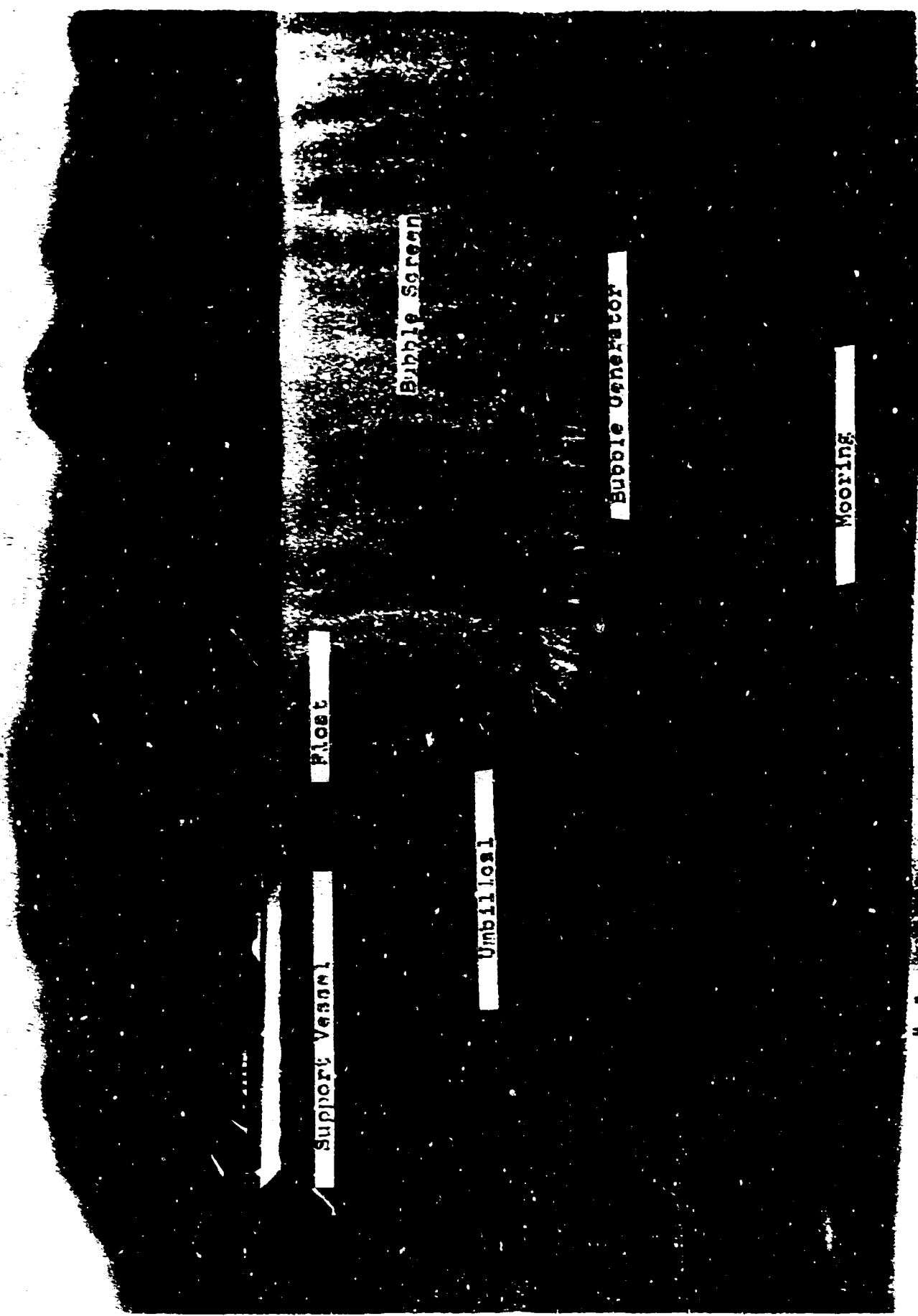
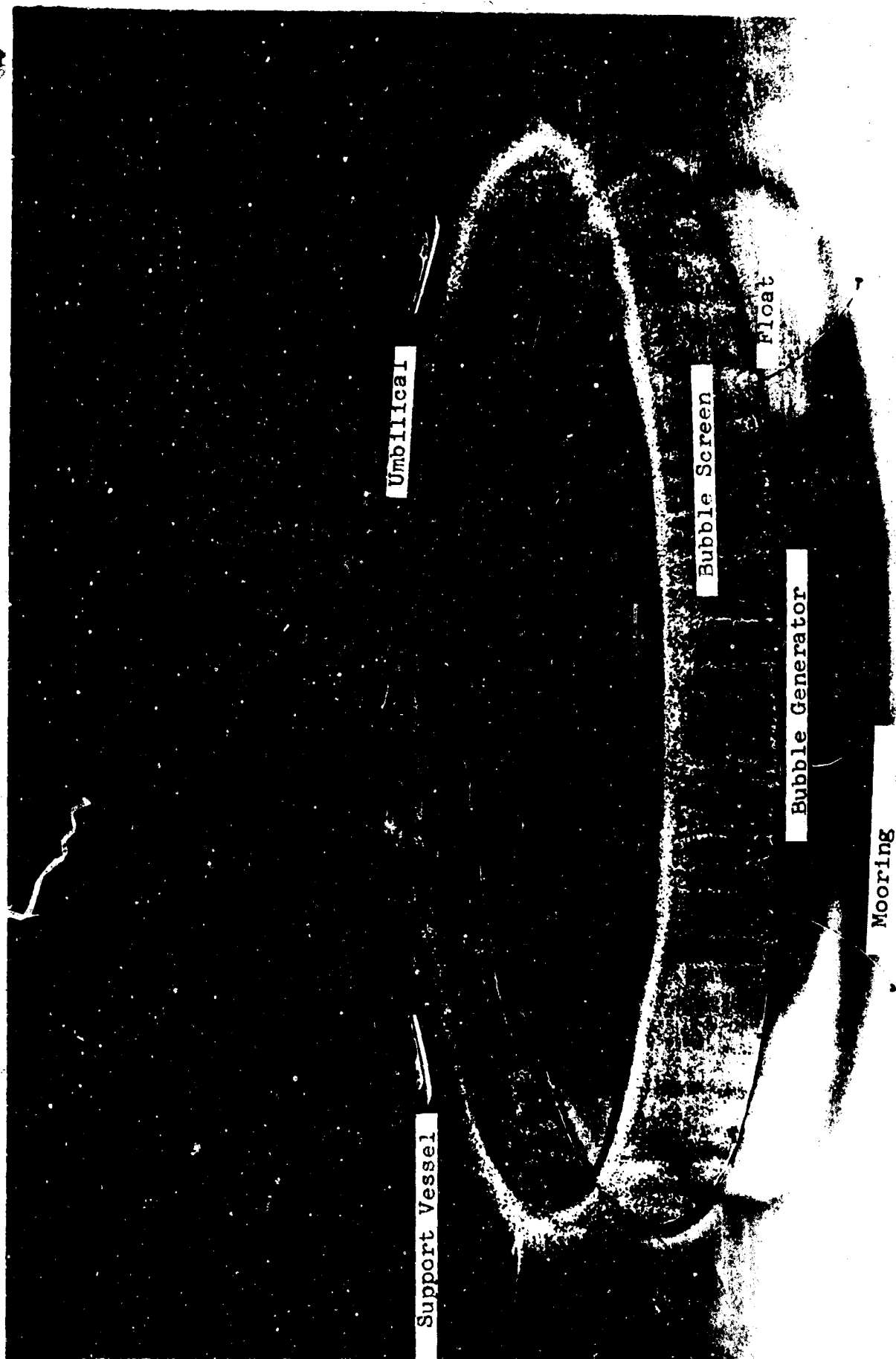


EXHIBIT "C"

- Fig. I-I-4 Pneumatic barrier deployed at sea.



I-1-5 Pneumatic barrier deployed at sea.



I-I-6 A ship passes over a pneumatic barrier.

estuary and it may be turned off during the ebb tide to permit oil or debris to leave the estuary. Floating debris can not cause the pneumatic system to fail.

2. Field Installations

The pneumatic barrier has been successfully used in Kornwerderzand, the Netherlands, to prevent salt water intrusion in existing navigation locks. A most dramatic application is also in the Netherlands at the four locks at IJmuiden⁶. During every complete lockage of the largest of the four locks (measuring 1200 x 150 x 44 ft.) some 3,000 tons of chloride entered the North Sea Canal before the pneumatic barriers were installed. It has been found that by using 210 cubic meters of atmospheric air the salt water intrusion was reduced by 50 percent.

In addition to preventing the salt water intrusion, the pneumatic barrier is said to be effective in separating floating matter from areas to be kept clear of pollution; repelling surface layers of oil, log floats, driftwood and drifting ice.

Outside of actual installations in the Netherlands, the pneumatic barrier to contain oil has not been evaluated in the laboratory or in the field. Following the Torrey Canyon accident, a 1200-ft. long pneumatic barrier was placed across the mouth of the Helford River^{7,8} to try to prevent incoming oil. However, the oil never reached the river mouth and the performance of the system could not be evaluated.

A 500-ft. long air curtain was installed across the

entrance to the boat basin at Santa Barbara, California. The manufacturer of the installation⁹ claimed that the pneumatic barrier divided and separated the oil slick 15 feet to either side of the barrier.

3. Large-Scale Model Tests

The Army Transportation Research Command¹⁰ conducted large-scale model tests of a pneumatic breakwater. The feasibility of pneumatic wave attenuation was evaluated in this study for the two following military applications:

- (a) To produce a relatively calm area immediately surrounding a cargo vessel. The air to be supplied by portable compressors temporarily installed on the vessel during discharge operations.
- (b) To produce a relatively calm passage through surf to permit small crafts to approach the beach without the danger of broaching and remain in the breaker-free zone produced by a pneumatic barrier.

The studies were conducted in a two-dimensional wave channel in water depths between 7 and 16 feet with wave heights of between 1 and 5 ft. which approached the near shore field conditions.

The major conclusions of the study were that the large-scale model tests indicated that approximately 1/6 less air horsepower was necessary than was predicted by small-scale tests and that cargo discharge capability should increase by approximately 25 percent for the case of 50 percent wave attenuation produced by the pneumatic breakwater.

4. Need for Study

There was sufficient evidence, both field and laboratory, to indicate that the pneumatic barrier should be considered as an alternative to any mechanical barrier for use at sea under certain, specified environment conditions.

It was also evident that hydrodynamic analysis as well as experimental model tests, both small and large scale, were needed to evaluate the effectiveness of the pneumatic barrier under specified sea conditions and to provide sufficient information to permit design of a pneumatic barrier to contain oil.

5. Previous Engineering Studies to Evaluate Basic Concepts

There has been little theoretical work published as to the reason why the pneumatic barrier is effective in attenuating deep-water waves. Taylor⁴ suggested that the damping of waves is caused by the horizontal current which spreads out from the region where the vertical current induced by the rising bubbles reaches the surface. The bubbles themselves do not dampen the waves any appreciable amount, as the change in density in the bubble region is very small. One part of Taylor's theory was concerned with the theoretical predictions of the surface-current velocity required to stop waves of given length. The second part provided a method of computing the surface currents induced by a curtain of air bubbles.

The experimental work conducted by Wetzel¹, Straub⁵, Bowers⁵, Tarapore⁵, and Herbich³ indicates that if the maximum velocity is measured at a distance of one water depth from

the barrier, then the agreement between theoretical and experimental values is good. However, the theoretical relationship between the generated surface current and the air flow rate could not be verified experimentally as the measured surface current was considerably smaller than that predicted by theory for a given air discharge.

Based on theoretical and experimental studies by many researchers, including Evans¹⁰, Radionov¹¹, Dmitriev¹² and Herbich², it appeared that a pneumatic barrier would be feasible from an engineering viewpoint and that it will be effective in containing oil at sea.

More recently, Sjoberg and Verner¹⁵ conducted a study on the application of pneumatic barriers to stop the spreading of oil on water. This particular study proved to be quite helpful to the investigations conducted at the Hydromechanics Laboratories of Texas A&M University and permitted a number of short-cuts in the experimental procedures.

6. Environmental Conditions Imposed by the Sponsor

Heavy duty system: Upper limit for effective performance

1. Wind: Hourly average 40 mph at standard height.

The corresponding wind speed at any height below 10 m can be found using the following table:

Height above mean water level, meters	Percentage of 10 m windspeed
0.5	65
1.0	72
2.0	79
3.0	84
5.0	90

See previous table for speed at any height.

Gusts up to 60 mph can be expected, lasting no longer than 5 seconds each hour.

Waves: Wave conditions are specified as follows:

Parameter	Deep Water	Shallow Water
Significant height, ft.	10	10
Significant period, sec.	7.5	6
Average height, ft.	6.4	6.4
Average period, sec.	6.3	---
Average length, ft.	134	100
Range of periods, sec	3.4-12	---
Period of energy maximum, sec.	8.9	---
Height of highest 1/10 of waves, ft	13	---

Current: Sea current (uniform over depth of barrier): 2 knots

Heavy duty system: Upper limit for physical integrity

1. Wind: Hourly average 60 mph at standard height. See table above for speed at any height.

Gusts up to 90 mph can be expected, lasting no longer than 5 seconds each hour.

2. Waves: Wave conditions are specified as follows:

Parameter	Deep Water	Shallow Water
Significant height, ft.	20	20
Significant period, sec.	10	8
Average height, ft.	14	14
Average period, sec.	8.6	--
Average length, ft.	250	200
Range of periods, sec.	5-17	--
Period of energy maximum, sec.	12.1	--
Height of highest 1/10 of waves, ft.	28	--

3. Current: Sea current (uniform over depth of barrier): 3 knots

Review of the above conditions indicated that some discrepancies between the values given above and those calculated existed. However, the Sponsor indicated that the values supplied should be used to provide a common basis for systems design and model testing.

The calculated values were as follows:

(a) Wave Conditions Specified:

Deep Water

Assume significant wave height, $H_{1/3}$ of
10 ft. is correct.

Calculate average wave ht. ft.

$$\bar{H} = 0.625 H_{1/3} = 6.25 \text{ ft.}$$

Calculate height of highest 1/10 of waves, ft.

$$H_{1/10} = 2.03\bar{H} = 1.27 H_{1/3} = 12.7 \text{ ft.}$$

For $H_{1/3} = 10 \text{ ft.}$, $T_{\text{mean}} = 6.2 \text{ sec.}$

$$T_{1/3} = 1.24 T_m = 7.70 \text{ sec.}$$

$$L_0 = 5.12 (6.2)^2 = 197.0 \text{ ft.}$$

(b) Upper Limit for Physical Integrity:

Deep Water

Assume significant wave height, $H_{1/3}$ of 20 ft.
is correct.

Calculate average wave ht. ft.

$$\bar{H} = 0.625 H_{1/3} = 12.5 \text{ ft.}$$

Calculate height of highest 1/10 waves, ft.

$$H_{1/10} = 2.03\bar{H} = 1.27 H_{1/3} = 25.4 \text{ ft.}$$

For $H_{1/3} = 20 \text{ ft.}$, $T_{\text{mean}} = 9.4 \text{ sec.}$

$$T_{1/3} = 1.24 T_m = 11.68 \text{ sec.}$$

$$L_0 = 5.12 T^2 = (5.12) (9.4)^2 = 452 \text{ ft.}$$

(c) Definitions

1. Significant wave ht. - The average height of one-third highest waves of a given wave group. (> 100 waves).
2. Significant wave period - Period of the one-third highest waves within a group.

7. Proposed System

The pneumatic barrier will consist of a manifold pipe made of steel and submerged at the required depth, air supply umbilical pipes, and compressors for providing the required amount of air at the desired pressure.

The main manifold pipe releasing air to produce a pneumatic barrier will be located about 25 feet below the water's surface. The hole spacing along the main pipe was determined in the hydrodynamics tests and was recommended to be six to 12 holes per foot of pipe. The hole size required will be between $1/32$ and $1/16$ inch. In the same part of the study, the air flow was determined to be in the range of one cubic foot per second per foot length of pipe. This rate of air flow would produce a surface current of five feet per second. The power required at the manifold will range between 5 and 12 horsepower per foot length of pipe depending on the overpressure in the pipe. Frictional losses in the supply pipes are considered negligible so that approximately the same power will be required at the compressor.

Initially, a flexible P.V.C. pipe was considered for the manifold pneumatic barrier. After serious consideration, it was decided that the pipe should be rigid to facilitate control of placement and floatation level and to provide the

necessary tensile load-carrying capability. The most suitable pipe will, therefore, be a steel pipe.

The size of pipe will depend on the type of compressor used and will be between 4.5 and 7.0 inches in diameter. A rotary, positive displacement, axial flow compressor driven by a gas turbine engine will supply 18,675 CFM at 49.7 PSIA and will require 2,255 BHP. This unit can supply air for 310 feet of pneumatic barrier at 7.27 HP per foot length of barrier. The weight of the unit may be excessive and further development of such a unit will be required to reduce its weight. Another type of unit is the gas turbine-driven air compressor which will deliver 20,000 CFM at 40.0 PSIG. This unit can supply air for 210 feet of pneumatic barrier and can be loaded on a C-130 aircraft. Since this type of unit will provide compressed air at pressures higher than required, the pneumatic barrier pipe can be reduced to 4 inches in diameter.

The connectors are of the hub and clamp type and are readily obtainable. The umbilical pipe can be made of nylon reinforced neoprene-covered flexible sleeves, also readily available.

The pneumatic barrier pipe will have a primary and secondary flotation system. The primary system will consist of fluidic logic devices and air bags, while the secondary flotation system will be composed of large polyethylene floats attached

to the pipe with 30-foot long nylon ropes.

The Heavy Duty System will be stored in four subsystem packages:

Package I Machinery - This package will consist of a turbine-driven compressor, a machinery hull, a cradle, and a pallet. The estimated weight will be 21,000 pounds.

Package II - Inflatable rubber fuel tanks.

Package III - Bubble Screen - This package will contain a complete set of 200 feet of pipe sections, clamps, one umbilical, and floats. Approximate weight is 3,000 pounds.

Package IV - Mooring - This package will contain four anchor and mooring lines to connect the bubble generators, and machinery hulls as shown in Fig. III.III.8. Approximate weight is 12,000 pounds.

All packages will be secured to standard C-130 aircraft pallets. The packages will be removed from storage and transported to the C-130 aircraft by a 25K aircraft cargo loading truck Fig. III.I.12. The packages will be ground winched onto the C-130. Three aircraft will be required for each 200 foot module of bubble barrier. The aircraft will fly to an airport near a port close to the oil spill. The packages will be off-loaded onto flatbed trucks for transportation to docks or Coast Guard station. Packages III and IV will be loaded onto

a buoy tender. Packages I and II will be set in the water. Jet fuel tank trucks will load 120,000 gallons of fuel into the fuel bags. This is an eight day fuel capacity. Estimated time for transport and loading will be two to four days depending on the availability of buoy tenders.

Because of the towing characteristics of the fuel tank, the tenders will require six to 24 hours to reach the spill site.

8. Adaptability of the System

The oil containment system should be designed for a number of possible combinations of waves, currents and wind. Two such combinations are selected as an example as shown in Fig. I-I-7.

(a) Case 1

Wave, current and wind coming from one quarter. In this case the pneumatic barrier need not be placed around the oil to be contained. The pneumatic barrier could be deployed by two U.S. Coast Guard ships in the manner shown in Fig. I-I-7.

(b) Case 2

In this case the waves and wind are coming from one quarter and the current from the opposite direction to the waves' direction.

The pneumatic barrier must enclose the oil spill in such a case.

The system is compatible with existing equipment and designed so that it can be deployed, wholly or in part, by

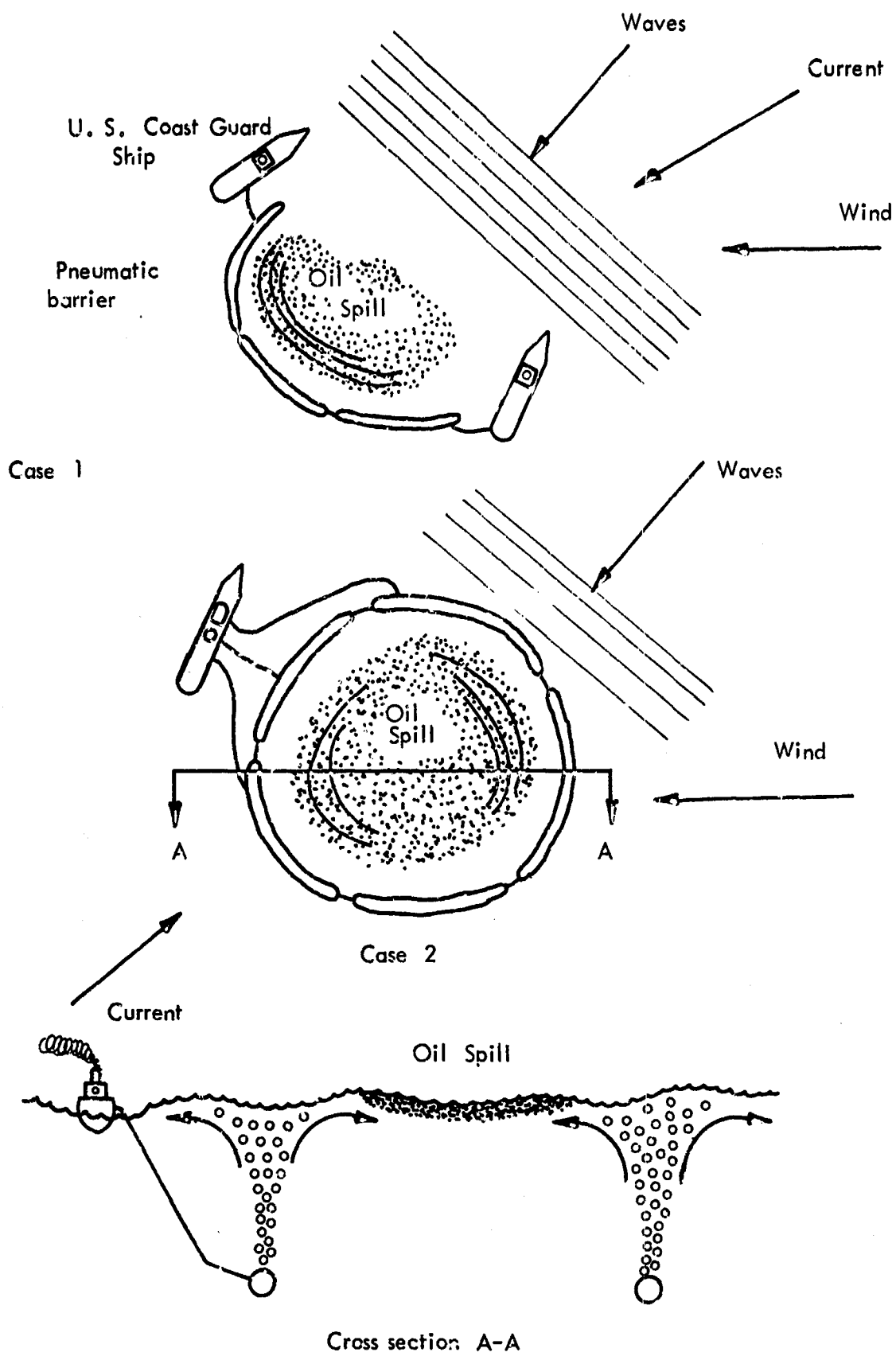


FIG. I-I-7 PNEUMATIC BARRIER CONTAINMENT SYSTEM

any of the existing ships or aircraft of the U.S. Coast Guard.

9. Emphasis on Unique and Significant Features of Design

The pneumatic system will be easily deployed and retrieved. The system can be operated by compressors on board existing ships or from floating platforms or barges placed at the site of the spill. The pneumatic system will allow ships or other craft to pass over the barrier without causing removal or shut down.

Additional side benefits are that certain amounts of wave attenuation will be achieved of the order of 5-10 percent. If environmental conditions are less than those specified, a much greater wave attenuation may be expected which will permit an easier and more efficient way of disposing of the oil from the contained area.

10. Summary

A pneumatic barrier concept has proven to be a most effective oil containment device to operate under environmental conditions specified. Its effectiveness was demonstrated in the laboratory at various water depths up to 7.5 feet. The air, power, etc. requirements have been based on the experimental studies. Since the tendency of the air discharge and power requirements decrease with the increase in model size, it can be expected that the air and power requirement may be further reduced for the prototype installation.

The most demanding environmental requirement is the 2 knot current. If the current is reduced to 1 knot, the air discharge and horsepower may be reduced from 1 cfs/ft to 0.5 cfs/ft. and from approximately 8.0 HP/ft. to 4.0 HP/ft., assuming one atmosphere overpressure in the manifold located 30 ft. below the surface.

I-II. Research Conducted

The engineering study to develop the basic design concept involved determination of the following factors:

1. Oil set-up by wind
2. Oil set-up by current
3. Hydrodynamics of the pneumatic system
 - (a) minimum surface velocity to contain oil
 - (b) optimum depth of pipe submergence
 - (c) optimum pipe size - orifice area combination
 - (d) air discharge, pressure discharge head, and power requirements at the orifice
4. Pneumatic supply
 - (a) supply pipe
 - (b) fluidic devices
 - (c) compressor and prime mover
 - (d) system strength
 - (e) physical characteristics
5. Deployment capability
6. Reliability standards
7. Maintenance
8. Suitability

1. Oil Set-Up by Wind

The two-dimensional wind set-up of oil retained by a barrier was investigated analytically and experimentally. The results may be incorporated with results of the investigation of set-up of oil by currents to give the total set-up due to the combined effects of wind and currents.

The shear stress, τ_o , at the air-oil interface may be written

$$\tau_o = C \rho_w U^2 \quad (\text{II-1})$$

where ρ_w is the density of water, U is the wind speed, and C is a drag coefficient that will vary with the surface roughness. From the equation of hydrostatics applied at the barrier; a summation of horizontal forces on the oil wedge; and the above equation for wind stress the following equations were developed.

$$d_o = \sqrt{\frac{2 \tau_o L}{g \rho_o (1 - \rho_o/\rho_w)}} = \sqrt{\frac{2C U^2 L \rho_w}{g \rho_o (1 - \rho_o/\rho_w)}} \quad (\text{II-2})$$

Here, d_o is the set-up at the barrier, L is the oil fetch length, ρ_o is the oil density and g is the acceleration due to gravity. This indicates that the oil wedge is parabolic in shape and that the volume of oil retained per length of barrier, V , is:

$$V = \frac{2}{3} d_o L \quad (\text{II-3})$$

The equation for set-up can also be written

$$d_o/L = \sqrt{2C \rho_w/\rho_o} \cdot \frac{U}{\sqrt{Lg (1 - \rho_o/\rho_w)}} \quad (\text{II-4})$$

which shows that the dimensionless set-up, d_o/L , depends upon a Froude number, $U/\sqrt{Lg (1 - \rho_o/\rho_w)}$, and the drag coefficient, C , which is constant if no waves are generated in the oil.

Plots of these values as a function of oil viscosity are presented in the main report as well as plots of set-up for all oils, wind velocity data, etc. Plots of set-up of oil as a function of distance along the oil wedge indicate that the wedge shape is parabolic and accordingly that volume predictions based on this are satisfactory.

In order to combine these results with current effects it is necessary to present an overall design wind stress equation. Using an envelope curve for all test data yields:

$$\tau_o = 6.9 \times 10^{-6} \rho_w U^2 \quad (\text{II-5})$$

for the air-oil interface stress including waves. Again, the wind velocity is for an evaluation of 0.7 ft.

Tests were run with three oils having the following properties.

<u>No.</u>	<u>Viscosity (centipoise)</u>	<u>Specific Gravity</u>
1	388	0.888
2	3.7	0.858
3	96	0.911

Each oil was placed in the 2 ft wide by 3 ft deep by 120 ft long wind-wave flume with 14 or 18 inches of water and subjected to a range of wind velocities. The oil wedge thickness at a retaining barrier and at 10 foot intervals upwind from this point was measured with a point gage and a specially designed stilling well. Wind velocities were measured at 0.1 ft intervals along a vertical line at the tank center and 5 ft upwind of the barrier. A reference velocity at 0.7 ft elevation was used for the flume experiments and was found to be related to the velocity at 10 meters elevation by $1.75 U_{0.7} = U_{10}$.

Below a critical wind velocity, U_c , the set-up of oil of any viscosity and density (less than 1.0) is given by

$$d_o/L = 2.3 \times 10^{-3} \sqrt{\frac{\rho_w}{\rho_o}} \cdot \frac{U}{\sqrt{gL(1 - \rho_o/\rho_w)}} \quad (\text{II-6})$$

For $U > U_c$ when waves cause an excess surface stress.

$$d_o = 2.3 \times 10^{-3} \frac{\rho_w L}{\rho_o g (1 - \rho_o/\rho_w)} U + \frac{2BL \rho_w}{\rho_o g (1 - \rho_o/\rho_w)} (U - U_c) \quad (\text{II-7})$$

where B and U_c have the following values

<u>Oil No.</u>	<u>$B \times 10^6$</u>	<u>U_c, fps</u>
1	49.3	32.6
2	7.7	11.7
3	14.1	24.0

2. Oil Set-Up by Current

The purpose of this research was to investigate the oil set-up due to current. More specifically, the objective was to study the behavior of oil floating on water and held in place by a barrier while the underlying water flowed past. Of particular interest was the oil geometry as a function of current velocity, oil density and viscosity. Also, a quantitative description of the entrainment of the oil by the flowing water was of interest.

The need for the study results from the need for a knowledge of the depth of the oil at the barrier. This set-up depth (as well as that contribution due to wind) is the primary consideration in the determination of the air requirements of the barrier. The entrainment of the oil by the flowing water is also of interest as a mode of failure of the barrier.

The specific objectives of the task concerned with oil set-up due to current was: (a) to determine the complete description of the set-up configuration as a function of current and fluid properties, (b) to study the entrainment of the oil due to the flowing water.

When an oil layer is subjected to a current and held in place by a fixed barrier, the resulting layer configuration appears similar to that shown in Fig. I-II-1. Three separate regions of the layer may be identified wherein the resulting configuration is dependent on different mechanisms.

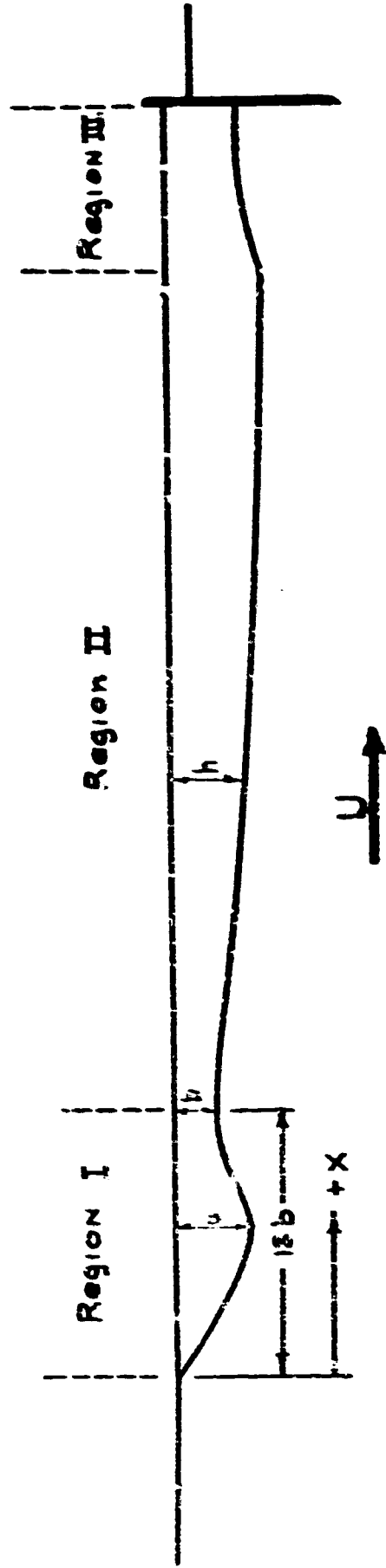


FIG. I-II-1
OIL SET-UP DUE ^{TO} A CURRENT

And, as a consequence of the different controlling mechanisms, it was impossible to model the complete flow phenomena at one time because Froude and Reynolds laws cannot be satisfied simultaneously. The general approach was to study the flow in parts by use of a semi-empirical theory. Once the experimental constants were evaluated the theory was extended to calculate prototype set-ups.

Region I

The shape of the head wave region (or Region I) is considered to be controlled primarily by gravity and inertia forces. Accordingly, a dimensional analysis of the variables involved indicates that the single dimensionless number, which is generally called the densiometric Froude number, should describe the flow,

$$\frac{U^2}{gb \left(1 - \frac{\rho_o}{\rho_w}\right)} = C_1 \quad (\text{II-8})$$

where U is the current velocity, $g = 32.2 \text{ ft/sec}^2$, b denotes the head wave thickness and ρ_o and ρ_w are the density of the oil and water, respectively.

In order to evaluate the constant occurring in equation II-8, a series of tests was conducted using oils of various densities. The head wave thickness and current velocities were recorded and the results of these tests were plotted in the form of U^2 versus $gb(1 - \rho_o/\rho_w)$.

A straight line drawn through this data shows that the constant has a value of approximately $C_1 = 3.5$. Thus, equation II-8 is plotted in Fig. I-II-2 showing the head wave thickness as a function of current velocity for oils of various specific gravities.

According to the laws of dimensional analysis, it is expected that the head wave would have a fixed shape independent of velocity or oil density. This shape can be demonstrated by plotting the coordinates of the head wave profile made dimensionless with the thickness, b . Although considerable scatter can be expected in this kind of plot, a characteristic shape does exist and is shown in Fig. I-II-3. According to the figure, the neck of the head wave occurs at approximately $x/b = 13$ and, therefore, Region I may be considered to extend to $x = 13 b$.

Region II

The geometry of the oil layer in Region II indicated in Fig. I-II-1 (i.e.) in the region where values of $x \geq 13b$, depends not only on gravity and inertia forces but also on viscous forces. The action of the water flowing under the oil layer causes a gradual build-up of the layer thickness with distance along the layer. This viscous shear stress at the interface is just offset by the gravitational forces tending to cause the oil layer to spread in the direction of the flow.

In order to describe the oil layer in Region II a

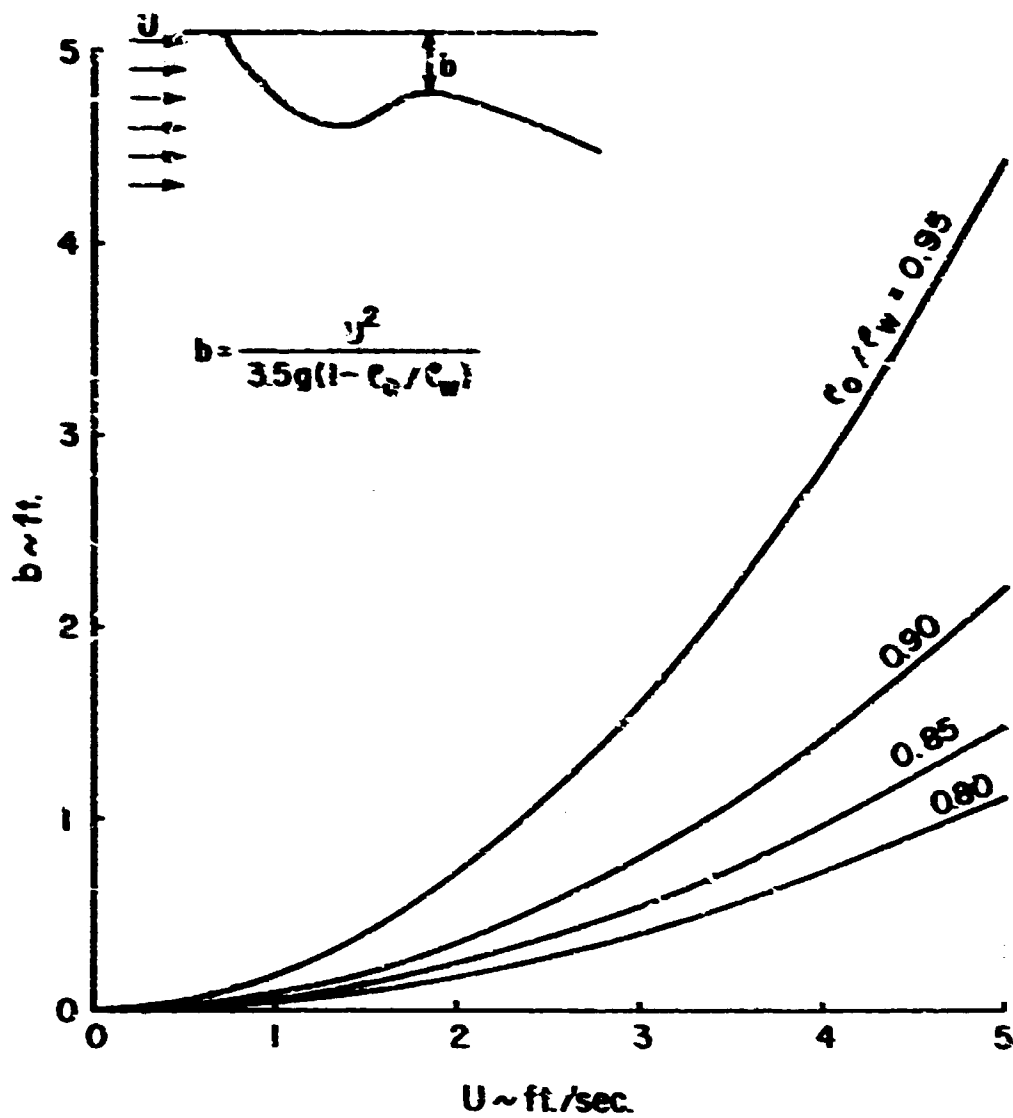


FIG. HEAD WAVE THICKNESS
I-II-2

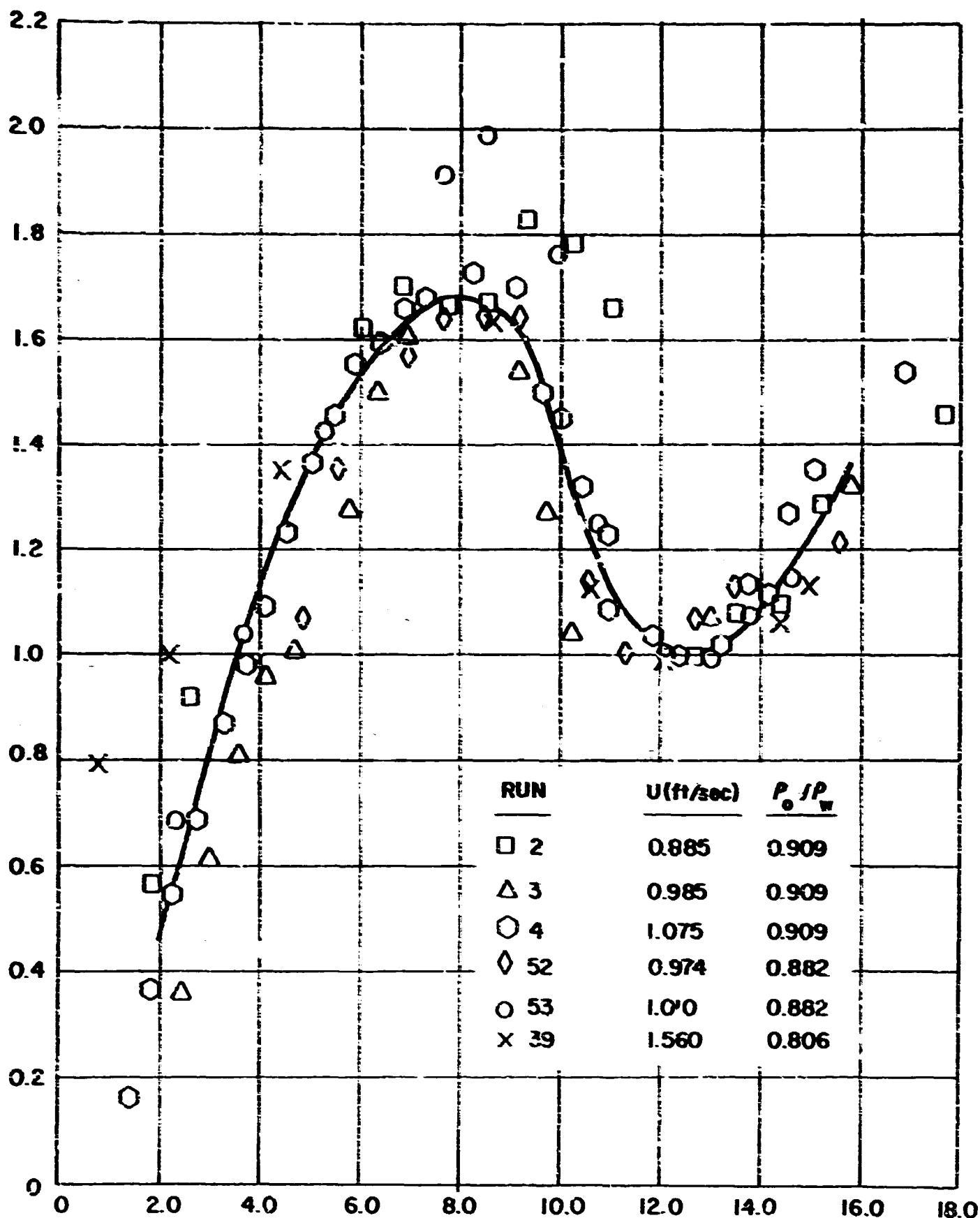


FIG. HEAD WAVE PROFILE
I-II-3

momentum analysis was applied to a control volume which included the hydrostatic pressure forces and shear stresses due to the under-flowing water. The result of this analysis yields the following relationship for the oil layer thickness as a function of distance along the layer:

$$h = \sqrt{\frac{U^2(x - 13b)}{g \frac{\rho_o}{\rho_w} (1 - \frac{\rho_o}{\rho_w})} \left[\frac{C_i}{\left(\frac{U(x-13b)}{\nu_w} \right)^{1/n}} + \frac{\tau_s}{\frac{1}{2} \rho_w U^2} \right] + b^2} \quad (\text{II-9})$$

where:

h = oil layer thickness

U = current velocity

ρ_o = density of the oil

ρ_w = density of the water

g = 32.2 ft/sec²

b = head wave thickness

ν_w = kinetic viscosity of water

C_i = shear stress coefficient

n = 5.0

τ_s = wind shear stress at the free surface

The two unknowns, C_i and n , occurring in equation (II-9) were introduced by assuming the following form for the shear stress at the oil water interface:

$$\frac{\tau_i}{\frac{1}{2} \rho_w U^2} = C_i \left[\frac{U(x - 13b)}{z_w} \right]^{-1/n}$$

where:

τ_i = Shear stress at the oil-water interface

C_i = Shear stress coefficient

n = constant

This form of the shear stress law is valid for flow past a flat plate with $C_i = 0.058$ and $n = 5.0$. In the present case, however, the equation was applied to the experimental data from the model tests and C_i and n were adjusted until the equation fit the data. In this manner a correlation between C_i and current velocity was determined and is presented in Fig. I-II-4. However, n was found to be equal to 5.0 as in the case of flow past a flat plate.

Prototype Oil Set-Ups

The complete geometry of the oil layer is described by a combination of the head wave shape present in Fig. I-II-3, where b is given by Fig. I-II-2, along with equation II-9 which describes the oil thickness in Region II. Using these results, the oil set-up corresponding to the prototype conditions of 0.5, 1.0, 1.5, 2.0 and 2.5 knots are presented in Figures I-II-5 through II-9.

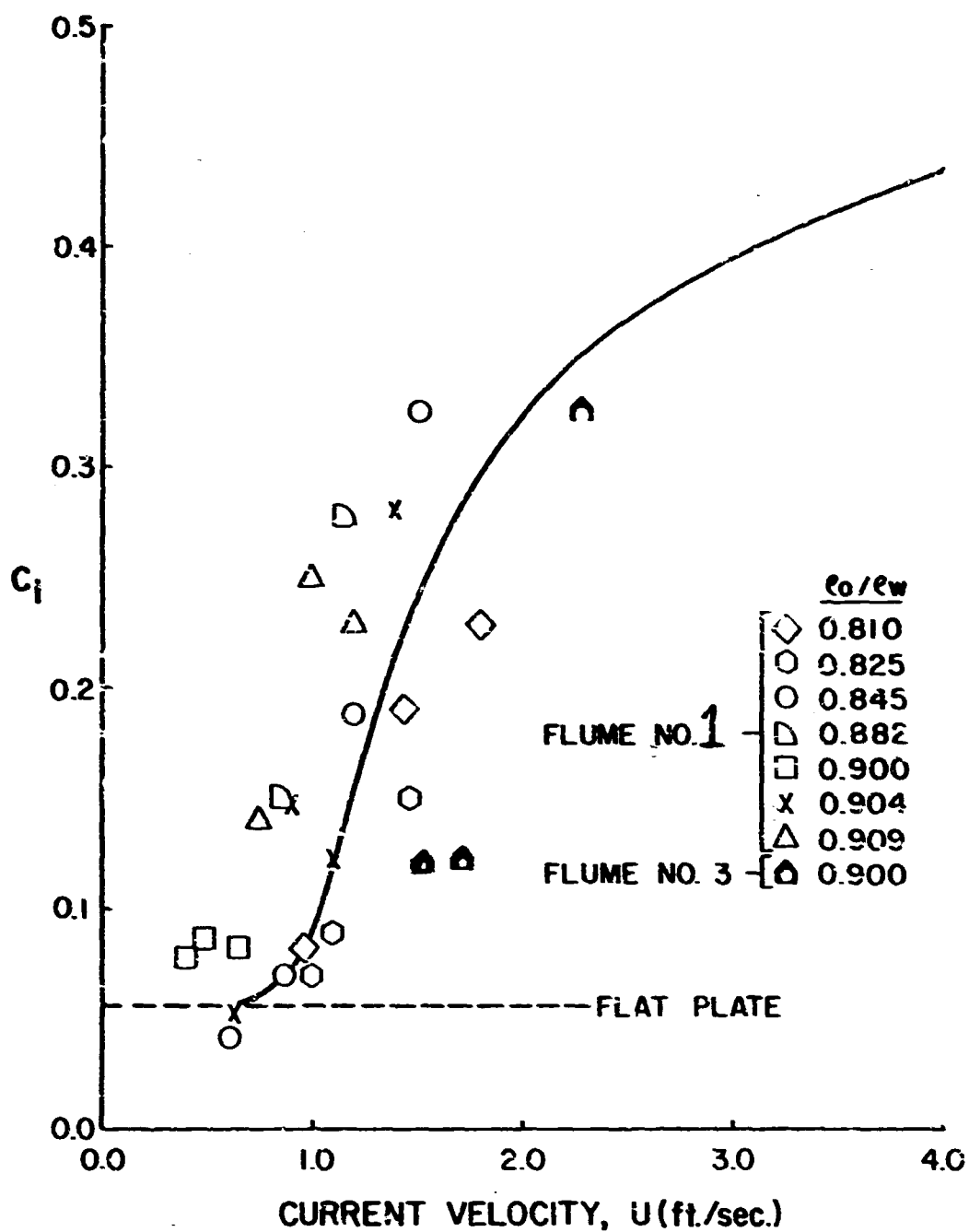


FIG. I-II-4 INTERFACIAL SHEAR STRESS COEFFICIENT versus CURRENT VELOCITY (CORRECTED FOR DEPTH EFFECT)

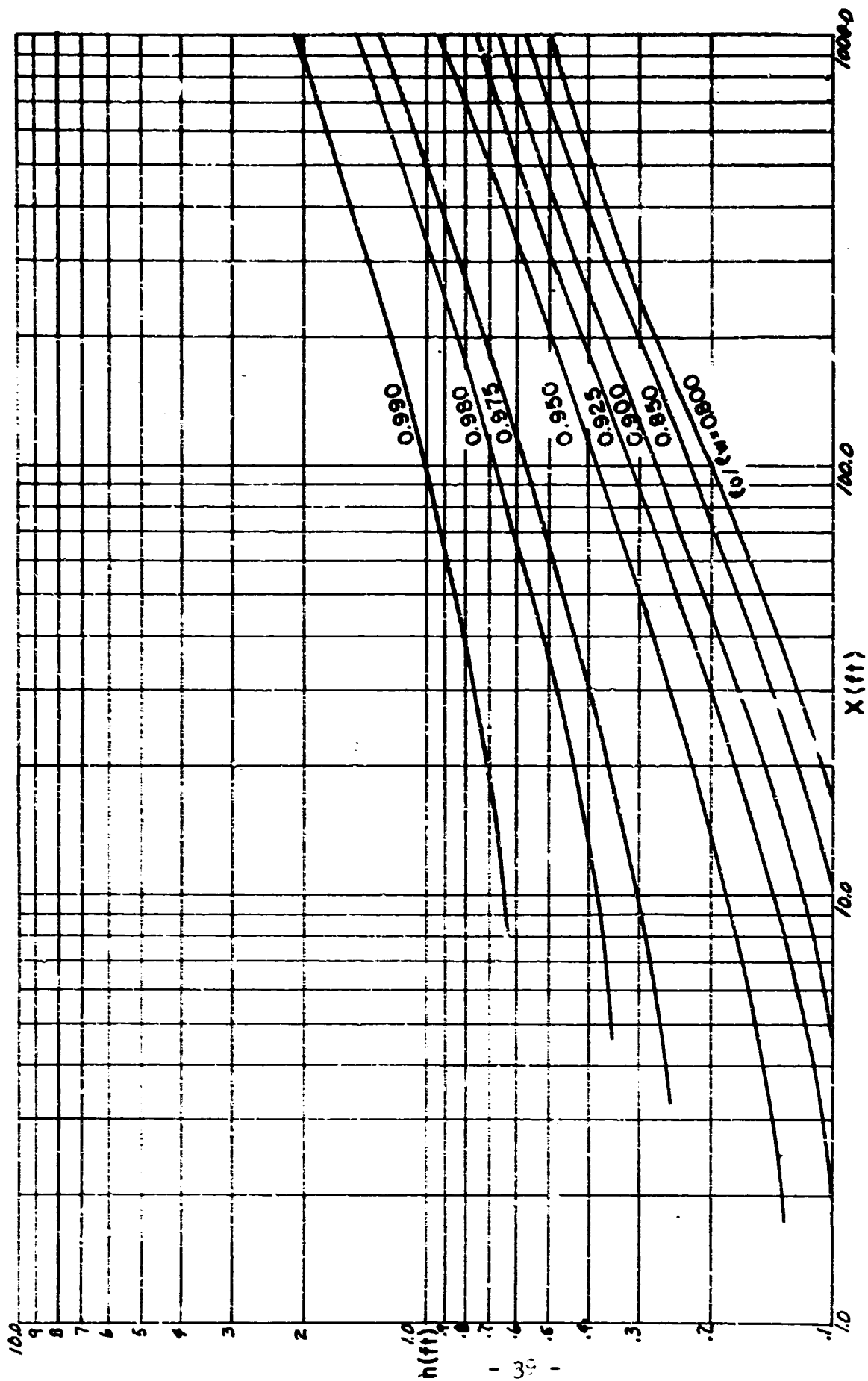


FIG. OIL LAYER CONFIGURATION FOR 0.5 KNOT CURRENT
I-II-5

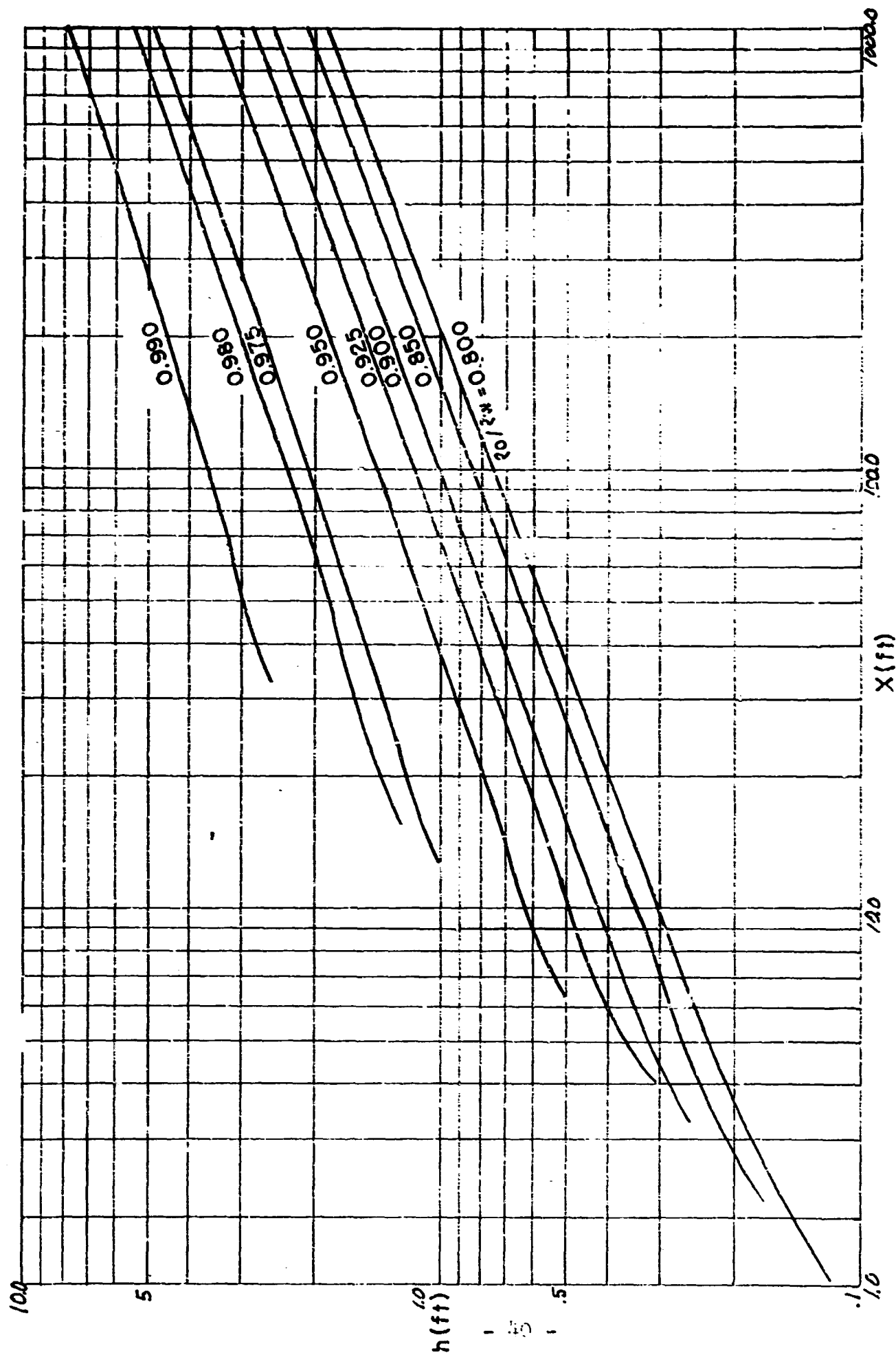


FIG. OIL LAYER CONFIGURATION FOR 1.0 KNOT CURRENT
I-II-6

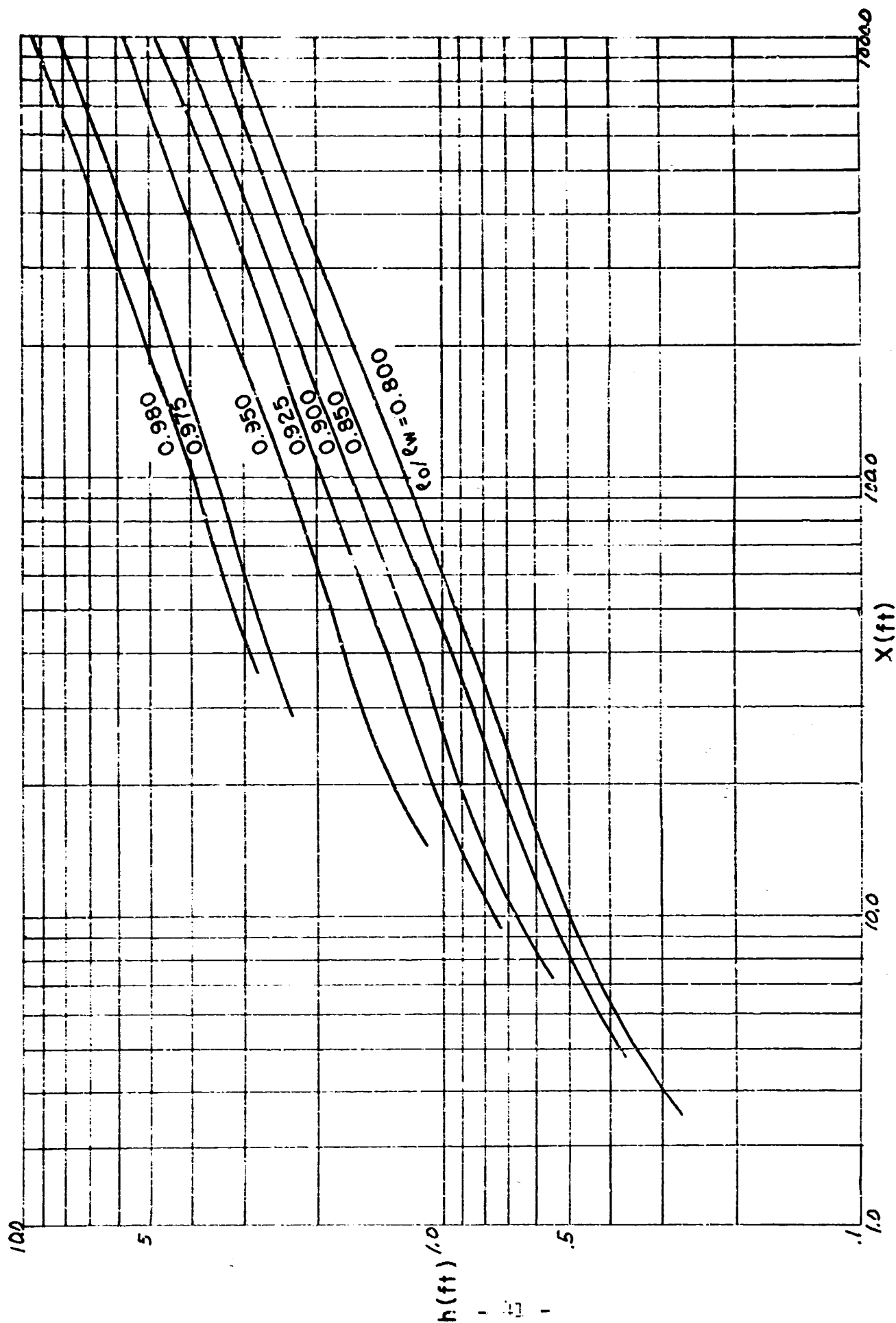


FIG. OIL LAYER CONFIGURATION FOR 1.5 KNOT CURRENT
I-II-7

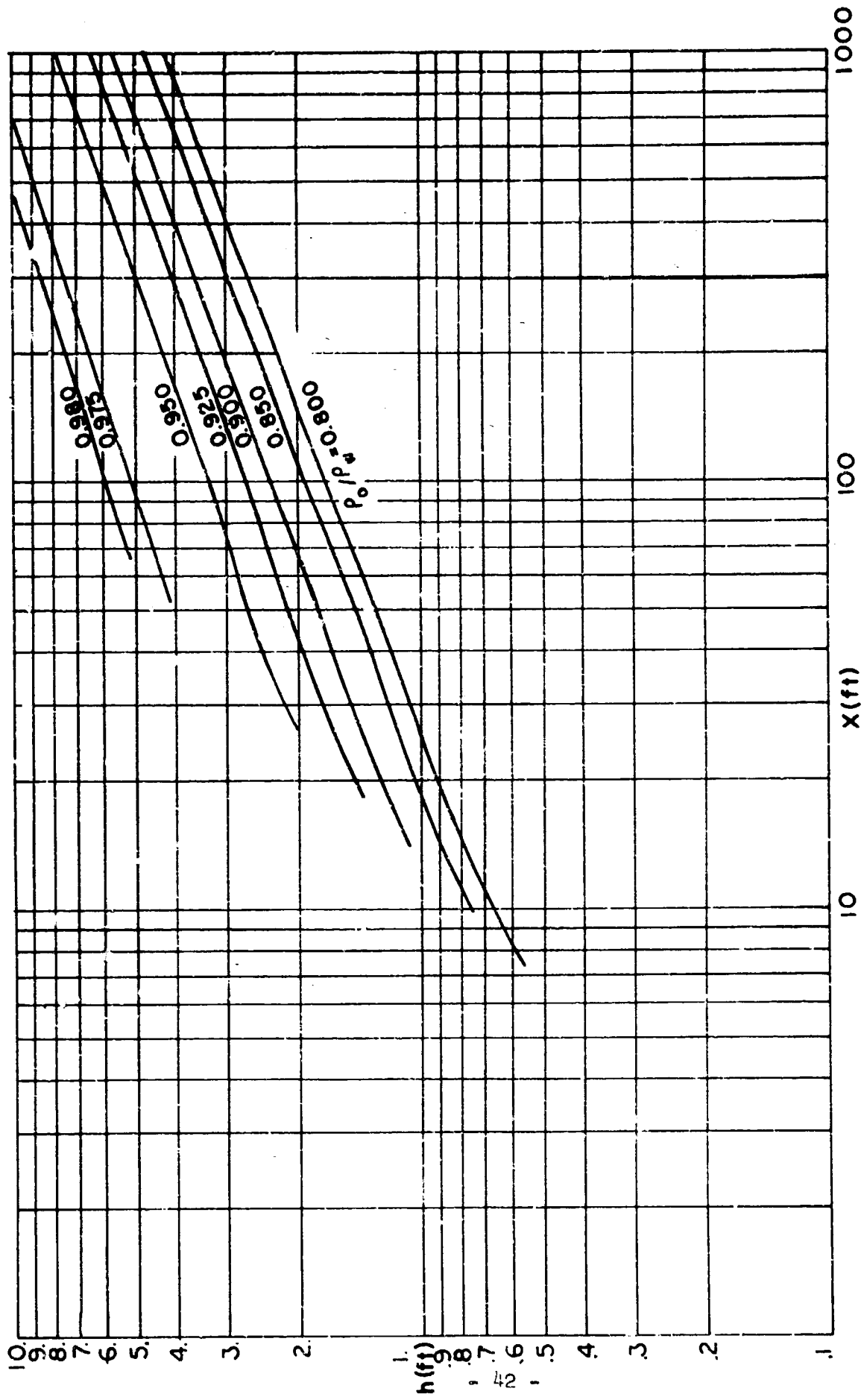


FIG. OIL LAYER CONFIGURATION FOR 2.0 KNOT CURRENT
I-II-8

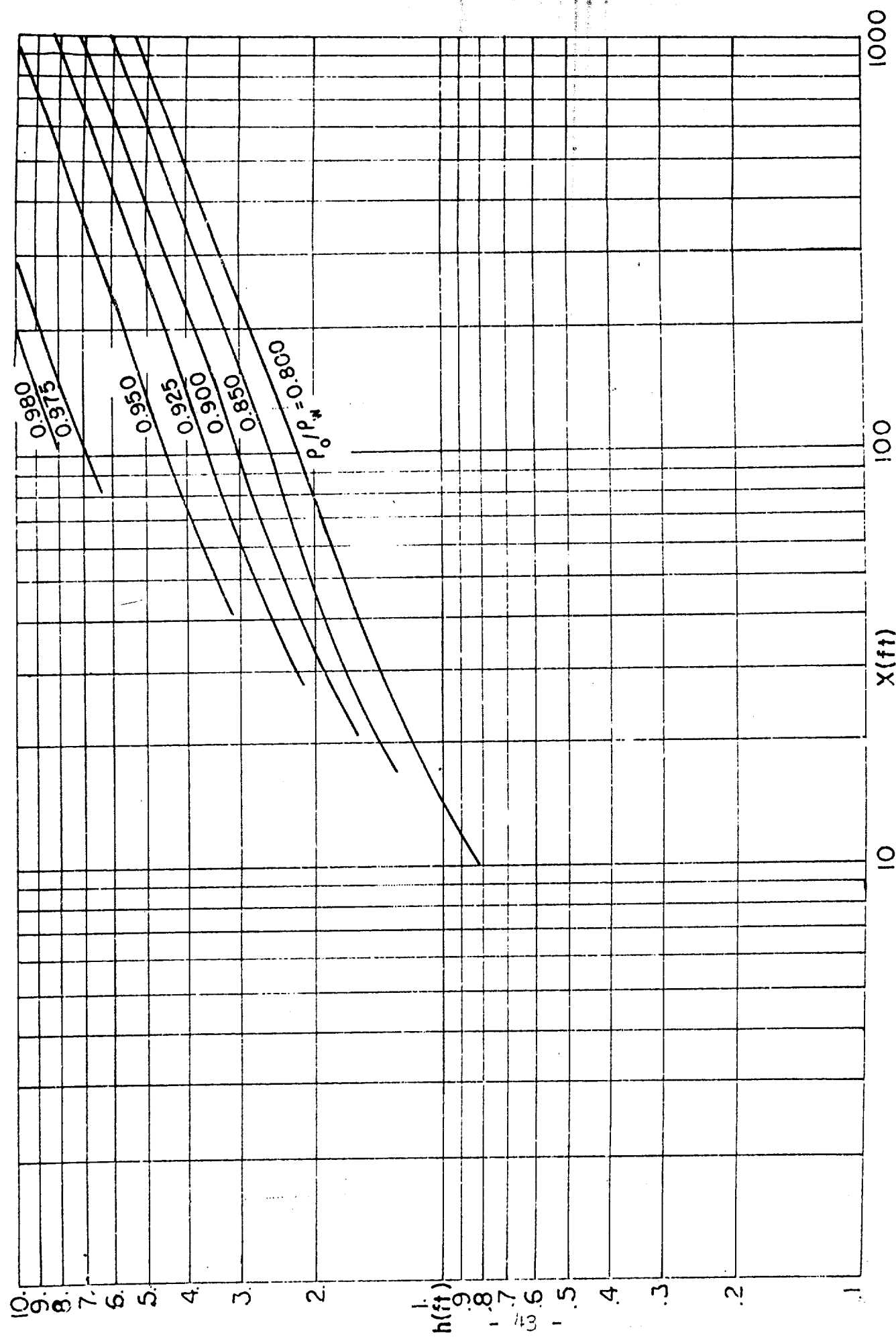


FIG. OIL LAYER CONFIGURATION FOR 2.5 KNOT CURRENT
I-II-9

Entrainment

At water velocities above 1.6 ft/sec, failure by entrainment became significant. The waves along the oil-water interface appeared to be unstable and there was a continuous formation of liquid particles along the interface. The particles had a core of water surrounded by a layer of oil. These particles had a density very near that of water and most of them flowed under the barrier. Those which were retained by the barrier were persistent and formed an oil-water froth behind the barrier. The failure rate due to the particles flowing under the fixed vertical barrier was significant. Failure rate measurements at a water velocity of 1.95 ft/sec indicated a loss rate of about 0.5 gal/min per foot of barrier length.

Entrainment tests were run with SAE 10 motor oil and with diesel fuel with similar results. The only difference was the size range of the particles. Using SAE 10 oil the range of diameter was $3/8$ in. to $3/4$ in., while with diesel fuel it was $1/8$ in. to $3/8$ in.

Results and Conclusions

A theoretical and experimental study has been made of the oil set-up due to current. The oil layer has been broken into two regions, a head wave region wherein the oil layer profile is controlled primarily by viscous and inertia forces. The thickness of this layer is described by the densimetric Froude number given as equation II-8. The characteristic shape of the head wave is shown in Fig. I-II-3.

A semi-empirical theory was developed using the form of the shear law for flow past a flat plate and the coefficient and exponent occurring therein was evaluated experimentally. The shear stress coefficient was found to increase with velocity and approach the limiting value of that associated with the flat plate for very low velocity.

Using the results obtained from the model tests and the semi-empirical theory, the oil layer configuration was calculated and plotted for oils of various density and at prototype current velocities of 0.5, 1.0, 1.5, 2.0 and 2.5 knots. These results, presented in Figs. I-II-5 to II-9 are one of the primary results of the study on oil set-up by current. These results show that for the case of light oils and low currents the set-up depths are quite reasonable. However, as the current and density of the oil increase the set-up depth increases quite rapidly.

Tests at water velocities greater than 1.6 ft/sec

showed that failure by entrainment will be significant at higher velocities.

3. Hydrodynamics of the Pneumatic System

An air bubble released below the surface of a liquid such as water will rise to the surface because its buoyant force is greater than the combination of fluid drag on the bubble and its weight. As the bubble rises it drags water along with it creating an upward flow. At the free surface, the air bubble dissipates itself. However, the upward liquid momentum is deflected and causes a surface current. If a number of small bubbles continuously flow from a submerged duct, a steady surface current can be used to oppose the potential energy of oil of a given depth. When equilibrium is established, the oil is essentially contained by the bubble generated current. This forms the basis of the pneumatic (air) barrier for oil containment. The objective of this task is to determine the relationship between the quantity and manner of air bubbles released and the kinematics of the generated surface flows, i.e., the "hydrodynamics of pneumatics".

Review of the literature indicated that most of the research work, both laboratory and in the field, was limited to the idea of using this system to attenuate waves, hence the name of the "pneumatic breakwater". The only reference pertaining to the study of pneumatic barrier as an oil containment device is fairly recent and is described in Reference 15.

However, the theoretical work conducted on the pneumatic breakwaters is applicable to the pneumatic barrier system and was fully utilized in the study at Texas A&M University.

SURFACE CURRENTS PRODUCED BY A PNEUMATIC BARRIER.

Taylor²⁰ used an analogy between the hot air flow from a heat source and the vertical current induced by the air bubbles. He found theoretically that the vertical current, U_{\max} (See Fig. I-II-10 is related to the unit discharge rate of air, q by the following relationship:

$$U_{\max} = K (gq)^{1/3} \quad (\text{II-11})$$

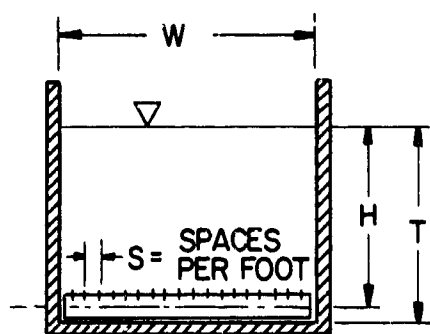
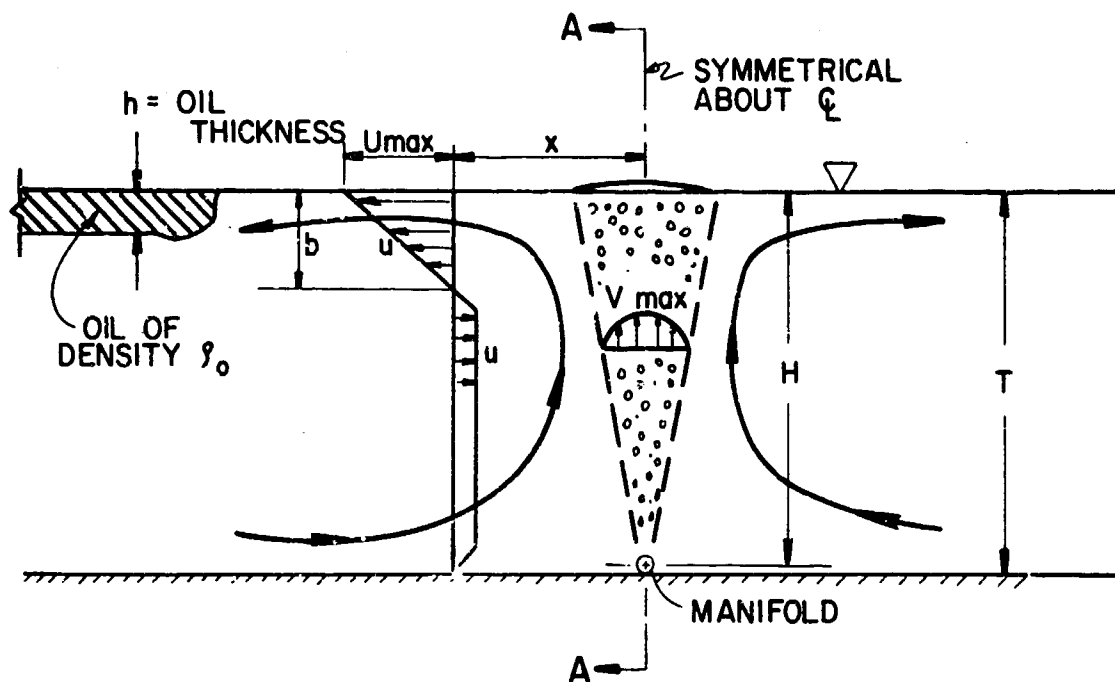
where: g = the gravity constant

K = an experimentally determined constant.

The constant K was found to be about 1.9 from the hot air analogy tests. If no energy loss occurs when the flow momentum changes to the horizontal direction at the surface then the theoretical surface velocity as determined by Taylor becomes:

$$U_{\max} = 1.9 (gq)^{1/3} \quad (\text{Theoretical}) \quad (\text{II-12})$$

Since 1955, many experiments have been performed in the laboratory and at prototype scale to determine the constant in Equation II-11. Those felt to be most significant have been plotted as Figure I-II-11 which also includes Taylor's theoretical result. Although the general trend of all experiments is similar, there was a wide variation in K values obtained. There are many reasons for the variation in the values of constants, but many involved inconsistencies where the current was measured and some were due to "scale effect" and experimental error.



SECTION A-A

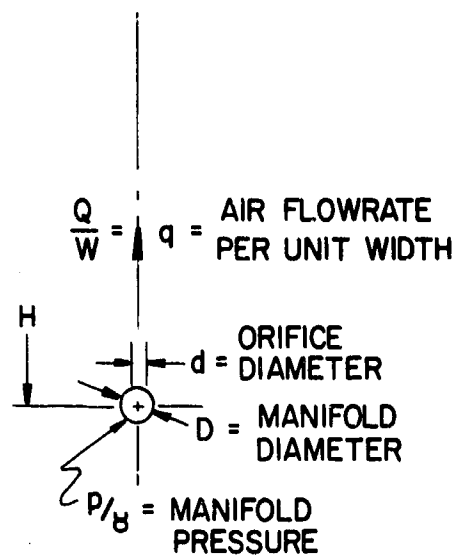
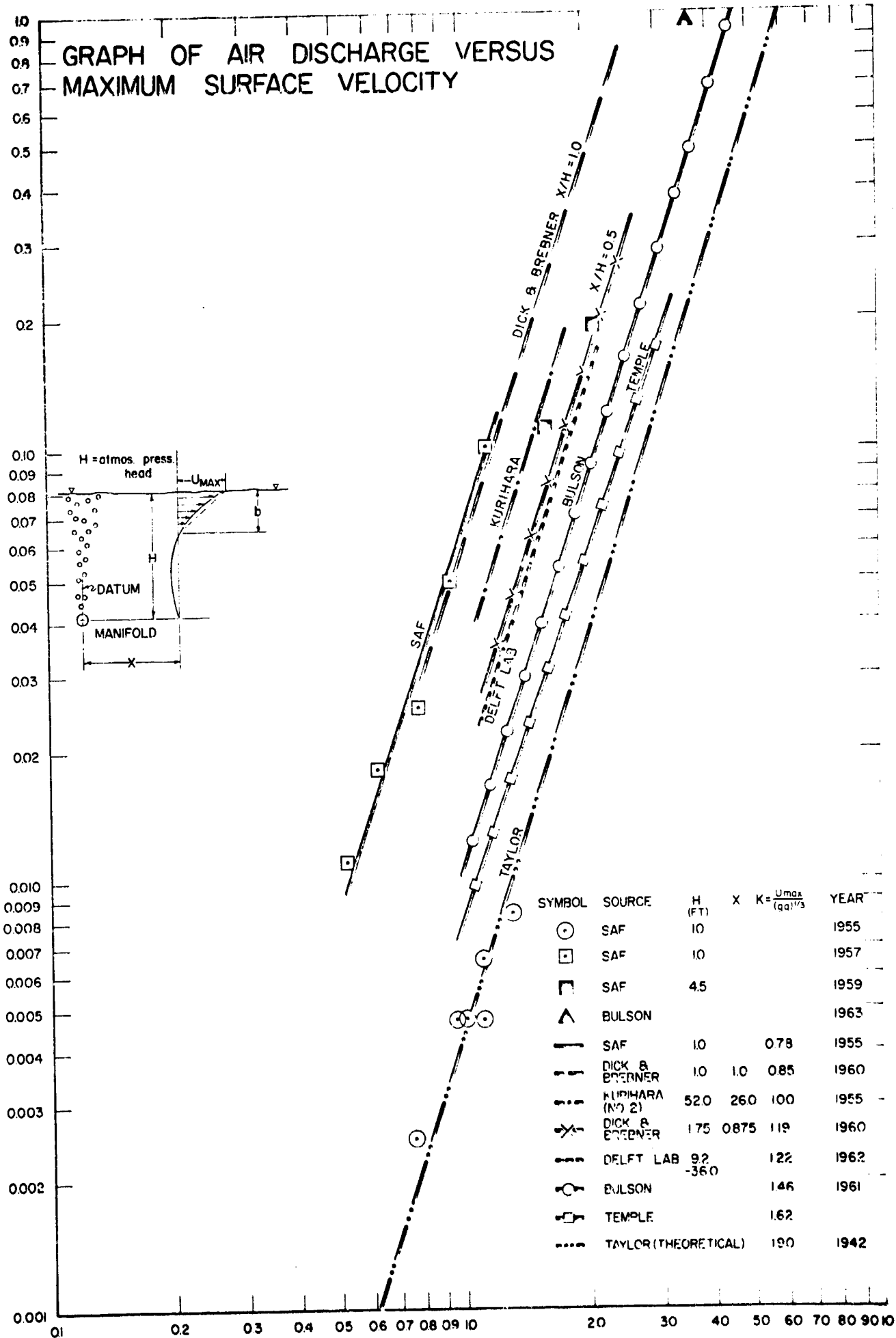


FIG. - DEFINITIONS OF GEOMETRIC, FLUID AND
I-II-10 FLOW VARIABLES



U_{MAX} , MAXIMUM SURFACE VELOCITY, FT/SEC

Bulson (1)* recognized that the volumetric air flowrate q , depended on the atmospheric pressure head, H_o and the manifold depth H . He defined q_o as the unit air flowrate of "free" air delivered under one atmosphere of absolute pressure head, i.e.

$$q_o = q \left(1 + \frac{H}{H_o}\right) \quad (\text{II-13})$$

Substituting the above in Equation II-11 gives

$$U_{\max} = K (gq_o)^{1/3} \left(1 + \frac{H}{H_o}\right)^{-1/3} \quad (\text{II-14})$$

Bulson experimentally deduced K to be about 1.46.

A recent report by Sjöberg and Verner⁽¹⁵⁾ confirmed the work at Delft (22) and by Dick and Brebner (23) and obtained a K value of approximately 1.3.

Surface Velocity Decay

The horizontal surface velocity, U_{\max} was found to decrease with increased distance from the manifold centerline. Due to the eruption of air bubbles the maximum U_{\max} usually occurred between $0.3H$ and $0.6H$ (1) (5) (14).

EXPERIMENTAL EQUIPMENT AND PROCEDURE

The TAMU Hydromechanics Laboratory tests were conducted in four separate flumes in order to study a wide range of water depths and test section widths. Since any water depth could be employed for the tests, the flumes have been designated by their width for this task report. All tests in the two-foot wave tank and eight-inch flume were conducted with a one-inch nominal diameter manifold. Tests in the deeper five-foot and 18-inch flumes used a two-inch manifold pipe. The orifice spacing was 24 holes per foot for all tests.

TEST RESULTS

Surface Currents Under Stagnant Conditions

Effect of Water Depth

The experimental results were obtained for U_{\max} as a function of q for four different water depths tested in four different flumes. In all tests U_{\max} was measured at x/H about 0.5 with 1/16-in. diameter holes. The trends in all cases followed the theoretical slope and the constant K appeared to increase slightly with water depth. The one exception was in the wide (5 foot) flume when there appeared to be very little change of U_{\max} with increased manifold depth, H . These results are summarized in Fig. I-II-12. The narrow, 18-in. flume might possibly explain the increase in U_{\max} at this depth. Further tests at prototype depths (25 to 30 ft.) and in wide flumes are needed to clarify this point.

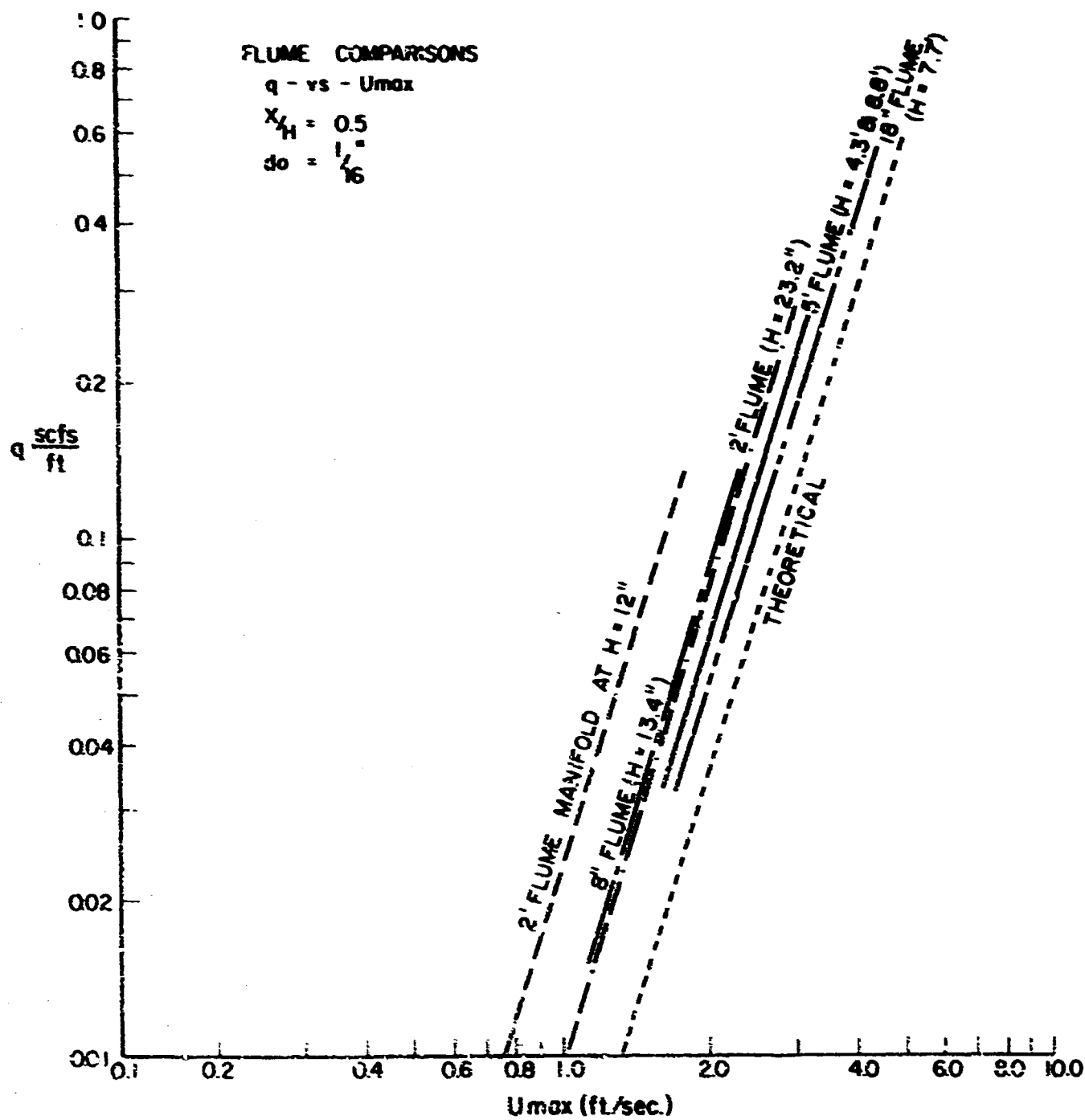


FIG. - FLUME COMPARISONS OF q versus U_{max}
 I-II-12

Effect of Orifice Size

Under identical test conditions the size of the orifice nozzles in the manifold pipe were varied. Fig. I-II-13 indicates a possible slight increase in the constant K with the smaller orifice tested. In many cases, however, experimental error was larger than the apparent differences noted. The manifold pressures were found to increase as hole size diminished.

Summary of Surface Current Tests

In stagnant water the results plotted in Fig. I-II-12 for U_{\max} versus q indicate a constant, K , of about 1.5 which is close to that reported by Bulson (24) (25). Little change in performance was noted with variation in orifice size which is also reported by Bulson (24). The floor boundary exhibited no effects for the limited range of tests performed.

Consequently based on these tests and those surveyed in the literature the following recommendations are made for preliminary design purposes of the prototype barrier.

<u>No.</u>	<u>Item</u>	<u>Remarks</u>
1	$U_{\max} = 1.5 (gq)^{1/3}$	Based on TAMU Lab Tests
2	Orifice Diam, $d = 1/16"$	Based on TAMU Tests and References
3	Orifice Spacing, $S = 12/\text{ft}$	Based on References
4	Manifold Pipe Diam, $D = 6"$	Based on References
5	Manifold Pipe Depth, $H = 25 \text{ ft.}$	Based on References

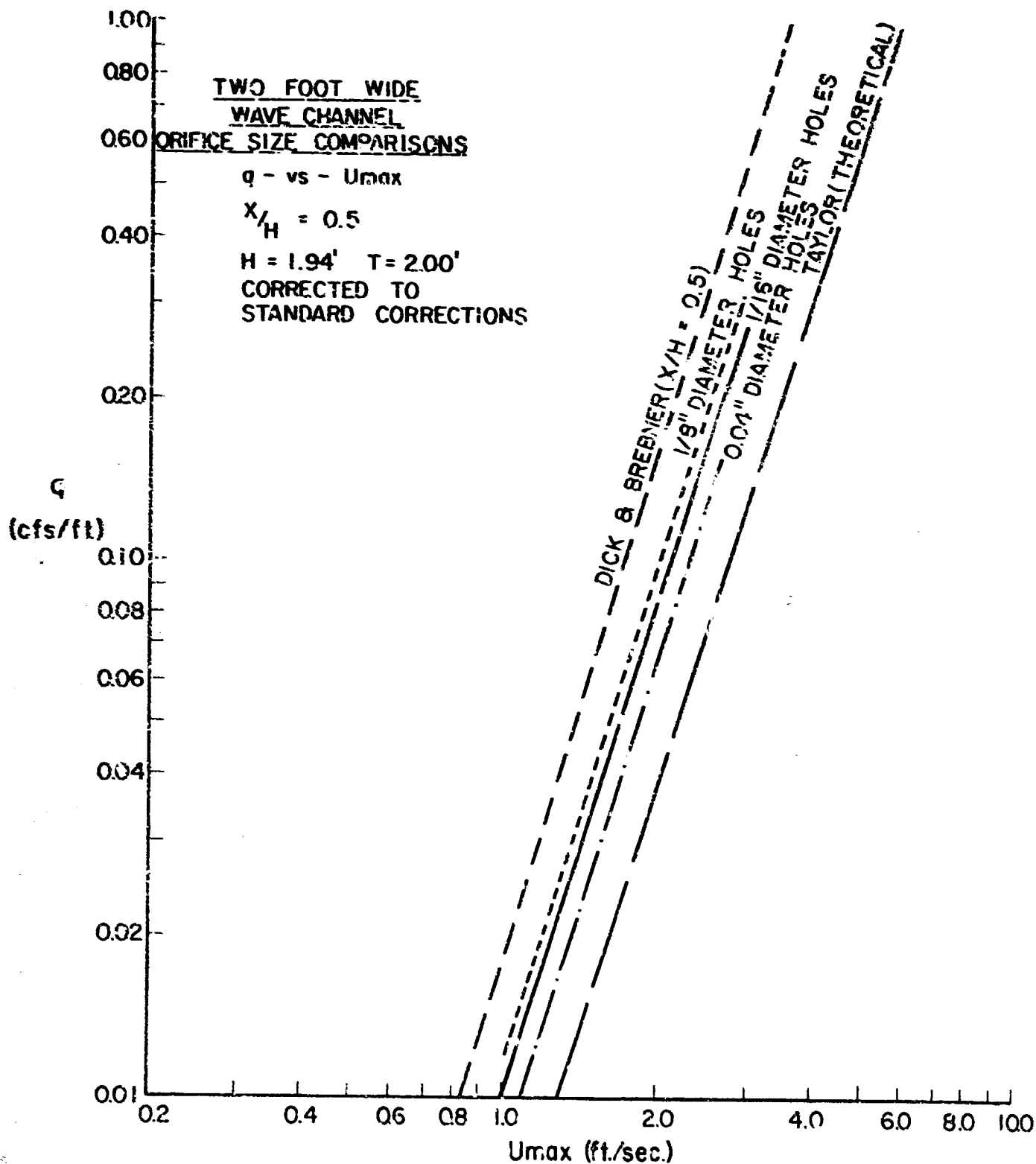


FIG. - ORIFICE SIZE COMPARISONS
 I-II-13

Effect of Steady Channel Flow on Bubble Current

A steady, uniform, open channel flow added to the bubble current has been found to shift the bubble pattern downstream. Consequently, instead of the center of bubble eruption occurring directly above the submerged pipe, it occurs some distance downstream.

It was postulated that the individual velocity profiles of open channel flow and bubble-generated current could be linearly superimposed together. If this theoretical supposition could be experimentally proven, then the resulting combined velocity profile could be theoretically estimated for any combination of channel flow and bubble current.

Since the stagnant bubble current was symmetrical about the centerline of bubble eruption, it was hypothesized that the channel flow would decrease the upstream bubble generated current and increase the downstream current by similar amounts. Thus the upstream decrease would be the critical case for oil containment and of most interest for this application.

Primary experimental tests were performed in the 18-in. wide flume with water depths of around 7.5 feet. Fig. I-II-14 presents two, measured, open channel flow, velocity profiles at the flume centerline with no bubble currents present. Although the profiles are characteristically non-uniform, in the region of interest where b is less than $0.25H$ the profiles are reasonably uniform and were tabulated mean values used for calculation purposes. The transverse profile was characteristically non-uniform due to the boundary layer

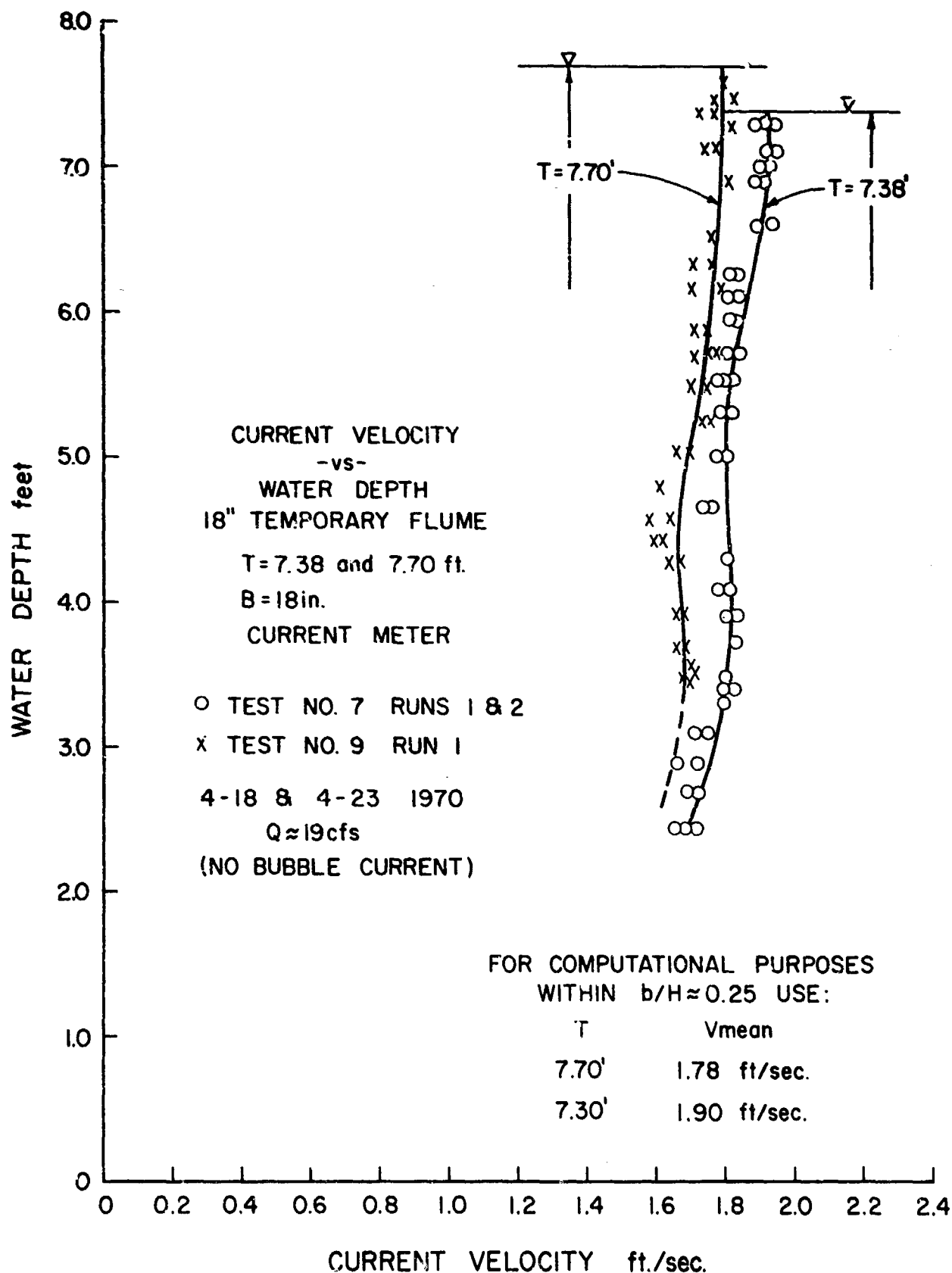


FIG. I-II-14 OPEN CHANNEL VELOCITY PROFILES IN 18 in. FLUME

so that the centerline velocity was used at the reference.

Next, an air flowrate of 0.436 cfs/ft was added in the flume which would normally create a U_{\max} of 4.1 ft/sec under stagnant conditions. Velocity profile measurements were then taken at five locations upstream of the shifted bubble eruption. The characteristic linear depth profile was still present and the resulting surface current generated, U_{\max} still decayed with distance from the centerline of eruption. This test was carried out with a mean flow current V_m between $d = 0$ and $d = b$ of about 1.78 ft/sec present in the open channel. There appeared to be excellent agreement between theory and experiment for all surface velocities of interest.

In Fig. I-II-15 the principle of linear superposition has been applied to simulate prototype conditions when H is 25 feet, U_{\max} generated is 5.0 ft/sec and the design 2 knot current opposes the bubble current. The resulting estimated surface current, U'_{\max} is 1.62 ft/sec and b' is about 2.0 ft. The prototype conditions were not possible to achieve in the laboratory.

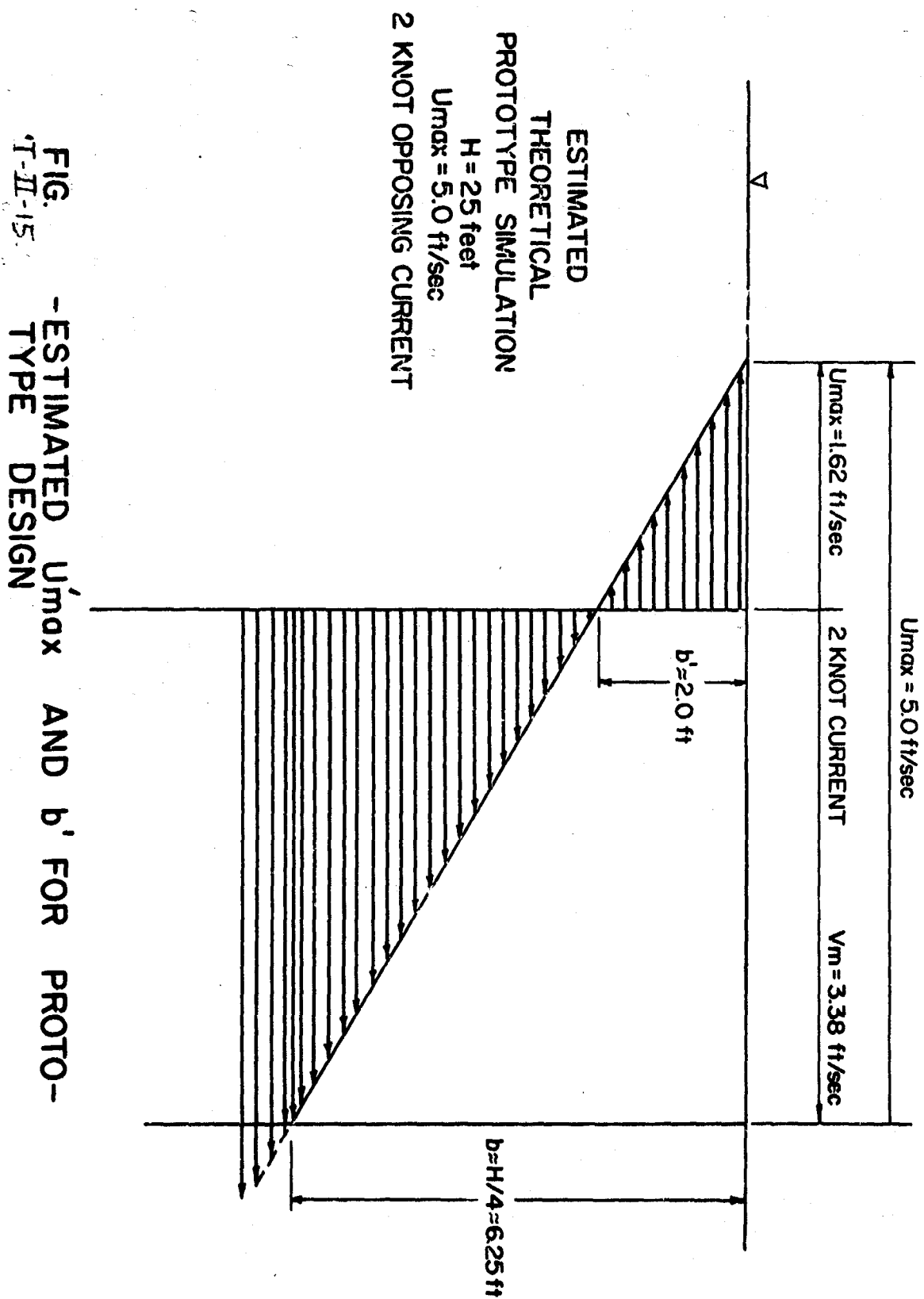


FIG. -ESTIMATED U_{max} AND b' FOR PROTO-
TYPE DESIGN

Oil Containment by Pneumatic Barrier

Oil flowing over water is a complex phenomenon. Being lighter than water, gravity forces "drive" the oil to "seek" its own uniform level above the water surface. In a system open to the atmosphere, the driving force is solely the hydrostatic pressure head of the oil, h . Thus a thick layer of oil will have a greater tendency to spread than the same oil of smaller depth.

Once the flow commences, the gravity forces which originated the motion soon give way and are dominated by viscous shear at the interface so that the viscous forces govern the dynamics of the motion. Spreading decreases the oil thickness.

At some further point when the oil becomes of "film" thickness, surface tension forces become dominant and this phenomenon determines the manner in which further spreading takes place. Superimposed wind and wave forces add considerable complexity to the situation.

EXPERIMENTAL TEST RESULTS

Stagnant Water

Initial tests were conducted in the two-foot wide wave channel with 2 ft. of water depth, T and the manifold located near the bottom, H so that H/T was about 1.0. With a constant air flowrate and U_{\max} being generated, the oil depth being contained was gradually increased until failure occurred.

Waves

Design waves had to be scaled to model sizes for laboratory tests. A wide range of wave conditions was specified and time limitations prevented testing all combinations. Therefore, the significant wave characteristics (height, length, etc.) were chosen as most representative for laboratory tests in the two-foot wide wave channel.

If a prototype manifold depth of 25 feet is assumed, the geometric scale ratio used became 25:1 since the model manifold was located one foot below the water surface. A maximum water depth of 2 feet was used for the tests resulting in the generation of "shallow water" wave forms. The following shallow water wave characteristics were employed at the 25:1 scale ratio.

	<u>PROTOTYPE</u>	<u>MODEL</u>
Significant Wave Height	10 ft	0.4 ft
Significant Wave Period	6 sec	1.2 sec
Significant Wave Length	185 sec	7.4 ft

Model surface velocities generated were near 1.0 ft/sec which scaled-up to about 5.0 ft/sec in the prototype.

As noted in the literature, the required U_{\max} to contain oil was also considered to depend on the height (H), and length (L), of the waves striking the barrier, i.e., on the wave steepness H/L . Waves of large steepness ratio approaching breaking conditions were found to impose additional forces on the barrier. Of primary interest for the laboratory tests was

the case with oil located on the side from which waves were generated so that the waves possibly moved the oil against the barrier. Fig. I-II-16 presents the results in the same U_{\max} versus $\sqrt{gh(1 - SGo)}$ form used previously.

Surprisingly, the long swell wave form modeled in the tests produced little change from stagnant conditions. The critical α was still between 1.0 and 1.2. In fact, when the waves were stopped during testing, the stagnant conditions present were noted to be closer to failure than when testing with waves.

Based on these laboratory tests α equal to 1.2 is recommended for preliminary design with waves.

Current

To test the principle of linear superposition of velocities, the 18-in. wide flume was used with 7.7 feet of water which gave a mean velocity, V_m of 1.78 ft/sec. A constant bubble generated velocity was introduced and the effects of the current tested by adding oil and noting the mean oil thickness at failure were determined. If the principle of superposition should hold under these conditions, then a plot of the effective surface velocity, U'_{\max} (U_{\max} minus V_m) versus $\sqrt{gh(1 - SGo)}$ should also result in a critical coefficient α of 1.2 near failure. The results generally indicated that this is precisely what happens. Sufficient time was not available to completely verify these results particularly at small values of U'_{\max} .

MODEL WAVES
1:25 SCALE RATIO
 $U_{max} - \text{vs} - \sqrt{gh(1-SG_0)}$

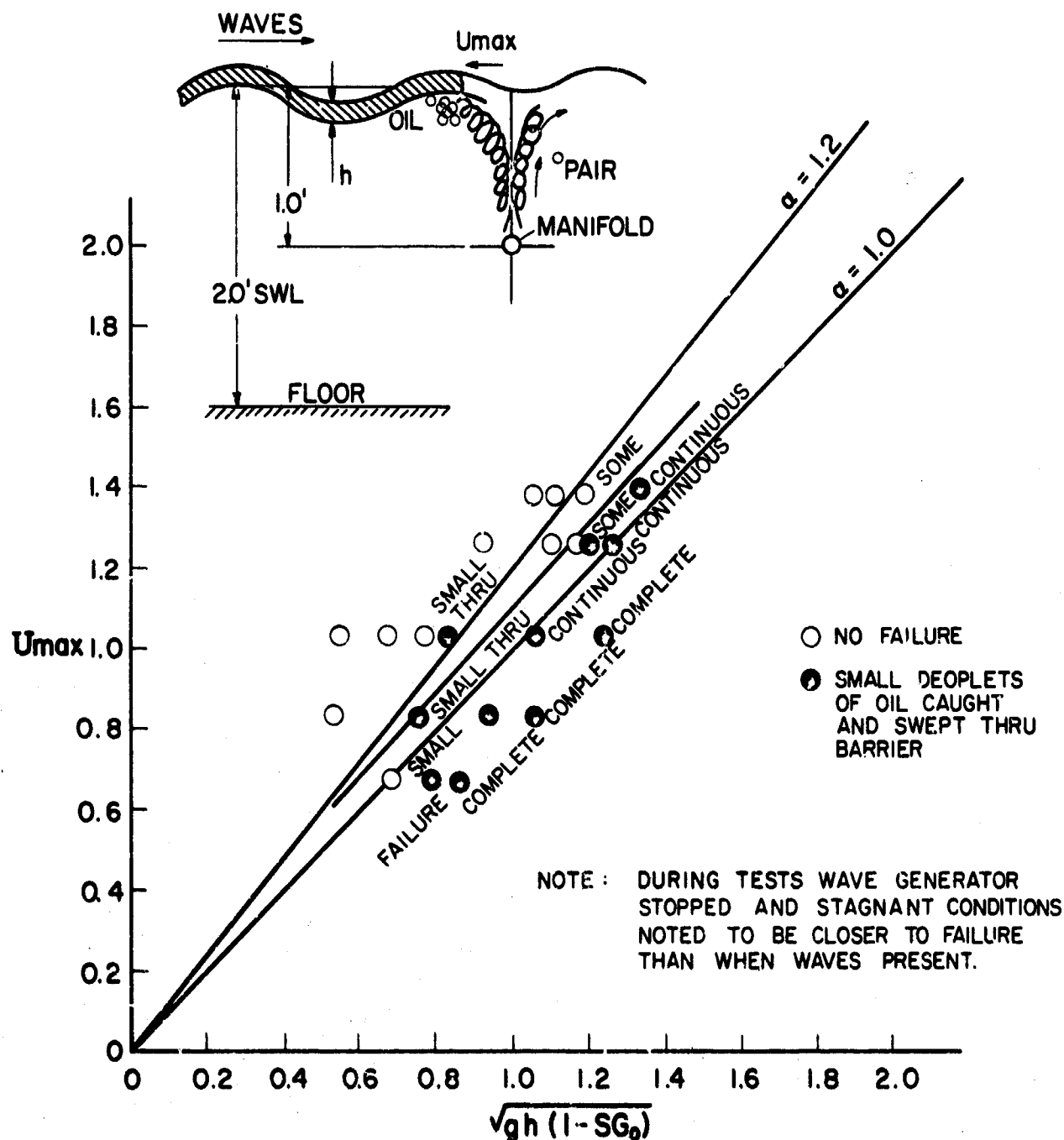


FIG. I-II-16 - U_{max} versus $\sqrt{gh(1-SG_0)}$ UNDER MODELED DESIGN WAVES

Failure was specified when masses of oil began to overtop the air barrier and move downstream. Significantly, it was also observed that a number of oil droplets were entrained near the head region of the contained oil and when located at depths greater than the effective barrier profile, b' were swept right through the deflected bubble region by the current. Time was unavailable to record any rates of this type of loss except to estimate that in all cases well over 95% of the oil remained contained by the air barrier.

Conclusions and Recommendations

1. The continual release of air below water creates a surface current of water near the surface.
2. The magnitude of the current at the surface decreases approximately linearly with distance from the submerged pipe. It is a maximum at a distance of around 0.3 to 0.5 pipe depths from the pipe.
3. The velocity generated by the bubbles decreases approximately linearly with water depth and is a maximum at the surface. The velocity reverses (current is zero) at a distance below the surface which is about one-quarter of the pipe depth.
4. The maximum surface current generated is proportional to the unit air flowrate raised to the one-third power. The constant of proportionality is strongly dependent on depth of manifold pipe and practically independent of manifold hole size.
5. The following formula was recommended for preliminary design purposes:
$$U_{\max} = 1.5 (q_a)^{1/3} \quad (\text{II-15})$$
6. The principle of linear superposition applied to combine stagnant U_{\max} and channel flow velocities was found to hold.
7. The results of the stagnant water, wave, and current tests were extrapolated to prototype conditions. Fig. I-II-17 presents the combined results in the form of a preliminary design chart. For any pneumatic generated velocity, U_{\max} ,

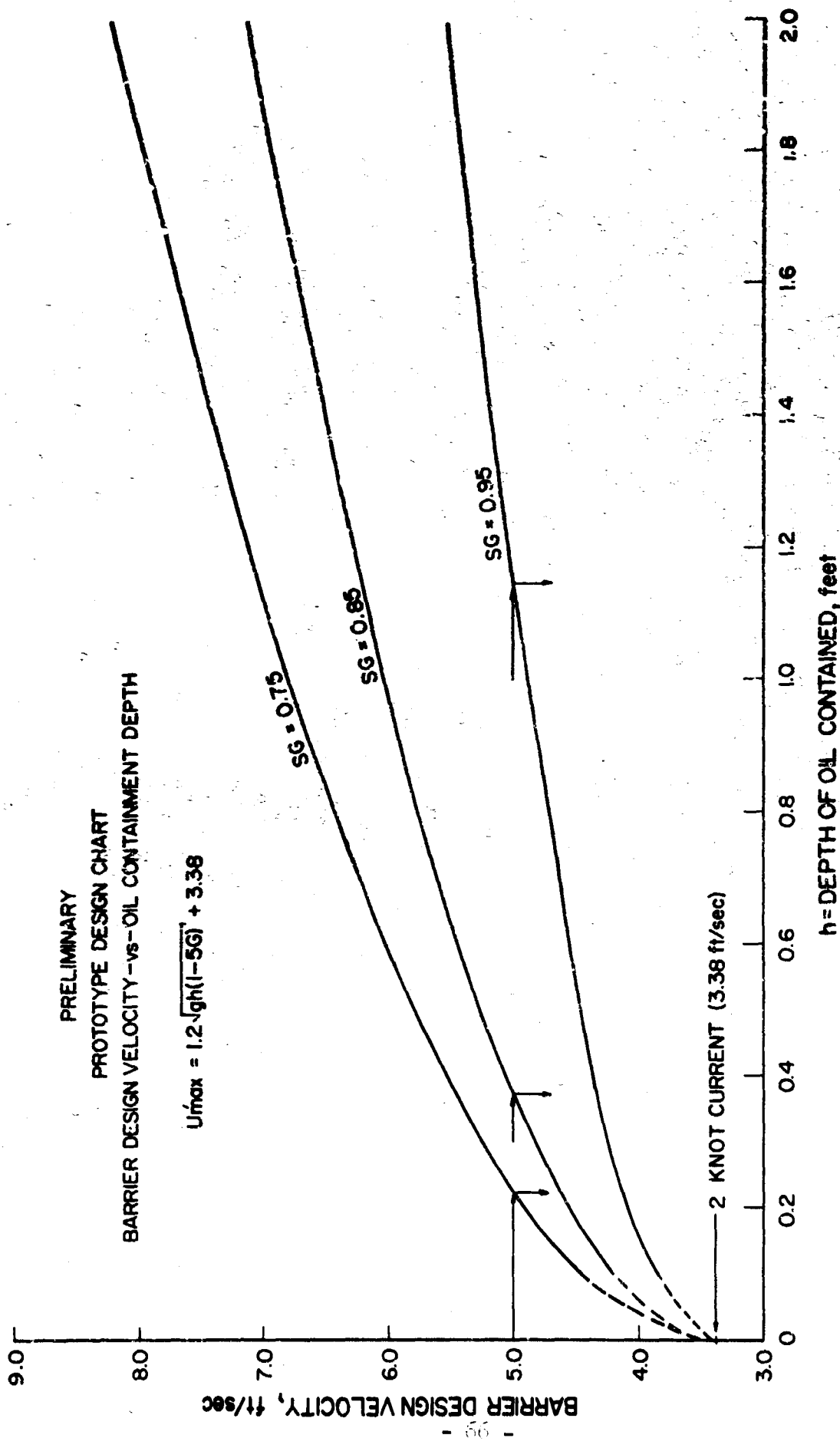


FIG. I-II-17 -RECOMMENDED PROTOTYPE DESIGN CHART
U_{max} versus h

the resulting mean oil depth contained can be determined for the range of specific gravity oils of interest. A 2 knot prototype current (3.38 ft/sec) is used in the plot. No wind set-up effects are included but mean oil containment depths can be estimated with wind by using only 2/3 of the values indicated. These results are tabulated below.

Barrier Design Velocity U_{max} (ft/sec)	SG of Oil	Mean Oil Depth Contained (Feet)	
		No Wind	Including Design Wind
5.0	0.75	0.225	0.15
5.0	0.85	0.370	0.295
5.0	0.95	1.140	0.76

Figure I-II-18 presents the combined results for a 1 knot prototype current (1.69 ft/sec). The results are as follows:

Barrier Design Velocity U_{max} (ft/sec)	SG of Oil	Mean Oil Depth Contained (Feet)	
		No Wind	Including Design Wind
5.0	0.75	0.95	0.63
5.0	0.85	1.55	1.03
5.0	0.95	4.60	3.05

It is recommended that complete verification of all of the above preliminary results be made under prototype conditions.

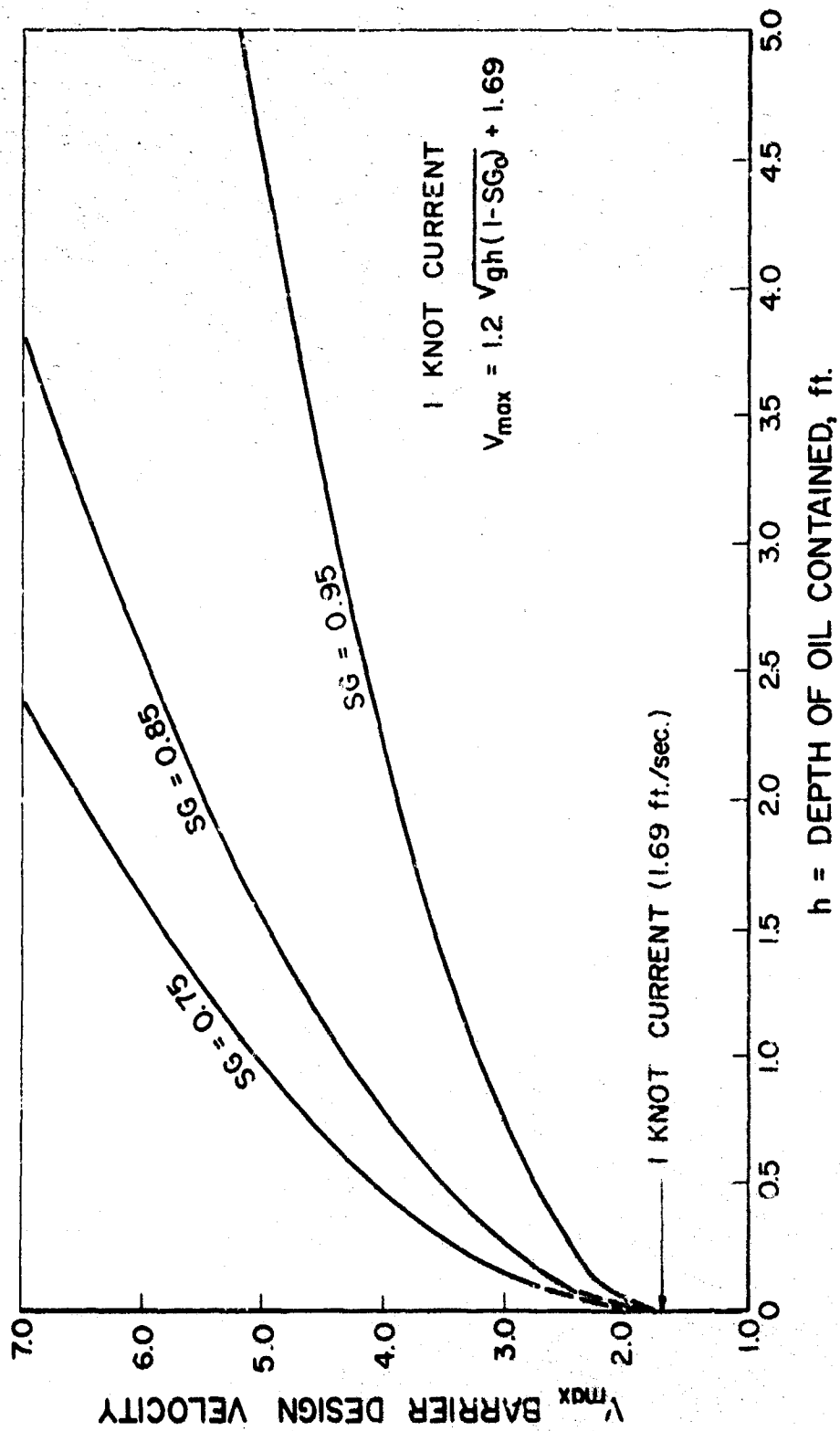


FIG. I-II-18



FIGURE I-II-19

Pneumatic barrier operating in waves and currents. Oil contained on the right. (Note droplets of water covered with a film of oil also being contained.)

4. General Comment

Since the air supply and associated equipment must be air transportable, blower size must be related to airflow requirements and pipe diameters to determine the maximum performance available from combinations of blower size and pipe diameter per unit length of manifold.

The interrelationship between these are relatively complex, involving friction and possible compressibility effects. Evaluations of these interrelationships are needed in order to be able to optimize the design of the pneumatic supply system.

This research, then, was intended to determine those parameters which would affect the design of air supply mechanisms and piping, present them in a form such that trade - offs of design parameters were available, then aid in the optimization of the design itself. In particular, relationships were needed between diameter of pipe leading down to the manifold, airflow velocity within this pipe, manifold depth, air supply power, overpressure needed within the pipe to maintain an outflow of air from the manifold, and numbers and size of holes in the manifold through which the air is blown into the water.

Determination of Pipe Diameter

In the determination of necessary pipe diameter for a given surface flow rate and depth, the following development was applied. Within the pipe, the area necessary to handle volumetric airflow rate is

$$A_p = \frac{Q_p}{V_p} \quad (\text{II-15})$$

where A_p = pipe area required per foot of manifold length

Q_p = volumetric airflow rate in the pipe per foot of manifold length

V_p = airflow velocity in the pipe

The airflow rate in the pipe may be related to that having been blown out of the pipe at the given depth by

$$Q_p = Q_d \frac{T_p}{T_d} \frac{P_d}{P_p} \quad (\text{II-16})$$

where Q_d = volumetric airflow rate at the depth pressure per foot

T = temperature

P = pressure

Substitution gives

$$A_p = \frac{Q_d}{V_p} \frac{T_p}{T_d} \frac{P_d}{P_p} \quad (\text{II-17})$$

But depth pressure, P_d , is the sum of atmospheric and that created by the head of water;

$$P_d = P_s + \gamma h \quad (\text{II-18})$$

where P_s = surface or atmospheric pressure

γ = specific weight of seawater

h = depth of the manifold below the surface

and the pressure in the pipe must be that depth pressure plus the necessary overpressure to push the air from the pipe into the water.

$$P_p = P_s + \gamma h + P_{op} \quad (\text{II-19})$$

Substitution gives

$$A_p = \frac{\pi D^2}{4} p = \frac{Q_d}{V_p} \frac{T_p}{T_d} \frac{(P_s + \gamma h)}{(P_s + \gamma h + P_{op})} \quad (\text{II-20})$$

Hence

$$D_p = \sqrt{\frac{4}{\pi} \frac{Q_d}{V_p} \frac{T_p}{T_d} \frac{(P_s + \gamma h)}{(P_s + \gamma h + P_{op})}} \quad (\text{II-21})$$

To estimate the temperature ratio in the above, the assumption is made of isentropic expansion through the holes, giving

$$\frac{T_p}{T_d} = \left(\frac{P_p}{P_d} \right)^{(k-1)/k} = \left(\frac{P_s + \gamma h + P_{op}}{P_s + \gamma h} \right)^{(k-1)/k} \quad (\text{II-22})$$

Substitution gives

$$D_p = \sqrt{\frac{4}{\pi} \frac{Q_d}{V_p} \frac{P_s + \gamma h}{P_s + \gamma h + P_{op}}^{1/k}}$$

Figure I-II-20 presents typical information for various values of pipe velocity.

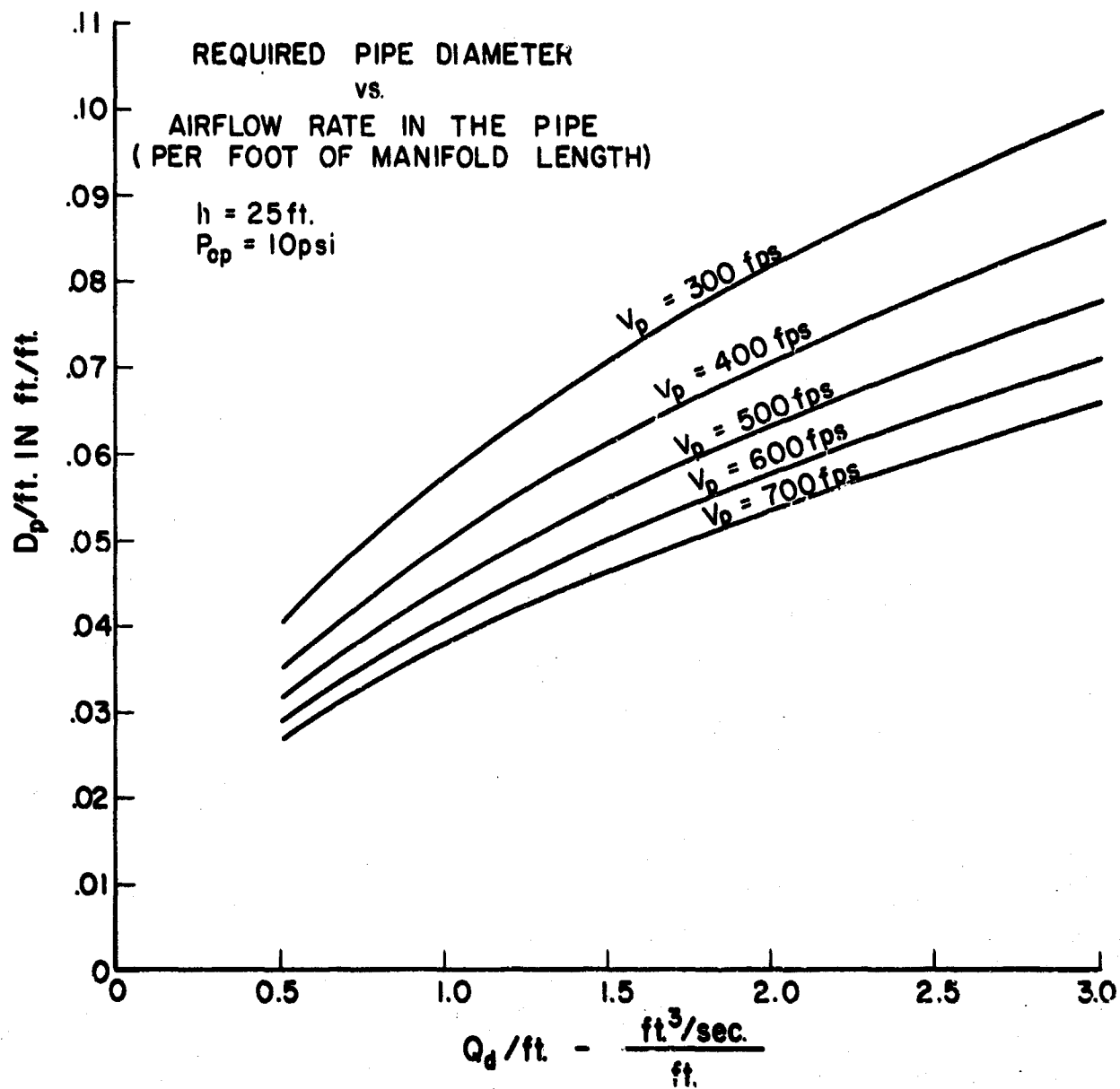


FIG. I-II-20

This airflow rate at depth is related to the surface current velocity generated by a constant. In order to have some idea of the relationship between pipe diameters and generated surface current it was assumed that

$$V_s = 1.57 (Q_{dg})^{1/3}$$

Figure I-II-21 includes this relation.

To determine required HP per foot of manifold length for the blowers, the relationship is

$$HP = \frac{Q_s \Delta P}{550 \eta} \quad (II-24)$$

where Q_s = volume flow rate in cfs at the surface of the sea per foot of pipe length

ΔP = the pressure increase through the blower in psf.

η = blower efficiency

The volume flow rate, Q_s , at the surface can be determined from the rate at the pipe depth by

$$Q_s = Q_d \frac{T_s}{T_d} \frac{P_d}{P_s} \quad (II-25)$$

The pressure increase, ΔP , needed through the pump will be created by a) friction in the pipe, b) pressure at the manifold water depth due to the head of water above the manifold and c) overpressure needed to force the air out through the manifold holes. ie:

$$\Delta P = P_f + P_h + P_{op} \quad (II-26)$$

where P_f = friction pressure drop

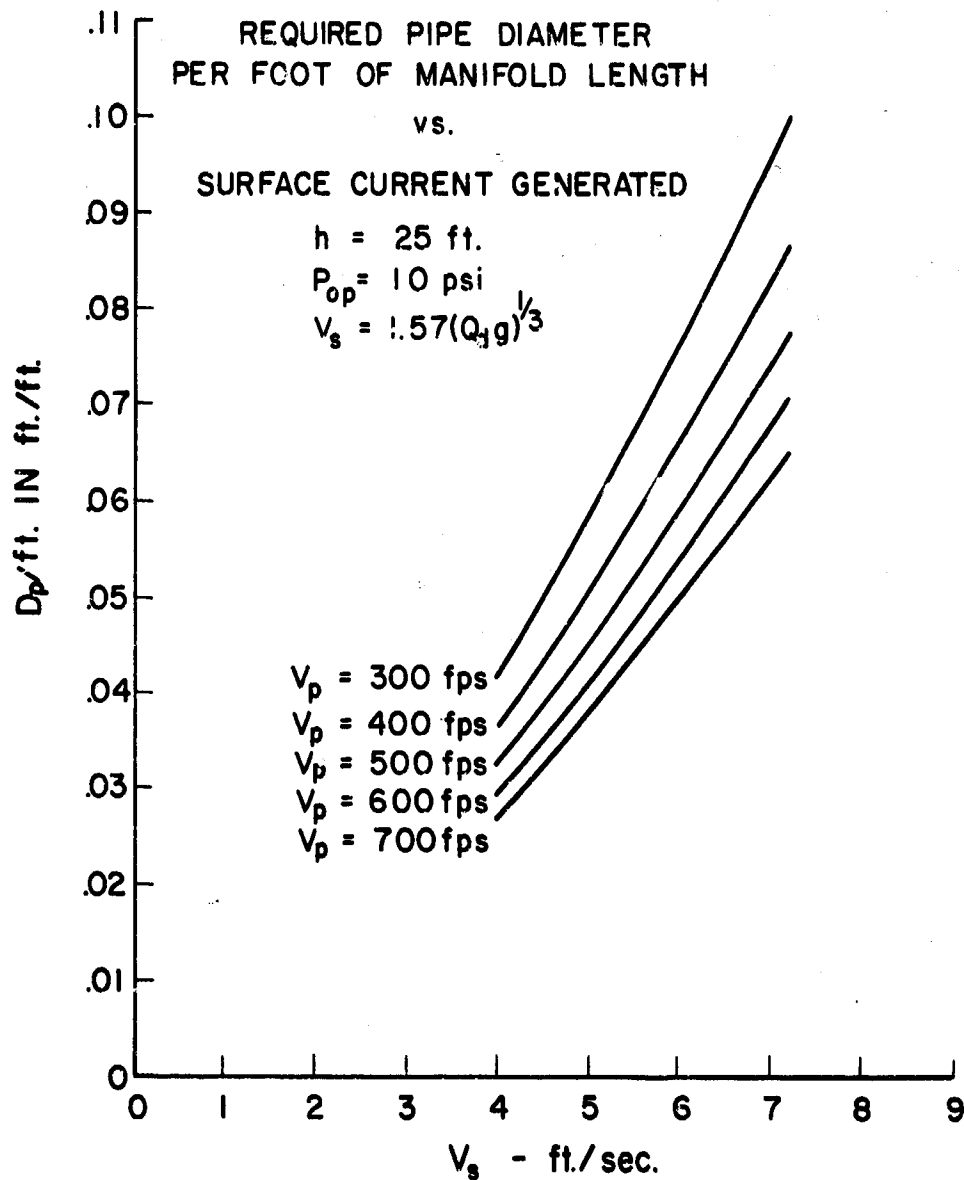


FIG. I-II-21

P_h = gage pressure at manifold depth ($P_h = \gamma h$, where γ is the specific weight of water and h is the water depth.)

P_{op} = required manifold overpressure.

Since $P_d = P_s + P_h$ the required HP can be expressed as;

$$HP = \frac{Q_d \frac{T_s}{T_d} \frac{(P_s + P_h)}{P_s} (P_f + P_h + P_{op})}{550 \eta} \quad (II-27)$$

To estimate the temperature ratio, T_s/T_d , one needs to know blower design parameters. In the absence of such information the assumption will be made here that the air loses half the temperature rise it would get isentropically as it flows through the pipe. ie:

$$\frac{T_s}{T_d} = \left(\frac{P_s}{P_d} \right)^{\frac{k-1}{k}} \quad (II-28)$$

hence

$$(T_d - T_s) = T_d \left[1 - \left(\frac{P_s}{P_d} \right)^{\frac{k-1}{k}} \right]$$

Assume the actual $T_d - T_s$ is half of this. Then

$$\frac{T_s}{T_d} = 1 - \frac{1 - \left(\frac{P_s}{P_d} \right)^{\frac{k-1}{k}}}{2}$$

On the basis, then, the HP required

$$HP = \frac{Q_d}{5500} \left\{ 2 - \left(\frac{P_s}{P_s + \gamma h} \right)^{\frac{k-1}{k}} \right\} \frac{1}{2} \left(\frac{F_s + \gamma h}{P_s} \right) (P_f + \gamma h + P_{op}) \quad (II-31)$$

Figures I-II-22, and I-II-23 contain typical values for these, relating the required HP per foot to depth of manifold and required overpressure.

In order to determine hole size and number for a given airflow rate the following analysis was used. Assuming each hole in the manifold pipe to be a short tube, the velocity of flow through it may be approximated by the Fanning equation:

$$V_h = \left\{ \frac{2d}{f} \frac{P_{op}}{L} \frac{1}{\rho_d} \right\}^{1/2} \quad (II-32)$$

where V_h = airflow velocity through the hole

d = hole diameter

L = pipe thickness

ρ_d = density at the given depth of air through the hole

f = friction factor, (a function of ρ , v , d , and air viscosity, and obtainable from a Moody diagram of Reynolds Number vs. ν)

P_{op} = required manifold overpressure

Figure I-II-24 contains the faired results of a reiterative application of the relation. The flow rate through each hole then will be

$$Q = A_h V_h$$

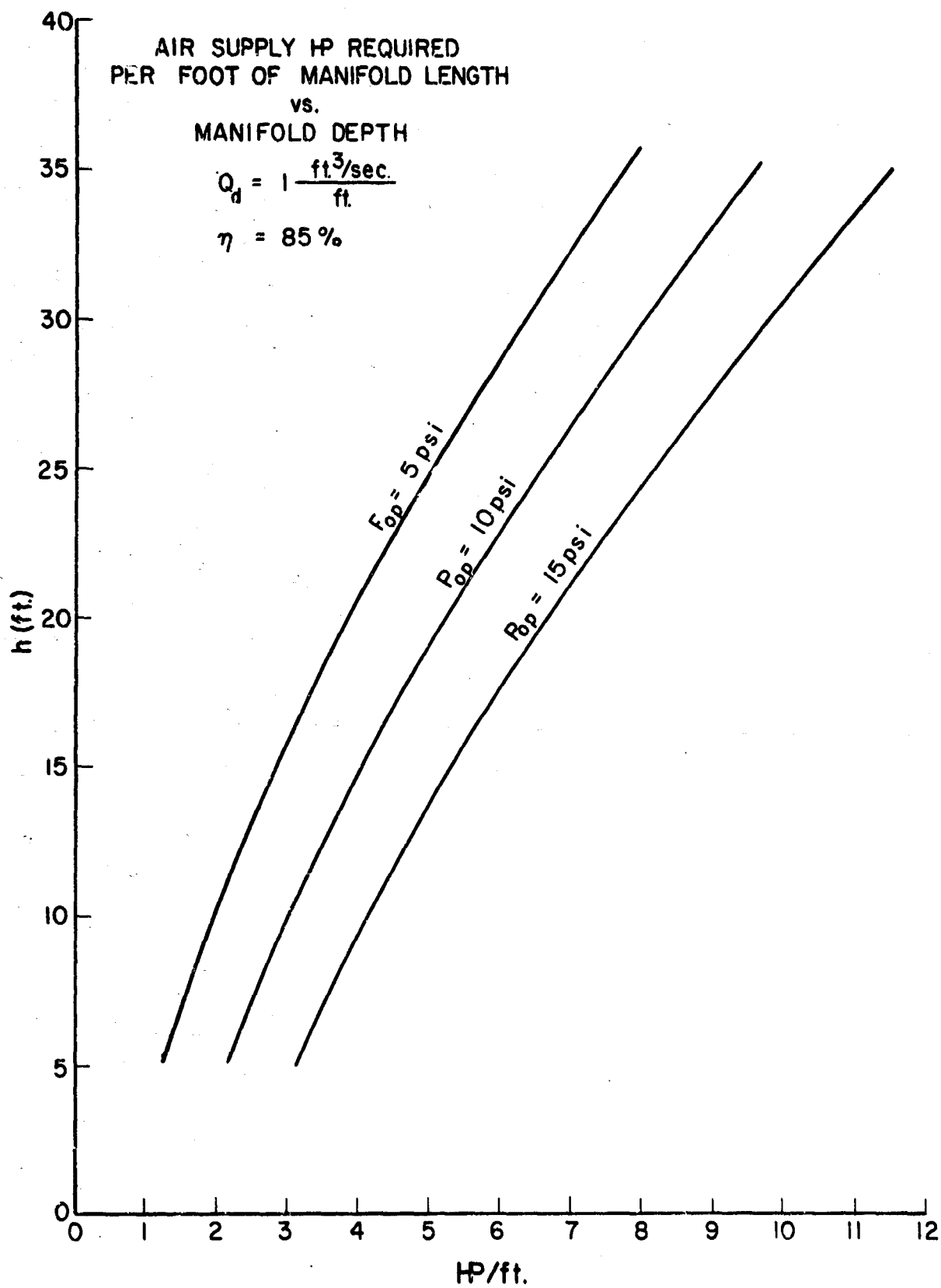


FIG. I-II-22

AIR SUPPLY HP REQUIRED PER
FOOT OF MANIFOLD LENGTH
vs.
OVERPRESSURE

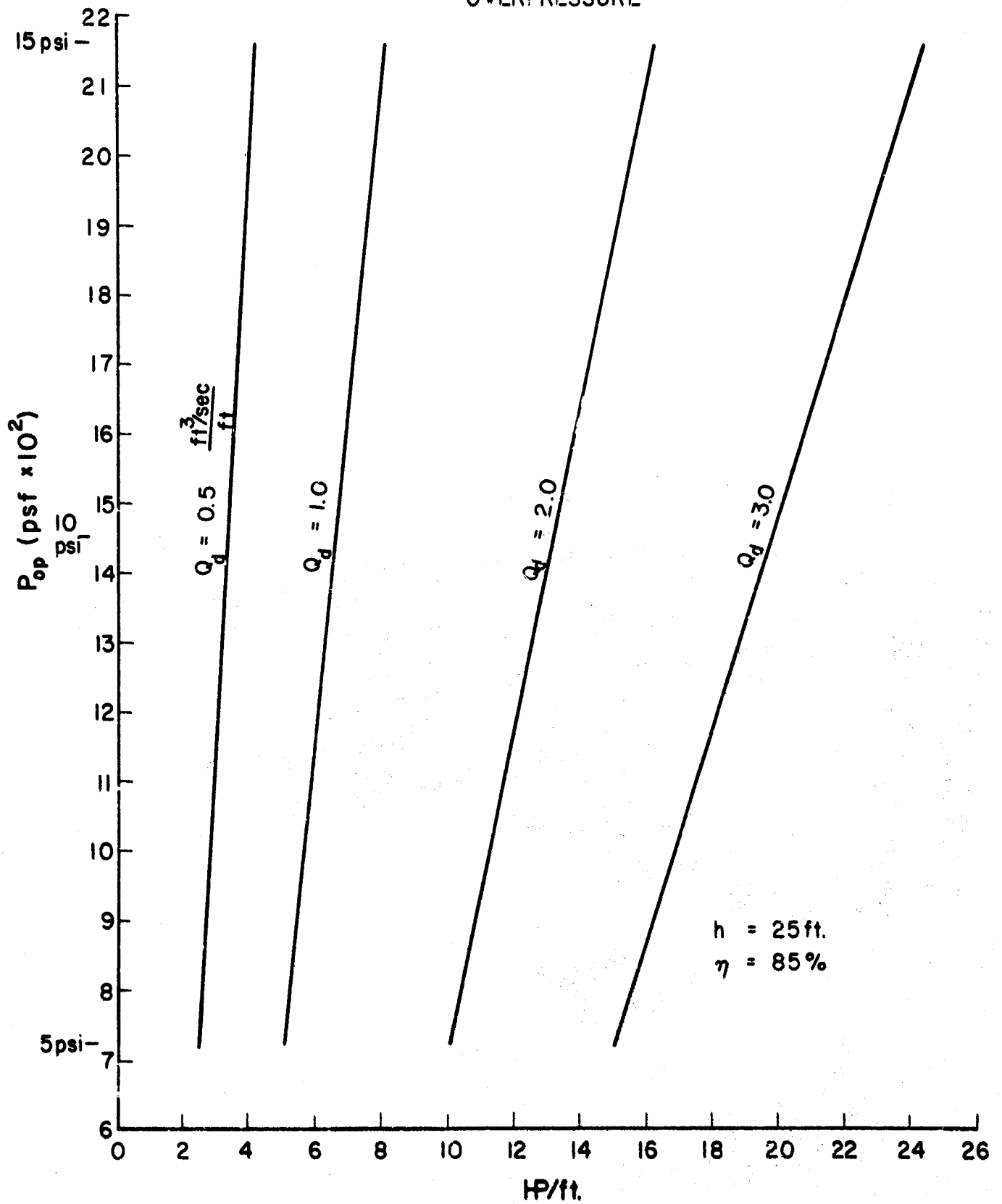


FIG. I-II-23

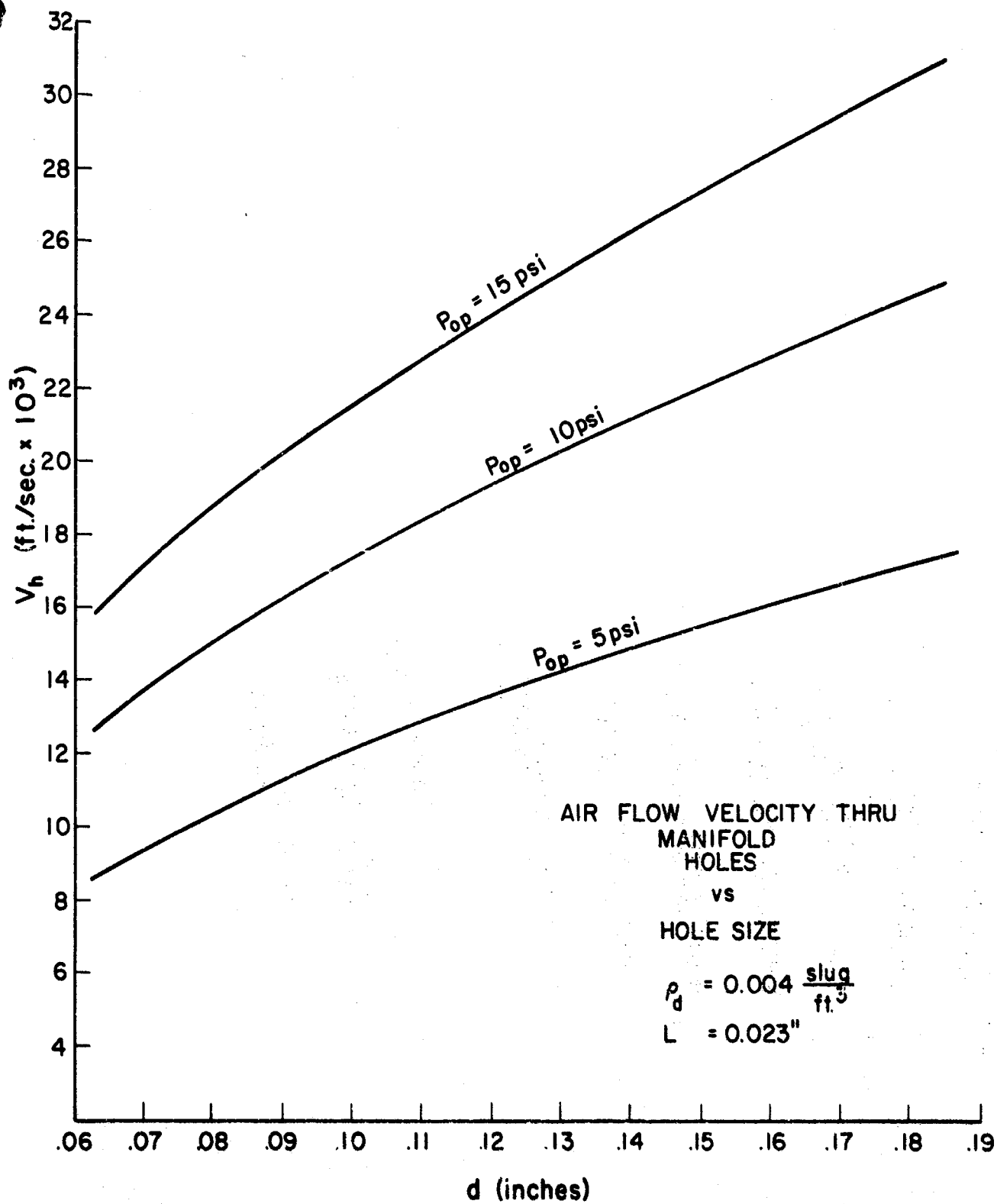


FIG. I-II-24

and combining this with the previous equation gives

$$Q_d/\text{hole} = \frac{\pi d^2}{4} \left\{ \frac{2d}{f} \frac{P_{op}}{L} \frac{1}{\rho_d} \right\}^{1/2} \quad (\text{II-33})$$

where the bracketed term is the V_h as determined from reiteration of the previous relation. The total airflow at depth into the water will then be

$$Q_d = N \frac{Q_d}{\text{hole}} = N \frac{\pi d^2}{4} \left\{ \frac{2d}{f} \frac{P_{op}}{L} \frac{1}{\rho_d} \right\}^{1/2} \quad (\text{II-34})$$

where N is the number of holes per foot, and the bracketed term is again the appropriate V_h for a given hole diameter.

Figures I-II-25 and I-II-26 presents examples of this data for various common hole diameters.

These may also be related to blower HP through the relation given earlier between Q_d and HP. Typical curves are shown in Figure I-II-27.

Summary

These results show that the number of parameters involved present no obvious choice of an air supply and piping system. Aside from the general requirement for a minimum power requirement and pipe size with a maximum airflow, trade - offs are necessary. The choice thus will be highly dependent on air supply system availability, and the specific piping system arrangement.

NUMBER OF MANIFOLD HOLES
PER FOOT OF MANIFOLD LENGTH

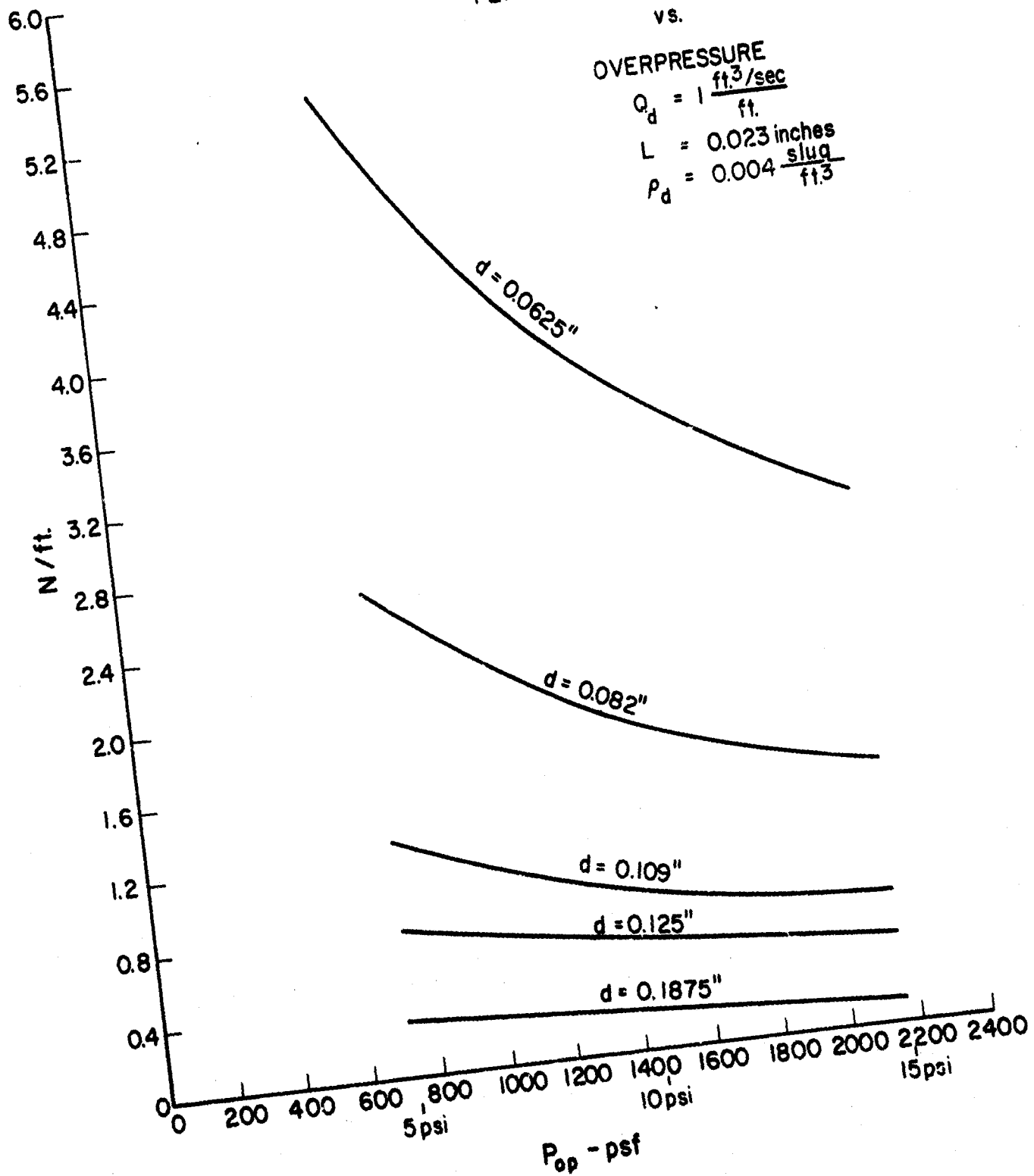
vs.

OVERPRESSURE

$$Q_d = 1 \frac{\text{ft}^3/\text{sec}}{\text{ft.}}$$

$$L = 0.023 \text{ inches}$$

$$P_d = 0.004 \frac{\text{slug}}{\text{ft}^3}$$



$P_{op} - \text{psf}$

FIG. I-II-25

- 82 -

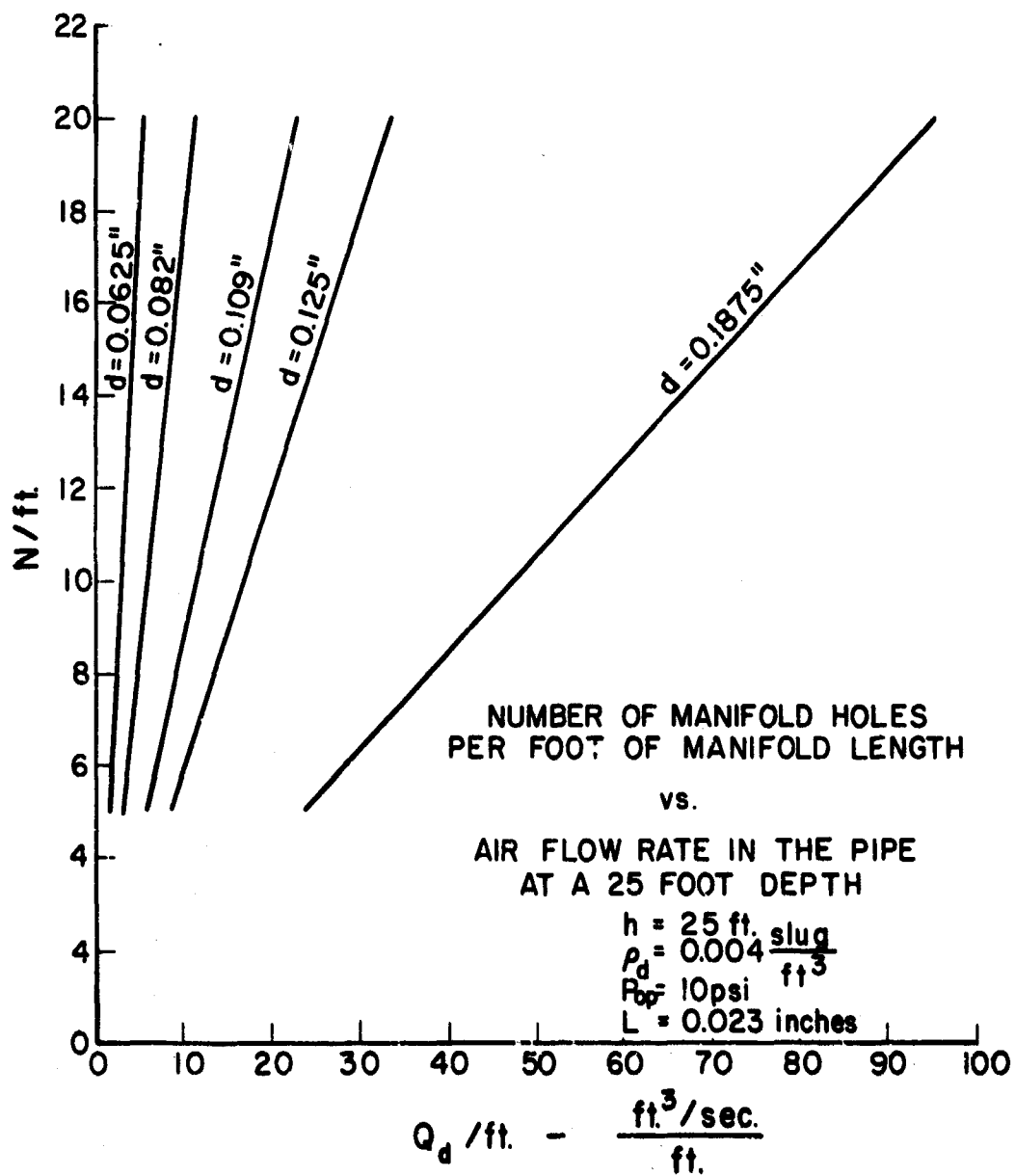


FIG. I-II-26

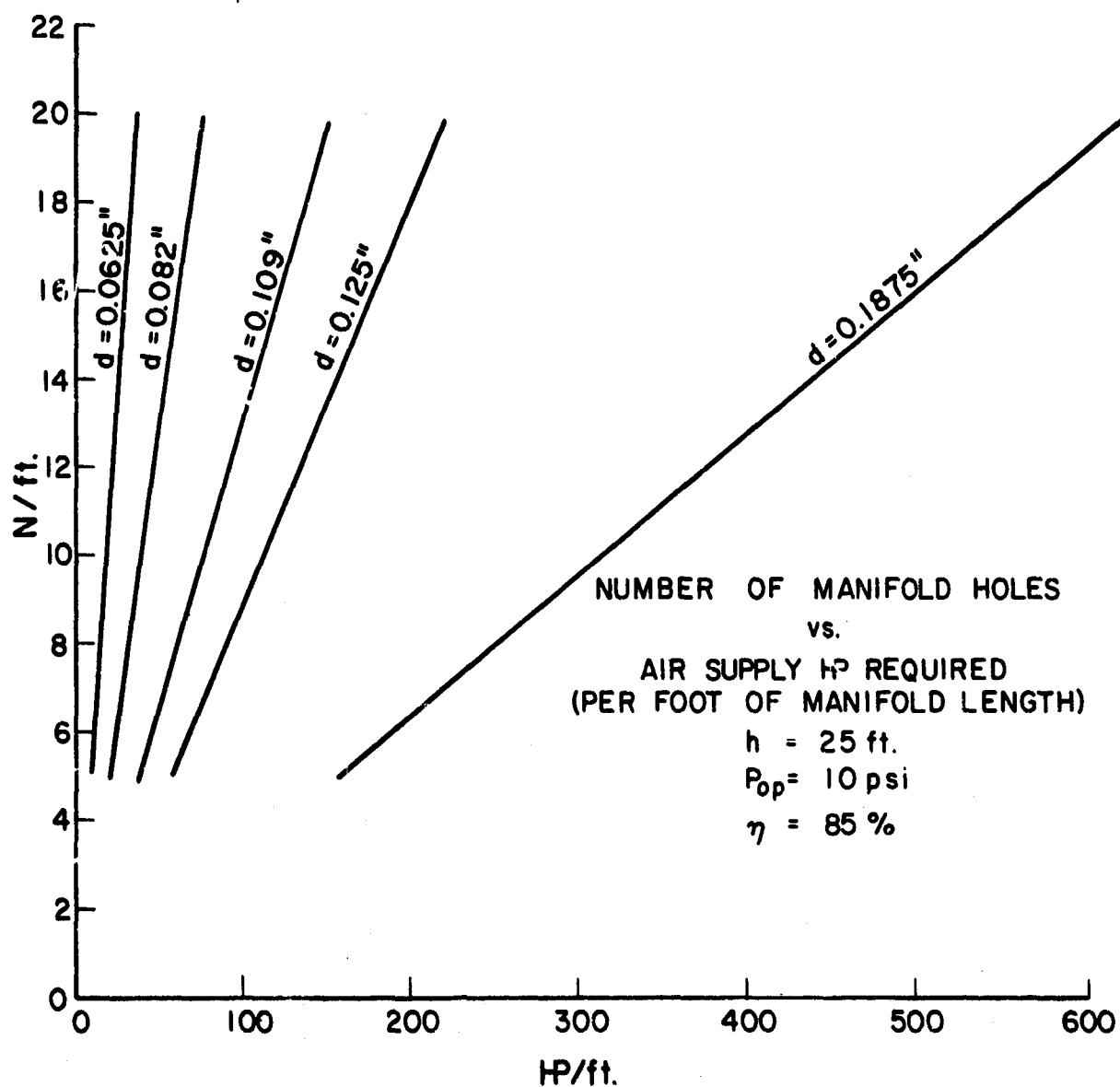


FIG. I-II-27

I-II-5 Study of Suitable Materials

General Comment

The purpose of this study was to establish the material's response to mechanical, thermal and environmental loading conditions and to assume structural integrity throughout the service and storage life. In each case where published information was lacking, or was questioned, experimental testing was carried out. The materials study program was in direct response to and in support of each of the major tasks in the program.

6. Major Design Decisions

Manifold Depth

Previous prototype uses of a pneumatic barrier for wave breaking deployed the manifold from 15 to 55 feet below the water surface. The imposed design conditions for physical integrity were for a significant wave height of 20 ft. and a 1/10 wave of 28 ft. Prototype and laboratory tests indicated some increase in surface velocities with increased manifold depths. Hence, it is recommended to design the prototype manifold to operate in 25 to 30 ft. of water.

Orifice Size

The literature survey of previous investigations indicated orifice diameters from 3/64 in. to 1/4 in. tested in the field. Laboratory tests indicated a slight increase in surface velocities as the orifice size (bubble diam. released) decreased. To keep the orifice from plugging and still keep it as small as possible it is recommended that a 1/16 in. diam. be used for design purposes.

Orifice Spacing

Although the laboratory spacing used for these tests was 24 per foot, previous prototype tests employed from 2 to 26 holes every foot. Since these tests revealed no apparent effects of spacing, it is recommended to use 12 holes per foot for economical reasons.

Orifice Location

No effects of orifice location were evident from previous prototype tests, therefore it is recommended to locate the holes at the top of the pipe.

Number of Manifolds

It is recommended to use one manifold for the preliminary design for economical reasons and ease of deployment.

Pneumatics and Containment

Laboratory tests and the previous work of other investigators indicated that for prototype design depths the surface velocity generated is approximately

$$U_{\max} = 1.5 (gq)^{1/3}$$

These investigations also revealed that the surface velocity required for containment can be approximated by the following formula for the design conditions of interest:

$$U_{\max} = 1.2 \sqrt{g h (1 - SGo)} + 3.38$$

Hence, based on these results a design U_{\max} of 5.0 ft/sec requiring about 1.0 cfs/ft of air supply is recommended for design.

The three main considerations on choosing the size of the manifold pipe are: 1) the air flow capabilities, 2) the buoyant forces, and 3) the drag forces. Since the air will be incrementally released along the pipe to form the bubbles, the mass flow rate along the pipe will continually decrease, but the initial section of pipe will have to carry the total amount of air to be released.

In order to avoid large energy losses due to shock waves, the velocity of the air in this initial section should be limited to about one half the speed of sound. Therefore, for a given air velocity, the length of manifold pipe that can be supplied is proportional to its diameter squared. This assumes that all the pipe is of the same diameter. The decision was made to keep the diameter constant so that no certain order was necessary in assembly.

The buoyant forces are proportional to the square of the diameter. The pipe must be heavy enough to sink. A 7 inch diameter pipe must weigh 17 lbs. per foot and a 24 inch pipe must weigh 200 lbs. per foot. In order to facilitate assembly, it was decided to make each joint of pipe light enough to be handled without the aid of machinery. This limits the length of each joint of pipe to 10 feet for a

7 inch diameter pipe or 5 feet for a 10 inch diameter pipe. The decision was made to use a 7 inch diameter pipe because of its longer length.

The above decisions were made based on the assumption that the necessary air movers could be obtained. As it evolved, this was not the case. The bids received were for air movers that would supply only 200 feet of manifold pipe.

One of these movers weighs 30 tons. This eliminates it. The other mover weighs only 10 tons which is very suitable. It supplies air at 45 psig. This is well above the pressure for which the original 7 inch pipe was designed.

From the above, it is obvious that the final pipe dimensions and the length between supply points will need to be determined after the air moving equipment is ascertained. This will also affect the overpressure in the pipe.

The original choice of material for the manifold pipe was polyvinyl chloride (P.V.C.). This was due to its rigidity and corrosion resistance. This had to be weighted and required an additional tension carrying member. Due to this, it was decided to build the pipe of steel. Since all of the steel in the manifold pipe system will be of the same type, corrosion should not be a major problem.

Supply Umbilicals

The final umbilical design cannot be completed until the manifold pipe is finally sized. The size and material will depend on the pressure and temperature of the outlet air from the compressor.

Power Supply

Design of the pneumatic system began under the assumption that the necessary air moving equipment could be obtained. This turned out to be not the case. Availability of air movers of the size necessary for the pneumatic barrier is limited and most are much too heavy to be used as a portable unit. The specifications for the unit to be used can be found from Gas Turbine Power, Inc., in Section III.

Section II

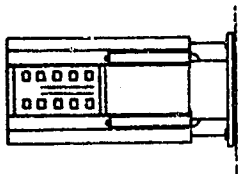
Experimental Apparatus and Procedures

II-I. Wind-Wave Channel

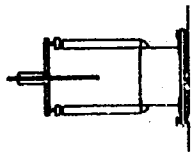
The wind set-up tests and some of the Pneumatic Barrier tests, including those with waves and currents, were performed in the 2 ft. wide by 3 ft. deep by 120 ft. long wind-wave channel shown in Fig. II-I-1. The combined wind-current set-up tests were also performed in this channel.

Waves were generated by a pendulum type paddle connected through pulleys and a variable stroke drive arm to a 3 h.p. Dynamatic variable speed motor. Waves could be generated from zero to approximately 12 inches in height and from less than a foot to in excess of 20 feet in length. These waves were absorbed at the opposite end of the channel by a series of perforated aluminum plates inclined at 15 degrees with the horizontal. The total working length of the channel was about 95 feet. A wave filter made of 1/4 in. opening wire mesh was inserted into the channel as needed to smooth minor irregularities out of larger waves.

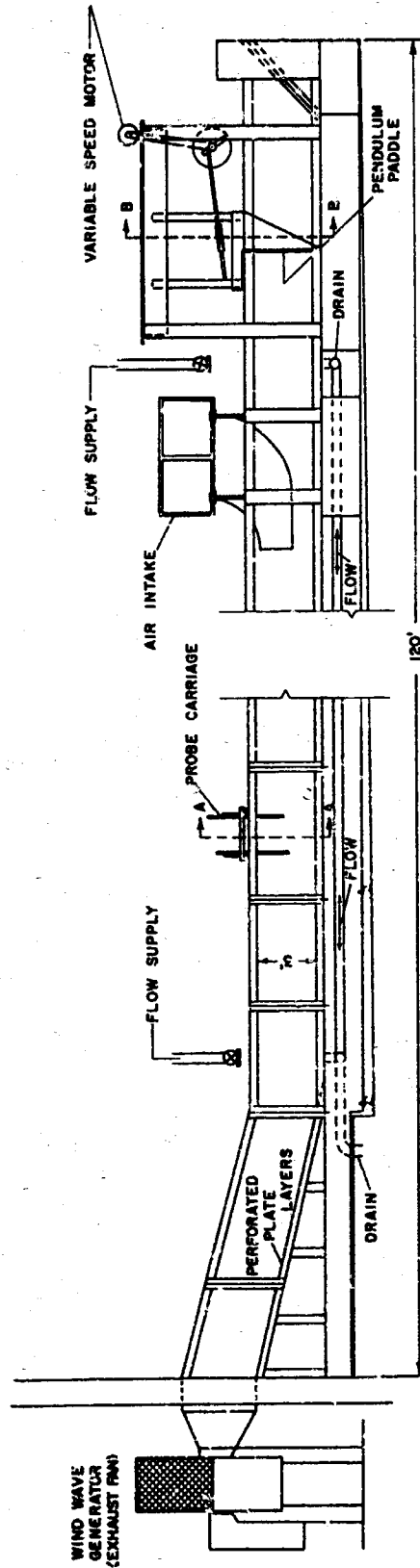
An air intake was located in front of the wave generator and could be adjusted vertically to any desired elevation. This consisted of eight large air filters placed on top of the intake to clean air emitted to the tank and a streamlined entry with guide vanes to emit air in a horizontal direction. A centrifugal blower located at the exterior of the laboratory exhausted the air from the tank. The magnitude of wind velocities that could be achieved depended on



CROSS SECTION B-B
(WAVE GENERATOR)



CROSS SECTION A-A



TEXAS A&M UNIVERSITY	
DEPARTMENT OF CIVIL ENGINEERING	
COASTAL AND OCEAN ENGINEERING DIVISION	
2' X 3' X 120' WAVE CHANNEL	
DRAWING NO. 4	DATE: JAN 10, 1969
SCALE	
DRAWN BY:	CHECKED BY:

FIG-II-I-1

the depth of water in the tank. With 14 in. water depth, average wind velocities of over 30 mph could be achieved. When generating winds, the channel was covered with plywood sections and all joints were taped to make the tank airtight.

Currents in the tank were generated with a 4.5 c.f.s. capacity axial flow pump. The pump lifted water from the main sump and delivered it to the channel in front of the wave paddle. The water flowed through the air filter and then out a 12 in. opening at the far end of the tank that leads back to the sump. With a water depth of 18 in. currents up to 1.5 f.p.s. were generated.

Air for the tests was provided by a 15 c.f.m. capacity air compressor. The air flowed through three Fisher-Porter flowrators connected in parallel, so that a variety of flow-rates could be accurately measured. The three flowrators had capacities of 1.1, 4.6, and 28 c.f.m.

II-II. Water-Wave Channel (Recirculating Flume)

The small recirculating flume is approximately 44.5 ft. long, 7.5 in. wide and 17 in. deep. This flume is sketched diagrammatically in Fig. II-II-1. The flume has both wave generating and current generating capabilities. A pneumatic generator may be readily installed by simply placing a manifold with desired orifice openings across the bottom of the channel and providing the necessary connecting lines to a compressed air supply. The small recirculating flume operates as a closed system; the water is recirculated through a 4-in. line by a centrifugal pump which is driven by a 20 horsepower electric motor. The walls of the flume are constructed of plexiglas, a feature which allows the flow pattern and oil set-up geometry to be visually observed and the measurements of the oil set-up to be readily obtained. Also, the flume is equipped with turning vanes at the ends and a series of flow-straighteners at the upstream in order to provide a reasonably uniform flow distribution over the cross-section of the channel.

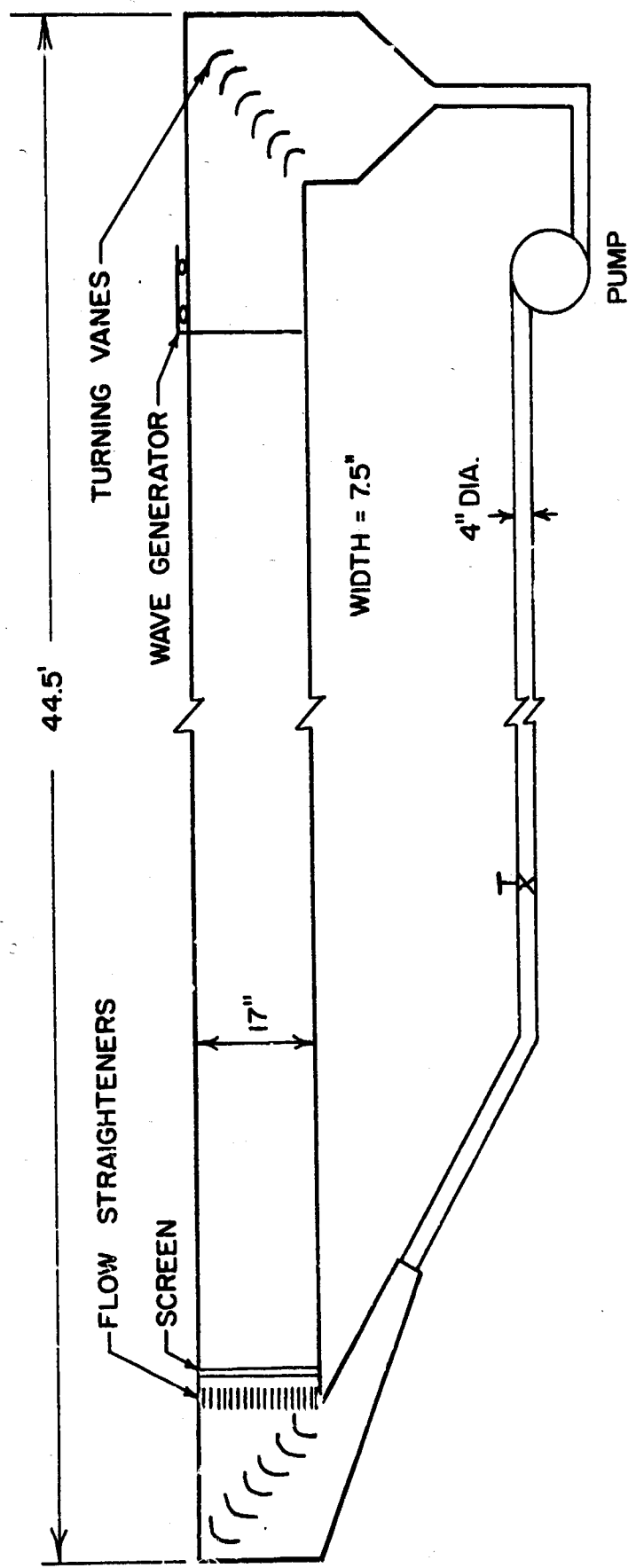
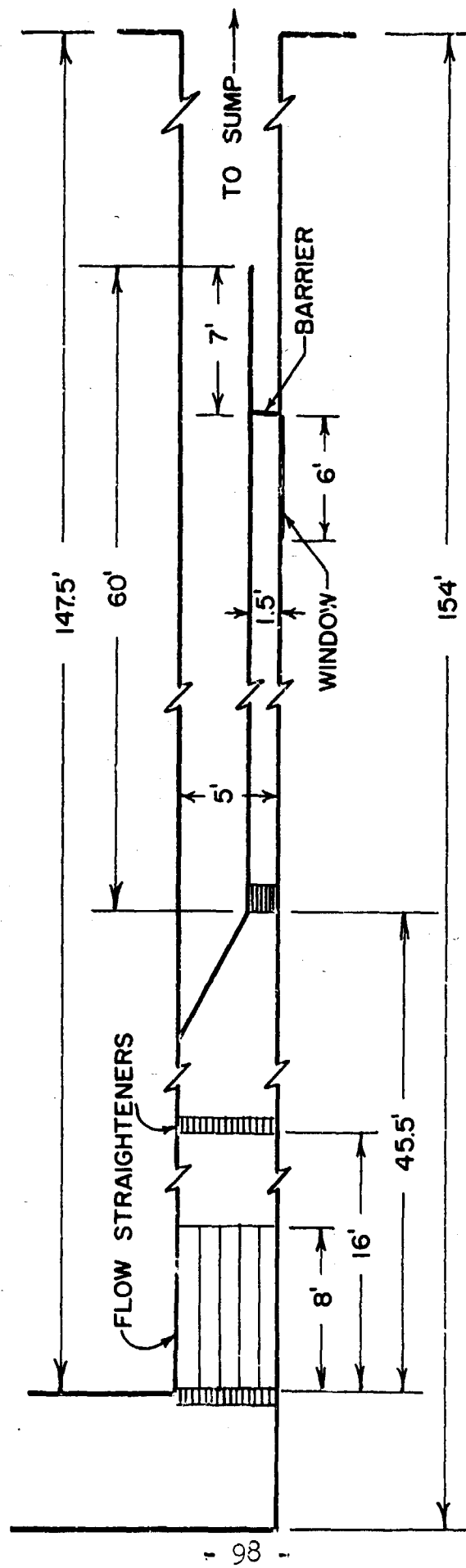


FIG. II-II-1
 DIAGRAMMATIC SKETCH OF THE SMALL RECIRCULATING FLUME

II-III. Current Channel (Recirculating Floor Channel)

The recirculating floor channel is 147.5 ft. long, 5 ft. wide and 10 ft. deep. A sketch of this facility is shown in Fig. II-III-1. The channel is connected to a sump and is operated as a closed system by the use of two centrifugal pumps which provide a combined maximum flow capacity of $19.5 \text{ ft}^3/\text{sec}$. The channel is made of concrete and is situated with its open top flush with the floor of the building. An observation window made of plexiglas and having approximate dimension of 6 ft. long and 4 ft. high is located in one side of the channel about 100 ft. from the upstream end. A pneumatic generator may be installed by inserting a manifold with the desired orifice openings across the channel and then providing the necessary connection lines to a compressed air supply.

In order to obtain relatively large values of water current a necked-down region was constructed in the floor channel. The overall dimensions of the narrowed region was 60 ft. long, 1.5 ft. wide and 8 ft. deep. A number of flow straighteners were installed upstream of the test section in order to provide a reasonably smooth velocity profile at the test area. The narrowed region and the location of the flow straighteners are depicted in Fig. II-III-1.

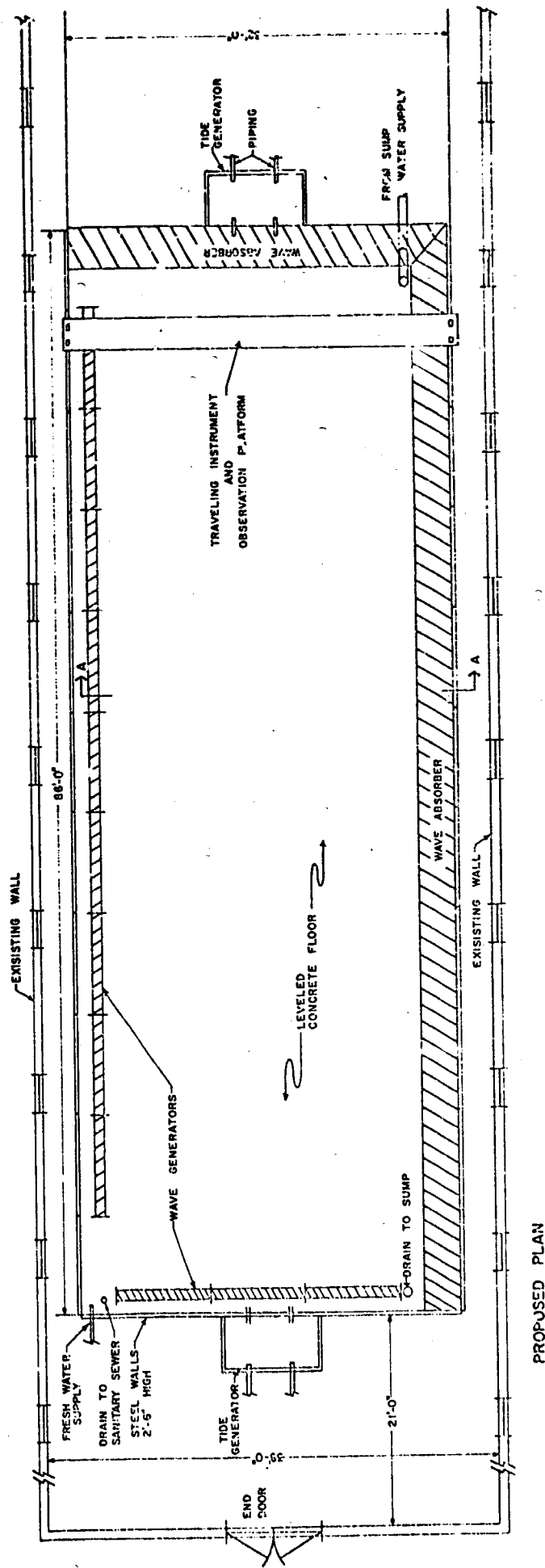


CHANNEL DEPTH = 10 ft.

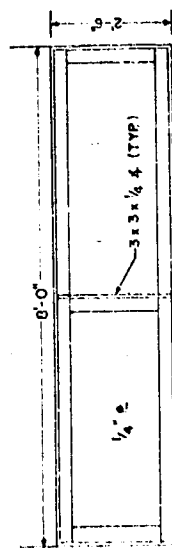
FIG. SKETCH OF RECIRCULATING FLOOR CHANNEL
II-III-1

II-IV. Three-Dimensional Wave Basin

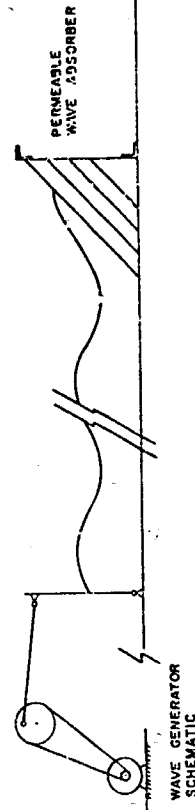
The three-dimensional wave basin is 86 ft. long, 32 ft. wide and 2 ft. deep. It has three wave generating plates which are powered by a variable speed motor. Currents may also be generated in one direction providing a capability of producing waves and currents at the same time. (Fig. II-IV-1).



PROPOSED PLAN



WALL PANEL (TYP)
SCALE: 3/8" = 1'-0"



SECTION A-A

TEXAS A&M UNIVERSITY			
DEPARTMENT OF CIVIL ENGINEERING			
COASTAL AND OCEAN ENGINEERING DIVISION			
32' x 86' x 2' 6" WAVE BASIN	DRAWING NO. 1	DATE	10 MAR 1969
SCALE 3/8" = 1'-0"	DRAWN BY	CHECKED BY	

FIG-II-IV-1

II-V. Research Instrumentation

Water-surface time-histories were measured to determine wave heights and periods (and thus wave lengths), with a capacitance-type wave gage mounted on a point gage. The gage consists of a mounted vertical wire coated with an insulator material. The wire acts as one dielectric and the water serves the other. As a wave passes the gage, the capacitance is varied. This capacitance is calibrated to water surface elevation, so that water surface elevation may be continuously recorded on a direct-writing recorder. Sanborn 150 amplifier-recorders were used to obtain wave records. The gage was calibrated by raising and lowering it in still water and noting the pen deflection on the recorder.

Wind velocities were measured with a Meriam Pitot tube connected to an air-water U-tube manometer inclined on a 1 to 48 slope to increase the accuracy with which velocities could be measured.

Water velocities were also measured with a pitot tube connected to an inclined U-tube water manometer. Also, an Ott-propeller current meter was used. This has a range from 0.2 f.p.s. up to velocities greatly in excess of those encountered in this research.

II-VI. Experimental Procedure and Analysis of Data

1. Oil Set-Up By Wind

Analytical Considerations

In order to gain further insight into the nature and degree of set-up (or set-down) of oil floating on water, subjected to a wind stress and retained by some mechanism, and to guide experiments on this problem; it is worthwhile to analytically develop equations that relate oil set-up volume, fetch length, and properties and wind stress.

An equation for the two-dimensional set-up of floating oil due to a wind generated surface stress can be developed by considering the schematic oil wedge shown in Fig. II-VI-1. It has been shown that for the set-up of water during coastal storm surges, convective and local accelerations can be neglected. As oil is less dense and more viscous than water, these accelerations will also be neglected for our problem. Due to the oil fetch lengths involved, horizontal pressure gradients in the air may also be neglected.

From a consideration of hydrostatics at the barrier,

$$\rho_o \frac{d_o}{\rho_a} = \rho_a \frac{d_a}{\rho_a}$$

or

$$\frac{d_a}{\rho_a} = \frac{\rho_o}{\rho_a} \frac{d_o}{\rho_a} \quad (VI-1)$$

where d_w and d_o are the water and oil depths at the barrier, ρ_w and ρ_o are the water and oil densities, and g is the acceleration of gravity.

A summation of horizontal forces acting on the oil and water control volume shown in Fig. II-VI-1 gives

$$\frac{1}{2} (\rho_w g d_w^2) + \tau_o L + \tau_w L - \frac{1}{2} (\rho_o g d_o^2) = 0 \quad (\text{VI-2})$$

The small angle between the air-oil interface and the horizontal has been neglected and τ_o and τ_w represent the average shear stresses over the fetch, L .

The stress at the oil-oil interface may be written

$$\tau_o = C' \rho_a U^2 \quad (\text{VI-3})$$

where ρ_a is the air density, U is the wind velocity and C' is a coefficient that depends on interface roughness, atmospheric stability and air Reynolds number. This can also be written

$$\tau_o = C \rho_w U^2 \quad (\text{VI-4})$$

where the drag coefficient C incorporates the ratio of air to water density. It is anticipated (see 17, 18) the C will just vary with surface roughness (i.e. waves on oil) at higher Reynolds numbers. This will be investigated and the value of C for wind over oil will be determined in the laboratory tests.

If we let

$$\tau_o + \tau_z = n \tau_o \quad (\text{VI-5})$$

and we combine Eqs VI-1, 2, 4 and 5 we have

$$d_o = \sqrt{\frac{2 n \tau_o L}{\epsilon \rho_o (1 - \rho_o / \rho_w)}} \quad (\text{VI-6})$$

and

$$d_o = \sqrt{\frac{2 n c J_L^2 \rho_z}{\epsilon \rho_o (1 - \rho_o / \rho_w)}} \quad (\text{VI-7})$$

Eq. VI-7 gives the oil set-up at the barrier in terms of the oil and water densities, fetch length, wind speed and an experimental coefficient nc .

Van Dorn (17) studied water set-up by wind in a 6 ft deep and 800 ft. long yacht pond and found n to be between 1.0 and 1.1 or essentially neglectable. As for our problem τ_z probably acts upwind over part of the fetch and downwind over the remainder of the fetch. As the stress should be less than if a solid bottom bounded the control volume, it is possible to neglect n in further equations.

In order to simplify the writing of Eqs. VI-6, VI-7, etc. we will use the densimetric acceleration of gravity, g ; defined as

$$g' = g(1 - \rho_o / \rho_w) \quad (\text{VI-8})$$

To indicate the vertical profile of the oil wedge, we can develop an equation similar to Eq. VI-7 in terms of the oil set-up, d_{ox} , at any point, x (see Fig. II-VI-1)

Thus

$$d_{ox} = \sqrt{\frac{2 C U^2 x \frac{\rho_w}{\rho_o}}{g'}} \quad (VI-9)$$

The total oil volume per unit width, v , is as follows:

$$v = \int_0^L d_{ox} dx$$

$$v = \frac{2}{3} \sqrt{\frac{2 C U^2 L^3}{g'} \frac{\rho_w}{\rho_o}} \quad (VI-10)$$

If we know the total volume of oil spill, the shape assumed by the retention mechanism and the wind speed, we can calculate the fetch length, L , at any location from Eq. VI-10 and the oil thickness at any location from Eq. VI-9.

Eq. VI-7 can be written in dimensionless form as follows:

$$\frac{d_o}{L} = \sqrt{2 C, \frac{\rho_w}{\rho_o}} \sqrt{\frac{U}{g' L}} \quad (VI-11)$$

which indicates that the dimensionless set-up, d_o/L , is a function of a densimetric Froude number, $U/\sqrt{g' L}$. Eq. VI-11 will be useful for the presentation of experimental results.

Experimental Arrangement and Tests

All tests on the wind set-up of oil were conducted in the 2 ft wide by 3 ft deep by 120 ft long wind-wave flume shown in Figures II-VI-2 and II-VI-3. Air enters a streamlined air intake that may be adjusted vertically to sit just above the water

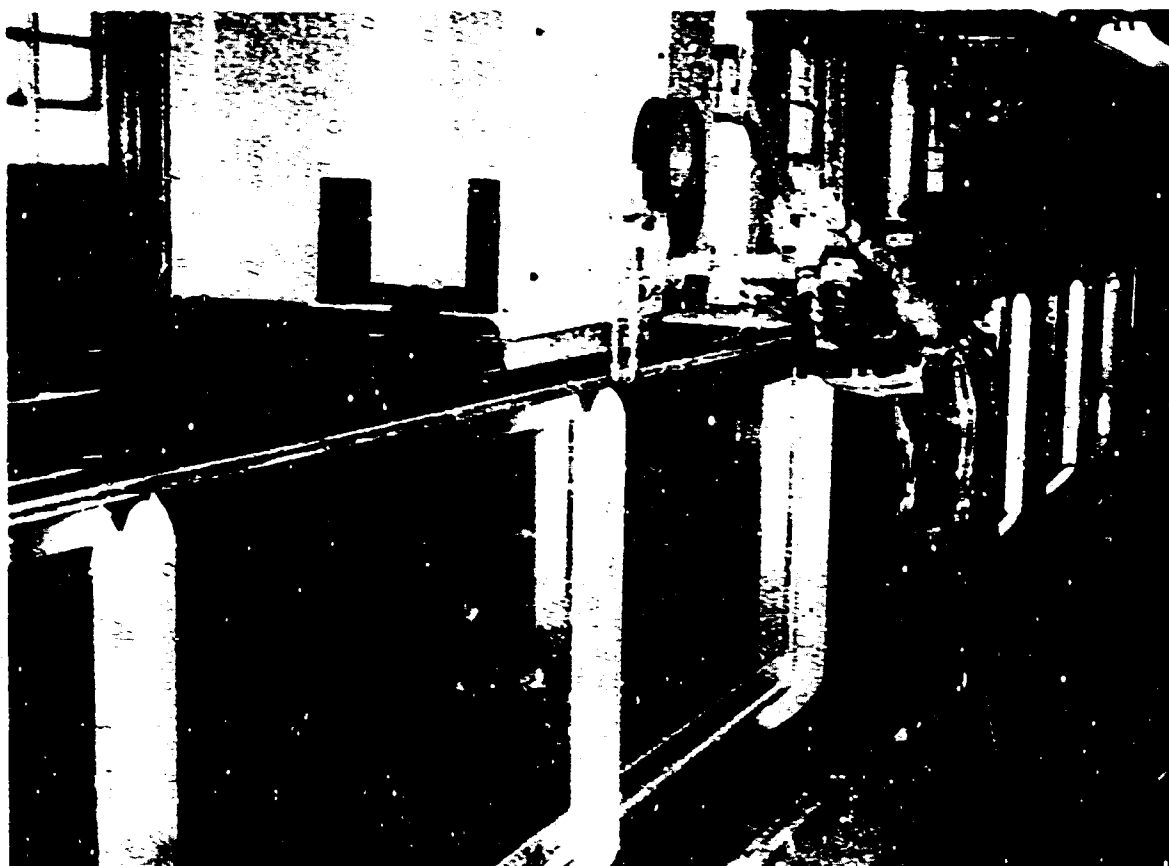


FIGURE II-VI- 2

INTERMEDIATE GLASS WALL FLUME (TESTS OF
PNEUMATIC BARRIER IN STAGNANT WATER)

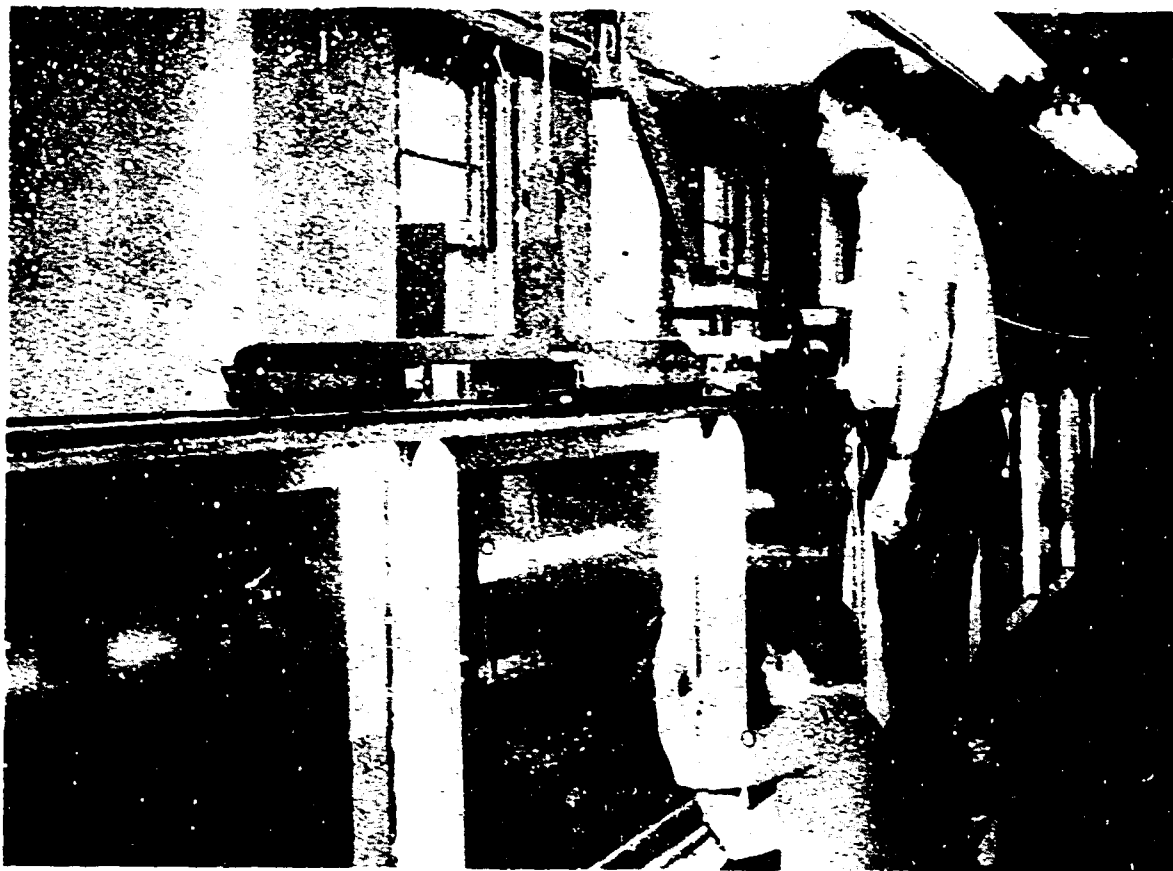


Figure II-7) Measurements taken of oil set-up by wind

surface and is evacuated by a centrifugal blower located at the exterior of the building. The tank has glass side walls which allow observation of the oil set-up and motion.

A series of tests was conducted with each of the three oils listed in Table I.

TABLE I - OIL PROPERTIES

<u>No.</u>	<u>Name</u>	<u>Viscosity, 60°F (centipoise)</u>	<u>Specific Gravity, 60°F</u>
1	Chevron RPM Delo Special	388	0.888
2	Gulf Diesel Fuel	3.7	0.858
3	Shell Legion 43	96	0.911

Each test series consisted of placing one, two, three or four barrels of one oil into the tank with fresh water and measuring the set-up for a range of about 30 wind speeds. The oil properties were determined by periodically collecting samples and measuring viscosity and density with a Saybolt viscometer and hydrometer, respectively.

Experimental results show a more viscous oil would have negligible surface waves at wind velocities of interest (up to 40 mph at ten meters elevation) and only during the existence of waves does the set-up differ from that predicted by the basic equation to be developed. (Figures II-VI-4, II-VI-5) As three different density oils all behaved as predicted in the previous section, the set-up of any density

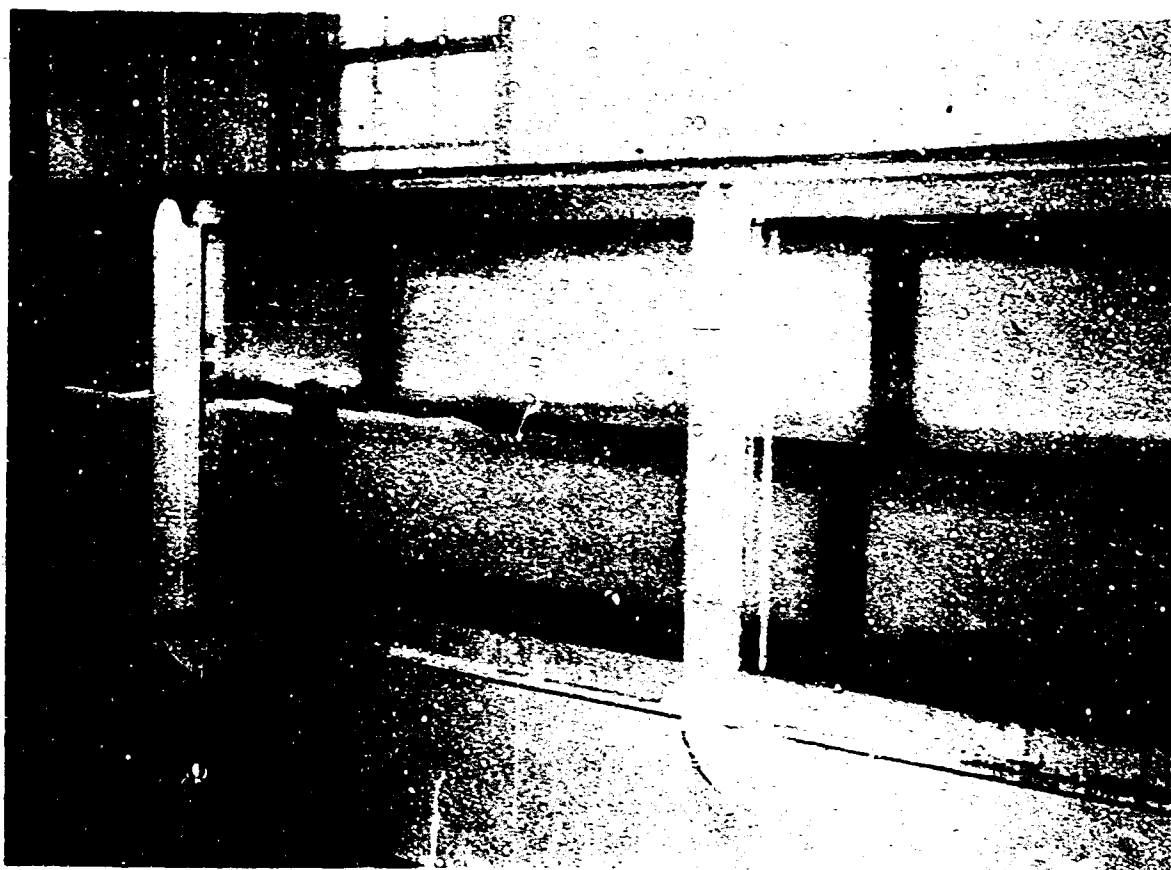


Figure II-VI-4 Oil set-up by wind (oil on the right - no surface waves, water on the left - surface waves) Oil No. 1, Viscosity 388 C.P. specific gravity 0.888



Figure II-VI-5 Oil set-up by wind

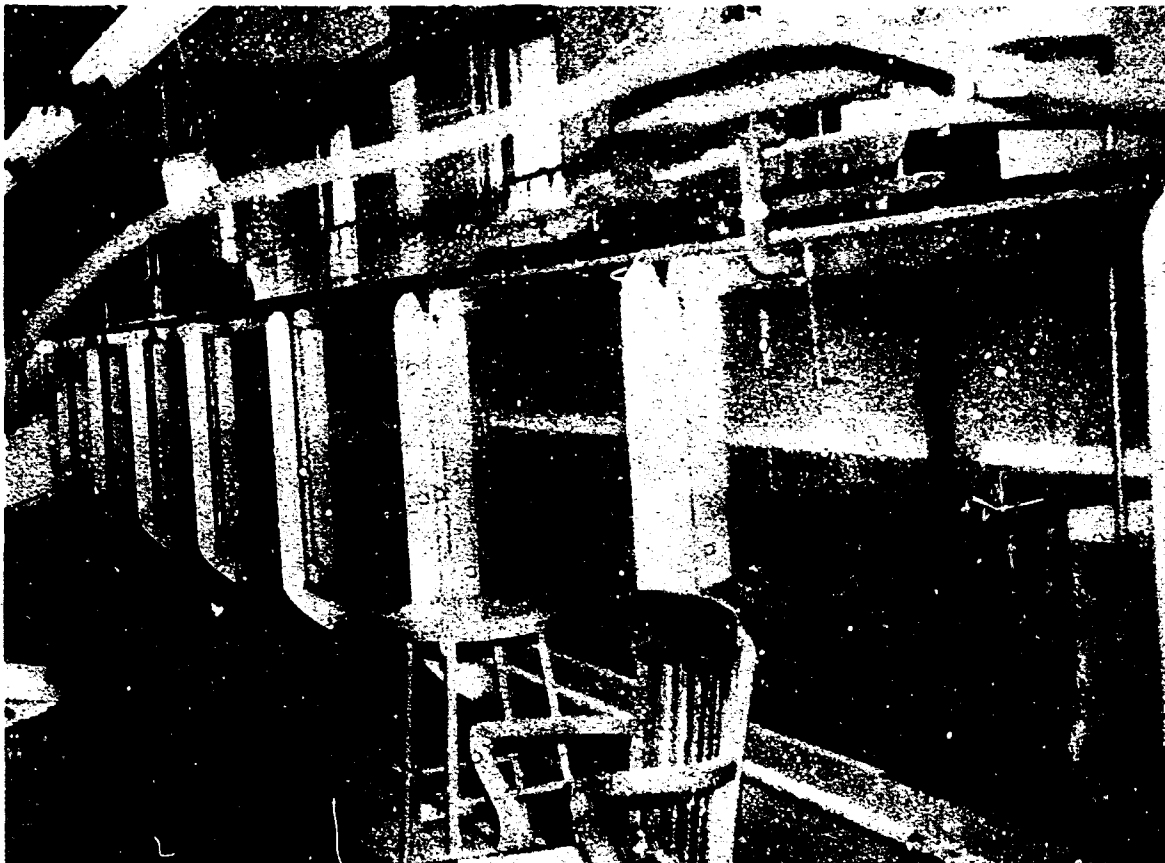


Figure II-VI-6 Oil set-up by wind (note the vertical barrier on the right and a gradual increase of oil thickness from left to right).

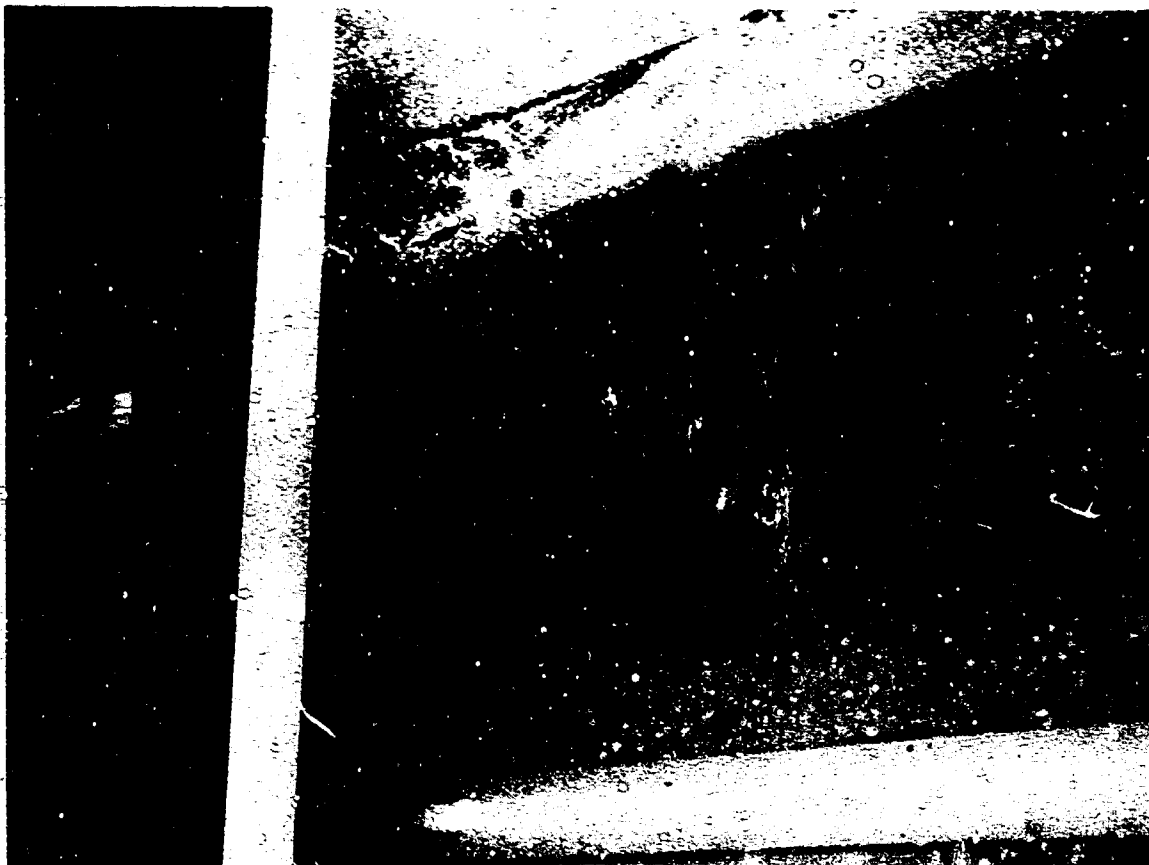


Figure II-VI-7 Tests on oil set-up by wind. (Viewed from below through glass wall of the wave tank, note the rough interface between oil and water)

oil that will be encountered can be predicted.

A one-foot high rigid vertical barrier was installed in the wind-wave flume at a point 70 ft. from the air-intake. (Figure II-VI-6) The barrier could be raised and lowered as desired and was generally set to extend 0.3 ft. above the still water surface. When waves developed on the oil surface, a gravel wave absorber was mounted on the barrier to prevent the formation of standing waves in the oil.

The set-up near the barrier and at various points along the oil wedge was measured by a point gage. The gage was mounted on a carriage above the tank and protruded through small openings in the tank cover. Set-up was determined by measuring the air-oil and oil-water interface elevations 2 ft. upwind of the barrier and at 10 ft. intervals upwind of this point. (Figure II-VI-7)

For tests with oil number one, a still water depth of 18 in. was used. The depth was changed to 14 in. for the remaining tests. This allowed for the development of better wind field patterns and helped verify the conclusion--set-up is independent of water depth for the water depths anticipated in practice.

Special stilling wells were developed to measure oil set-up when waves were generated in the oil. These wells consisted of vertical plexiglas tubes (1.5 in I.D.) with a number of

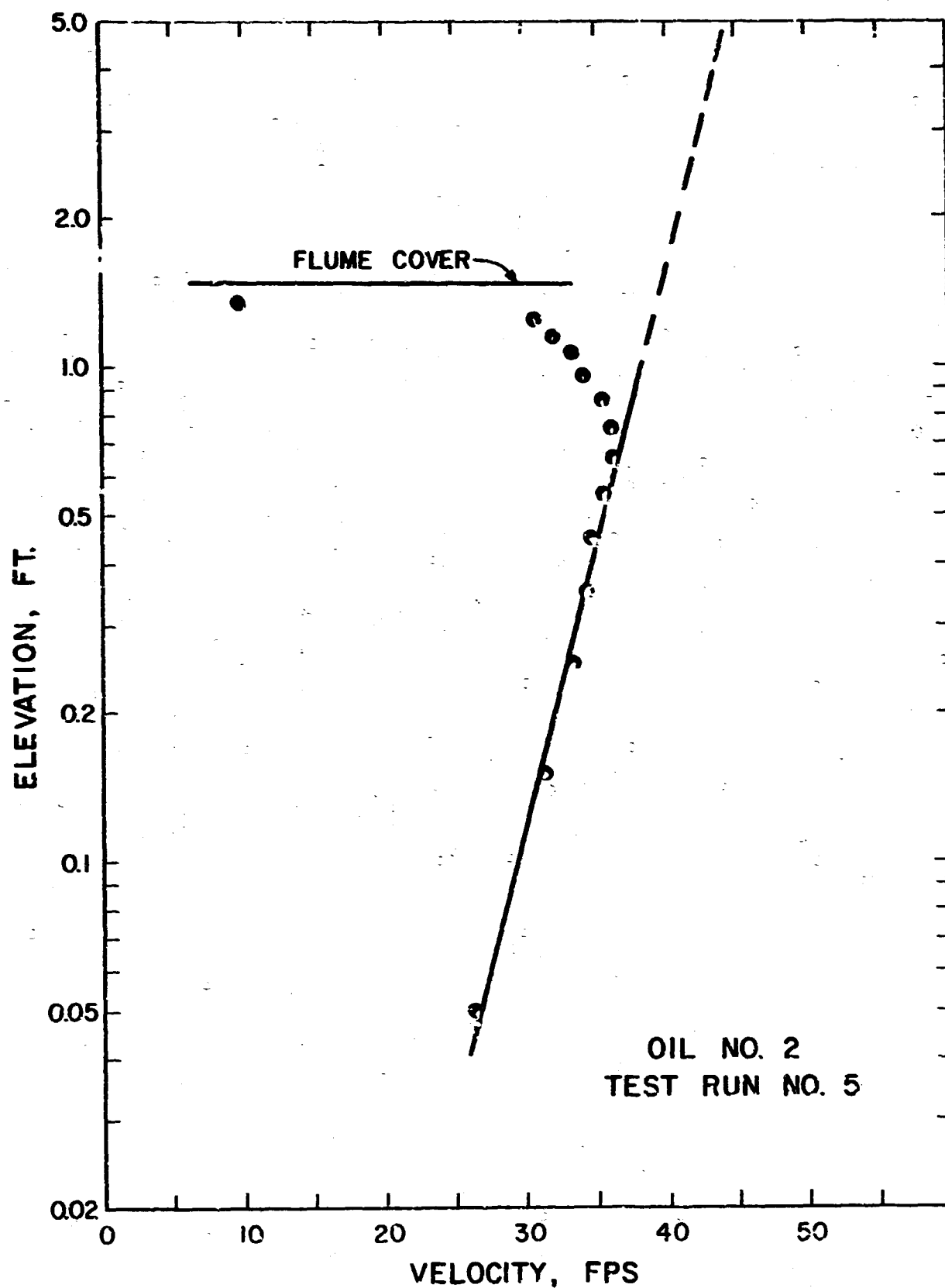


FIG. TYPICAL CENTERLINE VELOCITY PROFILE
II-VI-8

closely placed small holes on a vertical line on the downwind side that allowed the oil to enter the tubes and stand at its mean thickness. The wells functioned excellently for all oils used.

Wind velocities were measured by pitot tubes on moveable point gage staffs and connected to inclined air-water manometers. For each test run, wind velocities were measured at 0.1 ft intervals along a vertical line at the tank centerline 5 ft upwind of the barrier. In order to gain a better understanding of the wind patterns in the entire wind-wave tank with oil and water, a series of cross section velocity measurements were made to produce isovel patterns at three locations. The locations were 5, 25, and 45 ft upwind of the barrier and isovel patterns were determined for specific low, medium, and high wind velocities. The isovel patterns were incorporated in the reduction of wind velocity data as explained in the discussion of experimental results.

Experimental Results and Discussion

Fig. II-VI-8 shows a typical centerline wind velocity profile taken 5 ft upwind of the barrier. These data fit a semi-log curve above the oil surface up to a point where boundary effects from the flume cover cause the velocity to decrease with increasing elevation. Extrapolation of this lower curve yields a ratio of

1.5 for the velocity at 10 meters compared to the velocity at 0.7 ft which is the velocity used (i.e., U) in the flume data reduction. This ratio varies from approximately 1.4 to 1.9 for the range of tests. This ratio for the design wind profiles (Fig. II-VI-9) is 1.75. Thus, any design wind velocity chosen (e.g., 20 mph or 40 mph) should be divided by 1.75 to yield U for the charts and equations presented in the remainder of this section.

Due to boundary effects caused by the flume side walls, the wind velocity varied along any horizontal line normal to the tank axis. To adjust for this variation, a ratio of the root mean square velocity at 0.7 ft elevation for a cross section where isovels were measured to the centerline velocity at 0.7 ft elevation was established for different wind speeds. Centerline values of U were then corrected by this ratio. A root mean square velocity was used as wind stress is a function of wind velocity squared.

Using the format established by Eq. VI-11, the dimensionless wind set-up at the barrier, d_o/L , is plotted as a function of Froude number, $U/\sqrt{g'L}$, in Figs. II-VI-10, 11, 12 for all volumes of the three oils tested. The data between the origin and the break in the line are for no waves existing on the oil surface. The data from tests with all three oils fall on the same line when plotted in dimensionless form as is further demonstrated

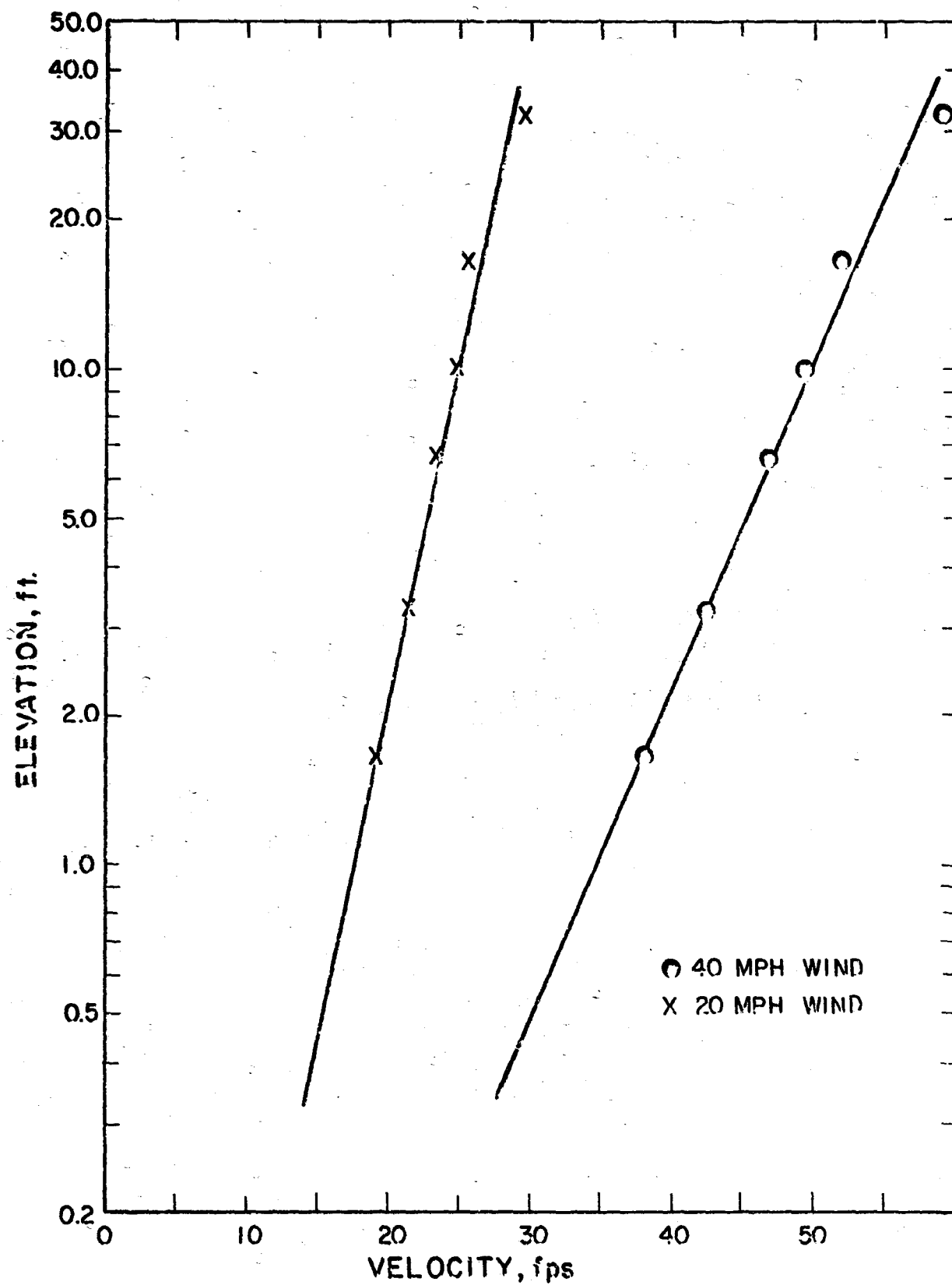
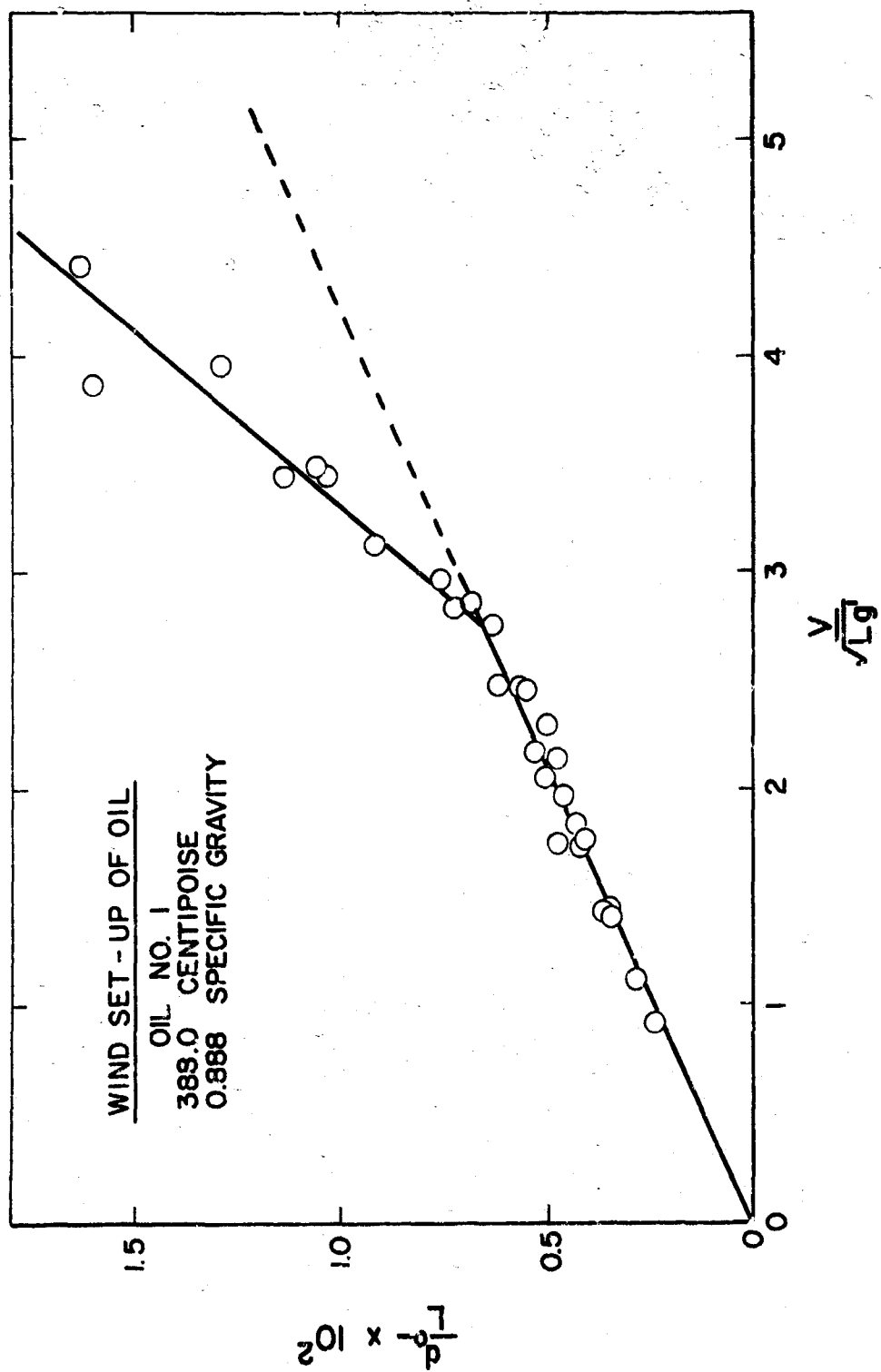


FIG. - GIVEN DESIGN WIND PROFILES
II-IV-9



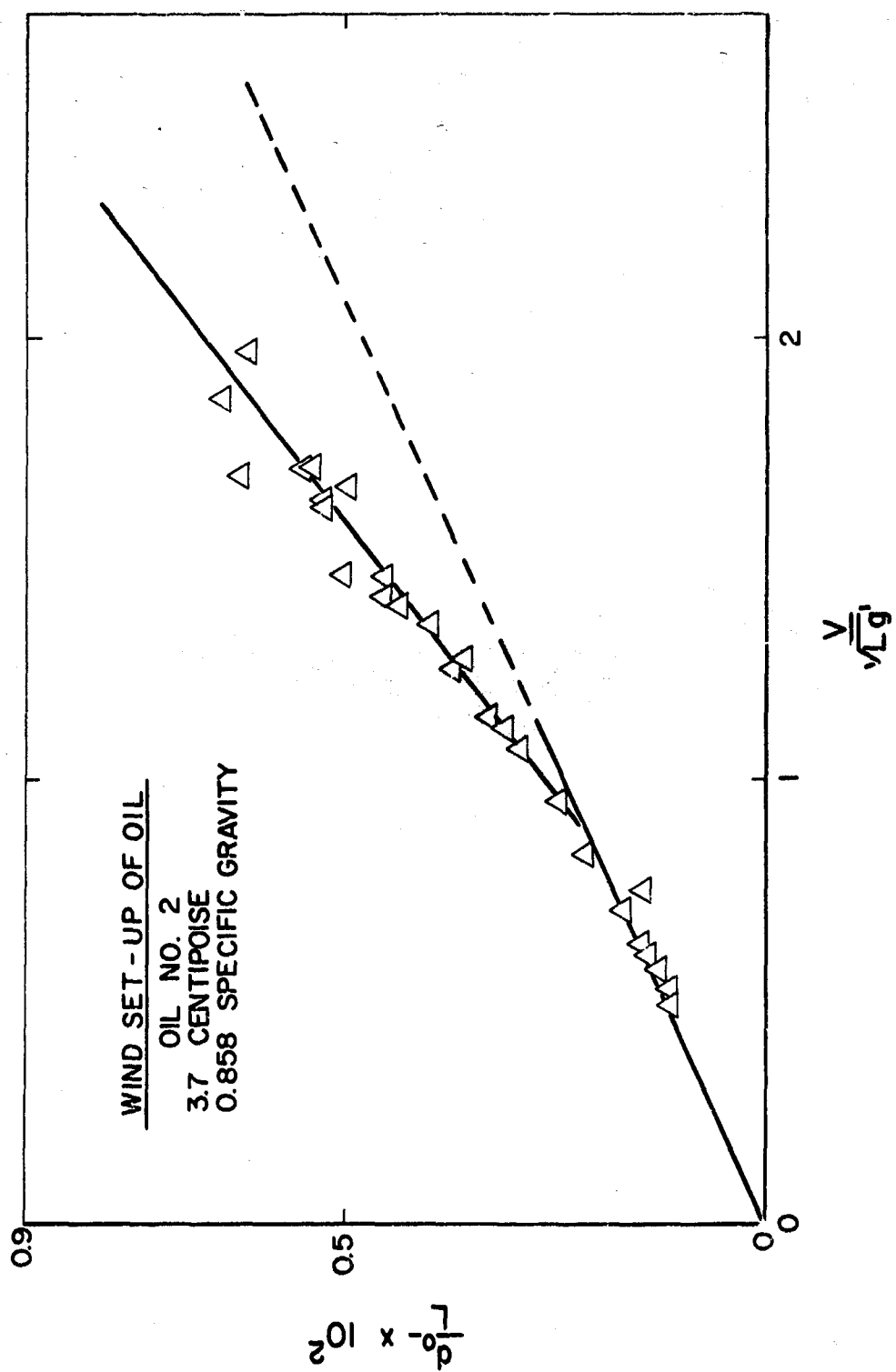


FIG. A-VI-11

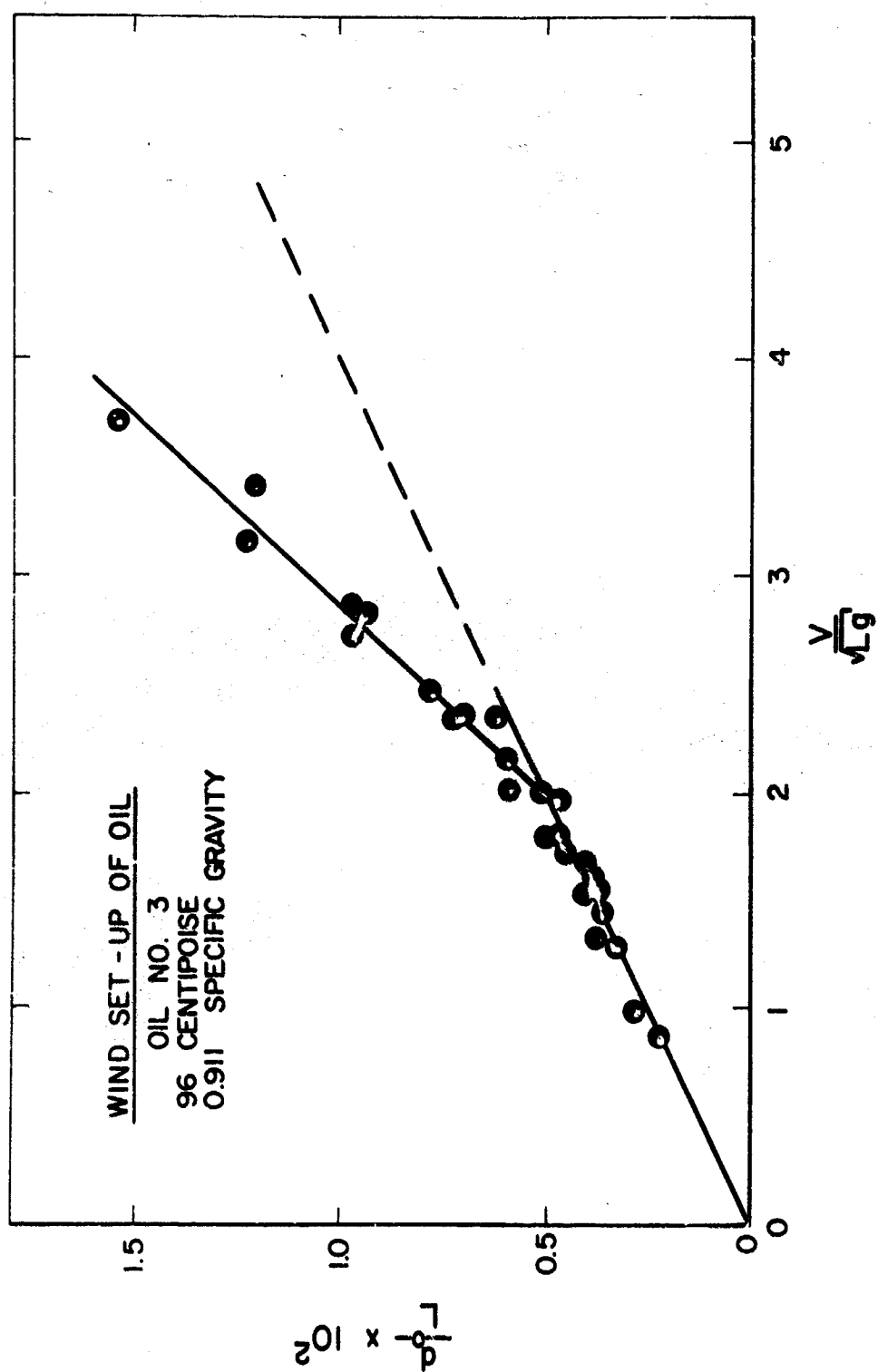


FIG. II-VI-12

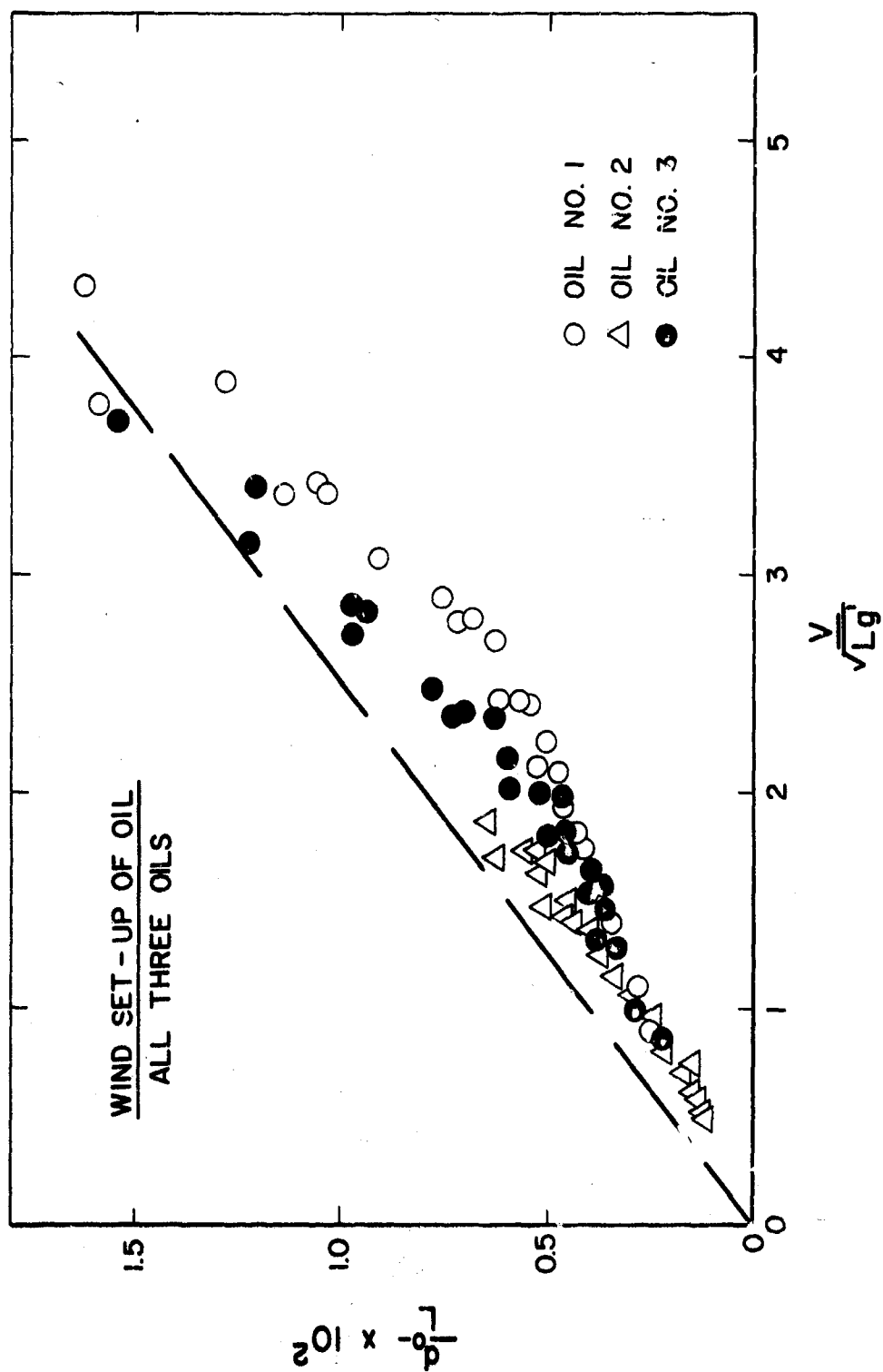


FIG. II-VI-13

in Fig. II-VI-13. Thus, for any oil with negligible surface waves, the set-up is given by Eq. VI-11 in the following form

$$\frac{d_o}{L} = 2.3 \times 10^{-3} \sqrt{\frac{\rho_x}{\rho_o}} U \sqrt{g' L} \quad (\text{VI-12})$$

In order to evaluate wave effects, the additional set-up caused by waves on the oil, d_{ow} , (i.e. the set-up in excess of that predicted by Eq. V-12) was determined. Thus, the total set-up, d_{ot} , is $d_o + d_{ow}$. From various plots of d_{ow} versus wind speed it was found that the additional set-up may be given by an equation of the form

$$d_{ow} = \sqrt{\frac{2 B L \rho_x}{g' \rho_o}} (U - U_c) \quad (\text{VI-13})$$

where U_c is the wind velocity at which wave set-up begins and B is a constant that depends on oil properties. Thus, the total set-up when $U > U_c$ is given by

$$d_{ot} = 2.3 \times 10^{-3} \sqrt{\frac{\rho_x L}{\rho_o g'}} U + \sqrt{\frac{2 B L \rho_x}{g' \rho_o}} (U - U_c) \quad (\text{VI-14})$$

Rearranging Eq. 13

$$\frac{d_{ow}}{\sqrt{L}} = \sqrt{\frac{2 B \rho_x}{g' \rho_o}} U - \sqrt{\frac{2 B \rho_x}{g' \rho_o}} U_c \quad (\text{VI-15})$$

which is the equation of a straight line. If this form is valid, a plot of d_{ow}/\sqrt{L} as a function of U will fit a straight line and B and U_c can be evaluated. A plot of this type for Oil No. 2 is shown in Fig. II-VI-14 from which $B = 7.7 \times 10^{-6}$ and $U_c = 11.7$ fps.

This value of U_c agrees very well with the velocity at which waves developed on the oil surface during the tests with Oil No. 2. For the other oils the following values were obtained.

<u>Oil</u>	<u>$B \times 10^6$</u>	<u>U_c, fps</u>
No. 1	49.3	32.6
No. 5	14.1	24.0

A plot of these values as a function of oil kinematic viscosity is given in Fig. II-VI-15. Thus, for a given oil, values of B and U_c can be estimated and the oil set-up can be calculated when U exceeds U_c . U_c is 32.6 fps or 22.3 mph in the flume and thus 39 mph at the 10 meter elevation. For oil with a viscosity in excess of 400 centipoise, no waves will be generated at the design wind speed of 40 mph or less. Set-up is given by Eq. VI-12.

It is of interest to reconsider the plot of all set-up data (Fig. II-VI-13). For design purposes, an envelope curve can be drawn on this plot and an apparent drag coefficient, C_a , can be estimated from this curve. This has a value of 6.9×10^{-6} giving a design air-oil interface stress with waves for any oil of

$$\begin{aligned}\tau_o &= C_a \rho_x U^2 \\ &= 6.9 \times 10^{-6} \rho_x U^2\end{aligned}\quad (V-16)$$

Remember, U in Eq. VI-16 is the design wind velocity at ten meters elevation divided by 1.75.

It is also interesting to check the analytical prediction (Eq. VI-9) that the oil wedge has a parabolic shape. Figs. II-VI-16 and II-VI-17 show typical plots of wedge thickness, d_{ox} , versus distance from the barrier, x , from experimental measurements and as predicted by Eq. 9. Agreement is acceptable so Eq. VI-10 for oil volume should give satisfactory values.

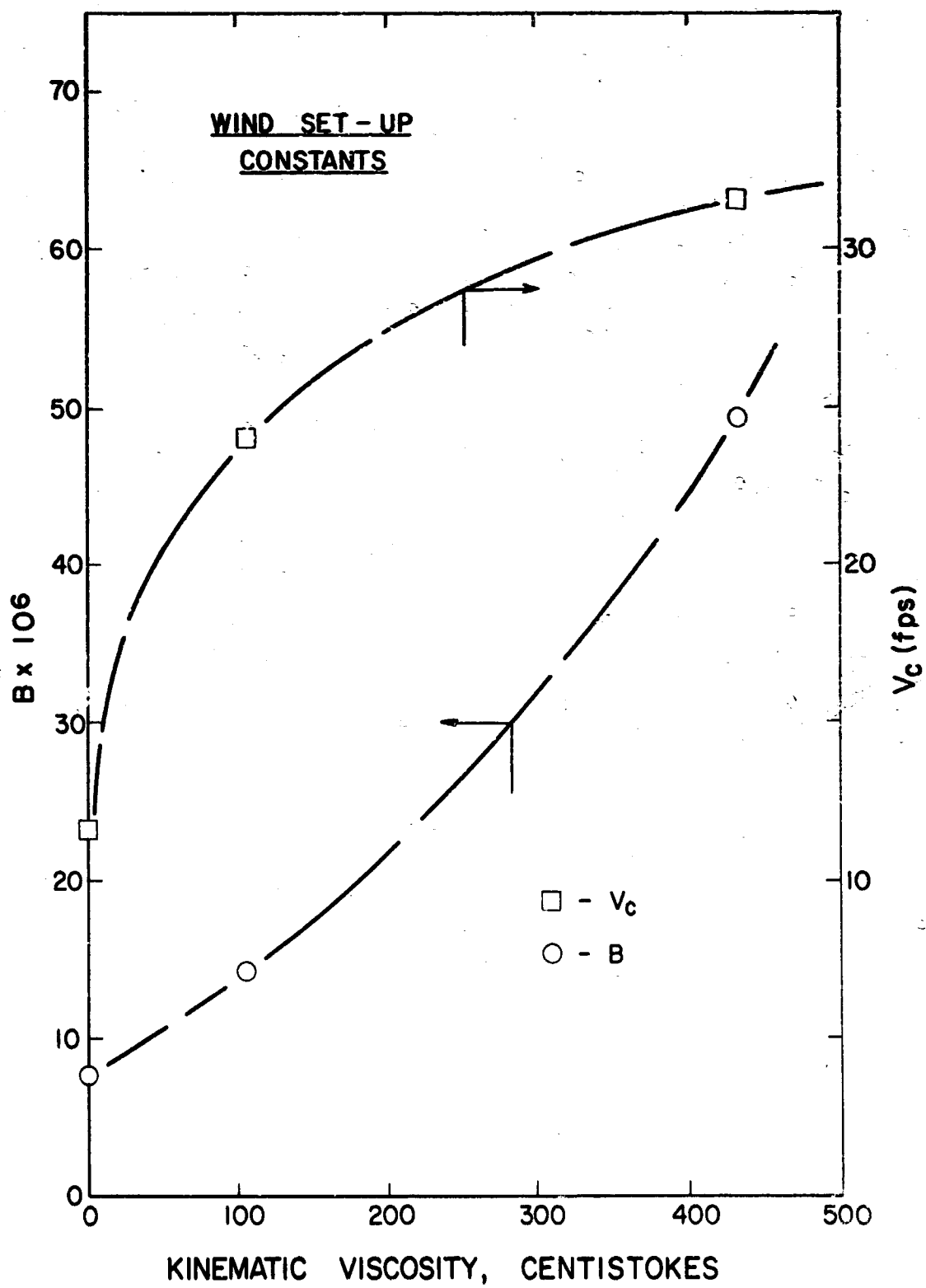


FIG. II-VI-15

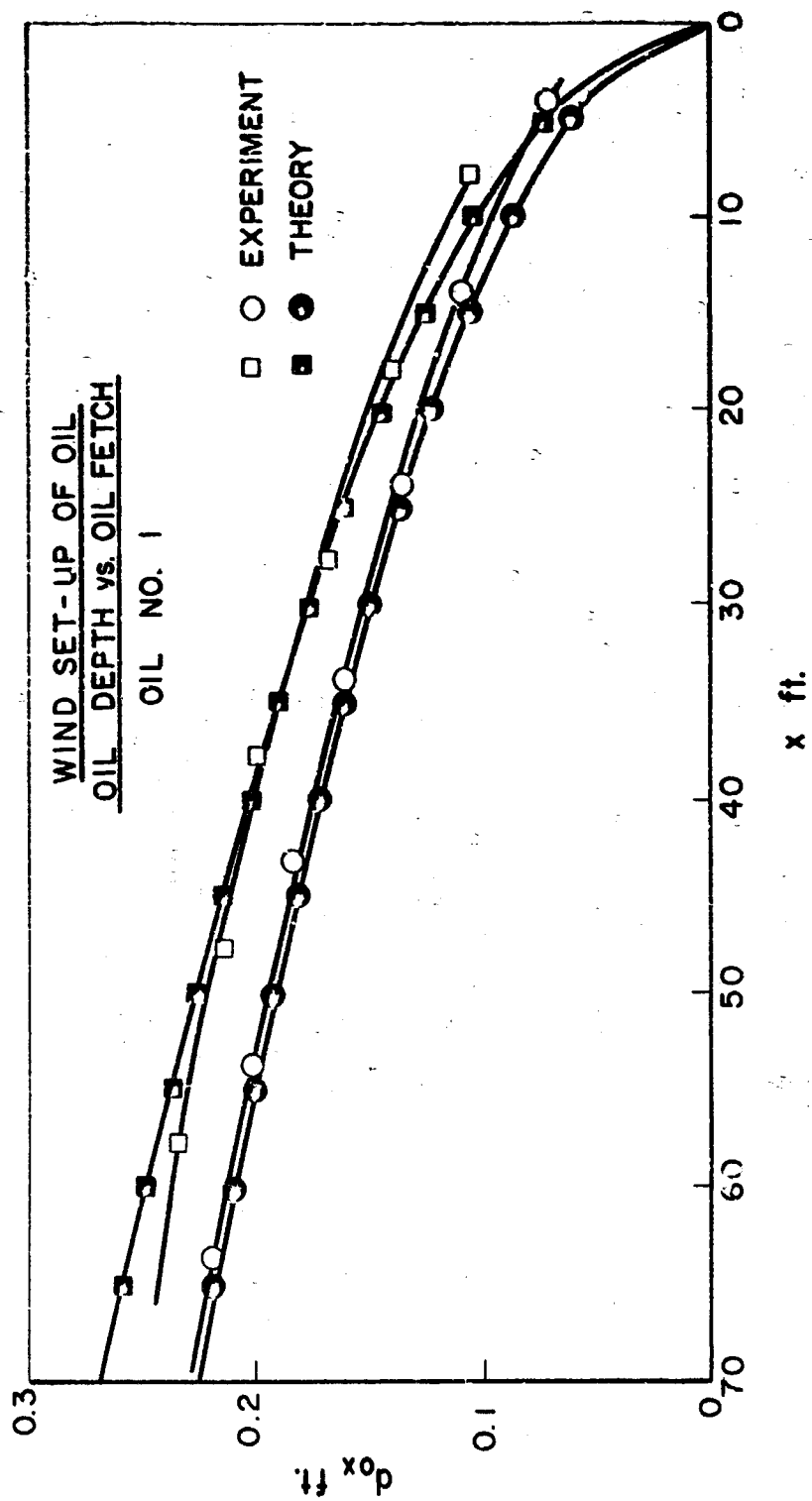


FIG. II-VI-16

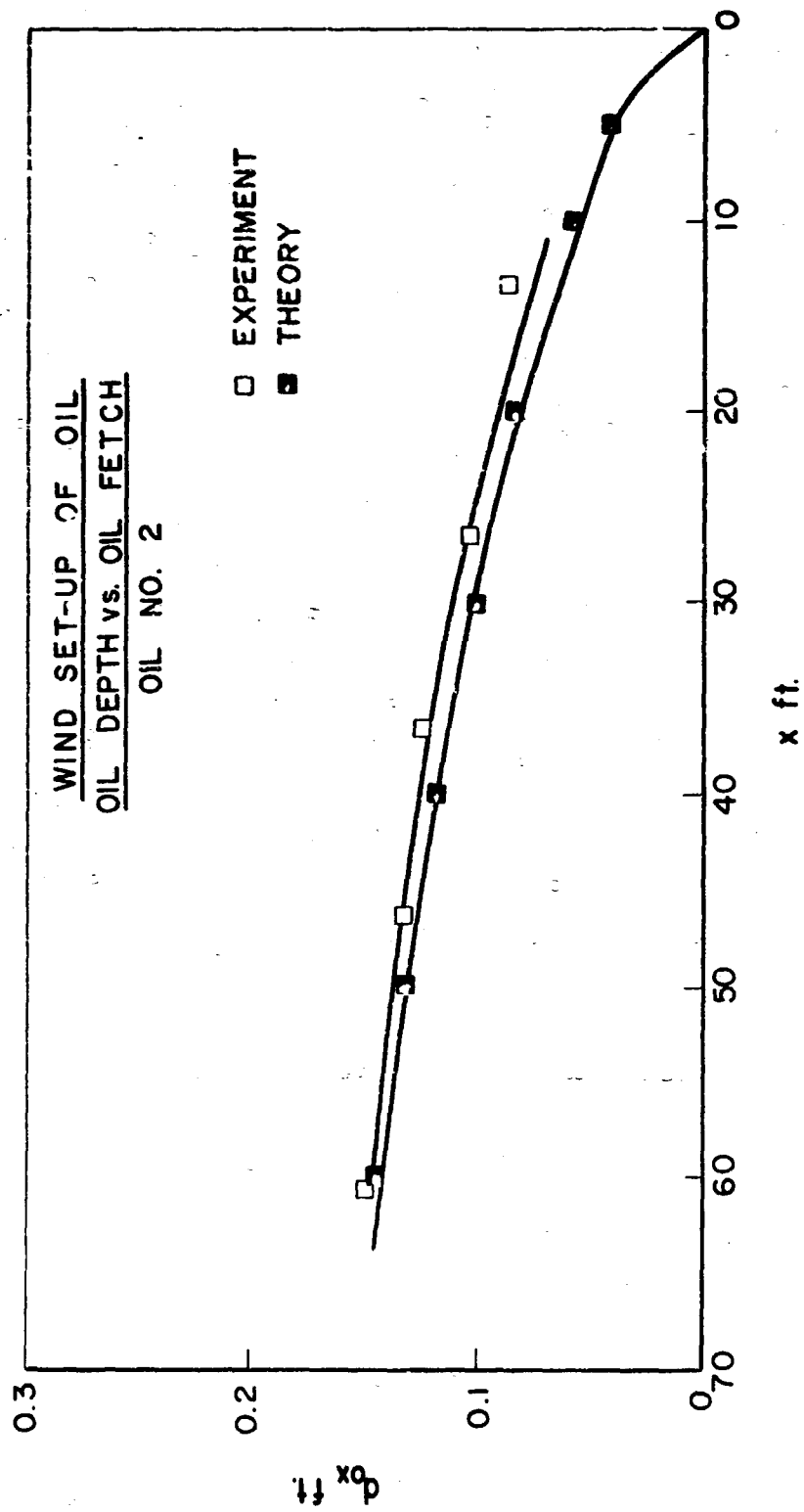


FIG. VI-17

2. Oil Set-Up Due to Current

Model Test Program

A test program was designed to study the set-up of oil due to current and the entrainment of the oil by the water. The bulk of the tests were conducted in the small glass-walled recirculating flume and others in the large concrete floor-flume. The number of tests conducted in the large flume were, however, limited because of the difficulty in working with large volumes of oil and in measuring set-up depth variation.

The oil set-up configuration tests were considered to be quite successful and reliable results can now be calculated. It was found, however, that set-ups could not be developed in the small flume with velocities which would produce entrainment. Thus, the small amount of results obtained came from the large concrete floor-flume. Since observation and testing in general were very difficult in this flume, the results are somewhat limited.

Experimental Studies

Experiments were conducted to study the behavior of an oil layer floating on a flowing stream of water. Specifically, experiments were designed to study the set-up due to the current and the entrainment at the water-oil interface. A discussion of the experiments carried out and the results obtained are contained in this section.

A series of tests was conducted in the small plexiglas-walled circulating flume to determine characteristics of the set-up. The length of the flume was approximately 4.5 feet and the width was approximately 7.5 inches. The depth of water was maintained at its maximum value of approximately 14.5 inches during all of the testing.

The tests were carried out by first starting the flow of water and then adding oil in front of the barrier. Once the flow was stabilized, the current velocity was measured using an Ott propeller-type flow meter. The oil set-up geometry was measured and recorded at various points along its length. A scale was held against the outside of the glass wall to measure the oil depth at various positions along the length of the layer. A plot of the oil thickness versus distance from the upstream start of the oil layer is shown in the Appendix for all of the runs made in the plexiglas-walled flume.

Although this flume had the capacity to provide large currents, it was limited to a 14.5 inch working depth. This indirectly restricted the maximum velocity of the tests because of the limitation on the maximum oil layer thickness. The oil layer tended to block the channel and thereby effectively increased the current velocity. Moreover, even for set-ups of 3.0 in. thickness, the correction for blockage due to the finite depth effect was nearly 50 percent of the set-up. Therefore, larger set-ups

not measured in this flume.

In order to conduct tests at higher velocities without the anomalies caused by the finite depth effect, tests were carried out in the large concrete floor-flume.

A section of the flume was necked down to an 18 in. width in order to increase the current velocity and still maintain a large depth. During the set-up tests conducted in this flume, the depth was maintained at 5 ft. which allowed a maximum velocity of 2.26 ft./sec.

The test procedure was like that conducted in the small recirculating flume, except for the method of measuring the oil layer depth. After the current was started, oil was allowed to flow into the channel until a sufficient amount collected in front of the barrier. The current was measured with an Ott propeller type current meter. The oil thickness was measured by use of a 3 ft. section of clear plastic tube approximately 1/4 inch inside diameter. The tube was left open on both ends and inserted very slowly into the oil surface. After the tube had been inserted beyond the oil-water interface, the upper end of the tube was sealed and it was withdrawn. The height of the oil column within the tube was then measured with an ordinary scale. The configuration of the oil layer obtained in these runs is shown in the Appendix.

When an oil layer held in place by a barrier is subjected to a current, the geometry of the layer produced is characteristic as shown in Fig. II-VI-18 as well as by the experimental data shown in the Appendix. Three separate regions of the layer may be identified wherein the resulting configuration is dependent on different mechanisms.

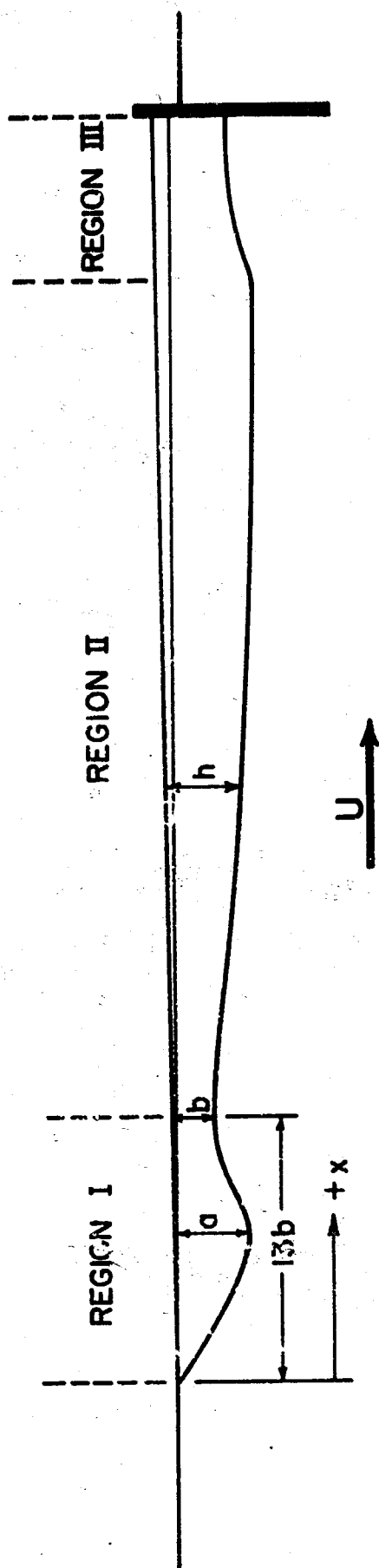


FIG. OIL SET-UP DUE TO CURRENT
II-VI-13

As a consequence of the different controlling mechanisms, it was impossible to model the complete flow phenomena at one time because Froude and Reynolds modeling cannot be obtained simultaneously. The general approach was to study the flow in parts by use of a semi-empirical theory. Once the experimental constants were evaluated, the theory was extended to prototype conditions.

Region I

The shape of the oil layer in Region I, indicated on Fig. II-VI-18 is considered to be controlled primarily by gravity and inertia forces. Accordingly, a dimensional analysis of the variables involved indicates that the single dimensionless number

$$\frac{U^2}{gb \left(1 - \frac{\rho_o}{\rho_w}\right)} = C_1 \quad \text{VI-1}$$

which is generally called the densiometric Froude number, should describe the flow, where U is the current velocity, $g = 32.2 \text{ ft/sec}^2$, and ρ_o and ρ_w are the density of the oil and water, respectively. The constant, C_1 , must be evaluated experimentally.

A second approach to the description of the head wave thickness can be obtained theoretically by application of Bernoulli's equation. Applying Bernoulli's equation between the point on the head wave at $x = h = 0$ where the velocity is zero and the point $h = b$ yields

$$\frac{P}{\rho_w g} + \frac{U^2}{2g} = b \quad (\text{VI-2})$$

P denotes the pressure at the lower edge of the layer where the thickness is b, U denotes the current velocity, and ρ_w denotes the density of the water. If, the pressure variation in the vertical direction through the oil is hydrostatic,

$$P = \rho_o g b \quad (\text{VI-3})$$

Substituting equation VI-3 into VI-2 then yields the relationship,

$$\frac{U^2}{g b \left(1 - \frac{\rho_o}{\rho_w}\right)} = 2.0 \quad (\text{VI-4})$$

Although obtained from a completely theoretical approach, equation VI-4 is identical in form to equation VI-1 and the constant has a theoretical value of 2.0.

Wicks has carried out experiments using oil on water similar to the experiments reported herein. Although he presents no experimental data, he advocates the use of the theoretical value of $C_1 = 2.0$.

A number of tests were carried out in the present research program to evaluate b as well as to determine the characteristic shape of the head wave region. A photograph of a typical head-wave profile is shown in Fig. II-VI-19. A tabulation of the velocities, oil densities and head wave thicknesses are presented in Table 1. It also may be noted in Table 1 that

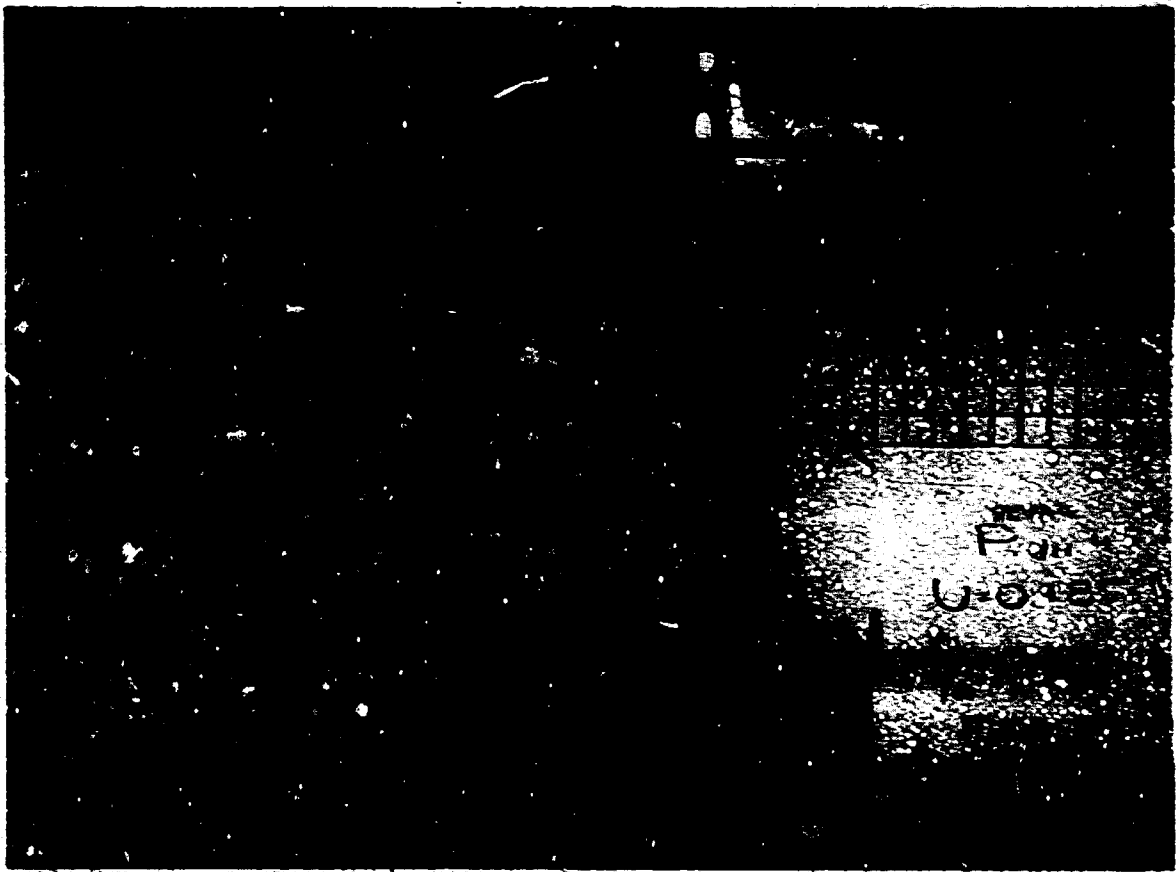


Figure II-VI-1: Oil Spill-U: See 91 Current, $\rho_0/\rho_w = 0.909$,
Current 7.5 m/s (15 mph) flow.

TABLE 1 HEAD WAVE DATA

RUN	b (ft)	U(fps)	U(fps)	ρ_o/ρ_w
			Corrected	
Small Flume # 1				
1	0.0525	0.692	0.760	0.909
2	0.1000	0.885	1.000	0.909
3	0.1500	0.985	1.200	0.909
5	0.1830	0.750	0.820	0.882
6	0.133	0.974	1.175	0.822
15	0.0125	0.348	0.353	0.904
16	0.0146	0.527	0.555	0.904
17	0.0350	0.603	0.535	0.904
18	0.1250	1.000	1.100	0.900
19	0.0834	0.782	0.880	0.900
20	0.0250	0.616	0.645	0.900
21	0.1340	1.130	1.385	0.900
22	0.171	1.153	1.550	0.900
24	0.0292	0.590	0.610	0.845
25	0.0375	0.820	0.850	0.865
26	0.0958	1.037	1.200	0.845
27	0.1500	1.263	1.540	0.845
29	0.0750	1.062	1.160	0.810
30	0.0567	1.291	1.450	0.810

31	0.1160	1.568	1.800	0.810
33	0.0330	0.947	1.000	0.825
34	0.0584	1.062	1.150	0.825
35	0.0816	1.288	1.460	0.825

Large Flume #3

58	0.117	1.456	1.456	0.900
59	0.250	1.695	1.695	0.900
60	0.333	2.261	2.261	0.900

a column labeled "U (corrected)" is tabulated for runs made in the small flume. Due to the small depth of the channel, considerable blockage occurred due to the oil layer thickness. Therefore, the velocity was corrected on the basis of the one-dimensional continuity equation using a blockage depth equal to the average value of the layer depth. A plot of the factor $gb \left(1 - \frac{\rho_o}{\rho_w}\right)$ as a function of velocity squared is shown in Fig. II-VI-20 for the experimental data corrected for the finite depth effect. As can be seen, equation VI-1 using $C_1 = 3.5$ represents a reasonable mean curve fit for the data and will be used subsequently to calculate the prototype oil set-ups due to current. Equation VI-1 is plotted in Fig. II-VI-21 to show the head wave thickness as a function of current velocity for oils of various specific gravities.

In general, the viscosity of the oil increased with density. Thus, although the test results represent a wide variation in viscosity, no consistent effect of viscosity could be detected in experimental data presented in Fig. II-VI-20.

According to the basic ideas of dimensional analysis, it may be expected that the head wave would have a characteristic's shape. That is, if the coordinates of the wave are made dimensionless with some characteristic dimension such as b , all of the wave profiles should plot on a single curve. Although considerable scatter can be expected in this kind of plot, a characteristic shape does in fact exist. Fig. II-VI-22 is a plot of the head wave profile where the coordinates are made dimensionless with the dimension b . According

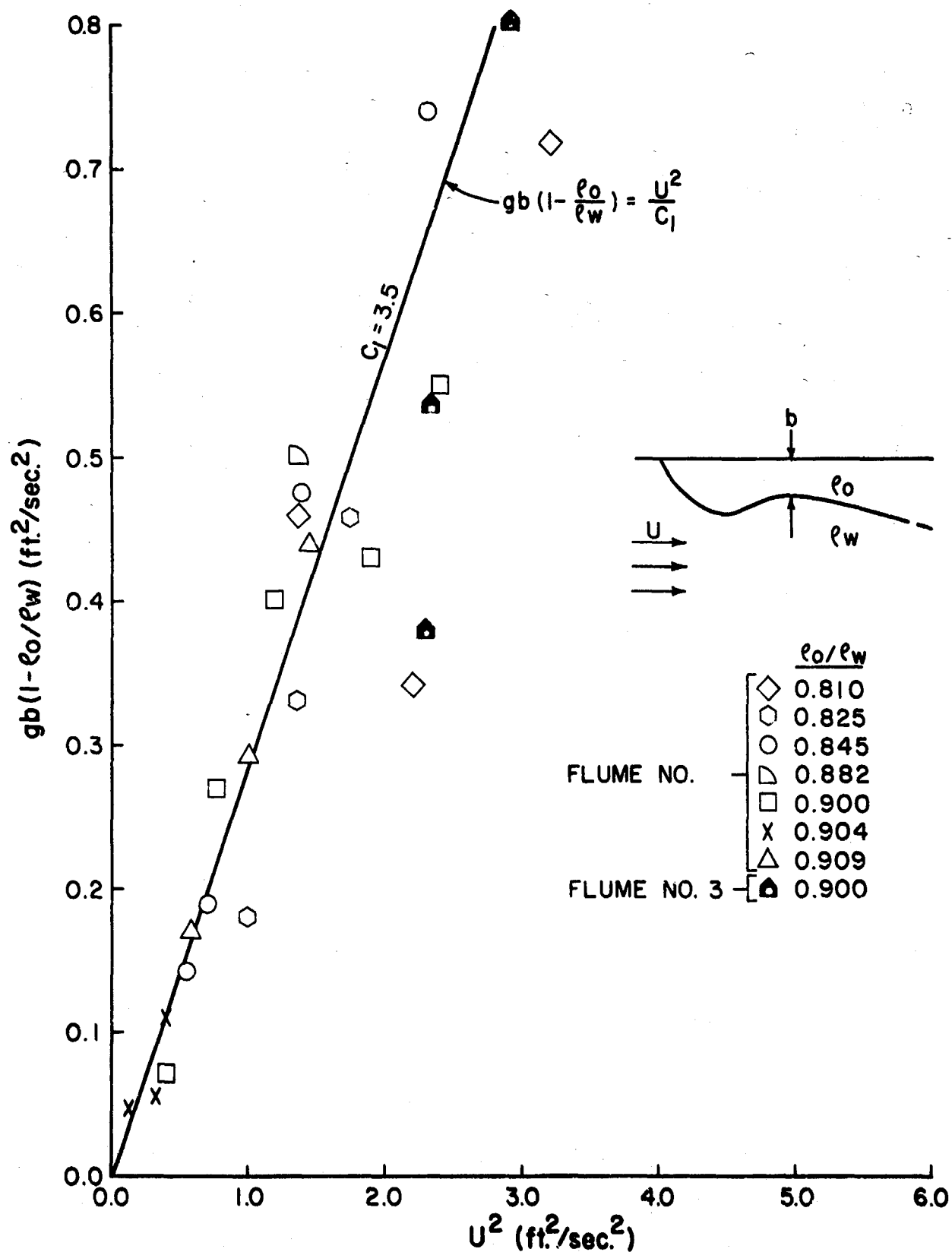


FIG. HEAD WAVE THICKNESS CORRELATION
II-VI-20

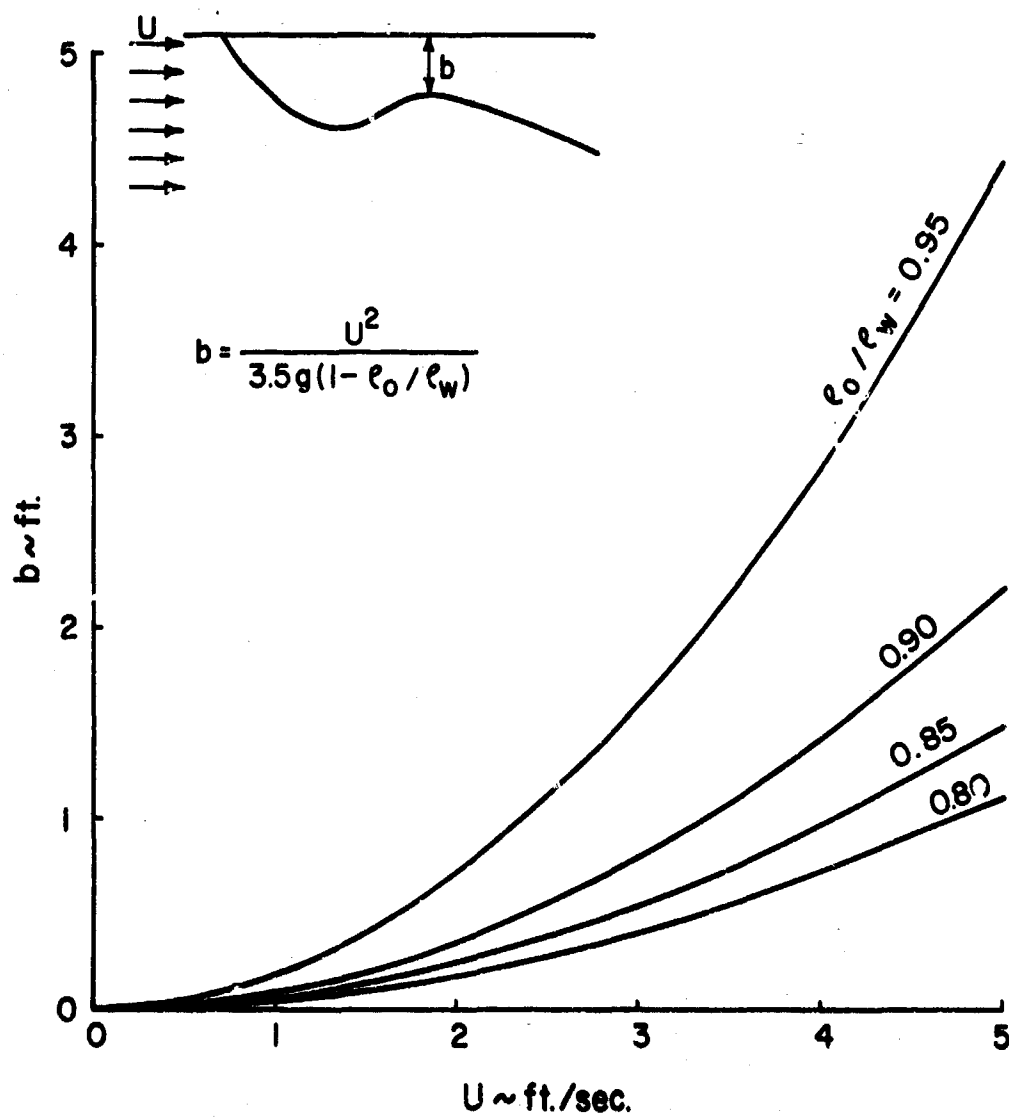


FIG. HEAD WAVE THICKNESS

II-VI-21

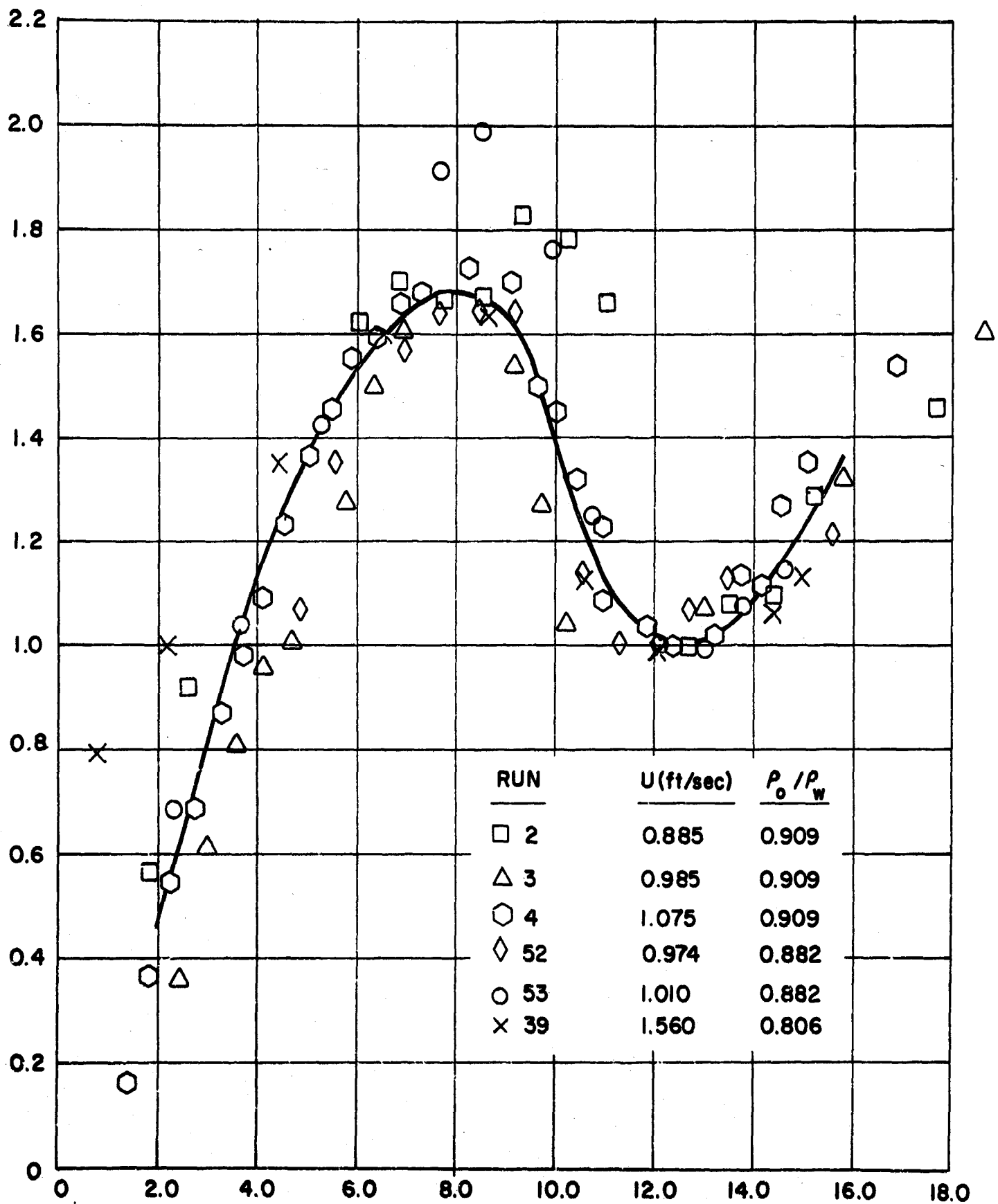


FIG. HEAD WAVE PROFILE

II-VI-22

to this figure, the neck in the wave occurs at approximately $x/b = 13$. Therefore, Region I may be considered to extend to $x = 13b$ where b is given in equation VI-1 as a function of current and oil specific gravity, ρ_o/ρ_w .

The oil lay geometry in Region I is completely defined by equation VI-1 and Fig. II-VI-22. The thickness can be obtained from equation VI-1 using $C_1 = 3.5$ (or Fig. II-VI-21) and Fig. II-VI-22. It then can be used to obtain the dimensional plot of oil depth versus distance. The head wave region is considered to extend a length of $13b$.

Region II

The flow in Region II is considered to be dependent not only on gravitational and inertia forces but also on viscous forces caused by the shear stress at the interface. The action of the water flowing under the oil layer causes a gradual build-up of the layer thickness with distance along the layer. This shearing action tends to pull the oil near the oil-water interface in the direction of the current. However, in order to maintain a steady state set-up, continuity considerations require that the oil velocity oppose the direction of the current near the air-oil interface so that the net flow across any cross section vanishes. Thus, a velocity profile similar to that shown in Fig. II-VI-23 is produced within the oil layer.

Theory - Region II

The theoretical development for the description of the

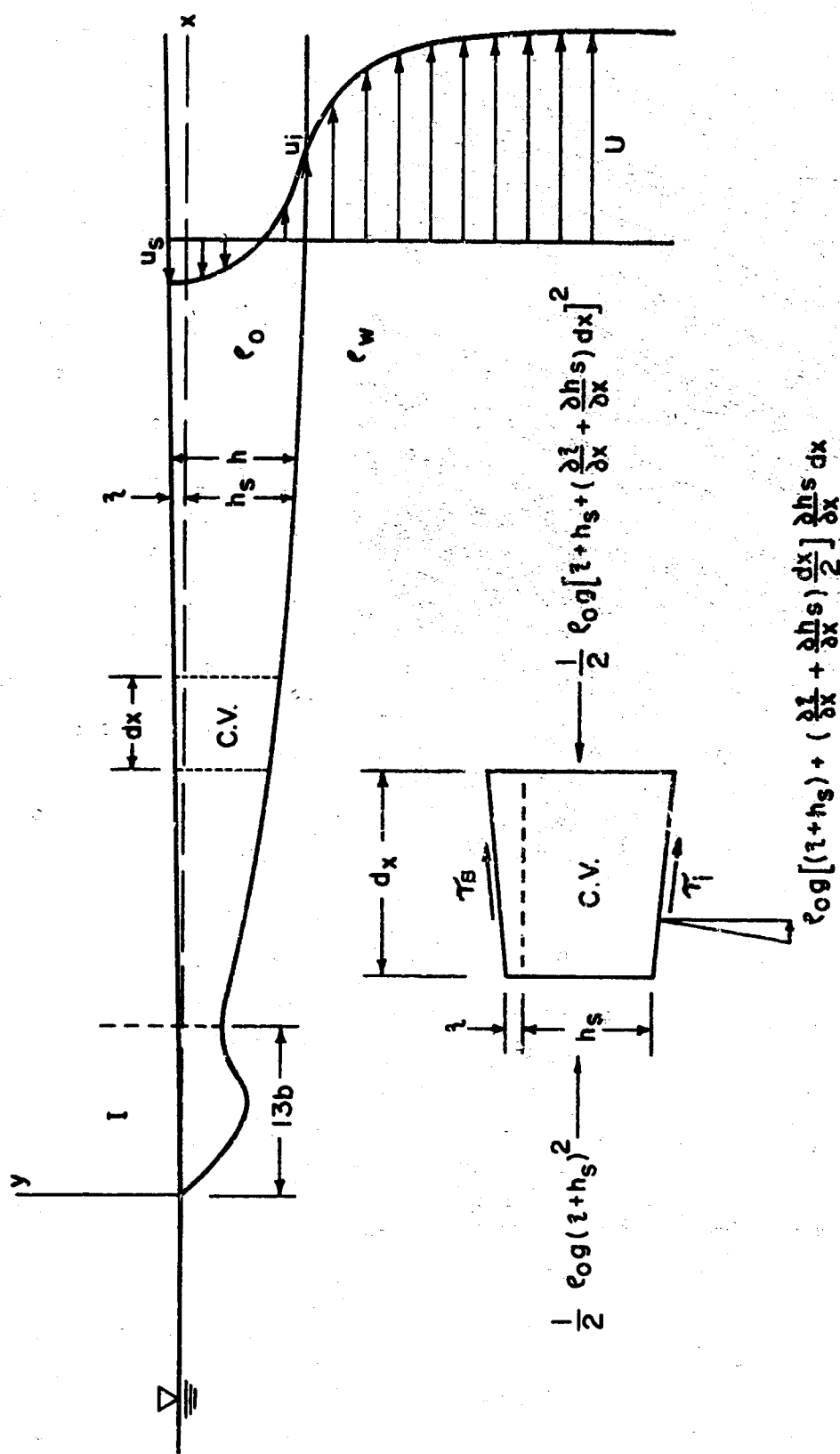


FIG. CONTROL VOLUME FOR APPLICATION
I-VI-23 OF MOMENTUM EQUATION

oil layer geometry in Region II is affected by applying the one-dimensional momentum equation to the control volume indicated in Fig. II-VI-23. The forces acting on the control volume consist of a net force due to the shear stress at both the oil-water interface and the free surface due to wind. Assuming that the pressure varies hydrostatically in the vertical direction, the forces as indicated in Fig. II-VI-23 are exerted on the ends of the control volume. Equating, then, the net force acting in the positive x - direction to the rate of increase of the momentum flux in that direction, the following relationship is obtained:

$$-\rho_o g h \frac{\partial \eta}{\partial x} + (\tau_s + \tau_i) = \frac{\partial}{\partial x} \left[\rho_o \int_{-h_s}^{\eta} u^2 dy \right] \quad (\text{VI-5})$$

where the symbols are defined in Fig. II-VI-23 and u is the local velocity which varies with both x and y.

Assuming that the pressure varies hydrostatically in the vertical direction through the oil as well as the water, $\partial \eta / \partial x$ may be written in terms of $\partial h / \partial x$ as

$$\frac{\partial \eta}{\partial x} = \left(1 - \frac{\rho_o}{\rho_w} \right) \frac{\partial h}{\partial x} \quad (\text{VI-6})$$

Substituting equation VI-6 into VI-5 gives

$$(\tau_s + \tau_i) = \frac{\partial}{\partial x} \left[\frac{1}{2} \rho_o g \left(1 - \frac{\rho_o}{\rho_w} \right) h^2 + \rho_o h u_{\eta}^2 \int_{-h_s/\eta}^{\zeta/h} (v/u_{\eta})^2 d(y/h) \right] \quad (\text{VI-7})$$

It is well known that in the case of flows where lateral variations are rapid and longitudinal variations are small, such as in the case of laminar and turbulent boundary layers and jets, the velocity profiles at different cross sections in the flow are similar. Since the flow within an oil layer is also of this type, it is reasonable to expect a similarity in velocity profiles at any cross section. Accordingly, it may be assumed that the velocity profile may be represented as

$$\frac{u}{u_{\eta}} = f(\xi) \quad (\text{VI-8})$$

where $\xi = (y+h_s)/h$. Substituting equation VI-8 into VI-7 gives

$$(\tau_s + \tau_i) = \frac{\partial}{\partial x} \left[\frac{1}{2} \rho_o g \left(1 - \frac{\rho_o}{\rho_w}\right) h^2 + \rho_o h u_{\eta}^2 \int_0^1 f^2(\xi) d\xi \right] \quad (\text{VI-9})$$

As a first approximation it is reasonable to assume that the velocity varies according to the quadratic expression,

$$\frac{u}{u_{\eta}} = f(\xi) = A + B \xi + C \xi^2 \quad (\text{VI-10})$$

Disregarding wind shear stress, τ_s , it is necessary that the slope of the velocity profile at the free surface vanish. Moreover, at the free surface $u = u_{\eta}$ and, in order that continuity be maintained, it is necessary that the net flow across any cross section vanish. These requirements can be

expressed by imposing on $f(\xi)$ the following boundary conditions:

$$f'(1) = 0 \quad (\text{VI-10a})$$

$$f(1) = 1 \quad (\text{VI-10b})$$

$$\int_0^1 f(\xi) d\xi = 0 \quad (\text{VI-10c})$$

These conditions yield the following values for the constants in equation VI-10:

$$A = -2$$

$$B = 6$$

$$C = -3$$

and, therefore, equation VI-10 becomes

$$\frac{u}{u_\eta} = f(\xi) = -2 + 6\xi - 3\xi^2 \quad (\text{VI-11})$$

Substituting equation VI-11 into equation VI-9 yields

$$\tau_1 = \frac{\partial}{\partial x} \left[\frac{1}{2} \rho_o \left(1 - \frac{\rho_o}{\rho_w} \right) gh^2 + .2\rho_o h u_1^2 \right] \quad (\text{VI-12})$$

where u_1 is the velocity of the oil-water interface and is related to the velocity at the free surface according to equation VI-11 as

$$u_1 = -2u_\eta \quad (\text{VI-13})$$

It is further expected that the velocity, u_i , at the interface would be small and, consequently, the second term in equation VI-12 can be neglected.

As a reasonable form for the shear stress at the oil-water interface, the general form of the relationship valid for a flat plate may be assumed as

$$\frac{\tau_i}{\frac{1}{2} \rho_w U^2} = C_i \left(\frac{U(x - 13b)}{\nu_w} \right)^{-1/n} \quad (\text{VI-14})$$

where C_i and n are constants having the values

$$C_i = .058$$

$$n = 5.0$$

for the case of flow past a flat plate, but for the present case, are evaluated experimentally. ν_w denotes the kinematic viscosity of the water, U denotes the current velocity and the factor $(x-13b)$ denotes the distance from the start of Region II.

Substituting equation VI-14 into equation VI-12, neglecting the second term on the right hand side of equation VI-12 and carrying out the integration with respect to x yields:

$$h = \sqrt{\frac{U^2 (x-13b)}{g \frac{\rho_o}{\rho_w} \left(1 - \frac{\rho_o}{\rho_w}\right)}} \left[\frac{C_i}{\left(\frac{U(x-13b)}{\nu_w}\right)^{1/n}} + \frac{\tau_s}{\frac{1}{2} \rho_w U^2} \right] + b^2 \quad (\text{VI-15})$$

Equation VI-15 describes the oil thickness in Region II, (i.e.), for $x \geq 13b$. The shear stress at the free surface, τ_s , is set equal to zero in the absence of wind velocity and the two parameters C_1 and n must be determined experimentally.

Model Test Results

Tests were conducted to determine the oil layer geometry due to current and thereby evaluate the parameters C_1 and n occurring in equation VI-15. The basic concept in testing was to experimentally determine the set-up shape and then adjust, by trial and error, the values of C_1 and n to make the equation fit the experimental data. As in the previous data reduction, a correction was made for the blockage effect due to the oil layer thickness. The corrected velocity was considered to be that resulting from a channel blockage equal to the average thickness of the oil layer.

The results of these experiments indicated, however, that unlike the case of a flat plate, the factor C_1 was not a constant, although n had a value of 5.0 as in the case of the flat plate. It was found that C_1 generally increased with velocity and the experimental correlation of C_1 versus U is shown in Fig. II-VI-24.

This general increase in C_1 with current velocity as indicated in Fig. II-VI-24 is, however, not unexpected. At low velocity, the interface is smooth and, as indicated, the value of C_1 appears to approach the smooth flat plate value of .058. As the velocity increases, however, the interface becomes wavelike, and it might be expected that this phenomenon would

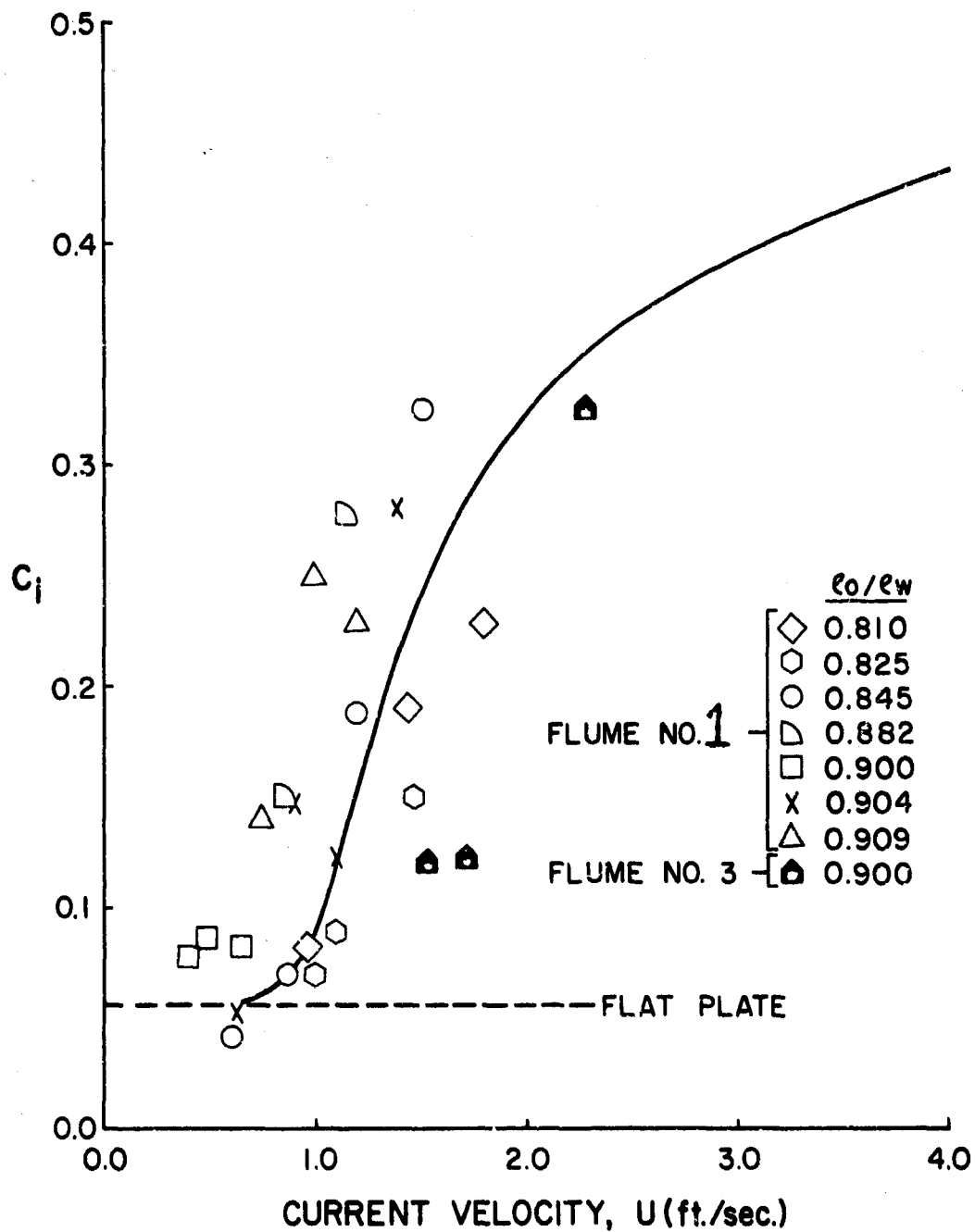


FIG. INTERFACIAL SHEAR STRESS
 II-VI-24 COEFFICIENT versus CURRENT VELOCITY
 (CORRECTED FOR DEPTH EFFECT)

tend to act as roughness and increase the shear stress coefficient. Yet, this increase in C_1 with velocity cannot continue indefinitely because eventually the interfacial waves break. Thus, although the data extended to current velocities of only 2.2 ft/sec the extrapolation of the data to higher velocities reflects this bias toward a flattening of the C_1 versus U .

It should also be noted that, in general, for the oils tested, the viscosity increased with density. However, no consistent effect of oil viscosity could be detected in the trend of the experimental data.

Prototype Set-Up Due to Current

Using the information discussed in the previous sections, the prototype oil set-up configuration due to current can be generated. Fig. II-VI-22 shows the head wave configuration made dimensionless with the head wave thickness b . The dimensional form of Region I can be obtained from this curve by simply evaluating b from equation VI-1 using $C_1 = 3.5$. In Region II the oil depth versus distance can be obtained from equation VI-15 where $n = 5.0$ and C_1 is obtained from Fig. II-VI-24.

Using this method, the oil set-up due to current for various oils has been plotted in Figs. I-II-5 through 9 of section II for $U = .5, 1.0, 1.5, 2.0$ and 2.5 knots, respectively.

Entrainment

Entrainment tests were conducted in the larger channel. The entrainment loss rate using a rigid barrier was determined by measuring the rate of movement of the head wave down the channel. This rate was combined with the average oil depth to give a volumetric loss rate. Data is shown in Table A.

TABLE A
ENTRAINMENT LOSS RATE

Specific Gravity = 0.90	Barrier Width = 18 in.
Water Velocity = 1.96 ft/sec	Average Oil Depth - 6.0 in.

Movement of Head Wave (inches)	Elapsed Time (min)
40	20
20	15
10	6

Results and Conclusions

A theoretical and experimental study has been made of the oil set-up due to current. The oil layer has been broken into two regions, a head wave region wherein the oil layer profile is controlled primarily by viscous and inertia forces, and a region where viscous effects are also important. The thickness of this layer is described by the densimetric Froude number given as equation VI-1 where C_1 was found experimentally to equal 3.5. The characteristic shape of the head wave was obtained by plotting the coordinates of the profile made dimensionless with the thickness b .

A semi-empirical theory was developed using the shear stress law for flow past a flat plate and the coefficient and exponent occurring therein were evaluated experimentally. shear stress coefficient was found to increase with velocity, and approach the limiting value of that associated with a flat plate for the case of very low velocity.

Using the results obtained from the model tests and the semi-empirical theory, the oil layer configuration was calculated and plotted for oils of various density and at prototype current velocities of .5, 1.0, 1.5, 2.0 and 2.5 knots. These results, presented in Figs. I-II-5 through 9, are one of the primary results of the present task on oil set-up by current. They show that for the case of light oils and low currents the set-up depths are quite reasonable. However, as the current and density of the oil increase the set-up depth increases quite rapidly.

3. Hydrodynamics of Pneumatics

Introduction

An air bubble released below the surface of a liquid such as water will rise to the surface because its buoyant force is greater than the combination of its fluid drag and its weight. As the bubble rises, dragging water along with it, it creates an upward flow. At the free surface, the air bubble dissipates and the upward liquid momentum is deflected and causes a surface current. If a number of small bubbles continuously flow from a submerged duct, a steady surface current can be used to oppose the potential energy of oil of a given depth. When equilibrium is established, the oil is essentially contained by the bubble-generated current. This forms the basis of the pneumatic (air) barrier for oil containment. The objective of this task was to determine the relationship between the quantity and manner of air bubbles released and the kinematics of the generated surface flows, i.e., the "hydrodynamics of pneumatics".

Literature Survey

The use of a bubble-induced surface current for wave attenuation has been proposed for many years. Fortunately, a number of laboratory scale and prototype studies are available in the

literature of the kinematics of the pneumatic system. A list of the more important publications appears as Table 1. The geometrical variables of interest are also shown in Table 1 and defined in Fig. II-VI-25 and where they first appear in this report.

Surface Currents

Taylor ²⁰ used an analogy between the hot air flow caused by heat source and the vertical current induced by the air bubbles. He found theoretically that the vertical current, V_{\max} (See Fig. II-VI-25) is related to the unit discharge rate of air, q by the following relationship:

$$V_{\max} = K (gq)^{1/3} \quad (\text{VI-16})$$

where: g = the gravity constant

K = an experimentally determined constant

The constant K was found to be about 1.9 from the hot air analogy tests. If no energy loss occurs when the flow momentum changes to the horizontal direction at the surface, then the theoretical surface velocity as determined by Taylor becomes:

$$U_{\max} = 1.9 (gq)^{1/3} \quad (\text{Theoretical}) \quad (\text{VI-17})$$

Since 1955, many experiments have been performed in the laboratory and at prototype scale to determine the constant in Equation VI-16. Those felt to be most significant have been plotted as Fig. II-VI-26 which also includes Taylor's theoreti-

Sec. II-VI:3

Table 1 LITERATURE SURVEY

NO.	TITLE	AUTHOR	PUBLICATION DATE	LABORATORY OR PROTOTYPE	H (PIPE DEPTH FEET)	D (PIPE DIAMETER INCHES)	d (ORifice DIAMETER INCHES)	S (ORifice SPACING FEET)	N (NUMBER OF PIPE MANIFOLD)	q ¹ (FLUID DISCHARGE CFS/FT)	P/h (PRESSURE)	T (DEPTH OF TANK FEET)	W (CHANNEL WIDTH FEET)
1	CURRENTS PRODUCED BY AN AIR CURRENT IN DEEP WATER	P. S. BULSON (SOUTHAMPTON)	DOCK & HARBOR AUTH. MAY 1961	PROTOTYPE	85.17 255.34	6	1/16, 1/8 1/4, 3/8		USUALLY ONE AT A TIME	0.05 TO 1.71		6 BELOW DATUM	100-150
2	EXPERIMENTAL STUDIES OF PNEUMATIC AND HYDRAULIC BREAKWATERS	STRAUD, BOWERS TANAPORE	S. A. F. T. R. NO. 25 AUG. 1959	LABORATORY	10 45		1/4, 3/8, 1/2	51	401 FEET	0.4-0.22		12 6	20 30
3	PNEUMATIC WAVE ATTENUATION FULL SCALE TANK TESTS	U. S. ARMY TRANSPORTATION RESEARCH COMP.	TRAC T. R. 50-26 DEC. 1960	PROTOTYPE	0 TO 16 INTER.	3	1/4 START 1/32	26	SINGLE OR DOUBLE	0.033 TO 0.78 SIN.	0 TO 70	PIPE CO. BOTTOM (WATER)	15.0
4	PNEUMATIC AND SIMILAN BREAKWATERS (MODEL EXPER. USING SURFACE CURRENTS)	J. T. EVANS DOCKS & INLAND W. W. SYA.	DOCK & HARBOR AUTH. DEC. 1955	LABORATORY	3		1/16	17	ONE	0.187	5 psi	4	4.0
5	REDUCTION OF SALT WATER INTRUSION THROUGH LOCKS BY PNEUMATIC BARRIERS	G. ABRAHAM & P. H. B. BURCH	DELFT HYD. LAB. PUB. NO. 28 AUG. 1942	PROTOTYPE	163.248 320	1 1/4	1/32 IN.	38		MAX. 103-05	1422 psi -57 psi	APPROX. 1/4	46-53
6	BREAKING UP WAVES BY AIR INJECTION	J. B. SCHUP	TRANS. WES. 1943 OCT. 1940	LABORATORY	0.75 TO 11	1 I.D.	3/8 & 1/2	30	ONE		MAX. 7 ATMOS.	1	24
7	FIRST TESTS ETC. JAPAN-USE PNEUMATIC BREAKWATER (I)	M. KURAHARA (1945)	U. S. CALIF. TRANS. AUG. 1956	PROTOTYPE	88.270 31.5	3	1/16 (-)	11	ONE	0.033 TO 0.19	APPROX. 2 ATMOS.	60 TO 85	OPEN SEA 300-700
8	SECOND TESTS ETC. JAPAN-USE PNEUMATIC BREAKWATER (II)	M. KURAHARA (1955-54)	U. S. CALIF. TRANS. NOV. 1956	PROTOTYPE	33.5	5	3/8 & 1/2 (-)	15	ONE	0.04 TO 0.75	APPROX. 1/4 ATMOS.	15	THREE ONEM- SIGNAL
9	ATLAS COPCO CO. (CHALMERS UNIV. - SWEDEN)	H. VERNER	1949	PROTOTYPE	30	6	1mm 0.039"	12					
10	LARGE SCALE BUBBLE BREAK WATER EXPERIMENTS-FELTHAM	P. S. BULSON	DOCK & HARBOR AUTH. OCT. 1963	PROTOTYPE	6.12 23.65	6	3/8 1/4	2 1	ONE AT A TIME	0.05, 0.04, 0.16		25	48
11	PNEUMATIC BREAKWATER	A. A. CHARLTON	BRITISH HYDRO. RESEARCH ASS. FEB. 1961	PROTOTYPE LABORATORY	2.5-1.5 5	3	1/8, 3/16, 1/4 1/8, 3/16, 1/4	2.75 4	3 AT 12' 1 TO 4	1.32 MAY 0.4-0.5		40 5	100 15
12	WAVE EXTINCTION BY PNEUMATIC BREAKWATER	A. A. CHARLTON T. Y. KONG A. V. TAYLOR	BRITISH HYDRO. RESEARCH ASS. 23-4-5 APR. 1961	LABORATORY	6.2	1/4 H	1/12 (-)	28	ONE			0.8	0.3
13	MOBILE BREAKWATER STUDIES	J. H. CARR	CAT. REPORT N-442 DEC. 1950	LABORATORY	11	2 1/2 3 1/2	0.039 0.040	15 32	1 TO 8	0.001 0.03			8
14	LABORATORY STUDIES OF PNEUMATIC BREAKWATERS	T. H. DICK & A. BROWN	QUEEN'S UNIV. C. S. RESEARCH REPORT NO. 2 JULY 1960	LABORATORY	2.75	3 1/2 IN.	3/32	74	ONE	0.1		2.75	10
	NOTE: 1. LUNGER ONE ATMOS.												

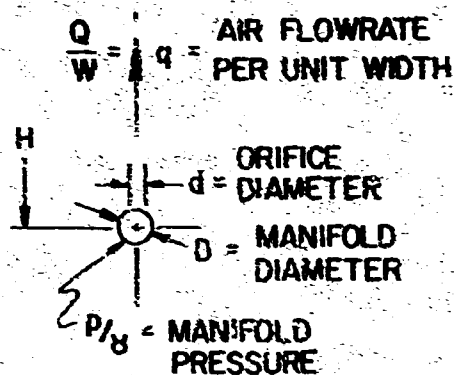
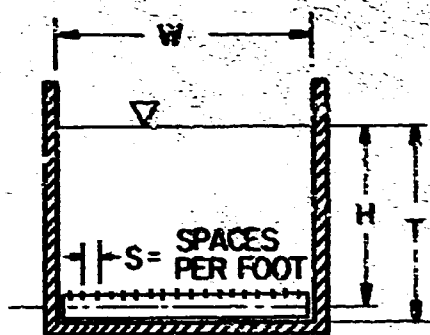
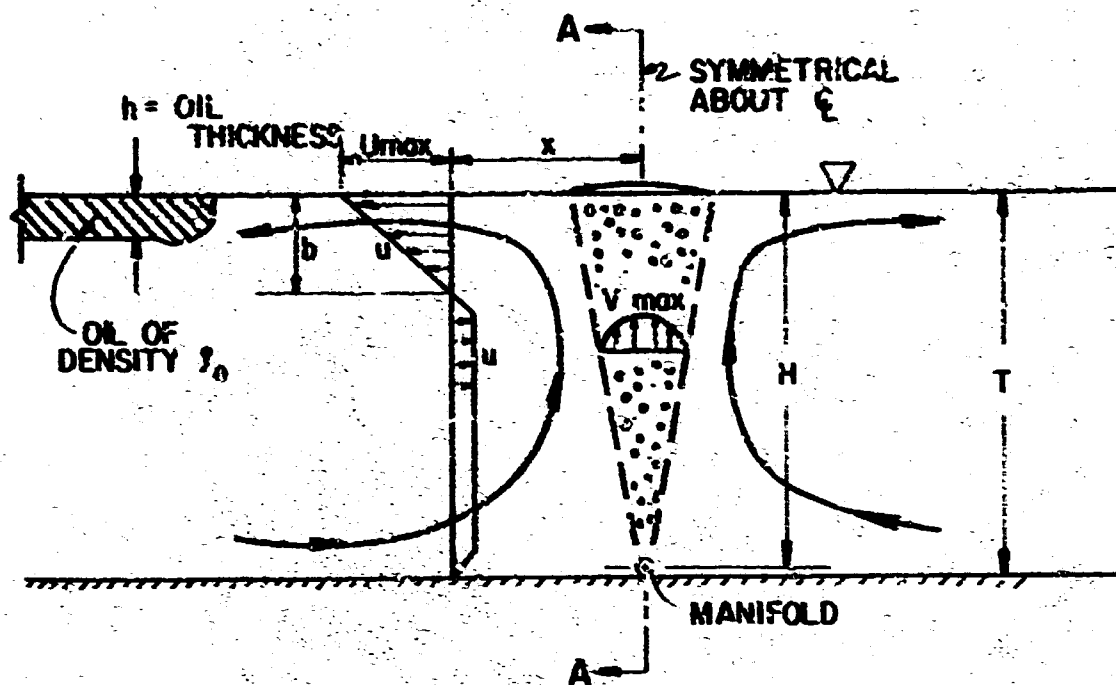


FIG. - DEFINITIONS OF GEOMETRIC, FLUID AND FLOW VARIABLES

II-VI-25

cal result. Although the general trend of all experiments is similar, there was a wide variation in K values obtained. Possible reasons for these variations are as follows:

1. Inconsistent location where U_{\max} is experimentally determined.
2. Failure of all investigators to correct test air flowrates to standard temperatures and pressures.
3. Differences in orifice size and number, i.e. variations in bubble size produced.
4. Scale effects possibly due to the depth of manifold pipe submergence.
5. Boundary effects of bottom and sides.
6. Experimental error.

Bulson (1) recognized that the volumetric air flowrate q , depended on the atmospheric pressure head, H_0 and the manifold depth H . He defined q_0 as the unit air flowrate of "free" air delivered under one atmosphere of absolute pressure head, i.e.

$$q_0 = q \left(1 + \frac{H}{H_0}\right) \quad (\text{VI-18})$$

Substituting the above in Equation (VI-16) gives

$$U_{\max} = K (gc_0)^{1/3} \left(1 + \frac{H}{H_0}\right)^{-1/3} \quad (\text{VI-19})$$

Bulson experimentally deduced K to be about 1.46. Since for laboratory tests H/H_0 is small, q_0 approximately equals q . Failure of researchers to consistently use either q or q_0 appar-

ently accounts for some of the differences in Fig. II-VI-26 and also may be responsible for some of the "scale effects" between laboratory and prototype scale tests.

Many researchers (1), (5), (9), (11), (14) have reported the decay of U_{\max} with distance from the center of bubble eruption. This is illustrated by Dick and Brebner's work (14) plotted in Fig. II-VI-26 for x/H equal to 0.5 and 1.0. Hence, those researchers that failed to specify where U_{\max} was measured negated the value of their results.

A recent report by Sjöberg and Verner¹⁵ confirmed the work at Delft (5) and by Dick and Brebner (14) and obtained a K value of approximately 1.3.

Velocity Profile Generated

All researchers essentially found that the current generated had a linear profile with depth. Taylor suggested that the distance from the surface to the point where the generated current was zero, i.e. b in Fig. II-VI-25 would be approximately $0.28H$. Sjöberg and Verner and others (5) (14) (4) suggested $0.25H$. Bulson (1) empirically determined:

$$b = 0.32 H_0 \ln \left(1 + \frac{H}{H_0} \right) \quad (\text{VI-20})$$

Surface Velocity Decay

The horizontal surface velocity, U_{\max} was found to decrease

q = AIR DISCHARGE FT³/SEC PER FOOT LENGTH OF PIPE

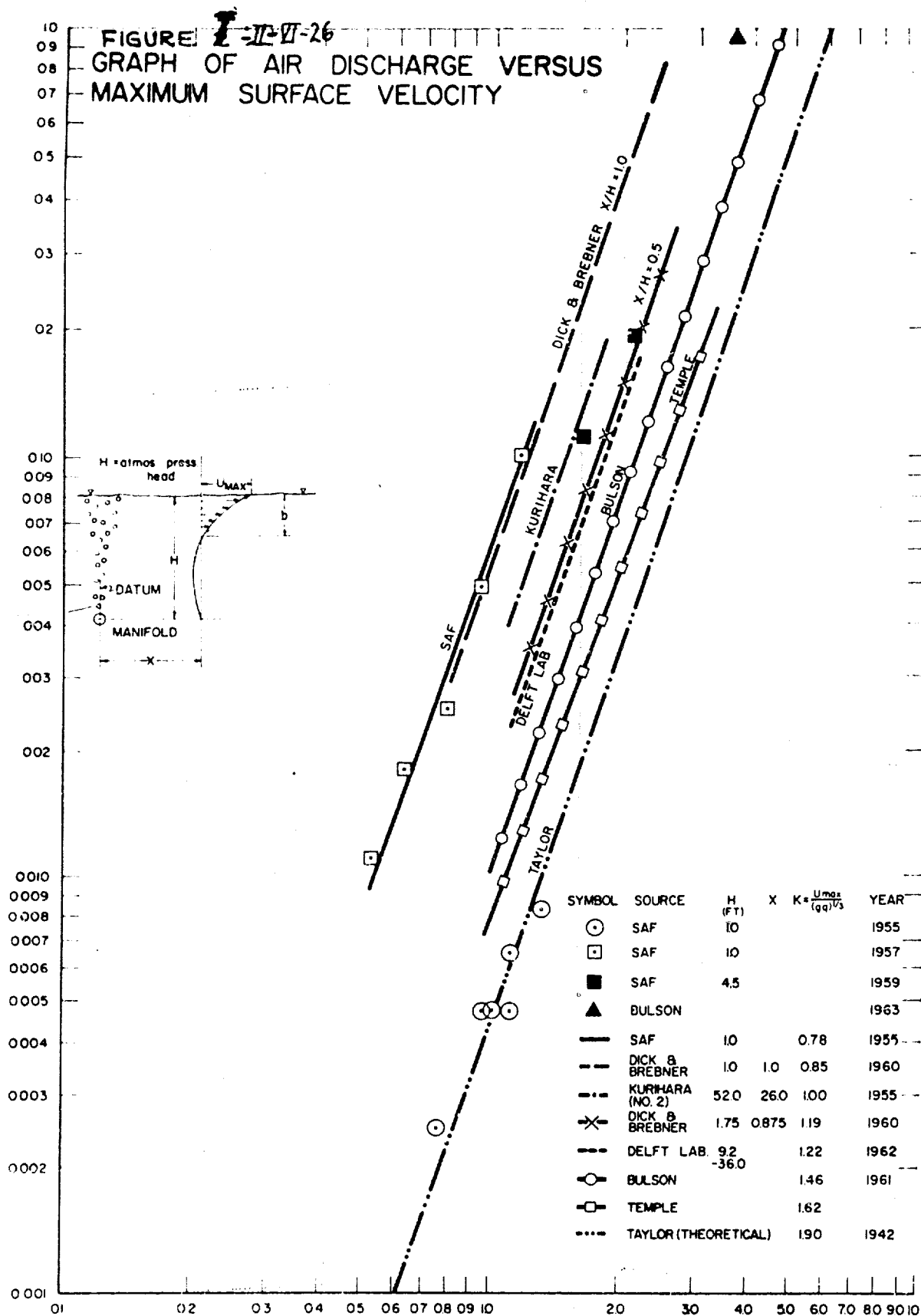


FIG. II-VI-26

U_{MAX}, MAXIMUM SURFACE VELOCITY, FT/SEC

with increased distance from the manifold centerline. Due to the eruption of air bubbles, the maximum U_{\max} usually occurred between $0.3H$ and $0.6H$ (1) (5) (14).

Miscellaneous Geometry Effects on U_{\max}

Bulson (1) reported that the orifice size and spacing based on laboratory tests showed essentially no effect on the magnitude of the surface current generated, provided the desired air discharge was uniform across the manifold. None of the articles reviewed considered the possible effects of floor boundary on the magnitude of U_{\max} produced.

EXPERIMENTAL EQUIPMENT AND PROCEDURE

The Texas A&M University (TAMU) Hydromechanics Laboratory tests were conducted in four separate flumes in order to study a wide range of water depths and test section widths. Since any water depth could be employed for the tests, the flumes have been designated by their width for this task report. All tests in the two-foot wave tank (Figure II-VI-27) and eight-inch flume (Figure II-VI-28) were conducted with a one-inch nominal diameter manifold. Tests in the deeper five-foot and 18-inch flumes used a two-inch manifold pipe. The orifice spacing was 24 holes per foot for all tests.

Bourdon type gages monitored the manifold pressures and were



FIGURE II-VI-27

INTERMEDIATE GLASS WALL FLUME (TESTS OF
PNEUMATIC BARRIER IN STAGNANT WATER)

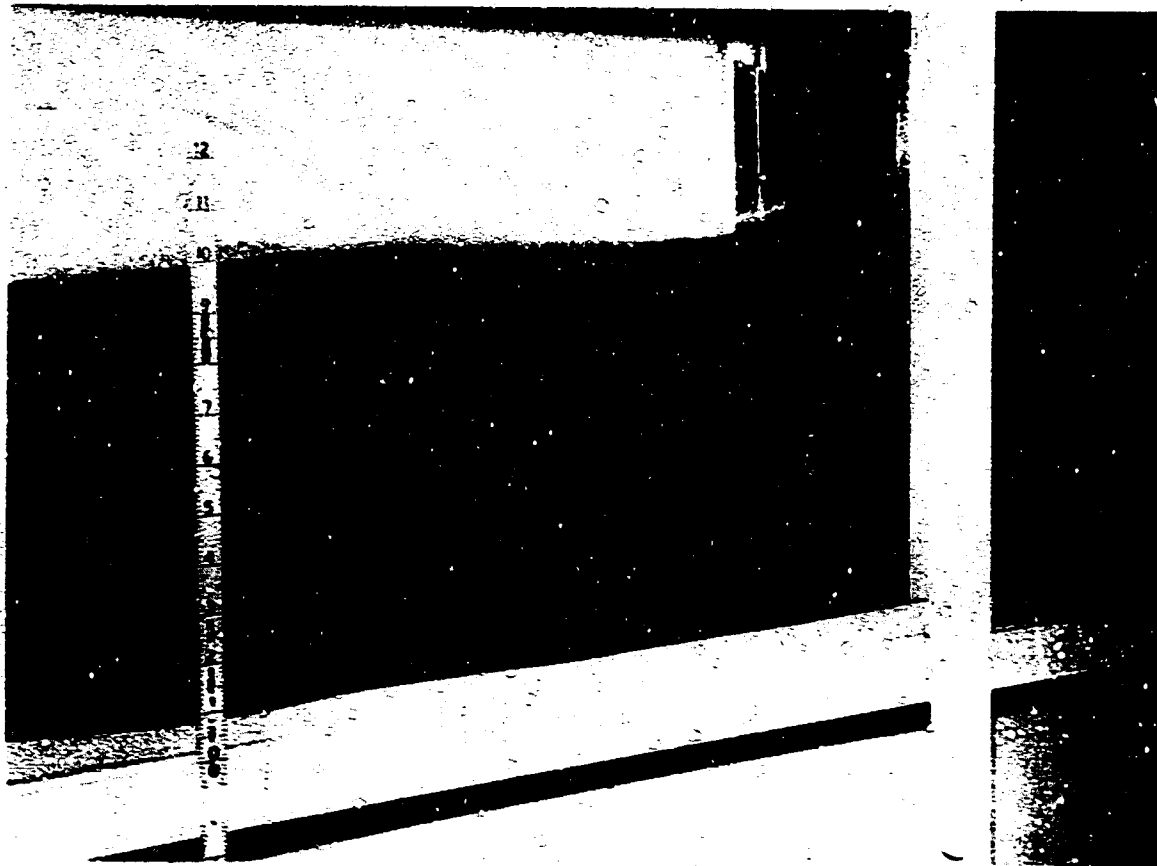


FIGURE II-VI-28

SMALL, PLEXIGLAS WALL FLUME
(TESTS OF PNEUMATIC BARRIER
IN WAVES)

located as close as possible to the manifold pipe. Laboratory and University compressors supplied the steady air flowrate which was first filtered and then metered on Fischer and Porter "rotameter" gages. In-line thermometers noted the supply temperatures (Figure II-VI-29).

All air flowrates were corrected to standard temperature (70°F) and pressure (14.7 psia) conditions. No attempt was made to correct the unit air flowrate, q to q_0 (Equation VI-18), since laboratory water depths were relatively shallow and the effects of water depths on the results were of interest in the study.

Air-water, inverted, differential manometers measured pressure differences across the pitot tube used to determine velocities in the 2-ft and 8-in flume studies. An Ott current meter was employed in the larger, deeper flume tests. Both meters are influenced by air bubbles. However, since all measurements were made outside the zone of bubble eruption, measurements were felt to be within the desired experimental accuracy.

TEST RESULTS

Surface Currents Under Stagnant Conditions

Effect of Water Depth

Figures II-VI-30, 31, 32 and II-VI-35 show experimental results of U_{max} plotted against q for four different water depths

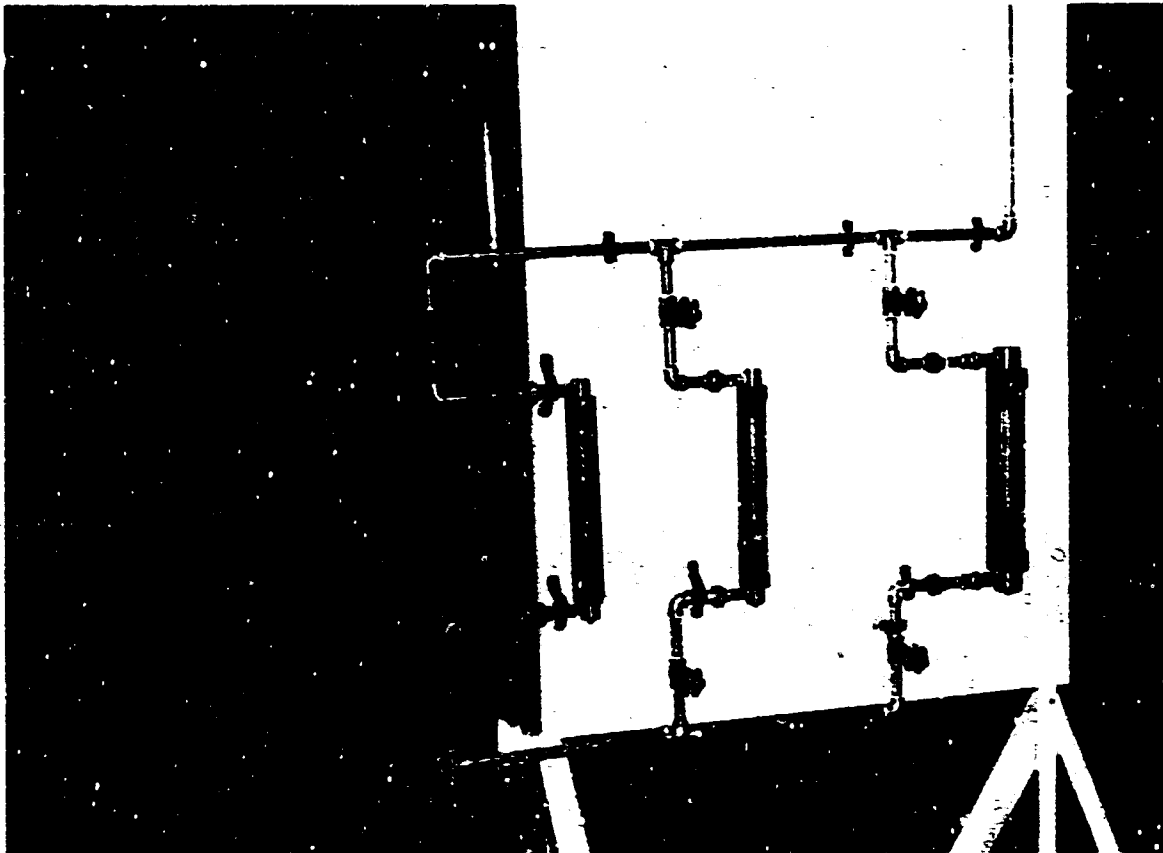


FIGURE II-VI-29

PRESSURE, TEMPERATURE AND AIR
FLOW RATE MEASUREMENT EQUIPMENT

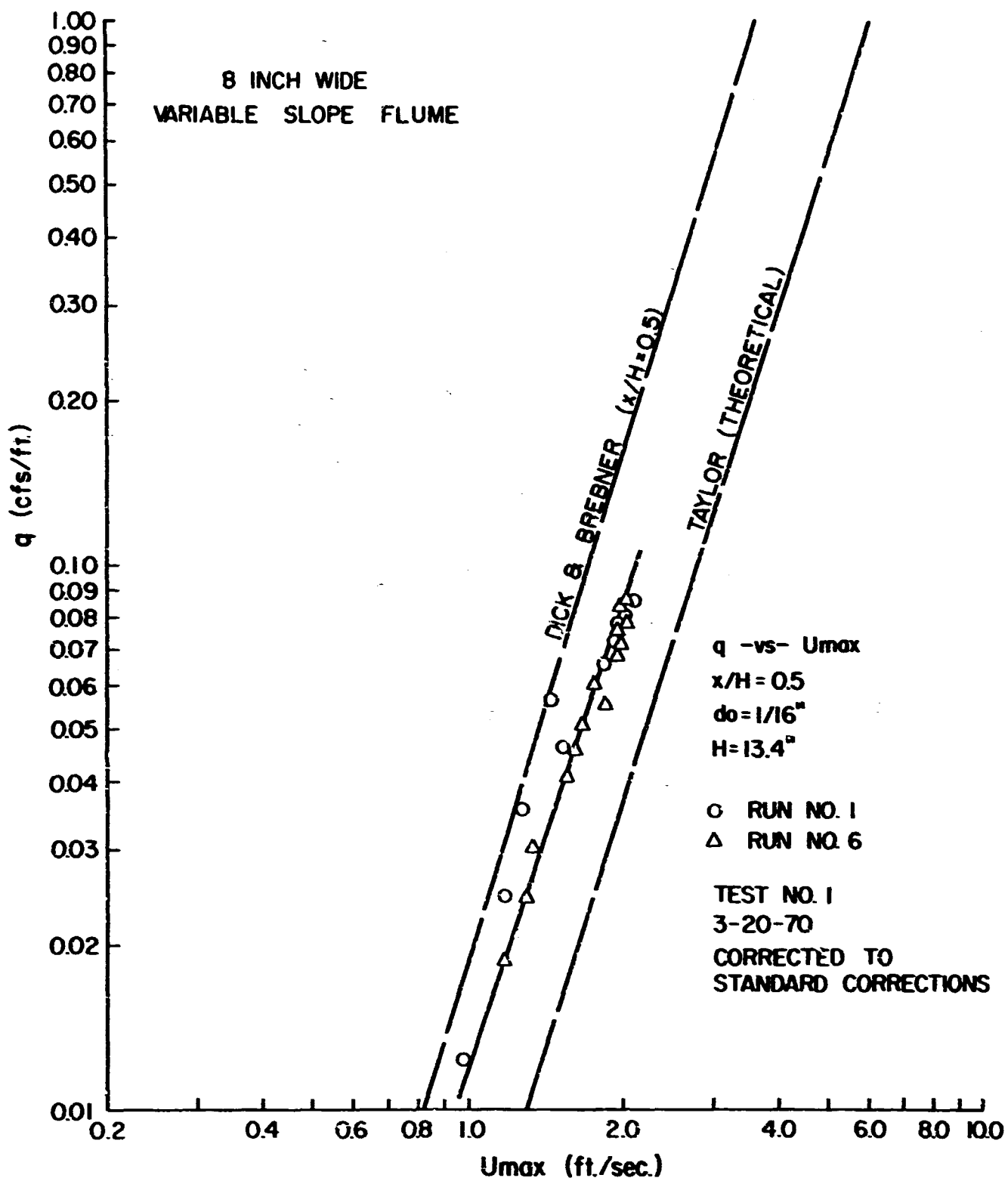


FIG. Umax versus q IN 8-INCH WIDE FLUME
II-VI-30-

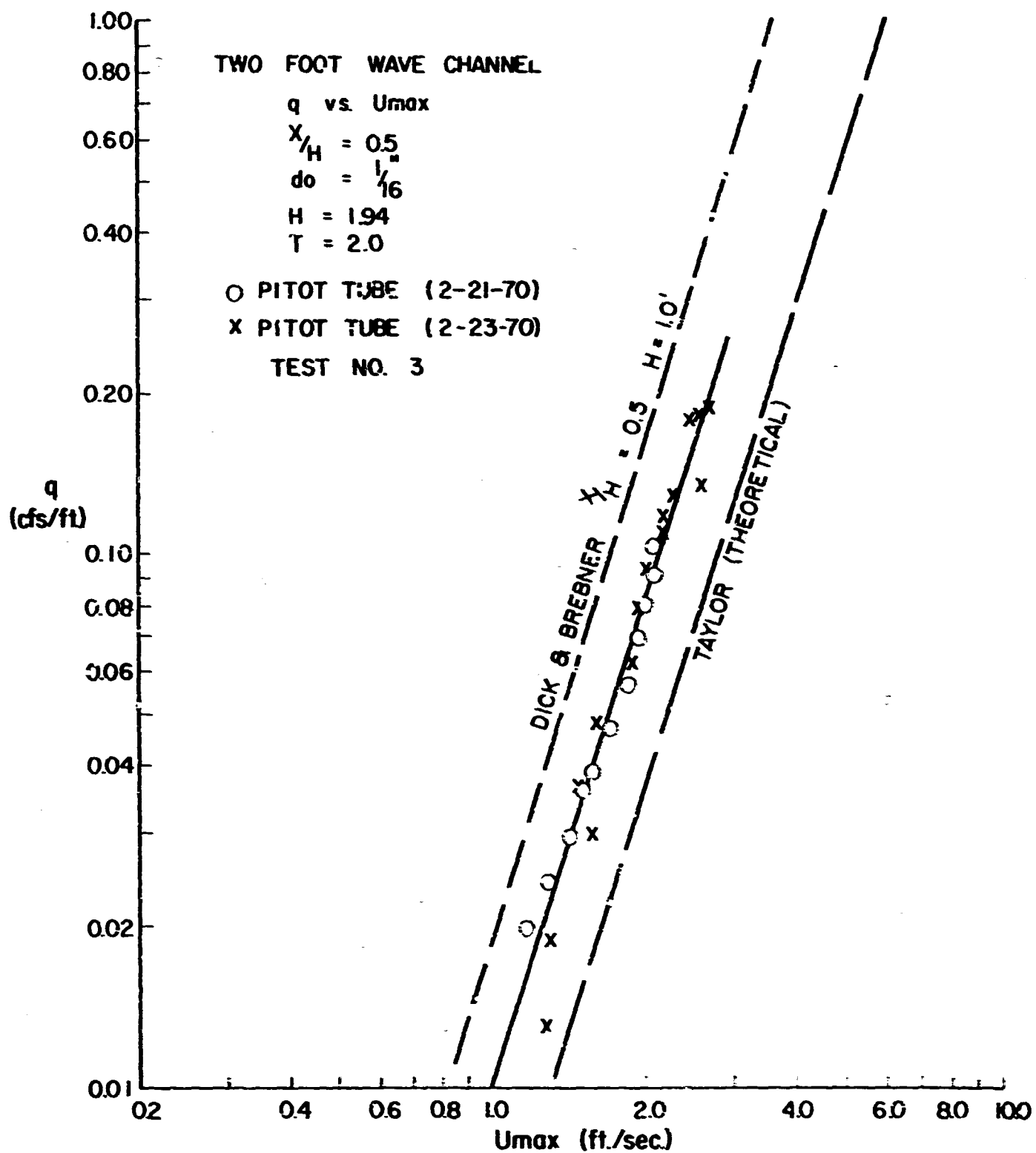


FIG. - U_{max} versus q IN TWO FOOT WAVE CHANNEL

II-VI-31

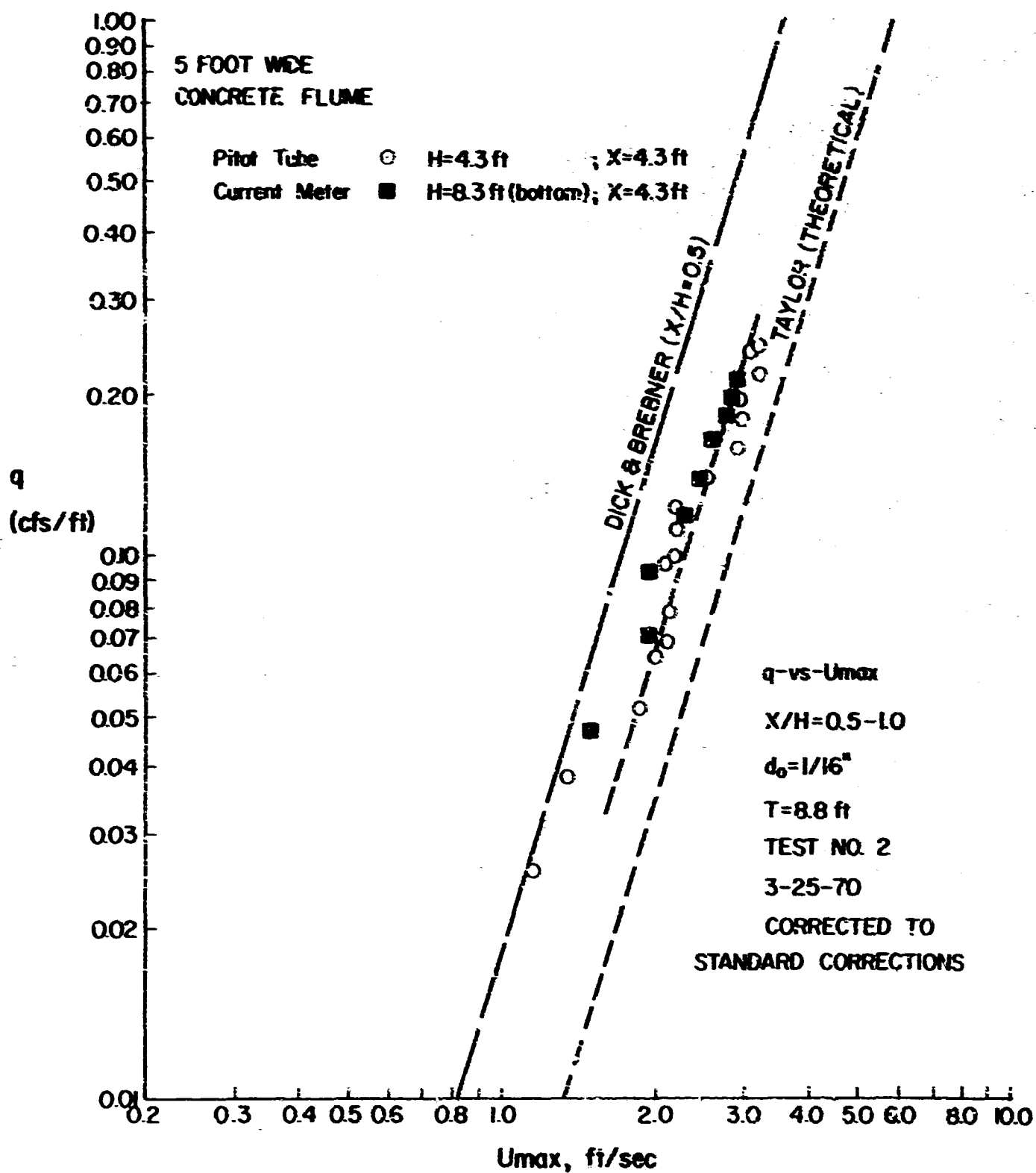


FIG. - U_{max} versus q IN 5 FOOT WIDE CONCRETE
II-VI-32- FLUME



FIGURE II-VI-33

MEASUREMENT OF SURFACE CURRENT PRODUCED
BY PNEUMATIC BARRIER IN 5 FT WIDE FLUME

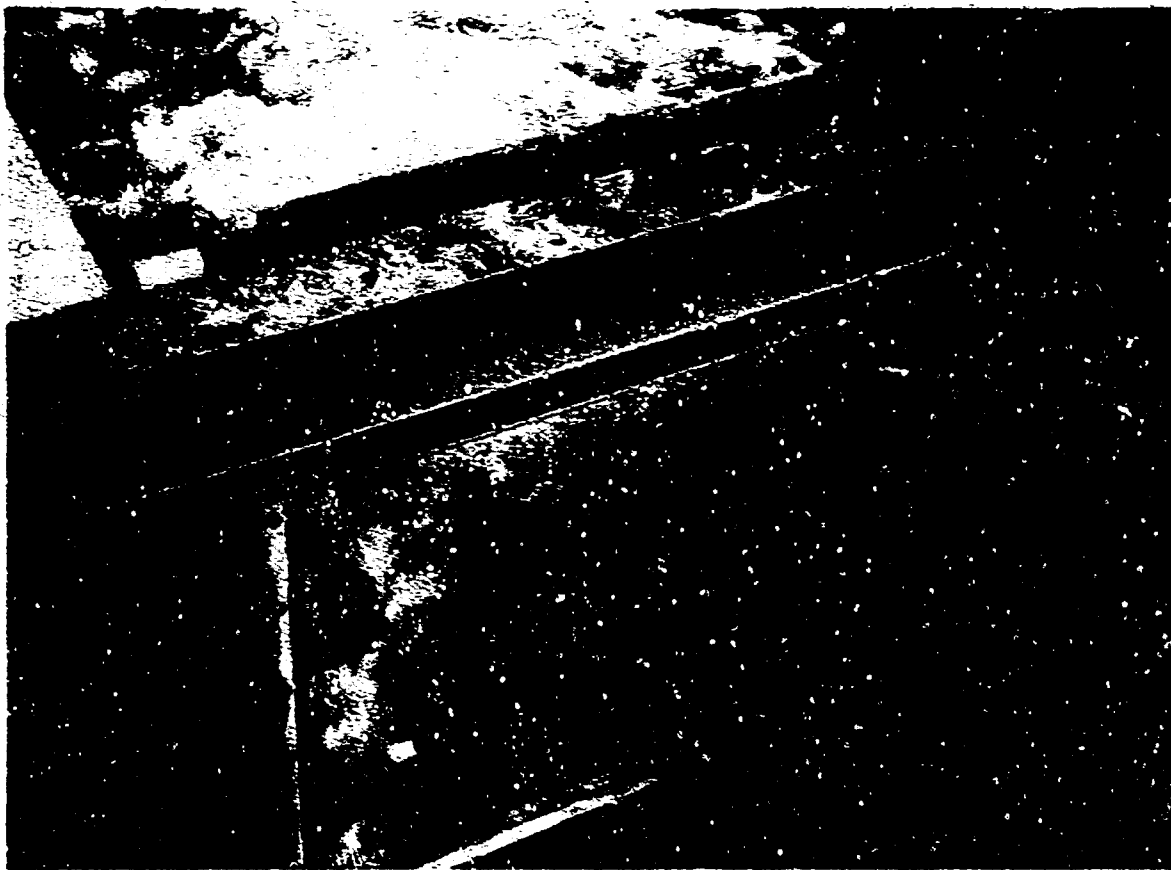


FIGURE II-VI-34

PNEUMATIC BARRIER IN OPERA-
TION IN 5 FT WIDE FLUME.

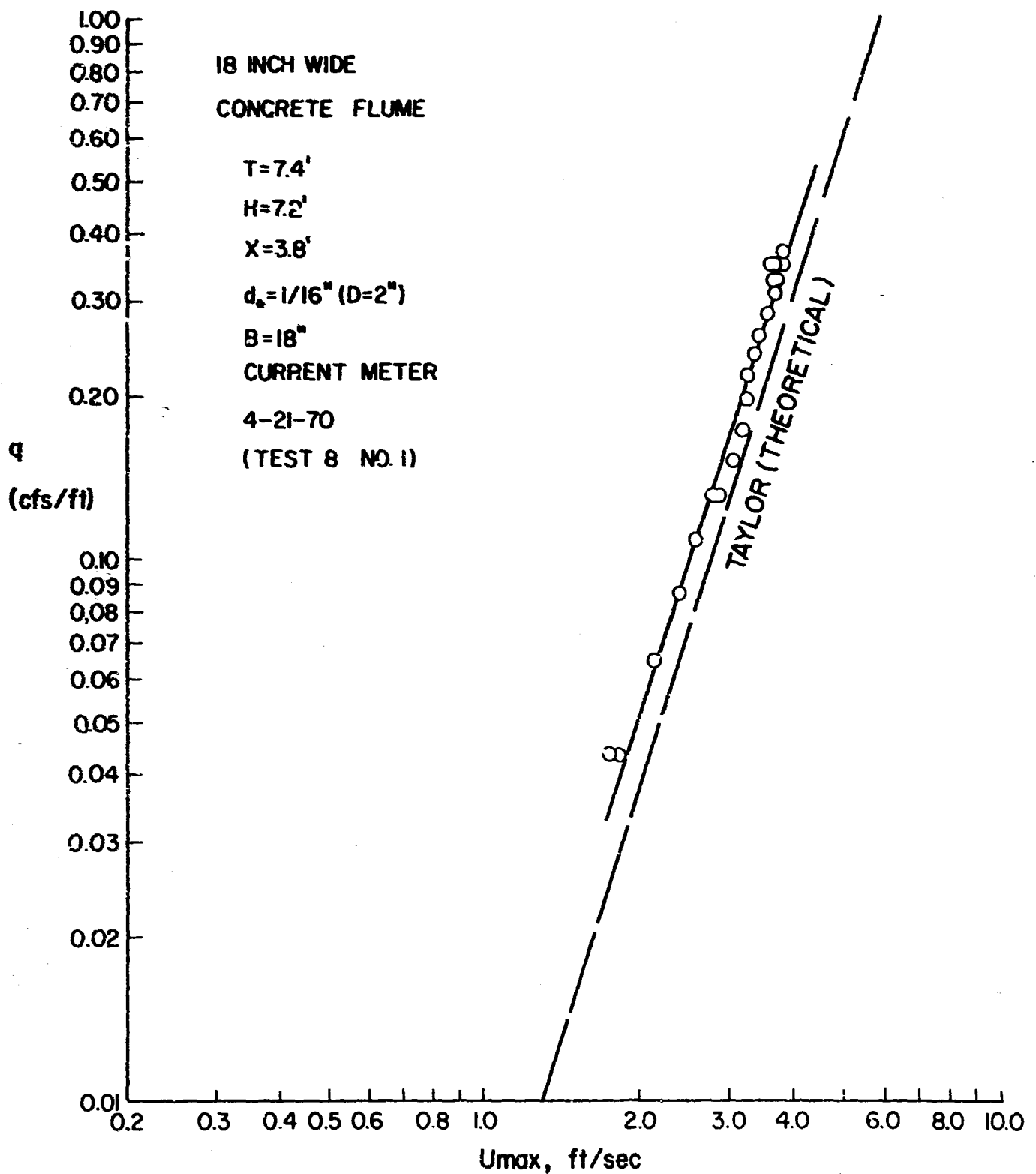


FIG. - Umax versus q IN 18 INCH WIDE
II-VI-35- TEMPORARY FLUME

tested in four different flumes. In all tests U_{\max} was measured at x/H about 0.5. The trends in all cases followed the theoretical slope and the constant K appeared to increase slightly with water depth. The one exception was in the wide 5 ft. flume when there appeared to be very little change of U_{\max} with increased manifold depth, H . (Figures II-VI-32, 33, 34). These results are summarized in Fig. II-VI-36. The narrow, 18 in. flume might possibly explain the increase in U_{\max} at this depth. Further tests at prototype depths (25 to 30 ft.) and in wide flumes are needed to clarify this point.

Effect of Orifice Size

Under identical test conditions, the size of the orifice nozzles in the manifold pipe were varied. Fig. II-VI-37 indicates a possible slight increase in the constant K with the smaller orifice tested. In many cases, however, experimental error was larger than the apparent differences noted. The manifold pressures were found to increase as hole size diminished.

Effect of Floor Boundary

In Fig. II-VI-38 the manifold is located at one-half the water depth of two feet and the results are similar to those for Diek and Brebner (14). When the water depth is lowered to one foot the results also fall in this range. (Fig. II-VI-39).

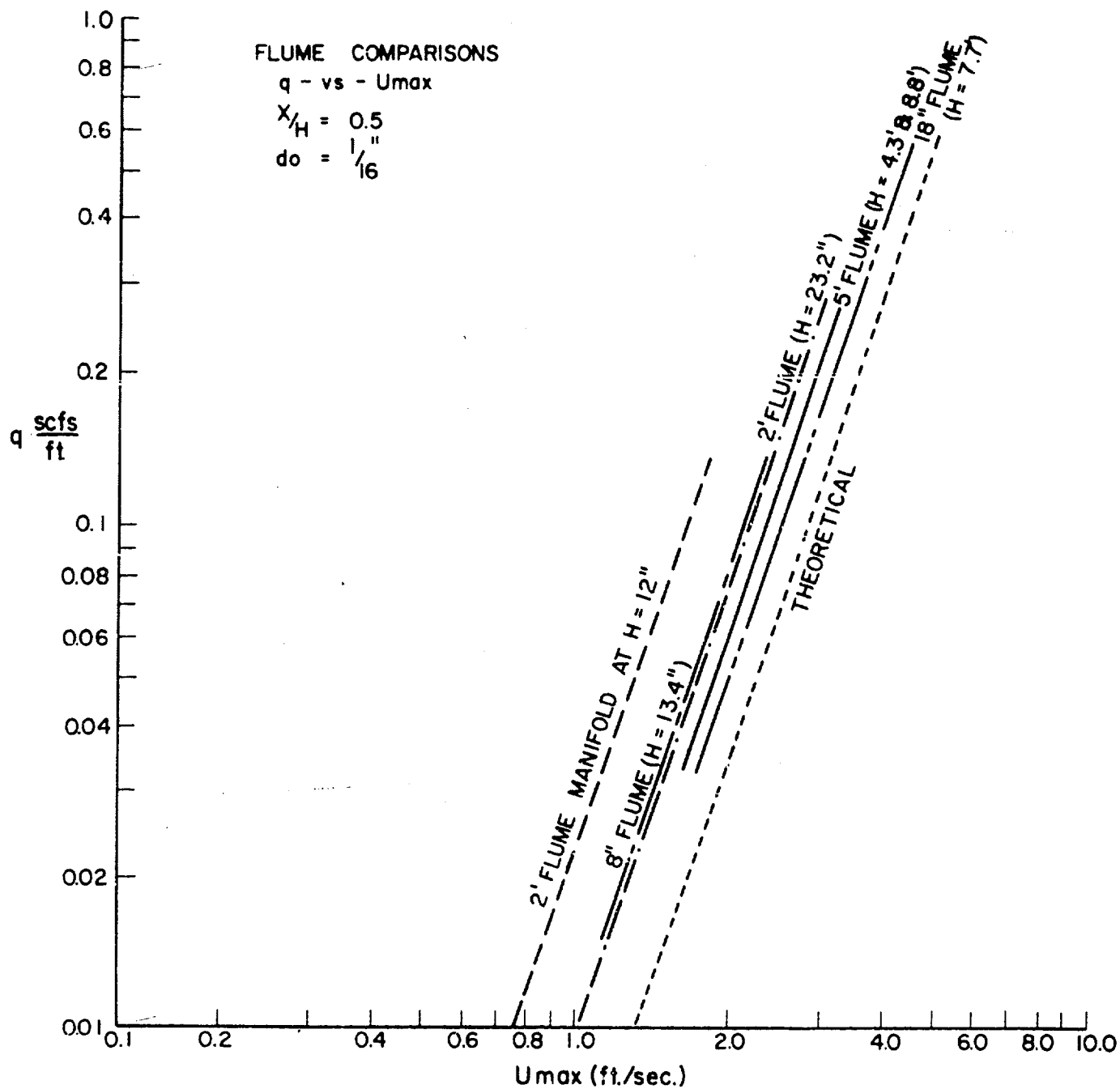


FIG. - FLUME COMPARISONS OF q versus U_{max}
 II-VI-36 - 173 -

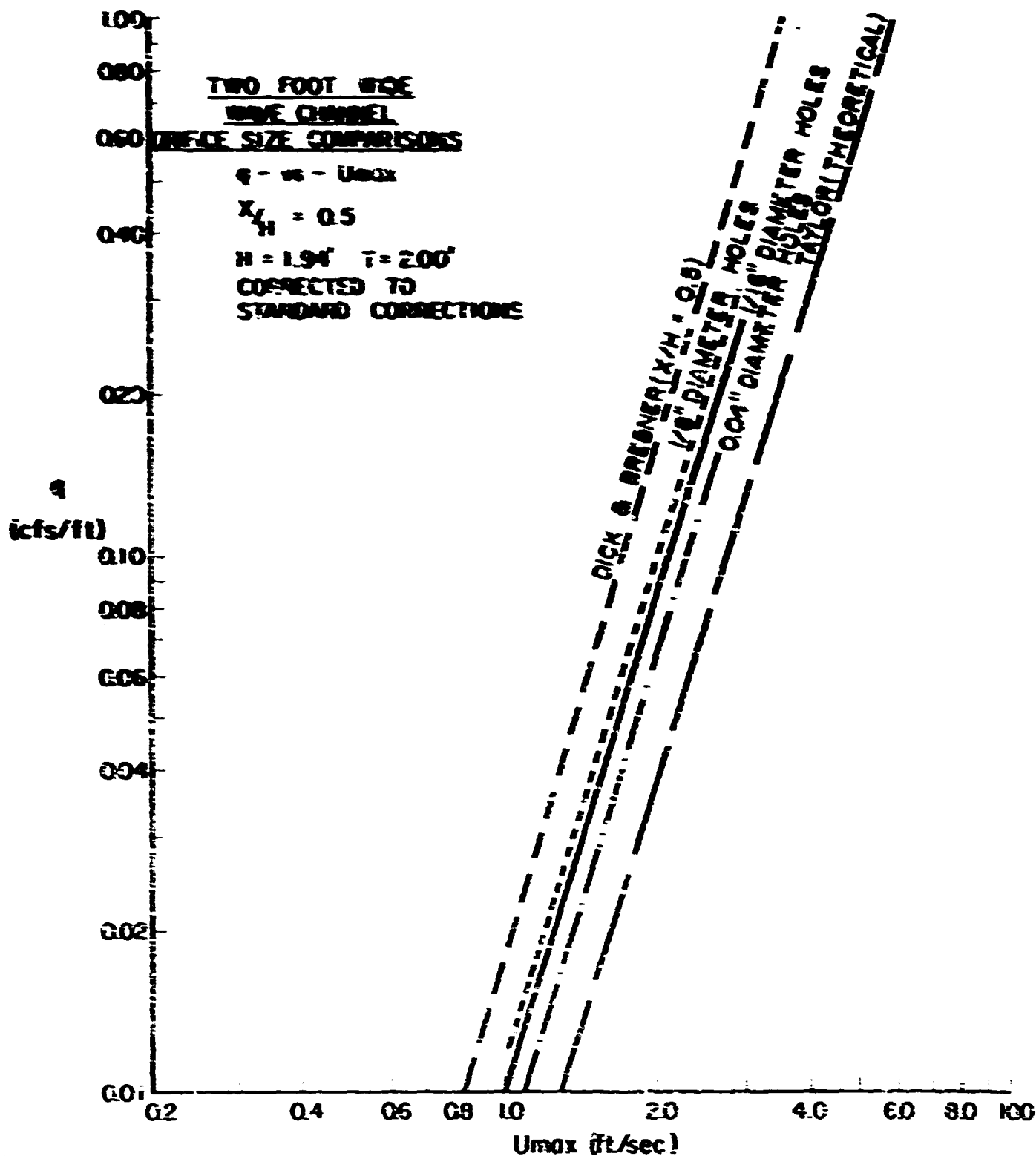


FIG. - ORIFICE SIZE COMPARISONS

11-11-37

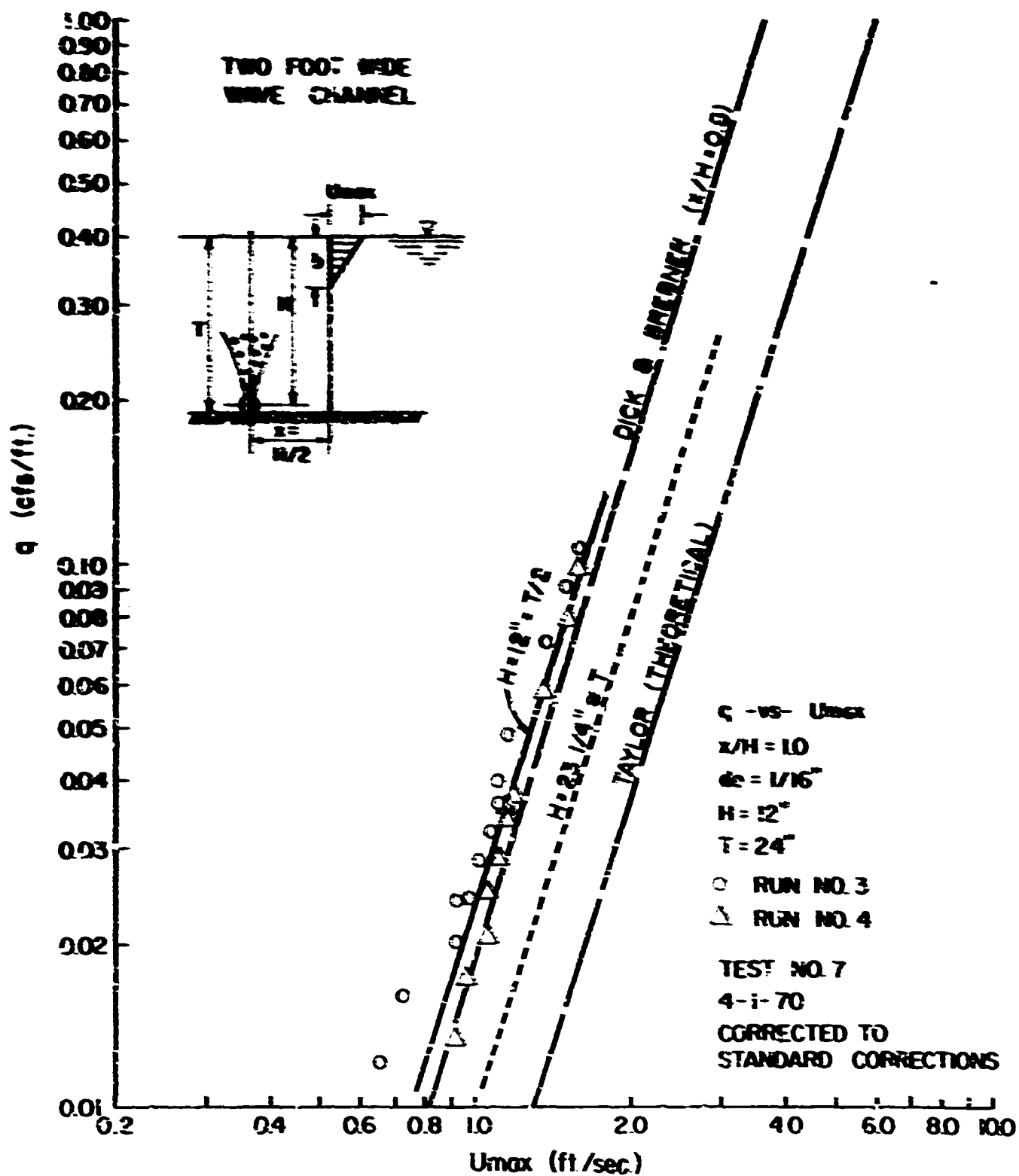


FIG. U_{max} versus q WITH $H = T/2$
II-VI-38 -

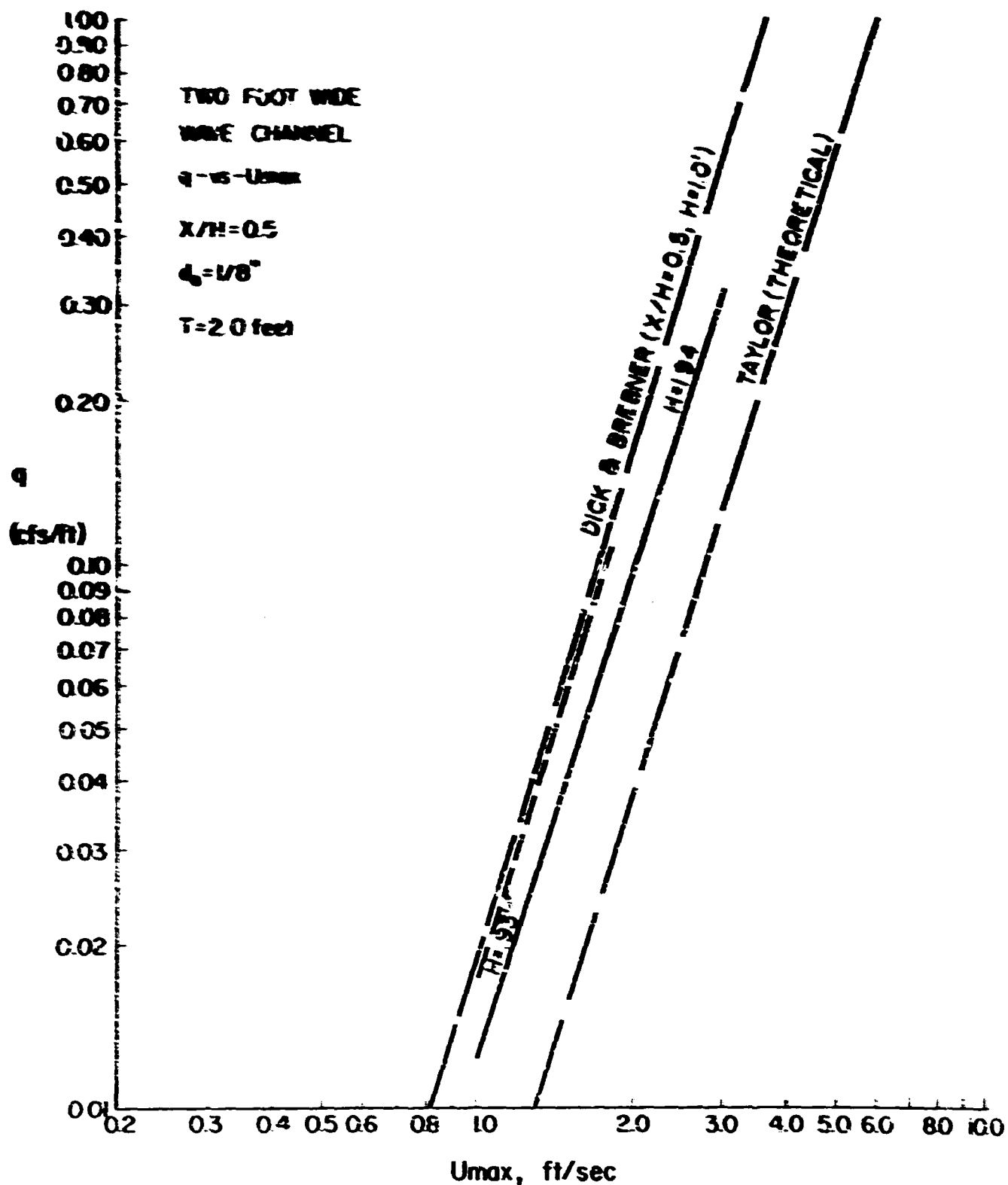


FIG. D-7-39 U_{max} versus q BOUNDARY EFFECTS

There appears to be little difference in the constant K based on these limited laboratory test results.

Summary of Surface Current Tests

In stagnant water, the results plotted in Fig. II-VI-36 for U_{\max} versus q indicate a constant K of about 1.5 which is close to that reported by Bulson (1) (10). Little change in performance was noted with variation in orifice size which is also reported by Bulson (1). The floor boundary exhibited no effects for the limited range of tests performed.

Consequently, based on these tests and those surveyed in the literature (Table 1) the following recommendations are made for preliminary design purposes of the prototype barrier.

<u>No.</u>	<u>Item</u>	<u>Remarks</u>
1	$U_{\max} = 1.5 (gq)^{1/3}$	TAMU Lab. Tests
2	Orifice Diam, $d = 1/16"$	TAMU Tests and See References (1) (5) (7) (8) (9)
3	Orifice Spacing, $S = 12/\text{ft}$	See References (7) (8) (9)
4	Manifold Pipe Diam. $D = 6"$	See References (1) (8) (9) (10) (11)
5	Manifold Pipe Depth, $H = 25 \text{ ft.}$	See References (1) (5) (7) (8) (9) (10) (11)

Surface Current Depth Profile Under Stagnant Conditions

Besides the measurement of U_{\max} at x/H equal to 0.5, for many tests a depth velocity profile was also established. Figs. II-VI-40 and II-VI-41 have been included as examples. The measured profile was approximately linear and the depth of velocity reversal, b , was approximately equal to one-quarter of the manifold depth, H . Fig. II-VI-42 summarizes the results of many tests at different air flowrates, water depths and manifold depths on a dimensionless basis. These results were consistent with those previously reported (5) (4) (14) for profiles measured at x/H about 0.5.

Decay of Surface Currents Under Stagnant Conditions

Many measurements were also taken to determine the reduction of U_{\max} as the distance from the bubble eruption increased. Fig. II-VI-43 is included as one example of the results. The decay was essentially linear with maximum surface currents found near x/H about 0.5. To facilitate a dimensionless plot, a U_{\max} at x equal to zero was established by extrapolation of each graphical plot of the results. The ratio of $U_{\max}/(U_{\max})_{x=0}$ plotted against x/H for a number of tests is presented as Fig. II-VI-44. Although a considerable amount of scatter existed, the solid line roughly indicates the trend of the results. If U_{\max} at x/H equal to 0.5 is used as reference the trend is indicated by

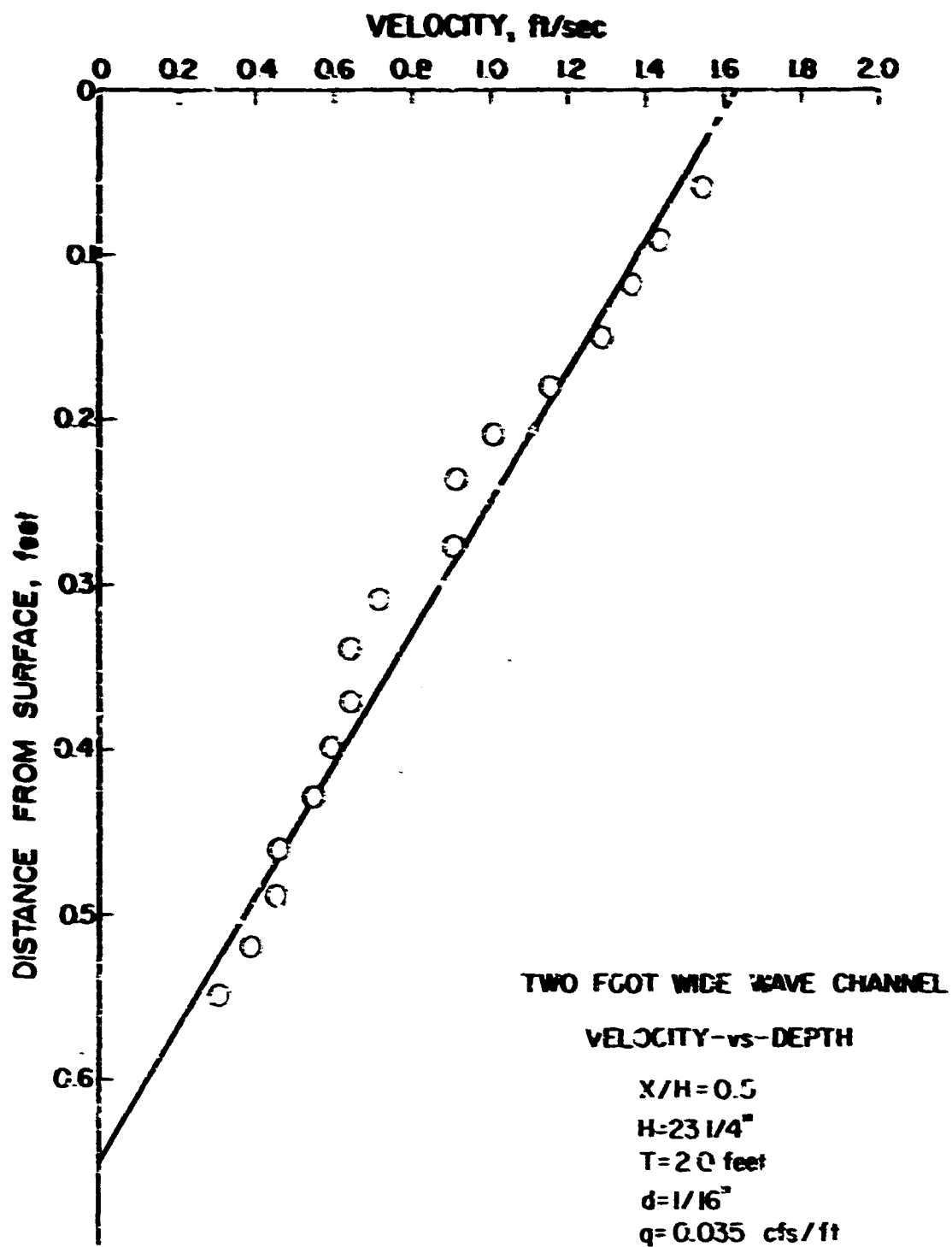


FIG. 11-10-VELOCITY versus DEPTH PROFILE TWO FOOT FLUME

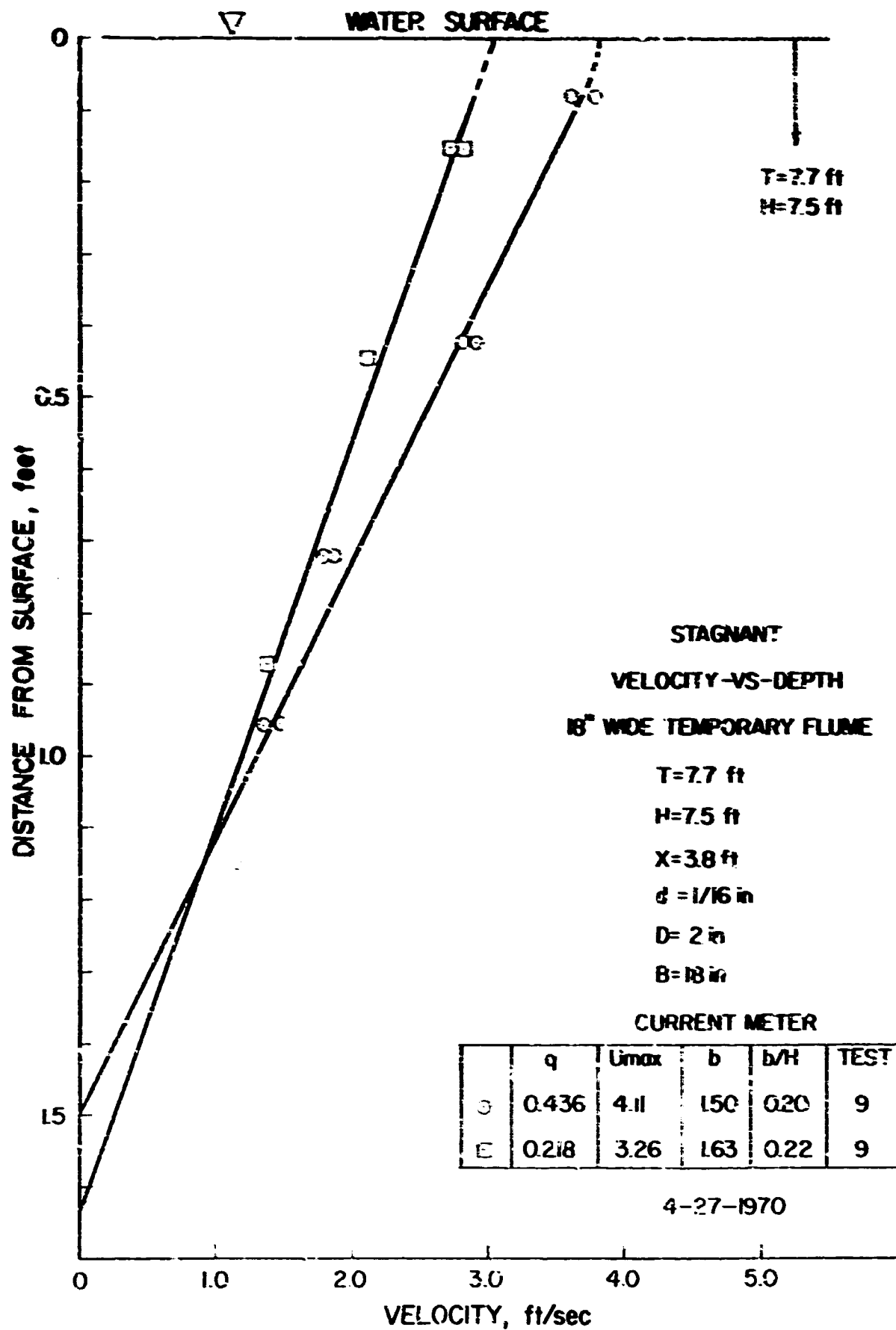


FIG. 17-4 - VELOCITY versus DEPTH PROFILE
18 INCH FLUME

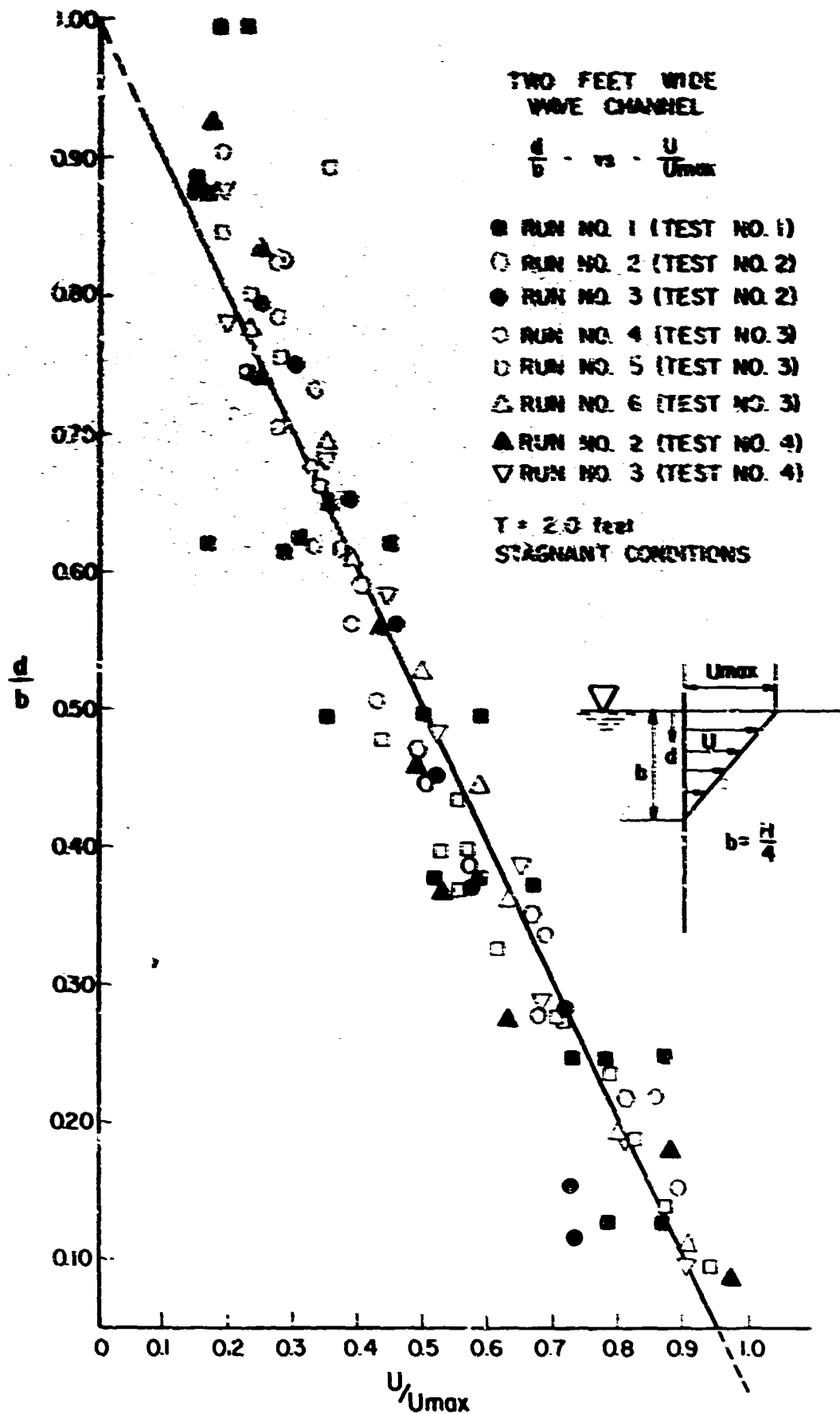


FIG. II-VI-42 - DIMENSIONLESS DEPTH PROFILE

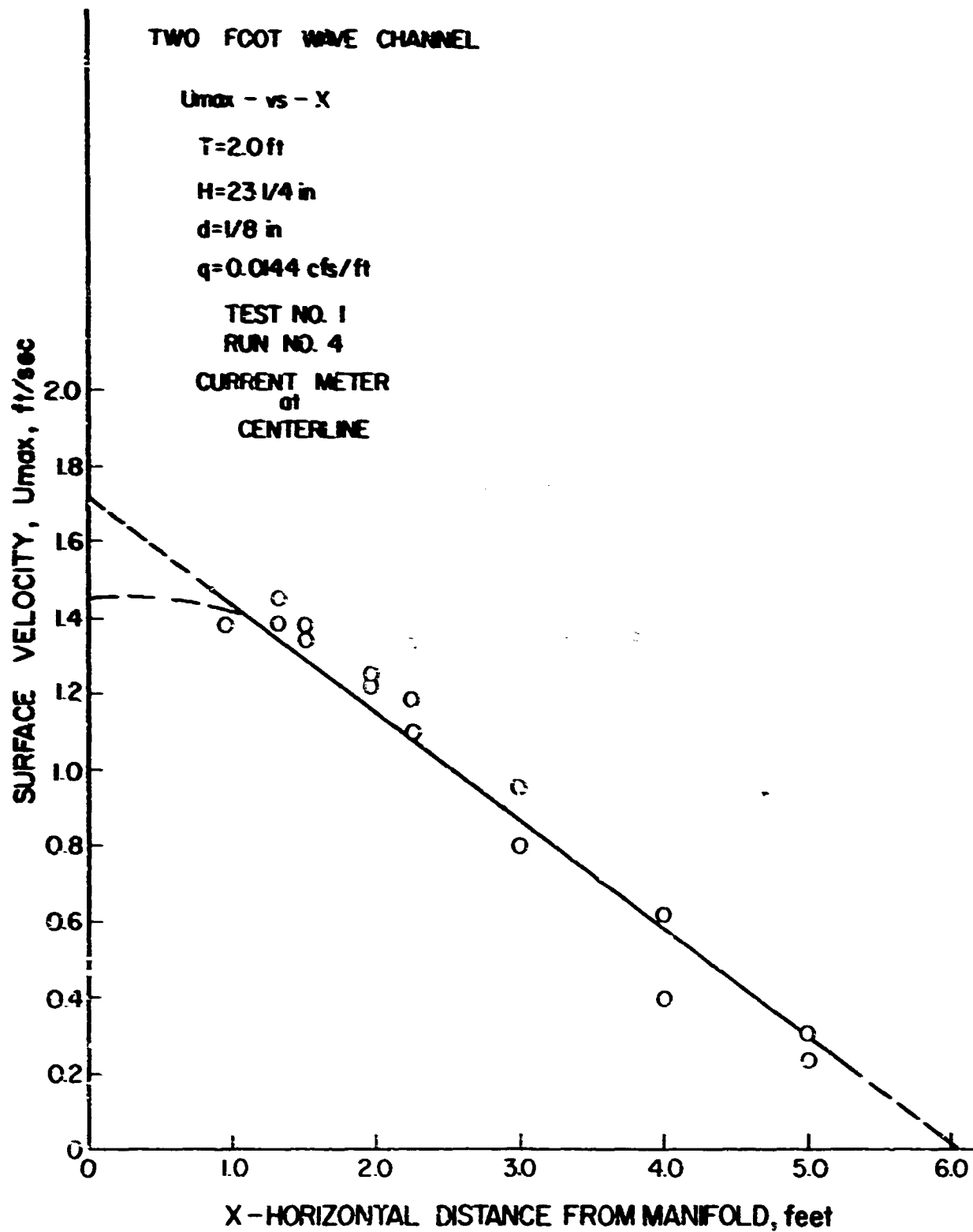


FIG. II-D-43 - TYPICAL DECAY OF U_{max} WITH X

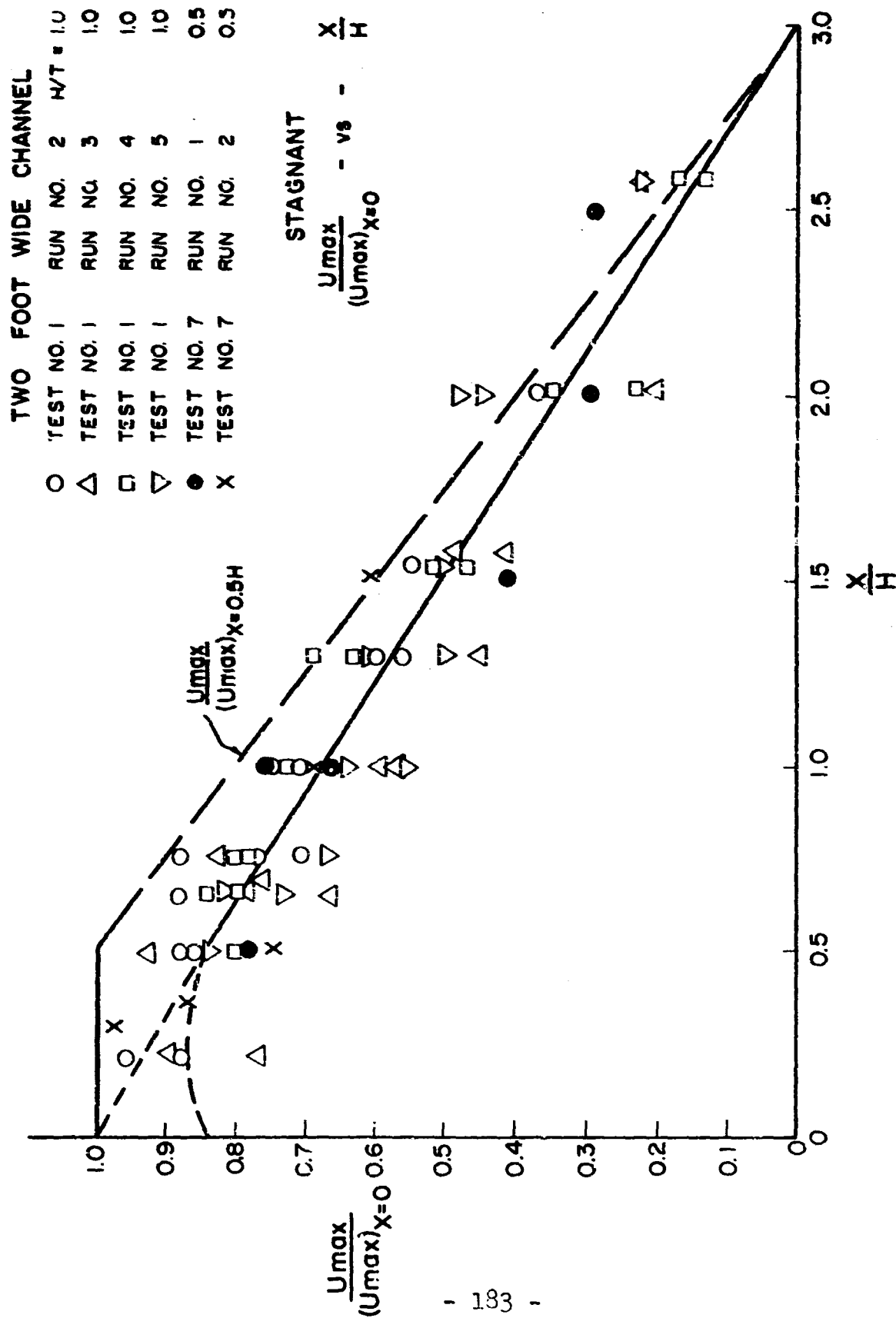


FIG. II-VI-44 - DIMENSIONLESS SURFACE VELOCITY RATIOS versus LOCATION

the dashed line of Fig. II-VI-44. The manifold location with respect to the floor boundary did not appear to be of importance.

Effect of Steady Channel Flow on Bubble Current

A steady, uniform, open channel flow added to the bubble current has been found to shift the bubble pattern downstream. Consequently, instead of the center of bubble eruption occurring directly above the submerged pipe, it occurs some distance downstream. (Figures II-VI-45, 46)

It was postulated that the individual velocity profiles of open channel flow and bubble-generated current could be linearly superimposed together. If this theoretical supposition could be experimentally proven, then the resulting combined velocity profile could be theoretically estimated for any combination of channel flow and bubble current.

Since the stagnant bubble current was symmetrical about the centerline of bubble eruption, it was hypothesized that the channel flow would decrease the upstream bubble-generated current and increase the downstream current by similar amounts. Thus the upstream decrease would be the critical case for oil containment and of most interest for this application.

Primary experimental tests were performed in the 18 in. wide flume with water depths of around 7.5 ft. (Figure II-VI-47).

Two, measured, open channel flow, velocity profiles



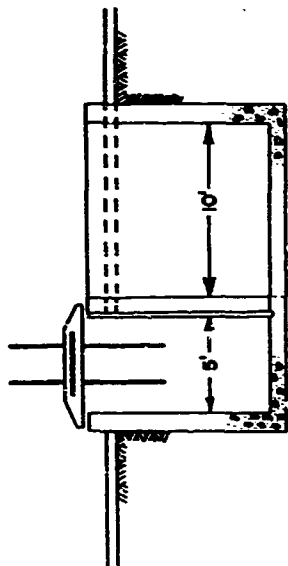
FIGURE II-VI-45

EFFECT OF STEADY CURRENT ON
PNEUMATIC BUBBLE CURTAIN



FIGURE II-VI-46

EFFECT OF STEADY CURRENT ON PNEUMATIC
BUBBLE CURTAIN. MEASUREMENT OF VELOCITIES.



CROSS SECTION AT GLASS WALL

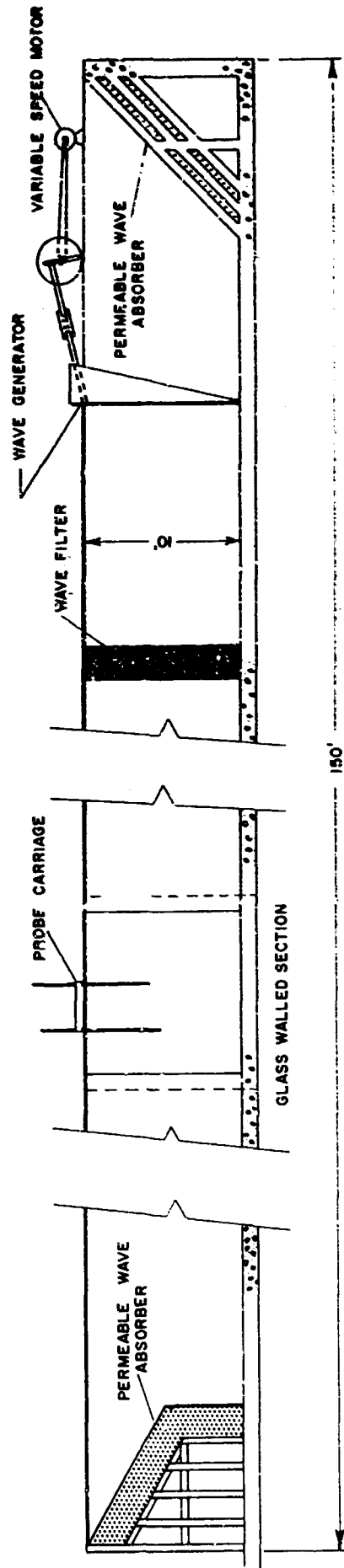


Fig. II-VI-47 5-ft wide, 10 ft deep 150 ft long
concrete flume

TEXAS A&M UNIVERSITY	
DEPARTMENT OF CIVIL ENGINEERING	
COASTAL AND OCEAN ENGINEERING DIVISION	
5'X10'X150' WAVE CHANNEL	
DRAWING NO. 4	DATE JAN 10, 1969
SCALE	
DRAWN BY:	CHECKED BY:

at the flume centerline with no bubble currents present are shown in Fig. II-VI-48. Although the profiles are characteristically non-uniform in the region of interest, where b is less than $0.25 H$ the profiles are reasonable uniform and are the tabulated mean values used for calculation purposes. The transverse profile was characteristically non-uniform due to the boundary layer so that the centerline velocity was used at the reference.

Next, an air flowrate of 0.436 cfs/ft was added in the flume which would normally create a U_{\max} of 4.1 ft/sec under stagnant conditions. Velocity profile measurements were then taken at five locations upstream of the shifted bubble eruption (Fig. II-VI-49). The characteristic linear depth profile was still present and the resulting surface current generated, U_{\max} still decayed with distance from the centerline of eruption. This test was carried out with a mean flow current V_m of about 1.78 ft./sec. present in the open channel.

With the aid of Figs. II-VI-35 and II-VI-42 the theoretical stagnant bubble-generated profiles were estimated at each location of interest and plotted as the triangular profiles in Fig. II-VI-50. Note that b was estimated as $0.25H$ or about 1.88 ft for all cases. Next, the opposing mean flow, V_m of about 1.78 ft/sec was superimposed at all locations. The resulting theoretical, surface current, U'_{\max} and depth to zero velo-

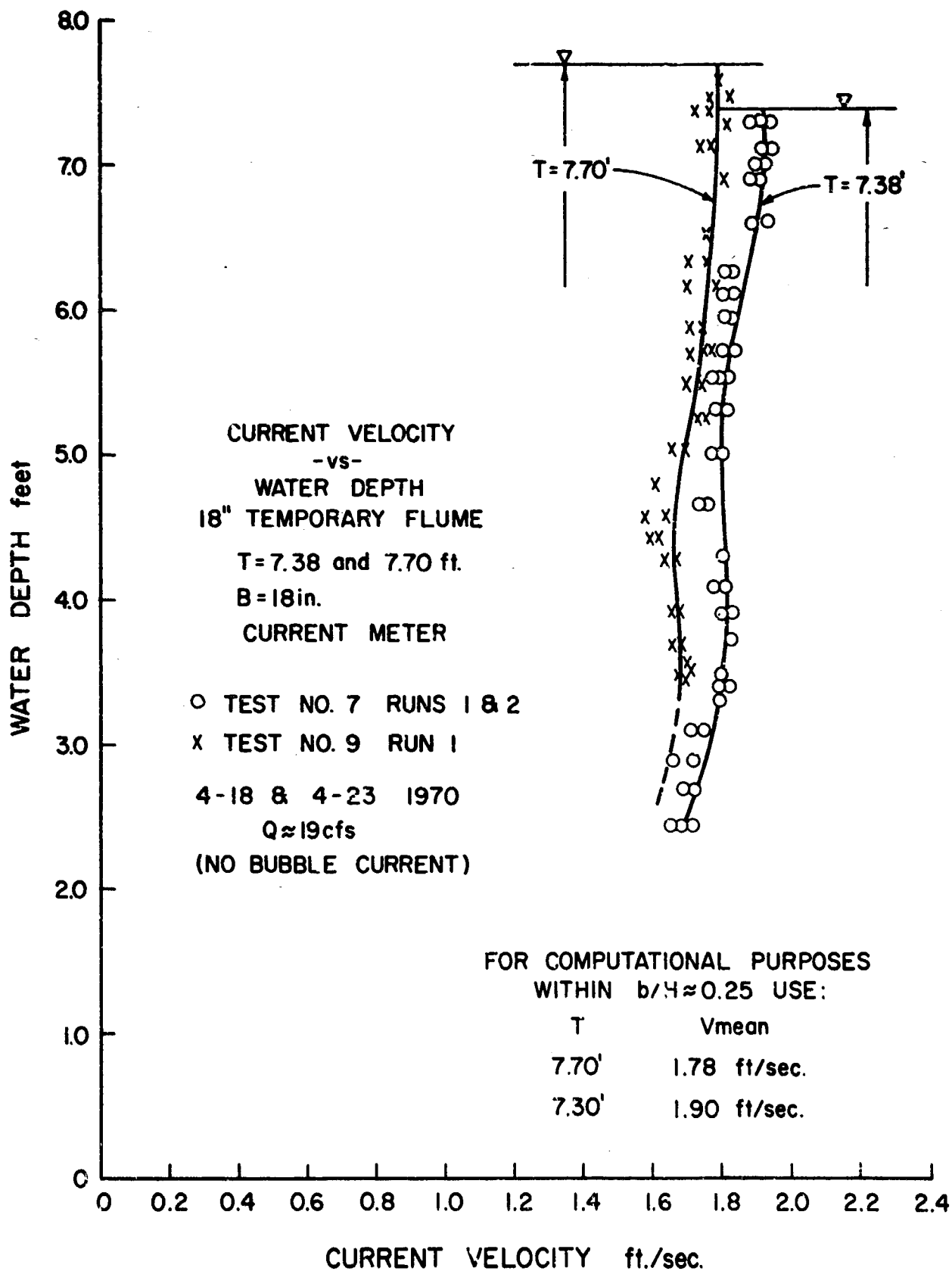


FIG. II-VI-48 OPEN CHANNEL VELOCITY PROFILES IN 18 in. FLUME

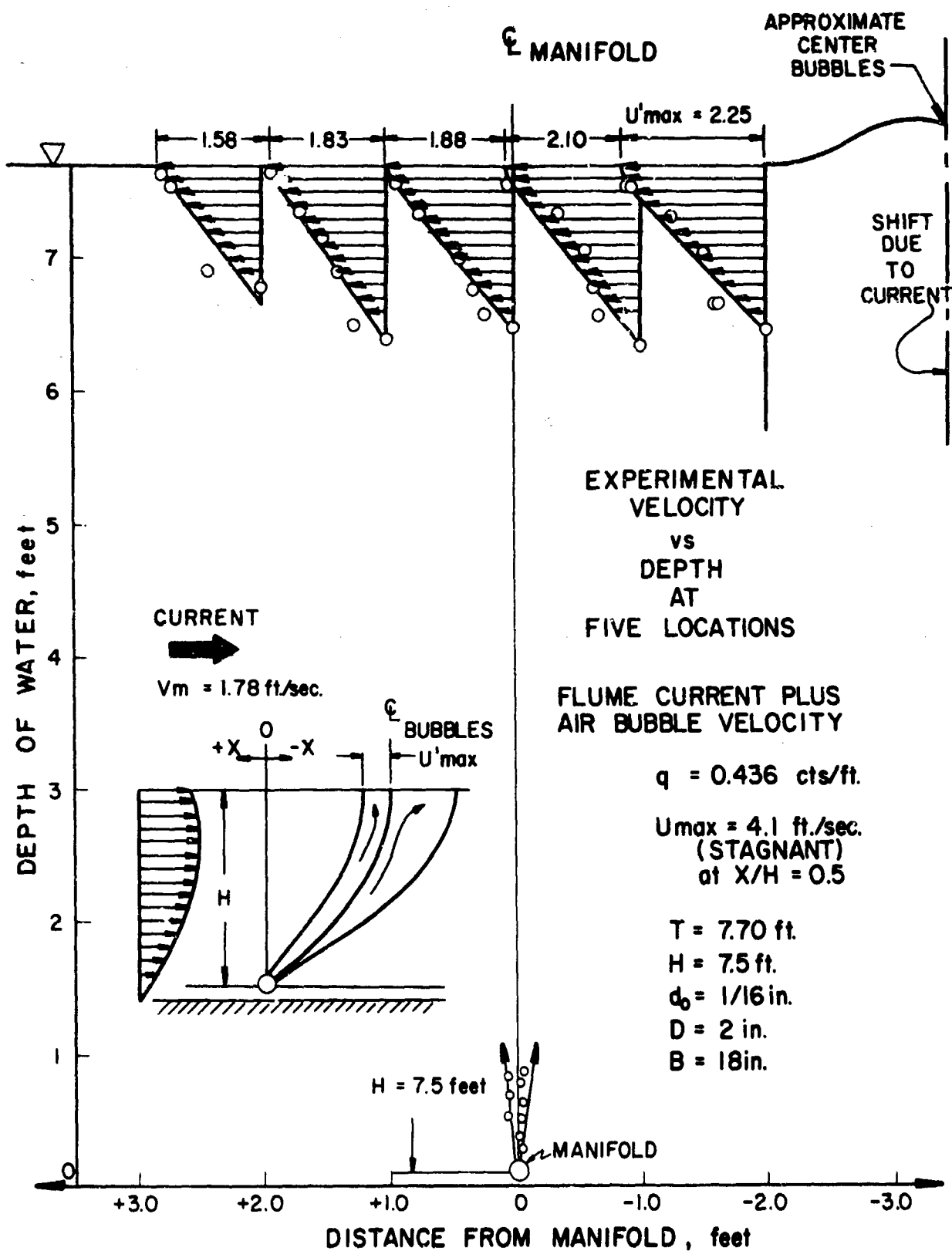


FIG. II-VI-49 - EXPERIMENTAL NET EFFECTIVE SURFACE VELOCITY

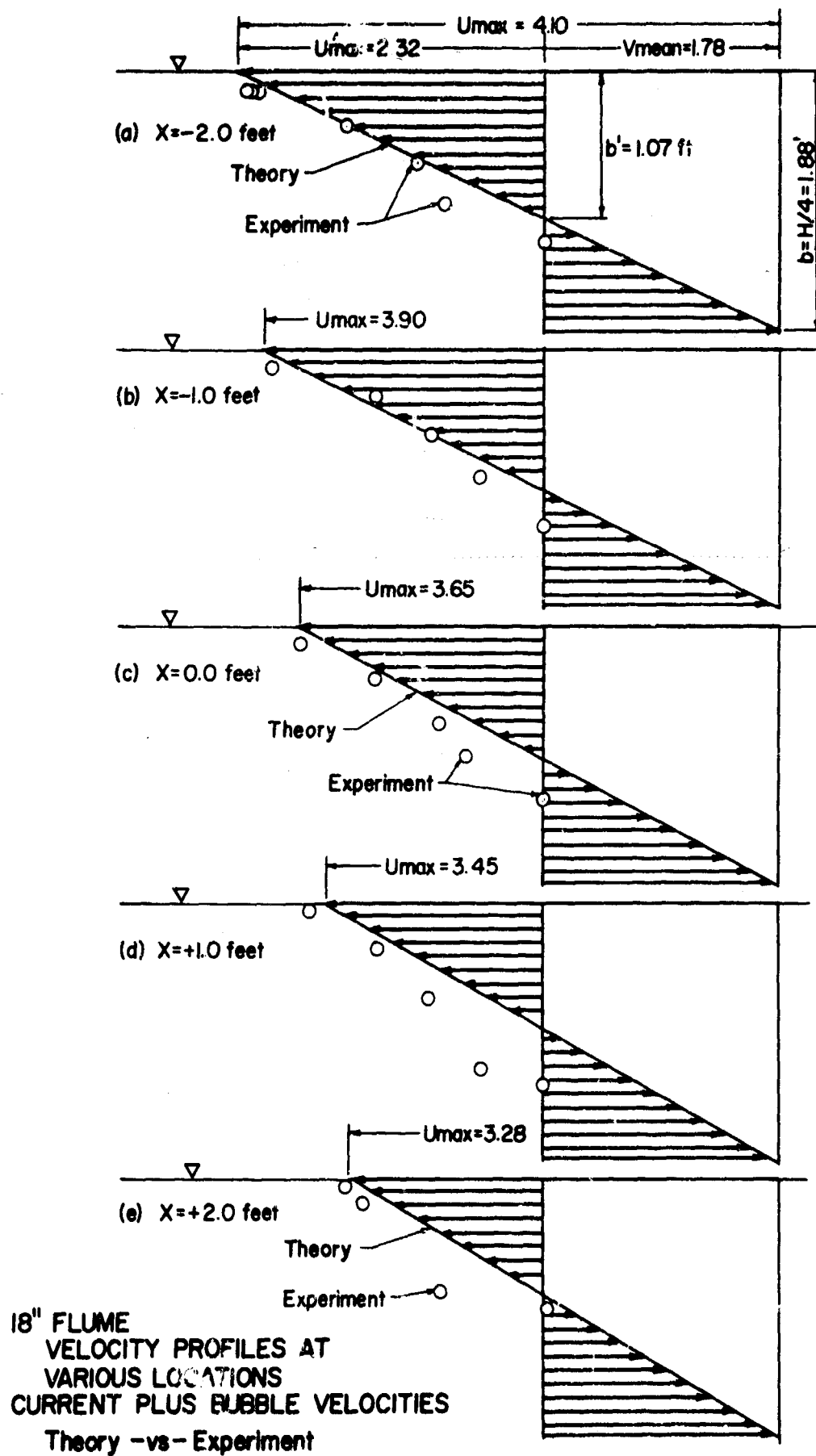


FIG. II-VI-50 - 191 -

city, b' are indicated in Fig. II-VI-50.

Finally, the experimental results of Fig. II-VI-49 have been added for comparison. There appeared to be excellent agreement between theory and experiment for all surface velocities of interest. Even the difficult estimation of b' showed fair correlation with the experimentally determined values being consistently greater than b' theoretical. Similar results were experienced for a different air flowrate in the 18 in. flume and for shallower water tests in the two foot wave channel.

In Fig. II-VI-51 the principle of linear superposition has been applied to simulate prototype conditions when H is 25 feet, U_{\max} generated is 5 ft/sec and the design two knot current opposes the bubble current. The resulting estimated surface current, U'_{\max} is 1.62 ft/sec and b' is about two feet. The prototype conditions were not possible to achieve in the laboratory.

CONCLUSIONS AND RECOMMENDATIONS

Based on the limited scale and range of the laboratory tests primarily discussed the following conclusions are drawn.

1. The continual release of air below water creates a surface current of water near the surface.
2. The magnitude of the current at the surface decreases approximately linearly with distance from the submerged pipe. It is a maximum at a distance of around 0.3 to

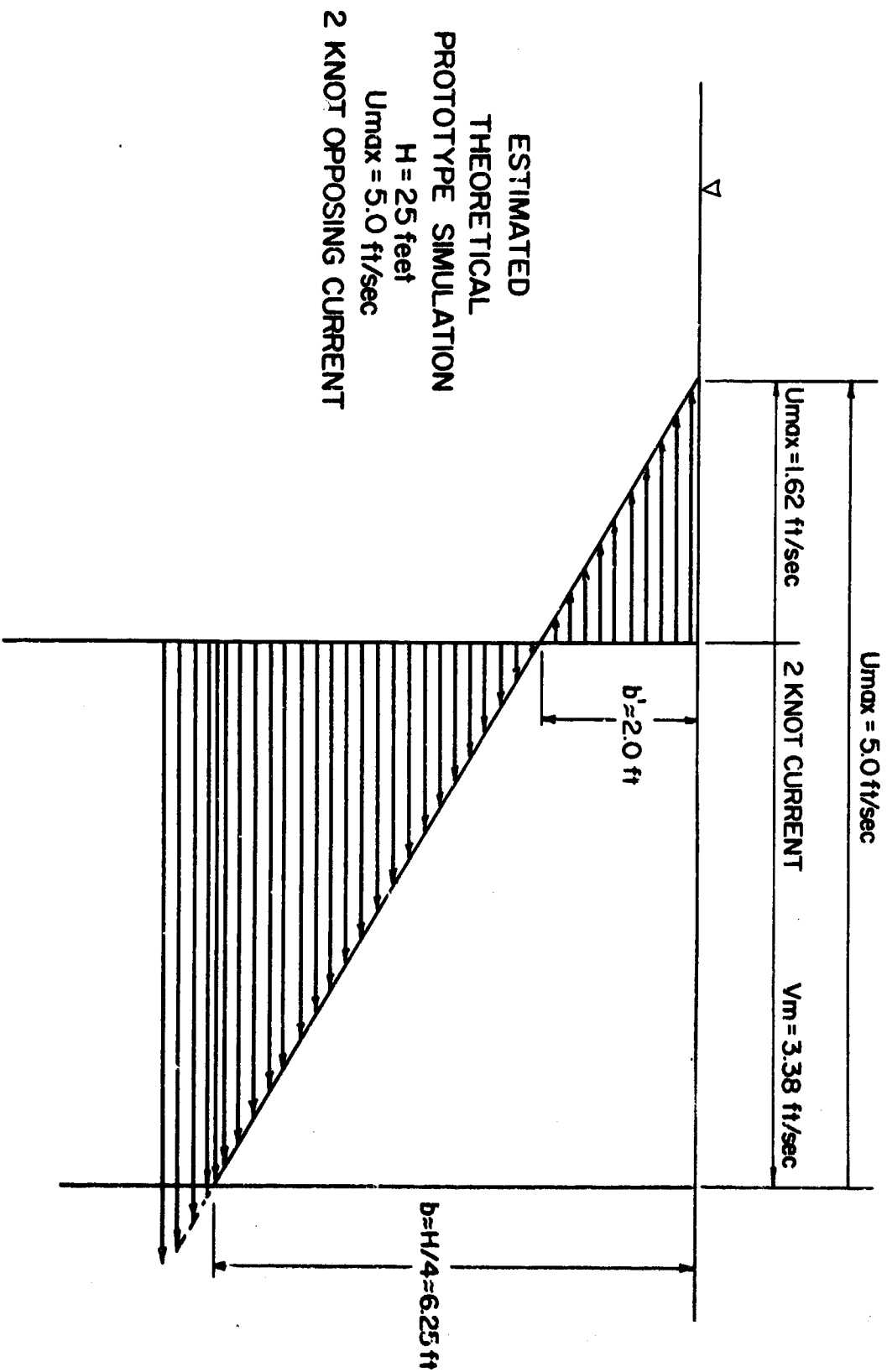


FIG. -ESTIMATED U'_{max} AND b' FOR PROTO-
TYPE DESIGN

II-VI-51

0.6 pipe depths from the pipe.

3. The velocity generated by the bubbles decreases approximately linearly with water depth and is a maximum at the surface. The velocity reverses (current is zero) at a distance below the surface which is about one-quarter of the pipe depth.
4. The maximum surface current generated is proportional to the unit air flowrate raised to the one-third power. The constant of proportionality is strongly dependent on depth of manifold pipe and practically independent of manifold hole size.
5. The following formula was recommended for preliminary design purposes:
$$U_{\max} = 1.5 (sq)^{1/3} \quad (6)$$
6. The principle of linear superposition, applied to combine stagnant U_{\max} and channel flow velocities, was found to hold.

It is recommended to determine the effects of prototype scale geometry and flow on the following results.

1. Manifold depth on the proportionality constant K in Equation (6).
2. Manifold depth on the rule that zero generated current is located at one-quarter the pipe depth.

3. Orifice hole size on the proportionality constant, K in Equations (6). Larger manifold orifices would reduce manifold pressures and power requirements.
4. Application of the linear superposition principle to combine U_{sax} and channel currents.

4. Model Tests Pneumatic Barrier

Introduction

Oil flowing over water is a complex phenomenon. Being lighter than water, gravity forces "drive" the oil to "seek" its own uniform level above the water surface. In a system open to the atmosphere, the driving force is solely the hydrostatic pressure head of the oil, h . Thus a thick layer of oil will have a greater tendency to spread than the same oil of smaller depth.

Once the flow commences, the gravity forces which originated the motion soon give way and are dominated by viscous shear at the interface, so that the viscous forces govern the dynamics of the motion. Spreading decreases the oil thickness.

At some further point when the oil becomes of "film" thickness, surface tension forces become dominant and this phenomenon determines the manner in which further spreading takes place. Superimposed wind and wave forces add considerable complexity to the situation.

Fortunately, under equilibrium conditions that must prevail during oil containment, the oil behind the barrier is essentially stationary so that the retarding viscous forces and surface tension forces are either not present or are very weak. Hence, analysis of the problem reduces to the case where the ratio of gravity forces to inertia forces describe the behavior.

And, since two liquids of differing densities are involved, the ratio of the two forces is characteristically described by the densiometric Froude number, F_D , i.e.,

$$F_D = \frac{\text{gravity forces}}{\text{inertia forces}} = \frac{V}{\sqrt{gL \frac{\Delta \rho}{\rho_w}}} \quad (\text{VI-21})$$

where: F_D = densiometric Froude number, dimensionless

V = characteristic reference velocity

g = gravity constant

L = characteristics reference length

$\Delta \rho = \rho_w - \rho_o$ = mass density difference

ρ_o = mass density of oil

ρ_w = mass density of water

Since

$$\rho_o = \gamma_o/g,$$

$$\rho_w = \gamma_w/g, \text{ and}$$

$$SG_o = \gamma_o/\gamma_w$$

where:

γ_o = unit weight of oil

γ_w = unit weight of water

SG_o = specific gravity of oil

Equation VI-22 can be written:

$$F_D = \frac{V}{\sqrt{gL (1 - SG_o)}} \quad (\text{VI-22})$$

For oil spill containment by pneumatic barrier, the maximum surface velocity generated by the bubbles, U_{\max} determined at a location approximately 0.5 pipe depths, H from the centerline of the submerged pipe can be used as reference. The characteristic reference length is naturally the mean oil depth contained, h . Consequently, Equation VI-22 becomes for oil containment.

$$F_D = \frac{U_{\max}}{\sqrt{gh(1 - SG_o)}} \quad (VI-23)$$

It is apparent that for a given oil as the driving force, h increases, the spreading tendency (velocity) increases. For equilibrium to be maintained, a "retarding" force primarily composed of the kinetic energy in the bubble-generated current must also be increased. To be determined therefore, is the critical ratio of $U_{\max}/\sqrt{gh(1 - SG_o)}$ at the crucial point when failure occurs or begins to occur. Letting α be a coefficient equal to (F_D) critical when failure occurs Equation VI-23 can be written.

$$U_{\max} = \alpha \sqrt{gh(1 - SG_o)} \quad (VI-24)$$

It is the primary purpose of this task to determine the value of the critical constant, α under stagnant water, wave and current conditions.

The method of solution will be essentially experimental, since the bubble-generated velocities retarding the oil are

not completely understood, particularly when oil is present in significant depths near the barrier. It is anticipated that α will be a true constant independent of the scale of the laboratory tests. Consequently, laboratory tests will be carefully analyzed to insure their similarity to prototype scale conditions.

LITERATURE SURVEY

Only one unpublished report dealing with the explicit use of pneumatically developed currents to retain oil was uncovered. This was the work of Sjöberg and Verner¹⁵ jointly undertaken by Chalmers University and the Atlas Copco AB, in Sweden.

Both laboratory and prototype size tests were performed under stagnant water and uniform wave conditions.

Stagnant Water Conditions

Sjöberg and Verner¹⁵ cited additional references indicating that the critical constant, α at failure was between 1.0 and 1.4. Their own tests gave an α equal to 1.2"....which is required to stop leakage of oil through the barrier."

Waves

Two distinct regions of failure were noted with the addition of uniform waves against the air barrier. In one region the waves were such that they were practically unaltered by the bubble-generated current against them. These waves were characteristically long period swells with low values of steepness

and the oil bobbed up and down on the water. Sjoberg and Verner obtained α values greater than 1.2 with this type of wave present and attributed the slight increase to "...the pumping effect of the waves, which press the oil front against the barrier."

The other, more critical case was characterized by waves of high steepness ratio which when moving against an adverse current created by the bubbles broke against the front of the bubble barrier (principle of pneumatic wave breaker). The potential energy in the wave is transferred to kinetic energy and a significantly increased surface velocity, U_{\max} is needed to contain the oil.

Tests by the authors indicated that the critical constant, α increased to about 2.7 when the waves broke at the barrier. They also indicated that the coefficient depended on the depth and profile of the generated current and the steepness of the oncoming wave train.

THEORY

An exact analytical solution is beyond the intended scope of this report. However, it was felt that a one-dimensional application of the equations of continuity, linear momentum, and energy using a control volume may give some idea as to the expected range of possible critical α values.

Conservation of Linear Momentum

Consider a control volume encompassing the surface current generated down to zero flow at depth b and containing oil at depth h . For the case when h is much less than b , it is assumed that the exit velocity profile beneath the oil is also zero at b and approximately triangular in shape, so that entrance and exit momentum coefficients for the control volume are identical. The shear along the bottom of the control volume at depth b can then also be neglected.

At equilibrium, the steady flow form of the linear momentum equation for a unit width can be written:

$$\Sigma F = \dot{m} (\bar{V}_2 - \bar{V}_1) \quad (\text{VI-25})$$

where: \dot{m} = mass flowrate per unit width

\bar{V}_1, \bar{V}_2 = mean velocities at the entrance and exit sections of the control volume, respectively.

Since,

$$\bar{V}_1 = U_{\max}/2 \quad (\text{VI-26})$$

by continuity

$$\bar{V}_2 = U_{\max}/2 \left(\frac{b}{b-h} \right) \quad (\text{VI-27})$$

if the circulation in the oil is neglected.

Also

$$\dot{m} = \rho_w \frac{U_{\max}}{2} b \quad (\text{VI-28})$$

The forces acting on the control volume are essentially hydrostatic, hence

$$\Sigma F = \frac{1}{2} \gamma_w b^2 - [\gamma_o (bh - h^2) + \frac{1}{2} \gamma_w b^2 - \gamma_w bh + \frac{1}{2} \gamma_w h^2] \quad (\text{VI-29})$$

which yields after some simplification

$$\overline{\Sigma F} = \gamma_w \frac{h}{2} (2b - h) - \gamma_o h (b - h) \quad (\text{VI-30})$$

Making the proper substitutions, simplifying and solving for

U_{\max} one obtains:

$$\left[4 - 6 \left(\frac{h}{b} \right) + 2 \left(\frac{h}{b} \right)^2 - SG_o \left\{ \left(1 - 2 \left(\frac{h}{b} \right) - \left(\frac{h}{b} \right)^2 \right) \right\} \right]^{1/2} \quad (\text{VI-31})$$

Equation VI-31 is similar in structure to Equation (4) when h/b approaches zero.

Conservation of Energy

When h is considerably less than b , the kinetic energy of the current can be expressed as the velocity head:

$$\alpha' \frac{(U_{\max})^2}{2g} \quad (\text{VI-32})$$

where α' is the energy correction factor due to the triangular velocity distribution.

The total energy in the bubble-generated current to a depth of water, h_w , equivalent to the oil thickness (assuming a hydrostatic pressure distribution) is then:

$$\alpha' \left(\frac{U_{\max}}{2g} \right)^2 + h_w \quad (\text{VI-33})$$

Since the oil is stationary, its total energy is simply the pressure head of oil, P/γ_o or h .

Applying the conservation of energy and neglecting any losses we obtain

$$\alpha' \left(\frac{U_{\max}}{2g} \right)^2 + h_w = \frac{P}{\gamma_o} = h \quad (\text{VI-34})$$

However, at equilibrium conditions

$$h_w SG_o = h \quad (\text{VI-35})$$

Consequently,

$$U_{\max} = \sqrt{2/\alpha'} \sqrt{gh (1 - SG_o)}$$

When $\alpha' = 1.0$, the critical failure, α is about 1.4. As α' increases due to the triangular shape of the velocity distribution, the α value decreases. This range of critical failure coefficients is approximately those obtained experimentally by Sjöberg and Verner.

EXPERIMENTAL TEST RESULTS

Stagnant Water

Initial tests were conducted in the two-foot wide wave channel with two feet of water depth, T and the manifold located near the bottom so that H/T was about 1.0. With a constant air flowrate and U_{\max} being generated, the oil depth being contained was gradually increased until failure occurred. The $\sqrt{gh (1 - SG_o)}$

value at failure was then computed and plotted against U_{\max} .

Fig. II-VI-52 with the \square symbol for these initial tests presents the results.

When the generated U_{\max} in this initial test series was raised near 2 ft/sec, failure was noted at a much smaller oil thickness than expected. It was discovered, however, that under these conditions, the oil failure thickness approached the thickness, b of the generated surface profile (Fig. II-VI-53). Since this condition was far from that expected in the prototype, high α factors for h/b conditions near 1.0 were considered to be due to scale effects and no further tests were performed in this range.

In the next series of tests the manifold was raised off the floor so that H/T equalled 0.5. These results are also plotted in Fig. II-VI-52 for two different specific gravity oils. In all cases, the critical α coefficients were found to lie in the 1.0 to 1.2 range.

Finally, stagnant water tests were performed in the 18 in wide flume with T about 7.7 feet to check failure in the higher U_{\max} range. These results are also plotted on Fig. II-VI-52 and appear to confirm those results previously obtained. In the tests the critical h/b ratios were well within the limits where no scale effects could be expected.

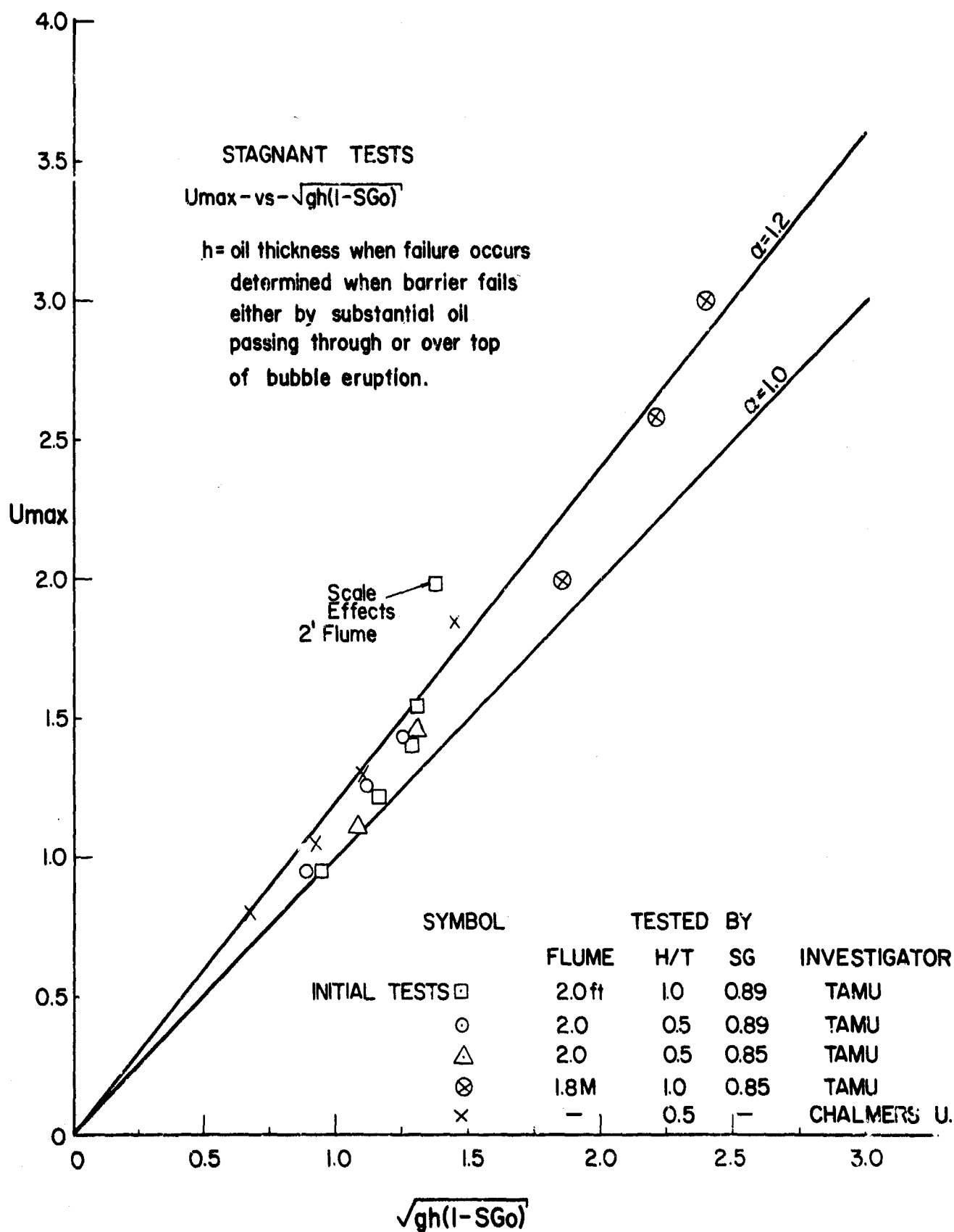
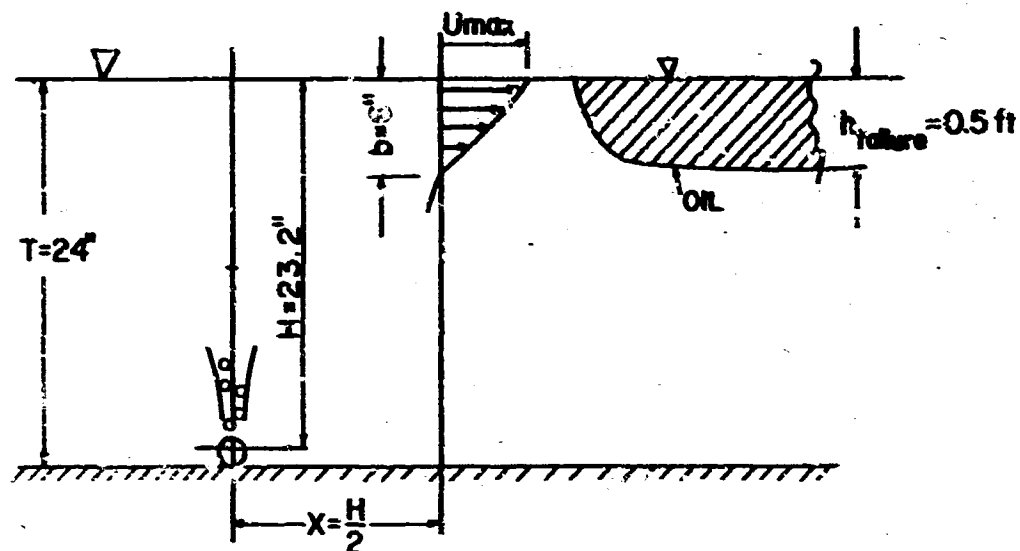


FIG. II-VI-52 - U_{max} versus $\sqrt{gh(1-SG_o)}$ FOR STAGNANT WATER

SCALE EFFECTS

LABORATORY $b = h_{\text{failure}}$



PROTOTYPE $b \gg h_{\text{failure}}$

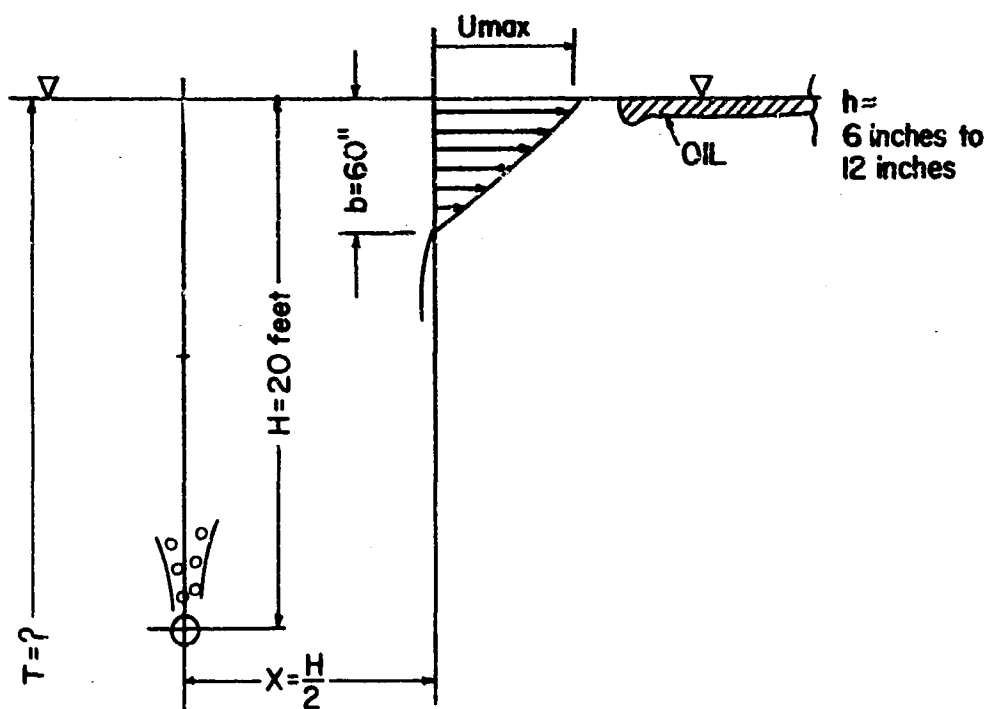


FIG. II-VI-53 -SCALE EFFECTS IN TWO FOOT WAVE CHANNEL

Four experimentally determined data points taken from the Chalmers University tests by Sjöberg and Verner¹⁵ are also shown in Fig. II-VI-52 for comparison. There was excellent agreement obtained. Consequently a critical coefficient of 1.2 was recommended for preliminary design under stagnant conditions.

As noted on Fig. II-VI-52, failure was considered to occur when masses of oil droplets began to pass through the barrier below the surface or when masses of oil over-topped the barrier.

Waves

Design waves had to be scaled to model sizes for laboratory tests. A wide range of wave conditions were specified and time limitations prevented testing all combinations. Therefore, the significant wave characteristics (height, length, etc.) were chosen as most representative for laboratory tests in the two-foot wide wave channel.

If a prototype manifold depth of 25 feet is assumed, the geometric scale ratio used became 25:1, since the model manifold was located one foot below the water surface. A maximum water depth of two feet was used for the tests resulting in the generation of "shallow water" wave forms. The following shallow water wave characteristics were employed at the 25:1 scale ratio.

	<u>PROTOTYPE</u>	<u>MODEL</u>
Significant Wave Height	10 ft	0.4 ft
Significant Wave Period	6 sec	1.2 sec
Significant Wave Length	185 ft	7.4 ft

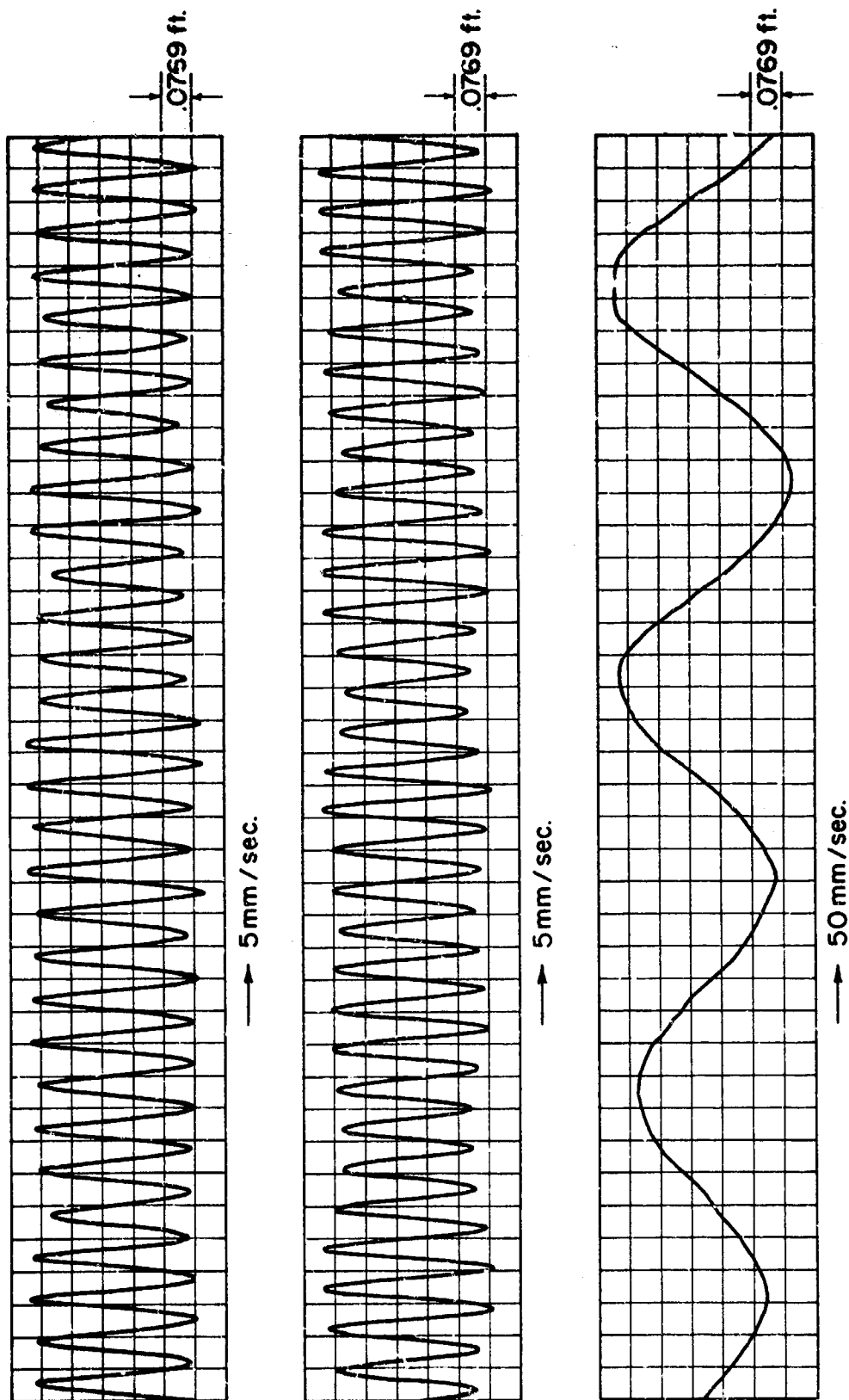
The measured model wave form is shown in Fig. II-VI-54.

Although some secondary harmonics existed, the wave used was essentially of a scaled size and period very close to that required. Model surface velocities generated were near 1 ft/sec which scaled-up to about 5 ft/sec in the prototype.

As previously noted in the literature, the required U_{\max} to contain oil was also considered to depend on the height, H and length, L , of the waves striking the barrier, (i.e., on the wave steepness H/L). Waves of large steepness ratio approaching breaking conditions were found to impose additional forces on the barrier.

In a theoretical analysis of a deep water wave entering an adverse, uniform current, Unna²¹ suggested that when the adverse current, U was about 25 percent of the wave celerity, C_1 , the deep water wave would be fully attenuated by the adverse current (hydraulic breakwater). Wave theory states that waves break when the steepness, H/L exceeds 0.14 in deep water.

Dick and Brebner²³ combined these results and determined the effects of an adverse current to aid in breaking waves. Fig. II-VI-57 reproduces the combined effects and shows at



WAVE PROFILE FOR $L_r = \frac{L_m}{L_p} = \frac{1}{25}$

$T_m = 1.2$ sec. - $T_p = 6$ sec.

$H_m = 0.40$ ft. - $H_p = 10$ ft. $d = 2.0$ ft.

SHALLOW WATER WAVE
RUN NO. 1 15 APRIL 1970

FIG. II-VI-54

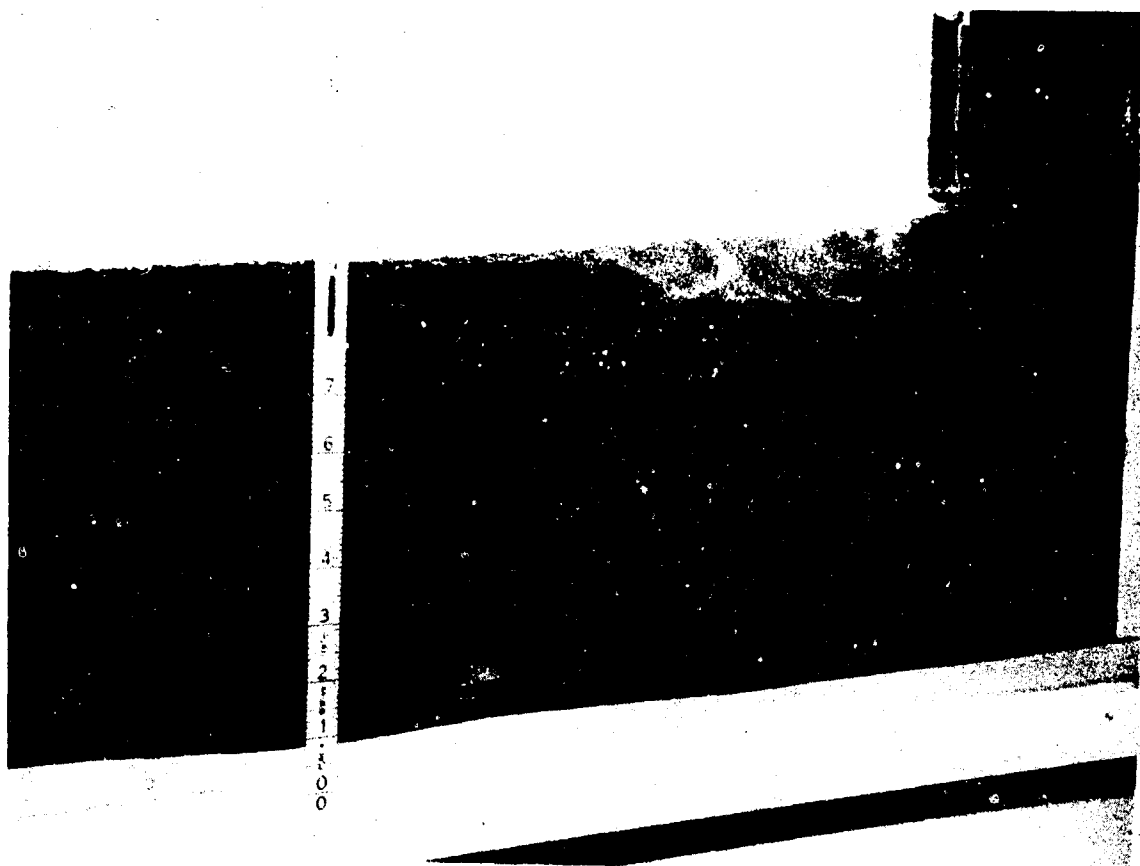


Fig. II-VI-55 Pneumatic barrier operating in waves-
small wave tank. (Oil retained on the right)

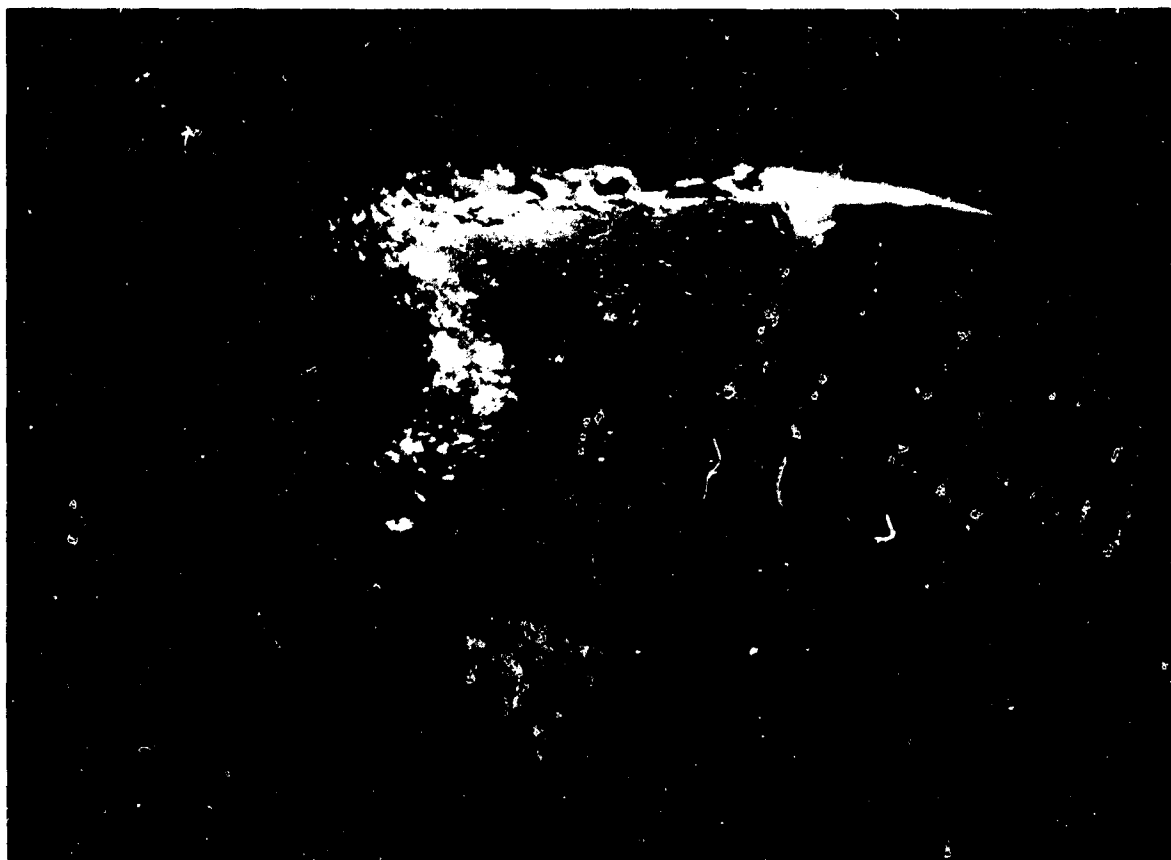


Fig. II-VI-56 Pneumatic Barrier operating in waves -
intermediate wave tank.

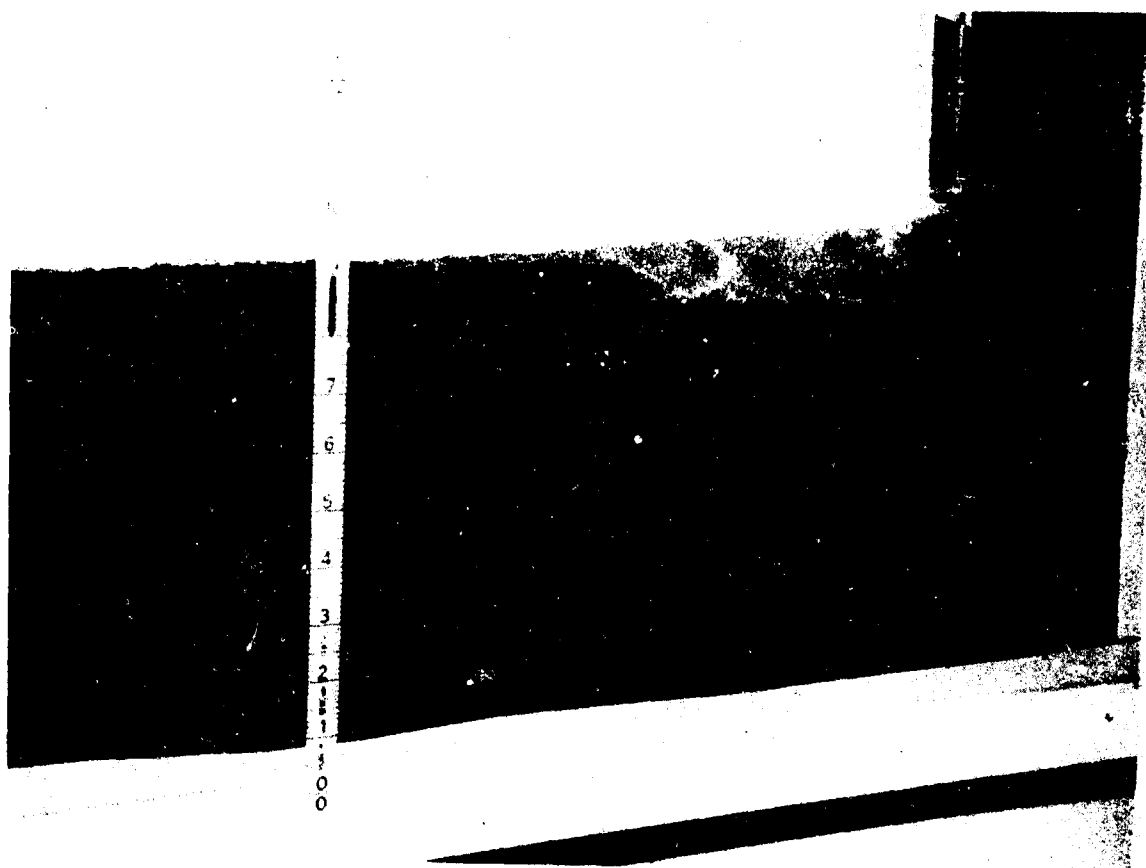


Fig. II-VI-55 Pneumatic barrier operating in waves-
small wave tank. (Oil retained on the right)



Fig. II-VI-56 Pneumatic Barrier operating in waves —
intermediate wave tank.

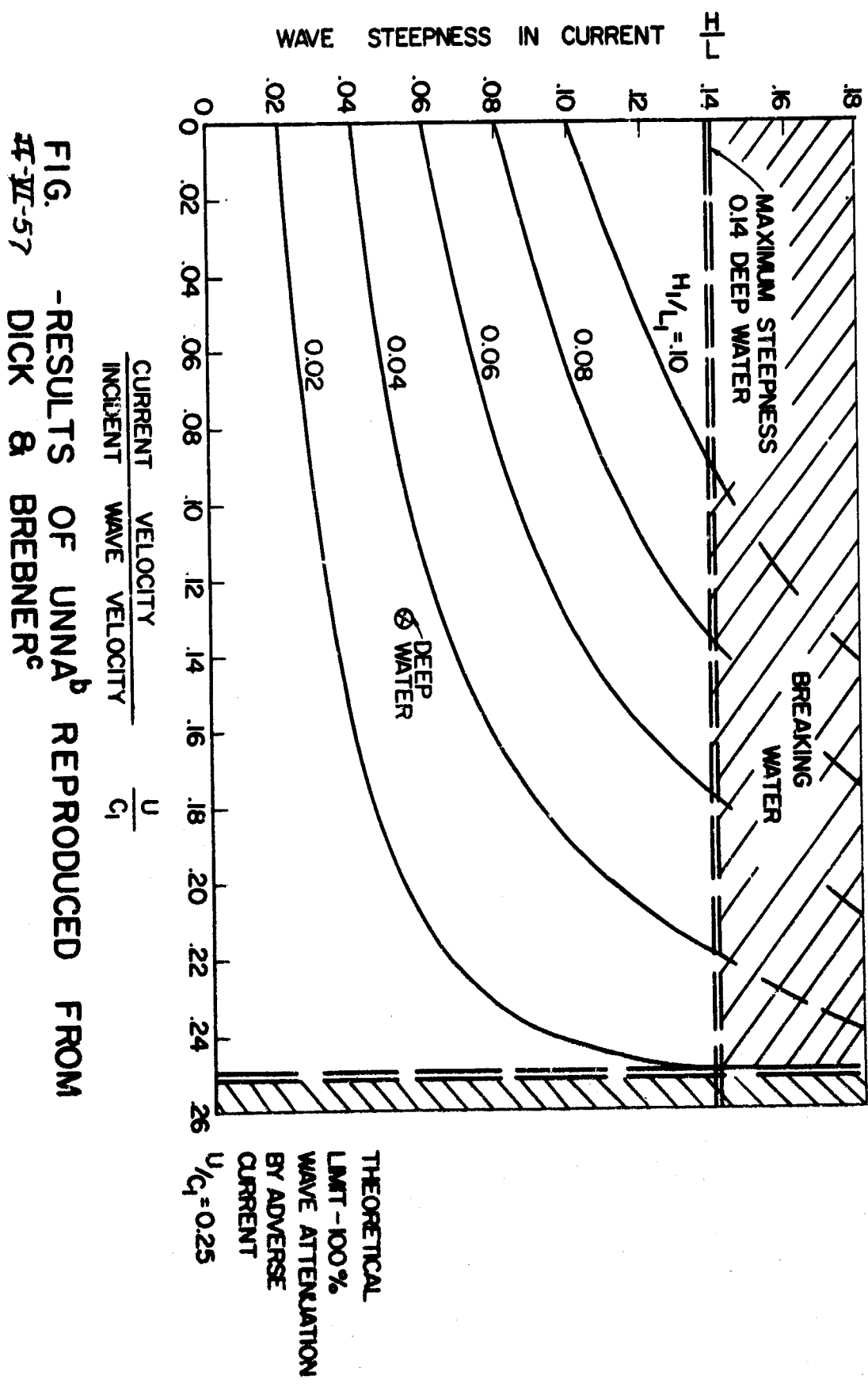


FIG. -RESULTS OF UNNA^b REPRODUCED FROM
 44-77-57 DICK & BREBNER^c

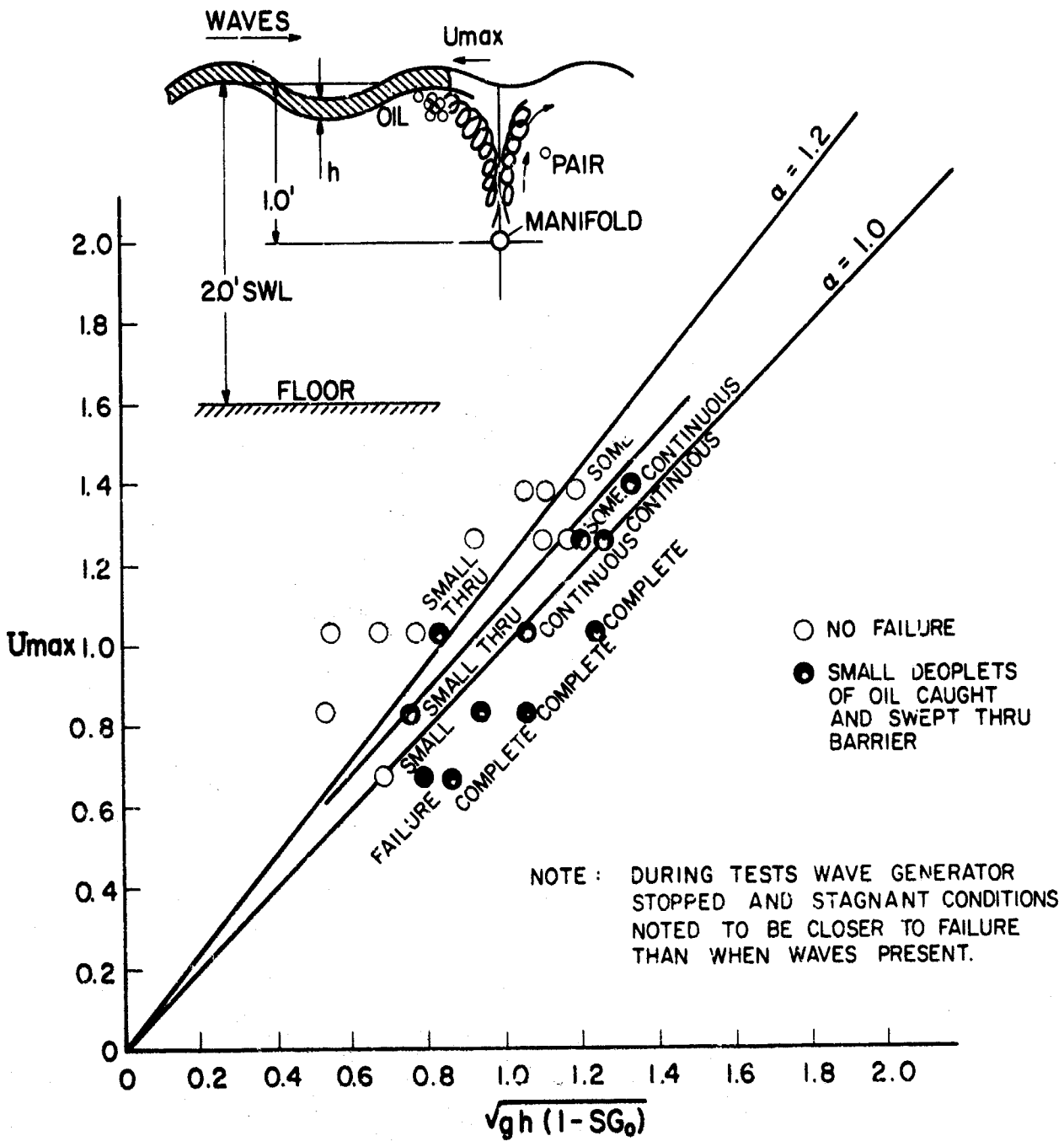
$$U_{\max} \text{ -- vs -- } \sqrt{gh(1-SG_0)}$$


FIG. II-VI-58 -U_{max} versus $\sqrt{gh(1-SGo)}$ UNDER
MODELED DESIGN WAVES

what U/C_1 ratios breaking occurs for varying wave steepness.

From the prototype design criteria in deep water, the wave celerity C_1 equals $\sqrt{gL/2\pi}$ or about 38.5 ft/sec. The prototype steepness ratio is about 0.0347 at significant height conditions. Assuming Fig. II-VI-57 is conservative when the velocity profile is triangular, (i.e. U_{\max} is less than a mean,) uniform velocity, U , the deep water H/L versus U_{\max}/C_1 point for the prototype design has been plotted in Fig. II-VI-57. A design U_{\max} of 5.0 ft/sec has been selected for this calculation.

Since this calculated point is far from the area where breaking occurs, the large swells characteristic of the significant design waves were felt to probably have little or no "pumping" effects on the pneumatic containment device.

Of primary interest for the laboratory tests was the case with oil located on the side from which waves were generated so that the waves possibly moved the oil against the barrier. Fig. II-VI-55, 56, & 58 presents the results in the same U_{\max} versus $\sqrt{gh(1 - SG_o)}$ form used previously.

Surprisingly, the long swell wave form modeled in the tests produced little change from stagnant conditions. The critical α was still between 1.0 and 1.2. In fact, when the waves were stopped during testing the stagnant conditions present were noted to be closer to failure than when testing with waves.

Laboratory conditions permitted testing only uniform wave shapes. Random waves present at sea would perhaps produce entirely different results.

Based on these laboratory tests, α equal to 1.2 is recommended for preliminary design with waves.

Current

To test the principle of linear superposition of velocities discussed in detail earlier in this part, the 18 in. wide flume was used with 7.7 feet of water which gave a mean velocity, V_m of 1.78 ft/sec. A constant bubble-generated velocity was introduced and the effects of the current were tested by adding oil and noting the mean oil thickness at failure. If the principle of superposition should hold under these conditions, then a plot of the effective surface velocity, $U_{\max} / (U_{\max} \text{ minus } V_m)$ versus $\sqrt{gh(1 - SG_o)}$ should also result in a critical coefficient α of 1.2 near failure. Fig. II-IV-59 shows the results which generally indicated that this is precisely what happens. Sufficient time was unavailable to completely verify these results particularly at small values of U_{\max} .

As noted in Fig. II-VI-59, failure depths were recorded when masses of oil began to over-top the air barrier and move downstream. Significantly, it was also observed that a number of

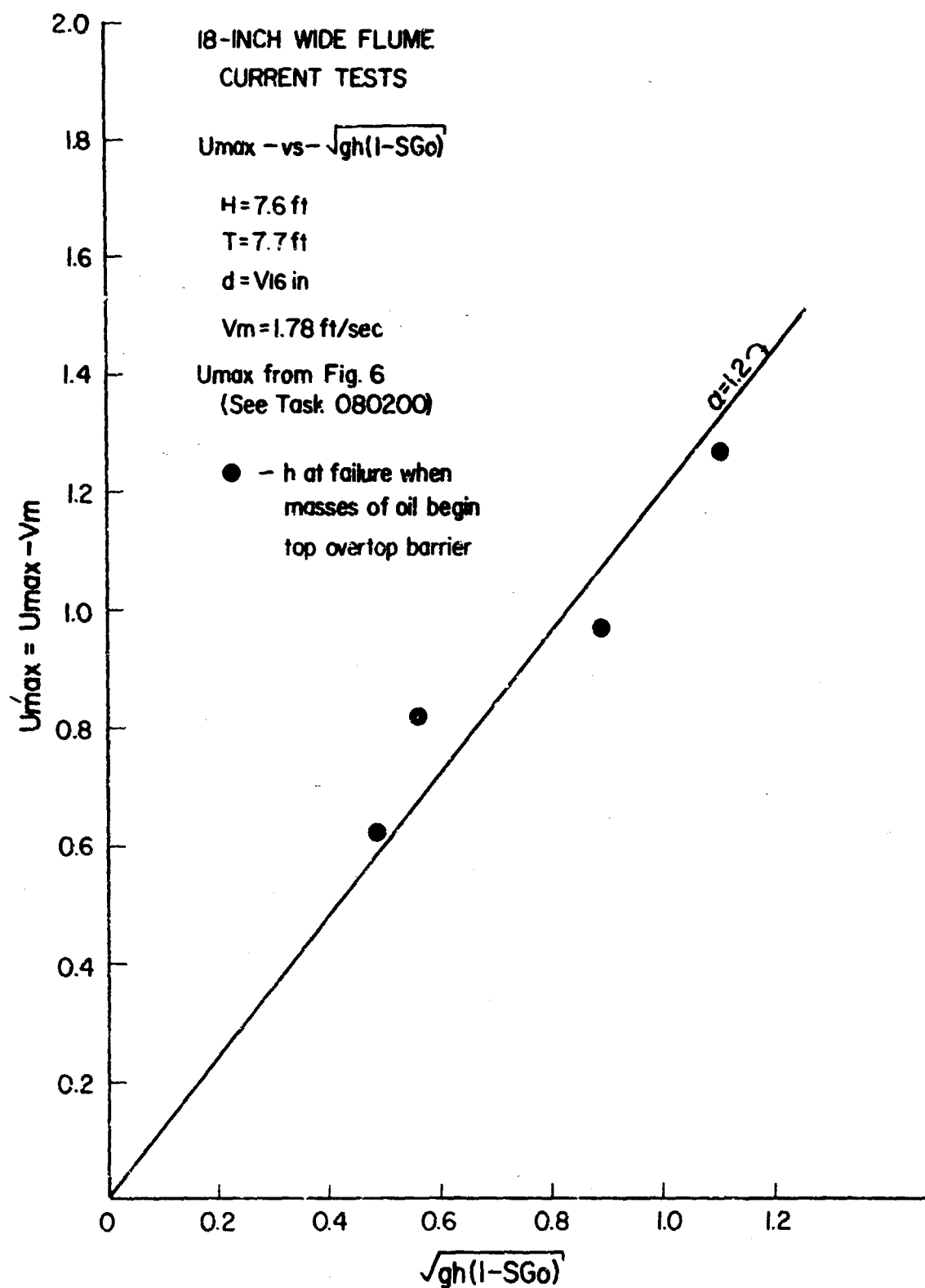


FIG. II-VI-59 - U_{max} versus $\sqrt{gh(1-SGo)}$ WITH CURRENT

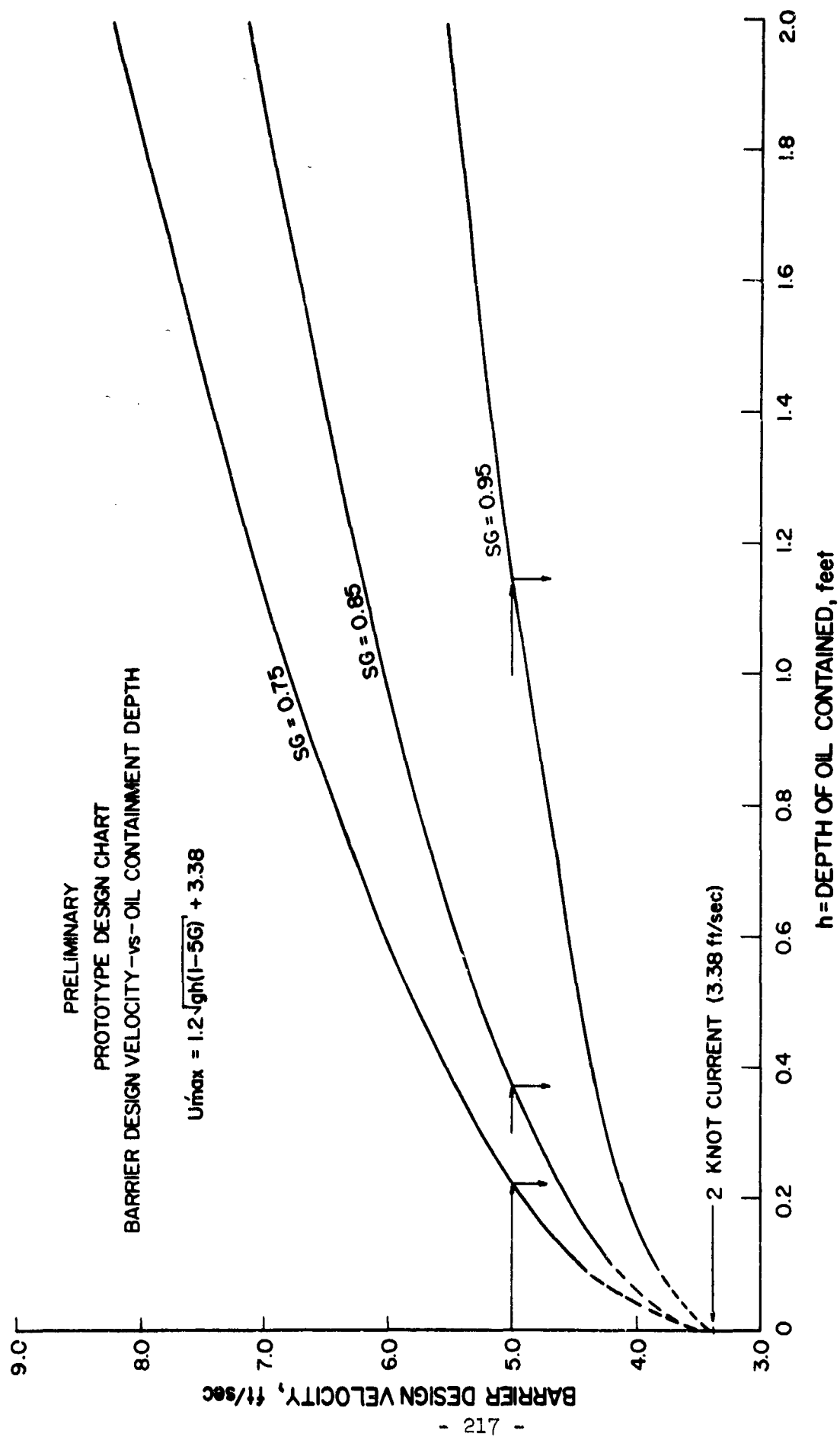
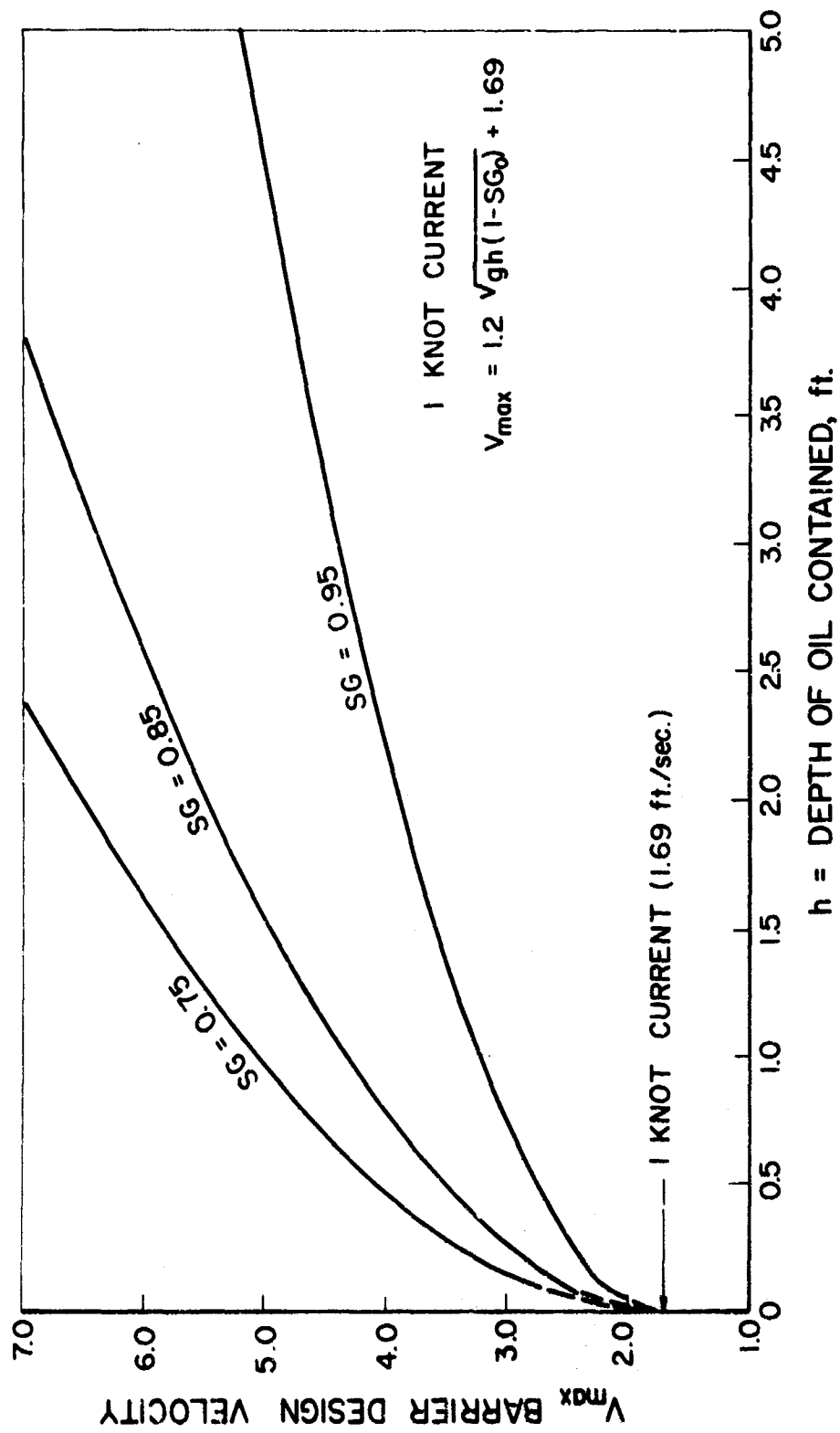


FIG. -RECOMMENDED PROTOTYPE DESIGN CHART

11-VI-60



II-VI-61

oil droplets were entrained near the head region of the contained oil and when located at depths greater than the effective barrier profile, b' , were swept right through the deflected bubble region by the current. Time was unavailable to record any rates of this type of loss except to estimate that in all cases well over 95% of the oil remained contained by the air barrier.

CONCLUSIONS & RECOMMENDATIONS

In conclusion, the results of the stagnant water, wave, and current tests were extrapolated to prototype conditions. Fig. II-VI-60 presents the combined results in the form of a preliminary design chart. For any pneumatic generated velocity, U_{max} , the resulting mean oil depth contained can be determined for the range of specific gravity oils of interest. A two knot prototype current (3.38 ft/sec) is used in the plot. No wind set-up effects are included, but mean oil containment depths can be estimated with wind by using only 2/3 of the values indicated. These results are tabulated below.

Barrier Design Velocity U_{max} ft/sec	SG of Oil	Mean Oil Depth Contained, (Feet)	
		No Wind	Including Wind
5.0	0.75	0.225	0.15
5.0	0.85	0.370	0.295
5.0	0.95	1.140	0.76

It is recommended that complete verification of all of the above preliminary results be made under prototype conditions.

For lower prototype current (1.69 ft/sec) the barrier design velocity is greatly reduced as indicated in the table below and in Fig. II-VI-61.

Barrier Design Velocity U_{\max} ft/sec	SG of Oil	Mean Oil Depth Contained, (Feet)	
		No Wind	Including Wind
3.25	0.75	0.225	0.15
3.25	0.85	0.370	0.295
3.25	0.95	1.140	0.76

Section III

Design of Major System

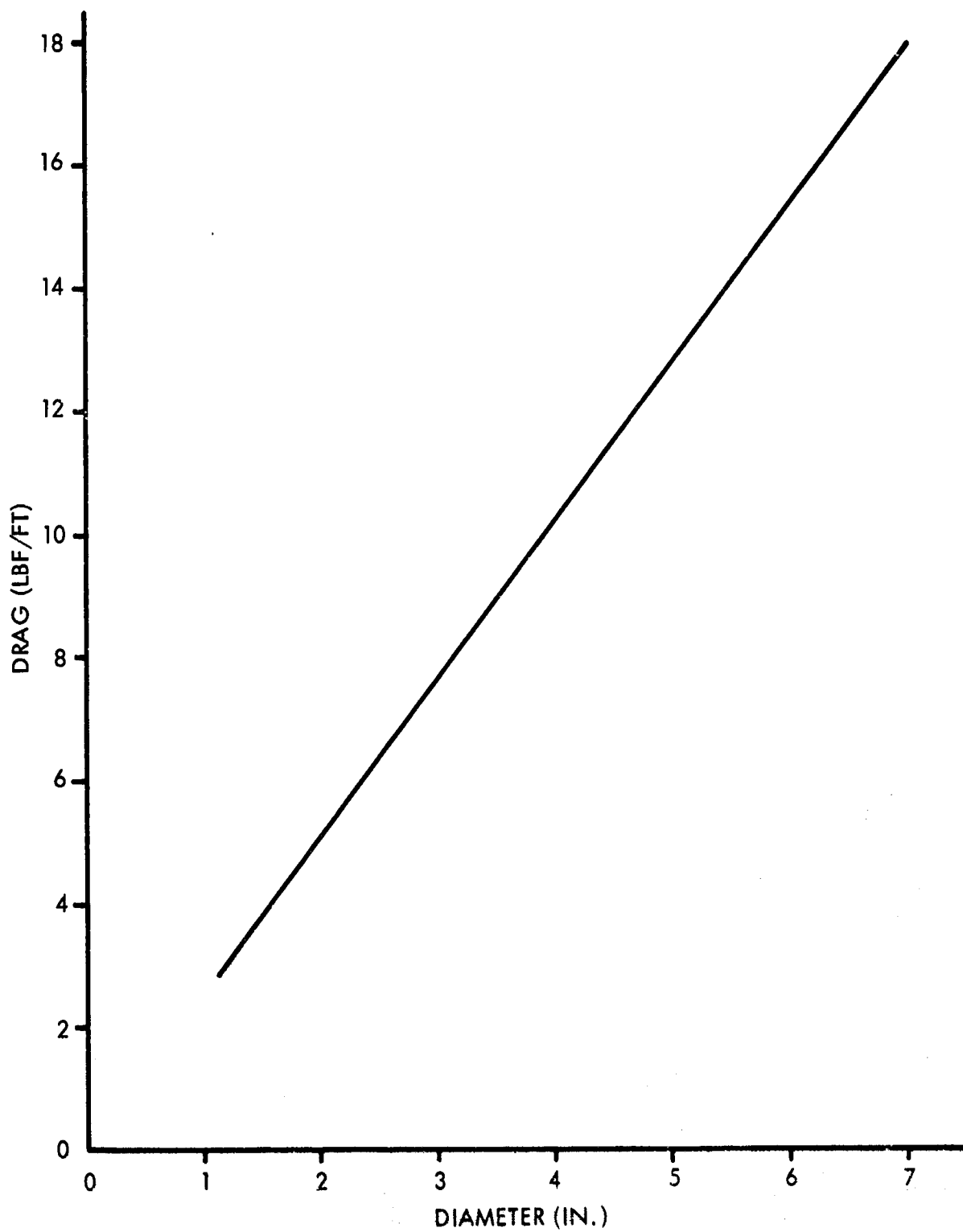
III-I-1. Bubble Screen Generator

The purpose of the manifold pipe is to carry and incrementally release the air that forms the bubble screen. The pipe will be located about 25 feet below the water surface and will be supplied with compressed air from above at given intervals. The hole spacing along the pipe was determined in the hydrodynamics tests and was recommended to be six to 12 holes per foot of pipe. In this same part of the study, the air flow rate was determined to be in the range of 1 c.f.s. per foot of pipe for a surface velocity of 5 ft/sec. This flow is measured at standard temperature and pressure and requires between 5 and 12 horsepower per foot, depending on the overpressure in the pipe. Frictional losses are negligible.

At the beginning of this project, a considerable amount of effort was devoted to finding materials which would not be harmfully affected by marine conditions over a period of several months without special treatment. This study was the basis for the initial choice of polyvinyl chloride (PVC) for a pipe material.

Having chosen a material for constructing the pipe, the next step was to determine the size of the pipe. This depended on several factors. The three most important factors were drag forces, buoyant forces, and supply lengths. Fig. III-I-1 shows the drag forces for various sizes of pipe in a 3 knot current. As can be seen in this plot, the forces on the pipe become very large as the diameter increases.

The next consideration is that of buoyancy. The pipe



PLOT OF DRAG FORCE VERSUS
PIPE DIAMETER FOR A 3 KNOT
CURRENT

FIG. III-I-1

must weigh enough to sink or it must be weighted on location. In either case, the necessary weight must be transported to the location. This necessary weight is plotted in Fig. III-I-2.

After considering the dynamics of wave actions and the sea conditions in which the pneumatic barrier is required to operate, it was decided that the pipe should be rigid. By being rigid, control of placement and floatation level would be much less difficult and the necessary tensile load carrying capability could be inherent. The method of floatation will be discussed later.

During one of the meetings, it was recommended that this pipe be rolled onto a large drum much the same as is done by some pipe laying concerns. Examining the procedure of putting the pipe on drums reveals that it is yielded during wrapping and then is reverse yielded during removal so that it will be approximately straight when unloaded. If the PVC pipe were wound on a large diameter drum in a relatively warm fabrication building and then taken out into a brisk 50°F wind to be unwound, the unwinders would very likely encounter considerable difficulty in laying the PVC pipe in a straight line. From this then, the most logical means of storing and transporting the pipe was in short straight sections. For optimum construction and assembly procedures, the pipe sections should be of the same dimensions. In this way, there would be no particular order for packaging, storing, or assembling.

The next consideration for determining the diameter of the bubble screen pipe, is the length of pipe that is between

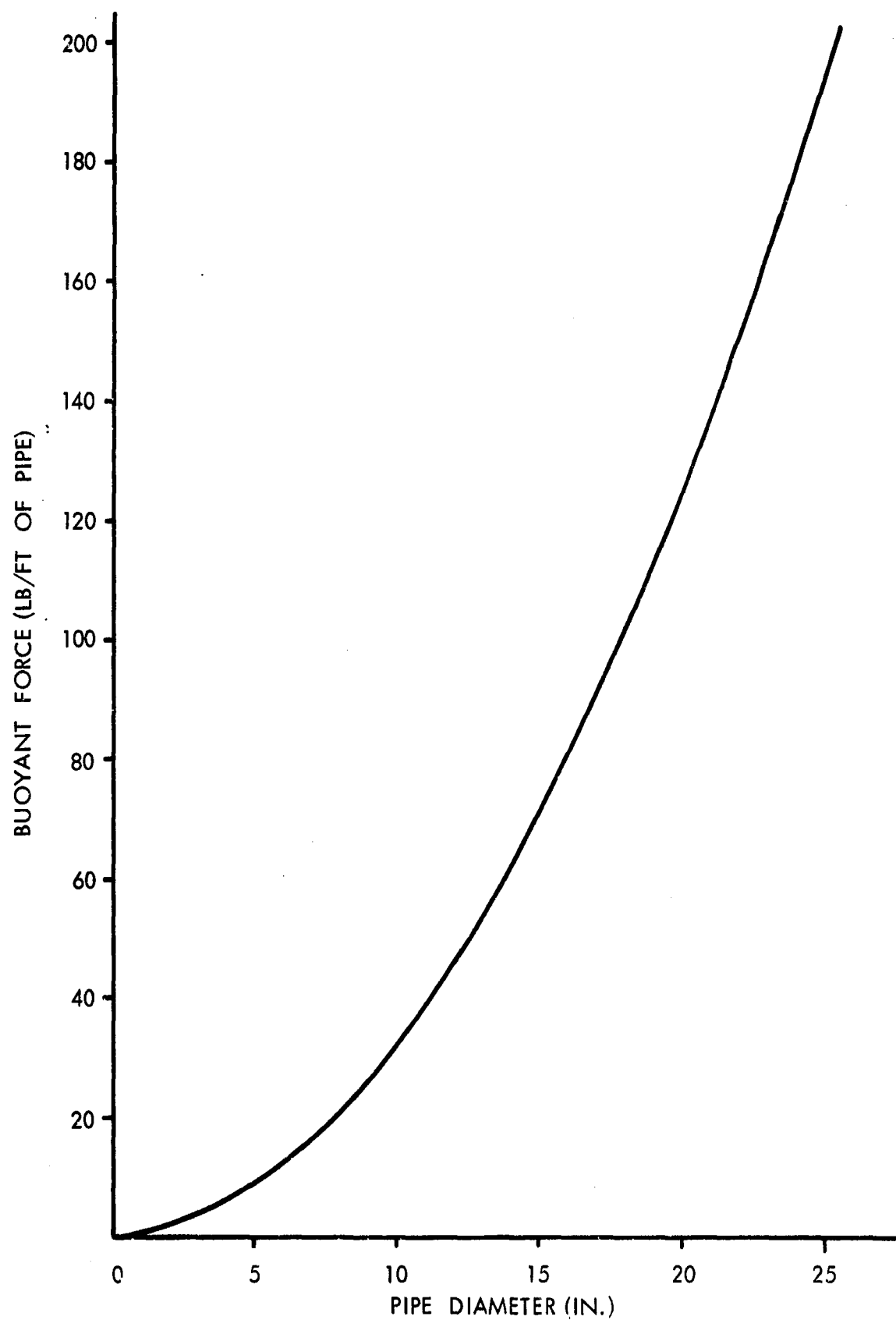


FIG. III-I-2

BUOYANT FORCE AS A FUNCTION
OF PIPE DIAMETER

the supply points. From these supply points, the air moves along the pipe with a decreasing mass flow rate because of the incremental release of the air forming the bubble screen. For a given diameter of pipe then, the length between the supply points is limited by the mass flow rate at the supply inlet.

The mass flow rate at the inlet is limited by the sonic velocity in the inlet air and by the cross sectional area of the pipe. The sonic velocity of the air is a function of temperature alone and is plotted in Fig. III-I-3. The cross sectional area is proportional to the inside diameter squared. Therefore, for a given temperature of supply air, the length between supply points is proportional to the diameter squared.

The deciding criterion for the pipe diameter was the weight of an individual section. An arbitrary figure of 200 lbs. was chosen as the maximum weight if the pipe sections were to be moved by hand. By having a 7 inch diameter pipe, the sections could be about 11 feet long and weigh about 200 lbs. An 8 inch section could be 9 feet long, or a 6 inch section could be 16 feet long. The diameter was chosen as 7 inches. This was about the largest that could be handled in 1000 foot lengths with a 16,000 lb. bollard pull.

All of the aforementioned design work had been performed with the assumption that a suitable air mover could be obtained. Soon after design began and the necessary amount of air volume per foot was realized, contacts were made for equipment that would do the job. Two answers (letters III-I-1 and 2) to these inquiries arrived during the week of May 18, 1970. (See Appendix V).

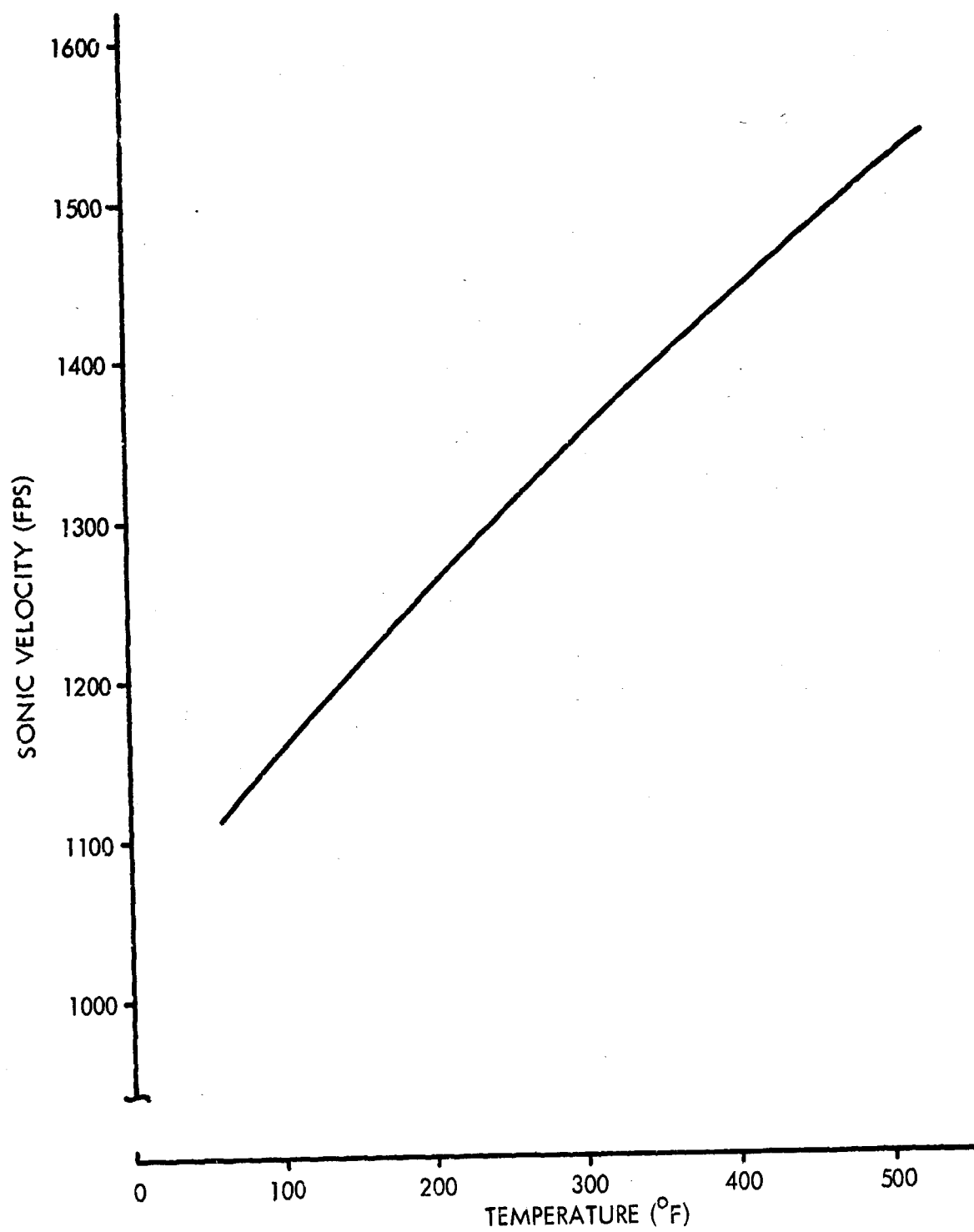


FIG. III-1-3 SONIC VELOCITY AS A FUNCTION OF TEMPERATURE

The first of these (letter III-I-1) is a turbine-driven rotary screw compressor weighing about 60,000 lbs. By weight alone, this unit is ruled out. The other answer (letter III-I-2), is from Gas Turbine Power, Inc., in Houston, Texas, for a Curtis Wright "Jet Air" Compressor package. (GTP 7850E) As can be seen in their letter, this unit is readily adaptable to use in this program.

Using the "Jet Air" package changes the design conditions for the bubble screen pipe. It has a much higher discharge pressure than the pipe was designed for. One cubic foot of air at conditions at the bubble screen pipe level weighs 0.132 lbs.; 22,000 standard cubic feet of air weighs 1,681 lbs. In other words, one GTP 7850E can supply air for 210 feet of bubble screen pipe. Remembering that the sonic velocity increases with temperature (Fig. III-I-3) and that the density increases with pressure (Fig. III-I-4), the discharge pressure and temperature greatly affect the necessary diameter of the bubble screen pipe (Fig. III-I-5). The pressure differential is the pressure inside the pipe above atmospheric plus 25 feet of water. The inlet air velocity is Mach 0.5. For these conditions, the best pipe diameter would be about 4 inches.

After some consideration as to how the PVC bubble screen pipe was to be connected and how the large tension loads were going to be carried, it was decided best to construct the pipe of steel. Since all the steel is of the same type and remains completely submerged, corrosion should not present any problem. Pipe of the size and weight needed can readily be purchased from United States Steel, Pittsburgh, Pa.

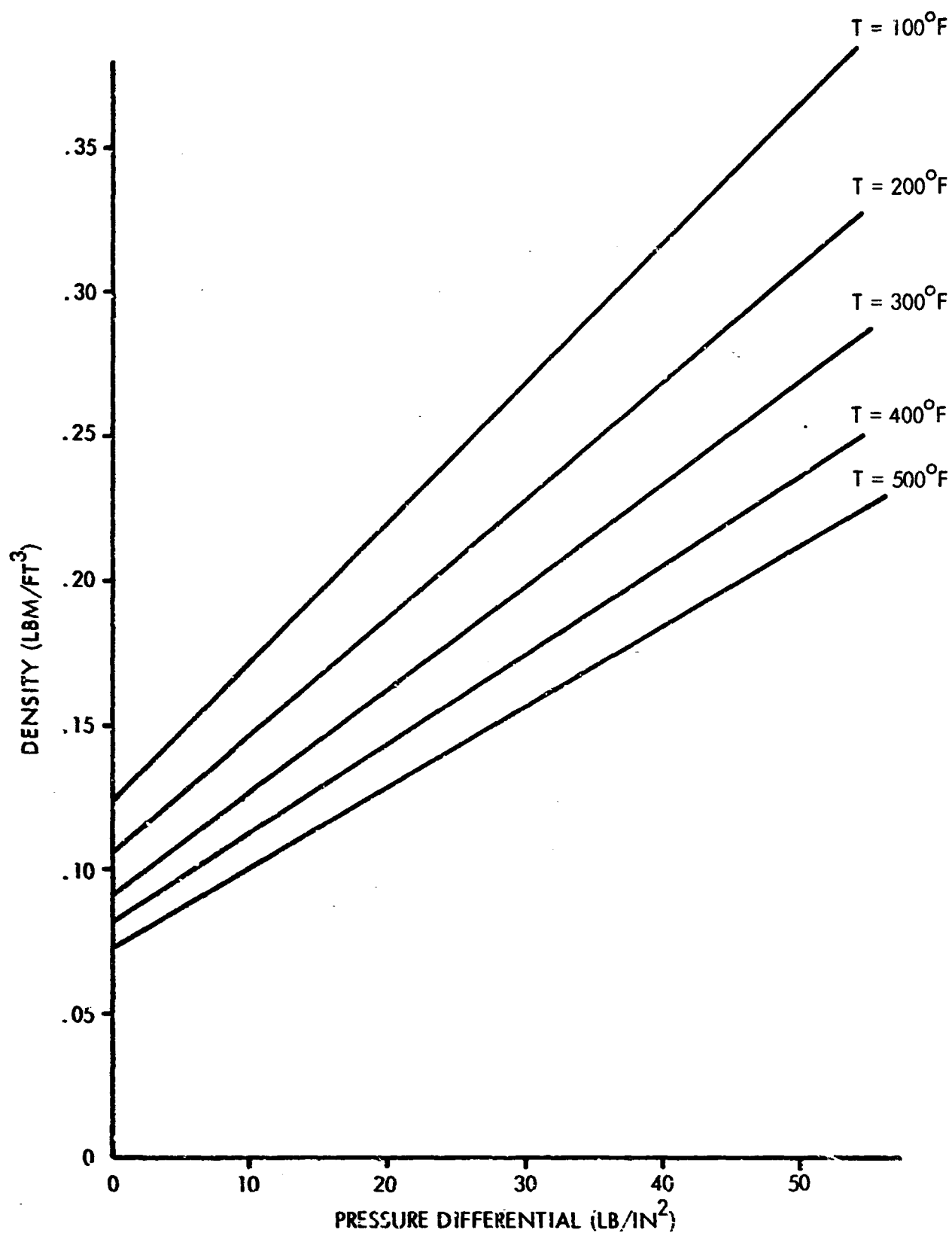
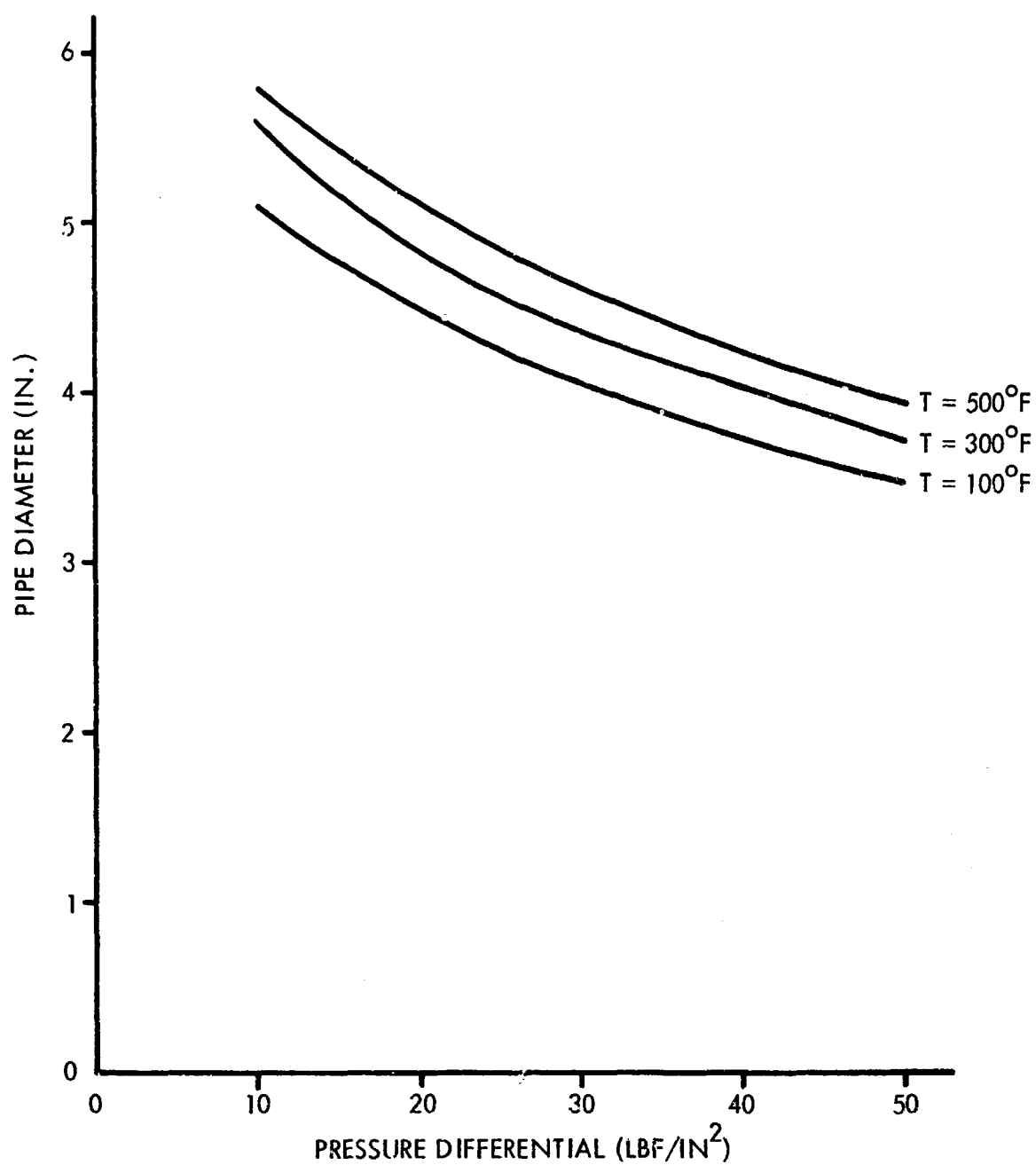


FIG. III-I-4 AIR DENSITY AS A FUNCTION OF PRESSURE DIFFERENTIAL IN MANIFOLD PIPE



PIPE DIAMETER AS A FUNCTION OF PRESSURE DIFFERENTIAL
AT VARIOUS TEMPERATURES

FIG. III-I-5

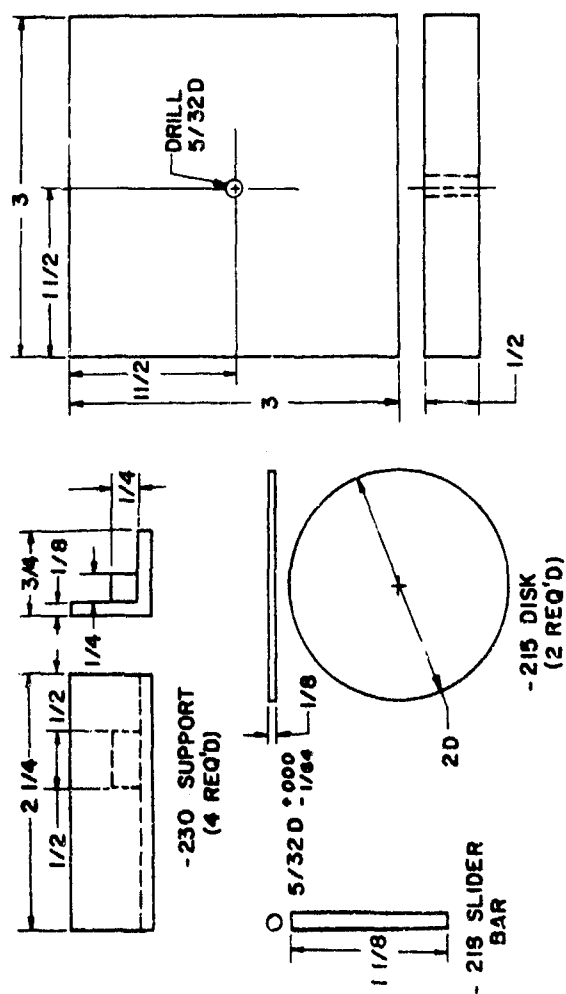
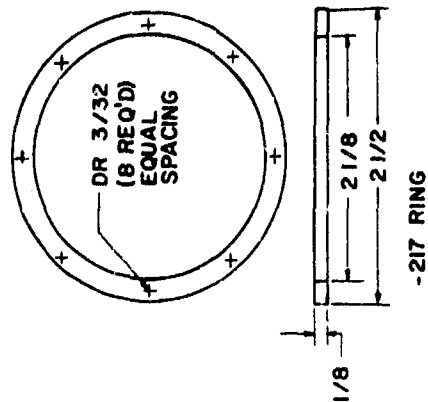
The connectors to be used are of the hub and clamp type and can be obtained from either Gray Tool Company or Cameron Iron Works, Houston, Texas. This hub and clamp unit was chosen because it is definitely stronger than the bubble screen pipe. Other types of quick pipe connectors are made by Thornhill-Craver Company, Houston, Texas, and by Victaulic Company of America, Elizabeth, New Jersey. Their connectors appear as though they might be suitable but strength tests would be required before they could be used. In any of the above cases, assembly would require a minimum of time.

The umbilical pipe will be made by the Action Flex Division of Schott Industries, Elkhart, Indiana. They have the facilities for the manufacture of nylon reinforced neoprene covered flexible sleeves. These sleeves differ from tubes in the absence of reinforcing wires which would hinder fast packaging of the tubing. These sleeves are specially fabricated to have reinforced ends for strength at the attachment points and will hold the design pressure. Each segment is coupled to another through standard hose clamps acting on a rigid tube inserted at the point of attachment. The cross sectional area of these sleeves will be twice that of the bubble screen pipe since they will be connected in a "T" fashion feeding the pipe in two directions.

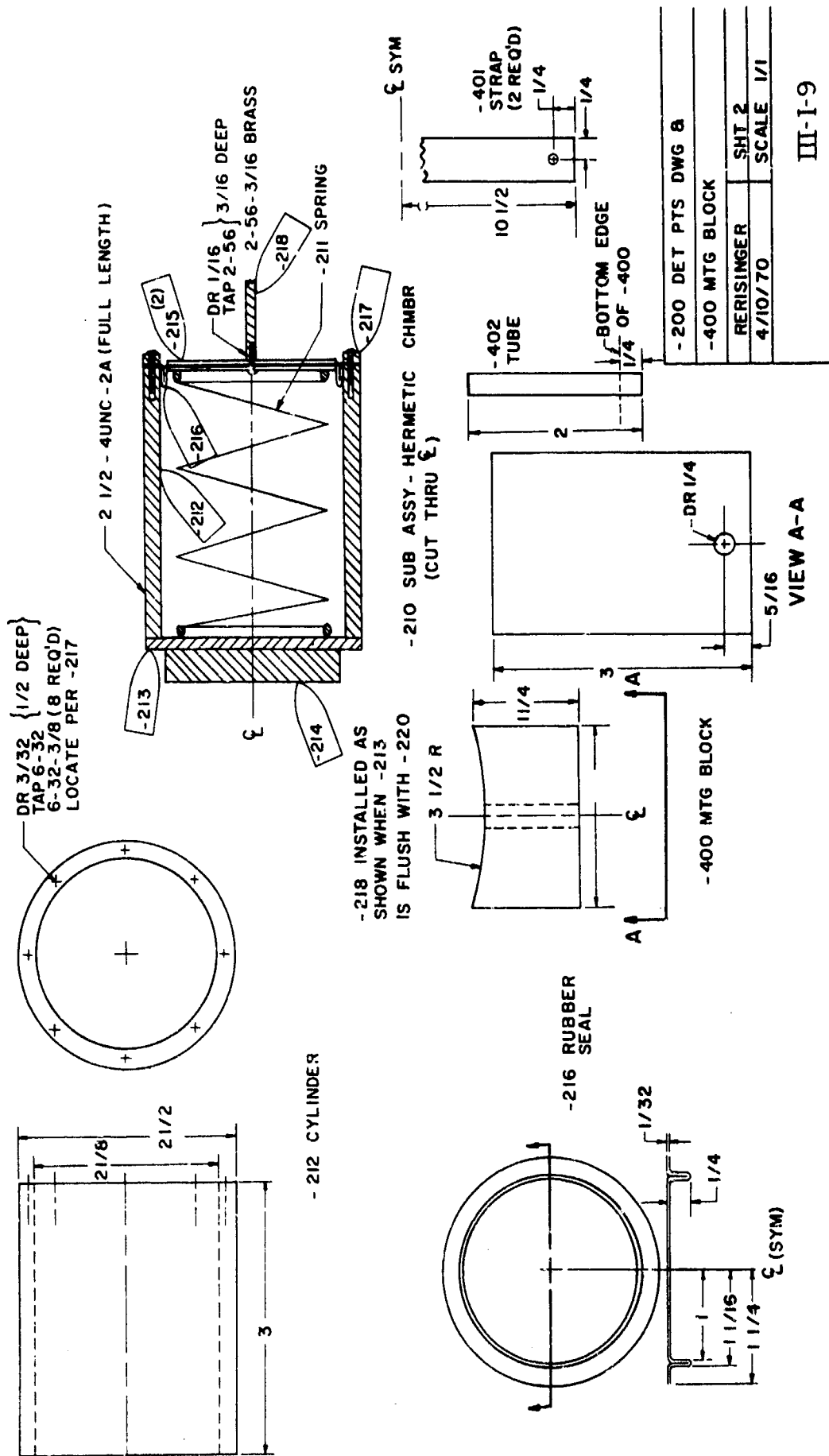
The bubble screen pipe will have a primary and a secondary floatation system. The primary system consists of fluidic logic devices and air bags. The fluidic logic device operates on the air supplied in the pipe and detects the depth. When the pipe sinks below 26 feet, the device switches the air flow

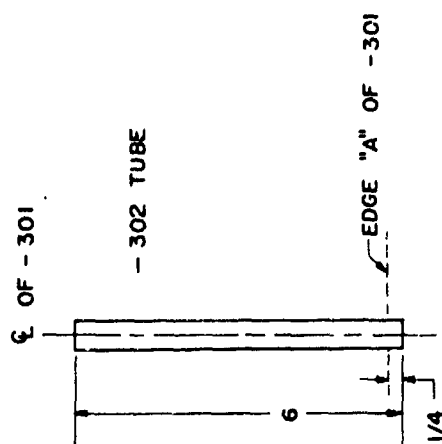
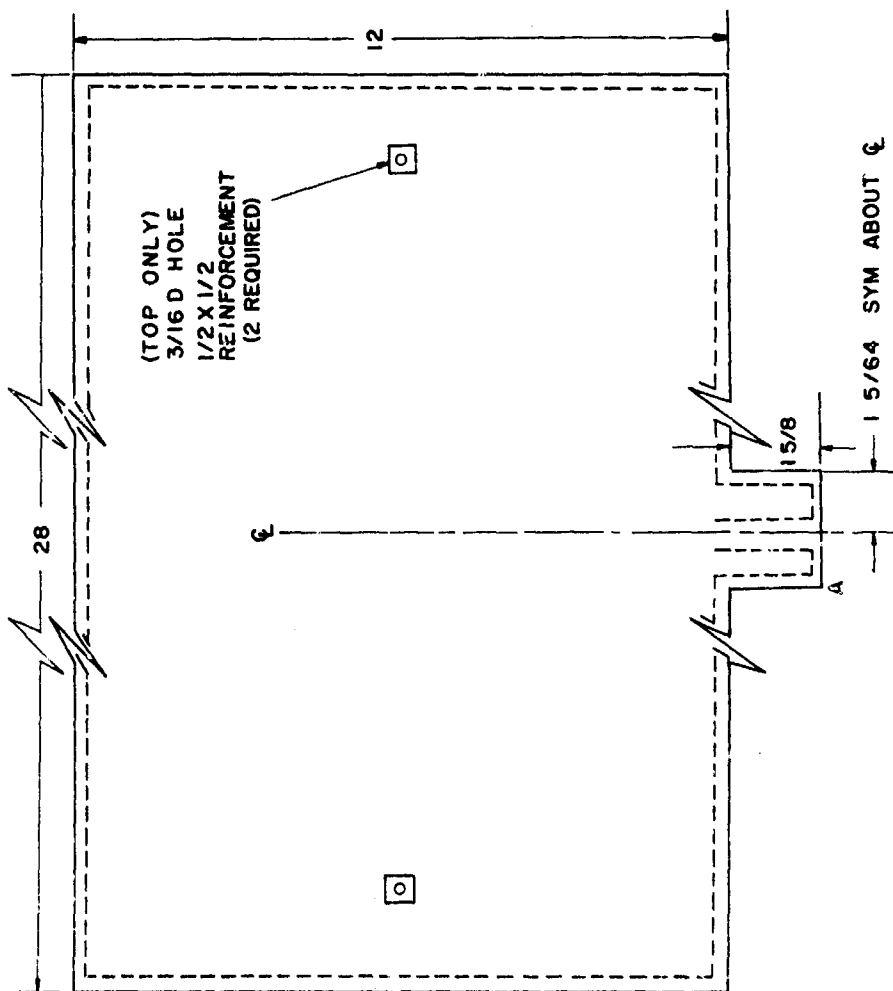
into the air bag, thereby increasing the floatation of the system. When the pipe rises to 24 feet, the air supply to the bag is switched off and it begins to sink again. This tolerance can be reduced with some minor sophistication of the logic device. Drawings for the fluidic logic device are shown in Figs. III-I-6 through 11.

The secondary floatation system is composed of large polyethylene floats attached to the pipe with 36 feet long nylon ropes to provide emergency floatation for the case when the bubble screen pipe is not in operation. The material for these floats is manufactured by Dow Chemical Co. and can be obtained from Kirkland Sales, Dallas, Texas.



- 200 PRESSURE DIFF.	
DETAIL PARTS DWG	
RE RISINGER	
4/9/70	SCALE 1/1
SHT 1 OF 2	





- 300	Float
DETAIL	DRAWING
R. E. RISINGER	
4/5/70	SCALE 1/2

III-I-10

- 301 Float Half
2 IDENTICAL SHTS SEALED ONLY AT
EDGES WHERE DASHED LINE APPEARS

NO	NAME	MATL. SIZE	QTY
101	BASE	2 X 3 X 1/2 PLEXIGLAS	1
102	COVER	2 X 3 X 1/2 PLEXIGLAS	1
103	PLATE	2 X 3 X 1/2 PLEXIGLAS	1
211	SPRING	D _W = 5/32 D _m = 1.35 Nc = 16 SQ = GND K = 2512 ASTM A227 HD	1
212	CYLINDER	3 X 2 1/2 OD X 2 1/8 ID PLEX	1
213	END PLATE	1/8 X 2 1/2 D PLEXIGLAS	1
214	INDICATOR	2 X 3/8 X 1/4 PLEXIGLAS	1
215	DISK	2 X 1/8 D PLEXIGLAS	2
216	SEAL	1/32 X 3 D RUBBER	1
217	RING	1/8 X 2 1/2 D PLEXIGLAS	1
218	SLIDER	1 1/2 X 5/32 D PLEX ROD	1
220	SHELL	3 X 3 X 3 PLEXIGLAS	1
230	SUPPORT	2 1/4 X 3/4 X 1/8 L-PLEX 1/4 X 1/4 X 1/2 PLEX	4 4
240	PLATE	3 X 3 X 1/2 PLEXIGLAS	1
301	FLOAT HALF	14 X 28 X 1/32 RUBBER	2
302	TUBE	6 X 1/2 OD X 3/8 ID FLEX VINYL	1
300	FLOAT	RUBBER CEMENT STITCH	
400	BLOCK	1 1/4 X 2 X 3 PLEXIGLAS	1
401	STRAP	1/8 X 1/2 X 21 VINYL STRAP	2
402	TUBE	2 X 1/4 OD X 1/8 ID FLEX VINYL	1
210	SCREW	5 - 32 - 3/8 BRASS MCH SCR	8
210	SCREW	2 - 56 - 3/16 BR MCH SCR	1

1
2
3
1

NO	NAME	MATL. SIZE	QTY
220	SCREW	8 - 32 - 3/4 BR MCH	1
220	NUT	8 - 32 WING NUT	1
ASSY	SCREW	8 - 32 - 3 BR MCH	2
ASSY	NUT	8 - 32 WING NUT	2
ASSY	SCREW	8 - 32 - 2 1/2 BR MCH	3
ASSY	PLEX BOND	ETHYLENE DICHLORIDE	

FLUIDIC DEPTH CONTROLLER
LIST OF MATERIALS
R.E. RISINGER
4/15/70
III-I-11

2. Packaging

The Heavy Duty System will be stored in four subsystem packages:

Package I - Machinery - This package will consist of a turbine-driven compressor, a machinery hull, a cradle and a pallet. The estimated weight will be 21,000 lbs.

Package II - Inflatable rubber fuel tanks.

Package III - Bubble Screen - This package will contain a complete set of 200 feet of pipe sections, clamps, one umbilical and floats. Approximate weight is 3,000 lbs.

Package IV - Mooring - This package will contain four anchor and mooring lines to connect the bubble generators, and machinery hulls as shown in Fig. III-I-1. Approximate weight is 12,000 lbs.

All packages will be secured to standard C-130 aircraft pallets. The packages will be removed from storage and transported to the C-130 aircraft by a 25K aircraft cargo loading truck, Fig. III-I-12. The packages will be ground-winched onto the C-130. Three aircraft will be required for each 200 foot module of bubble barrier. The aircraft will fly to an airport near a port close to the oil spill. The packages will be offloaded onto flat bed trucks for transportation to docks or Coast Guard station. Packages III and IV will be loaded onto a buoy tender. Packages I and II will be set in the water. Jet fuel tank

trucks will load 120,000 gallons of fuel into the fuel bags. This is an eight day fuel capacity. Estimated time for transport and loading will be two to four days depending on the availability of buoy tenders.

Because of the towing characteristics of the fuel tank, the tenders will require from six to 24 hours to reach the spill site.

Best Available Copy

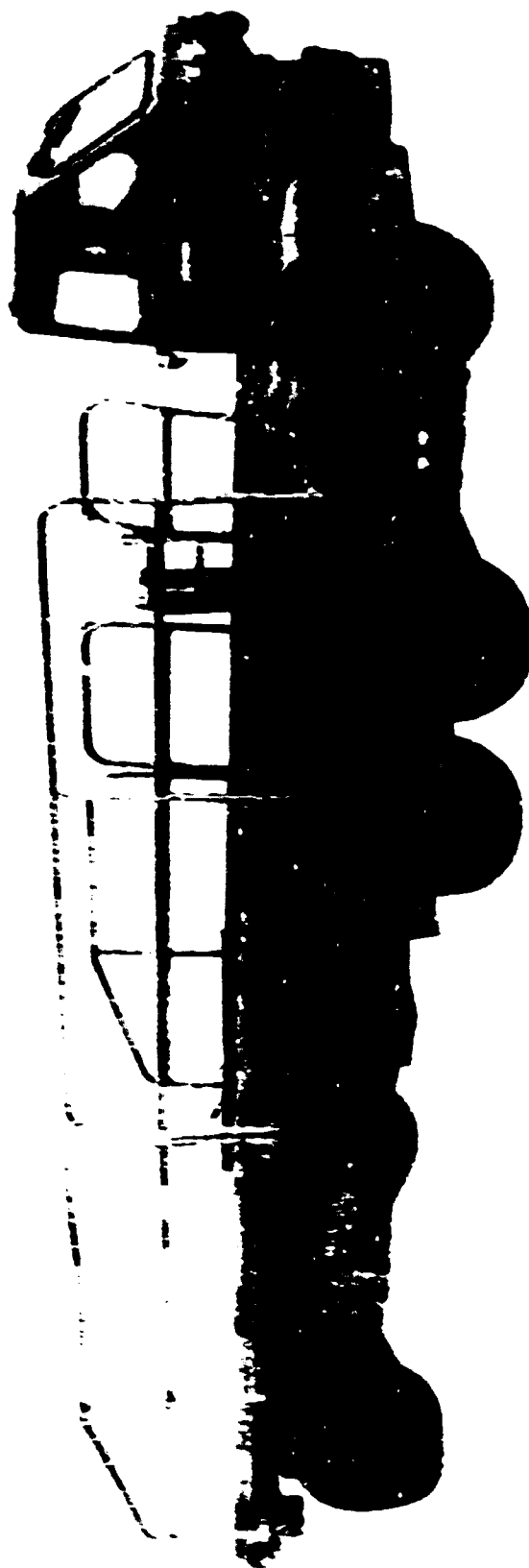


Figure 11-12
M541 Truck, Aircraft Cargo Loading - 35K

III-II. STUDY OF SUITABLE MATERIALS

General Comment

Material mechanical properties are, in general, dependent upon temperature, time (rate of load application or time in service), environment (chemical and organism effects), stress state (tension, compression, uni-, bi-, or triaxial loading conditions), and stress history (processing effects, number of load cycles, packaging forces).

In order to assess system structural integrity, it is necessary to know the structural behavior of the material of which the system is to be constructed. Material structural behavior is, as indicated above, a function of the type of system, its loads, environmental situation, etc., in which it is to be used.

Successful system designs result, therefore, from continuing iteration in design and materials selection. Design perturbations, fortunately, get smaller and smaller with each successive iteration.

Materials study tasks, thusly, never become "finished" until the "final" design is accomplished. Even then, and especially as the designs are implemented, service life data must continue to be accumulated so that both storage and service life may be precisely established.

Objectives

General statement of the principal task involved in

material testing: To establish the material's response to mechanical, thermal, and environmental loading conditions, and to assure structural integrity throughout the service and storage life. In each case where published data was in question or where data was lacking, separate tests were carried out. The materials study program was in direct response and in support of each of the major tasks in this program.

Specific Items to be Noted:

(a) Physical Properties

Density
Color (influences sunlight degradation properties:)
Refractive index n_p

(b) Mechanical Properties

Tensile strength, p.s.i.
Elongation, %
Tensile modulus, p.s.i.
Compressive strength, p.s.i.
Flexural yield strength, p.s.i.
Impact strength, ft. lb/inch of notch
Creep behavior
Fatigue life
Hardness
Flexural modulus, p.s.i.
Compressive modulus, p.s.i.

(c) Thermal Properties

Thermal conductivity, difference in temperature, cal./
sec./sq. cm./ $1(^{\circ}\text{C}/\text{cm.})$
Specific heat cal/ $^{\circ}\text{C}/\text{gm.}$
Thermal expansion $1/^{\circ}\text{C}$
Resistance to heat, $^{\circ}\text{F}$
Deflection temperature, $^{\circ}\text{F}$

- 1) 264 p.s.i. fiber stress
- 2) 66 p.s.i. fiber stress

(d) Environmental Resistance Characteristics

Water absorption, 24 hr., 1/8 in. thick., %
Burning rate (flammability), in./min.
Biological fouling potential
Marine boring potential
Marine microorganism attack
Effect of sunlight

Compilation of Data for Material Selection

1. A product guide was established for vendors supplying metals and elastomers of potential use in this program.
2. A directory of manufacturers, which when combined with the product guide, relates a company to a specific material and/or relates a material to companies supplying, and in what form (tubing, wire, sheet, foil, etc.).
3. An inventory of current literature available from manufacturers having to do with design properties, codes, design calculations, corrosion data, fabrication standards, dimensions, cost data, technical descriptions, reference tables, and sales offices.
4. A laminates chart cataloging physical, mechanical, thermal, electrical, and chemical properties of polymeric materials.
5. Creep properties of plastics specifying the nature of the test specimen, test conditions, and creep test data in terms of the creep apparent modules.
6. Temperature dependence of plastics measured by dynamic mechanical properties, dynamic shear modulus and damping factors versus temperature.
7. Charts of foamed plastics relating type of material to mechanical, physical, thermal and chemical properties.

8. Plastics properties charts listing processing characteristics, physical, mechanical, thermal, and electrical properties and the important resistance characteristics such as water absorption, effects of sunlight, effect of oil and other organic solvents.
9. Film charts essentially similar to (8) but specifically for film and sheets.
10. Effects of marine organisms including listings of coatings and encapsulants useful for marine environment.
11. Modes and mechanisms of the deterioration of metals in a marine environment.
12. Charts of foaming agents for all types of plastics.
13. Extensive bibliography on marine, chemical and mechanical degradative influences on materials.

Less general compilations were as follows: (1) catalog of wire rope and cables suitable for a marine environment, (2) methods of welding plastics - heat welding, high frequency heat sealing, and ultrasonic assembly, (3) plastic design guides and (4) engineering reviews of plastics.

The use of plastics in the Texas A&M Heavy Duty Barrier System necessitates that an evaluator have a somewhat sophisticated understanding of plastics and their various interlocking aspects. As it is not feasible to provide insights into the basics of polymer science and technology at every point within this report, the following brief introduction to polymer science is offered. It is designed to provide a basic insight into plastics so that assimilation

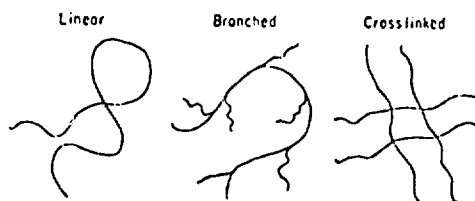
of all that follows is possible. A good general reference for polymer science is found in the Modern Plastics Encyclopedia, 1969-1970, created by the publishers of Modern Plastics Magazine and offered once each year as an encyclopedic volume.

NOT REPRODUCIBLE

What polymers are and associated definitions

The covalent bonding of carbon to carbon, starting with relatively small chemical units (called monomers) which are capable of reacting with one another, results in relatively large molecules called polymers. The unique properties associated with these materials are due to sizeable interactions between the molecules over extended lengths, and over large surfaces.

The repetition of the units in the molecule may be structures *linear* and *chain-like*, and with or without appendage segments called *branches*, or *crosslinked* structures which form three-dimensional, network-type molecules:



It should be noted that the chain-like molecules may have degrees of flexibility and that the primary interactions between the molecules are physical—either in the form of weak van der Waals forces, or the stronger electrical forces associated with polar groups if they are present. The molecules may also be physically entwined one in another, especially when they are quite long and relatively coiled. In this instance, they may be thought of as being represented by a bowl of cooked spaghetti.

The application of energy in the form of heat to such an assembly of molecules causes increased molecular motions, first in the form of segmental motion and later with increased heat, a liquid-like flow where the molecules are free to slide over one another. Such materials are referred to as thermoplastics. Common examples are polyethylene, polystyrene, and nylon.

If, on the other hand, we consider the *crosslinked* structures, where the individual chain segments are chemically attached to one another, then the application of thermal energy does not result in extensive chain mobility, and the polymers do not soften with heat. This type of material is commonly referred to as a *thermoset*. Examples are the phenol or urea formaldehyde polymers, and crosslinked polyethylene. These materials are usually formed initially

in a linear, flowable stage, and then set or crosslinked into final, intractable non-flowing form by application of heat and pressure, radiation, or chemical crosslinking agents.

Our mention of the notion of molecule length or size immediately raises the question of quantifying this characteristic so that it may be significantly discussed in terms of effects on properties. The accepted procedure for referring to this property is through the *molecular weight (MW)* or *degree of polymerization (DP)*. The latter is simply defined as the number of monomer units in the polymer molecule. Its relationship to molecular weight is as shown in the following expression:

$$MW(\text{polymer}) = DP \times MW(\text{monomer})$$

Since every polymer sample actually consists of a mixture of molecular weights, our concern is really with the average molecular weight. Depending upon the method of measurement, we may obtain different averages. The two most commonly considered are the number average, M_n , and the weight average, M_w . The former is derived from measurements which effectively count the number of particles, while the latter is based on such methods as light scattering where large sized particles contribute more strongly to the observed effect. Thus the average is weighted toward higher values.

For an idealized case where all molecules are of the same size, M_n would equal M_w . However, since this is not true,

in practice, the ratio is of $\frac{M_w}{M_n}$ gives an indication of the breadth of distribution of molecular weight species in a sample. As $\frac{M_w}{M_n}$ increases, the molecular weight distribution is broader.

The DP or the molecular weight can have an important effect on properties. As either increases, the molecular size increases and provides greater opportunity for molecular interactions.

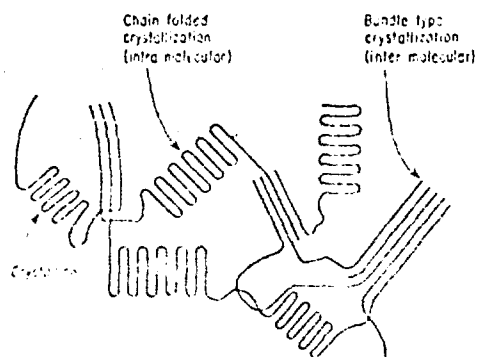
For the sake of orientation, we may consider a series of linear polymers based on the gas ethylene C_2H_4 . In the low DP range, the polymers are liquids; as the DP rises, the products become greases and waxy solids; only when we get to a DP of several hundred do we start to achieve the characteristic properties associated with a plastic—toughness along with strength and flexibility. If we assume a molecular model where each ethylene unit is 1.2-in. long, a 600 DP molecule fully extended would have a length of 72 feet. One can now see how appropriate it is to think of these molecules as long, thread-like or chain-like structures, and it becomes easy to visualize that a mass of such molecules would, indeed, have great probability of physical entanglement and interaction.

NOT REPRODUCIBLE

Amorphous polymers do not exhibit structural order among the chains. There are not regular repeating spacings or distances between the molecules. These polymers are usually made up of molecules which are irregular in shape, which cannot pack in an ordered fashion, and which may be thought of as a mass of cooked spaghetti:



Crystalline polymers are characterized by the capability of their molecules, or more correctly segments in their molecules, to form three-dimensionally ordered arrays exhibiting characteristic inter- or intra-molecular spacings:



It must be recognized that because of the lengths of the crystalline molecules, polymers almost never achieve a degree of order equivalent to those observed in low molecu-

lar weight crystalline materials. The normal chain entanglements, crossovers, and kinks which, incidentally, increase with chain length or molecular weight, cause a degree of disorder, even in polymers which are highly crystallizable. This disorder is equivalent to amorphous structure, and may constitute from about 5% to 95% of the total volume. Further, it must be noted that the melt of a crystallizable polymer may be quenched (cooled rapidly) to a temperature below its melting point, and thereby freeze in the disordered amorphous structure associated with the melt. If the molecules are then kept at a temperature where they are capable of limited segmental motion (above T_g , as discussed later) this will eventually result in development of crystallinity.

The size, shape, and amount of crystalline material within a polymer plays an important role in affecting properties, and will be discussed later.

Another important structural state is oriented polymer molecules, developed by subjecting the molecules to uniaxial stress, thereby aligning them in the direction of the stress.



This may be done with amorphous or crystalline polymers, and in both cases the properties in the direction of molecular alignment differ from those at right angles to the alignment direction. This is the basis of fibers, where advantage is taken of high strengths in the direction of orientation achieved by stretching the polymer fibers.

Mechanical properties

To a large extent polymers find their usefulness due to their mechanical properties, and these include their stress-strain (or tensile elongation) and stress relaxation (or ten-

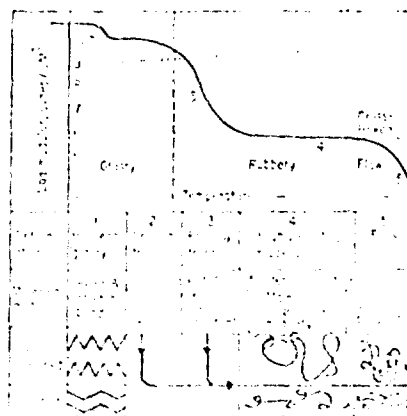


Fig. 2 A characteristic curve of modulus vs. elasticity vs. temperature, and of associated molecular motions of polymer chain.

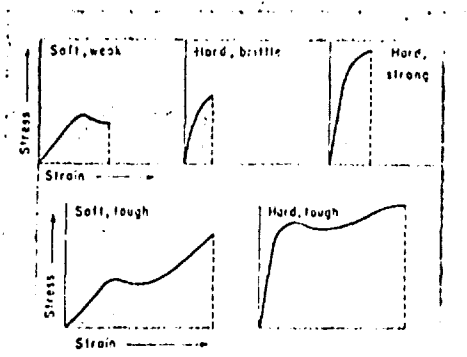


FIG. 2. Sample stress-strain curves for different types of plastics materials.

sile-time) behaviors. The latter often manifests itself as creep properties, and is essentially a manifestation of the visco elastic property of polymers. The former is usually represented by stress-strain curves, and may conveniently be separated into various types of behavior such as those indicated in Fig. 2.

It should be noted that soft, weak materials (amorphous polymers at a temperature above T_g) show low stress values (low tensile) accompanied by relatively low strain (elongation). The initial slope is rather shallow, indicating a low modulus. In marked contrast, a hard, brittle material (amorphous polymer below T_g) shows moderate tensile, but very low elongation, and a high initial slope which is an index that the modulus is very high. The area under the curves is the integral of force acting through a distance, and therefore is an index of the energy absorption capability of the material before failure. The greatest area under a curve is for the hard, tough material which is capable of having its chains straightened out under the influence of the stress, yet maintains enough molecular entangling points so as not to slip, thereby giving high elongation along with high strength.

This latter type curve is most usually found for high molecular weight crystalline materials. Here the long chain length maximizes entanglement and tie points between crystalline regions. The latter, of course, provide the high strength because of the constructive effect of the intra and inter molecular crystalline forces. Most of the other important properties may be equally well understood on the basis of the structure of the polymer.

Hardness is related to T_g and crystallinity. Below T_g , materials tend to be hard because molecular motion is frozen in. But above T_g the materials tend to be softer. For crystalline materials, however, because of the close packing of chains, hardness usually is related to degree of crystallinity. Since lower molecular weight materials may crystallize more readily with a given thermal treatment, they tend to be harder than a higher molecular weight version of the same polymer.

Elasticity depends upon the ability of *disordered*, kinked chain segments to be straightened out under influence of stress, and is associated with materials above T_g . Thus highly crystalline materials would be expected to exhibit less elasticity than would materials having lesser crystallinity.

Impact strength is related to energy absorption. Materials below T_g are generally low in impact strength. There is a notable exception in bisphenol polycarbonate, which has a high impact strength at room temperature in spite of having a T_g of about 150° C. This phenomenon has been explained by the energy absorption capability associated with the rotation of the phenyl rings in the backbone of the chain.

From a structural property point of view, we may summarize some more important properties features as follows:

1) *Stiff chains* (those containing large side groups or phenyl groups within the chain) tend to have a higher T_g and, if they are crystallizable, tend to have high melt temperatures. Chains that can crystallize, and which have polar groups, have high melting points.

2) *Regular chains* (those having stereoregular structure or simple regular structure) can crystallize most readily.

3) *Effect of molecular weight*:

a) *on crystallinity*: shorter chains are more mobile and may crystallize more rapidly and to a greater extent;

b) *on melt flow properties*: longer chains have a very large effect on (M_v) in increasing melt viscosity;

c) *on physical properties*: many properties, such as density, increase with molecular weight and reach relatively constant value at moderate molecular weight. Toughness, however, increases with increasing molecular weight because of the greater tendency to have chain interactions.

NOT REPRODUCIBLE

Mechanical Behaviour of Plastics*

Direct use of most data presented in the majority of available physical properties of plastics charts can cause serious problems if the behaviour of a material and the effect of time, temperature, and other variables are not understood.

Plastics materials, unlike metals, are not elastic; they are viscoelastic. As a result, stress-strain curves determined by standard ASTM tests are difficult to interpret correctly because ultimate properties and time at failure do not give a true indication of the performance of plastic material.

Thus, a plastic material may follow any one of the time-stress-strain curves in Fig. 1 depending on temperature conditions. This figure shows the proportional limit, the point at which the modulus line determined in tensile tests diverges from the

actual curve, which determines the continuous loading possible for a particular plastics material. All parts designed to this proportional limit will be 100% safe; all parts designed to the yield point strength or break point will fail.

Creep. Engineers have always needed an equation by which long-term creep of any material could be predicted, but such an equation is not completely possible because of the many factors which must be considered. At present, the most precise method of determining such data is the long-term test of various levels of stress and temperature. For example, Fig. 2 gives comparative creep curves under one set of conditions; curves for different conditions are available from manufacturers of the materials.

Apparent modulus. Determined in conjunction with creep, apparent modulus represents the actual strain at a given stress level over a designated per-

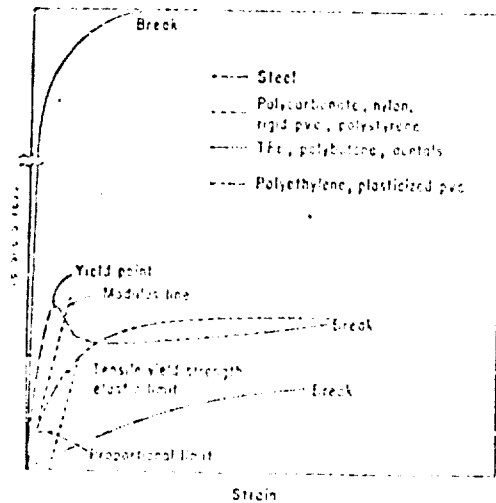


FIG. 1: Three typical stress-strain curves.

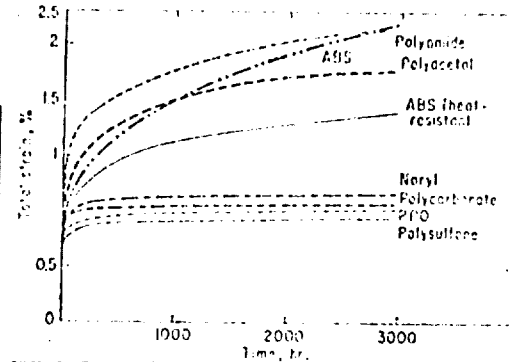


FIG. 2: Comparative creep behavior at 73° F.

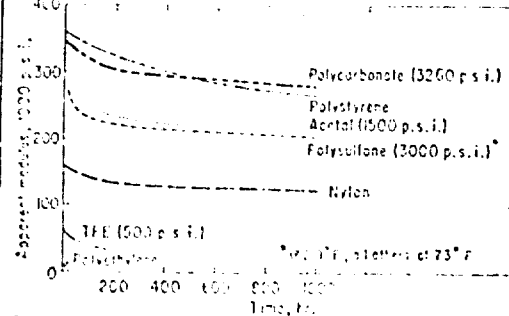


FIG. 3: Variation of apparent modulus with time.

NOT REPRODUCIBLE

iod of time. Figure 3 gives apparent modulus vs. time at room temperature for different materials.

Creep and apparent modulus can be used to determine deflections over a given period. A true creep-resistant material would have no change in deflection, and its apparent modulus would be equal to an instantaneous modulus. Figures 2 and 3 indicate that plastics materials differ greatly and that, if creep is important for a particular application, the various materials should be checked to determine which one will give best results.

Tensile modulus: Figure 4 shows how tensile modulus (by ASTM procedures) varies from plastic to plastic. Tensile, compressive, flexural, and shear strengths of these materials vary greatly with temperature. It must be remembered that strengths shown in property charts are instantaneous values at room temperature.

Impact: Data on impact strengths of various

plastics and metals are valid only for direct comparisons; they have little value otherwise because impact resistance of a finished part depends so much on part shape, impact rate, and other considerations. Prototyping testing is far more important.

Allowable working stresses: In general, working stress values are not included in available properties charts, so Fig. 5 compares some of the engineering plastics according to values obtained from the various manufacturers. It demonstrates the changes which occur when temperature is raised. The curves show how the allowable continuous load of a part decreases with rising temperature, and that the allowable continuous stresses for plastics are far below the instantaneous strength values shown in properties charts. Yet, the continuous stress limits are the values to which plastic parts must be designed if short-term part failure is to be avoided.

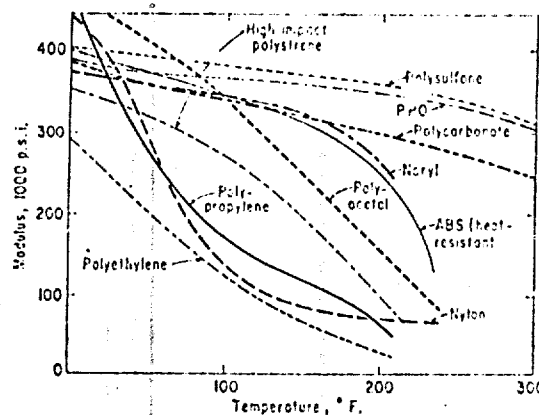


FIG. 4: Tensile modulus vs. temperature.

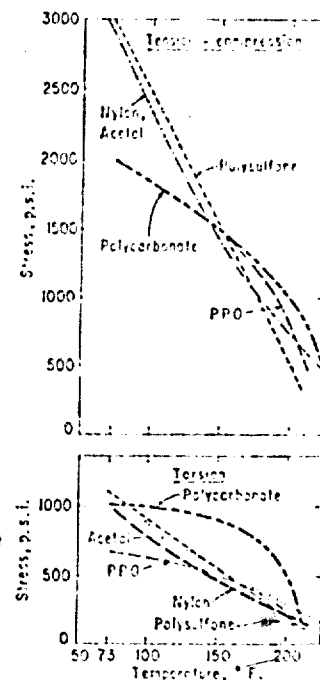


FIG. 5: Continuous allowable stress vs. temperature.

NOT REPRODUCIBLE

Main floor material

the urethane foams

Urethane foam has become one of the

most versatile materials in the entire spectrum of plastics. Foams generally are produced by mixing two or more liquids which expand to form the cellular structure. By varying the propor-

NOT REPRODUCIBLE

tions or components of the liquids, and by the inclusion of various additives, foams may be produced which have densities ranging upward from less than 1 lb./cu. ft. to about 70 lb./cu. ft.,

with an almost limitless range of chemical and mechanical properties.

Contributing to urethane's usefulness is the simplicity with which it is produced. The liquid components may be mixed by hand in paper containers and poured into a cavity where they foam and adhere with great tenacity to the inside walls. This foam can be poured into a mold that has been treated with a wax or other releasing compound; it is adaptable to mass production with the use of foam-producing machinery; it can be sprayed on horizontal, vertical, or convolute surfaces, or applied as preformed slab stock.

Because of these qualities and its ease of application, urethane is now being used in scores of industries where it has proved to be unsurpassed.

Foams can be produced that have flexible, open cell structures like that of foam rubber, or produced with closed cell structures that tend to be completely rigid.

There are two basic types, polyether-based and polyester-based. The polyether class is generally less susceptible to the effects of humidity; the polyesters are losing their positions of higher temperature stability and strength-to-weight ratio to the newer polyethers. Both types may be produced in densities from less than 2 lb./cu. ft. up to the solid polymer weighing 75 lb./cubic foot.

Rigid foams

Rigid foams have an excellent strength-to-weight ratio, extremely low thermal conductivity, and a range of remarkably useful compressive, shear, tensile, and flexural strengths.

Other qualities which make the rigid foam desirable in many fields are its high dielectric strength, resistance to flame (with additives), very low water vapor transmission and water absorption, good vibration resistance and resistance to oxygen, and to most solvents and dilute acids. It is not attacked by fungus, is inert and non-abrasive, that will not adversely affect substrates or metals which it contacts.

Some of its more striking applications include use in the crushable landing pads of the Surveyor moon ship, for increasing the stopping power of naval armor, at the same time making the ships unsinkable; for raising of sunken ships; for component support in atomic warheads, and in construction of houses.

Urethane foam's most important and useful application is in the field of ther-

mal insulation. It is the most efficient insulation known today, with a K Factor (Btu in./sq. ft. °F. hr. at 75 °F.) ranging between 0.11 and 0.14 in densities from 1.5-3 lb./cu. foot.

Almost equally important attributes are such as effective operation as measured by production, compatibility (cost in time, labor and energy—all of which mean money), and end use efficiency (effectiveness, long term integrity, maintenance, resistance to various environments, and effect on operational costs), in which urethane insulation excels.

These advantages have led those industries whose efficient operations are linked closely to precise temperature control, to specify urethane foam for nearly all their insulation needs. These industries include manufacturers of household refrigerators and freezers, commercial walk-in and reach-in coolers, refrigerated vans and railway cars, hot and cold service rail and truck tankers, and storage vessels and piping for refineries, liquefied gas plants, and the chemical process industries.

The marine industries are incorporating rigid urethane foams for insulation and flotation into both new work and renovation. The construction industry is turning, although slowly, to urethane foams for the solution of problems with which traditional materials have been unable to cope.

Flexible foams

Flexible foams to date have almost replaced foam rubber as cushioning in mattresses, pillows, and in various other applications. This revolution in the furniture field was brought about by the superior chemical and physical qualities of the flexible urethane, in much the same manner as rigid urethanes have replaced many materials in other areas.

As with the rigid foams, there are two types of flexible foams—polyether-based and polyester-based. Both have many similar properties, but often have wide differences in resistance to the various environments in which they are placed.

Polyethers are noted for their resilience and are therefore used primarily as furniture cushioning, whereas polyesters are used mainly in packaging because of their superior shock absorbing characteristics.

The densities of both types range from about 1-30 lb./cu. ft., thus giving consumers a wide range of choices. Both flexible foams are available as

white or colored slab stock in sizes up to 76 in. wide by 30 in. deep in unlimited lengths, in a wide range of densities and flexibility. These slabs, or "buns," can be cut to any dimension within these limitations and in thicknesses down to less than 1/8-inch. The materials can be cut with a knife or common woodworking power tools, but more usually are cut with specially designed slitters, and can be cemented together with almost any type of adhesive. Both flexible foams now also may be molded or foamed-in-place in large volume.

Chemical and physical properties which make the use of flexible urethane foams so advantageous include:

Light weight and high strength-to-weight ratio; an even cell structure and smooth texture; a high resilience and elasticity under dynamic pressures, with excellent resistance to tearing, abrasion, creep, and flexural stresses. There is little compression set. Foams may suffer no permanent degradation of physical properties from exposure to temperatures from 30-250° F.

Polyether-based foams have been the general choice in the furniture industry over the past several years because they are less flammable, and have greater stiffness and tensile strength than synthetic rubber foams. Flame retardants may be added to both polyethers and polyesters so that they can be classified as "self-extinguishing."

Unlike rigid foams which generally have the same overall resistance to various chemicals and solvents, the two types of flexible foams react in different degrees to various chemical environments. Both foams are swollen when immersed in chlorinated solvents, aromatics, ketones, esters, and alcohol, but generally return to their original shape when removed from these liquids and dried. Polyesters have a better resistance to these solvents than polyethers, and are relatively unaffected by hydrocarbons and vegetable oils. Both foams are considerably damaged by strong acids and bases, often to the point of destruction, because of their better solvent resistance; and, therefore, cleanability—polyester flexible foams are widely used in textiles.

Marine applications

The extraordinary flotation properties of rigid urethane foam account for its widespread use in the marine field. Two-lb. density urethane has about 60 lb. of buoyancy for every cu. foot. It is not affected by salt water, gasoline or oil, and absorbs no water.

It is now used as a construction material for boats, pontoons, buoys, and floats and docks, generally in conjunction with a polyester-impregnated glass fiber covering.

The potential of the foam in this area has proven to be so provocative that one of the basic goals of the Navy's new SEALAB was the testing of urethane in underwater environments. Most of the tests concerned the salvage of boats, aircraft, and other equipment from the ocean floor. All of these tests proved successful.

Miscellaneous applications

Miscellaneous uses of urethane also are legion. It is now being used to construct lightweight radar antennas up to 60 ft. in diameter and having high resolution, ease of maintenance, and the advantage of being manufacturable on-site, in remote areas, with appropriate machinery. In more than 200 mines throughout the nation urethane is applied by the spray method to inhibit weathering of coal ribs, to improve ventilation by sealing off areas of gas seepage, for preventing the freezing of pipes during winter, for caulking shafts, for erecting fire seals, etc.

The foam also is now an indispensable material for creating such diverse products as model terrains, replacing papier mache, and is used as a medium

by sculptors . . . and even as a fishing lure. A piece of flexible urethane impregnated with crushed salmon eggs has been found to be irresistible to steelhead trout.

Urethane also is proving its worth in the oil industry. Hot oil tanks and associated equipment are increasingly being insulated with urethane, either by applying battens to the tanks or by spraying the tanks with foam. In one test, distillate pumped into a urethane insulated tank maintained a required

temperature of 180° F. or above for 3 wks., without the company having to activate its steam heating equipment.

Though relatively more expensive than conventional packaging materials, urethane foams—both flexible and rigid—are slowly invading areas of the packaging field where their physical properties are needed, or where the foam-in-place technique is advantageous. A special friable foam is used to package large objects containing delicate equipment. The foam crushes at a

predetermined rate during heavy shock, protecting parts from destructive vibration. The packaging of the Polaris missile is an example.

A new method of packaging military equipment destined for areas without docking facilities has been developed. The equipment is placed in a sealed polyethylene bag suspended in a carton, and the voids around it are foamed in-place. Such a carton may be jettisoned overboard during an incoming tide, and will float ashore—End

NOT REPRODUCIBLE

Handy product

Summary of Properties

POLYTETRAFLUOROETHYLENE (Teflon)

Specific gravity (density)	2.14 - 2.20
Specific volume, cu. in./lb.	12.9 - 12.5
Tensile strength, p.s.i.	2000 - 5000
Elongation, %	200. - 400.
Tensile Modulus, 10^5 p.s.i.	0.5
Impact strength ft. lb./in. of notch (1ZOD Test)	No break
Hardness, Rockwell	R25
Thermal expansion, $10^{-5}/^{\circ}\text{C}$	8.0 - 10.5
Resistance to heat, $^{\circ}\text{F}$ continuous	400
Water absorp., 24 hr., 1/8 in. thick %	0.01
Burning rate (flammability), in./min.	None
Effect of sunlight	None
Effect of organic solvents	None

POLYURETHANES

Specific gravity (density)	1.11 - 1.25
Specific volume, cu. in./lb.	24.0 - 22.0
Tensile strength, p.s.i.	5,000 - 9,000
Elongation, %	10 - 650
Tensile modulus, 10^5 p.s.i.	0.1 - 3.5
Compressive strength, p.s.i.	20,000
Flexural yield strength, p.s.i.	700 - 9,000
Impact strength, ft. lbs./in. of notch (IZOD Test)	Does not break
Hardness, shore	48A - 8CD
Flexural modulus, p.s.i. x 10^5	3.2 - 3.5
Compressive modulus, p.s.i. x 10^5	0.04 - 0.09
Thermal conductivity, 10^{-4} cal./sec./ sq.cm., / 1(degrees centigrade./cm.)	1.7 - 7.4
Thermal expansion, $10^{-5}/^{\circ}\text{C}$	10.0 - 20.0
Resistance to heat, $^{\circ}\text{F}$ continuous	190
Water absorption, 24 hrs., 1/8 in. thick %	0.7 - 0.9
Burning rate (flammability), in./min.	Slow to self extinguishing
Effect of sunlight	None - yellows slightly
Effect of organic solvents	Resists most solvents

POLYETHYLENE

Specific gravity (density)	0.941 - 0.965
Specific Volume cu. in./lb.	29.6 - 28.8
Tensile strength, p.s.i.	3,100 - 5,500
Elongation, %	20.0 - 1000.0
Tensile Modulus, 10^5 p.s.i.	0.6 - 1.8
Compressive strength, p.s.i.	2,700 - 3,600
Impact strength, ft. lbs./in. of launch (IZOD Test)	0.5 - 20
Hardness, shore	D60 - 70
Flexural modulus, p.s.i. $\times 10^5$	1.0 - 2.6
Thermal expansion, $10^{-5}/^{\circ}\text{C}$	11.0 - 13.0
Resistance to heat, $^{\circ}\text{F}$ continuous	250
Water absorption, 24 hrs., 1/8 thick %	less 0.01
Burning rate (flammability), in./min.	Very slow to self extinguishing
Effect of sunlight	Unprotected material crazes rapidly. Requires light for complete protection but weather resistant grades are available in natural and color
Effect of organic solvents	Very resistant to oils and seawater below 80°C

NYLON

Specific gravity (density)	1.12 - 1.14
Specific volume, cu. in./lb.	24.8 - 24.2
Tensile strength, p.s.i.	7,000 - 13,000
Elongation, %	100 - 320
Tensile modulus, 10^5 p.s.i.	1.1 when saturated with water to 4.5 when dry
Compressive strength, p.s.i.	6,700 - 13,000
Flexural yield strength, p.s.i.	5,000 - 15,000
Impact strength, (IZOD Test)	0.8 - 5.5
Hardness, Rockwell	R103 - R119
Flexural modulus, p.s.i. $\times 10^5$	0.8 - 1.4 (2.5% H_2O) to 3.7 - 4.0 (0.2% H_2O)
Compressive modulus, p.s.i. $\times 10^5$	2.45 - 2.48
Thermal expansion, $10^{-5}/^{\circ}C$	8.3
Resistance to heat, $^{\circ}F$ continuous	175 - 250
Water absorption, 24 hrs., 1/8 in. thick %	1.3 - 1.9
Burning rate (flammability), in./min.	Self extinguishing
Effect of sunlight	Discolors slightly
Effect of organic solvents	Resistant to oil and seawater

POLYVINYL CHLORIDE

Specific gravity (density)	1.35 - 1.45
Specific volume, cu. in./lb.	20.5 - 19.1
Tensile strength, p.s.i.	5,000 - 9,000
Elongation, %	2.0 - 40.0
Tensile modulus, 10^5 p.s.i.	3.5 - 6.0
Compressive strength, p.s.i.	8,000 - 13,000
Flexural yield strength, p.s.i.	10,000 - 16,000
Impact strength, ft. lbs./in. (IZOD Test)	0.4 - 20
Hardness, Shore A:	50 - 100
Thermal expansion - 10^{-5} °C	7.0 - 25.0
Resistance to heat, °F continuous	150 - 175
Water absorption, 24 hrs, 1/8 in. thick %	0.15 - 0.75
Burning rate (flammability) in./min.	Slow to self extinguishing
Effect of sunlight	Slight
Effect of organic solvents	Extremely resistant to alcohols, aliphatic hydrocarbons and oils

III-III System Characteristics

1. Barrier's Oil Retention Capability

The pneumatic barrier proved to be substantially effective for the imposed environmental conditions specified by the U. S. Coast Guard. The depths of oil contained for different pneumatic barrier design conditions and for three different oil specific gravities are presented in Figs. III-III-1 and III-III-2. For example in Fig. III-III-1 which is valid for the design conditions, the depth of oil contained will depend greatly on the specific gravity of the oil as shown in the following table:

TABLE III-III-1.1
FOR 2 KNOT CURRENT

Specific Gravity of Oil	Depth of Oil Contained (ft.)
0.75	0.225
0.85	0.370
0.95	1.140

If a 50% design current value is used (or a current of 1 knot instead of 2 knots) the following depths of oil will be contained:

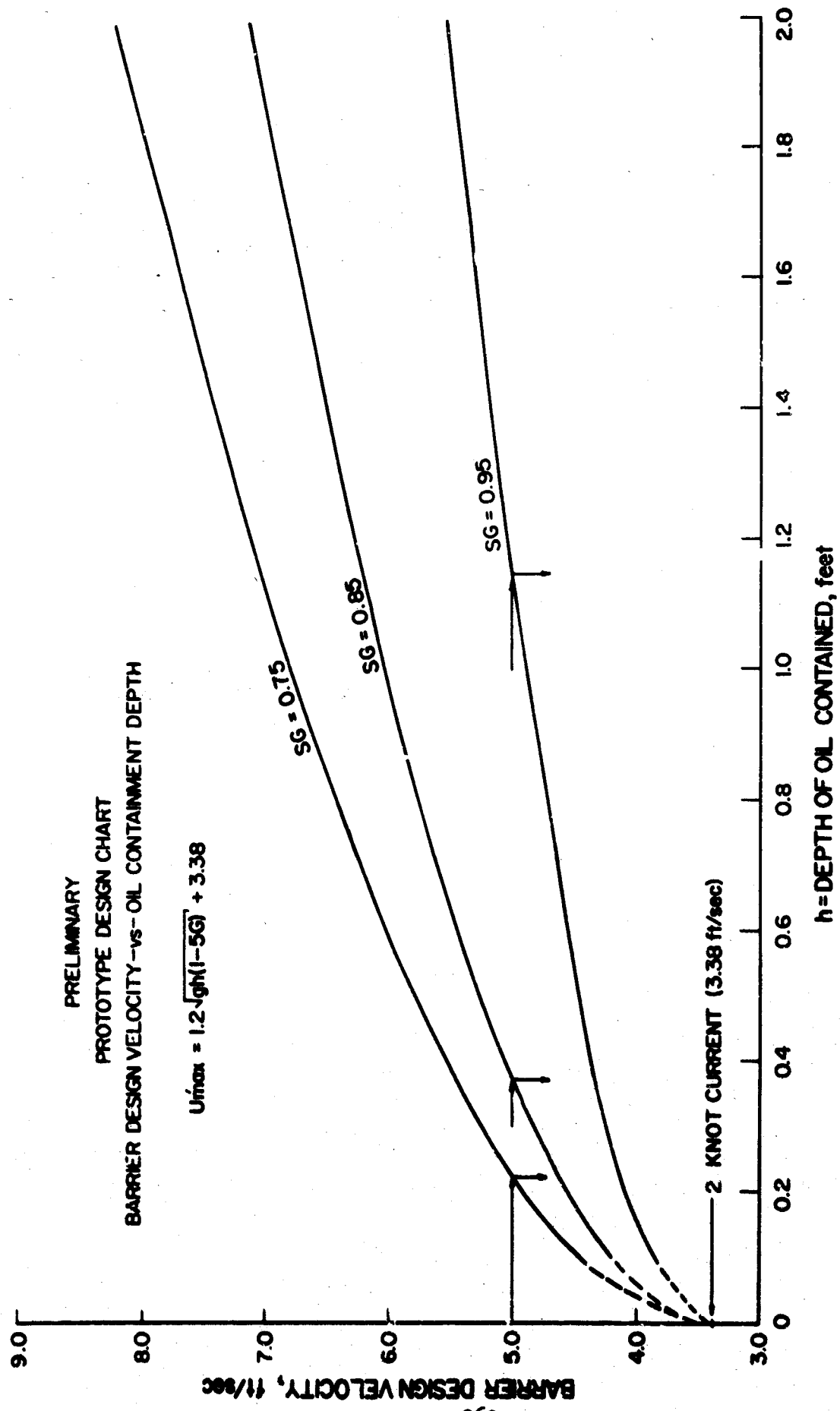
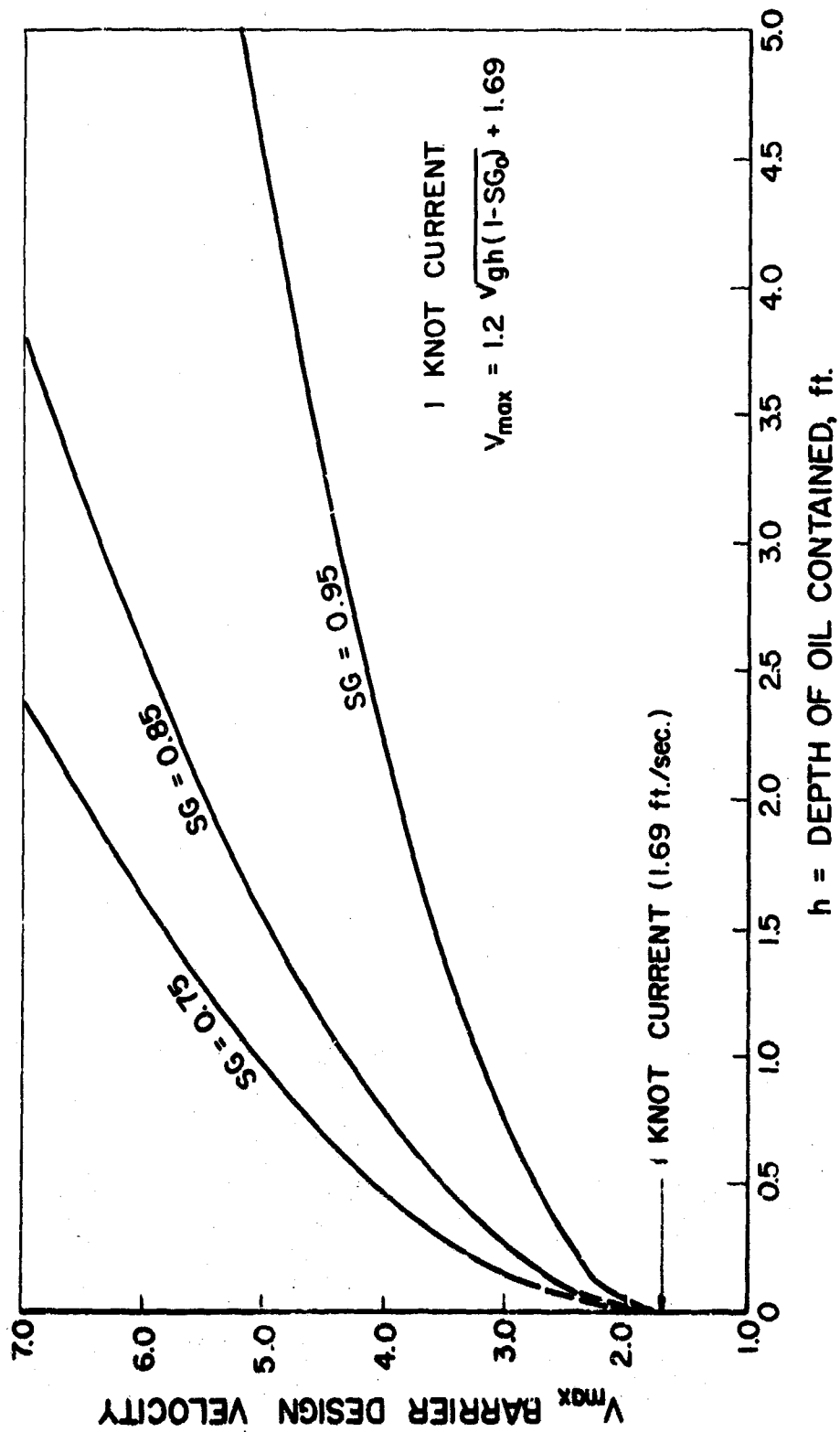


FIG. -RECOMMENDED PROTOTYPE DESIGN CHART
III-III-1 U_{max} versus h



III-III-2

TABLE III-III-1.2

FOR 1 KNOT CURRENT

Specific Gravity of Oil	Depth of Oil Contained (ft.)
0.75	0.95
0.85	1.55
0.95	4.60

If the current produced by the pneumatic barrier is reduced to one-half (thus reducing the air discharge and horsepower requirements) the following table would apply:

TABLE III-III-1.3

FOR 1 KNOT CURRENT

Specific Gravity of Oil	Depth of Oil Contained (ft.)
0.75	0.29
0.85	0.48
0.95	1.33

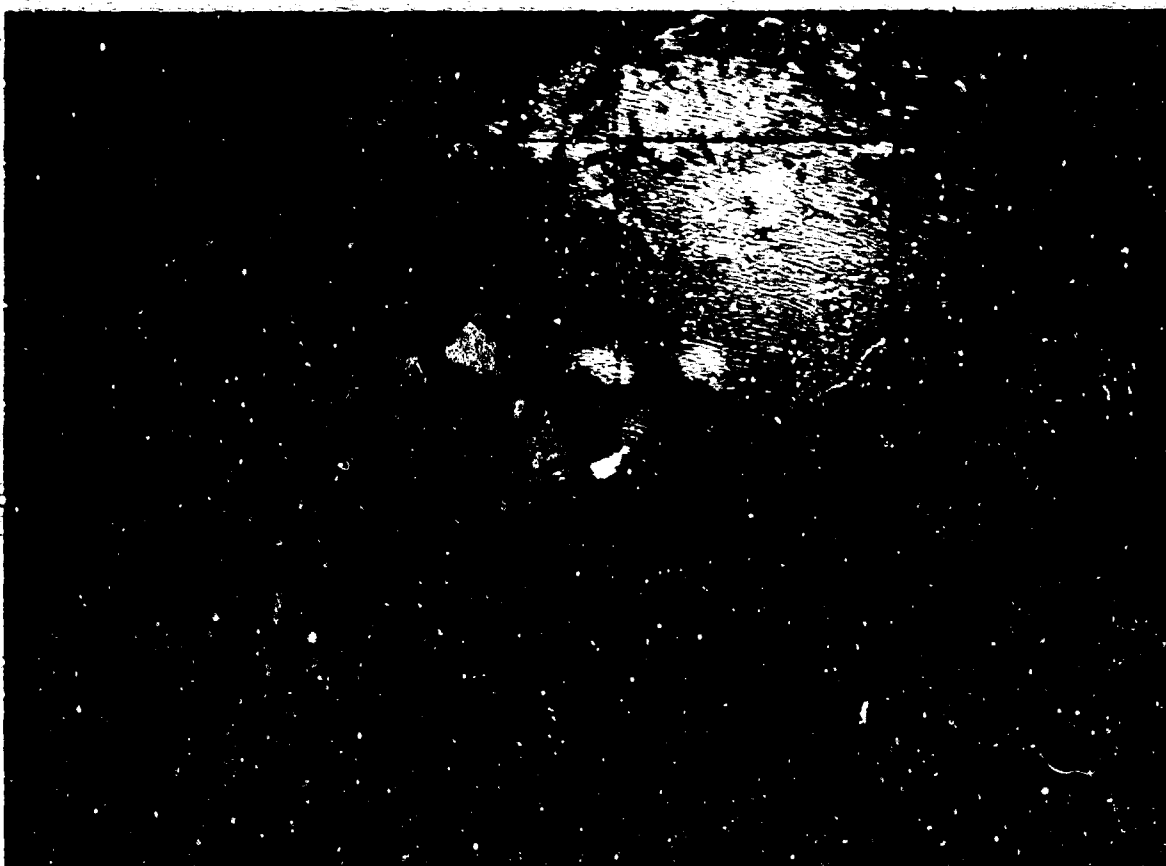


FIG. III-III-3

Pneumatic barrier operating in waves and currents. Oil contained on the left. Note that a few droplets of water encased in oil pass through the barrier (this occurs at more severe environmental conditions than the design conditions).

2. System Strength

Materials Selection

Based upon the considerations of Section III-II, the compilation of critical data and, in many cases, through actual testing, the following materials have been selected as being completely satisfactory for use in the Texas A&M Heavy Duty Oil Containment System.

Main Floats

Polyurethane
Polyethylene

Air Supply Umbilical Hose

Polyvinyl chloride

Umbilical Connectors

Flexible steel tubing,
Plastic insulators

Main Manifold

Low carbon steel pipe

Nozzles for Main Manifold

Polytetrafluoroethylene (teflon)
Polyamide (nylon)

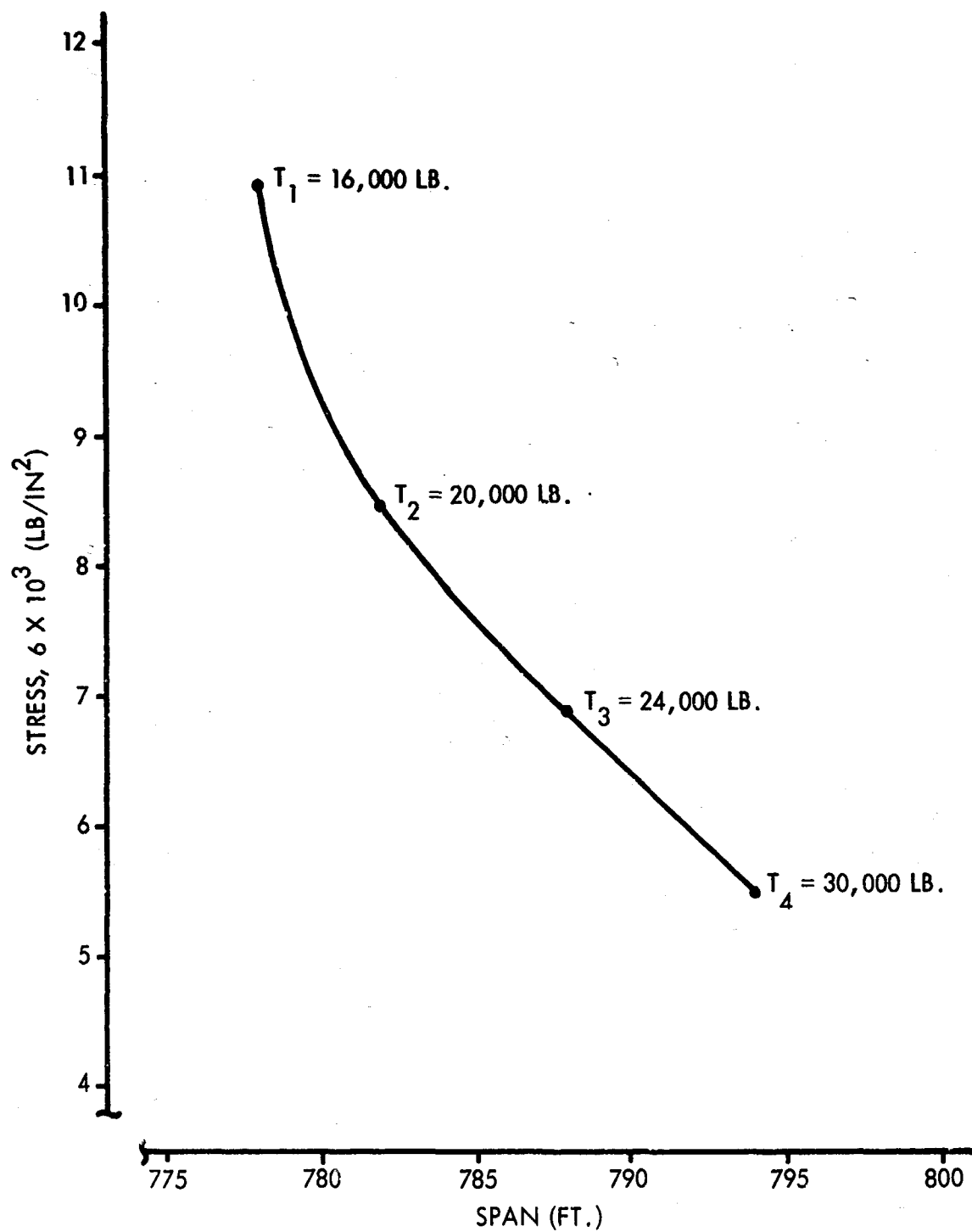
Main Manifold Stresses

Stress calculations were performed for all components of the 7 inch diameter steel pipe. It was found that the maximum stresses in all of the parts were well below the allowable. Since the present trend is to decrease the diameter to 4.5 inches, the stresses will not be any problem. This is

due to the decrease in drag force from 18 pounds per foot to 11.5 pounds per foot and the decrease in the rigidity of the pipe. Final stress calculations will be performed when the procurement of an air supply allows final sizing of the pipe.

Plots of stresses as a function of span for an 800 ft., 1000 ft., and 1200 ft. length of pipe are presented in Figs. III-III-4, 5, and 6. Stresses as a function of length for various bollard pulls are also summarized in Fig. III-III-7.

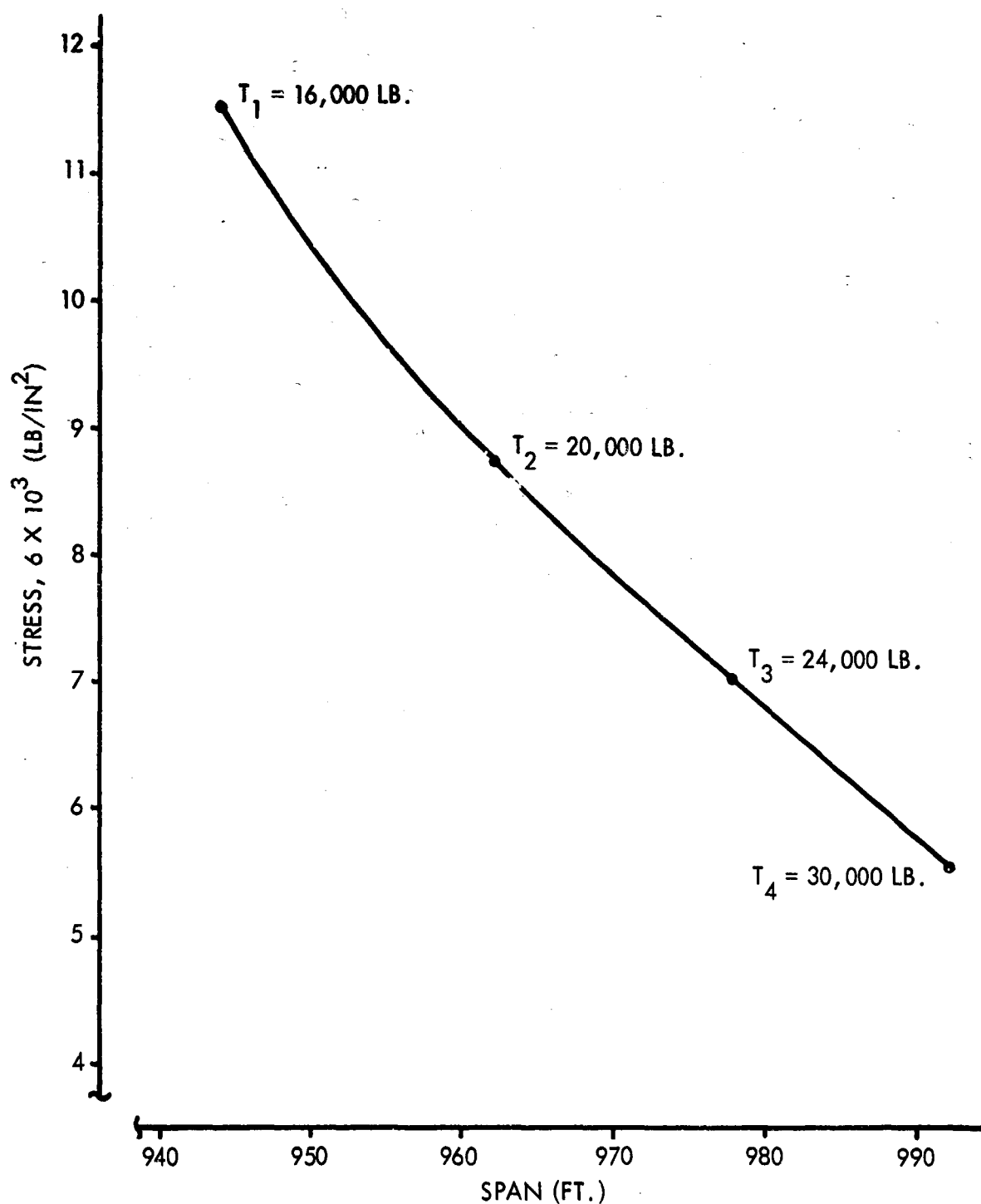
Similar stress calculations may be performed for any size of pipe finally selected in Stage II of the study.



PLOT OF STRESS AS A FUNCTION OF SPAN
FOR 7 IN. O.D. PIPE (STEEL)

CURRENT = 3 KNOTS
LENGTH = 800 FT.

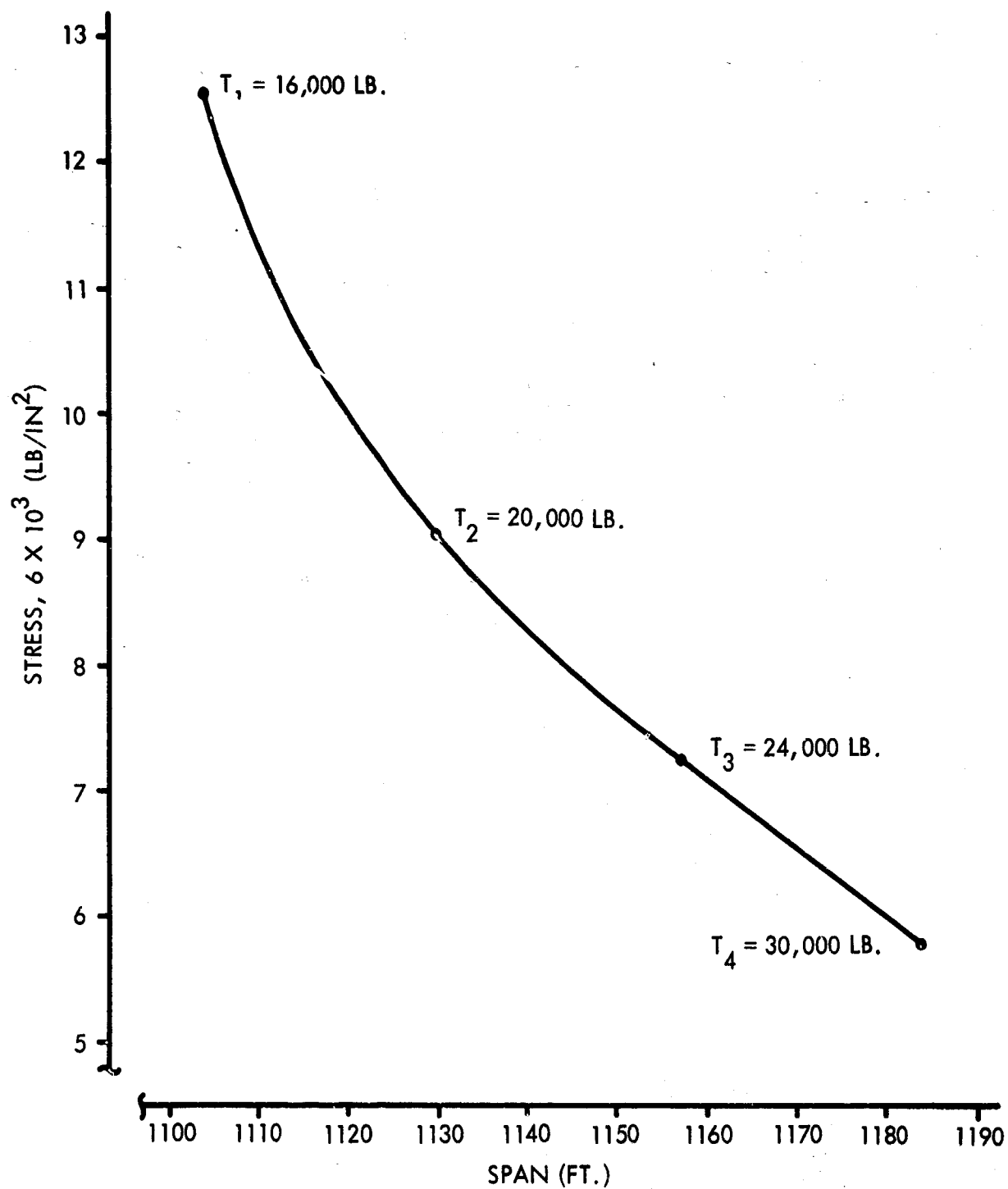
FIG. III-III-4



PLOT OF STRESS AS A FUNCTION OF SPAN
FOR 7 IN. O.D. PIPE (STEEL)

CURRENT = 3 KNOTS
LENGTH = 1000 FT.

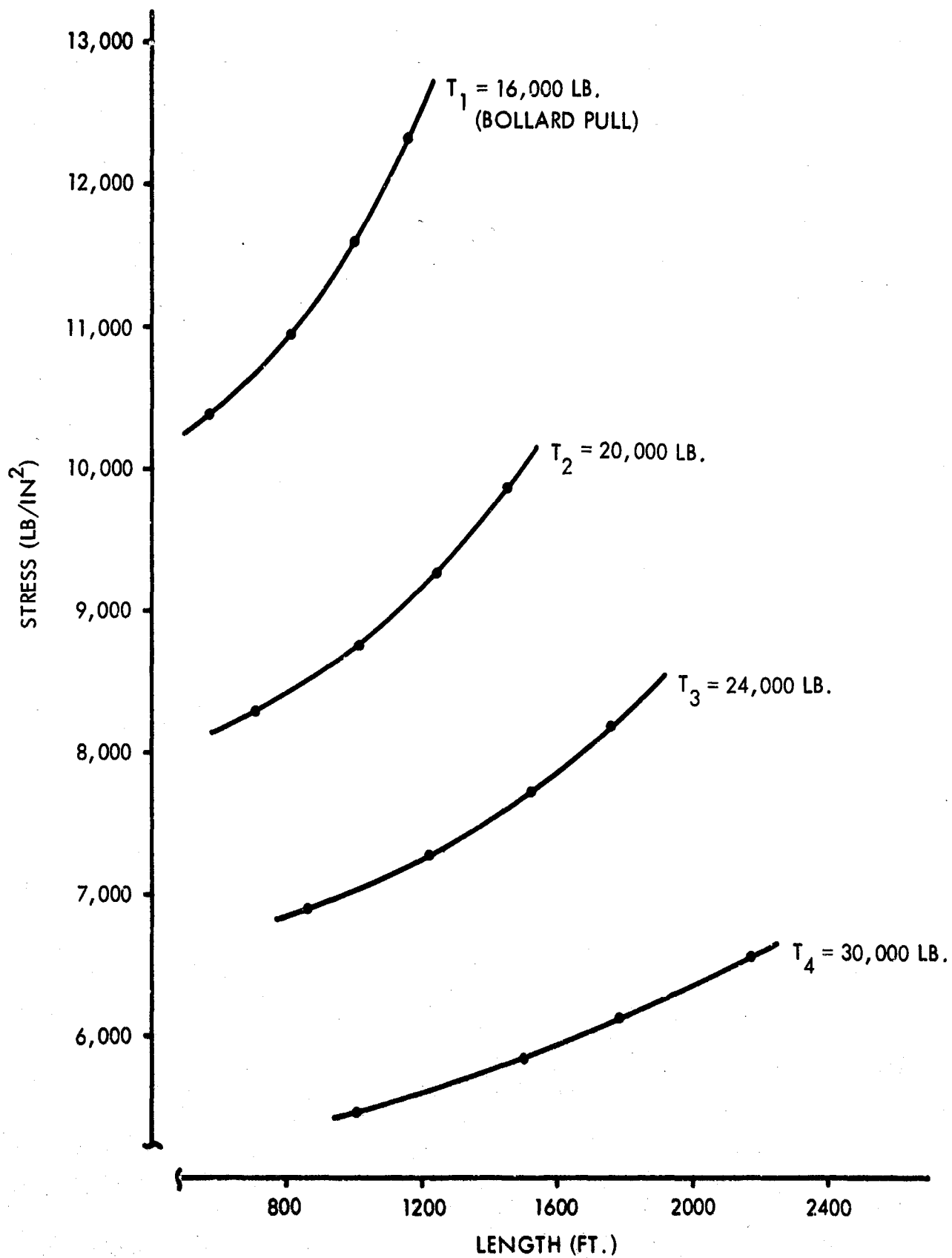
FIG. III-III-5



PLOT OF STRESS AS A FUNCTION OF SPAN
FOR 7 IN. O.D. PIPE (STEEL)

CURRENT = 3 KNOTS
LENGTH = 1200 FT.

FIG. III-III-6



PLOT OF STRESS VERSUS LENGTH
FOR 7 IN. O.D. PIPE (STEEL)
CURRENT = 3 KNOTS
DRAG = 18 LB/FT

FIG. *N-III-7*

3. Deployment Capability

It is estimated that the Heavy Duty System can be deployed in four to seven days depending on the availability of Coast Guard vessels at the time of the spill and the availability of eight C-130s to provide air transport. These estimates are based on the following times. Approximately one hour is required for the loading of each of the four packages on the C-130 for each 200 foot module of bubble barrier. The aircraft will then fly to an airport near a port close to the oil spill. The time for transport and loading for packages would be two to four days depending on the availability of buoy tenders. Because of the towing characteristics of the fuel tanks, the tenders will require 6 to 24 hours to reach an oil spill site at the reduced speed required for towing. At the site of the spill, approximately four hours deployment time will be required for each 200 feet of bubble barrier. It is estimated that the barrier can be deployed in seas of up to ten foot significant wave height.

4. Reliability Standards

The reliability of the overall system for the retention of oil is very high due to the redundancy of the gas generator. At maximum capability, a gas turbine is required for every 200 feet of pipe. The loss of a single gas turbine would reduce the effective back current and total amount of oil that can be retained but it would continue to act as an effective barrier and would have the ability to retain oil. Redundancy of anchor systems is provided by the use of two anchors on each end of the system. (Fig. III-III-8). The fluidic valves to adjust the depth of the pipe are also designed so that if one fails the pipe is rigid enough to bridge between the next two fluidic devices which have a capacity to replace the failed fluidic device. A major problem would be the maintenance of the inflatable rubber fuel tanks during high seas. However, if the tanks break away, they can be replaced with other tanks or attached by a fuel line to the tank at another compressor station until repairs can be made. No reliability capacity has been established for the operation of the gas turbine engine under possible breaking wave conditions. However, it is not anticipated that sufficient spray can enter the engine to impair its operation. It injects large volumes of fuel and air under normal operation.

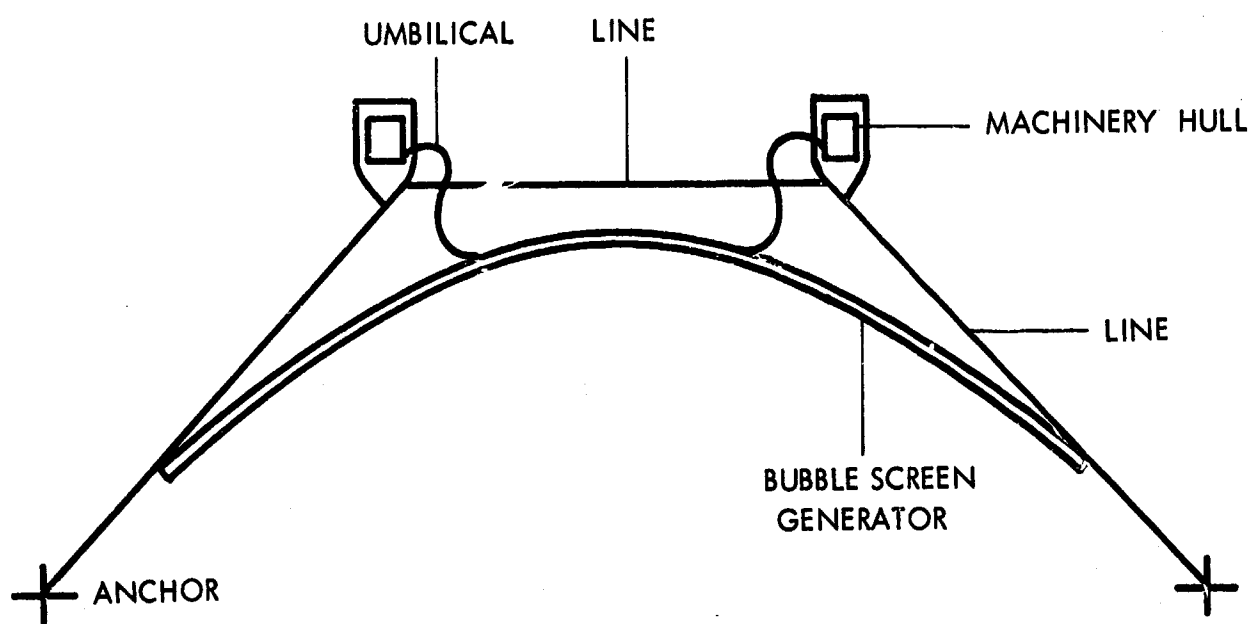


FIG. III-III-8 Anchor System.

5. Biological Effects

General Comment

If materials are to perform their service function in a marine environment for an extended period of time, they must withstand (a) mechanical forces, (b) chemical activity, and (c) biological activity. Where short service life is the only requirement, the resistance of materials to mechanical forces and chemical attack may be the only considerations necessary. Ability to withstand biological activity becomes an important consideration where extended service life is required. As a part of the materials task, a literature survey has been concluded to insure that biological considerations are recognized in the materials selection process for an oil spill containment barrier. Some of the more important considerations are discussed below.

The general effect of detrimental change in materials appearance or characteristics caused directly or induced by biological activity is referred to as biodeterioration. Limiting this review to the marine environment, biodeterioration may be considered to include (a) biological fouling (b) boring and (c) microbial degradation.

Biological fouling

Biological fouling is the accumulation of adhering organisms

on the surface of materials exposed to sea water. The most familiar example of fouling is the accumulation of barnacles on the subsurface hulls of ships. However, any object exposed to sea water is subject to fouling unless its surface will not allow the adherence of organisms; the material itself is toxic to the organisms, or the surface has been coated with a toxic material. Biological fouling may have the following effects:

1. Reduced functional efficiency.
2. Acceleration of localized corrosion.
3. Destruction of corrosion protection coatings.

Firstly, accumulation of organisms obviously changes the design surface geometry and increases frictional drag. In a Pneumatic Barrier System, dependent on release of compressed air through small orifices, fouling might cause plugging of the orifices as an example of functional impairment.

Secondly, accumulation of barnacles or other organisms on a metal surface would very likely lead to the creation of localized anodic areas beneath the shells, greatly accelerating pitting type corrosion in an aerobic, salt water environment. This would be particularly true for ferrous metals.

Thirdly, barnacles or other hard shell organisms may destroy a corrosion protection coating by wedging into the coating as they grow. Also they may become so firmly attached

as to cause peeling of the protective coating if they are inadvertently broken loose.

Factors Contributing to Fouling

In general, fouling may be expected to be most severe and buildups occur most rapidly in shallow, near-coast waters and particularly in the warmer climates. Waters must provide sufficient nutrients for organisms growth, but heavily polluted waters apparently decrease the growth of fouling organisms. Although the shallow, warm waters may contribute to most severe fouling conditions, it nevertheless will occur in all sea waters and at depths below 5,000 feet.

Control of Fouling

Copper or copper-nickel alloys are effective antifouling metals unless the copper is rendered passive by coupling to zinc or iron to form a galvanic couple. For other metals an antifouling coating may be required. Fouling may be effectively retarded by the application of toxic copper or mercury containing paints. The formulation for extended periods of protection must be such as to allow slow leaching of the toxic substance; for copper this may be not less than 10 micrograms per square centimeter per day. A successful paint system used on Navy ships consists of one coat of wash primer (Mil-P-153281B),

multiple coats of red-lead vinyl primer (Mil-P-15929B), and two coats of vinyl antifouling paint (Mil-P-15931B).

Marine Boring

Boring organisms in marine waters are the principal causes of wood deterioration, although test plastic specimens of various types have also shown some damage when placed in couple with a wood bait specimen. The primary specie is a crustacean, Limnoria tripunctate, although various molluscan species in rocky and coral areas also may cause severe wood damage.

Control of Boring Organisms

Wood pilings, the most susceptible material to borer deterioration, is generally pressure treated with coal-tar creosote. This is effective against Teredo and Bankia, but provides little protection against Limnoria or the rock boring mollusc, Martesia. A toxic wood preservative effective against the latter organisms is lacking. Barrier systems on wooden pilings consisting of flexible FVC sheet (20 to 30 mils thick), 90:10 cupro: nickel alloy and concrete have been found to be effective in preventing attack providing stagnant conditions are maintained between the barrier and the piling.

Marine Microorganisms

Of the many species of microorganisms which inhabit the sea, probably the most damaging to materials, particularly metals, is the sulfate-reducing bacteria Desulfavibrio desulfuricans. Through its metabolic activity, this organism produces highly corrosive hydrogen sulfide gas. It is a strict anaerobic bacteria, however, and therefore the most effective barrier against it is an aerobic environment. It would not flourish in shallow waters unless such waters were so polluted as to be devoid of oxygen. With a Pneumatic Barrier System, employing continued aeration, anaerobic bacteria would automatically be controlled. Aerobic bacterial or algal forms would probably not attack metals directly, but might establish colonies or anchor on any surface, as do the larger fouling organisms. They would contribute to metallic corrosion through the creation of localized oxygen concentration cells or through the excretion of acidic metabolic products. Antifouling paint should also be an effective barrier against such micro-organism activity.

Most plastics are resistant to microbial activity unless the extracellular enzymes can hydrolyze the polymeric bonds. Microorganisms may, however, bring about some changes in properties of certain plastics, (as may grades of polyvinyl chloride), by attacking the plasticizer molecules. Before specifying PVC for use in an environment conducive to microbial growth, information

should be obtained on plasticizer resistance. This would presumably be true also of other plasticized polymers. Butyl rubber and natural rubber have been shown to support aerobic and anaerobic microorganisms, the aerobic ones being also able to attack the rubbers GR-S, GR-A, and neoprene.

Related studies

Investigations in the field of biodeterioration have received considerable impetus since World War II. The following bibliography is, of necessity, not complete; however, it is felt that the necessary information as it is presently known is available within the references cited below. Also many further references may be obtained within these books and articles.

Marine Fouling and Its Prevention

Prepared for Bureau of Ships, Navy Department, by Woods Hole Oceanographic Institution, Woods Hole, Mass.; United States Naval Institute, Annapolis, Maryland (1952)

This is a somewhat dated, but very comprehensive, compilation of 22 articles concerned with the problems of fouling, the biology of fouling, and the prevention of fouling. A basic reference.

Materials Performance and the Deep Sea

ASTM Special Technical Publication 445, American Society for Testing and Materials, 1916 Race Street, Philadelphia, Penn., (1969)

A symposium presented at the 71st Annual Meeting ASTM, San Francisco, California, June 23 - 29, 1968. Contains 10 articles at least three of which are concerned with biodeterioration. One article includes effects of boring organisms on plastics.

Biodeterioration of Materials

Microbiological and Allied Aspects, Ed. A. Harry Walters and John J. Elphich, Elsevier Publishing Co., New York (1963).

Contains 67 articles concerned with many aspects of biodeterioration of a wide range of materials, but it is not concerned specifically with the marine environment. A basic reference.

The Microbiology of Fabricated Materials

J. N. Turner, Little, Brown and Company, Boston, Mass. (1967).

Eleven general discussion chapters on the microbiology of timber, woodpulp, paper, textiles, hides and skins, plastics, rubber, paints, and assorted materials. Contains numerous literature citations.

Marine Boring and Fouling Organisms

Ed. Dixy Lee Ray, University of Washington Press, Seattle (1959). A Friday Harbor Laboratory Symposium Volume primarily dealing with the biology of the boring and fouling organisms. Contains thirty-nine articles.

"Effects of Marine Organisms", J.S. Muraoka. Machine Design, 184-187, January 18, 1968. A short, but informative, paper on the effects of fouling and recommendations for protective treatment.

"Protective Coatings", J.R. Saroyan, Machine Design, 188-192, January 18, 1968. This paper provides some specific information on coatings application for corrosion and fouling retardation.

"Coatings and Encapsulants - Preservers in the Sea", J.R. Saroyan, Ocean Energy, 1, 435-456, Pergamon Press, Great Britain (1969). Extensive and very specific information for anticorrosion and antifouling coatings application.

"Bacterial Corrosion", G.H. Booth, Discovery, 24-27, May 1964. A general discussion of the mechanisms of aerobic and anaerobic microbial corrosion and recommendations for its prediction.

"Deterioration of Organic Materials by Marine Organisms", Waldimero Coscarelli, Principles and Application of Aquatic Microbiology, Ed. Heukelekian and Dondero, Wiley and Sons (1964).

An extensive report of investigations by Bell Telephone Laboratories on the resistance of over 70 materials including natural and synthetic fibers, plastics, rubbers, and casting compounds to marine boring and microbial organisms.

Additional references are listed as No. 27 to 128.

Microbiological Degradation

The microbiological degradation of organic materials, and particularly of natural micromolecular substances, such as cellulose or rubber, is now a well established area of study. An understanding of the durability, utility and appearance of any part of the oil containment system requires some knowledge of the affects on biological systems on these materials.

The entire phenomenon of microbial degradation of materials, including polymers, hinges on the natural food cycle of marine life. A constant solubilization operates to reduce all materials to some stage in which they can be utilized as nutritional elements. In conjunction with the basic physical and chemical degradation mechanisms of polymers, the microbiological component-vector can be considered as one with a minor or major role depending on circumstances. The dynamics of total degradation can properly be considered as continuous, involving chemical, physical and biological conversions among

the chemical forces, arbitrarily isolated from the physical forces, that contribute to the shortening of the useful life of commercial and experimental plastics. One can recognize such processes as hydrolysis, oxidation, cyclization, etc. Among the physical forces are high energy radiation, pressure or vacuum, flexural stress, thermal or mechanical shock, and diffusion, which illustrate in part still other possible degradative influences.

All the components of any plastic system may be ranked for specific resistance to microbiological degradation. Plasticisers, extenders, mold release agents, binders, laminating materials, resins, and other substances or components or inclusions have been studied in this respect. Plasticizers, in particular, which have been extensively evaluated in rankings by specific venerability, are available.

Testing of Polymers

The essential philosophy of testing the resistance of plastics to microbial organisms is suitably expressed in the American Society for Testing and Materials (ASTM) document (D 1924-63) entitled "Recommended Practices for Determining Resistance of Plastics to Fungi". This procedure was published as a tentative method from 1961 until 1963, at which time it was adopted as a recommended practice.

This technique has also been approved as American Standard K 65.20-1965 by the American Standards Association.

Effect on Polymer Properties

When biological attack occurs, either in nature or in assay procedures, several groups of effects may be observed. In the event of purely surface type attack, the growth of a fungus or fungi will produce staining, discoloration, opacity, and possible etching, where an imprint of the fungus as it grows across the surface of the test material. Where a heavy growth occurs, a serious loss of plasticizer or other property modifiers may occur and flexibility, weight, or dimensional losses, and similar voiding may result. Attack on specific ingredients in the formulation, the accumulation of metabolic products of bacterial growth, and the absorption and retention of moisture by the fungled mat, may create and maintain regions of highly localized moisture attack on the material where none before existed.

Corrosion

Corrosion is defined as the destruction of a metal by chemical or electro-chemical reaction with its environment. Corrosion as a chemical reaction is a characteristic of metals that goes along with the freedom of the valance electrons. It is this very

freedom that produces a metallic bond and allows electronic conduction to take place. Hence, the property which makes metals so useful also accounts for their main weakness.

Being loosely bound to their atoms, the electrons in metals are usually removed in chemical reactions. In the presence of non-metals such as oxygen, sulphur, or chlorine, with their incomplete valance shells, there is almost always a tendency for metals to form a compound. Stated another way, the free energy of such compounds is almost always lower than that of the metal in the metallic state. Consequently, only the most inactive or noble metals like gold or platinum are found in the metallic state. The rest are almost always found in the form of ore in which the compounds are bonded by covalence or ionic bonds.

The constant tendency of refined metals to return to their natural state accounts for corrosion. The rate at which corrosion reactions take place is governed largely by the relative activity or passivity of the metal which in turn depends on many factors. As already mentioned a few metals like gold and platinum are found only in metallic states because they are truly inert. Other metals, because of their electron structure, have an apparent tendency to be passive. Still others are frequently made passive by the product of corrosion itself. Some of the products of corrosion are usually deposited on the corroded surface and interfere to some degree with the

further progress of corrosion. The degree of interference is extremely variable. However, under certain conditions a tightly adhering, impenetrable film of only a few angstroms thickness is formed at once, effectively stopping further corrosion. Under other conditions the corrosion products are loose and porous. In corrosion by liquids the products may be precipitated at some distance from the surface being corroded. Thus the progress of corrosion is primarily a surface phenomenon, although the reactions involved at the start depend on the electron structure of the atoms in the bulk of the material.

Because of the constant thermal agitation of the ions in a metal, there is always a tendency for some of the surface ions to escape into the surrounding medium. The presence of ions and molecules of a liquid at the metal surface causes significant numbers of the metal ions to escape or dissolve in the liquid. The loss of positive ions leaves the metal with a slight negative charge. Thus the metal ions are attracted back to the metal, and an equilibrium is reached in which as many ions return as leave. The negative charge on the metal is known as the solution potential.

If two different metals are placed in contact with a liquid they will dissolve at different rates and set up different potentials.

The relative ease with which metals lose their valance electrons is shown by the electromotive force series (Table below).

Electromotive Force Series

METAL	METAL
(anodic)	
Lithium	Cobalt
Potassium	Nickel
Calcium	Tin
Sodium	Lead
Magnesium	Hydrogen
Beryllium	Bismuth
Aluminum	Copper
Manganese	Mercury
Zinc	Silver
Chromium	Palladium
Gallium	Platinum
Iron	Gold
Cadmium	(cathodic)
Iridium	
Thallium	

Those at the beginning of the list are more prone to dissolve in electrolytes because it is easier for the ions to break away from their valence electrons.

Galvanic Cells Involved in Corrosion

Metals in contact with electrolytes form galvanic cells in many unexpected ways. The most obvious situation would probably be two dissimilar metals, connected and immersed in the same solution. Ships' propeller shafts made of steel

and running in bronze bearings immersed in sea water, which makes an excellent electrolyte because of the dissolved salts, constitutes a most destructive corrosion cell.

Corrosion can take place when only one metal is involved through differences in the electrolyte. A single electrolyte can vary from one location to another by having different concentrations of ions. Generally speaking, at the place where the concentration is lowest the metal becomes anodic, forming a galvanic cell. This type of galvanic cell is called a concentration cell. It occurs in places where the electrolyte is flowing past discontinuities. Ions tend to concentrate in corners and holes, and the difference in concentration produces corrosion.

Many factors complicate the oxidation of metals. For detailed information on oxidation of specific metals in specific environments the student is referred to the Corrosion Handbook.*

Protection Against Corrosion

Corrosion-Resisting Materials: Copper and copper alloys have long been used in applications where the corrosive environment consists of water or salt air. Other metals, such as stainless steel, monel metal, and lead, are used in special

environments. Newer metals include titanium and zirconium, which are outstanding in their resistance to chlorine and chlorine compounds as well as certain other media. The high first cost of such metals can be more than compensated by the increased service life and resulting lower annual replacement costs.

Nonmetallic materials are also becoming available in larger numbers as replacement for metals. Plastics in general are highly resistant to many of the corrosive environments which attack metals.

Coatings: It is frequently impractical to use the most corrosion-resistant materials because of high cost, lack of strength, or some other limitation. An alternative is the use of protective coatings. Coatings can be classified as those offering purely mechanical protection, separating the electrode from the electrolyte or atmosphere; those offering galvanic protection by being anodic to the base metal; and passivators, which in effect shift the base metal toward the cathodic end of the electromotive series.

Cathodic Protection: In corrosion of metals by liquids, galvanic cells are formed in which certain areas become anodes and others cathodes. Electric currents flow from anodic to cathodic areas through the electrolyte. As the currents flow, the metal at the anode is dissolved or corroded.

Cathodic protection reverses these currents and thereby makes cathodic all the metal to be protected. The mechanism is to insert a new anode in the system, the potential of which is adjusted to overcome the potential of the original anodes plus the resistance of the circuit elements (electrolyte, metal parts, connections, etc.). In this way corrosion is concentrated in the new anode, which can be replaced from time to time.

The Weatherability and Aging of Plastics

The term weatherability, although commonly used in plastics technology, is a poorly defined concept since it refers to long term service under complex and variable conditions and because different properties of a plastic are effected to different degrees by a given environment. Improvement in the ability to predict weatherability, therefore, requires careful redefinition of the problem as well as a refinement of experimental technique. A review of the extensive literature on outdoor and artificial exposure of plastics shows that no simple correlation exists between these two modes of testing. Further, because the rates and mechanisms of deterioration are different when produced by visible light, ultraviolet, heat, or moisture, an arbitrary "accelerated" weathering test will distort the balance of responses observed

in the slower, actual, in-service exposure of plastics. Analytical approaches to predicting the resistance of plastics to degradation are considered at some length in an applied polymer symposia paper written by Musa R. Kamal and Robert Saxon (Plastics and Resins Division, American Cyanamide Co., Wallingford, Connecticut - within the text entitled "Weatherability of Plastic Materials" edited by M. R. Kamal 1967 Interscience Publishers, Division of John Wiley and Sons).

In the procedures suggested by the above authors, the effects of specific weathering parameters are established for specific properties of a given material using controlled artificial environments; the make-up of the environment at any given location is analyzed in terms of the critical parameters; and finally, by suitable mathematical models, the results to be expected on an exposure of this material to a given composition of environment can be computed. While this approach is admittedly complex, its feasibility has been demonstrated. There are no universal artificial weathering and aging tests. Thus, materials for which long term behavior must be determined must be themselves subjected to the actual environment in question and their responses recorded.

Creep Properties of Plastics

Creep properties are fundamental, mechanical engineering properties of plastics because they realistically predict plastics rigidity and strength under constant load as a function of time which is an in-use condition for nearly all applications of plastics. They have the same primary importance in measuring performance of plastics that stress-strain tests have for steel and similar Hookean elastic materials.

Definitions and Terminology

Creep: When a plastic is subjected to a constant load such as in storage or in deployment it deforms quickly to a strain roughly predicted by its stress-strain modulus, and then continues to deform slowly with time, indefinitely, or until rupture or yielding causes failure.

Creep Rupture: In a tensile and usually in a bending creep cast at relatively high stresses - i.e., close to the short time yield, tensile, or flexural strength - a plastic will fail after a short time under load either by catastrophic rupture or by yielding followed by rupture, depending upon whether the plastic tends to be ductile or nonductile at the temperature of interest. If the test is repeated at a lower increment of stress, the time to failure increases until at

some stress it becomes indefinite, beyond practical testing. By making creep tests at several stress levels we can determine a creep rupture inflow which broadly establishes the useful working stress range of a plastic at a particular temperature.

Creep (Apparent) Modulus: To discuss creep modulus, it is first necessary to define what we mean by creep strain. In polymer science it is convenient to visualize the deformation of plastics under load as being made up of the sum of Hookean elastic (like steel) components and time dependent, liquid like (viscus) components. In the scientific literature the term creep is sometimes used to mean only the time dependent components of formation. However, for engineering purposes it is much more practical to work with the total deformation at any time, regardless of the polymer mechanisms that give rise to it. In the following discussion, as in plastics engineering practice generally, the term "creep strain" means total deformation in a creep test, and its use permits us to define a simple creep modulus.

Data taken from creep curves of creep strain vs. time are awkward to use in design because in the most frequently used mechanical design formulas, the material constant required is a modulus, not a strain. Therefore, it is advan-

tageous to convert creep strain curves to modulus curves. This is readily done by dividing the initial applied stress by the creep strain at any time in the cases of tension and compression, or by substituting measured deflection at any time in the beam ending formula for modulus in the case of the simple beam test.

Use of Data in the Creep Modulus Table

All of the data and information listed in the table for each grade of plastic was contributed by the manufacturer of that grade exactly in the form which it appears, except for some nominal editing. The creep modulus data is presented in tabular form for the sake of clarity. Where extra calculation is required, the data should be plotted on logarithmic coordinates and the best fit line drawn through the data.

Factors Responsible for Polymer Degradation

Ultraviolet, Radiant Energy

Sunlight is a major source of radiant energy. At ground level, the wave lengths which cause the most degradation of polymers (oxidation, scission, cross linking) are in the near ultraviolet, 3000-4000 A., even though these comprise only about 5% of the total sunlight at the earth's surface.

In order for radiant energy to initiate such chemical

reactions, it must first be absorbed. The solution, therefore, to the ultraviolet radiant problem is to shield or screen the material from sunlight.

Oxygen

Residual double bonds in some molecules such as polyethylene are especially susceptible to attacks by atmospheric oxygen, although most polymers react very slowly with oxygen. However, oxidation is greatly promoted by elevated temperatures and ultraviolet radiation, and the reactions of polymers with oxygen under these conditions can be very complex. Most degradation phenomena occur at the surface of the plastic which is in equilibrium with its environment. The solution to the oxidation problem is straightforward. All polymeric, and for that matter, metallic materials composing the oil containment system are to be bagged in an opaque material filled with an oxygen free inert gas such as argon.

Moisture

Water can have at least three kinds of effects which are important for the degradation of polymers. One is chemical, hydrolysis of labile bonds such as those of polyesters or polyamides; a second is physical, destroying the bond between a polymer and a filler like glass fiber or pigment and resulting in chalking or fiber bloom; and a third is photochemical,

involving the generation of hydroxyl radicals or other reactive species which can then promote a host of free radical reactions. To solve the moisture problem the same packaging material used to exclude the ultraviolet radiant energy and oxidation can also be used and expected to exclude moisture. If the oil containment system is stored in a dry environment these long term moisture effects will be eliminated.

Thermal Energy

Under extreme outdoor exposure conditions, a plastic sample may reach 170°F. In an opaque and thermally absorbent package the internal temperatures may reach 200 to 250°F. Thermal energy is generally not sufficient to promote long cleavage of any structures likely to be found in commercial plastics. However, the principal role of heat in the degradation of plastics is in accelerating processes otherwise induced, such as hydrolysis, secondary photochemical reactions, or the oxidation of trace contaminants like hydroquinone. Thermal effects will thusly be minimized if not eliminated by the simple expedients of packaging which eliminates ultraviolet energy, oxygen, and moisture, all of which would have to be stimulated by increased temperatures. The problem generated by the temperature is that of long term creep or permanent set within the packaged oil containment system.

6. Maintenance

General Comment

Maintenance and storage is affected by a number of factors, some of these are of environmental and some of physical, or physico-chemical nature. The information is summarized in the following order:

- (a) Biological effects
- (b) Microbiological degradation
- (c) Corrosion
- (d) Weatherability and aging of plastics
- (e) Creep properties of plastics
- (f) Factors responsible for polymer degradation

The Storage Problem

In extended storage in a humid environment, materials may be subject to biodeterioration caused by fungal growths. This has been particularly noted with regard to plasticized polyvinyl chloride polymers, where the fungus grows at the expense of the plasticizers, thereby causing a detrimental change in the mechanical characteristics of the material. Virtually all organic material, however, have been observed to support fungal growth to some degree.

Control of such fungal attack of stored materials must be based on biocidal or environmental methods. The biocidal

method of control suggests the inclusion of a preservative within the material.

Formulation

Organotin compounds are used as stabilizers for plastic compounds and as rodent repellants and fungicides. Mercapto-benzothiazole and other organic sulfur compounds are rubber stabilizers as well as fungicides. The selection of a specific fungicide is in many cases based on trial and error screening techniques with a large number of chemicals. There has as yet been no direct method developed for relating toxicity to molecular structure. General classes of compounds which may serve well as fungicide, however, are organometallics, particularly organotin or organomercurials; chlorinated phenol derivative, pentachlorophenyl esters, and some organosulfur compounds.

Environmental control may be effective if the packaging environment is completely dry and anaerobic. In a completely inert atmosphere, maintained at low humidity through the use of desiccants, fungal growth would be inhibited. A very effective system for fungal control would incorporate a biocide in the material formulation with environmental control of packaging and storage conditions.

Factors Influencing Storage and Service Life

Factors which could influence the storage and service life of the system have been identified and solutions for each potential problem area have been formulated. Some of these factors and solutions are:

Problem: Radiant Energy -- ultraviolet

Solution: Opaque packaging for storage and solar incorporated within the plastic formulation to minimize effect.

Problem: Oxygen

Solution: Exclude it in packaging through use of an inert atmosphere. Oxidation is relatively slow and will not influence in-service life.

Problem: Moisture

Solution: Exclude it in packaging through use of a desiccant. In-service saturation will constitute no problem in mechanical strength although some swelling of various components can occur which, in fact, can be argued as being beneficial, not detrimental.

Problem: Thermal energy

Solution: Packaging should be highly reflective so as to minimize heat retention. Packages of dark colors can reach 200° to 250°F in direct sunlight. In-service conditions never reach temperatures high enough to ever cause degradation. Packaging will be such as to minimize sharp and flat folds which could permanently set.

Problem: Microbiological degradation

Solution: Biocides and desiccants. During in-service conditions, a biocidal and antifouling paint will provide protection.

Problem: Corrosion

Solution: Knowledge of the nature of corrosion - cathodic protection where necessary and avoidance of dissimilar metals in contact in sea water or in packaging.

7. Suitability

The Heavy Duty System has been designed so that it consists of packages small enough to be handled by existing Coast Guard aircraft. A 25-K aircraft cargo loading truck is required to load the pallets aboard eight C-130 aircraft. Commercial trucking equipment is required to transport from the airport to dockside. Dockside cranes of 13 ton capacity are required to off-load the equipment into the water or onto the deck of the buoy tender. A 180-foot or larger Coast Guard buoy tenders are required for towing and transportation of the subsystems to the oil spill site. A commercial tank truck to deliver the jet fuel for filling of the inflatable fuel tanks is required. The inflatable fuel tank would be the type that has been developed by the Coast Guard for off-loading tankers. If the Heavy Duty System is required to operate for more than eight days it will be necessary to refuel the inflatable tanks which would require a tanker of 12,000 barrel capacity to transfer jet fuel at the site of the installation.

8. Physical Characteristics

The exact dimensions for the component parts of the bubble screen generator are very dependent upon the type of air supply. The size of the pipe will be between four and seven inches, depending upon the pressure and temperature of the outlet air from the compressor. Since the size has changed several times during the project, the procedures for determining the other variables are well known and can be obtained soon after knowing the compressor size.

9. Deployment and Pick-Up

After the system has been towed to the location of the oil spill and the location of the deployment position is established, the deployment will probably take the following procedure:

1. Open Package IV (mooring), and secure two anchors to the bottom or secure a mooring line to the mooring.
2. Open Package III (bubble screen), remove a first pipe section and secure it in Deck Vise One in the aft section.
3. Secure the mooring line to the first pipe section. This will have a plugged end and an attachment for securing the line. Clamp second pipe section to the first pipe section and then secure this section in Deck Vise Two.
5. Release Deck Vise One from the pipe.
6. Fasten a pillow float to the first pipe section.
7. Move Deck Vise Two with captive pipes to aft station.
8. Reset Deck Vise One in forward station.
9. Clamp third pipe section to second pipe section and secure this section in Deck Vise One. Proceed in this manner to connect and extend pipe sections until 200 feet of pipe has been connected. Use pillow floats to support each section of pipe as it is deployed on the sea surface.
10. Connect a Tee-section and umbilical in a similar

manner. The blower end of the umbilical will have a plug and a float so it can be recaptured for attachment later.

11. Continue to connect pipe sections, umbilicals, and mooring lines as before. When the last pipe section of the last set is in a Deck Vise at the aft station, connect its plug and mooring line and drop the two remaining anchors or heave the line to another mooring tug.

12. Using an additional tug, move the machinery and fuel tank into position at the first set point. Secure the mooring line to the hull, retrieve the umbilical and connect it to the blower. Start the prime mover. Continue this procedure with each machinery hull until the complete heavy duty barrier is deployed.

13. Release the pillow float to allow the bubble screen generator to descend to operating depth.

14. Commence station keeping.

The pick-up procedures would reverse the deployment procedures. The pick-up procedures would be to pull the two anchors, have a diver carry a pillow float package and compressed gas bottle to the bubble screen generator and deploy pillow floats on each pipe section inflating the floats with compressed gas. After the bubble screen is floated to the surface, it would be brought on board, clamped in the Deck

Vises and each section removed from the adjacent section.

The tugs would separate the machinery hulls and fuel tanks for towing back to the appropriate dock.

Section IV

Prototype Design

IV-I Technical Problems

One technical problem is the final sizing of the pipes, clamps, and umbilical tubes. This can be done rapidly after the decision is made on the air compressor to be used.

Another technical problem is the deployment of the fluidic logic flotation device. This will be subcontracted to a commercial firm which is active in this field.

Finally, an important technical problem remaining is to locate the most suitable and economical air mover. Considerable effort has been expended in searching for a compressor or blower that will provide a sufficient air supply. The type of compressor or blower required is a unit which will deliver a large volume of air at low pressure. Only one unit which will be suitable for this application has been located to date. Another unit was located but its weight would prohibit deployment by C-130 aircraft. Further inquiries will be made before final choice is made for the air mover. No doubt more commercial interest will be generated when acquisition funds are available. It appears from contacts with industry that such units will be available on a rental basis for field testing.

IV-II Future Studies

A. Mechanics of Oil Set-Up

At the conclusion of Stage I of the project, a number of questions concerning oil set-up and barrier failure remain unanswered. More specifically, due to time limitations in Stage I, it was not possible to study thoroughly the oil loss rate due to entrainment or the draining action, if any, near the pneumatic barrier. Further testing will be conducted during Stage II. Although it is doubtful that these factors will affect the pneumatic barrier design, they will affect the volume of oil containment and, therefore, should be done as early in Stage II of the project as possible.

On the basis of our findings in Stage I, an effective and efficient test program can be planned and executed. However, due to the great complexity of these phenomena, full-scale velocities and size should be used in these tests.

The phenomenon of entrainment was found to begin at current velocities of approximately one knot and increase with increasing velocity. Since the scaling of this phenomenon depends on such a large number of factors - including current, oil viscosity, wave motion, surface tension, density and set-up length, - the most efficient route to understanding this problem is through full-scale laboratory testing. For this purpose the five-foot wide channel will be used with a pneumatic barrier. A representative group of oils will be tested and the rate of oil loss will be measured as a function of velocity.

A second group of tests will be used to evaluate the combined effect of the pneumatic barrier in waves, current and wind. These additional experiments will be conducted in the Hydromechanics Laboratory in the three-foot deep glass wave channel and in the 10-foot deep wave channel. Also, it is proposed to continue evaluation of the effects of waves of various steepness ratios (H/L) on oil containment. Of particular interest is whether the pumping action significantly changes the α_{failure} values obtained in Stage I, since there was some discrepancy with test results reported by Chalmers University.

Further tests are also planned to confirm the linear superposition principle to combine current and air bubble velocity profiles. Additional tests to support the oil failure depths determined under current and air bubble conditions are also proposed.

The efficiency of a two-manifold system with manifolds placed in "parallel" will also be investigated briefly to see if passage of entrained oil can be eliminated. This would involve a second manifold, perhaps with a much lower discharge rate, placed below and offset from the main manifold. The objective of this and other studies should be aimed at reducing the total air discharge and horsepower requirements for satisfactory retention of oil.

B. Preliminary Field Tests

Preliminary field tests will include a full-size section of the pneumatic barrier, but its length will be restricted

to not more than 150 feet. Such tests can be conducted at Lake Somerville (25 miles from College Station) or at another, sufficiently deep-water lake located near College Station. Results of these tests will be incorporated, as needed, in the main testing program.

The reasons for these tests are as follows:

1. To investigate the effect of manifold depth of prototype scale (25 to 30 feet) on the maximum surface current produced, U_{max} . Maximum laboratory depth was 8.8 feet. Surface and depth velocity profiles will also be checked.

2. To study the scale effects, if any, on the oil failure depths under stagnant conditions as determined in the laboratory. These can be performed on a two-dimensional scale using a bio-degradable vegetable oil.

3. To study the current effects on the bubble velocity profile under nearly prototype conditions. (The outlet works stilling basin of the dam will be employed for these tests.)

4. To familiarize operating and technical personnel with the equipment to be used in the main testing program. In particular:

- a. Test pipe connection technique;
- b. Test umbilical connection;
- c. Test power package, blower;
- d. Make flotation checks;

2. Determine deployment procedures;

3. Make minor design changes before the main test.

5. To familiarize Texas A&M personnel with the specialized instruments and equipment, calibration techniques, and recording procedures that will be employed for the main test.

Instrumentation required for these preliminary tests are as follows and can be reused for the main tests when applicable:

1. Air supply flowrate meter,
2. Pressure gauges to monitor manifold pressures,
3. Air temperature gage,
4. Velocity current meters,
5. Depth measuring device.

IV-III. System Performance

The pneumatic system will basically satisfy the design criteria, in that it will retain anticipated oil volumes under given environmental conditions of wind, waves and currents. Some minor losses of oil by entrainment may occur. Further tests are planned to better evaluate these quantities and to seek possible methods of reducing or eliminating entrainment losses as mentioned in the previous section.

IV-IV Optimization of System

The primary trade-offs in the design of the bubble screen manifold were between the pipe size and the air supply pressure. The lower the supply pressure, the larger the manifold pipe required and the larger the supply pipe required. Also, the larger the pipe size, the greater the weight of the pipe.

After several conferences with the manufacturers of air moving equipment, it was found that the suitable size (and weight) compressor or blower would supply only about 200 feet of pneumatic breakwater. But, the output pressure was higher than that required for release of air bubbles, so that the diameter of the manifold could be substantially reduced.

Section V

Plan for Detailed Design for Construction of the Full-Scale Prototype

Detailed plans for the design of a full-scale prototype are described in Part II of the report (Proposed Final Management Plan) under Tasks B - G.

Specifications for various parts of the pneumatic barrier such as the manifold pipe, umbilical, supply pipe and connectors, power plant, fluidic logic, anchors, etc., will be prepared as soon as various tasks are completed.

No problems of acquiring or fabricating the various parts are anticipated. The air mover will be rented from the manufacturer; it is anticipated that the four air mover units required to provide air for a 1000 foot pneumatic oil containment device will be made available in three to five months from the award of the contract. One air mover will be required for preliminary tests at Lake Somerville. If the air mover is not available in time for this preliminary test, other types of compressors will be rented for this preliminary test.

References

1. Wetzel, J. M., "Experimental Studies of Pneumatic and Hydraulic Breakwaters", Project Report No. 46, St. Anthony Falls Hydraulic Laboratory, University of Minnesota, 56 pp., May 1955.
2. Herbich, J. B., Ziegler, J. and Bowers, C. E., "Experimental Studies of Hydraulic Breakwaters", Project Report No. 51, St. Anthony Falls Hydraulic Laboratory, University of Minnesota, 103 pp., June 1956.
3. Straub, L. G., Herbich, J. B. and Bowers, C. E., "An Experimental Study of Hydraulic Breakwaters", Chapter 43, Coastal Engineering, pp. 715-723, 1958.
4. Taylor, G. I., "Note on the Possibility of Stopping Sea Waves by Means of a Curtain of Bubbles", Admiralty, Scientific Research Department, (Great Britain) ATR/Misc/1258, 1943.
5. Straub, L. G., Bowers, C. E. and Tarapore, Z. S., "Experimental Studies of Pneumatic and Hydraulic Breakwaters", St. Anthony Falls Hydraulic Laboratory, University of Minnesota, Technical Paper No. 25, Series B., Aug. 1956.
6. Anonymous, "Pneumatic Barriers," Hydro. Delft, the Netherlands, No. 8, pp. 11-13, July 1967.
7. Anonymous, "Oil Spillage Study", Literature Search and Critical Evaluation for Selection of Promising Techniques to Control and Prevent Damage, Report of Battelle Memorial Institute, Nov. 20, 1967.
8. Dudley, B. L., "Harbourmaster's Visit to Cornwall to Study Anti-Oil Pollution Measures", Milford Haven Conservancy Board, April 25, 1967.
9. Sherk, S. M., "Offshore Discharge (Pneumatic Wave Attenuation Full-Scale Tank Tests)", U. S. Army Transportation Research Command, Fort Eustis, Virginia, Engineering Report, Project PR38-05-010, 98 pp., Dec. 1960.

10. Evans, J. T., "Pneumatic and Similar Breakwaters", Proc. Royal Society, A., Vol. 231, pp. 457-466, 1955.
11. Radionov, S. I., "Wave Dissipation by Compressed Air", translated by H. Arnesen; Wave Research Projects Report No. 104-9, University of California, Berkeley, 47 pp., 1960.
12. Dmitriev, A. A., Bonchkovskaya, T.V. and Teplov, A. V., "Wave Extinction by Pneumatic Breakwater", translated by H. Arnesen; Wave Research Projects Report No. 104-10, University of California, Berkeley, 28 pp., 1961.
13. Kurihara, Michinori, "Japanese Study of a Pneumatic Breakwater. Third Full-Scale Test Under Natural Conditions During the 11th Typhoon at Tsurumi Shipyard, Yokohama, Japan." Vol. 40, No. 466; London, Aug. 1959.
14. Kyushu University Research Institute for Applied Mechanics, 1955-59, on the Study of a Pneumatic Breakwater. I-IV by Research Committee for Hydrology (Part I by M. Kurihara reprinted from Reports of Research Institute of Applied Mechanics, Vol. 3, No. 12; Vol. 4, No. 16; Vol. 5, No. 20; Vol. 7, Nos. 25 and 26. Sukeroka, Japan; 1955-59.
15. Sjöberg, A. and Verner, B., "Pneumatic Barriers Against the Spreading of Oil on Water", Technical Report, Division of Hydraulics, Chalmers University of Technology, Gothenburg, Sweden.
16. Ippen, A. T., Estuary and Coastline Hydrodynamics (McGraw-Hill Co., Inc.); chapter 5, 1966.
17. Van Dorn, W. G., "Wind Stress on an Artificial Pond," Journal of Marine Research, Vol. 12, No. 3, 1953, pp. 249-276.
18. Keulegan, G. H., "Wind Tides in Small Closed Channels", Journal of Research, National Bureau of Standards, Vol. 46, No. 5, 1951, pp. 353-361.
19. Wilson, B. W., "Note on Surface Wind Stress Over Water at Low and High Wind Speeds", Journal of Geophysical Research, Vol. 65, No. 10, 1960, pp. 3377-3382.

20. Taylor, Geoffrey, "The Action of a Surface Current Used as a Breakwater", Proceedings, Royal Society of London, Ser. A, 231, 1955.
21. Unna, P. J. H., "A Laboratory Study of Pneumatic Breakwaters", Report No. 12, C. E. Dept.; Queen's University at Ontario, July 1960.
22. Abraham, G. and Burgh, V. D., "Reduction of Salt Water Intrusion Through Locks by Pneumatic Barriers", Delft Hydraulic Publication, No. 28, Aug. 1928.
23. Dick, T. M. and Brebner, A., "A Laboratory Study of Pneumatic Breakwaters", Report No. 12, C.E. Dept.; Queen's University at Ontario, July 1960.
24. Bulson, P. S., "Currents Produced by an Air Current in Deep Water", Dock and Harbour Authority, May 1961.
25. Bulson, P. S., "Large Scale Bubble Breakwater Experiments-Feltham", Dock and Harbour Authority, Oct. 1963.
26. Wicks, M. III, "Fluid Dynamics of Floating Oil Containment by Mechanical Barriers in the Presence of Water Currents," American Petroleum Institute and Federal Water Pollution Control Administration Joint Conference on Prevention and Control of Oil Spills, New York; Dec. 1969.
27. Brown, B. F., "Metals and Corrosion", Machine Design, Jan. 18, 1968.
28. Anonymous, "Plastics Properties Chart", Modern Plastics Encyclopedia, 1969-70.
29. Longinow, A. W. and Brickner, K. G., "Designing with a New Stainless Steel", Chemical Engineering, Sept. 8, 1969.
30. Kolb, Don J., "Ultrasonic Assembly", Modern Plastics Encyclopedia, 1969-70.
31. Kaminsky, Stanley J., "Welding Thermoplastics", Modern Plastics Encyclopedia, 1969-70.
32. Fenner, Otto H., "Plastic Materials of Construction", Chemical Engineering, Nov. 4, 1968.
33. Fenner, Otto H., "Directory of Manufacturers", Chemical

Engineering, Nov. 4, 1968.

34. Fenner, Otto H., "Listing of Basic Manufacturers", Chemical Engineering, Nov. 4, 1968.
35. Fenner, Otto H., "Inventory of Current Literature", Chemical Engineering, Nov. 4, 1968.
36. Anonymous, "Product Guide for Ferrous and Nonferrous Metals Vendors", Sweet's Industrial Division, Catalog Systems, 1969.
37. Anonymous, "Product Guide for Plastics, Elastomers, and Other Non-Metals Vendors", Sweet's Industrial Division, Catalog Systems, 1969.
38. Saroyan, John R., "Protective Coatings", Machine Design, Jan. 18, 1968.
39. Muraoka, James S., "Effects of Marine Organisms", Machine Design, Jan. 18, 1968.
40. Saroyan, John R., "Coatings and Encapsulants-Preservers in the Sea", Ocean Engineering, Vol. 1, pp. 435-456, 1969.
41. Anonymous, "Wire Rope Design Specifications in Product Designs", Hackensack Cable Corporation.
42. Kennedy, J. G., "Protecting Marine Structures from Corrosion", Oct. 1967.
43. Lederman, Peter B. and Kallas, "Materials: Key to Exploiting the Oceans", Chemical Engineering, June 3, 1968.
44. Anonymous, "Performance of Exceptional Metals in Corrosive Environments", Materials Protection, Oct. 1967.
45. McIlhenny, W. F. and Zeitoun, M. A., "A Chemical Engineer's Guide to Seawater" (Part 1), Chemical Engineering, Nov. 3, 1969.
46. McIlhenny, W. F. and Zeitoun, M. A., "A Chemical Engineer's Guide to Seawater" (Part 2), Chemical Engineering, Nov. 17, 1969.
47. Garside, Dr. J. E., "The Economics of Corrosion Prevention", Anti-Corrosion, Jan. 1966.

48. Hom, Kenneth, "Composite Materials for Pressure Hull Structures", Ocean Engineering, Vol. 1, pp. 315-324, 1969.
49. Tyson, Samuel E., "Sure Shortcut to Stainless-Steel Specification", Chemical Engineering, Oct. 6, 1969.
50. Pollock, Kenneth G., "Glassy Materials for Hydrospace", Machine Design, Jan. 18, 1968.
51. Anonymous, "Down to the Sea", Machine Design, Jan. 18, 1968.
52. Gillam, W. S., "Materials Problems in Desalination", Ocean Engineering, Vol. 1, pp. 137-142, 1968.
53. Baron, Thomas, "Materials Problems in the Utilization of Marine Non-Biological Resources", Ocean Engineering, Vol. 1, pp. 143-148, 1968.
54. Fried, N., "Structures of Reinforced Plastics", Machine Design, Jan. 18, 1968.
55. Woodland, B. T., "Deep-Submergence Metal Structures", Machine Design, Jan. 18, 1968.
56. LaQue, F. L., "Deterioration of Metals in an Ocean Environment", Ocean Engineering, Vol. 1, pp. 299-312, 1969.
57. Nielson, L. E., "Mechanical Properties of Polymers," (Reinhold: N.Y.); 1962.
58. O'Toole, J. L. and Koo, G. P., "Engineering Properties of 'Plastics", Modern Plastics Encyclopedia, (McGraw-Hill, Inc.: N.Y.); 1966.
59. Smack, K. G. and O'Toole, J. L., "High Temperature Thermo-Setting Molding Compounds", Spe. Retec., Automatic Molding of Thermosets, New Haven, Conn.; Nov. 1967.
60. Turner, S., "A System of Deformation Data for Rational Engineering Design with Plastics", Polymer Engineering and Science, April 1968.
61. Bergen, R. L., "Creep of Thermoplastics in the Glassy Region: Stress as a Reduced Variable", Oct. 1967.
62. Koo, G. P., Riddell, E. D., and O'Toole, J. L., "Engineering Properties of a New Polytetrafluoroethylene," SPE Journal,

Sept. 1965 and "Application of Time-Temperature Superposition Principle to Long Term Engineering Properties of Plastics Materials", Seitz, J. T. and Aalazs, C. F., Polymer Engineering and Science, April, 1968.

63. Tobolski, A. V., "Properties and Structure of Polymers", (New York); 1960.
64. Ferry, J. D., "Viscoelastic Properties of Polymers, (New York); p. 201, 1960.
65. Bergen, R. L., "Environmental Resistance of Plastics", SPE Journal; July 1964.
66. Calderon, O. H., "Colonization of Silicone Rubber by Microorganisms", Int. Biodeter. Bull., pp. 33-37; 1965.
67. Crum, M. G., Reynolds, R. J. and Hendrick, H. G., "Effect of Surfactants and Additives on the Progress of Microbiological Corrosion of Aluminum Alloys", Devel. Incl. Micro.; pp. 253-359, 1967.
68. Doochin, H. D., "Marine Doring and Fouling in Relation to Velocity of Water Currents", Bull. Mar. Sci. of Gulf and Carib.; pp. 196-298, 1951.
69. Eisenschine, R. and Bauer, W. H., "Microbial Degradation of Plasticized Polyvinyl Chloride Films", Am. Chem. Soc., Div. Incl & Eng. Chem., 53rd Meeting, Miami, Fla, 1967.
70. Ferris, A. P., "Synthetic Resins Resistant to Fungal Attack", Nature 212, 1039; 1966.
71. Freiburger, A., Cologer, C.P. Liquori, V. R., and Nigralli, R. F., "Some New Approaches to the Study of Barnacles", Ocean Engineering, pp. 469-474; 1969.
72. Gauger, G. W., Spradlin, B. C., Easterday, J. L., Knuth, D. T., Davidson, R. S., Litchfield, J. H.; "Microbial Degradation of Electronic Components I. Selected Components and Materials of Construction", Devel. Incl. Micro. pp. 372-394, 1967.
73. Hazen, I. W., "Results of First Inter-Laboratory Experiment

- on Biodeterioration of Plastics", Int. Biodeter. Bull., pp. 15-19; 1967.
74. Hedrick, H. G. and Gilmartin, J. N., "A Detection Study of Microbiological Penetration of Aircraft Fuel Tank Coatings", Devel. Ind. Micro.; pp. 124-132, 1965.
 75. Hedrick, H. G., Reynolds, R. J. and Crum, M. G., "Factors Influencing the Mechanism of Corrosion of Aluminum Alloys by Aerobic Bacteria", Devel. Ind. Micro., pp. 267-274, 1967.
 76. Hong, Van S., "Microbial-Metal Corrosion - Literature Report", Final Technical Report, Army Weapons Command, Rock Island, Ill., Research and Engineering Division, RTA-67-534; 1967.
 77. Hueck, E., "A Survey of Biological Test Methods for Microbial Deterioration of Materials", Int. Biodeter. Bull., pp. 38-45; 1965.
 78. Johnson, G. L. and Hayeu, B. C., "Natural Hazards to Submarine Cables", Ocean Engineering, pp. 535-443; 1969.
 79. Klausmeir, R. E. and Jones, W. A., "Microbial Degradation of Plasticizers", Devel. Ind. Micro. pp. 47-54; 1961.
 80. LaQue, F. L., "Deterioration of Metals in an Ocean Environment", Ocean Engineering, pp. 299-312; 1969.
 81. Leeflang, K. W., "Degradation of Rubber Gaskets Used for Sealing Pipe Joints", J. Amer. Water Wks. Assoc., pp. 1070-1076; 1968.
 82. Muraska, J. S., "Deep Ocean Biodeterioration of Materials- Part V. Two Years at 5,640 Feet", Technical Report TR-R-495, Naval Civil Engineering Lab., Port Hueneme, Calif, 1966.
 83. Muraoka, J. S. "Plastic Film Coatings for Protection from Marine Fouling and Corrosion", Technical Report Uul 67 - Aug. 1968, Naval Civil Engineering Lab., Port Hueneme, Calif.; Report No. NCEL-TR-612, 1969.
 84. Pequegnat, W. E., "Biofouling Studies of Panama City, Florida", Texas A&M University Department of Oceanography Project 286-1; 1966.

85. Smith, R. L., "Control of Microbial Damage to Hull Tanks and Linings with 8-Azaquinoline", Devel. Ind. Micro., pp. 360-366.
86. Staffeldt, E. E., "Possible Degradation of Metals by Micro-Organism", pp.321-326; 1967.
87. Tiller, A. K. and Booth, G. K., "Anaerobic Corrosion of Aluminum by Sulfate Reducing Bacteria", Corrosion Science, pp. 547-556; (1968).
88. Wallen, I. S., "Materials Problems in the Utilization of Marine Biology Resources", Ocean Engineering, pp. 149-157, 1968.
89. Anonymous, "An Annotated Bibliography of Marine Fouling for Marine Scientists and Engineers", U.S. Government Clearinghouse for Federal Science and Technical Information, Springfield, Va., 1969.

APPENDIX

	Page
I. Oil Set-up due to current	2a
II. Oil Set-up by wind	42a
III. Hydromechanics of pneumatics	73a
IV. Model tests of pneumatic barrier	173a
V. Miscellaneous	209a

APPENDIX I

RAW DATA

OIL SET-UP BY CURRENT

RUN 1

U=0.692 fps

$\rho_o/\rho_w=0.909$

X(2N)

h(zn)

0	0.0
1	0.1
2	0.8
3	1.0
4	1.1
5	1.1
6	1.0
7	0.9
8	0.8
9	0.75
10	0.75
20	0.9
30	1.1
40	1.25
50	1.35
60	1.45
70	1.50
80	1.60
90	1.70
100	1.75
110	1.80
120	1.90
130	1.90
140	1.5

RUN 2

U=0.885

$\rho_o/\rho_w=0.909$

X(2N)

h(in)

1	0.68
2	1.10
3	1.30
4	1.50
5	1.60
6	1.70
7	1.90
8	2.00
9	2.00
10	2.20
11	2.15
12	2.00
13	1.50
14	1.20
15	1.30
16	1.32
17	1.55
18	1.60
19	1.70
20	1.75
30	2.10
40	2.30
50	2.30
60	2.50
70	2.75
80	2.75
84	2.30
90	2.2
94	2.1

RUN 3
 $U=0.985\text{fps}$ $\rho_o/\rho_w=0.909$

RUN 5
 $U=0.750\text{fps}$ $\rho_o/\rho_w=0.882$

X(in)	h(in)	X(in)	h(in)
1	0.65	0	0
2	1.10	2	1.0
3	1.45	4	1.3
4	1.72	6	1.5
5	2.00	9	1.1
6	2.45	11	1.0
7	2.30	14	1.2
8	2.70	26	1.3
9	2.90	38	1.4
10	3.00	50	1.5
11	3.10	62	--
12	3.00	74	1.6
13	2.75	98	1.8
14	2.30	122	1.9
15	1.90	146	2.1
20	1.95	158	2.0
25	2.40	170	1.7
30	2.90		
35	3.10		
40	2.90		
45	2.70		
50	2.90		
55	3.20		
60	3.45		
65	3.65		
66	3.40		
67	3.00		
68	2.70		
69	2.60		
70	2.50		
71	2.50		
72	2.40		
73	2.40		
74	2.40		
75	2.40		

U=0.974fps

RUN 6

$\rho_o/\rho_w=0.882$

U=0.348fps

RUN 15

$\rho_o/\rho_w=0.904$

X(in)	h(in)	X(in)	h(in)
0	0	0	0
3	1.6	10	0.20
6	2.1	20	0.25
9	2.4	30	0.30
12	1.6	40	0.32
15	1.7	50	0.41
21	1.9	60	0.42
27	2.1	70	0.53
31	2.2	80	0.60
45	2.4	90	0.61
69	2.7	100	0.61
93	3.0	110	0.70
105	3.2	120	0.70
117	2.5	130	0.72
		140	0.75
		150	0.75
		160	0.77
		170	0.78
		180	0.75
		190	0.70
		200	0.70
		210	0.68
		218	0.62

RUN 16		RUN 17	
U=0.527fps		U=0.603	
$\rho_o/\rho_u=0.904$		$\rho_o/\rho_w=0.904$	
X(in)	h(in)	X(in)	h(in)
0.5	0.25	0	0
1.0	0.26	1	0.25
1.5	0.28	2	0.30
2.0	0.30	3	0.31
12.0	0.30	4	0.30
22.0	0.55	5	0.31
30.0	0.60	10	0.40
42.0	0.62	20	0.45
52.0	0.70	30	0.60
62.0	0.73	40	0.69
72.0	0.75	50	0.72
82.0	0.76	60	0.79
92.0	0.80	70	0.86
102.0	0.85	80	0.91
112.0	0.88	90	0.97
122.0	0.82	100	1.00
132.0	0.82	110	0.96
142.0	0.85	120	0.92
152.0	0.85	123	0.90
162.0	0.88		
165.5	0.76		

RUN 18
U-1.00fps $\rho_o/\rho_w=0.900$

X(in)	h(in)
0	0
1	0.8
2	1.0
3	1.1
5	1.5
6	1.6
7	1.8
8	1.8
9	1.9
10	1.8
15	1.5
20	1.7
30	1.9
40	2.0
50	2.1
60	2.3
70	2.5
80	2.7
90	2.9
100	3.1
110	2.5

RUN 19
U=0.782 $\rho_o/\rho_w=0.900$

X(in)	h(in)
0	0
1	0.9
2	1.0
3	1.2
4	1.4
5	1.5
6	1.5
7	1.2
8	1.0
10	1.2
15	1.2
20	1.3
30	1.3
40	1.4
50	1.6
60	1.7
70	1.8
80	1.8
10	1.9
100	2.0
110	2.0
120	2.1
130	2.1
140	2.2
150	1.8
161.5	1.7

RUN 20
U=0.616fps

$\rho_o/\rho_w=0.900$

RUN 21
U=1.130ft/sec $\rho_o/\rho_w=0.900$

X(in)	h(in)	X(in)	h(in)
1	.22	1	.6
2	.25	2	.9
3	.28	3	1.1
4	.3	4	1.5
5	.3	5	1.8
6	.3	6	2.0
9	.33	7	2.2
12	.40	8	2.5
15	.39	9	2.8
18	.42	10	2.9
21	.45	11	2.8
24	.50	12	2.7
30	.52	13	2.4
40	.59	14	2.1
50	.6	15	1.9
60	.75	18	1.6
70	.78	21	1.7
80	.8	24	1.8
90	.85	27	2.1
100	.9	30	2.4
110	1.0	40	2.6
120	1.05	50	2.8
130	1.15	60	3.1
140	1.15	70	3.5
150	1.18	80	3.0
160	1.20	85.5	2.6
170	1.25		
180	1.28		
190	1.30		
200	1.35		
210	1.38		
220	1.40		
230	1.45		
240	1.48		
250	1.35		
253	1.25		

RUN 22
 $U=1.153\text{fps}$ $\rho_o/\rho_w=0.900$

RUN 24
 $U=0.590\text{fps}$ $\rho_o/\rho_w=0.845$

X(in)	h(x)	X(in)	h(in)	X(in)	h(in)
1.0	0.7	3	0.29	210	1.03
2.0	1.0	6	0.33	220	1.04
3.0	1.3	9	0.35	230	1.05
4.0	1.5	12	0.40	240	1.06
5.0	1.6	15	0.41	250	1.06
6.0	1.8	18	0.42	260	1.07
7.0	2.0	21	0.44	270	1.07
8.0	2.4	24	0.45	280	1.08
9.0	2.6	30	0.46	290	1.00
10.0	2.7	36	0.49	295	0.90
11.0	2.9	42	0.51	298	0.85
12.0	3.1	50	0.52		
13.0	3.1	60	0.56		
14.0	3.2	70	0.59		
15.0	3.2	80	0.64		
16.0	3.0	90	0.68		
17.0	2.7	100	0.75		
18.0	2.6	110	0.78		
21.0	2.1	120	0.81		
24.0	2.1	130	0.83		
30.0	2.5	140	0.87		
40.0	3.1	150	0.90		
45.0	3.5	160	0.94		
50.0	3.4	170	0.97		
58.5	2.5	180	0.99		
		190	1.02		
		200	1.03		

U=0.823 fps $\rho_0/\rho_1=0.845$

U=1.037 fps $\rho_0/\rho_2=0.845$

X(in)	h(in)	X(in)	h(in)
2	.30	1	.70
5	.35	2	.90
6	.40	3	1.00
8	.50	4	1.24
12	.60	5	1.30
15	.63	6	--
18	.60	7	--
21	.63	8	1.40
24	.65	9	1.60
30	.68	10	1.65
36	.73	11	1.50
42	.80	12	1.45
50	.86	13	--
60	.93	14	--
70	.92	15	1.15
80	.95	18	1.20
90	.98	21	1.40
100	1.01	24	1.60
110	1.03	30	1.60
120	1.13	40	1.65
130	1.15	50	1.70
140	1.21	60	2.00
150	1.26	70	2.00
160	1.30	80	2.20
170	1.33	90	2.20
180	1.35	100	2.40
190	1.38	103	2.70
198	1.47	110	1.70
200	1.42	115	1.30

RUN 27
U=1.263fps

$\rho_0/\rho_\infty=0.845$

X(in)	h(in)	X(in)	h(in)
1	0.426	50	21.276
2	0.851	55	23.404
3	1.276	60	25.532
4	1.702	65	27.660
5	2.128	67	28.511
6	2.553	70	29.737
7	2.979	75	31.439
8	3.404		
9	3.830		
10	4.255		
11	4.681		
12	5.106		
15	6.383		
16	6.880		
17	7.234		
18	7.660		
19	8.085		
20	8.511		
21	8.936		
22	9.362		
23	9.787		
24	10.213		
25	10.638		
26	11.064		
27	12.489		
28	11.815		
29	12.340		
30	12.766		
31	13.191		
32	13.617		
33	14.042		
36	15.319		
40	17.021		
45	19.149		

RUN 29
U=1.062fps $\rho_0/\rho_\infty=0.806$

X(in)	h(in)
1	0.30
2	0.68
3	0.79
4	0.92
7	0.95
10	0.99
15	0.90
20	0.95
25	1.00
30	1.06
35	1.12
40	1.21
45	1.19
50	1.20
55	1.25
60	1.19
65	1.10
70	1.20
80	1.20
90	1.20
100	1.41
103	1.40
104	1.31
105	1.25
106	1.12
107	1.10
108	1.10
109	1.00
110	0.90
111	0.91
112	0.90
113	0.85

U=.947ft/sec RNN 33 $\rho_0/\rho_1=.825$

X(in)	h(in)
1	.2
2	.3
3	.3
4	.4
5	.5
6	.5
7	.4
8	.5
9	.5
10	.6
15	.6
20	.65
25	.70
30	.70
35	.75
40	.75
50	.85
60	.90
70	.90
80	.90
90	1.00
100	1.00
110	1.00
112	1.15
115	1.00
116	.95
117	.90
118	.9
119	.8
120	.8
121	.8
122	.8
123	.7
124	.7
125	.6

U=1.062fps RNN 34 $\rho_0/\rho_1=.825$

X(in)	h(in)
1	.25
2	.25
3	.30
4	.30
5	.35
6	.50
7	.60
8	.85
9	.85
10	.95
11	1.00
12	.90
13	.90
14	.75
15	.70
20	.90
25	.85
30	.90
35	.95
40	.95
45	1.20
50	1.10
60	1.20
70	1.30
80	1.35
85	1.20
91	1.30
92	1.20
93	1.00
94	1.00
95	1.00
96	.90
97	.90
98	.90
99	.90
100	.80
101	.90

RUN 35
U=1.228fps

$\rho_o/\rho_w=0.825$

X(in)	h(in)	X(in)	h(in)
1.0	0.35	55.0	1.2
3.0	0.55	56.0	1.1
4.0	0.65	57.0	1.1
5.0	0.80	58.0	1.1
6.0	0.90	59.0	0.9
7.0	1.10	60.0	0.8
8.0	1.10	61.0	0.7
9.0	1.20	61.5	0.7
10.0	1.30		
11.0	1.30		
12.0	1.40		
13.0	1.40		
14.0	1.50		
15.0	1.50		
16.0	1.30		
17.0	1.30		
18.0	1.10		
19.0	1.00		
20.0	1.00		
21.0	1.10		
22.0	1.30		
23.0	1.40		
24.0	1.50		
25.0	1.50		
26.0	1.60		
27.0	1.60		
28.0	1.60		
29.0	1.60		
30.0	1.60		
35.0	1.40		
40.0	1.50		
45.0	1.70		
50.0	1.60		
52.0	1.50		
53.0	1.50		
54.0	1.30		

RUN 58 (Flume #3)
U=1.456fps $\rho_o/\rho_w=0.900$

X(ft)	h(in)	X(ft)	h(in)
		26.0	4.8
0.5	1.5	27.0	4.0
1.0	1.5	28.0	3.8
1.5	1.7	29.0	3.7
2.0	1.7	30.0	4.7
2.5	1.5	31.0	4.0
3.0	1.0	32.0	5.2
3.5	2.8	33.0	3.9
4.0	3.3	34.0	5.1
4.5	2.8	35.0	4.9
5.0	1.5	36.0	4.6
5.5	1.8	37.0	4.8
6.0	3.2	38.0	4.0
6.5	3.0	39.0	4.0
7.0	3.0	40.0	4.7
7.5	2.6	41.0	4.4
8.0	3.0	42.0	4.6
8.5	2.7	43.0	4.2
9.0	3.8	44.0	4.0
9.5	3.1	45.0	3.8
10.0	2.9	46.0	3.7
10.5	3.8	47.0	4.3
11.0	3.8	48.0	4.5
12.0	3.7	49.0	5.3
13.0	2.7		
14.0	3.4		
15.0	3.9		
16.0	4.1		
17.0	3.8		
18.0	4.6		
19.0	3.4		
20.0	2.8		
21.0	3.0		
22.0	3.9		
23.0	3.8		
24.0	4.4		
25.0	3.6		

RUN 30
U=1.291 $\rho_o/\rho_w=0.81$

X(in)	h(in)
1	.3
2	.4
3	.48
4	.52
5	.68
8	.75
12	1.23
16	.69
20	.90
25	1.30
30	1.45
40	1.65
50	1.68
60	1.80
65	1.88
67	1.70
68	1.62
69	1.35
70	1.20
71	--
72	1.10
73	1.15
74	.90
75	.85
76	.80
77	.90

RUN 31
U=1.568 $\rho_o/\rho_w=0.810$

X(in)	h(in)
1	.50
2	.70
3	.78
4	.81
5	1.20
6	1.31
7	1.25
8	1.25
9	1.50
10	1.60
11	1.80
15	2.30
18	1.65
21	1.39
24	1.40
27	1.62
30	1.85
35	2.15
40	2.10
45	2.10
48	2.05
49	2.18
50	2.30
51	2.29
52	2.09
53	1.75
54	1.70
55	1.50
56	1.50
57	1.49
58	1.30

U=1,695fps RUN 59

$\rho_o/\rho_w=.900$

X(ft)	h(in)	X(ft)	h(in)
1/2	4.6	32	6.0
1	4.6	33	4.9
1 1/2	3.4		
2	2.2		
2 1/2	3.6		
3	3.7		
3 1/2	3.5		
4	2.7		
4 1/2	3.0		
5	3.2		
5 1/2	3.2		
6	3.7		
7	3.4		
8	4.4		
9	5.1		
10	3.7		
11	4.6		
12	4.4		
13	5.5		
14	4.0		
15	4.0		
16	5.0		
17	4.8		
18	4.8		
19	5.4		
20	5.0		
21	4.1		
22	4.8		
23	3.8		
24	3.3		
25	4.6		
26	4.5		
27	5.0		
28	6.2		
29	4.6		
30	5.0		
31	5.9		

U=2.261fps RUN 60
 $\rho_o/\rho_w=.900$

X(ft)	h(in)
1/2	6.5
1	6.0
1 1/2	5.2
2	5.2
2 1/2	6.0
3	4.3
4	4.5
5	4.0
6	6.9
7	5.3
8	6.8
9	7.4
10	7.6
11	5.9
12	4.9
13	7.3
14	5.0
15	7.2
16	7.1

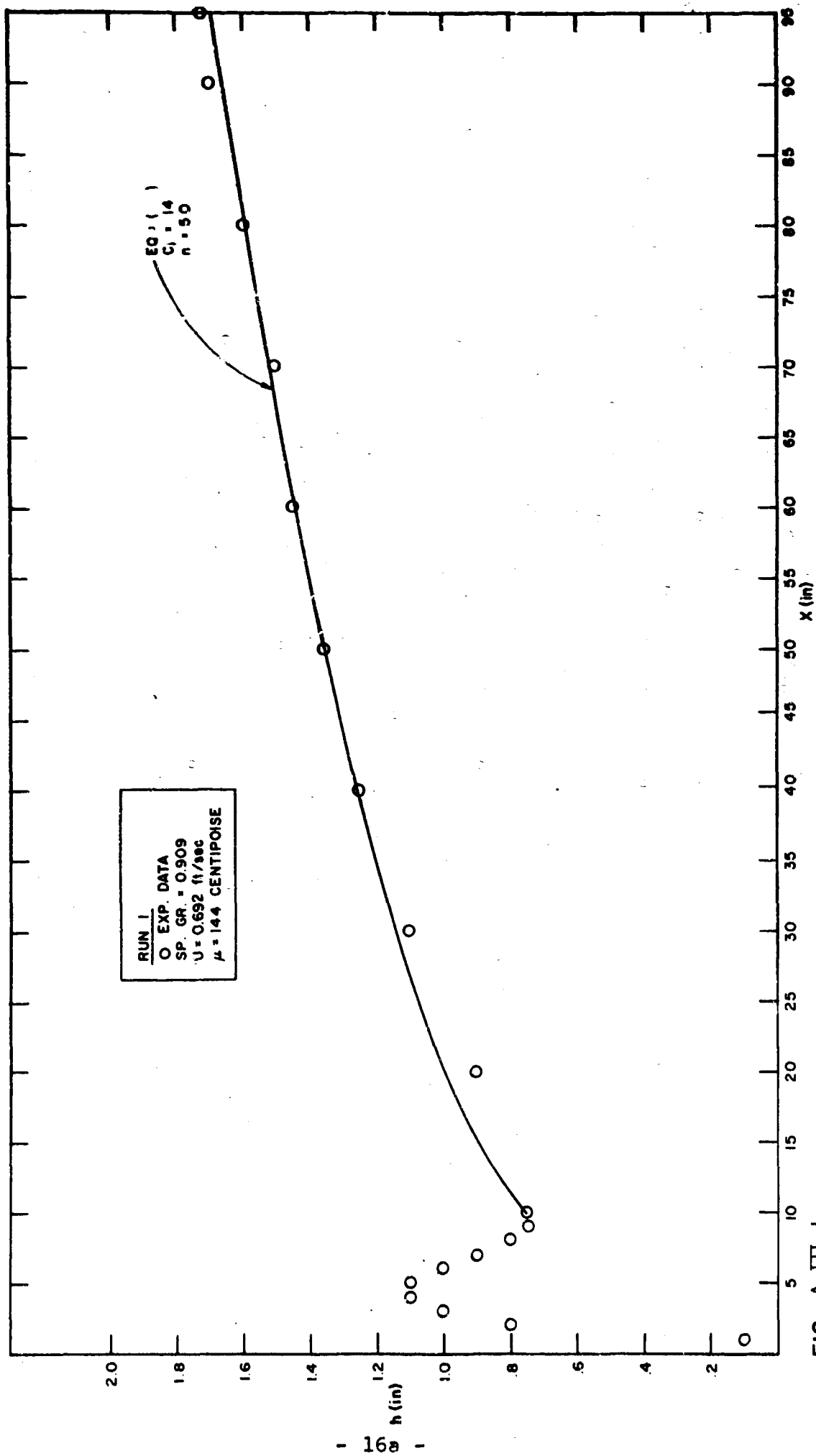


FIG. A-III-1

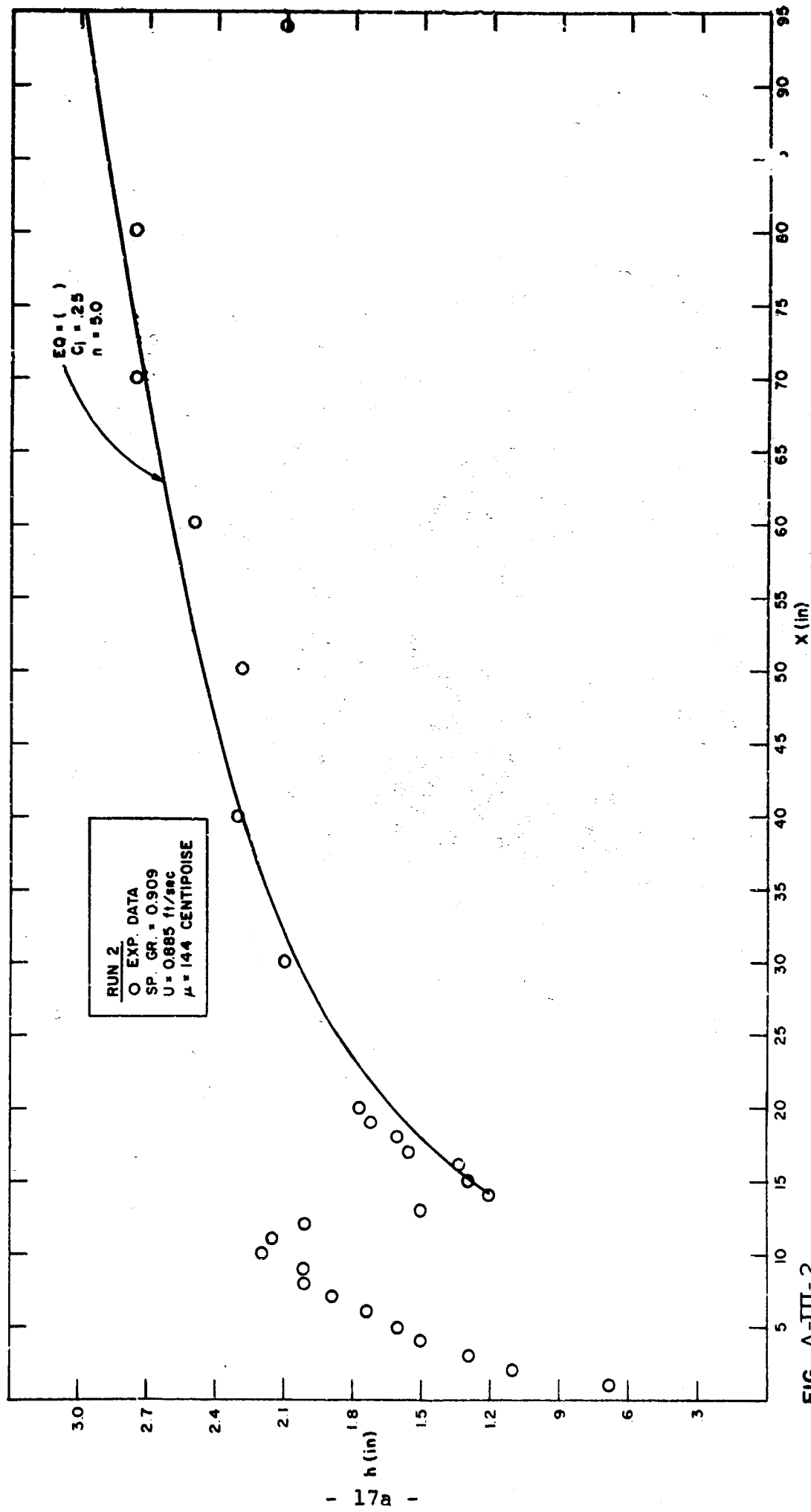


FIG. A-III-2

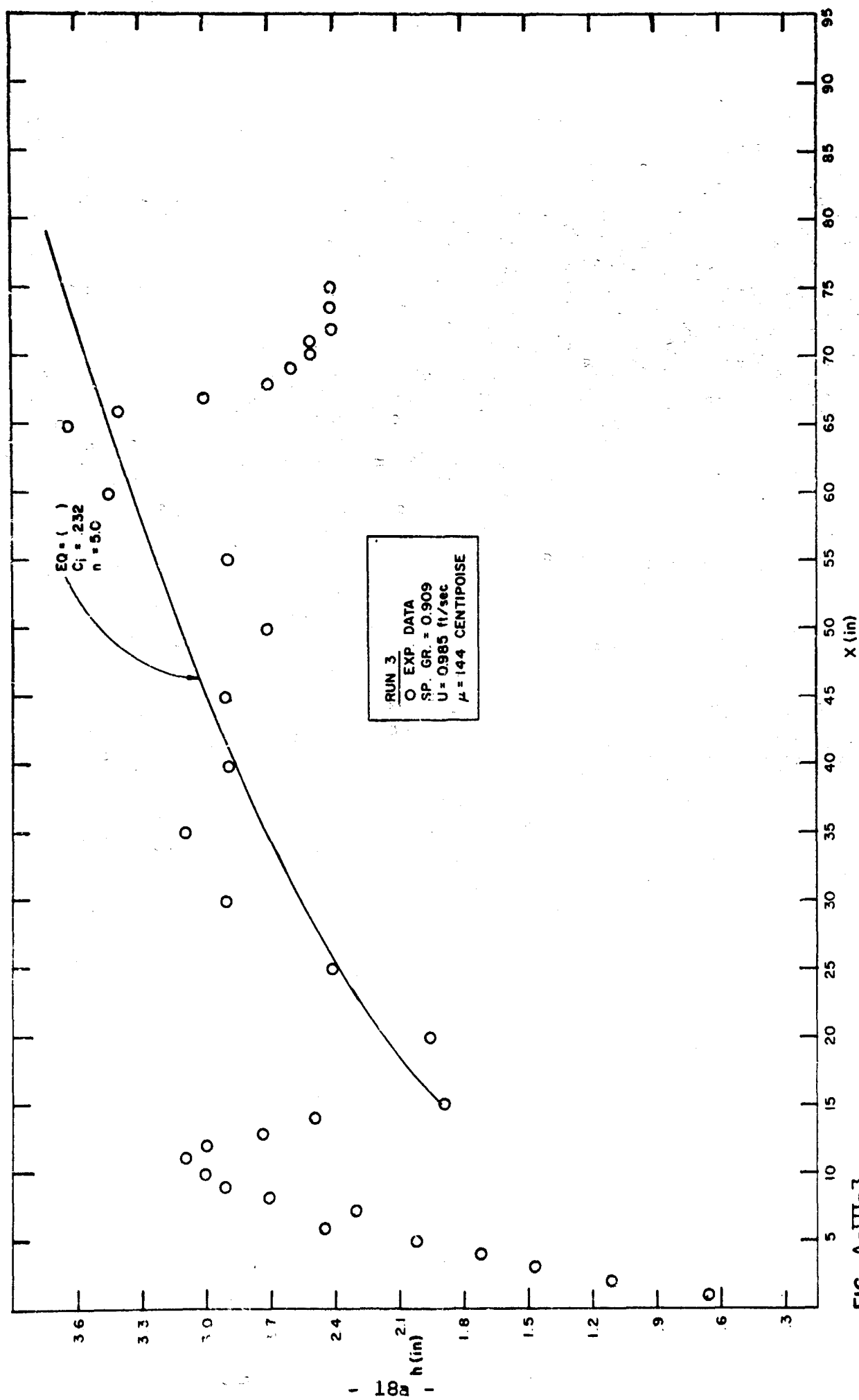


FIG. A-III-3

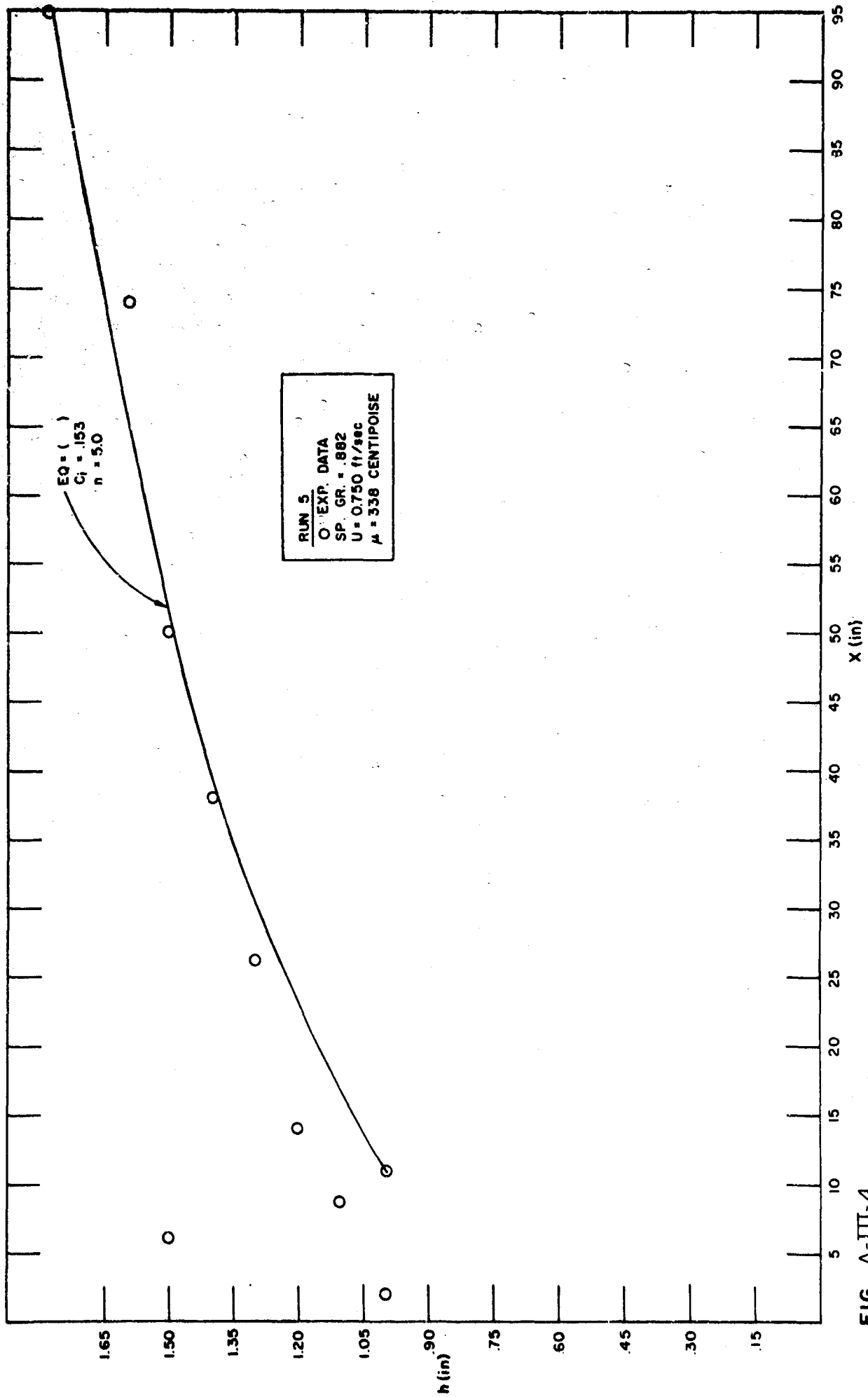


FIG. A-III-4

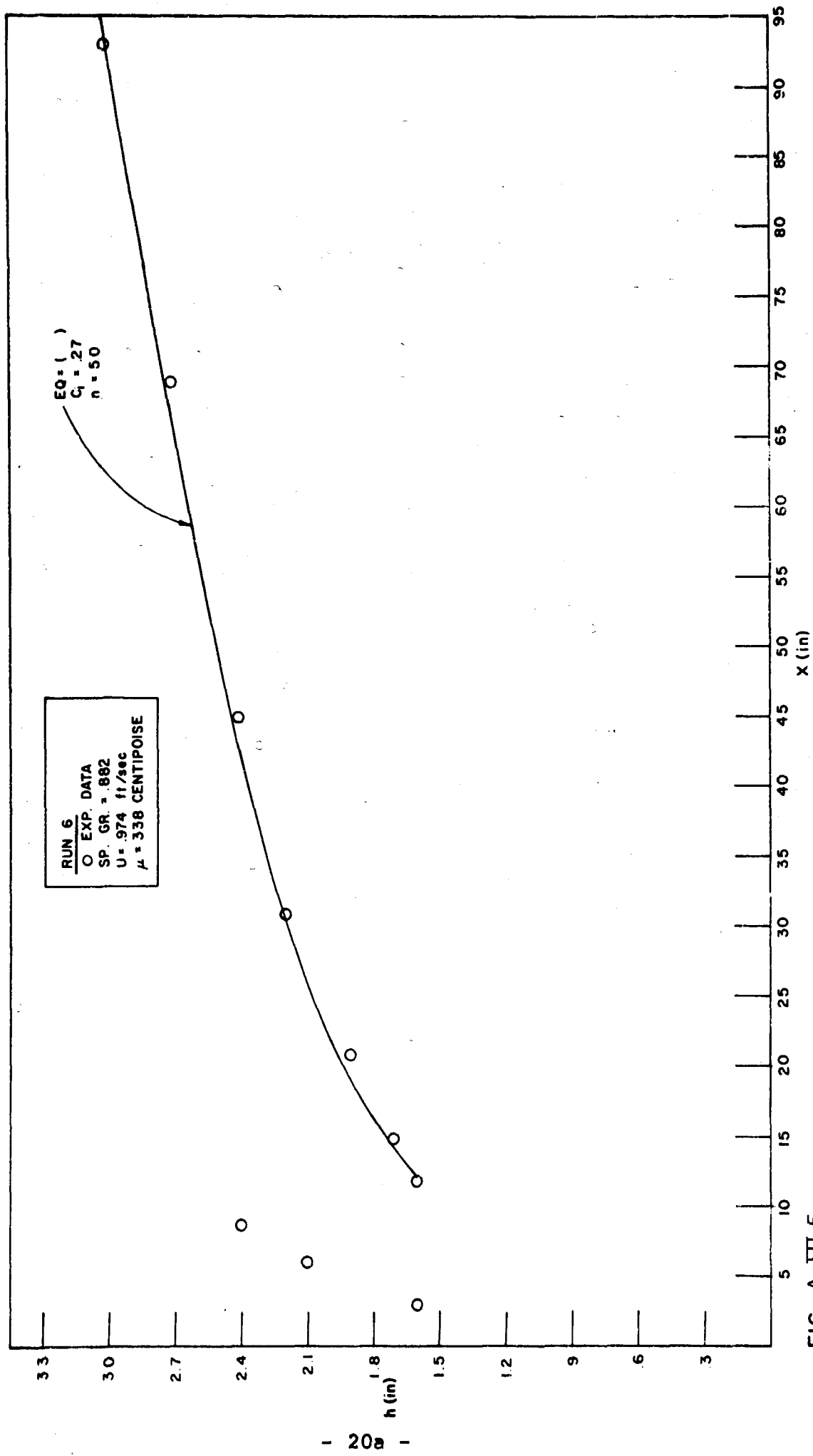


FIG. A-III-5

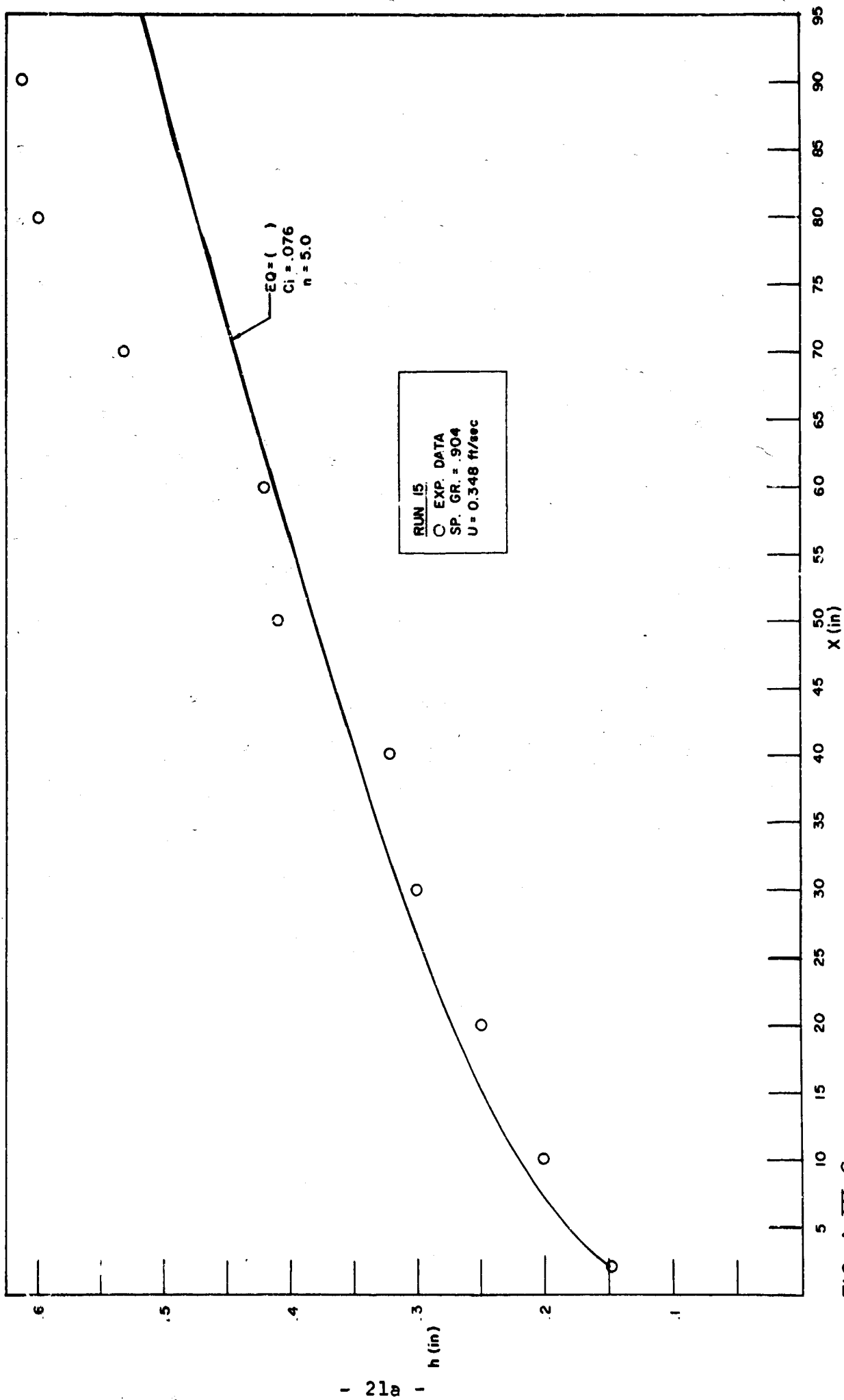


FIG. A-III-6

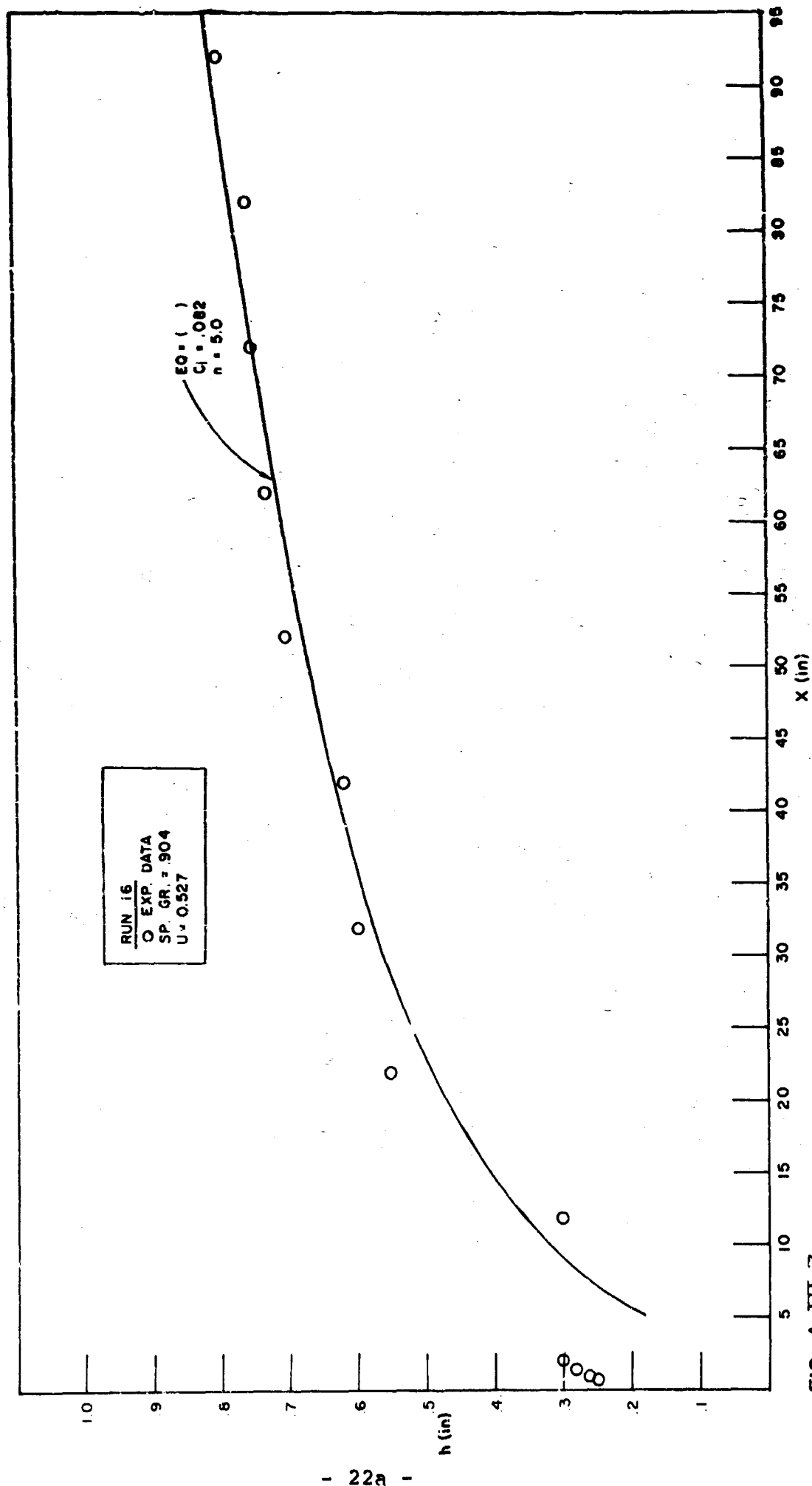


FIG. A-III-7

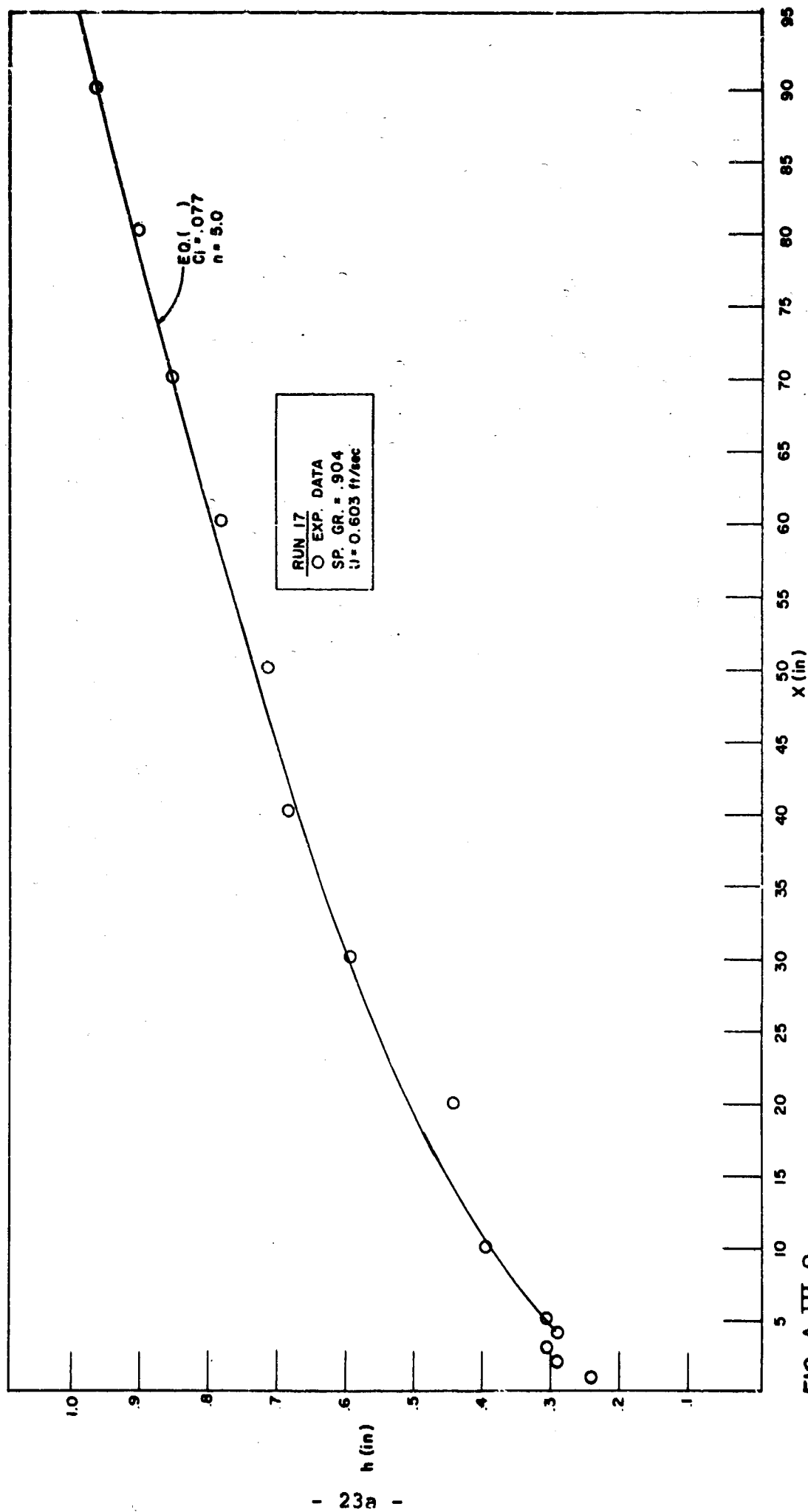


FIG. A-III-8

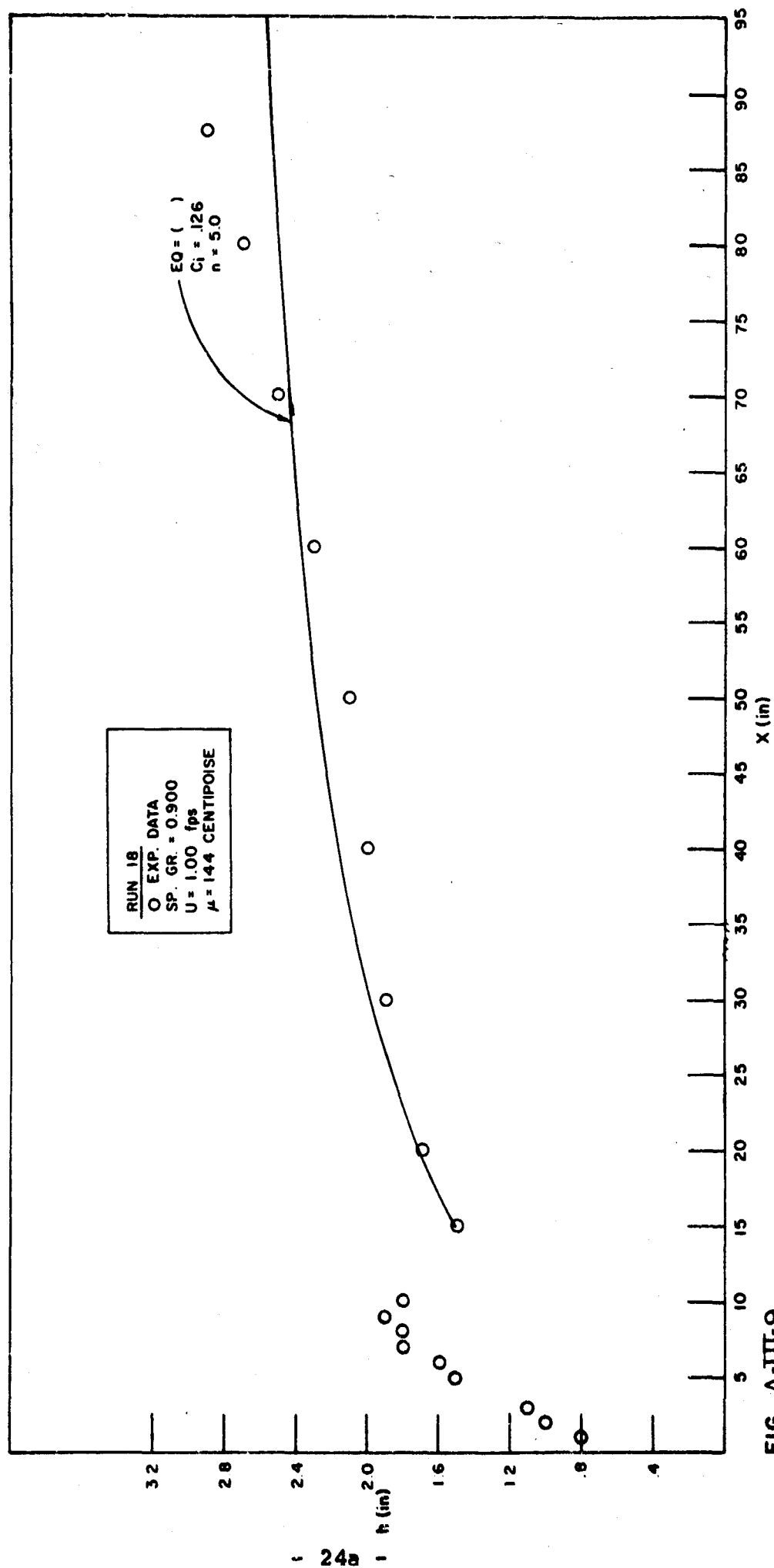


FIG. A-III-9

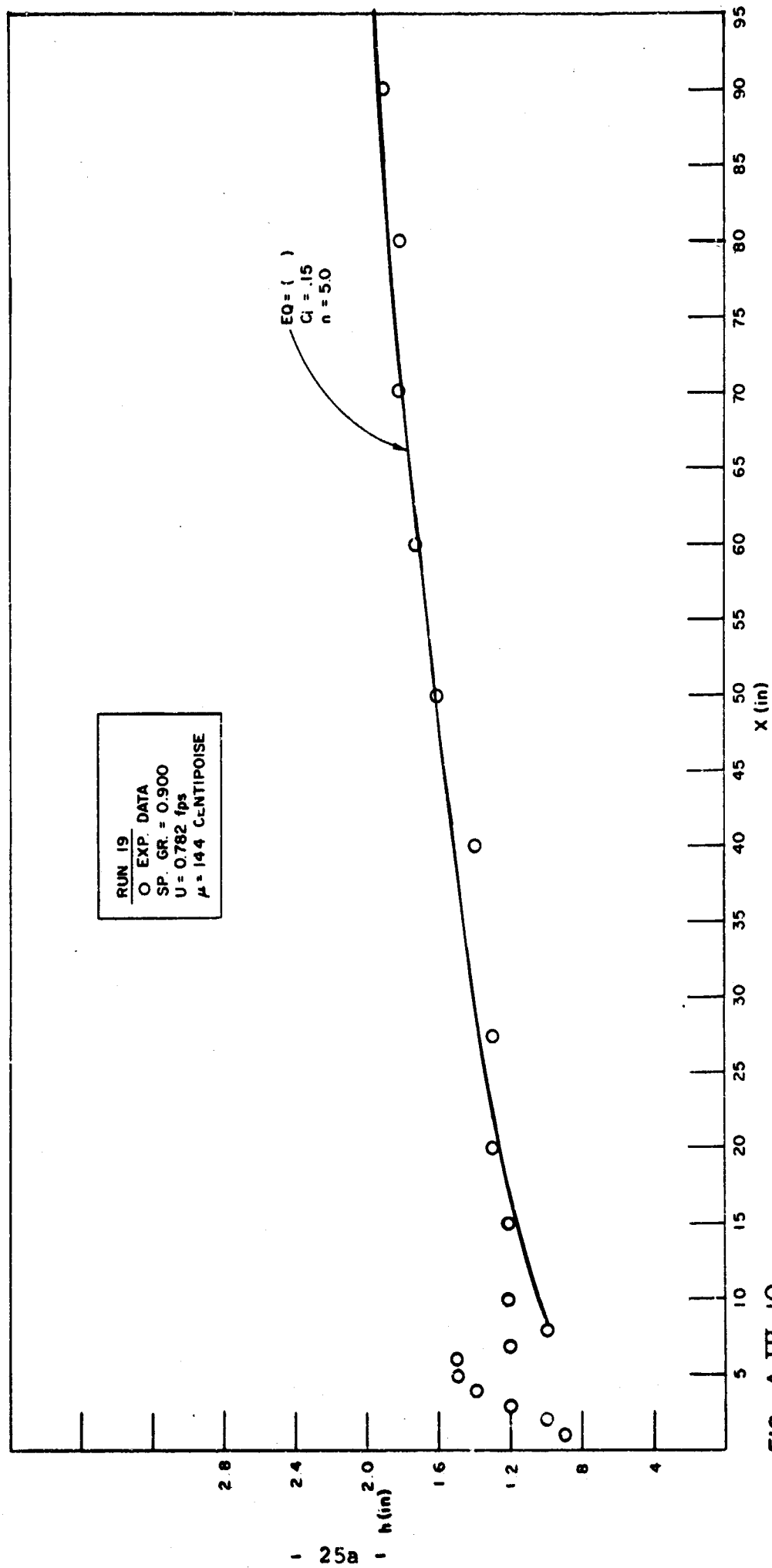


FIG. A-III-10

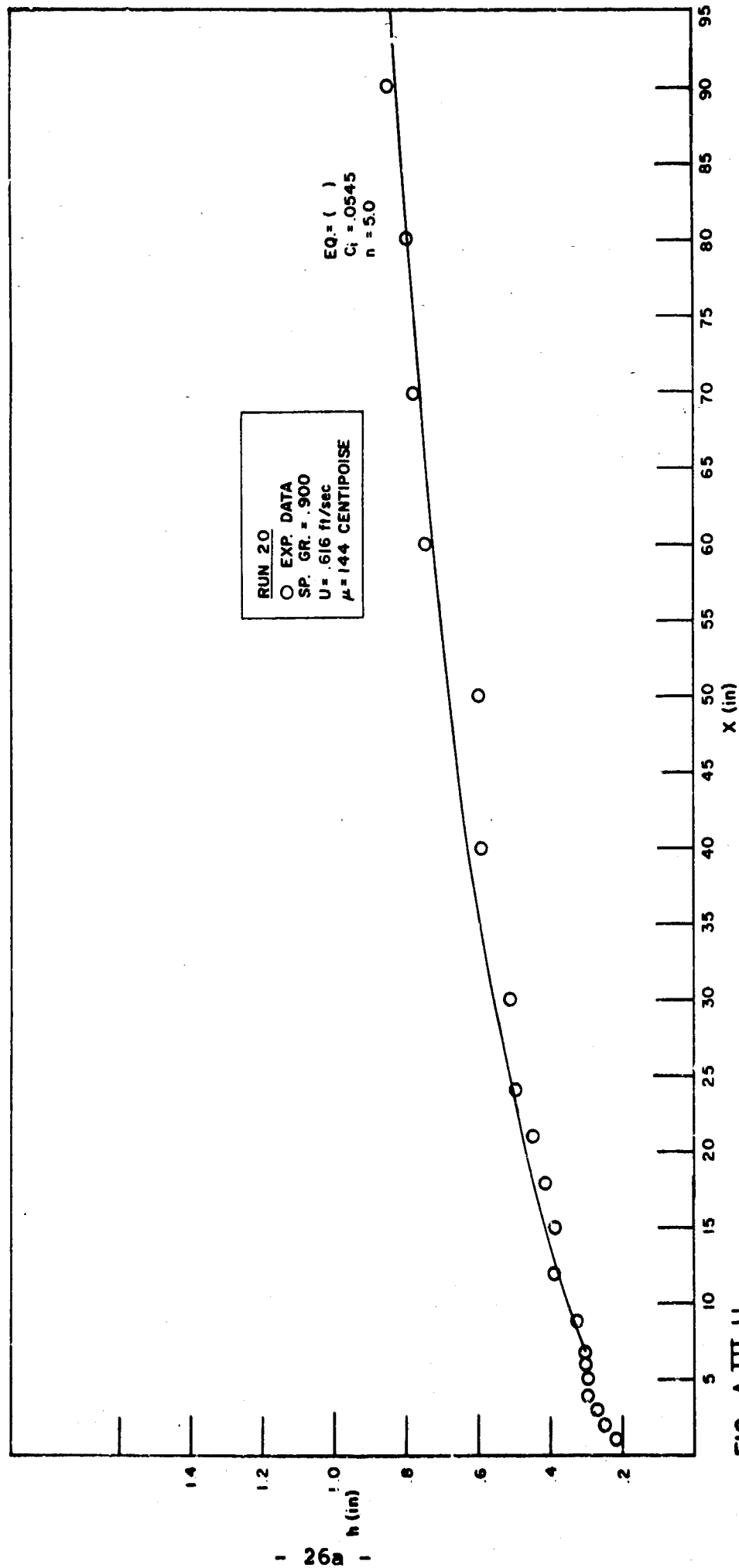


FIG. A-III-11

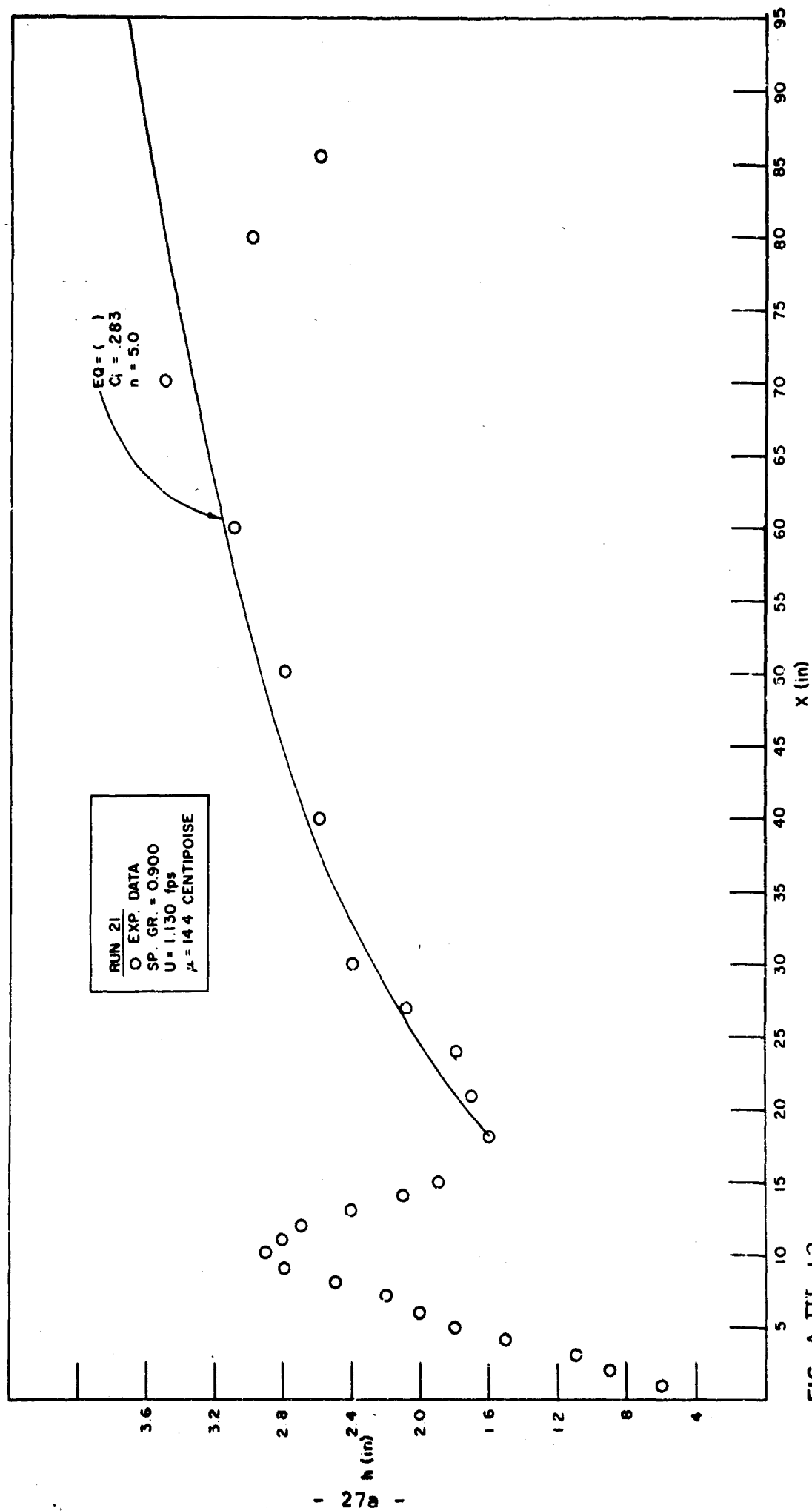


FIG. A-III-12

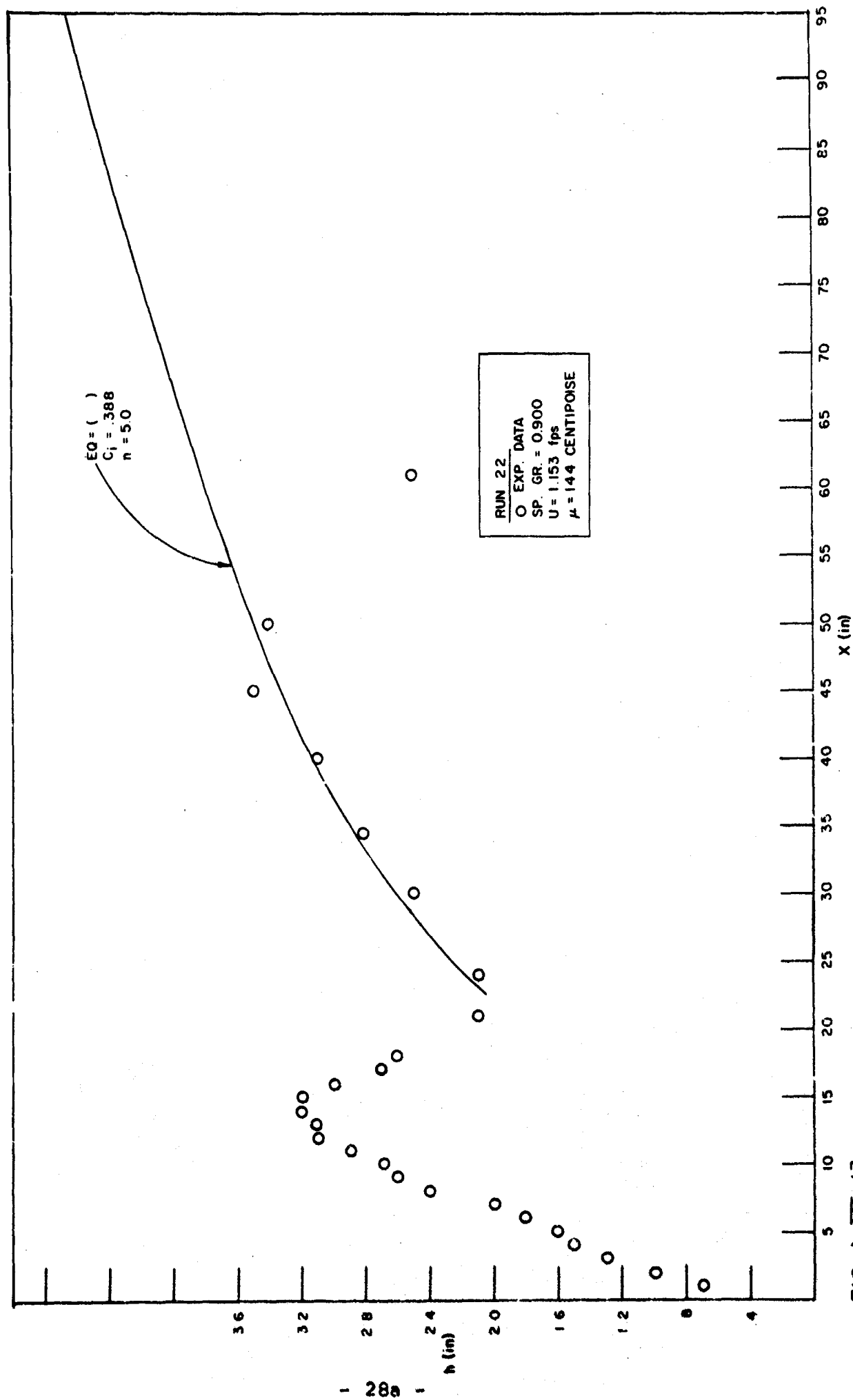


FIG. A-III-13

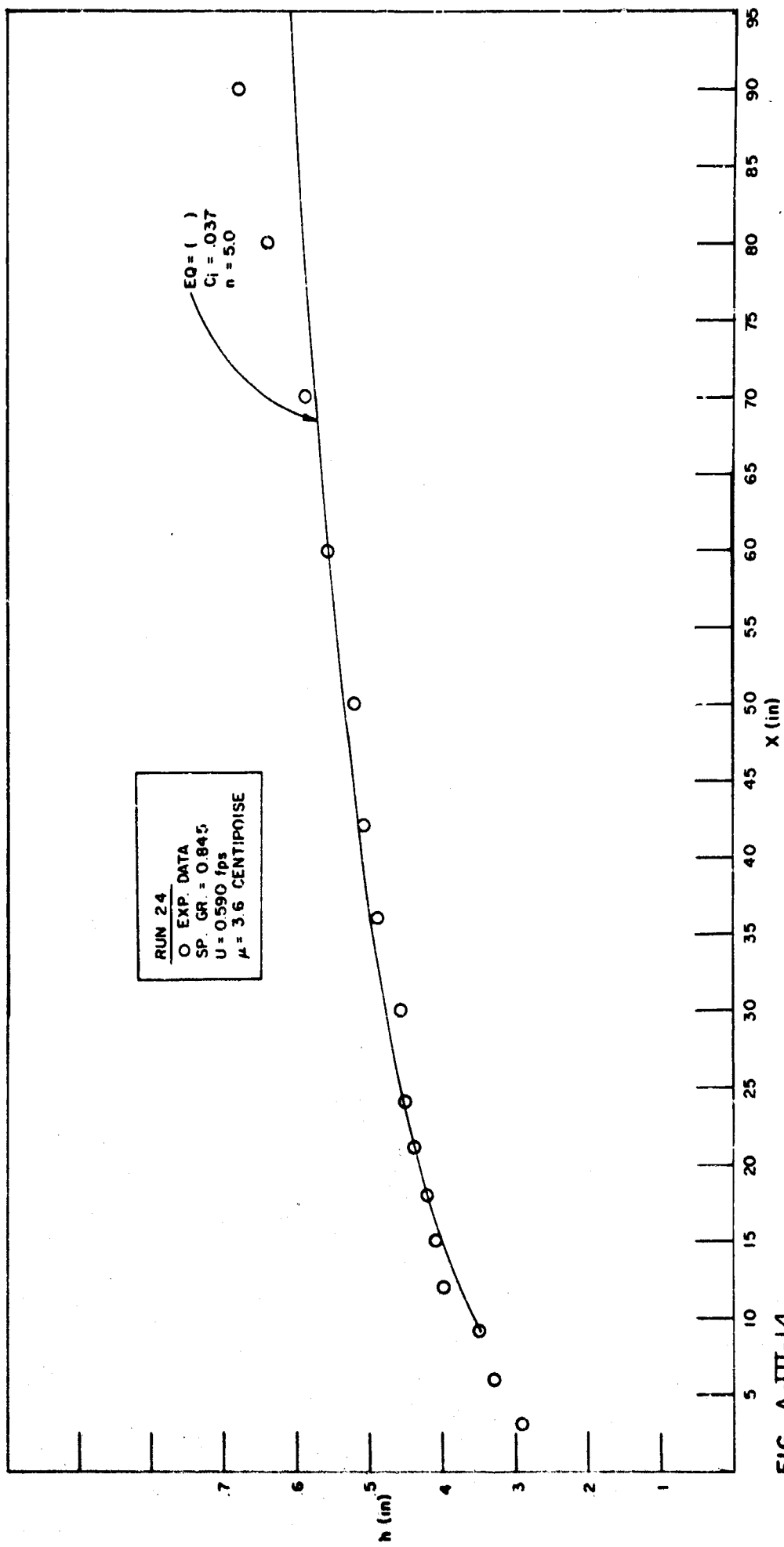


FIG. A-III-14

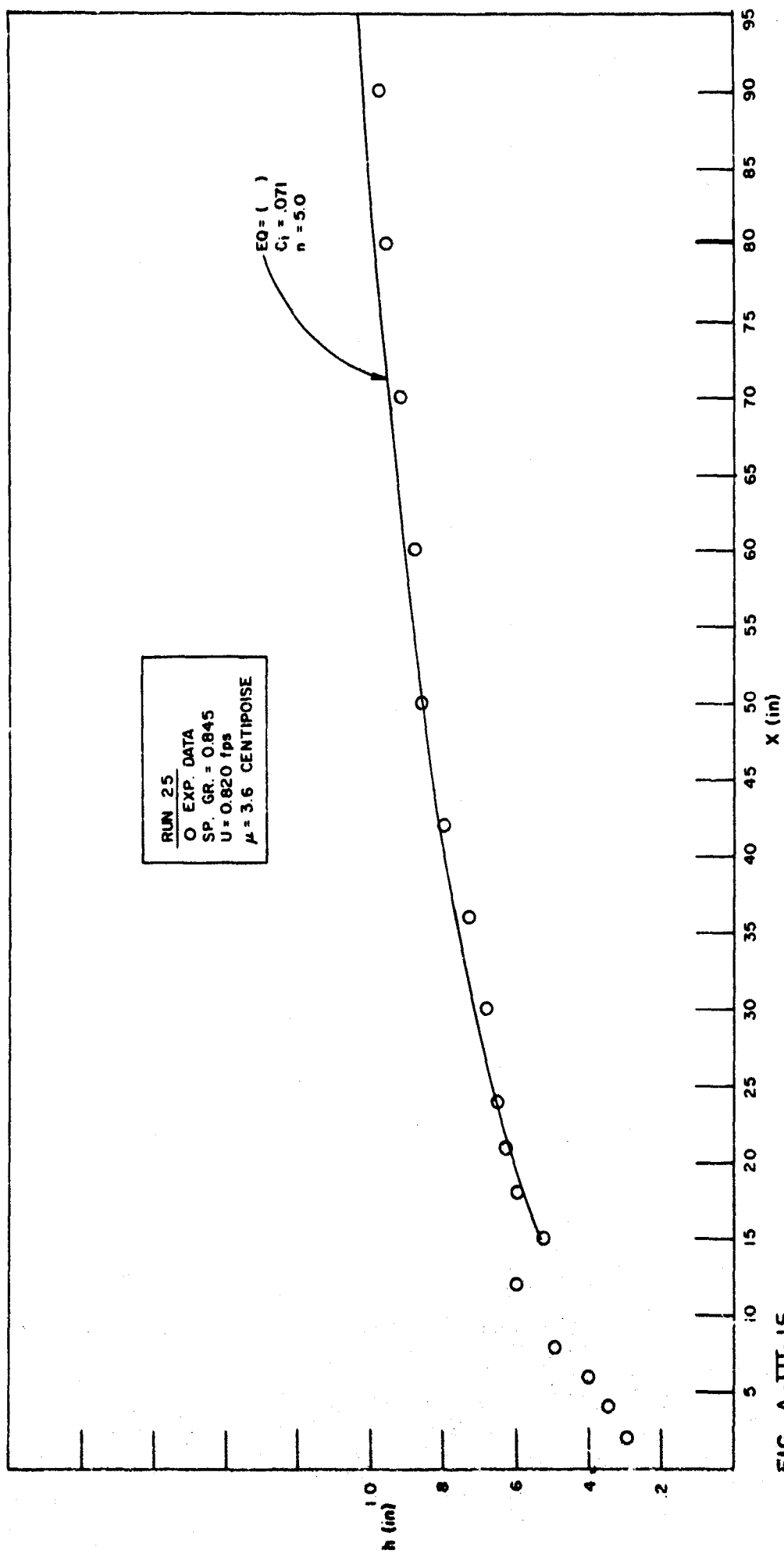


FIG. A-III-15

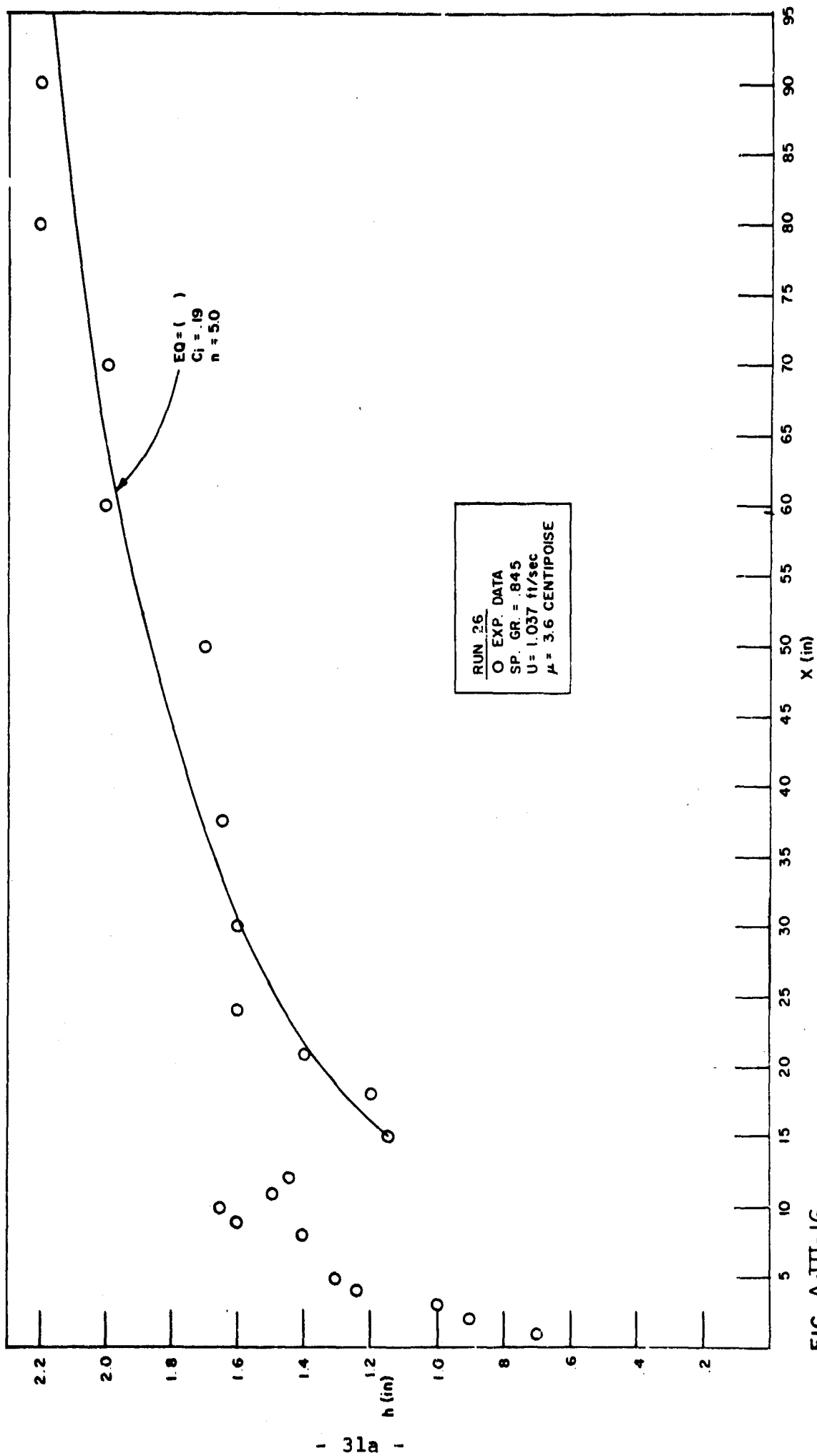


FIG. A-III-16

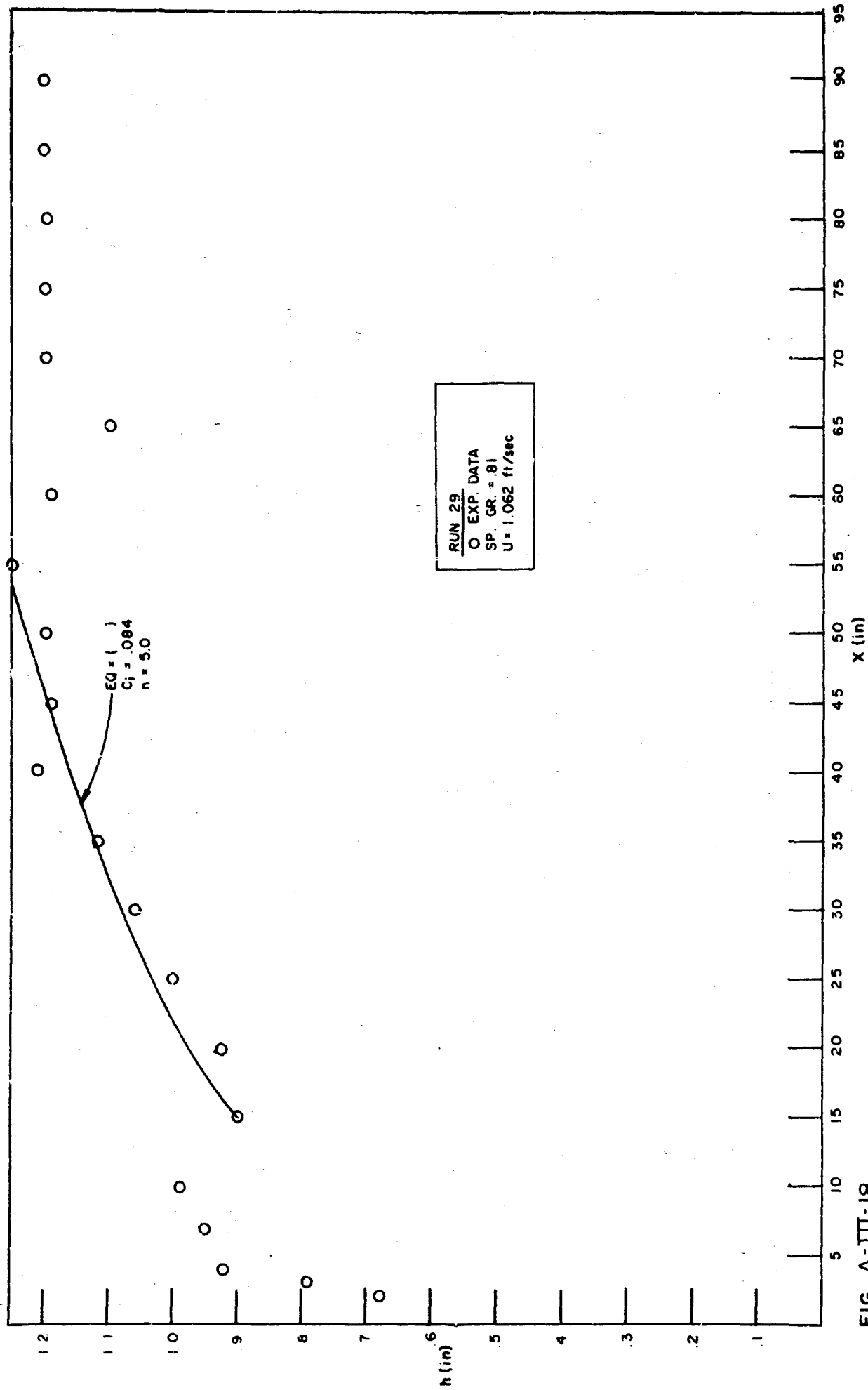


FIG. A-III-18

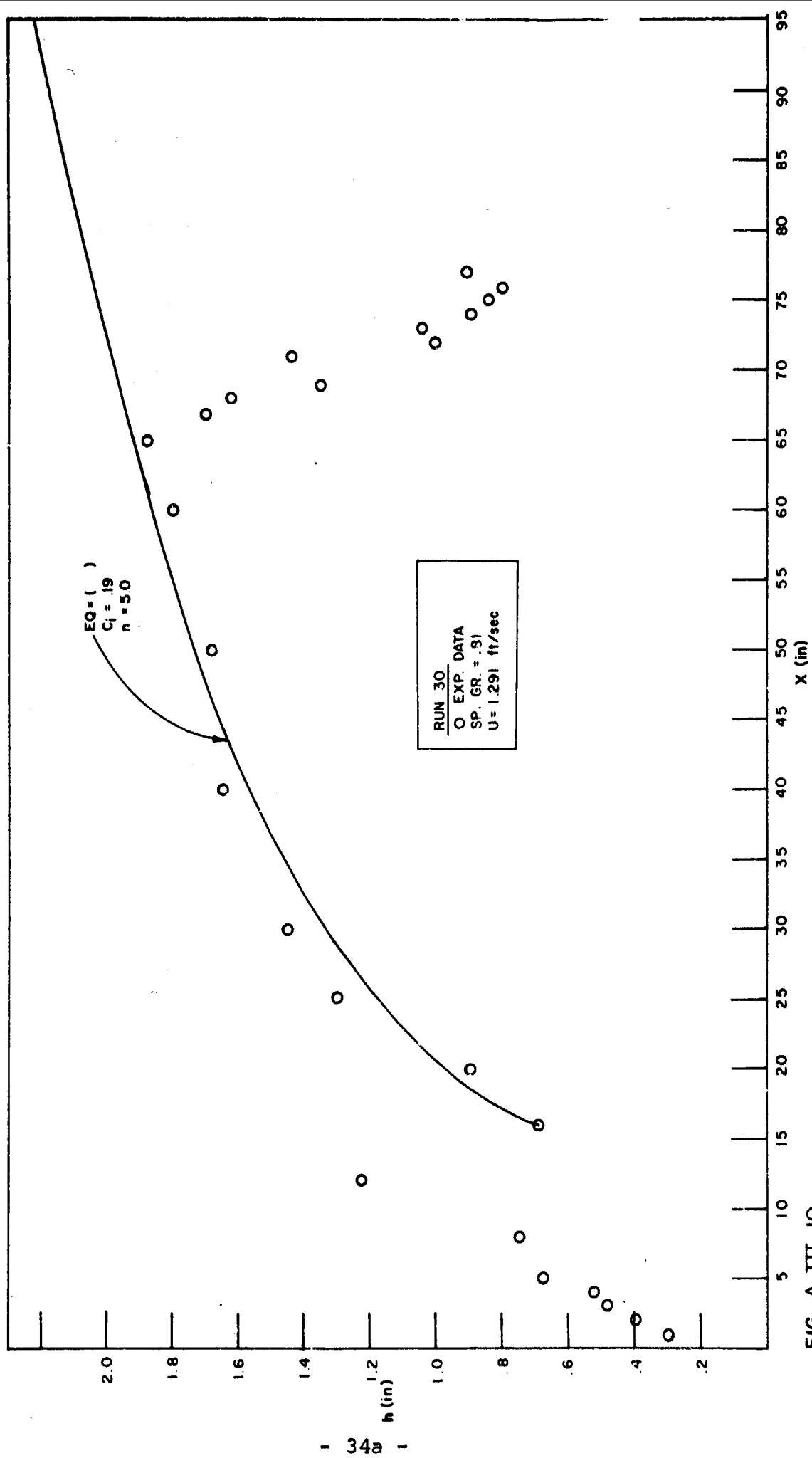


FIG. A-III-19

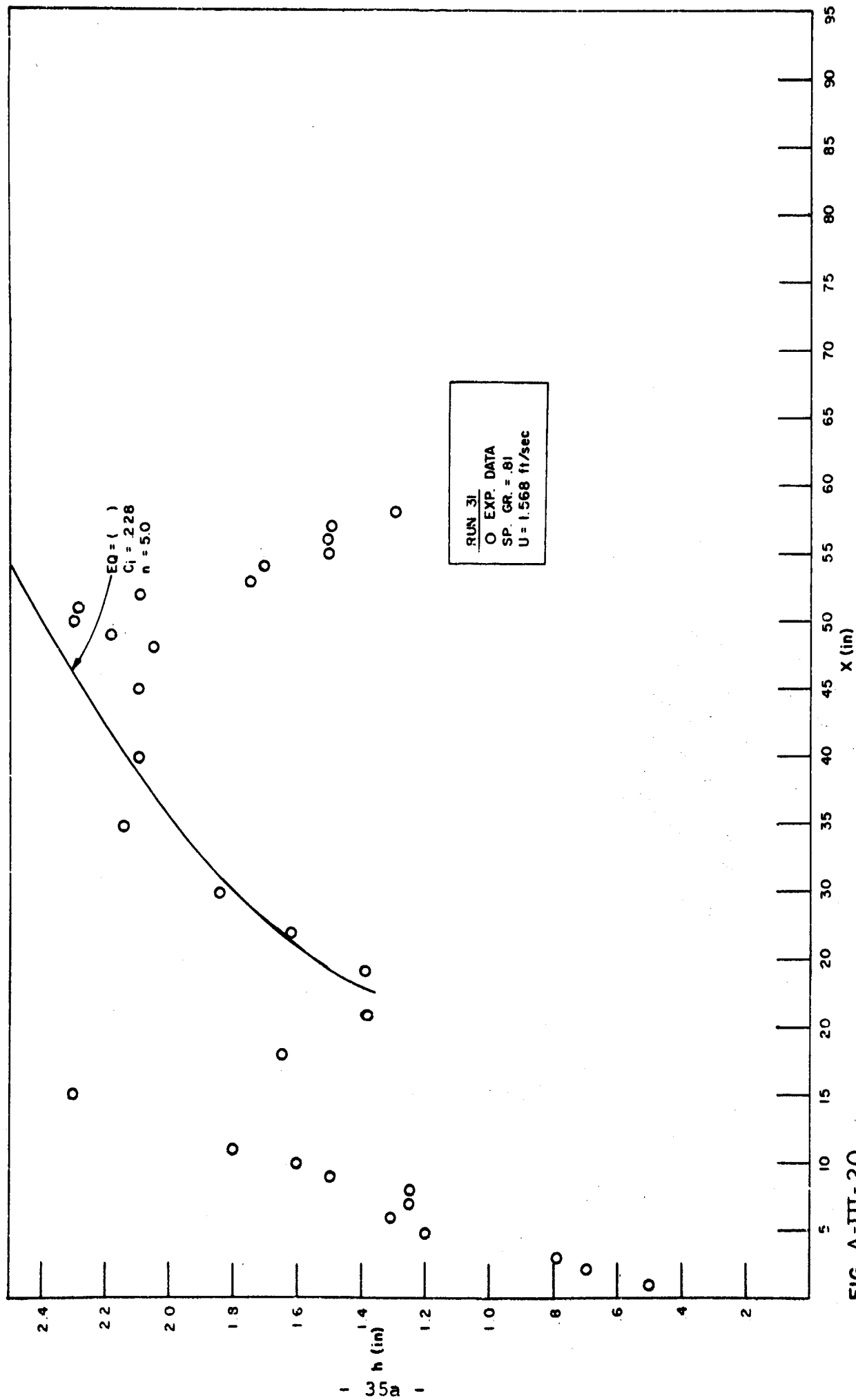


FIG. A-III-20

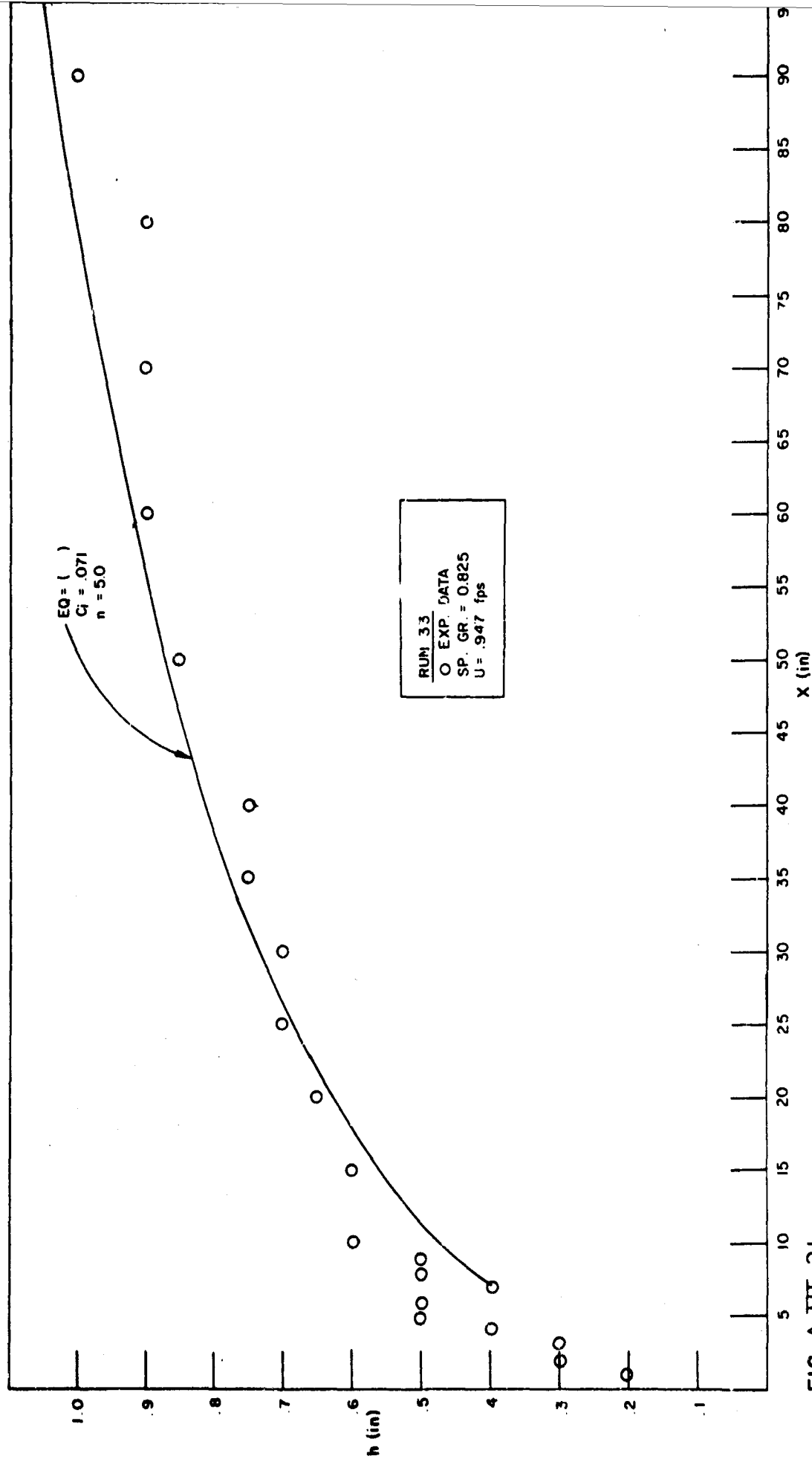


FIG. A-III-21

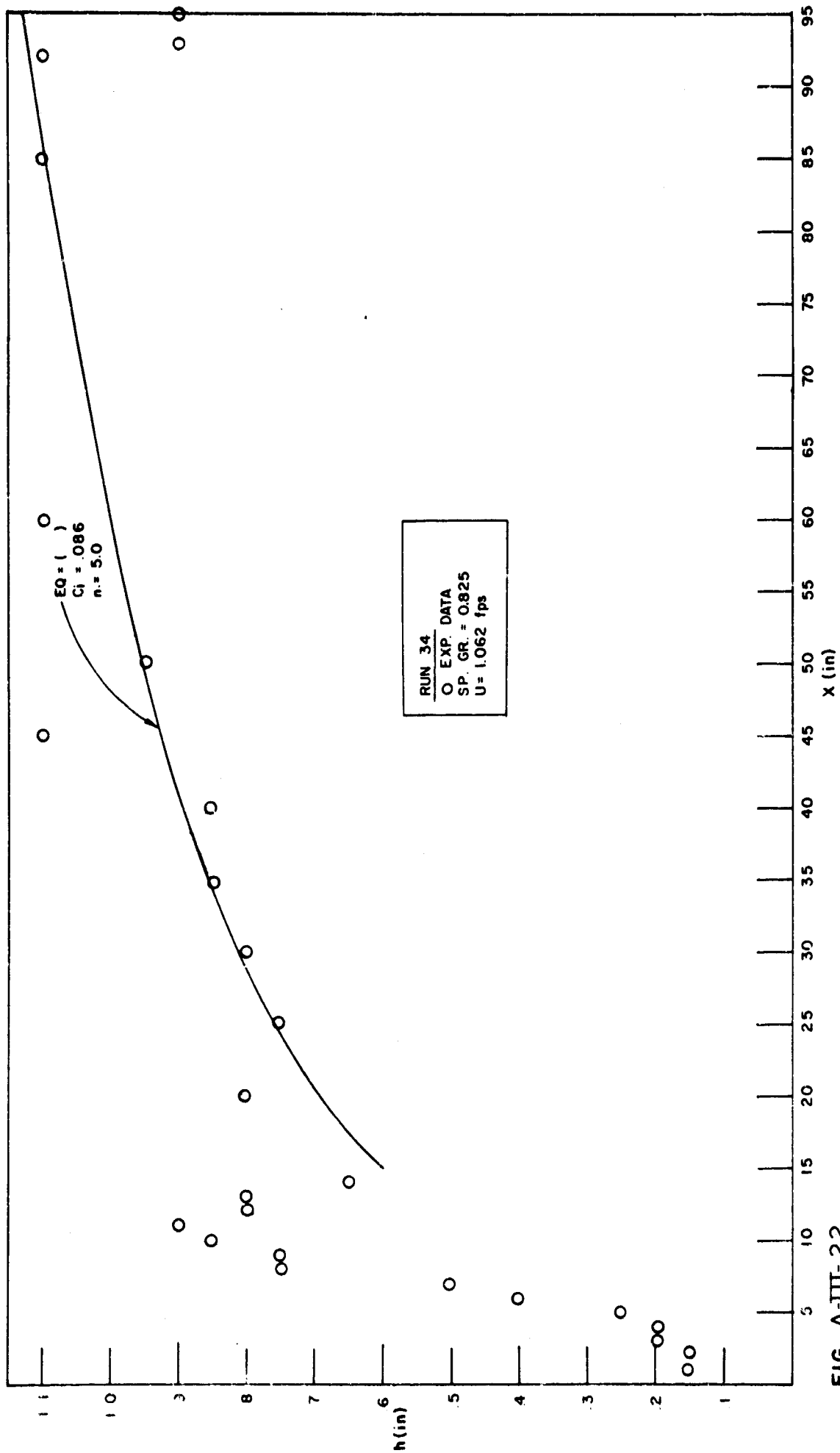


FIG. A-III-22

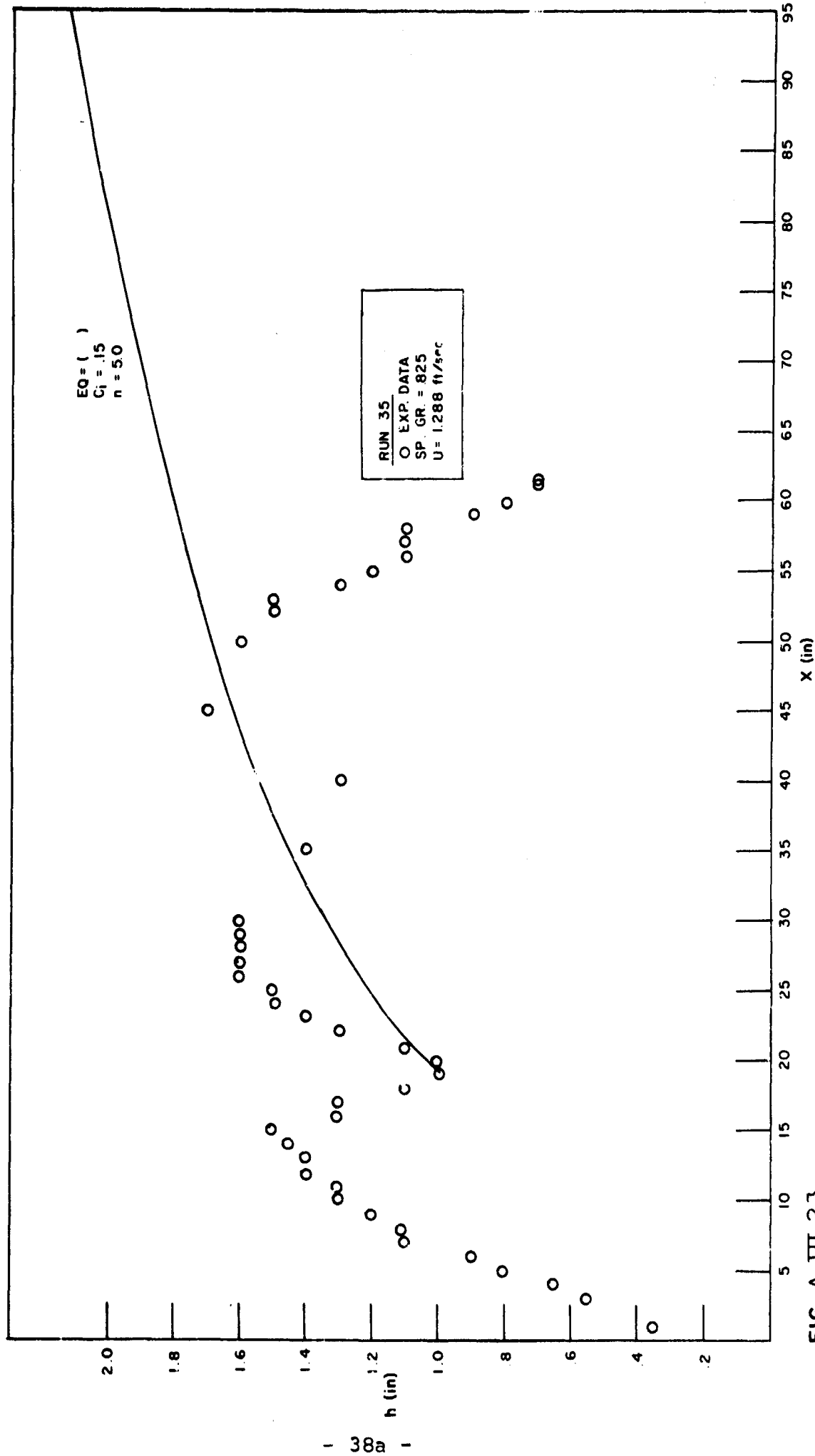


FIG. A-III-23

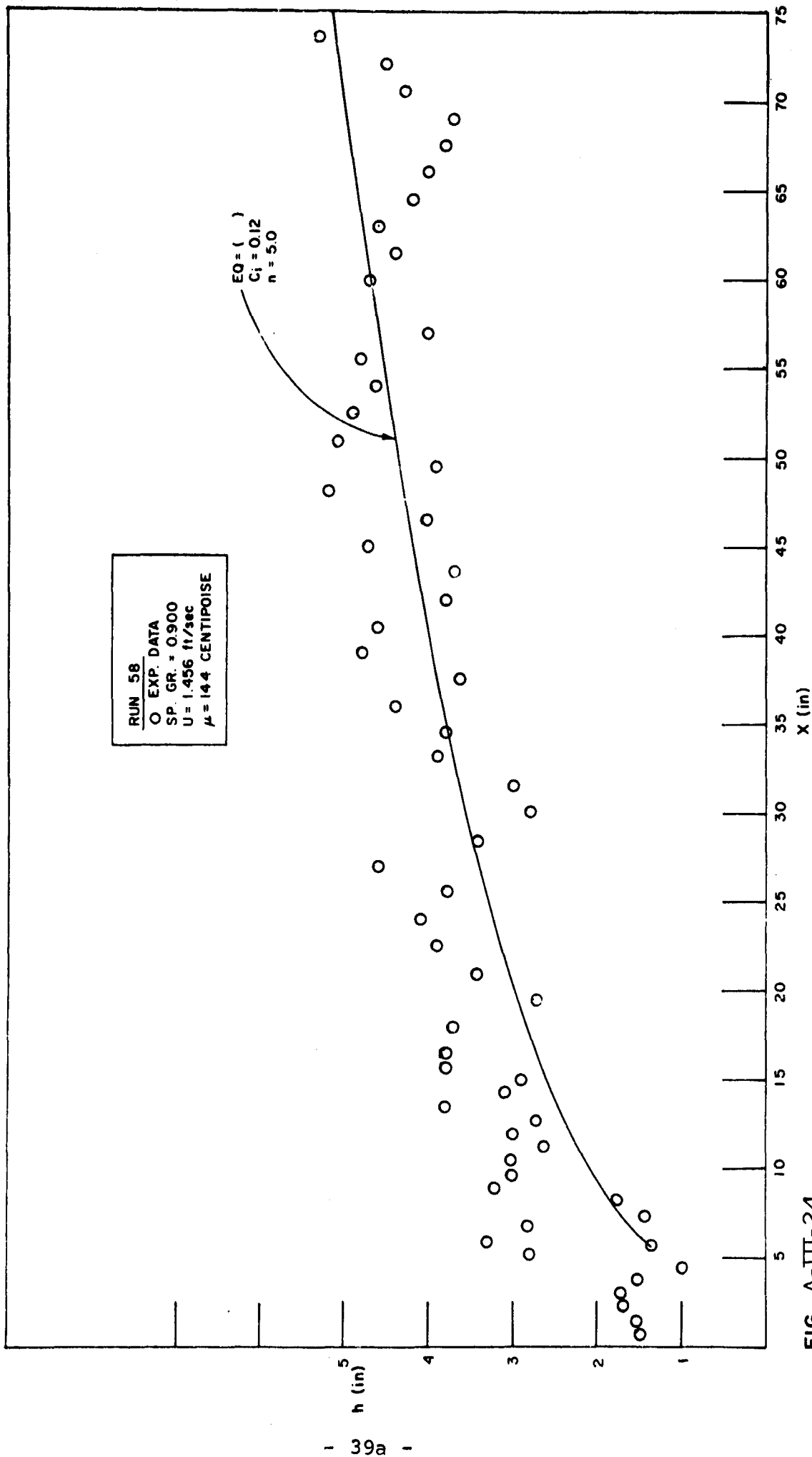


FIG. A-III-24

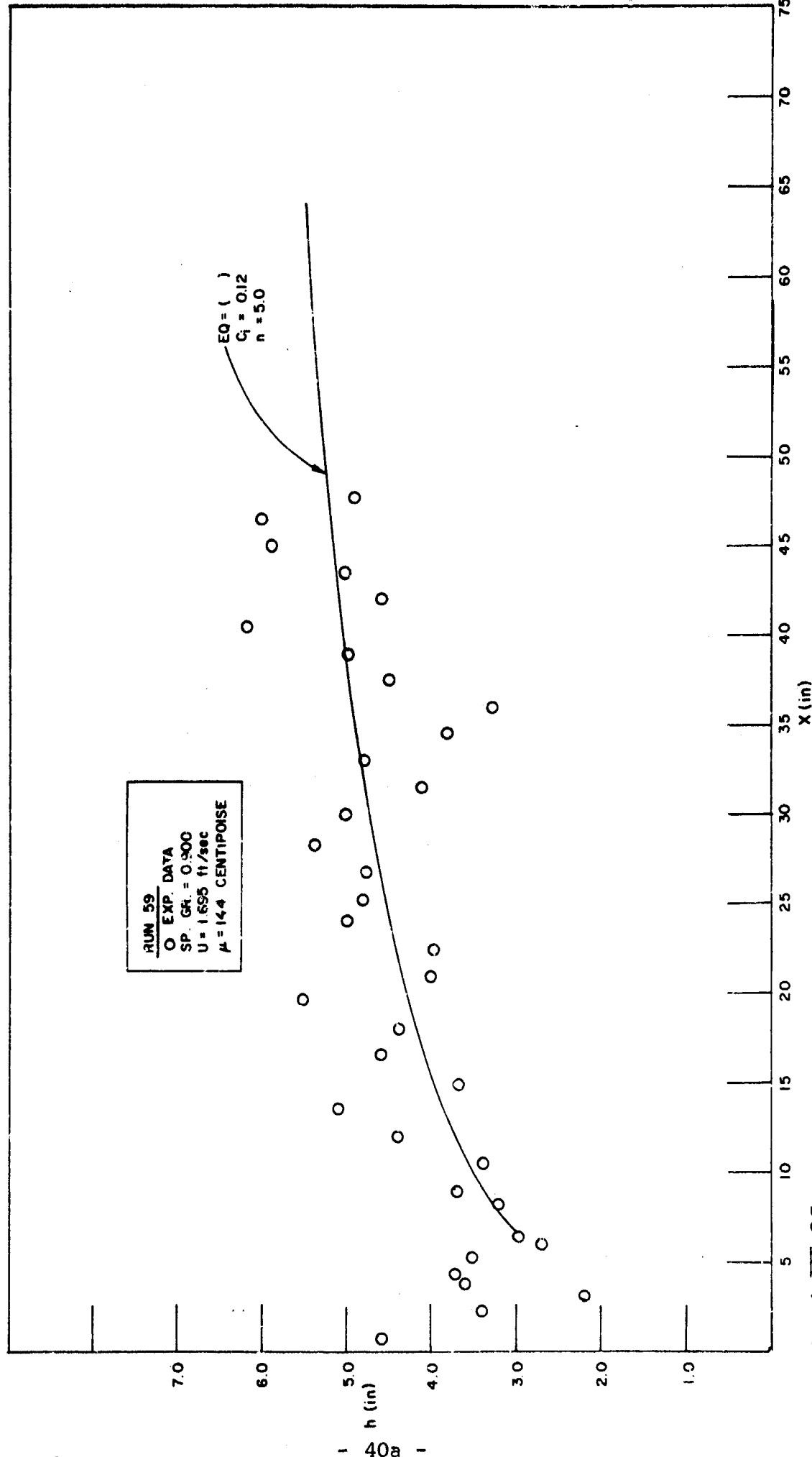


FIG. A-III-25

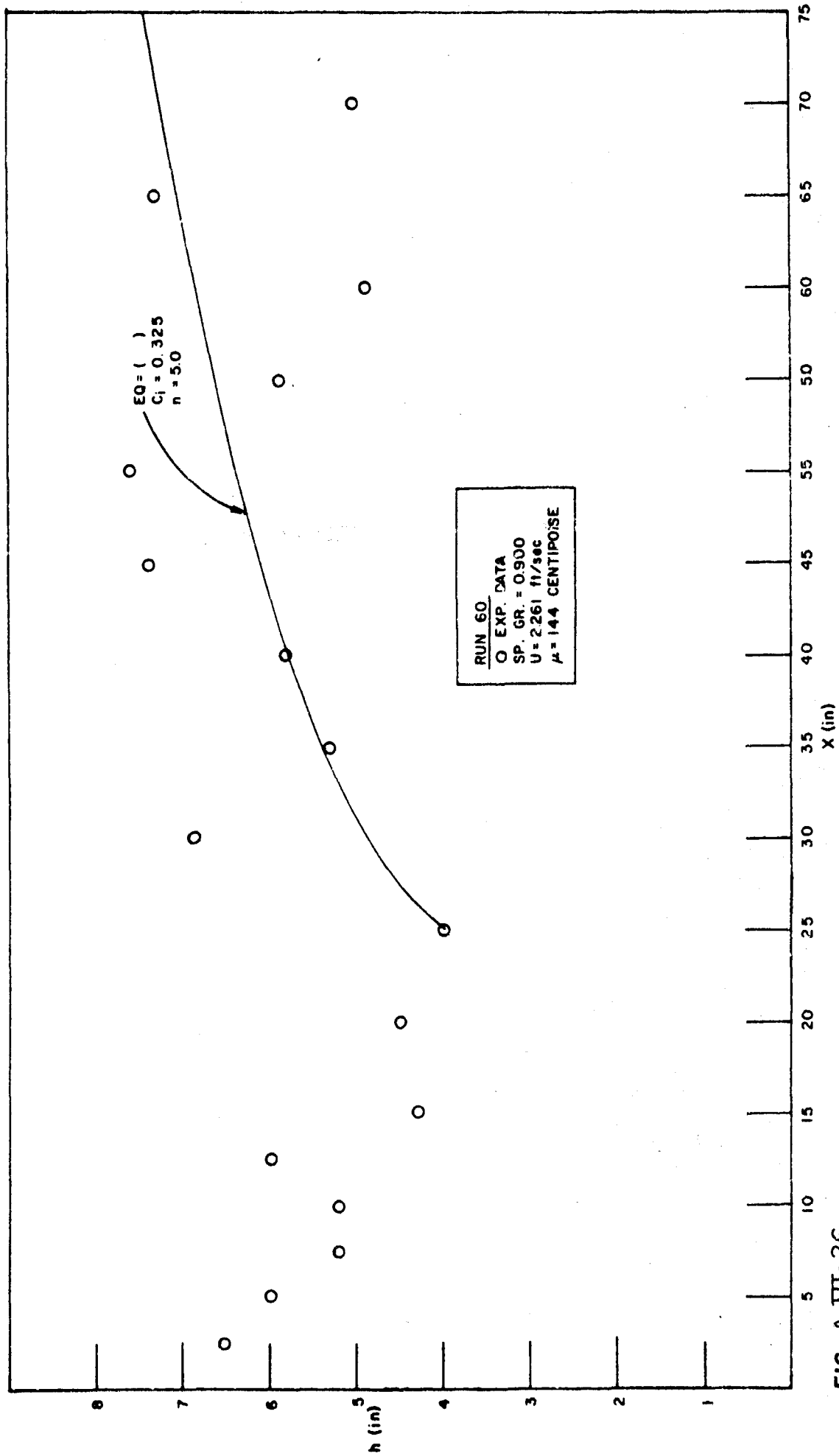


FIG. A-III-26

APPENDIX II

OIL DEPTH PROFILES

Run # 1-1-1

x (ft)	29.416	19.478	9.54
d (ft)	0.223	0.195	0.173

Run # 1-1-2

x (ft)	35.167	26.229	16.291	6.353
d (ft)	0.216	0.194	0.166	0.134

Run # 1-1-3

x (ft)	40.33	30.39	20.45	10.51
d (ft)	0.201	0.173	0.160	0.131

Run # 1-1-4

x (ft)	45.92	35.98	26.04	16.10	6.16
d (ft)	0.190	0.172	0.152	0.124	0.082

Run # 1-1-5

x (ft)	48.25	38.31	28.37	18.43	8.49
d (ft)	0.176	0.158	0.139	0.114	0.090

Run # 1-1-6

x (ft)	56.83	46.89	35.95	26.01	16.07	6.13
d (ft)	0.159	0.147	0.129	0.111	0.089	.061

Run # 1-1-7

x (ft)	61.77	51.83	41.89	31.95	22.01	12.07	2.13
d (ft)	0.145	0.133	0.121	0.106	0.090	0.068	.033

Run # 1-1-8

x (ft)	20.5	10.56
d (ft)	0.53	0.32

Run # 1-1-9

x (ft)	22.92	12.98
d (ft)	0.293	0.266

Pun # 1-1-19

x (ft)	25.75	15.81	5.87
d (ft)	0.271	0.240	0.235

Run # 1-2-1

x (ft)	47.33	37.39	27.45	17.51	7.57
d (ft)	.267	.237	.212	.176	.134

Run # 1-2-2

x (ft)	49.20	39.26	29.32	19.38	9.44
d (ft)	.256	.232	.205	.178	.143

Run # 1-2-3

x (ft)	57.60	47.66	37.72	27.78	17.84	7.90
d (ft)	.234	.213	.199	.167	.139	.104

Run # 1-2-4 (a)

x (ft)	63.69	53.75	43.81	33.87	23.93	13.99	4.05
d (ft)	.219	.201	.183	.160	.134	.107	.070

Run # 1-2-4 (b)

x (ft)	63.50	53.56	43.62	33.68	23.74	13.80	3.86
d (ft)	.220	.204	.185	.164	.139	.111	.065

Run # 1-2-5

x (ft)	40.17	30.23	20.29	10.35
d (ft)	.239	.258	.229	.195

Run # 1-2-6

x (ft)	35.25	25.31	15.37	5.43
d (ft)	.321	.287	.257	.230

Run # 1-2-7

x (ft)	33.00	23.06	13.13
d (ft)	.342	.308	.278

Run # 1-3-1

x (ft)	66.17	56.23	46.29	36.35	26.41	16.47	6.53
d (ft)	.270	.248	.226	.203	.167	.143	.098

Run # 1-3-2

x (ft)	64.58	54.64	44.70	34.76	24.82	14.88	4.94
d (ft)	.274	.255	.228	.202	.179	.142	.092

Run # 1-3-3

x (ft)	62.25	52.31	42.37	32.43	22.49	12.55	2.61
d (ft)	.283	.258	.234	.201	.170	.137	.090

Run # 1-3-4

x (ft)	60.17	50.23	40.29	30.35	20.41	10.47	0.53
d (ft)	.284	.261	.236	.208	.174	.135	.086

Run # 1-3-5

x (ft)	58.92	48.98	39.04	29.10	19.16	9.22
d (ft)	.296	.268	.241	.205	.173	.134

Run # 1-3-6

x (ft)	56.42	46.48	36.54	26.60	16.66	6.72
d (ft)	.307	.275	.246	.213	.175	.126

Run # 1-3-7

x (ft)	49.92	39.98	30.04	20.16	10.16
d (ft)	.312	.283	.253	.222	.186

Run # 1-3-8

x (ft)	49.33	39.39	29.45	19.51	9.57
d (ft)	.334	.295	.253	.219	.133

Run # 1-3-9

x (ft)	35.67	25.73	15.79
d (ft)	.305	.262	.216

Run # 1-3-10

x (ft)	30.50	20.56
d (ft)	.335	.305

Run # 2-1-1

x (ft)	60.03	45.70	35.87	25.83	12.75
d (ft)	0.068	0.059	0.051	0.048	0.037

Run # 2-1-2

x (ft)	59.54	45.21	35.38	25.34	12.26
d (ft)	0.069	0.059	0.054	0.048	0.033

Run # 2-1-3

x (ft)	56.63	42.30	32.47	22.43	9.35
d (ft)	0.072	0.064	0.057	0.048	0.034

Run # 2-1-4

x (ft)	53.96	39.63	29.80	19.76	6.68
d (ft)	0.078	0.064	0.055	0.046	0.030

Run # 2-1-5

x (ft)	57.29	42.96	33.13	23.09	10.01
d (ft)	0.089	0.068	0.054	0.042	0.032

Run # 2-1-6

x (ft)	51.67	37.34	27.51	17.47	4.39
d (ft)	0.074	0.061	0.053	0.035	0.015

Run # 2-1-7

x (ft)	47.25	32.92	23.09	13.05	
d (ft)	0.080	0.067	0.059	0.039	

Run # 2-1-8

x (ft)	45.17	30.84	21.01	10.97	
d (ft)	0.097	0.073	0.058	0.036	

Run # 2-1-9

x (ft)	33.17	18.34	9.01		
d (ft)	0.103	0.072	0.058		

Run # 2-1-10

x (ft)	32.08	17.75	7.92
d (ft)	0.115	0.087	0.063

Run # 2-2-1

x (ft)	60.67	46.34	36.51	26.47	13.39
d (ft)	0.149	0.132	0.125	0.104	0.086

Run # 2-2-2

x (ft)	56.25	41.92	32.09	22.05	8.97
d (ft)	0.164	0.143	0.133	0.106	0.077

Run # 2-2-3

x (ft)	54.83	40.50	30.67	20.63	7.55
d (ft)	0.181	0.155	0.136	0.104	0.072

Run # 2-2-4

x (ft)	49.58	35.25	25.42	15.38	2.30
d (ft)	0.184	0.162	0.143	0.109	0.071

Run # 2-2-5

x (ft)	47.00	32.67	22.84	12.80
d (ft)	0.204	0.163	0.146	0.098

Run # 2-2-6

x (ft)	45.83	31.50	21.67	11.63
d (ft)	0.208	0.169	0.145	0.096

Run # 2-2-7

x (ft)	43.00	28.67	18.84	8.80
d (ft)	0.215	0.176	0.099	0.087

Run # 2-2-8

x (ft)	41.50	27.17	17.34	7.30
d (ft)	0.223	0.183	0.146	0.074

Run # 2-2-9

x (ft)	38.50	24.17	14.34	4.30
d (ft)	0.238	0.188	0.148	0.050

Run # 2-3-1

x (ft)	61.67	47.34	37.51	27.47	14.39
d (ft)	0.220	0.207	0.191	0.152	0.124

Run # 2-3-2

x (ft)	58.17	43.84	34.01	23.97	10.89
d (ft)	0.237	0.213	0.188	0.158	0.126

Run # 2-3-3

x (ft)	56.50	42.17	32.34	22.30	9.22
d (ft)	0.256	0.220	0.191	0.155	0.108

Run # 2-3-4

x (ft)	54.50	40.17	30.34	20.30	7.22
d (ft)	0.275	0.233	0.190	0.155	0.103

Run # 2-3-5

x (ft)	52.75	38.42	28.59	18.55	5.47
d (ft)	0.277	0.232	0.192	0.150	0.105

Run # 2-3-6

x (ft)	52.50	38.17	28.34	18.30	5.22
d (ft)	0.275	0.226	0.205	0.156	0.101

Run # 2-3-7

x (ft)	51.67	37.34	27.51	17.47	4.39
d (ft)	0.283	0.238	0.198	0.148	0.077

Run # 2-3-8

x (ft)	49.25	34.92	25.09	15.05	1.97
d (ft)	0.306	0.238	0.202	0.156	0.073

Run # 2-3-9

x (ft)	48.17	33.84	24.01	13.97	0.89
d (ft)	0.313	0.250	0.198	0.148	0.068

Run # 3-1-1

x (ft)	51.50	40.46	29.67	20.21	7.17
d (ft)	0.114	0.094	0.076	0.064	0.043

Run # 3-1-2

x (ft)	46.10	35.06	24.27	14.81	1.77
d (ft)	0.129	0.101	0.085	0.071	0.032

Run # 3-1-3

x (ft)	39.17	28.13	17.34	7.88
d (ft)	0.132	0.110	0.093	0.069

Run # 3-1-4

x (ft)	30.50	19.46	8.67
d (ft)	0.155	0.126	0.105

Run # 3-1-5

x (ft)	29.17	17.13	6.34
d (ft)	0.165	0.139	0.107

Run # 3-1-6

x (ft)	25.17	14.13	3.34
d (ft)	0.18	0.160	0.111

Run # 3-1-7

x (ft)	21.83	10.79
d (ft)	0.205	0.164

Run # 3-1-8

x (ft)	19.25	8.21
d (ft)	0.233	0.138

Run # 3-1-9

x (ft)	17.50	6.46
d (ft)	0.269	0.193

Run # 3-2-1

x (ft)	55.25	44.21	33.42	23.96	10.92
d (ft)	0.187	0.166	0.145	0.126	0.092

Run # 3-2-2

x (ft)	52.17	41.13	30.34	20.88	7.84
d (ft)	0.192	0.163	0.154	0.126	0.097

Run # 3-2-3

x (ft)	50.75	39.71	28.92	19.46	6.42
d (ft)	0.204	0.177	0.155	0.133	0.092

Run # 3-2-4

x (ft)	46.58	35.54	24.75	15.29
d (ft)	0.214	0.186	0.160	0.137

Run # 3-2-5

x (ft)	42.67	31.62	20.84	11.38
d (ft)	0.219	0.191	0.167	0.133

Run # 3-1-6

x (ft)	49.50	38.46	27.67	18.21
d (ft)	0.228	0.201	0.175	0.138

Run # 3-2-7

x (ft)	38.50	27.46	16.67	7.21
d (ft)	0.239	0.208	0.183	0.137

Run # 3-2-8

x (ft)	37.83	26.79	16.00	6.54
d (ft)	0.266	0.223	0.194	0.135

Run # 3-2-9

x (ft)	39.75	19.71	8.92
d (ft)	0.299	0.240	0.203

Run # 3-2-10

x (ft)	28.42	17.38	6.59
d (ft)	0.347	0.266	0.212

Run # 3-3-1

x (ft)	64.08	53.04	52.75	32.79	19.75	7.91
d (ft)	0.239	0.218	0.199	0.183	0.157	0.095

Run # 3-3-2

x (ft)	60.50	49.46	38.67	29.21	15.17	4.33
d (ft)	0.245	0.222	0.202	0.179	0.156	0.092

Run # 3-3-3

x (ft)	63.58	52.54	41.75	32.29	19.25	11.41
d (ft)	0.246	0.221	0.203	0.180	0.145	0.104

Run # 3-3-4

x (ft)	60.33	49.29	38.50	29.04	16.00	3.16
d (ft)	0.253	0.228	0.204	0.161	0.142	0.105

Run # 3-3-5

x (ft)	57.24	46.20	35.41	25.95	12.91
d (ft)	0.264	0.231	0.215	0.187	0.148

Run # 3-3-6

x (ft)	54.67	43.63	32.84	23.38	10.34
d (ft)	0.279	0.241	0.221	0.138	0.138

Run # 3-3-7

x (ft)	50.50	39.46	28.67	19.21	6.17
d (ft)	0.301	0.259	0.229	0.196	0.147

Run # 3-3-8

x (ft)	45.92	34.88	24.09	14.63	1.59
d (ft)	0.327	0.279	0.240	0.201	0.113

Run # 3-3-9

x (ft)	44.25	33.21	22.42	12.96
d (ft)	0.344	0.287	0.240	0.200

Run # 3-3-10

x (ft)	39.00	27.96	17.17	7.71
d (ft)	0.373	0.313	0.282	0.203

APPENDIX
VELOCITY PROFILES

Run # 1-1-1

U (fps)	25.30	29.80	30.10	31.50	32.50	31.90	31.10
y (ft)	0.058	0.188	0.288	0.388	0.488	0.588	0.688
	31.95	31.48	30.37	28.84	28.35	27.21	10.00
	0.788	0.288	0.988	1.088	1.188	1.288	1.388

Run # 1-1-2

U (fps)	24.50	27.40	28.53	28.55	30.20	30.20	29.01
y (ft)	0.088	0.188	0.288	0.388	0.488	0.588	0.688
	29.15	29.18	27.70	27.02	26.10	24.60	11.60
	0.788	0.888	0.988	1.088	1.188	1.288	1.388

Run # 1-1-3

U (fps)	21.78	24.65	25.06	26.22	26.44	26.22	26.47
y (ft)	0.088	0.188	0.288	0.388	0.488	0.588	0.688
	27.20	28.03	25.30	25.39	23.30	21.15	12.20
	0.788	0.888	0.988	1.088	1.188	1.288	1.388

Run # 1-1-4

U (fps)	20.20	22.55	23.26	23.50	23.90	24.17	24.55
y (ft)	0.088	0.188	0.288	0.388	0.488	0.588	0.688
	24.55	26.20	22.60	22.41	21.82	20.92	11.23
	0.788	0.388	0.988	1.088	1.188	1.288	1.388

Run # 1-1-5

U (fps)	16.90	19.00	20.10	20.43	20.48	20.75	20.95
y (ft)	0.088	0.188	0.288	0.388	0.488	0.588	0.688
	21.00	20.75	20.37	19.40	18.60	17.50	10.37
	0.788	0.888	0.988	1.088	1.188	1.288	1.388

Run # 1-1-6

U (fps)	14.38	16.09	17.13	17.36	18.43	18.10	18.40
y (ft)	0.088	0.132	0.283	0.323	0.423	0.583	0.688
	18.30	18.40	18.40	17.58	18.75	16.75	9.51
	0.783	0.883	0.983	1.083	1.183	1.283	1.383

Run # 1-1-7

U (fps)	12.36	13.91	14.55	14.12	13.61	15.35	15.90
y (ft)	0.088	0.133	0.283	0.388	0.423	0.583	0.688
	16.05	16.05	15.62	14.40	14.10	12.32	6.47
	0.783	0.883	0.983	1.083	1.183	1.283	1.383

Run # 1-1-8

U (fps)	35.40	37.60	35.95	38.35	28.40	37.42
y (ft)	0.183	0.283	0.383	0.483	0.583	0.683
	36.40	34.75	33.60	32.60	31.20	30.60
	0.783	0.883	0.983	1.083	1.183	1.283

Run # 1-1-9

U (fps)	35.20	36.65	37.05	36.20	26.40	34.40
y (ft)	0.183	0.283	0.383	0.483	0.583	0.683
	32.80	33.20	31.80	30.80	28.50	12.56
	0.783	0.883	0.983	1.083	1.183	1.283

Run # 1-1-10

U (fps)	28.72	32.70	35.05	35.20	34.08	35.40	35.80
y (ft)	0.083	0.183	0.283	0.383	0.483	0.583	0.683
	34.05	33.10	31.95	31.10	29.80	29.25	12.95
	0.783	0.883	0.983	1.083	1.183	1.283	1.383

Run # 1-3-1

x (ft)	66.17	56.23	46.29	36.35	26.41	16.47	6.53
d (ft)	.270	.248	.226	.203	.167	.143	.098

Run # 1-3-2

x (ft)	64.98	54.64	44.70	34.76	24.82	14.88	4.94
d (ft)	.274	.255	.228	.202	.179	.142	.092

Run # 1-3-3

x (ft)	52.25	52.31	42.37	32.43	22.49	12.55	2.61
d (ft)	.233	.253	.234	.201	.170	.137	.090

Run # 1-3-4

x (ft)	60.17	50.23	40.29	30.35	20.41	10.47	0.53
d (ft)	.254	.261	.236	.208	.174	.135	.086

Run # 1-3-5

x (ft)	58.92	48.98	39.04	29.16	19.16	9.22
d (ft)	.296	.268	.241	.205	.173	.134

Run # 1-3-6

x (ft)	56.42	46.48	36.54	26.60	16.66	6.72
d (ft)	.307	.275	.246	.213	.175	.126

Run # 1-3-7

x (ft)	49.92	39.98	30.04	20.10	10.16
d (ft)	.312	.287	.253	.222	.186

Run # 1-3-8

x (ft)	49.33	39.39	29.45	19.51	9.57
d (ft)	.334	.295	.253	.219	.188

Run # 1-3-9

x (ft)	35.67	25.73	15.79
d (ft)	.305	.362	.316

Run # 1-3-10

x (ft)	30.50	20.56
d (ft)	.485	.405

Run # 1-2-1

U (fps)	23.90	29.20	30.62	32.40	32.95	33.80	34.40
y (ft)	0.050	0.150	0.250	0.350	0.450	0.550	0.650
	34.40	34.05	33.50	32.40	31.21	31.19	19.20
	0.750	0.850	0.950	1.050	1.150	1.250	1.350

Run # 1-2-2

U (fps)	23.02	25.03	28.20	29.70	30.20	31.40	31.10
y (ft)	0.050	0.150	0.250	0.350	0.450	0.550	0.650
	31.10	30.80	30.15	28.96	28.20	26.50	15.30
	0.750	0.850	0.950	1.050	1.150	1.250	1.350

Run # 1-2-3

U (fps)	19.20	23.40	24.85	25.70	26.60	27.40	28.80
y (ft)	0.050	0.150	0.255	0.355	0.455	0.555	0.655
	28.60	27.20	26.92	26.00	25.30	23.00	15.40
	0.750	0.850	0.950	1.050	1.150	1.250	1.350

Run # 1-2-4 (a)

U (fps)	17.90	21.10	22.05	22.80	23.70	24.12	24.15
y (ft)	0.050	0.150	0.250	0.350	0.450	0.550	0.650
	24.12	24.01	23.80	23.10	22.70	19.22	12.74
	0.750	0.850	0.950	1.050	1.150	1.250	1.350

Run # 1-2-4 (b)

U (fps)	17.90	21.30	22.20	23.15	24.00	24.10	24.80
y (ft)	0.050	0.150	0.250	0.350	0.450	0.550	0.650
	24.75	24.20	23.90	23.05	22.30	21.40	16.85
	0.750	0.850	0.950	1.050	1.150	1.250	1.350

Run # 1-2-5

U (fps)	26.20	31.40	33.38	34.35	34.80	35.78	36.30
y (ft)	0.050	0.150	0.250	0.350	0.450	0.550	0.650
	36.22	35.61	34.02	33.29	32.10	30.70	9.72
	0.750	0.850	0.950	1.050	1.150	1.250	1.350

Run # 1-2-6

U (fps)	27.80	34.08	36.00	36.60	37.30	37.18	36.80
y (ft)	0.050	0.150	0.250	0.350	0.450	0.550	0.650
	35.80	35.40	33.80	32.90	31.60	30.20	11.02
	0.750	0.850	0.950	1.050	1.150	1.250	1.350

Run # 1-2-7

U (fps)		35.00	37.00	38.05	39.03	39.05	38.04
y (ft)		0.150	0.250	0.350	0.450	0.550	0.650
	37.25	35.58	34.60	33.45	32.20	31.40	9.72
	0.750	0.850	0.950	1.050	1.150	1.250	1.350

Run # 1-3-1

U (fps)	20.71	21.70	26.61	27.70	28.40	29.10	29.58
y (ft)	0.050	0.150	0.250	0.350	0.450	0.550	0.650
	29.42	29.20	28.60	27.60	26.90	25.82	10.47
	0.750	0.850	0.950	1.050	1.150	1.250	1.350

Run # 1-3-2

U (fps)	21.50	26.60	28.40	28.65	29.70	30.12	30.70
y (ft)	0.050	0.150	0.250	0.350	0.450	0.550	0.650
	30.60	30.09	29.30	28.60	27.60	26.40	8.20
	0.750	0.850	0.950	1.050	1.150	1.250	1.350

Run # 1-3-3

U (fps)	23.70	23.80	29.70	30.80	31.60	32.00	32.10
y (ft)	0.050	0.150	0.250	0.350	0.450	0.550	0.650
	31.40	31.60	31.00	30.04	28.95	27.20	11.08
	0.750	0.850	0.950	1.050	1.150	1.250	1.350

Run # 1-3-4

U (fps)	24.25	28.10	31.30	33.10	33.28	33.65	33.80
y (ft)	0.050	0.150	0.250	0.350	0.450	0.550	0.650
	33.70	33.28	32.40	31.58	30.20	28.90	11.90
	0.750	0.850	0.950	1.050	1.150	1.250	1.350

Run # 1-3-5

U (fps)	23.90	30.40	32.00	33.60	34.20	34.75	35.40
y (ft)	0.050	0.150	0.250	0.350	0.450	0.550	0.650
	36.95	35.45	34.20	33.40	32.40	30.50	21.60
	0.750	0.850	0.950	1.050	1.150	1.250	1.350

Run # 1-3-6

U (fps)	24.95	31.82	33.40	35.20	36.00	36.90	37.10
y (ft)	0.050	0.150	0.250	0.350	0.450	0.550	0.650
	36.90	36.50	35.60	34.80	33.30	32.00	29.60
	0.750	0.850	0.950	1.050	1.150	1.250	1.350

Run # 1-3-7

U (fps)	26.18	34.30	35.90	36.90	37.80	38.35	38.50
y (ft)	0.050	0.150	0.250	0.350	0.450	0.550	0.650
	38.12	37.90	37.10	35.50	34.60	32.90	17.22
	0.750	0.850	0.950	1.050	1.150	1.250	1.350

Run # 1-3-8

U (fps)	31.60	34.20	35.90	36.60	39.20	39.55	39.95
y (ft)	0.100	0.150	0.250	0.350	0.450	0.550	0.650
	39.60	39.20	38.05	37.30	35.82	34.40	14.55
	0.750	0.850	0.950	1.050	1.150	1.250	1.350

Run # 1-3-9

U (fps)	28.00	33.60	37.40	39.60	40.49	40.40	40.25
y (ft)	0.100	0.150	0.250	0.350	0.450	0.550	0.650
	39.50	38.80	37.20	36.20	35.21	34.06	10.08
	0.750	0.850	0.950	1.050	1.150	1.250	1.350

Run # 1-3-10

U (fps)	33.70	37.20	40.60	40.95	41.15	41.08
y (ft)	0.150	0.250	0.350	0.450	0.550	0.650
	40.50	39.40	38.60	37.65	37.00	36.20
	0.750	0.850	0.950	1.050	1.150	1.250
						15.50
						1.350

Run # 2-1-1

U (fps)	7.04	7.66	7.94	7.94	7.94	7.94	7.94	7.66	7.66
y (ft)	0.094	0.194	0.294	0.394	0.494	0.594	0.694	0.794	0.894

	7.66	7.66	7.94	7.66	7.36	7.04	6.72	6.38	6.38
	0.994	1.094	1.194	1.294	1.394	1.494	1.594	1.694	1.794

Run # 2-1-2

U (fps)	7.36	8.21	8.21	8.21	8.50	8.50	8.21	8.21	7.94
y (ft)	0.094	0.194	0.294	0.394	0.494	0.594	0.694	0.794	0.894

	7.66	7.94	7.66	7.66	7.66	7.36	7.04	6.72	6.38
	0.994	1.094	1.194	1.294	1.394	1.494	1.594	1.694	1.794

Run # 2-1-3

U (fps)	8.50	8.76	8.76	8.76	8.76	9.02	9.02	9.02	9.02
y (ft)	0.094	0.194	0.294	0.394	0.494	0.594	0.694	0.794	0.894

	8.76	8.50	8.50	8.21	8.21	7.94	7.66	7.36	6.72
	0.994	1.094	1.194	1.294	1.394	1.494	1.594	1.694	1.794

Run # 2-1-4

U (fps)	8.76	9.26	9.51	9.51	9.51	9.51	9.51	9.51	9.51
y (ft)	0.094	0.194	0.294	0.394	0.494	0.594	0.694	0.794	0.894

	9.26	9.02	9.02	8.76	8.50	8.21	7.94	7.66	7.04
	0.994	1.094	1.194	1.294	1.394	1.494	1.594	1.694	1.794

Run # 2-1-5

U (fps)	7.36	8.21	8.76	9.72	9.72	9.72	9.72	9.51	9.51
y (ft)	0.094	0.194	0.294	0.394	0.494	0.594	0.694	0.794	0.894

	9.26	8.76	9.26	8.76	8.76	8.76	7.66	7.66	7.04
	0.994	1.094	1.194	1.294	1.394	1.494	1.594	1.694	1.794

Run # 2-1-6

U (fps)	9.51	9.51	8.50	10.40	11.62	11.23	11.23	11.62	9.51
y (ft)	0.094	0.194	0.294	0.394	0.494	0.594	0.694	0.794	0.894

	9.02	9.02	11.23	9.51	10.82	9.51	9.02	10.40	9.51
	0.994	1.094	1.194	1.294	1.394	1.494	1.594	1.694	1.794

(continued Run # 2-1-6)

8.50
1.894

Run # 2-1-7

U (fps)	6.70	9.02	10.82	9.96	9.51	9.96	9.02	10.82	8.50
y (ft)	0.080	0.180	0.280	0.380	0.480	0.580	0.680	0.780	0.880

10.40	9.96	9.51	10.82	10.82	9.96	9.51	9.51	8.50
0.980	1.080	1.180	1.280	1.380	1.480	1.580	1.680	1.780

7.36
1.880

Run # 2-1-8

U (fps)	9.96	11.23	12.02	12.02	12.40	12.40	11.62	11.62	11.62
y (ft)	0.080	0.180	0.280	0.380	0.480	0.580	0.680	0.780	0.880

12.40	11.23	11.23	10.82	9.96	9.96	9.51	9.02	7.94
0.980	1.080	1.180	1.280	1.380	1.480	1.580	1.680	1.780

Run # 2-1-9

U (fps)	10.82	13.45	14.08	14.40	14.40	14.08	14.40	13.45	13.45
y (ft)	0.080	0.180	0.280	0.380	0.480	0.580	0.680	0.780	0.880

13.75	13.08	13.75	13.08	13.08	12.73	12.02	11.23	9.51
0.980	1.080	1.180	1.280	1.380	1.480	1.580	1.680	1.780

Run # 2-1-10

U (fps)	13.45	15.60	15.19	16.47	16.47	16.19	16.19	15.89	15.89
y (ft)	0.080	0.180	0.280	0.380	0.480	0.580	0.680	0.780	0.880

15.89	15.60	15.60	15.01	14.70	14.40	13.75	13.08	12.40
0.980	1.080	1.180	1.280	1.380	1.480	1.580	1.680	1.780

Run # 2-2-1

U (fps)	14.70	16.19	16.73	17.00	16.73	16.73	16.73	16.47	16.47
y (ft)	0.10	0.20	0.30	0.40	0.50	0.60	0.70	0.80	0.90

16.73	15.89	15.60	15.30	15.01	14.08	13.45	11.62
1.00	1.10	1.20	1.30	1.40	1.50	1.60	1.70

Run # 2-2-2

U (fps)	15.83	17.50	17.78	18.26	18.26	18.54	18.26	17.97	17.78
y (ft)	0.10	0.20	0.30	0.40	0.50	0.60	0.70	0.80	0.90

17.50	15.70	17.31	16.74	15.88	15.31	14.46	12.74
1.00	1.10	1.20	1.30	1.40	1.50	1.60	1.70

Run # 2-2-3

U (fps)	17.50	18.73	19.21	19.21	19.21	19.02	19.21	19.02	18.54
y (ft)	0.150	0.250	0.350	0.450	0.550	0.650	0.750	0.850	0.950

18.26	17.97	17.78	17.50	17.02	15.88	15.02	13.12
1.050	1.150	1.250	1.350	1.450	1.550	1.650	1.750

Run # 2-2-4

U (fps)	18.54	19.21	20.35	20.35	20.35	20.35	20.35	20.35	19.50
y (ft)	0.150	0.250	0.350	0.450	0.550	0.650	0.750	0.850	0.950

19.02	19.02	18.26	17.97	17.78	17.31	15.88	14.46
1.050	1.150	1.250	1.350	1.450	1.550	1.650	1.750

Run # 2-2-5

U (fps)	19.68	21.68	22.35	22.06	22.06	22.06	22.35	21.68	21.49
y (ft)	0.150	0.250	0.350	0.450	0.550	0.650	0.750	0.850	0.950

21.30	20.83	20.35	19.97	19.50	18.54	17.50	15.88
1.050	1.150	1.250	1.350	1.450	1.550	1.650	1.750

Run # 2-2-6

U (fps)	18.54	19.47	21.49	22.06	22.06	22.35	22.06	22.06	22.06
y (ft)	0.150	0.250	0.350	0.450	0.550	0.650	0.750	0.850	0.950

22.35	21.87	21.49	21.30	21.02	20.35	19.97	17.97
1.050	1.150	1.250	1.350	1.450	1.550	1.650	1.750

Run # 2-2-7

U (fps)	21.68	22.92	24.06	25.20	25.30	25.49	25.49	25.49	25.30
y (ft)	0.150	0.250	0.350	0.450	0.550	0.650	0.750	0.850	0.950

24.32	24.44	24.25	23.68	22.92	21.87	20.64	19.02
1.050	1.150	1.250	1.350	1.450	1.550	1.650	1.750

Run # 2-2-8

U (fps)	20.64	22.35	23.87	24.25	25.49	25.68	25.68	25.87	25.68
y (ft)	0.150	0.250	0.350	0.450				0.850	0.950

25.49	25.01	24.82	25.01	24.96	23.68	22.92	19.68
1.050	1.150	1.250	1.350	1.450	1.550	1.650	1.750

Run # 2-2-9

U (fps)	24.63	26.92	27.33	28.34	28.82	29.03	28.82	28.53
y (ft)	0.250	0.350	0.450	0.550	0.650	0.750	0.850	0.950

28.24	27.58	27.20	26.91	25.37	25.01	23.68	21.49
1.050	1.150	1.250	1.350	1.450	1.550	1.650	1.750

Run # 2-3-1

U (fps)	20.12	21.65	22.45	23.05	23.05	22.87	22.87	22.65
y (ft)	0.150	0.250	0.350	0.450	0.550	0.650	0.750	0.850
	22.22	21.90	21.02	21.02	20.80	19.45	18.50	17.00
	0.950	1.050	1.150	1.250	1.350	1.450	1.550	1.650

Run # 2-3-2

U (fps)	21.22	22.65	23.80	24.00	24.00	23.80	23.80	23.41
y (ft)	0.150	0.250	0.350	0.450	0.550	0.650	0.750	0.850
	22.47	22.22	22.08	21.43	21.02	20.38	19.45	18.50
	0.950	1.050	1.150	1.250	1.350	1.450	1.550	1.650

Run # 2-3-3

U (fps)	22.87	24.60	25.30	25.80	25.80	25.80	25.42	25.15
y (ft)	0.150	0.250	0.350	0.450	0.550	0.650	0.750	0.850
	24.60	24.20	23.61	23.41	22.87	22.22	20.60	19.45
	0.950	1.050	1.150	1.250	1.350	1.450	1.550	1.650

Run # 2-3-4

U (fps)	20.38	22.45	23.61	24.60	25.00	25.15	25.15	25.00
y (ft)	0.150	0.250	0.350	0.450	0.550	0.650	0.750	0.850
	24.80	24.80	24.80	24.20	24.00	23.61	22.45	21.22
	0.950	1.050	1.150	1.250	1.350	1.450	1.550	1.650

Run # 2-3-5

U (fps)	23.41	25.15	26.55	27.68	27.55	27.20	27.20	26.65
y (ft)	0.150	0.250	0.350	0.450	0.550	0.650	0.750	0.850
	26.00	25.61	25.00	24.60	24.00	23.41	22.45	21.02
	0.950	1.050	1.150	1.250	1.350	1.450	1.550	1.650

Run # 2-3-6

U (fps)	23.61	25.42	26.65	27.38	27.68	27.82	27.55	27.00
y (ft)	0.150	0.250	0.350	0.450	0.550	0.650	0.750	0.850
	26.65	26.20	25.42	25.15	24.40	23.22	22.45	21.22
	0.950	1.050	1.150	1.250	1.350	1.450	1.550	1.650

Run # 2-3-7

U (fps)	23.22	25.15	27.55	28.53	28.80	28.80	28.53	28.02
y (ft)	0.150	0.250	0.350	0.450	0.550	0.650	0.750	0.850
	27.55	27.00	26.55	26.00	25.15	24.40	23.61	22.08
	0.950	1.050	1.150	1.250	1.350	1.450	1.550	1.650

Run # 2-3-8

U (fps)	22.22	24.50	25.42	26.20	27.26	27.63	27.68	27.68
y (ft)	0.150	0.250	0.350	0.450	0.550	0.650	0.750	0.850
	27.38	27.38	27.20	26.55	26.60	24.42	24.80	22.87
	0.950	1.050	1.150	1.250	1.350	1.450	1.550	1.650

Run # 2-3-9

U (fps)	27.93	28.61	29.77	30.30	30.45	31.02	29.59	29.10
y (ft)	0.150	0.250	0.350	0.450	0.550	0.650	0.750	0.850
	28.61	28.61	28.02	27.87	27.70	26.70	24.80	23.61
	0.950	1.050	1.150	1.250	1.350	1.450	1.550	1.650

Run # 3-1-1

U (fps)	3.50	9.07	10.40	10.40	10.40	10.40	10.82	10.40	10.40
y (ft)	0.05	0.15	0.25	0.35	0.45	0.55	0.65	0.75	0.85
	10.40	10.40	10.40	10.40	9.00	9.00	3.50	7.45	
	0.95	1.05	1.15	1.25	1.35	1.45	1.55	1.65	

Run # 3-1-2

U (fps)	10.40	12.04	12.40	12.04	12.04	12.40	12.40	12.40	11.63
y (ft)	0.05	0.15	0.25	0.35	0.45	0.55	0.65	0.75	0.85
	11.25	12.04	11.25	11.75	11.25	10.32	10.40	8.50	
	0.95	1.05	1.15	1.25	1.35	1.45	1.55	1.65	

Run # 3-1-3

U (fps)	12.04	14.10	14.40	14.40	14.40	14.40	14.40	14.40	14.10
y (ft)	0.05	0.15	0.25	0.35	0.45	0.55	0.65	0.75	0.85
	13.77	13.45	13.45	12.72	12.40	12.40	12.40	10.82	
	0.95	1.05	1.15	1.25	1.35	1.45	1.55	1.65	

Run # 3-1-4

U (fps)	15.35	17.50	18.50	18.50	18.50	18.50	18.50	18.50	18.00
y (ft)	0.05	0.15	0.25	0.35	0.45	0.55	0.65	0.75	0.85
	17.50	16.72	16.20	16.20	15.90	15.35	15.01	14.10	
	0.95	1.05	1.15	1.25	1.35	1.45	1.55	1.65	

Run # 3-1-5

U (fps)	17.00	18.50	19.95	19.95	19.95	19.50	19.27	19.02	19.02
y (ft)	0.05	0.15	0.25	0.35	0.45	0.55	0.65	0.75	0.85
	19.02	18.50	18.00	17.50	17.30	16.72	15.90	15.35	
	0.95	1.05	1.15	1.25	1.35	1.45	1.55	1.65	

Run # 3-1-6

U (fps)	20.80	21.30	22.10	22.10	22.10	22.10	21.65	21.65
y (ft)	0.15	0.25	0.35	0.45	0.55	0.65	0.75	0.85
	21.42	21.30	20.80	20.40	20.40	19.27	19.02	17.80
	0.95	1.05	1.15	1.25	1.35	1.45	1.55	1.65

Run # 3-1-7

U (fps)	21.87	23.85	24.40	24.90	24.90	24.65	24.40	23.65
y (ft)	0.15	0.25	0.35	0.45	0.55	0.65	0.75	0.85
	23.65	23.45	22.50	22.30	21.87	21.65	21.00	20.19
	0.95	1.05	1.15	1.25	1.35	1.45	1.55	1.65

Run # 3-1-8

U (fps)	24.40	26.35	27.20	28.00	28.15	28.15	28.28	27.65
y (ft)	0.15	0.25	0.35	0.45	0.55	0.65	0.75	0.85
	27.20	27.20	26.57	25.70	25.15	23.85	23.30	22.90
	0.95	1.05	1.15	1.25	1.35	1.45	1.55	1.65

Run # 3-1-9

U (fps)	24.90	27.90	28.53	29.25	29.25	29.25	29.25	28.80
y (ft)	0.15	0.25	0.35	0.45	0.55	0.65	0.75	0.85
	28.28	28.15	28.00	27.37	27.90	26.57	26.20	24.40
	0.95	1.05	1.15	1.25	1.35	1.45	1.55	1.65

Run # 3-2-1

U (fps)	17.90	18.40	18.62	18.62	18.62	18.62	18.40	18.62
y (ft)	0.10	0.20	0.30	0.40	0.50	0.60	0.70	0.80
	18.33	18.15	17.90	16.85	16.85	16.05	15.75	14.84
	0.90	1.00	1.10	1.20	1.30	1.40	1.50	1.60

Run # 3-2-2

U (fps)	19.35	19.77	20.25	19.77	20.09	19.77	19.77	19.65
y (ft)	0.10	0.20	0.30	0.40	0.50	0.60	0.70	0.80
	19.65	19.65	18.62	18.15	18.15	16.84	16.30	15.18
	0.90	1.00	1.10	1.20	1.30	1.40	1.50	1.60

Run # 3-2-3

U (fps)	20.93	21.45	21.55	21.55	21.55	21.55	21.45	21.19
y (ft)	0.10	0.20	0.30	0.40	0.50	0.60	0.70	0.80
	20.93	20.93	20.50	19.77	19.35	18.88	17.65	17.15
	0.90	1.00	1.10	1.20	1.30	1.40	1.50	1.60

Run # 3-2-4

U (fps)	20.43	21.75	22.05	22.05	22.05	22.05	21.55	21.45
y (ft)	0.10	0.20	0.30	0.40	0.50	0.60	0.70	0.80
	20.43	20.71	20.71	20.71	20.22	19.77	18.83	18.40
	0.90	1.00	1.10	1.20	1.30	1.40	1.50	1.60

Run # 3-2-5

U (fps)	22.75	24.25	24.42	24.42	24.42	24.25	24.25	24.25
y (ft)	0.10	0.20	0.30	0.40	0.50	0.60	0.70	0.80
	24.25	23.90	23.72	23.55	22.98	22.05	21.19	20.22
	0.90	1.00	1.10	1.20	1.30	1.40	1.50	1.60

Run # 3-2-6

U (fps)	23.35	25.10	25.75	26.22	26.10	25.55	25.90	25.90
y (ft)	0.10	0.20	0.30	0.40	0.50	0.60	0.70	0.80
	25.75	24.82	24.42	24.25	23.35	22.75	22.05	20.71
	0.90	1.00	1.10	1.20	1.30	1.40	1.50	1.60

Run # 3-2-7

U (fps)	24.42	26.21	26.91	27.10	27.42	27.42	27.42	26.48
y (ft)	0.10	0.20	0.30	0.40	0.50	0.60	0.70	0.80
	26.21	25.10	25.10	25.10	24.42	23.55	22.75	21.55
	0.90	1.00	1.10	1.20	1.30	1.40	1.50	1.60

Run # 3-2-8

U (fps)	24.25	26.43	27.75	28.08	28.08	28.08	27.96	27.75
y (ft)	0.10	0.20	0.30	0.40	0.50	0.60	0.70	0.80
	27.42	27.42	27.10	26.43	25.35	24.25	23.72	22.57
	0.90	1.00	1.10	1.20	1.30	1.40	1.50	1.60

Run # 3-2-9

U (fps)	28.79	28.90	30.08	30.20	30.20	30.08	29.60
y (ft)	0.20	0.30	0.40	0.50	0.60	0.70	0.80
	29.42	29.31	28.75	28.66	28.00	26.91	25.75
	0.90	1.00	1.10	1.20	1.30	1.40	1.50

Run # 3-2-10

U (fps)	27.42	30.43	31.50	31.80	31.80	31.90	31.80
y (ft)	0.20	0.30	0.40	0.50	0.60	0.70	0.80
	31.16	30.55	30.43	30.20	30.08	28.90	29.31
	0.90	1.00	1.10	1.20	1.30	1.40	1.50

Run # 3-3-1

U (fps)	21.65	22.96	23.95	23.30	23.30	22.96	22.50	22.10
y (ft)	0.10	0.20	0.30	0.40	0.50	0.60	0.70	0.80
	21.30	21.65	21.00	21.00	20.60	20.40	19.50	18.80
	0.90	1.00	1.10	1.20	1.30	1.40	1.50	1.60

Run # 3-3-2

U (fps)	22.96	24.05	24.65	24.65	24.65	24.65	24.65	24.65
y (ft)	0.10	0.20	0.30	0.40	0.50	0.60	0.70	0.80
	24.40	23.65	23.30	23.30	23.30	22.10	21.42	20.40
	0.90	1.00	1.10	1.20	1.30	1.40	1.50	1.60

Run # 3-3-3

U (fps)	22.10	23.65	24.40	24.90	24.05	23.85	23.65	23.85
y (ft)	0.10	0.20	0.30	0.40	0.50	0.60	0.70	0.80
	23.65	23.65	23.30	23.30	22.50	21.65	20.80	19.95
	0.90	1.00	1.10	1.20	1.30	1.40	1.50	1.60

Run # 3-3-4

U (fps)	23.65	25.15	25.52	25.70	25.70	25.70	25.52	25.52
y (ft)	0.10	0.20	0.30	0.40	0.50	0.60	0.70	0.80
	25.52	24.99	24.40	23.85	23.30	22.50	21.65	21.00
	0.90	1.00	1.10	1.20	1.30	1.40	1.50	1.60

Run # 3-3-5

U (fps)	23.65	25.30	26.00	26.20	25.82	26.00	26.00	26.20
y (ft)	0.10	0.20	0.30	0.40	0.50	0.60	0.70	0.80
	25.70	25.30	24.96	24.65	24.40	23.45	22.30	21.30
	0.90	1.00	1.10	1.20	1.30	1.40	1.50	1.60

Run # 3-3-6

U (fps)	24.05	26.57	27.38	27.57	27.65	28.00	27.87	27.57
y (ft)	0.10	0.20	0.30	0.40	0.50	0.60	0.70	0.80
	27.20	26.90	26.20	26.00	24.96	24.22	23.30	22.50
	0.90	1.00	1.10	1.20	1.30	1.40	1.50	1.60

Run # 3-3-7

U (fps)	26.57	28.00	28.30	29.08	29.08	29.22	28.80
y (ft)	0.20	0.30	0.40	0.50	0.60	0.70	0.80
	28.80	27.97	27.57	26.71	26.57	24.96	24.65
	0.90	1.00	1.10	1.20	1.30	1.40	1.50
							1.60

Run # 3-3-8

U (fps)	26.90	29.05	30.42	30.52	30.10	30.00	30.00
y (ft)	0.20	0.30	0.40	0.50	0.60	0.70	0.80
	30.10	29.80	29.08	28.68	27.75	27.02	25.67
	0.90	1.00	1.10	1.20	1.30	1.40	1.50
							1.60

Run # 3-3-9

U (fps)	26.43	26.75	30.42	31.12	31.12	31.12	30.98
y (ft)	0.20	0.30	0.40	0.50	0.60	0.70	0.80
	30.52	30.10	29.08	29.05	27.90	26.94	26.60
	0.90	1.00	1.10	1.20	1.30	1.40	1.50
							1.60

Run # 3-3-10

U (fps)	26.90	29.62	31.38	32.09	32.40	32.20	32.00
y (ft)	0.20	0.30	0.40	0.50	0.60	0.70	0.80
	32.00	31.60	31.38	30.80	30.10	29.71	28.03
	0.90	1.00	1.10	1.20	1.30	1.40	1.50
							1.60

APPENDIX III
Table of Tests Performed

FLUME DEPTH	TEST NO.	RUN NO.	TEST TYPE	WATER DEPTH T	ORIFICE SIZE d	MANIF DEPTH H	VELOCITY PROBE LOCATION, x	REMARKS
2.0'	1	1	Stag	2.0'	1/8 "	23 1/4"	x=11 5/8"	Depth Profile
"	"	2	"	"	"	"	vary	Surface Profile
"	"	3	"	"	"	"	vary	" "
"	"	4	"	"	"	"	vary	" "
"	"	5	"	"	"	"	vary	" "
"	"	6	"	"	"	"	11 5/8"	Depth Profile
"	"	7	"	"	"	"	11 5/8"	q-vs-U _{max}
"	"	8	"	"	"	"	11 5/8"	"
2.0'	2	1	Stag	2.0'	1/8"	11 1/8"	5 9/16"	q-vs-U _{max}
"	"	2	"	"	"	"	5 1/8"	Depth Profile
"	"	3	"	"	"	"	vary	" "
"	"	4	"	"	"	"	vary	Surface Profile
2.0'	3	1	Stag	2.0'	1/16"	23 1/4"	11 5/8	q-vs-U _{max}
"	"	2	"	"	"	"	vary	Surface Profile
"	"	3	"	"	"	"	vary	" "
"	"	4	"	"	"	"	11 5/8	Depth Profile
"	"	5	"	"	"	"	23 1/4	" "
"	"	6	"	"	"	"	11 5/8	" "
"	"	7	"	"	"	"	11 5/8	q-vs-U _{max}
2.0'	4	1	Stag	2.0'	0.04"	23 1/4"	11 5/8	q-vs-U _{max}
"	"	2	"	"	"	"	11 5/8	Depth Profile
"	"	3	"	"	"	"	23 1/4	" "
"	"	4	"	"	"	"	11 5/8	q-vs-U _{max}
2.0'	5	See Task 080402						
2.0'	6	See Task 080402						
2.0'	7	1	Stag	2.0'	1/16"	12"	vary	Surface Profile
"	"	2	"	"	"	"	vary	" "
"	"	3	"	"	"	"	12"	q-vs-U _{max}
"	"	4	"	"	"	"	12"	"
2.0'	8	See Task 080402						
2.0'	9	See Task 080402						
2.0'	10	1	Stag	2.0'	1/16"	11 5/8"	11 5/8"	q-vs-U _{max}

FLUME WIDTH	TEST NO.	RUN NO.	TEST TYPE	WATER DEPTH T	ORIFICE SIZE d	MANIF. DEPTH H	VELOCITY PROBE LOCATION, x	REMARKS
"	"	2		"	"	"	"	"
"	"	3		"	"	"	"	void
"	"	4		"	"	"	"	void
2.0'	11	1	Current	2.0'	None	None	Near Manif.	Current Profile
"	"	2	"	"	"	"	"	"
"	"	3	"	"	"	"	"	"
"	"	4	"	"	"	"	"	Surface Profile
"	"	5	both	"	1/16"	12"	+0.5 ft.	Depth Profile
"	"	6		"	"	"	-1.0 ft.	" "
"	"	7	"	"	"	"	-1.5 ft.	" "
"	"	8	"	"	"	"	-1.5 ft.	" "
"	"	9	"	"	"	"	+0.5 ft.	" "
"	"	10	"	"	"	"	vary	Surface Profile
2.0'	12	1		2.0'	1/16"	12"	0	void
"	"	2		"	"	"	0	void
2.0'	13	See Task 080402						
8.0"	1	1	Stag	13 5/8"	1/16"	13 3/8"	5 11/16"	q-vs-U _{max}
"	"	2	"	13 5/8"	"	"	5 11/16"	Depth Profile
"	"	3	"	13 5/8"	"	"	5 11/16"	" "
"	"	4	"	13 3/4"	"	13 1/4"	vary	Surface Profile
"	"	5	"	"	"	13 1/4"	vary	" "
"	"	6	"	"	"	13 1/4"	5 11/16"	q-vs-U _{max}
"	"	7	"	"	"	13 1/4"	-	"
"	"	8	"	"	"	13 1/4"	-	"
"	2	1	Stag					void
"	3	1	Stag					void
5.0'	1	1	Stag	8.5	1/16"	4.3	4.3'	Depth Profile
"	"	2	"	8.6	"	"	"	" "
5.0'	2	1	Stag	8.6	1/16"	4.3	vary	Surface Profile
"	"	2	"	8.7	"	"	"	" "
5.0'	3	1	Stag	8.7	1/16"	4.3	4.3	q-vs-U _{max}
5.0'	4	1	Stag	8.3	1/16"	8.3	4.3	Depth Profile
"	"	2	"	"	"	8.3	"	" "
5.0	5	1	Stag	8.7	1/16"	8.7	vary	Surface Profile
"	"	2	"	"	"	"	"	" "
5.0	6	1	Stag	8.3	1/16"	8.3	4.3	q-vs-U _{max}

FLUME WIDTH	TEST NO.	RUN NO.	TEST TYPE	WATER DEPTH T	ORIFICE SIZE d	MANIF. DEPTH H	VELOCITY PROBE LOCATION, x	REMARKS
1.5	7	1	Current	7.4	None	None	on near manifold	Depth Profile
"	"	2	"	"	"	"	"	" "
"	"	3	"	"	"	"	"	Cross Sect. at Surf.
1.5	8	1	Stag	7.4	1/16"	7.4	3.8	q-vs-U _{max}
1.5	9	1	Both	7.7	1/16"	7.7	Variable	Depth Profile
"	"	2	"	"	"	"	since	" "
"	"	3	"	"	"	"	Current	" "
"	"	4	"	"	"	"	Deflects	" "
"	"	5	"	"	"	"	Bubbles	" "
1.5	10	See Task 080402						
1.5	11	See Task 080402						

TEST NO. 1

DATE February 19, 1970

RUN NO. 1

Stevens Current Meter

q 0.019cfs/ft

MANIFOLD DIAMETER 1 in.

ORIFICE SPACING 1/2 in.

t_{H₂O} 18.6°C

GAGE READING AT SURFACE .490 ft.

LINE PRESSURE .94 psig.

t_{air} 74 °F

GAGE READING (ft)	DISTANCE FROM SURFACE (ft)	REV/SEC	VELOCITY (fps)	REMARKS
.439	.051	.9	.83	*
.391	.099	.9	.83	
.342	.148	.67	.65	Stevens Current Meter
.291	.199	.5	.48	
.245	.245	.33	.34	9° blade
.245	.245	.27	.28	
.440	.050	.94	.85	
.291	.199	2.8	.34	
.291	.199	2.8	.34	
.240	.250	2.33	.293	
.240	.250	2.33	.293	
.192	.298	1.5	.214	
.192	.298	1.5	.214	60° blade
.141	.349	1.0	.167	
.141	.349	.84	.150	
.091	.399	1.53	.218	
.091	.399	1.2	.184	
.439	.051	.9	.82	
.439	.051	.8	.75	
.392	.098	.73	.70	
.392	.098	.8	.75	90° blade
.339	.151	.53	.5	
.339	.151	.57	.56	
.292	.198	.6	.57	

TEST NO. 1

DATE February 19, 1970

RUN NO. 1

Stevens Current Meter

q 0.019cfs/ft

MANIFOLD DIAMETER 1 in.

ORIFICE SPACING 1/2 in.

t_{H_2O} 18.6° C

GAGE READING AT SURFACE .490 ft.

LINE PRESSURE .94 psig.

t_{air} 74 °F

GAGE READING (ft)	DISTANCE FROM SURFACE (ft)	REV/SEC	VELOCITY (fps)	REMARKS
.292	.198	.6	.57	
.242	.248	.43	.43	90° blade
.242	.248	.14	.17	

*At a distance of .199 ft below the water surface and below the current began fluctuating and only clicks registered by current away from the air pipe were counted.

TEST NO. 1

DATE February 19, 1970

RUN NO. 2

Stevens Midget Current Meter

q 0.019 cfs/ft

MANIFOLD DIAMETER 1 in.

ORIFICE SPACING 1/2 in.

t_{H2O} 20 °C

GAGE READING AT SURFACE .490 ft.

LINE PRESSURE .92 psig.

t_{air} 74 °F

GAGE READING (ft)	DISTANCE FROM SURFACE (ft)	x (in.)	REV/SEC	VELOCITY (fps)	REMARKS
.443	.047	5 3/16	1.03	.93	*
.443	.047	11 5/8	1.03	.93	
.443	-	12	-	-	
.443	.047	15 9/16	1.03	.93	
.443	.047	18	1.03	.93	
.443	.047	23 1/4	.8	.75	
.443	-	24	-	-	
.443	.047	30	.77	.64	
.443	.047	36	.6	.58	
.443	.047	48	.4	.40	
.443	-	60	-	-	
.443	-	72	-	-	
.443	.047	5 3/16	1.13	1.02	
.443	.047	11 5/8	1.00	.91	
.443	-	12	-	-	
.443	.047	15 9/16	.93	.85	
.443	.047	18	.83	.75	
.443	.047	23 1/4	.87	.80	
.443	-	24	-	-	
.443	.047	30	.63	.60	
.443	.047	36	.57	.55	

* Using Stevens Midget Current Meter (9° blade).

Alot of static was encountered on readings over

36 in.

- 77a' -

TEST NO. 1

DATE February 19, 1970

PLS NO. 3

Stevens Current Meter

q 0.019 cfs/ft

MANIFOLD DIAMETER 1 in.

ORIFICE SPACING 1/2 in.

t_{H2O} 20.2 °C

GAGE READING AT SURFACE .490 ft.

LINE PRESSURE .94 psig.

t_{AIR} 73 °F

GAGE READING (ft)	DISTANCE FROM SURFACE (ft)	x (ft)	VELOCITY KEY/SEC (fps)	REMARKS
.483	.007	.484	1.2	1.25
.483	.007	.967	1.23	1.1 Using Stevens
.477	.013	1.45	1.25	1.1 Current Meter
.477	.013	1.5	1.3	1.16 (9° blade)
.477	.013	1.94	.9	.82
.477	.013	2.5	.77	.70
.477	.013	3.0	.63	.59
.477	.013	4.0	2.44	.31 Used 60° blade
.483	.007	.484	1.2	1.08
.483	.007	.967	1.43	1.30
.477	.013	1.45	1.03	.93
.477	.013	1.5	1.07	.97 Wheel half in &
.477	.013	1.94	.87	.80 half out of water
.477	.013	2.5	.67	.63
.477	.013	3.0	.73	.69
.477	.013	4.0	2.5	.31

TEST NO. 1

DATE February 19, 1970

RUC NO. 4

Stevens Hidget Current Meter

q .029 cfs/ft

MANIFOLD DIAMETER 1 in.

ORIFICE SPACING 1/2 in.

 t_{H_2O} 20.2 °C

GAGE READING AT SURFACE .490 ft.

LINE PRESSURE 1.01 psig.

 t_{air} 75 °F

GAGE READING (ft)	DISTANCE FROM SURFACE (ft)	X (in.)	REV/SEC	VELOCITY (fps)	REMARKS
		5 3/16			Too close to air
.480	.01	11 5/8	1.57	1.38	
.480	.01	15 9/16	1.63	1.45	Using Stevens
.480	.01	18	1.5	1.34	Current Meter
.477	.013	23 1/4	1.4	1.25	(9° blade)
.477	.013	30	1.3	1.18	
.477	.013	36	1.03	.95	
.477	.013	48	.47	.40	
.477	.013	60	1.67	.30	
		5 3/16			Too close to air
.480	.01	11 5/8	1.57	1.38	
.480	.01	15 9/16	1.57	1.38	
.480	.01	18	1.57	1.38	
.477	.013	23 1/4	1.37	1.22	
.477	.013	30	1.23	1.10	
.477	.013	36	.87	.80	
.477	.013	48	.67	.61	
.477	.013	60	1.67	.23	

TEST NO. 1

DATE February 19, 1970

RUN NO. 5

Stevens Hidget Current Meter

q .038 cfs/ft

MANIFOLD DIAMETER 1 in.

ORIFICE SPACING 1/2 in.

t_{H_2O} 20.2 °C

GAGE READING AT SURFACE .490 ft.

LINE PRESSURE 1.16 psig.

t_{air} 75 °F

GAGE READING (ft)	DISTANCE FROM SURFACE (ft)	x (in.)	REV/SEC	VELOCITY (fps)	REMARKS
.470	.02	11 5/8	1.43	1.27	Using Steven
.470	.02	15 9/16	1.23	1.10	Hidget Current
.470	.02	18	1.07	1.15	meter (9° blade)
.470	.02	23 1/4	1.07	.96	
.470	.02	30	.80	.75	
.459	.031	36	.87	.80	
.480	.02	48	.73	.70	
.480	.01	60	.33	.33	
.470	.02	11 5/8	1.3	1.18	
.470	.02	15 9/16	1.37	1.21	
.470	.02	18	1.1	1.0	
.470	.02	23 1/4	.93	.84	
.470	.02	30	1.0	.91	
.459	.031	36	.90	.82	
.480	.01	48	.80	.73	
.480	.01	60	.33	.33	

TEST NO. 1

DATE February 20, 1970

RUN NO. 6

MANOMETER WITH 1:5 SLOPE

q .038 cfs/ft

MANIFOLD DIAMETER 1 in.

ORIFICE SPACING 1/2 in.

t_{H₂O} 19.4°C

GAGE READING AT SURFACE 1.34 ft.

LINE PRESSURE 1.16 psig.

t_{air} 73 °F

GAGE READING (ft)	DISTANCE FROM SURFACE (ft)	ΔH (ft)	VELOCITY (fps)	REMARKS
1.277	.067	.04	1.58	Diff = R.R.-
1.223	.121	.0316	1.40	L.R. - I.D.
1.174	.170	.0183	1.06	
1.123	.221	.0133	0.91	1.84 ft. depth
1.078	.266	.0117	0.85	at gage reading
1.021	.323	.0083	0.72	1.184 ft.
0.971	.377	.0050	0.56	
0.926	.418	.0033	0.46	
0.872	.472	.0033	0.46	
0.825	.519	.0017	0.32	
0.780	-	-	-	
0.814	.530	0	0	

TEST NO. 1

DATE February 20, 1970

RUN NO. 7

Manometer Slope 1:5

MANIFOLD DIAMETER 1 in.

ORIFICE SPACING 1/2 in.

t_{H₂O} 19.4 °C

GAGE READING AT SURFACE 1.34 ft.

LINE PRESSURE (psig)	t _{air} (°F)	GAGE READING (ft)	q (cfs) (ft)	Δh (ft)	VELOCITY (fps)	REMARKS
1.16	74°	1.275	0.0383	.0322	1.45	
.95	74°	1.275	0.0192	.0216	1.15	
1.04	74°	1.275	0.0234	.0300	1.36	
1.41	75°	1.275	0.0467	.0425	1.66	
1.95	75°	1.275	0.070	.0533	1.82	
2.80	75°	1.275	0.0934	.0600	1.94	

Oil began seeping into the
flowmeter when a flow of 8.4
was being measured. Meter was
cleaned and test resumed.

3.52	74°	1.275	0.117	.0650	2.03	
4.35	74°	1.232	0.14	.0624	1.98	
5.30	74°	1.232	0.164	.0700	2.11	
6.64	74°	1.232	0.187	.0783	2.24	
8.20	75°	1.232	0.21	.0833	2.31	

TEST NO. 1

DATE 21 Feb. 1970

RUN NO. 8

Manometer Slope 1:5

MANIFOLD DIAMETER 1 in.

ORIFICE SPACING 1/2 in. ORIFICE DIAMETER 1/8 in.

t_{H_2O} 18.6 °C

GAGE READING AT SURFACE 1.363 ft.

LINE PRESSURE (psig)	t_{air} (°F)	GAGE READING (ft)	q $\left(\frac{cfs}{ft}\right)$	ΔH (ft)	VELOCITY (fps)	REMARKS
0.91	74	1.308	0.0192	0.027	1.29	
1.00	74	1.308	0.029	0.032	1.41	
1.12	74	1.308	0.0383	0.040	1.58	
1.00	74	1.308	0.0234	0.033	1.43	
1.15	74	1.308	0.035	0.040	1.57	
1.34	74	1.308	0.047	0.045	1.67	
1.55	74	1.308	0.058	0.050	1.77	
1.80	74	1.308	0.070	0.055	1.85	
2.10	74	1.308	0.082	0.058	1.91	
2.44	74	1.276	0.093	0.060	1.94	
2.75	75	1.276	0.105	0.062	1.98	
3.10	77	1.276	0.117	0.067	2.06	
3.40	79	1.276	0.128	0.070	2.11	
3.90	81	1.276	0.140	0.073	2.16	

TEST NO. 2

DATE 21 Feb. 1970

RUN NO. 1

Manometer with Slope 1:5

MANIFOLD DIAMETER 1 in.

ORIFICE SPACING 1/2 in.

t_{H_2O} 18.4 °C

GAGE READING AT SURFACE .37 ft.

LINE PRESSURE (psig)	t_{air} (°F)	GAGE READING (ft)	q ($\frac{cfs}{ft}$)	ΔH (ft)	VELOCITY (fps)	REMARKS
0.50	74	.357	0.0192	0.020	1.11	
0.58	74	.357	0.0287	0.025	1.26	
0.70	74	.357	0.0383	0.0317	1.41	
0.49	74	.357	0.0234	0.0234	1.20	
0.68	74	.357	0.0467	0.0283	1.32	
0.84	74	.357	0.0583	0.035	1.48	
1.04	74	.357	0.0700	0.0367	1.51	
1.36	74	.357	0.0816	0.0383	1.55	
1.73	75	.345	0.0933	0.0383	1.55	

TEST NO. 2

DATE 21 Feb. 1970

RUN NO. 2

MANOMETER WITH 1:5 SLOPE

q .0383 cfs/ft

MANIFOLD DIAMETER 1 in.

ORIFICE SPACING 1/2 in.

t_{H_2O} 19.2°C

GAGE READING AT SURFACE .400 ft.

LINE PRESSURE .70 psig.

t_{air} 74 °F

GAGE READING (ft)	DISTANCE FROM SURFACE (ft)	ΔH (ft)	VELOCITY (fps)	REMARKS
.345	.055	.0267	1.29	
.311	.089	.0183	1.06	
.280	.120	.010	.79	
.251	.149	.0067	.65	
.222	.178	.0033	.45	
.190	.210	.0033	.45	
.160	.240	-	-	

$$b = .254'$$

TEST NO. 2

DATE 21 Feb. 1970

RUN NO. 3

MANOMETER WITH 1:5 SLOPE

q .07 cfs/ft

MANIFOLD DIAMETER 1 in.

ORIFICE SPACING 1/2 in.

t_{H_2O} 19.4°C

GAGE READING AT SURFACE .399 ft.

LINE PRESSURE 1.35 psig.

t_{air} 78 °F

GAGE READING (ft)	DISTANCE FROM SURFACE (ft)	Δh (ft)	VELOCITY (fps)	REMARKS
.363	.036	.030	1.36	
.341	.048	.0292	1.34	
.310	.089	.0284	1.32	
.282	.117	.0183	1.06	
.257	.142	.0150	0.96	
.222	.177	.0117	0.85	
.193	.206	.0083	0.71	
.162	.237	.005	0.56	
.150	.249	.0033	0.45	

TEST NO. 2

DATE 21 Feb. 1970

RUN NO. 4

MANOMETER WITH 1:5 SLOPE

q 0.07 cfs/ft

MANIFOLD DIAMETER 1 in.

ORIFICE SPACING 1/2 in.

t_{H2O} 19.4°C

GAGE READING AT SURFACE .399 ft.

LINE PRESSURE 1.35 psig.

t_{air} 82 °F

GAGE READING (ft)	DISTANCE FROM SURFACE (ft)	x (ft)	ΔH (ft)	VELOCITY (fps)	REMARKS
.329	.070	.464	.033	1.43	
.350	.049	.928	.03	1.36	
.350	.049	1.85	.0117	.85	
.350	.049	2.5	.0067	.65	
.350	.049	3.0	.0033	.45	

TEST NO. 3

DATE 21 Feb 1970

RUN NO. 1

Manometer Slope 1:5

MANIFOLD DIAMETER 1 in.

ORIFICE SPACING 1/2 in. ORIFICE DIAMETER 1/16 in.

t_{H_2O} 19.6 °C

GAGE READING AT SURFACE 1.41 ft.

LINE PRESSURE (psig)	t_{air} (°F)	GAGE READING (ft)	q ($\frac{cfs}{ft}$)	ΔH (ft)	VELOCITY (fps)	REMARKS
0.86	75	1.350	.0096	.0133	.91	
0.99	75		.0132	.0216	1.16	
1.12	75		.0288	.0333	1.44	
1.32	75		.0384	.0399	1.59	
1.11	75		.0233	.0266	1.28	
1.35	75		.0350	.0366	1.51	
1.64	75		.0466	.0482	1.73	
1.97	75		.0583	.0549	1.85	
2.34	75		.0700	.0582	1.91	
2.75	76		.0816	.0632	2.0	
3.19	77		.0934	.0682	2.08	
3.77	81		.1050	.0682	2.08	

TEST NO. 3

DATE February 23, 1970

RUN NO. 2

MANOMETER WITH 1:5 SLOPE

q 0.04 cfs/ft

MANIFOLD DIAMETER 1 in.

ORIFICE SPACING 1/2 in.

t_{H2O} 20.2 °C

GAGE READING AT SURFACE 1.41 ft.

LINE PRESSURE 1.30 psig.

t_{air} 74 °F

GAGE READING (ft)	DISTANCE FROM SURFACE (ft)	x (in)	ΔH (ft)	VELOCITY (fps)	REMARKS
1.368	.042	11 5/8	.0350	1.48	
1.368	.042	17 7/16	.0334	1.44	
1.368	.042	23 1/4	.0300	1.36	
1.368	.042	30	.0234	1.20	
1.368	.042	36	.0200	1.11	
1.368	.042	48	.0133	0.91	
1.368	.042	60	.0100	0.79	

TEST NO. 3

DATE 23 Feb 1970

RUN NO. 3

MANOMETER WITH 1:5 SLOPE

q 0.07 cts/ft

MANIFOLD DIAMETER 1 in.

ORIFICE SPACING 1/2 in.

t_{H2O} 25.2 °C

GAGE READING AT SURFACE .92 ft.

LINE PRESSURE 2.37 psig.

t_{air} 77 °F

GAGE READING (ft)	DISTANCE FROM SURFACE (ft)	x (in)	Δh (ft)	VELOCITY (fps)	REMARKS
.876	.046	60	.0083	.72	
.856	.056	48	.0133	.91	
.856	.066	36	.0234	1.21	
.856	.066	30	.0333	1.44	
.856	.066	23 1/4	.0350	1.48	
.856	.066	17 7/16	.0417	1.62	
.856	.066	11 5/8	.0500	1.77	
		5 13/16			In air bubbles

TEST NO. 3

DATE 23 Feb. 1970

RUN NO. 4

MANOMETER WITH 1:5 SLOPE

q 0.05 cfs/ft

MANIFOLD DIAMETER 1 in.

ORIFICE SPACING 1/2 in.

t_{H₂O} 20.2°C

GAGE READING AT SURFACE .922 ft.

LINE PRESSURE 1.62 psig.

t_{air} 80 °F

GAGE READING (ft)	DISTANCE FROM SURFACE (ft)	Δh (ft)	VELOCITY (fps)	REMARKS
.856	.066	.0367	1.5	
.826	.096	.0334	1.44	
.800	.122	.0217	1.16	
.775	.147	.0217	1.16	
.752	.170	.015	.96	
.726	.196	.0117	.85	
.700	.222	.0083	.72	
.675	.247	.0067	.65	
.650	.272	.005	.56	
.625	.297	.005	.56	
.600	.322	.005	.56	
.575	.347	.0033	.46	
.550	.372	.0033	.46	
.525	.397	.0017	.32	
.500	.422	.0008	-	
.475	.447	-	-	

TEST NO. 3

DATE 24 Feb. 1970

RUE NO. 5

MANOMETER WITH 1:5 SLOPE

q 0.07 cfs/ft

MANIFOLD DIAMETER 1 in.

ORIFICE SPACING 1/2 in.

t_{H_2O} 20.2°C

GAGE READING AT SURFACE .97 ft.

LINE PRESSURE 2.32 psig.

t_{air} 75 °F

GAGE READING (ft)	DISTANCE FROM SURFACE (ft)	ΔH (ft)	VELOCITY (fps)	REMARKS
.910	.060	.0383	1.55	
.880	.090	.0333	1.44	
.850	.120	.0300	1.36	
.820	.150	.0267	1.29	
.790	.180	.0217	1.16	
.760	.210	.0167	1.01	
.730	.240	.0133	.91	
.690	.280	.0133	.91	
.660	.310	.0083	.72	
.630	.340	.0067	.65	
.600	.370	.0067	.65	
.570	.400	.0058	.60	
.540	.430	.0050	.56	
.510	.460	.0033	.46	
.480	.490	.0033	.46	
.450	.520	.0025	.39	
.420	.550	.0017	.31	
.390	.580	b=	.58'	

TEST NO. 3

DATE 24 Feb. 1970

RUN NO. 6

MANOMETER WITH 1:5 SLOPE

q 0.02 cfs/ft

MANIFOLD DIAMETER 1 in.

ORIFICE SPACING 1/2 in.

t_{H_2O} 20.3°F

GAGE READING AT SURFACE .970 ft.

LINE PRESSURE 0.96 psig.

t_{air} 77 °F

GAGE READING (ft)	DISTANCE FROM SURFACE (ft)	ΔH (ft)	VELOCITY (fps)	REMARKS
.930	.040	.0225	1.18	
.900	.070	.0175	1.04	
.870	.100	.0142	.93	
.839	.131	.0108	.82	
.810	.160	.0092	.76	
.780	.190	.0067	.65	
.750	.220	.0042	.51	
.720	.250	.0033	.46	
.69	.280	.0017	.31	
.66	.310	.0008	-	
.63	.340	.0008	-	
.60	.370	.0008	-	
.57	.400	.0000	.00	

$$b = .4'$$

TEST NO. 3

DATE 24 Feb. 1970

RUN NO. 7

Manometer with Slope 1:5

MANIFOLD DIAMETER 1 in.

ORIFICE SPACING 1/2 in.

t_{H2O} 20.2 °C

GAGE READING AT SURFACE .985 ft.

LINE PRESSURE (psig)	t _{air} (°F)	GAGE READING (ft)	q ($\frac{cfs}{ft}$)	ΔH (ft)	VELOCITY (fps)	REMARKS
.98	78	.941	.0176	.0250	1.24	
1.15	78	.941	.0184	.0283	1.33	
1.42	78	.941	.0364	.0350	1.48	
1.35	78	.932	.0291	.0384	1.55	
1.86	77	.932	.0466	.0467	1.70	
2.50	77	.932	.0619	.0567	1.88	
3.27	77	.916	.0794	.0617	1.97	
4.38	78	.916	.0984	.0667	2.06	
5.40	79	.875	.117	.0734	2.17	
6.14	82	.875	.128	.0750	2.19	
7.21	83	.849	.143	.0817	2.29	
8.20	84	.849	.158	.0891	2.59	
8.21	88	.849	.206	.0950	2.47	
9.41	88	.858	.214	.1032	2.57	
11.80	88	.858	.224	.1182	2.69	

TE NO. 4

DATE 26 Feb. 1970

RUN NO. 1

Manometer with Slope 1:5

MANIFOLD DIAMETER 1 in.

ORIFICE SPACING 1/2 in.

t_{H₂O} 19.4 °C

GAGE READING AT SURFACE 1.05 ft.

LINE PRESSURE (psig)	t _{air} (°F)	GAGE READING (ft)	q ($\frac{\text{cfs}}{\text{ft}}$)	ΔH (ft)	VELOCITY (fps)	REMARKS
.90	72	1.004	.00555	.0008	.2	
.99	72	1.004	.00912	.0017	.32	
.91	72	1.004	.00595	.0008	.2	
1.05	72	1.004	.01064	.0008	.2	
1.29	73	1.004	.01611	.0075	.69	
1.52	73	1.004	.02066	.0117	.85	
1.81	73	1.004	.02476	.0317	1.40	
2.14	73	1.004	.02866	.0383	1.55	
2.49	73	1.004	.03246	.0400	1.59	
2.98	73	1.004	.03734	.0433	1.65	
2.14	73	1.004	.02326	.0383	1.55	
4.52	73	1.004	.04354	.0500	1.77	
11.00	73	.955	-	.0667	2.05	
7.19	74	.955	.07720	.0584	1.91	
14.49	75	.955	-	.0766	2.21	
19.1	77	.955	-	.0850	2.33	
24.46	79	.955	-	.1000	2.53	
27.75	80	.95	-	.1050	2.59	

TEST NO. 4

DATE 26 Feb. 1970

RUN NO. 2

MANOMETER WITH 1:5 SLOPE

q .047 cfs/ft

MANIFOLD DIAMETER 1 in.

ORIFICE SPACING 1/2 in.

t_{H_2O} 19.4°C

GAGE READING AT SURFACE 1.046 ft.

LINE PRESSURE 4.3 psig.

t_{air} 81 °F

GAGE READING (ft)	DISTANCE FROM SURFACE (ft)	ΔH (ft)	VELOCITY (fps)	REMARKS
.45	.596	.0000	-	
.50	.546	.0008	.2	
.55	.496	.0017	.32	
.60	.446	.0033	.46	
.65	.396	.0033	.46	
.70	.346	.0067	.65	
.75	.296	.0100	.79	
.80	.246	.0133	.91	
.85	.196	.0150	.97	
.90	.146	.0217	1.16	
.95	.096	.0417	1.62	
1.00	.046	.0516	1.79	

TEST NO. 4

DATE 26 Feb. 1970

RUN NO. 3

MANOMETER WITH 1:5 SLOPE

q .047 cfs/ft

MANIFOLD DIAMETER 1 in.

ORIFICE SPACING 1/2 in.

t_{H_2O} 19.4°C

GAGE READING AT SURFACE 1.05 ft.

LINE PRESSURE 4.20 psig.

t_{air} 85 °F

GAGE READING (ft)	DISTANCE FROM SURFACE (ft)	ΔH (ft)	VELOCITY (fps)	REMARKS
.500	.546	.00	-	
.55	.496	.00	-	
.60	.446	.0017	.32	
.65	.396	.0017	.32	
.70	.346	.0050	.56	
.75	.296	.0083	.72	
.80	.246	.0117	.85	
.85	.196	.0183	1.06	
.90	.146	.0200	1.11	
.95	.096	.0283	1.32	
1.00	.046	.0350	1.48	

TEST NO. 4

DATE 26 Feb. 1970

RUN NO. 4

Manometer with Slope 1:5

MANIFOLD DIAMETER 1 in.

ORIFICE SPACING 1/2 in.

t_{H_2O} 19.4 °C

GAGE READING AT SURFACE 1.05 ft.

LINE PRESSURE (psig)	t_{air} (°F)	GAGE READING (ft)	q ($\frac{cfs}{ft}$)	ΔH (ft)	VELOCITY (fps)	REMARKS
.87	84	1.00	0.72	.0083	.72	
.98	83	1.00	0.97	.0150	.97	
.90	83	1.00	1.36	.0300	1.36	
1.11	83	1.00	1.20	.0233	1.20	
1.30	83	1.00	1.33	.0284	1.33	
1.67	82	1.00	1.48	.0350	1.48	
2.24	82	1.00	1.62	.0417	1.62	
2.81	82	1.00	1.70	.0467	1.70	
2.06	81	1.00	1.51	.0367	1.51	
4.29	80	1.00	1.85	.0550	1.85	
7.62	80	.969	.061	.0684	2.09	
11.84	82	.957	.074	.0766	2.21	
16.65	83	.957	.081	.0900	2.41	
27.35	83	.957	.010	.122	2.79	
23.10	87	.930	.096	.0984	2.51	

TEST NO. 7

DATE 1 April 1970

RUN NO. 1

MANOMETER WITH 1:5 SLOPE

q 0.07 cfs/ft

MANIFOLD DIAMETER 1 in.

ORIFICE SPACING 1/2 in.

t_{H2O} 20 °C

GAGE READING AT SURFACE 1.67 ft.

LINE PRESSURE 2.4 psig.

t_{air} 83 °F

GAGE READING (ft)	DISTANCE FROM SURFACE (ft)	x (ft)	ΔH (ft)	VELOCITY (fps)	REMARKS
1.60					Original
1.60	.07	.5	.0367	1.51	
1.60	.07	1.0	.0350	1.48	
1.60	.07	3.0	-	-	
1.60	.07	2.5	.005	.56	
1.60	.07	2.0	.005	.56	
1.60	.07	1.5	.0100	.79	
1.60	.07	1.0	.0267	1.29	
1.575	.095	.5	.0367	1.51	

TEST NO. 7

DATE 1 April 1970

RUN NO. 2

MANOMETER WITH 1:5 SLOPE

q .013 cfs/ft

MANIFOLD DIAMETER 1 in.

ORIFICE SPACING 1/2 in.

t_{H2O} 20 °C

GAGE READING AT SURFACE 1.66 ft.

LINE PRESSURE .64 psig.

t_{air} 76 °F

GAGE READING (ft)	DISTANCE FROM SURFACE (ft)	x (ft)	ΔH (ft)	VELOCITY (fps)	REMARKS
1.630	.03	3.5	.005	.56	Original
1.630	.03	3.0	.005	.56	
1.630	.03	2.5	.005	.56	
1.630	.03	2.0	.008	.705	
1.630	.03	1.5	.008	.705	
1.630	.03	1.0	.0100	.79	
1.630	.03	.5	.0117	.85	
1.630	.03	.35	.0167	1.01	
1.630	.03	-.30	.020	1.11	

TEST NO. 7

DATE

RUN NO. 3

Manometer with Slope 1:5

MANIFOLD DIAMETER 1 in.

ORIFICE SPACING 1/2 in.

t_{H2O} 20 °C

GAGE READING AT SURFACE 1.34 ft.

LINE PRESSURE (psig)	t _{air} (°F)	GAGE READING (ft)	q ($\frac{\text{cfs}}{\text{ft}}$)	ΔH (ft)	VELOCITY (fps)	REMARKS
Original						
.48	74	1.37	.00383	.005	.56	
.51	74	1.37	.00767	.005	.56	
.56	74	1.37	.0115	.0067	.65	
.60	74	1.37	.0153	.0083	.72	
.65	74	1.37	.0192	.0133	.91	
.69	74	1.37	.0230	.0133	.91	
.70	74	1.37	.0268	.0167	1.01	
.72	74	1.37	.0307	.0183	1.06	
.72	74	1.37	.0345	.0167	1.01	
.76	74	1.37	.0383	.0200	1.11	
.64	74	1.37	.0233	.0150	.96	
.96	74	1.37	.0466	.0217	1.15	
1.28	74	1.37	.0700	.0283	1.32	
3.04	75	1.37	.0933	.0350	1.48	
5.32	78	1.37	.1167	.0400	1.59	

TEST NO. 7

DATE

RUN NO. 4

Manometer with Slope 1:5

MANIFOLD DIAMETER 1 in.

ORIFICE SPACING 1/2 in.

t_{H2O} 20 °C

GAGE READING AT SURFACE 1.72 ft.

LINE PRESSURE (psig)	t _{air} (°F)	GAGE READING (ft)	q ($\frac{cfs}{ft}$)	ΔH (ft)	VELOCITY (fps)	REMARKS
		1.685				
.52	72	1.685	.00575	.00833	.72	
.53	72	1.685	.00958	.0100	.79	
.56	72	1.685	.01342	.0133	.91	
.60	72	1.685	.01725	.0150	.96	
.63	72	1.685	.02108	.0183	1.06	
.66	72	1.685	.02492	.0183	1.06	
.89	75	1.685	.02875	.0200	1.11	
.95	78	1.65	.03258	.0217	1.15	
1.11	79	1.65	.03642	.0233	1.20	
1.17	78	1.65	.0350	.0217	1.15	
2.04	80	1.65	.05833	.0300	1.36	
3.21	86	1.65	.08167	.0367	1.51	
4.42	90	1.65	.09975	.0400	1.59	

TEST NO. 10

DATE 9 April 1970

RUN NO. 1

Manometer with Slope 1:5

MANIFOLD DIAMETER 1 in.

ORIFICE SPACING 1/2 in.

t_{H_2O} 19.6 °C

GAGE READING AT SURFACE 1.38 ft.

LINE PRESSURE (psig)	t_{air} (°F)	GAGE READING (ft)	q ($\frac{cfs}{ft}$)	Δh (ft)	VELOCITY (fps)	REMARKS
.5	74	1.42	.0105	.0067	.643	
.55	74	1.42	.0175	.0067	.643	
.75	74	1.42	.0263	.0117	.850	
.84	74	1.42	.0350	.0135	.915	
.62	74	1.42	.0234	.0100	.790	
.82	74	1.42	.0350	.0150	.960	
1.12	74	1.42	.0467	.0184	1.06	
1.61	74	1.42	.0584	.0217	1.16	
2.38	74	1.42	.0700	.0267	1.28	
3.66	74	1.42	.0817	.0300	1.36	
5.21	74	1.42	.0952	.0350	1.48	
7.07	74	1.42	.105	.0350	1.48	
8.10	74	1.42	.117	.0417	1.62	

TEST NO. 10

DATE 9 April 1970

RUN NO. 2

Manometer Slope with 1:5

MANIFOLD DIAMETER 1 in.

ORIFICE SPACING 1/2 in.

t_{H_2O} 19.6 °C

GAGE READING AT SURFACE 1.38 ft.

LINE PRESSURE (psig)	t_{air} (°F)	GAGE READING (ft)	q ($\frac{cfs}{ft}$)	ΔH (ft)	VELOCITY (fps)	REMARKS
0.54	77	1.42	.0192	.0117	.850	
0.62	77	1.42	.0288	.0167	1.01	
0.76	77	1.42	.0384	.0200	1.11	
0.62	77	1.42	.0234	.0167	1.01	
0.84	77	1.42	.0350	.0217	1.16	
1.10	77	1.42	.0467	.0267	1.28	
1.38	77	1.42	.0584	.0267	1.28	
2.38	77	1.42	.0700	.0334	1.42	
3.40	77	1.42	.0819	.0384	1.55	
4.84	77	1.42	.0950	.0434	1.66	
6.91	78	1.42	.1050	.0500	1.76	
8.0	78	1.42	.1170	.0584	1.92	

TEST NO. 10

DATE 10 April 1970

RUN NO. 3

MANOMETER WITH 1:5 SLOPE

q 0 cfs/ft

MANIFOLD DIAMETER 1 in.

ORIFICE SPACING 1/2 in.

t_{H_2O} 19.6°C

GAGE READING AT SURFACE 1.90 ft.

LINE PRESSURE psig.

t_{air} - °F

GAGE READING (ft)	DISTANCE FROM SURFACE (ft)	Δh (ft)	VELOCITY (fps)	REMARKS
1.871	.033	.0045	.53	
1.670	.234	.0045	.53	
1.459	.445	.0045	.53	
1.347	.557	.0043	.52	
1.049	.855	.0040	.50	
0.838	1.006	.0040	.50	
0.650	1.254	.0035	.47	
0.450	1.454	.0035	.47	
0.249	1.655	.0032	.44	
0.028	1.932	.0020	.34	

TEST NO. 10

DATE 10 April 1970

RUN NO. 4

MANOMETER WITH 1:5 SLOPE

q 0 cfs/ft

MANIFOLD DIAMETER 1 in.

ORIFICE SPACING 1/2 in.

t_{H₂O} 19.6°C

GAGE READING AT SURFACE .077 ft.

LINE PRESSURE psig.

t_{air} - °F

GAGE READING (ft)	DISTANCE FROM SURFACE (ft)	ΔH (ft)	VELOCITY (fps)	REMARKS
0.077		.0033	.46	
0.162		.00483	.55	
0.418		.00558	.59	
0.705		.00608	.62	
0.981		.00642	.63	
1.190		.00666	.65	
1.507		.00793	.70	
1.655		.0075	.73	
1.828		.00683	.64	
1.850		.00666	.65	

TEST NO. 11

DATE

RUN NO. 1

Ott Current Meter

q - cfs/ft

MANIFOLD DIAMETER 1 in.

ORIFICE SPACING 1/2 in.

 t_{H_2O} 19.6°C

GAGE READING AT SURFACE 1.906 ft.

LINE PRESSURE - psig.

 t_{air} - °F

GAGE READING (ft)	DISTANCE FROM SURFACE (ft)	REV/SEC	VELOCITY (fps)	REMARKS
Surface	0	3.39	.78	
Surface	0	3.57	.81	
1.686	.220	4.54	.99	
1.686	.220	4.56	1.00	
1.521	.385	4.79	1.05	
1.521	.385	4.82	1.03	
1.349	.557	4.86	1.05	
1.349	.557	4.75	1.03	
1.200	.706	4.75	1.03	
1.200	.706	4.66	1.01	
1.050	.856	4.46	.97	
1.050	.856	4.36	.95	
.880	1.026	4.14	.91	
.880	1.026	4.16	.92	
.720	1.186	4.16	.92	
.720	1.186	4.06	.90	
.581	1.325	4.14	.91	
.581	1.325	4.14	.91	
.419	1.487	4.36	.95	
.419	1.487	4.36	.95	
.230	1.676	3.99	.89	
.230	1.676	4.06	.90	
.645	1.261	4.22	.93	
.645	1.261	4.18	.92	

- 107a -

TEST NO. 11 (continued)
RUN NO. 1

DATE

q cfs/ft

MANIFOLD DIAMETER in.

ORIFICE SPACING 1/2 in.

t_{H_2O}

GAGE READING AT SURFACE ft.

LINE PRESSURE psig.

t_{air} °F

GAGE READING (ft)	DISTANCE FROM SURFACE (ft)	REV/SEC	VELOCITY (fps)	REMARKS
1.373	.533	4.75	1.03	
1.642	.264	4.66	1.01	
1.845	.061	4.29	.94	Fully submerged

TEST NO. 11

DATE 11 April 1970

RUN NO. 2

Ott Current Meter

q - cfs/ft

MANIFOLD DIAMETER 1 in.

ORIFICE SPACING 1/2 in.

 t_{H_2O} 19.6°C

GAGE READING AT SURFACE 1.893 ft.

LINE PRESSURE - psig.

 t_{air} - °F

GAGE READING (ft)	DISTANCE FROM SURFACE (ft)	REV/SEC	VELOCITY (fps)	REMARKS
Surface	0	4.21	.93	
Surface	0	4.19	.92	
1.773	.120	5.01	1.075	
1.773	.120	5.05	1.08	
1.517	.376	5.09	1.09	
1.517	.376	5.09	1.09	
1.362	.531	5.05	1.08	
1.362	.531	5.04	1.08	
1.224	.669	4.87	1.05	
1.224	.669	4.90	1.055	
1.137	.756	4.74	1.025	
1.137	.756	4.85	1.045	
1.029	.864	4.48	.98	
1.029	.864	4.52	.985	
.956	.937	4.05	.90	
.956	.937	4.09	.91	
1.843	.050	5.18	1.105	
1.843	.050	5.19	1.110	
1.777	.116	4.99	1.07	
1.777	.116	4.91	1.06	
1.637	.256	4.95	1.07	
1.637	.256	4.99	1.07	
1.486	.407	5.06	1.08	
1.486	.407	4.99	1.07	

- 109a -

TEST NO. 11 (continued)
RUN NO. 2

DATE

q cfs/ft

MANIFOLD DIAMETER in.

ORIFICE SPACING 1/2 in.

t_{H_2O}

GAGE READING AT SURFACE ft.

LINE PRESSURE psig.

t_{air} °F

GAGE READING (ft)	DISTANCE FROM SURFACE (ft)	REV/SEC	VELOCITY (fps)	REMARKS
1.375	.518	4.98	1.07	
1.375	.518	4.99	1.07	

TEST NO. 11

DATE 11 April 1970

RUN NO. 3

Ott Current Meter

q - cfs/ft

MANIFOLD DIAMETER 1 in.

ORIFICE SPACING 1/2 in.

 t_{H_2O} 19.6°C

GAGE READING AT SURFACE 1.892 ft.

LINE PRESSURE - psig.

 t_{air} - °F

GAGE READING (ft)	DISTANCE FROM SURFACE (ft)	REV/SEC	VELOCITY (fps)	REMARKS
1.842	.050	4.29	.94	
1.842	.050	4.39	.96	
1.611	.281	4.66	1.01	
1.611	.281	4.66	1.01	
1.459	.433	4.74	1.025	
1.459	.433	4.78	1.035	
1.188	.704	4.47	.98	
1.188	.704	4.52	.985	
1.001	.891	4.28	.94	
1.001	.891	4.26	.94	
.840	1.052	4.14	.915	
.840	1.052	4.26	.935	
.650	1.242	4.26	.935	
.650	1.242	4.16	.915	
.500	1.392	4.19	.925	
.500	1.392	4.23	.93	
.399	1.493	4.28	.93	
.399	1.493	4.24	.93	
.250	1.642	4.11	.91	
.250	1.642	4.11	.91	
.177	1.715	3.85	.86	
.177	1.715	3.79	.85	
.103	1.789	3.57	.81	
.103	1.789	3.59	.81	

- 111a -

TEST NO. 11 (continued)
RUN NO. 3

DATE

q cfs/ft

MANIFOLD DIAMETER in.

ORIFICE SPACING 1/2 in.

t_{H_2O}

GAGE READING AT SURFACE ft.

LINE PRESSURE psig.

t_{air} °F

GAGE READING (ft)	DISTANCE FROM SURFACE (ft)	REV/SEC	VELOCITY (fps)	REMARKS
-.002	1.894	3.19	.74	
-.002	1.894	3.02	.715	

TEST NO. 11

DATE 11 April 1970

RUN NO. 4

Ott Current Meter

q - cfs/ft

MANIFOLD DIAMETER 1 in.

ORIFICE SPACING 1/2 in.

t_{H2O} 19.6 °C

GAGE READING AT SURFACE 1.90 ft.

LINE PRESSURE - psig.

t_{air} - °F

GAGE READING (ft)	DISTANCE FROM SURFACE (ft)	DISTANCE OFF CL (ft)	REV/SEC	VELOCITY (fps)	REMARKS
1.855	.049	.9	2.58	.64	
1.855	.049	.9	2.76	.67	
1.855	.049	.8	3.00	.71	
1.855	.049	.8	3.08	.72	
1.855	.049	.7	3.53	.80	
1.855	.049	.7	3.52	.77	
1.855	.049	.6	3.68	.83	
1.855	.049	.6	3.78	.85	
1.855	.049	.5	4.01	.89	
1.855	.049	.5	3.96	.89	
1.855	.049	.4	4.19	.91	
1.855	.049	.4	4.25	.94	
1.855	.049	.3	4.48	.98	
1.855	.049	.3	4.55	.99	
1.855	.049	.2	4.89	1.05	
1.855	.049	.2	4.77	1.03	
1.855	.049	.1	5.14	1.10	
1.855	.049	.1	5.18	1.10	
1.855	.049	.0	5.29	1.13	
1.855	.049	.0	5.18	1.11	
1.855	.049	.1	5.05	1.08	
1.855	.049	.1	5.07	1.08	
1.855	.049	.2	4.96	1.07	

TEST NO. 11 (continued)

DATE

RUN NO. 4

q cfs/ft

MANIFOLD DIAMETER in.

ORIFICE SPACING in.

t_{H2O} °C

GAGE READING AT SURFACE ft.

LINE PRESSURE psig.

t_{air} °F

GAGE READING (ft)	DISTANCE FROM SURFACE (ft)	DISTANCE OFF CL (ft)	REV/SEC	VELOCITY (fps)	REMARKS
1.855	.049	.2	4.99	1.07	
1.855	.049	.3	4.75	1.03	
1.855	.049	.3	4.77	1.03	
1.855	.049	.4	4.52	.99	
1.855	.049	.4	4.60	1.00	
1.855	.049	.5	4.46	.98	
1.855	.049	.5	4.40	.96	
1.855	.049	.6	4.19	.90	
1.855	.049	.6	4.12	.90	
1.855	.049	.7	3.98	.88	
1.855	.049	.7	4.07	.89	
1.855	.049	.8	3.64	.83	
1.855	.049	.8	3.74	.84	
1.802	.046	.9	3.16	.74	
1.802	.046	.9	2.72	.66	

TEST NO. 11

DATE 11 April 1970

RUN NO. 5

Ott Current Meter

q .070 cfs/ft

MANIFOLD DIAMETER 1 in.

ORIFICE SPACING 1/2 in.

 t_{H_2O} 19.6°C

GAGE READING AT SURFACE 1.845 ft.

LINE PRESSURE - psig.

 t_{air} - °F

GAGE READING (ft)	DISTANCE FROM SURFACE (ft)	REV/SEC	VELOCITY (fps)	REMARKS
1.845	0	0	0	
1.781	.046	2.22	.57	
1.739	.106	2.01	.53	
1.739	.106	2.72	.66	
1.739	.106	2.96	.71	
1.700	.145	3.74	.84	
1.700	.145	3.43	.79	
1.700	.145	3.43	.79	
1.650	.105	3.56	.81	
1.650	.105	3.68	.83	
1.650	.105	3.66	.83	
1.600	.245	3.78	.85	
1.600	.245	3.79	.85	
1.600	.245	3.72	.84	
1.550	.300	3.32	.88	
1.550	.300	3.86	.86	
1.550	.300	3.83	.86	
1.500	.345	3.89	.87	
1.500	.345	4.03	.90	
1.500	.345	3.90	.90	
1.45	.305	4.12	.91	
1.45	.305	4.05	.90	
1.45	.305	4.25	.94	
1.40	.445	4.24	.94	

TEST NO. 11

DATE

RUN NO. 5 (continued)

q cfs/ft

MANIFOLD DIAMETER in.

ORIFICE SPACING 1/2 in.

 t_{H_2O}

GAGE READING AT SURFACE ft.

LINE PRESSURE psig.

 t_{air} °F

GAGE READING (ft)	DISTANCE FROM SURFACE (ft)	REV/SEC	VELOCITY (fps)	REMARKS
1.40	.445	4.12	.91	
1.40	.445	4.14	.91	
1.35	.495	4.33	.95	
1.35	.495	4.32	.95	
1.35	.495	4.32	.95	
1.30	.545	4.32	.95	
1.30	.545	4.42	.97	
1.30	.545	4.34	.95	
1.25	.595	4.45	.97	
1.25	.595	4.45	.97	
1.25	.595	4.32	.95	

TEST NO. 11

DATE 11 April 1970

RUN NO. 6

Ott Current Meter

q .07 cfs/ft

MANIFOLD DIAMETER 1 in.

ORIFICE SPACING - 1/2 in.

 t_{H_2O} 19.6°C

GAGE READING AT SURFACE 1.817 ft.

LINE PRESSURE - psig.

 t_{air} - °F

GAGE READING (ft)	DISTANCE FROM SURFACE (ft)	REV/SEC	VELOCITY (fps)	REMARKS
1.764	.053	4.32	.95	In Air Bubbles
1.764	.053	4.52	.99	"
1.764	.053	4.29	.94	"
1.700	.117	4.12	.91	"
1.700	.117	4.09	.91	"
1.700	.117	4.86	1.05	"
1.650	.167	4.27	.94	"
1.650	.167	5.02	1.07	"
1.650	.167	4.51	.98	"
1.55	.267	5.29	1.08	"
1.55	.267	5.13	1.10	"
1.55	.267	5.33	1.13	"
1.45	.367	4.83	1.04	
1.45	.367	5.64	1.19	
1.45	.367	5.13	1.10	
1.35	.467	4.92	1.07	
1.35	.467	4.59	1.00	
1.35	.467	4.82	1.04	
1.25	.567	3.26	.76	Cannot see meter,
1.25	.567	4.06	.89	maybe in turbulent
1.25	.567	3.06	.71	region of mixing
1.15	.667	1.20	.40	"
1.15	.667	1.12	.39	"
1.15	.667	2.20	.57	

- 117a -

TEST NO. 11

DATE 11 April 1970

RUN NO. 7

Ott Meter

q .07 cfs/ft

MANIFOLD DIAMETER 1 in.

ORIFICE SPACING 1/2 in.

t_{H_2O} 19.6°C

GAGE READING AT SURFACE 1.800 ft.

LINE PRESSURE - psig.

t_{air} - °F

GAGE READING (ft)	DISTANCE FROM SURFACE (ft)	REV/SEC	VELOCITY (fps)	REMARKS
1.744	.056	9.41	1.86	
1.744	.056	9.22	1.82	
1.650	.150	7.20	1.46	
1.650	.150	7.56	1.53	
1.550	.250	5.83	1.23	
1.550	.250	5.81	1.22	
1.450	.350	4.57	.99	
1.450	.350	4.13	.92	
1.350	.450	3.18	.75	
1.350	.450	2.72	.66	
1.350	.450	2.33	.59	
1.250	.550	1.34	.43	
1.250	.550	.87	.45	
1.250	.550	1.00	.37	
1.150	.650	.37	.27	
1.150	.650	.53	.30	
1.150	.650	.53	.30	
1.050	.750	.57	.31	
1.050	.750	.43	.28	
1.050	.750	.47	.29	
.950	.850	1.60	.47	
.950	.850	1.49	.45	
.950	.850	2.13	.56	
.850	.950	3.30	.70	

TEST NO. 11 (continued)

DATE

RUN NO. 7

q cfs/ft

MANIFOLD DIAMETER in.

ORIFICE SPACING 1/2 in.

t_{H_2O}

GAGE READING AT SURFACE ft.

LINE PRESSURE psig.

t_{air} °F

GAGE READING (ft)	DISTANCE FROM SURFACE (ft)	REV/SEC	VELOCITY (fps)	REMARKS
.850	.950	3.15	.74	
.850	.950	3.44	.79	
.750	1.050	5.10	1.09	
.750	1.050	4.97	1.07	
.750	1.050	5.25	1.12	
.650	1.150	5.59	1.18	
.650	1.150	5.66	1.19	
.650	1.150	5.65	1.19	
.550	1.250	5.71	1.20	
.550	1.250	5.66	1.21	
.550	1.250	5.68	1.22	
.450	1.350	5.42	1.15	
.450	1.350	5.65	1.19	

TEST NO. 11

DATE 11 April 1970

RUN NO. 8

Ott. Current Meter

q .023 cfs/ft

MANIFOLD DIAMETER 1 in.

ORIFICE SPACING 1/2 in.

 t_{H_2O} 19.6°C

GAGE READING AT SURFACE 1.842 ft.

LINE PRESSURE - psig.

 t_{air} - °F

GAGE READING (ft)	DISTANCE FROM SURFACE (ft)	REV/SEC	VELOCITY (fps)	REMARKS
1.800	.042	6.43	1.33	x = -1.5 ft
1.800	.042	6.47	1.33	"
1.700	.142	5.57	1.18	"
1.700	.142	5.60	1.18	"
1.600	.242	5.36	1.14	"
1.600	.242	5.30	1.13	"
1.500	.342	5.07	1.09	"
1.500	.342	4.98	1.07	"
1.400	.442	4.43	.97	"
1.400	.442	4.66	1.01	"
1.300	.542	4.10	.91	"
1.300	.542	3.40	.78	"
1.200	.642	2.65	.65	"
1.200	.642	2.12	.56	"
1.100	.742	2.22	.57	"
1.100	.742	2.35	.60	"
1.000	.842	1.65	.47	"
1.000	.842	1.78	.49	"
1.792	.050	3.76	.85	x = +0.5 ft
1.792	.050	3.76	.85	"
1.696	.146	4.01	.89	"
1.696	.146	4.08	.90	"
1.600	.242	4.10	.91	"
1.600	.242	3.91	.89	"

TEST NO. 11

DATE

RUN NO. 8 (continued)

q cfs/ft

MANIFOLD DIAMETER in.

ORIFICE SPACING 1/2 in.

 t_{H_2O}

GAGE READING AT SURFACE ft.

LINE PRESSURE psig.

 t_{air} °F

GAGE READING (ft)	DISTANCE FROM SURFACE (ft)	REV/SEC	VELOCITY (fps)	REMARKS
1.500	.342	4.16	.92	q = +0.5 ft
1.500	.342	4.15	.92	"
1.400	.442	4.33	.95	"
1.400	.442	4.27	.94	"
1.300	.542	4.26	.94	"
1.300	.542	4.28	.94	"
1.200	.642	4.40	.96	"
1.200	.642	4.37	.96	"
1.100	.742	4.31	.95	"
1.100	.742	4.35	.95	"
1.00	.842	4.45	.97	"
1.00	.842	4.47	.98	"

TEST NO. 11

DATE 13 April 1970

RUN NO. 9

Ott Meter

q - cfs/ft

MANIFOLD DIAMETER 1 in.

ORIFICE SPACING 1/2 in.

 t_{H_2O} - °C

GAGE READING AT SURFACE 1.500 ft.

LINE PRESSURE - psig.

 t_{air} - °F

GAGE READING (ft)	DISTANCE FROM SURFACE (ft)	x (ft)	REV/SEC	VELOCITY (fps)	REMARKS
1.457	.043	2.0	4.730	1.025	q=.07 cfs/ft
1.457	.043	1.5	4.328	.950	P _{air} = .53
1.457	.043	1.0	3.245	.751	
1.457	.043	.5	1.171	.400	
1.457	.043	.0	-1.985	-.530	
1.457	.043	-.5	-4.128	-.915	
1.492	.008	-1.0	4.660	1.010	*
1.439	.061	-1.5	10.39	2.027	
1.439	.061	-2.0	8.693	1.73	
1.439	.061	-2.5	8.600	1.71	
1.439	.061	-3.0	7.923	1.59	
1.439	.061	-3.0	7.667	1.55	q=.465 cfs/ft
1.439	.061	-2.5	7.733	1.56	P _{air} = .51
1.439	.061	-2.0	8.548	1.70	
1.439	.061	-1.5	7.479	1.60	
1.439	.061	-1.0	3.333	.771	*
1.452	.048	-0.5	-5.719	-1.22	
1.452	.048	.0	-1.987	-.531	
1.469	.031	.5	2.200	.570	
1.469	.031	1.0	4.106	.91	
1.469	.031	1.5	4.651	1.01	
1.469	.031	2.0	4.987	1.07	
1.469	.031	2.0	4.978	1.085	q=.0583 cfs/ft
1.469	.031	1.5	4.585	.990	P _{air} = .52

TEST NO. 11 (continued)
 RUN NO. 9

DATE

q cfs/ft

MANIFOLD DIAMETER in.

ORIFICE SPACING in.

t_{H2O} °C

GAGE READING AT SURFACE ft.

LINE PRESSURE psig.

t_{air} °F

GAGE READING (ft)	DISTANCE FROM SURFACE (ft)	x (ft)	REV/SEC	VELOCITY (ips)	REMARKS
1.469	.031	1.5	4.585	.990	
1.469	.031	1.0	4.211	.936	
1.469	.031	.5	2.209	.572	
1.469	.031	.0	-1.187	-.409	
1.465	.035	-.5	-4.472	-.990	
1.523	-.023	-1.0	4.630	1.065	
1.481	.019	-1.5	9.273	1.83	
1.477	.023	-2.0	8.843	1.75	
1.477	.023	-2.5	8.100	1.63	
1.477	.023	-3.0	8.189	1.64	
1.477	.023	-3.0	6.729	1.38	q=.035 cfs/ft P _{air} = .49
1.477	.023	-2.5	7.267	1.47	
1.477	.023	-2.0	7.785	1.57	
1.477	.023	-1.5	7.764	1.56	
1.489	.011	-1.0	2.258	.580	*
1.462	.058	-.5	-4.467	-.980	
1.462	.058	.0	-.8013	-.230	
1.450	.070	.5	3.327	.771	
1.450	.070	1.0	4.291	.94	
1.450	.070	1.5	4.936	1.06	
1.450	.070	2.0	4.903	1.05	
1.488	.032	2.0	4.764	1.03	q=.0383 cfs/ft P _{air} = .3

TEST NO. 11 (continued)

DATE

RUN NO. 9

q cfs/ft

MANIFOLD DIAMETER in.

ORIFICE SPACING in.

 t_{H_2O} °C

GAGE READING AT SURFACE ft.

LINE PRESSURE psig.

 t_{air} °F

GAGE READING (ft)	DISTANCE FROM SURFACE (ft)	r (ft)	REV/SEC	VELOCITY (fps)	REMARKS
1.488	.032	1.5	4.663	1.01	
1.488	.032	1.0	3.970	.88	
1.507	.013	.5	1.300	.42	
1.507	.013	.0	2.201	-.58	
1.507	.013	-.5	6.183	-1.28	
1.497	.023	-1.0	3.612	-.82	
1.497	.023	-1.5	9.428	1.86	
1.497	.023	-2.0	8.449	1.69	
1.497	.023	-2.5	8.482	1.69	
1.497	.023	-3.0	8.360	1.67	
1.497	.023	-3.0	7.640	1.54	q=.031 cfs/ft P _{air} = .72
1.497	.023	-2.5	8.074	1.60	
1.497	.023	-2.0	8.311	1.66	
1.497	.023	-1.5	8.050	1.60	
1.497	.023	-1.0	2.015	.53	*
1.515	.005	-.5	-3.112	-.74	
1.515	.005	.0	-.8053	-.34	
1.508	.012	.5	2.818	.68	
1.508	.012	1.0	3.915	.87	
1.508	.012	1.5	4.551	.98	
1.508	.012	2.0	4.584	1.00	
1.508	.012	2.0	4.788	1.03	q=.023 cfs/ft P _{air} = .69
1.508	.012	1.5	4.864	1.05	

TEST NO. 11 (continued)
RUN NO. 9

DATE

q cfs/ft

MANIFOLD DIAMETER in.

ORIFICE SPACING in.

t_{H_2O} °C

GAGE READING AT SURFACE ft.

LINE PRESSURE psig.

t_{air} °F

GAGE READING (ft)	DISTANCE FROM SURFACE (ft)	x (ft)	REV/SEC	VELOCITY (fps)	REMARKS
1.508	.012	1.0	4.545	.99	
1.508	.012	.5	3.661	.83	
1.523	.003	.0	1.282	.42	
1.515	.005	- .5	- .9960	- .37	
1.515	.005	-1.0	1.861	.51	*
1.510	.010	-1.5	6.445	1.33	
1.510	.010	-2.0	7.052	1.44	
1.510	.010	-2.5	6.962	1.42	
1.510	.010	-3.0	7.029	1.43	

* in air bubbles

TEST NO. 11

DATE 14 April 1970

RUN NO. 10

Ott Meter

q - cfs/ft

MANIFOLD DIAMETER 1 in.

ORIFICE SPACING 1/2 in.

 t_{H_2O} 20 °C

GAGE READING AT SURFACE ft.

LINE PRESSURE - psig.

 t_{air} 77 °F

GAGE READING (ft)	DISTANCE FROM SURFACE (ft)	x (ft)	REV/SEC	VELOCITY (fps)	REMARKS
1.257	.066	2.0	4.729	1.025	q=.019 cfs/ft P _{air} = .65
1.257	.066	1.5	4.720	1.022	
1.257	.066	1.0	4.500	.980	
1.257	.066	.5	4.047	.900	
1.257	.066	.0	2.591	.640	
1.257	.066	- .5	.7973	.340	
1.257	.066	-1.0	2.599	.641	*
1.257	.066	-1.5	6.338	1.31	
1.257	.066	-2.0	6.455	1.33	
1.257	.066	-2.5	6.445	1.33	
1.257	.066	-3.0	6.440	1.33	
1.257	.066	-3.0	6.375	1.31	q=.0153 cfs/ft P _{air} = .6
1.257	.066	-2.5	6.380	1.32	
1.278	.045	-2.0	6.353	1.35	
1.278	.045	-1.5	6.190	1.29	
1.278	.045	-1.0	2.191	.565	*
1.278	.045	- .5	.9868	.371	
1.278	.045	.0	3.539	.81	
1.278	.045	.5	4.400	.963	
1.278	.045	1.0	4.719	1.02	
1.278	.045	1.5	4.780	1.030	
1.278	.045	2.0	4.857	1.047	
1.278	.045	2.0	5.006	1.075	q=.0096 cfs/ft P _{air} = .53
1.278	.045	1.5	4.863	1.045	

TEST NO. 11 (continued)
RUN NO. 10

DATE

q cfs/ft

MANIFOLD DIAMETER in.

ORIFICE SPACING in.

t_{H_2O} °C

GAGE READING AT SURFACE ft.

LINE PRESSURE psig.

t_{air} °F

GAGE READING (ft)	DISTANCE FROM SURFACE (ft)	x (ft)	REV/SEC	VELOCITY (fps)	REMARKS
1.278	.045	1.0	4.727	1.025	
1.295	.028	.5	4.510	.982	
1.295	.028	.0	3.992	.890	
1.295	.028	- .5	3.225	.752	
1.295	.028	-1.0	2.582	.640	*
1.295	.028	-1.5	5.765	1.215	
1.295	.028	-2.0	6.015	1.26	
1.295	.028	-2.5	5.912	1.24	
1.295	.028	-3.0	5.933	1.245	

* in air bubbles

TEST NO. 12

DATE 17 April 1970

RUN NO. 1

MANOMETER WITH 1:5 SLOPE

q cfs/ft

MANIFOLD DIAMETER 1 in.

ORIFICE SPACING 1/2 in.

t_{H_2O} 19.6°C

GAGE READING AT SURFACE 1.48 ft.

LINE PRESSURE psig.

t_{air} 77 °F

GAGE READING (ft)	DISTANCE FROM SURFACE (ft)	ΔH (ft)	VELOCITY (fps)	REMARKS
1.41	.067	.0033	.46	
1.341	.136	.0033	.46	
1.272	.205	.0033	.46	
1.200	.277	.0025	.39	
1.125	.352	.0025	.39	
1.058	.419	.0025	.39	
1.013	.464	.0017	.32	
.945	.532	.0017	.32	
.901	.576	.0017	.32	
.541	.936	.0133	.91	
.700	.777	.0100	.79	
.825	.652	.00417	.51	
.982	.495	.0025	.39	

TEST NO. 12

DATE 17 April 1970

RUN NO. 2

MANOMETER WITH 1:5 SLOPE

q .07 cfs/ft

MANIFOLD DIAMETER 1 in.

ORIFICE SPACING 1/2 in.

t_{H_2O} 19.6°C

GAGE READING AT SURFACE 1.48 ft.

LINE PRESSURE 2.38 psig.

t_{air} 77 °F

GAGE READING (ft)	DISTANCE FROM SURFACE (ft)	ΔH (ft)	VELOCITY (fps)	REMARKS
1.391	.086	.0033	.46	
1.309	.168	.00583	.72	
1.360	.117	.00583	.72	
1.418	.059	.00583	.72	
1.118	.359	.00583	.72	
.865	.612	.00583	.72	
.526	.951	.01333	.91	
1.318	.159	.0092	.76	
1.130	.347	.01417	.93	
.995	.482	.00583	.72	
1.377	.100	.00417	.51	
.748	.729	.01417	.93	
1.418	.059	.0008	.70	
1.159				No Bubbles
1.157	.320	.00417	.51	
1.371	.106	.0033	.46	
1.330	.147	.0033	.46	
1.268	.209	.00583	.72	
1.213	.264	.00583	.72	
1.071	.406	.00583	.72	

TEST NO. 1

DATE 20 March 1970

RUN NO. 1

Manometer with Slope 1:5

MANIFOLD DIAMETER 1 in.

ORIFICE SPACING 1/2 in.

t_{H_2O} 19.5 °C

GAGE READING AT SURFACE 1.304 ft.

LINE PRESSURE (psig)	t_{air} (°F)	GAGE READING (ft)	q ($\frac{cfs}{ft}$)	ΔH (ft)	VELOCITY (fps)	REMARKS
.61	72	1.276	.0124	.0167	1.01	
1.06	72	1.266	.0247	.0233	1.20	
1.74	72	1.262	.0362	.0267	1.29	
2.65	72	1.249	.0468	.0400	1.59	
3.81	73	1.245	.0568	.0434	1.46	
5.16	73	1.238	.0658	.0550	1.85	
6.79	73	1.229	.0737	.0583	1.91	
9.92	73	1.214	.0790	.0617	1.97	
11.66	73	1.200	.0813	.0667	2.06	
14.09	73	1.200	.0866	.0717	2.14	

TEST NO. 1

DATE 21 March 1970

RUN NO. 2

MANOMETER WITH 1:5 SLOPE

q .082 cfs/ft

MANIFOLD DIAMETER 1 in.

ORIFICE SPACING 1/2 in.

t_{H_2O} 19.5°C

GAGE READING AT SURFACE 1.304 ft.

LINE PRESSURE 8.64 psig.

t_{air} 72 °F

GAGE READING (ft)	DISTANCE FROM SURFACE (ft)	ΔH (ft)	VELOCITY (fps)	REMARKS
1.224	.08	.0667	2.06	
1.180	.124	.0483	1.73	
1.147	.157	.0317	1.40	
1.130	.174	.0283	1.32	
1.056	.248	.0233	1.20	
1.100	.204	.0133	.91	
1.200	.104	.0317	1.40	
1.160	.144	.0233	1.20	
1.120	.184	.0167	1.01	
1.162	.142	.030	1.56	
1.056	.248	.0250	1.24	
1.088	.216	.0133	.91	
1.161	.143	.0300	1.36	
1.233	.071	.0667	2.06	
1.200	.104	.0533	1.82	
1.221	.083	.0650	2.03	
.520	.784	.00333	.46	
.608	.696	.00167	.32	
.710	.594	.00167	.32	
.785	.514	.00167	.32	
.810	.494	.00167	.32	
.910	.394	.00167	.32	
.895	.409	.00167	.32	

TEST NO. 1 (continued)

DATE

RUN NO. 2

MANOMETER WITH 1:5 SLOPE

q cfs/ft

MANIFOLD DIAMETER in.

ORIFICE SPACING in.

t_{H_2O}

GAGE READING AT SURFACE ft.

LINE PRESSURE psig.

t_{air} °F

GAGE READING (ft)	DISTANCE FROM SURFACE (ft)	ΔH (ft)	VELOCITY (fps)	REMARKS
1.018	.286	.00333	.45	
1.057	.247	.00667	.65	
1.086	.218	.01168	.86	

TEST NO. 1

DATE 21 March 1970

RUN NO. 3

MANOMETER VITE 1:5 SCALE

q .041 cfs/ft

MANIFOLD DIAMETER 1 in.

ORIFICE SPACING 1 1/2 in.

t_{H_2O} 15.5°C

CAGE READINGS AT SURFACE 1.36 ft.

LINE PRESSURE 1.20 psig.

t_{air} 72 °F

CAGE READINGS (ft.)	DISTANCE FROM SURFACE (ft.)	DE (ft.)	VELOCITY (fps)	REMARKS
.520	.835	0	0	
.600	.735	0	0	
.700	.655	0	0	
.800	.555	0	0	
.920	.455	0	0	
1.00	.355	.00167	.32	
1.10	.255	.00167	.32	
1.150	.205	.00500	.56	
1.175	.180	.00833	.72	
1.200	.155	.0183	1.04	
1.225	.135	.0183	1.04	
1.240	.115	.0200	1.11	
1.260	.095	.0283	1.32	
1.280	.075	.0333	1.44	
1.300	.055	.0384	1.55	
1.160	.195	.0500	1.77	
.520	.835	0	0	

TEST NO. 1

DATE 21 March 1970

RUN NO. 4

MANOMETER WITH 1:5 SLOPE

q .0429 cfs/ft

MANIFOLD DIAMETER 1 in.

ORIFICE SPACING 1/2 in.

t_{H_2O} 19.5 °C

GAGE READING AT SURFACE 1.40 ft.

LINE PRESSURE 3.25 psig.

t_{air} 72 °F

GAGE READING (ft)	DISTANCE FROM SURFACE (ft)	x (ft)	Δh (ft)	VELOCITY (fps)	REMARKS
1.354	.043	.549	.0533	1.82	
1.354	.043	1.11	.0250	1.24	
1.354	.043	1.66	.0183	1.08	
1.354	.043	2.22	.0117	.85	
1.354	.043	-	.005	.56	
1.354	.043	.75	.0417	1.62	

TEST NO. 1

DATE 21 March 1970

RUN NO. 5

MASCHESTER WITH 1:5 SLOPE

q .082 cfs/ft

MANIPULATED DIAMETER 1 in.

ORIFICE SPACING 1/2 in.

t_{H_2O} 19.5°C

GAGE READING AT SURFACE 1.4 ft.

LINE PRESSURE 9.6 psig.

t_{air} 73 °F

GAGE READING (ft)	DISTANCE FROM SURFACE (ft)	Δh (ft)	VELOCITY (fps)	REMARKS
1.252	.145	.0400	1.57	
1.348	.048	.0367	1.51	
1.348	.048	.0317	1.40	
1.349	.048	.0183	1.06	
1.349	.048	.0150	.96	
1.349	.048	.0467	1.70	

TEST NO. 1

DATE 21 March 1970

RUN NO. 6

Manometer with Slope 1:5

MANIFOLD DIAMETER 1 in.

ORIFICE SPACING 1/2 in.

t_{H_2O} 20 °C

GAGE READING AT SURFACE 1.202 ft.

LINE PRESSURE (psig)	t_{air} (°F)	GAGE READING (ft)	q ($\frac{cfs}{ft}$)	ΔH (ft)	VELOCITY (fps)	REMARKS
.85	74	1.141	.0187	.0233	1.20	
1.53	75	1.141	.0304	.0300	1.36	
2.35	75	1.141	.0416	.0400	1.58	
3.50	75	1.123	.0516	.0467	1.70	
4.80	77	1.123	.0610	.0500	1.77	
6.39	77	1.112	.0694	.0583	1.91	
8.06	77	1.112	.0770	.0617	1.95	
10.05	77	1.103	.0840	.0633	2.00	
11.97	77	1.089	.0852	.0650	2.33	
1.10	77	1.159	.0246	.0283	1.32	
2.90	77	1.157	.0467	.0450	1.67	
4.10	77	1.148	.0565	.0567	1.88	
7.45	77	1.138	.0728	.0617	1.97	
9.45	77	1.112	.0797	.0667	2.36	

TEST NO. 1

DATE 21 March 1970

RUN NO. 7

Manometer with Slope 1:5

MANIFOLD DIAMETER 1 in.

ORIFICE SPACING 1/2 in.

t_{H_2O} 19.4 °C

GAGE READING AT SURFACE 1.4 ft.

LINE PRESSURE (psig)	t_{air} (°F)	GAGE READING (ft)	q ($\frac{cfs}{ft}$)	ΔH (ft)	VELOCITY (fps)	REMARKS
1.16	74	1.35	.0294		1.45	
.95	74	1.35	.0192		1.15	
1.04	74	1.35	.0242		1.36	
1.41	75	1.35	.0475		1.66	
1.95	75	1.35	.0705		1.82	
2.80	75	1.35	.0915		1.94	
3.52	74	1.35	.112		2.03	
4.35	74	1.35	.131		1.98	
5.30	74	1.35	.15		2.11	
6.64	74	1.35	.165		2.24	
8.20	75	1.35	.18		2.31	

TEST NO. 1

DATE 21 March 1970

RUN NO. 8

Manometer with Slope 1:5

MANIFOLD DIAMETER 1 in.

ORIFICE SPACING 1/2 in.

CH₂O 19.4 °C

GAGE READING AT SURFACE 1.4 ft.

LINE PRESSURE (psig)	t _{air} (°F)	GAGE READING (ft)	q ($\frac{cfs}{ft}$)	ΔH (ft)	VELOCITY (fps)	REMARKS
.91	74	1.3	.0192		1.29	
1.00	74	1.3	.029		1.41	
1.12	74	1.3	.0283		1.58	
1.00	74	1.3	.0234		1.43	
1.15	74	1.3	.035		1.57	
1.34	74	1.3	.047		1.67	
1.55	74	1.3	.058		1.77	
1.80	74	1.3	.070		1.85	
2.10	74	1.3	.082		1.91	
2.44	74	1.3	.093		1.94	
2.75	75	1.3	.105		1.98	
3.10	77	1.3	.117		2.06	
3.40	79	1.3	.128		2.11	
3.90	81	1.3	.140		2.16	

TEST NO. 2

DATE 21 March 1970

RUN NO. 1

Manometer with Slope 1:5

MANIFOLD DIAMETER 1 in.

ORIFICE SPACING 1/2 in.

t_{H_2O} 19.4 °C

CASE READING AT SURFACE 1.4 ft.

LINE PRESSURE (psig)	t_{air} (°F)	CASE READING (ft)	q ($\frac{cfs}{ft}$)	ΔH (ft)	VELOCITY (fps)	REMARKS
.50	74	1.35	.0192		1.11	
.58	74	1.35	.0287		1.26	
.70	74	1.35	.0383		1.41	
.49	74	1.35	.0234		1.20	
.68	74	1.35	.0467		1.32	
.84	74	1.35	.0583		1.48	
1.04	74	1.35	.0700		1.51	
1.36	74	1.35	.0816		1.55	
1.73	75	1.35	.0933		1.55	

TEST NO. 3

DATE 21 March 1970

RUN NO. 1

Manometer with Slope 1:5

MANIFOLD DIAMETER 1 in.

ORIFICE SPACING 1/2 in.

t_{H_2O} 19.4 °C

GAGE READING AT SURFACE 1.4 ft.

LINE PRESSURE (psig)	t_{air} (°F)	GAGE READING (ft)	q ($\frac{cfs}{ft}$)	ΔH (ft)	VELOCITY (ips)	REMARKS
.86	75	1.35	.0096		.21	
.99	75	1.35	.0192		1.16	
1.12	75	1.35	.0288		1.44	
1.32	75	1.35	.0384		1.59	
1.11	75	1.35	.0233		1.28	
1.35	75	1.35	.0350		1.51	
1.64	75	1.35	.0466		1.73	
1.97	75	1.35	.0583		1.85	
2.34	75	1.35	.0700		1.91	
2.75	76	1.35	.0816		2.0	
3.19	77	1.35	.0934		2.08	
3.77	81	1.35	.1050		2.08	

TEST NO. 1

DATE 1 April 1970

RUN NO. 1

Manometer with Slope 1:5

q .0653 cfs/ft

MANIFOLD DIAMETER 2 in.

ORIFICE SPACING 1/2 in.

t_{H₂O} 24.8°C

GAGE READING AT SURFACE - ft.

LINE PRESSURE 31.1 psig.

air 74 °F

GAGE READING (ft)	DISTANCE FROM SURFACE (ft)	REV./MIN	VELOCITY (fps)	REMARKS
	.2	118	1.65	
	.2	108	1.51	
	.2	105	1.47	
	.4	67	.97	
	.4	54	.80	
	.4	58	.85	
	.6	48	.72	
	.6	52	.78	
	.6	61	.89	
	.8	46	.70	
	.2	111	1.55	
	.2	127	1.77	
	.2	124	1.73	
	.4	84	1.17	
	.4	58	.85	
	.4	67	.97	
	.6	61	.89	
	.6	51	.76	
	.6	50	.75	
	.6	40	.62	
	.6	42	.65	
	.8	35	.56	
	.8	32	.52	
	.8	49	.74	
	1.0	37	.58	
	1.0	21	.38	
	1.0	31	.51	

TEST NO. 1
 RUN NO. 1 (continued)

DATE

q cfs/ft

MANIFOLD DIAMETER in.

ORIFICE SPACING 1/2 in.

t_{H_2O}

GAGE READING AT SURFACE ft.

LINE PRESSURE psig.

t_{air} °F

GAGE READING (ft)	DISTANCE FROM SURFACE (ft)	REV/MIN	VELOCITY (fps)	REMARKS
	1.2	20	.36	
	1.2	13	.27	
	1.2	22	.39	
	1.2	13	.27	
	1.4	10	.23	
	1.4	6	.18	
	1.4	33	.53	
	1.6	10	.23	
	1.6	17	.33	
	1.6	17	.33	
	1.8	22	.39	
	1.8	32	.52	
	1.8	10	.23	
	1.8	9	.22	
	2.0	14	.29	
	2.0	10	.23	
	2.0	9	.22	
	2.5	10	.23	
	2.5	8	.21	
	2.5	7	.20	
	2.0	13	.27	
	2.0	9	.22	
	2.0	15	.30	
	1.8	19	.35	
	1.8	32	.52	
	1.8	17	.33	
	1.6	6	.18	
	1.6	30	.49	
	1.6	13	.27	

TEST NO. 1 (continued)
RUN NO. 1

DATE

q cfs/ft

MANIFOLD DIAMETER in.

ORIFICE SPACING 1/2 in.

t_{H_2O}

GAGE READING AT SURFACE ft.

LINE PRESSURE psig.

t_{air} °F

GAGE READING (ft)	DISTANCE FROM SURFACE (ft)	REV/MLH	VELOCITY (fps)	REMARKS
	1.4	7	.20	
	1.4	14	.29	
	1.4	13	.27	
	1.2	14	.29	
	1.2	25	.43	
	1.2	14	.29	
	1.0	27	.46	
	1.0	14	.29	
	1.0	29	.48	
	.8	25	.43	
	.8	45	.70	
	.8	34	.55	
	.6	49	.74	
	.6	79	1.12	
	.6	55	.81	
	.4	71	1.02	
	.4	83	1.06	
	.4	100	1.40	
	.2	148	2.06	
	.2	130	1.81	
	.2	113	1.58	

TEST NO. 1

DATE 2 April 1970

RUN NO. 2

Ott Met.

q .198 cfs/ft

MANIFOLD DIAMETER 1 in.

ORIFICE SPACING 1/2 in.

 t_{H_2O} 24°C

GAGE READING AT SURFACE - ft.

LINE PRESSURE 67 psig.

 t_{air} 68 °F

GAGE READING (ft)	DISTANCE FROM SURFACE (ft)	REV/MIN	VELOCITY (fps)	REMARKS
	.2	144	2.0	
	.2	152	2.12	
	.2	171	2.38	
	.4	123	1.72	
	.4	102	1.42	
	.4	144	2.0	
	.6	102	1.42	
	.6	103	1.44	
	.6	82	1.15	
	.8	51	.76	
	.8	43	.66	
	.8	61	.89	
	1.0	45	.69	
	1.0	45	.69	
	1.0	52	.77	
	1.2	38	.60	
	1.2	23	.40	
	1.2	37	.58	
	1.4	9	.22	
	1.4	15	.30	
	1.4	24	.42	
	1.6	14	.29	
	1.6	15	.30	
	1.6	19	.35	
	1.8	18	.34	
	1.8	16	.32	
	1.8	18	.34	

TEST NO. 1
RUN NO. 2

(continued)

DATE

q cfs/ft

MANIFOLD DIAMETER in.

ORIFICE SPACING 1/2 in.

t_{H_2O}

GAGE READING AT SURFACE ft.

LINE PRESSURE psig.

t_{air} °F

GAGE READING (ft)	DISTANCE FROM SURFACE (ft)	REV/ MIN	VELOCITY (fps)	REMARKS
	2.5	11	.25	
	2.5	17	.33	
	2.5	30	.49	

TEST NO. 2

DATE 2 April 1970

RUN NO. 1

Ott Meter

q .198 cfs/ft

MANIFOLD DIAMETER 2 in.

ORIFICE SPACING 1/2 in.

t_{H₂O} 24 °C

GAGE READING AT SURFACE - ft.

LINE PRESSURE 7.35 psig.

t_{air} 76 °F

GAGE READING (ft)	DISTANCE FROM SURFACE (ft)	x (ft)	REV/MIN	VELOCITY (fps)	REMARKS
	.2	1.0	201	2.80	
	.2	1.0	207	2.88	
	.2	1.0	190	2.65	
	.2	2.0	181	2.52	
	.2	2.0	228	3.17	
	.2	2.0	209	2.91	
	.2	3.0	209	2.91	
	.2	3.0	218	3.05	
	.2	3.0	203	2.83	
	.2	4.0	189	2.63	
	.2	4.0	185	2.57	
	.2	4.0	184	2.56	
	.2	5.0	147	2.05	
	.2	5.0	158	2.20	
	.2	5.0	174	2.42	

TEST NO. 2

DATE 2 April 1970

RUN NO. 2

Ott Meter

q .0653 cfs/ft

MANIFOLD DIAMETER 2 in.

ORIFICE SPACING 1/2 in.

t_{H2O} 24.8 °C

GAGE READING AT SURFACE - ft.

LINE PRESSURE 2.92 psig.

t_{air} 76 °F

GAGE READING (ft)	DISTANCE FROM SURFACE (ft)	x (ft)	REV/MIN	VELOCITY (fps)	REMARKS
	.2	5.0	113	1.58	
	.2	5.0	101	1.41	
	.2	5.0	101	1.41	
	.2	4.0	120	1.67	
	.2	4.0	117	1.64	
	.2	4.0	115	1.60	
	.2	3.0	138	1.92	
	.2	3.0	135	1.88	
	.2	3.0	147	2.05	
	.2	2.0	154	2.14	
	.2	2.0	160	2.23	
	.2	2.0	137	1.91	
	.2	1.0	172	2.40	
	.2	1.0	173	2.41	
	.2	1.0	162	2.26	

TEST NO. 3

DATE 5 April 1970

REV NO. 1

Ott Meter

MANIFOLD DIAMETER 2 in.

ORIFICE SPACING 1/2 in.

t₂₀ 21.2°C

GAGE READING AT SURFACE - ft.

LINE PRESSURE (psig)	t _{air} (°F)	GAGE READING (ft)	q (cfs) ft	SLV/SEC	VELOCITY (fps)	REMARKS
8.1	84	.2	.248	187	2.60	
8.1	84	.2	.248	205	2.85	
8.1	84	.2	.248	173	2.41	
8.1	84	.2	.248	192	2.67	
6.95	92	.2	.223	163	2.27	
6.95	92	.2	.223	157	2.33	
6.95	92	.2	.223	158	2.20	
5.8	96	.2	.1985	132	1.82	
5.8	96	.2	.1985	157	2.19	
5.8	96	.2	.1985	166	2.31	
4.55	99	.2	.1735	129	1.80	
4.55	99	.2	.1735	129	1.80	
4.55	99	.2	.1735	139	1.94	
3.8	99	.2	.1489	103	1.42	
3.8	99	.2	.1489	123	1.72	
3.8	99	.2	.1489	111	1.55	
3.25	96	.2	.124	104	1.45	
3.25	96	.2	.124	80	2.13	
3.25	96	.2	.124	95	1.33	
2.68	93	.2	.099	100	1.40	
2.68	93	.2	.099	96	1.34	
2.68	93	.2	.099	98	1.37	
2.40	93	.2	.0744	66	1.20	
2.40	93	.2	.0744	76	1.07	
2.40	93	.2	.0744	80	1.13	
2.2	91	.2	.0496	76	1.07	
2.2	91	.2	.0496	66	.95	
2.2	91	.2	.0496	79	1.11	

TEST NO. 4

DATE 3 April 1970

TEST NO. 1

Orr Meter

q .37 cfs/ft

MANIFOLD DIAMETER 2 in.

GRIFICE SPACING 1/2 in.

t_{H2O} 22°C

GAGE READING AT SURFACE - ft.

LINE PRESSURE 3.65 psig.

t_{air} 66 °F

GAGE READING (ft)	DISTANCE FROM SURFACE (ft)	REV/MIN	VELOCITY (ft/s)	REMARKS
	.2	115	1.60	
	.2	113	1.65	
	.2	115	1.60	
	.4	80	1.13	
	.4	95	1.33	
	.4	109	1.52	
	.6	53	.79	
	.6	80	1.13	
	.6	77	1.10	
	.6	74	1.06	
	.8	61	.89	
	.8	66	.95	
	.8	47	.61	
	1.0	67	.97	
	1.0	40	.62	
	1.0	46	.70	
	1.0	54	.80	
	1.2	44	.67	
	1.2	44	.67	
	1.2	46	.70	
	1.4	34	.54	
	1.4	29	.48	
	1.4	41	.64	
	1.6	23	.40	
	1.6	19	.33	
	1.6	25	.43	
	2.0	12	.26	
	2.0	16	.31	
	2.0	18	.34	

- 140a -

TEST NO. 4 (continued)

DATE

RUN NO. 1

q cfs/ft

MANIFOLD DIAMETER in.

ORIFICE SPACING 1/2 in.

t_{H₂O}

GAGE READING AT SURFACE ft.

LINE PRESSURE psig.

t_{air} °F

GAGE READING (ft)	DISTANCE FROM SURFACE (ft)	REV/MIN	VELOCITY (fps)	REMARKS
	2.5	8	.21	
	2.5	10	.24	
	2.5	17	.33	

TEST No. 4-

DATE 4 April 1970

RUN NO. 2

Ctt Meter

q .198 cfs/ft

MANIFOLD DIAMETER 2 in.

ORIFICE SPACING 1/2 in.

t_{H₂O} 22°C

GAGE READING AT SURFACE - ft.

LINE PRESSURE 6.95 psig.

t_{air} 81 °F

GAGE READING (ft)	DISTANCE FROM SURFACE (ft)	REV/MIN	VELOCITY (fps)	REMARKS
	.20	205	2.85	
	.70	220	3.06	
	.20	218	3.03	
	.40	189	2.63	
	.40	163	2.27	
	.40	179	2.49	
	.60	156	2.17	
	.60	135	1.88	
	.60	156	2.17	
	.80	109	1.52	
	.80	126	1.76	
	.80	129	1.80	
	1.0	86	1.20	
	1.0	96	1.34	
	1.0	96	1.34	
	1.2	75	1.07	
	1.2	76	1.08	
	1.2	78	1.10	
	1.4	69	1.00	
	1.4	52	.78	
	1.4	41	.64	
	1.6	32	.52	
	1.6	43	.66	
	1.6	45	.69	
	2.0	26	.44	
	2.0	21	.38	
	2.0	28	.47	

TEST NO. 4 (continued)

DATE

RUN NO. 2

q cfs/ft

MANIFOLD DIAMETER in.

ORIFICE SPACING 1/2 in.

t_{H₂O}

GAGE READING AT SURFACE ft.

LINE PRESSURE psig.

t_{air} °F

GAGE READING (ft)	DISTANCE FROM SURFACE (ft)	REV/ MIN	VELOCITY (fps)	REMARKS
	2.5	19	.35	
	2.5	22	.39	
	2.5	25	.43	

TEST NO. 5

DATE 5 April 1970

RUN NO. 1

Ott Meter

q .065 cfs/ft

MANIFOLD DIAMETER 2 in.

ORIFICE SPACING 1/2 in.

t_{H_2O} 21.2 °C

GAGE READING AT SURFACE - ft.

LINE PRESSURE 4.2 psig.

t_{air} 78 °F

GAGE READING (ft)	DISTANCE FROM SURFACE (ft)	x (ft)	REV MIN	VELOCITY (fps)	REMARKS
	.2	1.0	128	1.73	
	.2	1.0	112	1.56	
	.2	1.0	107	1.50	
	.2	2.0	164	2.28	
	.2	2.0	151	2.10	
	.2	2.0	168	2.34	
	.2	3.0	160	2.23	
	.2	3.0	145	2.02	
	.2	3.0	155	2.16	
	.2	4.0	162	2.26	
	.2	4.0	158	2.20	
	.2	4.0	165	2.30	
	.2	4.5	104	1.45	
	.2	4.5	103	1.44	
	.2	4.5	110	1.54	

TEST NO. 5

DATE 5 April 1970

RUN NO. 2

Ott Meter

q .1982 cfs/ft

MANIFOLD DIAMETER 2 in.

ORIFICE SPACING 1/2 in.

t_{H_2O} 21.2 °C

GAGE READING AT SURFACE - ft.

LINE PRESSURE 7.25 psig.

t_{air} 83 °F

GAGE READING (ft)	DISTANCE FROM SURFACE (ft)	x (ft)	REV/MIN	VELOCITY (fps)	REMARKS
	.2	1.0	143	1.99	
	.2	1.0	140	1.95	
	.2	1.0	146	2.03	
	.2	2.0	216	3.01	
	.2	2.0	218	3.13	
	.2	2.0	200	2.78	
	.2	3.0	219	3.05	
	.2	3.0	225	3.13	
	.2	3.0	221	3.08	
	.2	4.0	230	3.20	
	.2	4.0	223	3.50	
	.2	4.0	231	3.22	
	.2	5.0	208	2.90	
	.2	5.0	228	3.17	
	.2	5.0	206	2.87	

TEST NO. 6

DATE 4 April 1970

RUN NO. 1

Ott Meter

MANIFOLD DIAMETER 2 in.

ORIFICE SPACING 1/2 in.

 t_{H_2O} 22 °C

GAGE READING AT SURFACE - ft.

LINE PRESSURE (psig)	t_{air} (°F)	GAGE READING (ft)	q ($\frac{cfs}{ft}$)	REV/MIN	VELOCITY (fps)	REMARKS
8.4	95	.2	.248	215	2.99	
8.4	95	.2	.248	227	3.16	
8.4	95	.2	.248	208	2.90	
7.35	98	.2	.223	208	2.90	
7.35	98	.2	.223	200	2.78	
7.35	98	.2	.223	210	2.92	
6.3	99	.2	.1985	204	2.84	
6.3	99	.2	.1985	201	2.60	
6.3	99	.2	.1985	199	2.77	
5.4	98	.2	.1735	177	2.46	
5.4	98	.2	.1735	201	2.80	
5.4	98	.2	.1735	182	2.54	
4.9	96	.2	.1489	178	2.48	
4.9	96	.2	.1489	172	2.39	
4.9	96	.2	.1489	173	2.41	
4.4	95	.2	.124	152	2.12	
4.4	95	.2	.124	166	2.31	
4.4	95	.2	.124	164	2.29	
3.9	92	.2	.099	134	1.87	
3.9	92	.2	.099	146	2.03	
3.9	92	.2	.099	131	1.82	
3.75	91	.2	.0744	138	1.92	
3.75	91	.2	.0744	140	1.95	
3.75	91	.2	.0744	141	1.96	
3.5	88	.2	.0496	109	1.52	
3.5	88	.2	.0496	96	1.34	
3.5	88	.2	.0496	105	1.46	

TEST NO. 7

DATE 18 April 1970

RUN NO. 1

Ott Current Meter

q - cfs/ft

MANIFOLD DIAMETER 2 in.

ORIFICE SPACING 1/2 in.

t_{H_2O} 19.6°C

GAGE READING AT SURFACE 4.10 ft.

LINE PRESSURE - psig.

t_{air} - °F

GAGE READING (ft)	DISTANCE FROM SURFACE (ft)	REV/SEC	VELOCITY (fps)	REMARKS
4.01	.09	2.32	1.95	
4.01	.09	2.26	1.89	
3.61	.49	2.29	1.91	
3.61	.49	2.26	1.89	
2.98	1.12	2.18	1.82	
2.98	1.12	2.19	1.83	
2.64	1.46	2.18	1.82	
2.64	1.46	2.19	1.83	
2.24	1.86	2.13	1.78	
2.24	1.86	2.18	1.82	
2.24	1.86	2.14	1.79	
1.73	2.37	2.16	1.80	
1.73	2.37	2.12	1.77	
1.02	3.08	2.16	1.80	
1.02	3.08	2.16	1.80	
.62	3.48	2.16	1.80	
.62	3.48	2.19	1.83	
.20	3.90	2.16	1.80	
.20	3.90	2.17	1.81	
.03	4.07	2.16	1.80	
.03	4.07	2.14	1.79	
.39	4.49	1.99	1.66	
.39	4.49	2.06	1.72	
.75	4.85	1.98	1.65	

TEST NO. 7
RUN NO. 1

(continued)

DATE

q cfs/ft

MANIFOLD DIAMETER in.

ORIFICE SPACING 1/2 in.

t_{H_2O}

GAGE READING AT SURFACE ft.

LINE PRESSURE psig.

t_{air} °F

GAGE READING (ft)	DISTANCE FROM SURFACE (ft)	REV/SEC	VELOCITY (fps)	REMARKS
.75	4.85	2.06	1.72	
.75	4.85	2.01	1.68	

TEST NO. 7

DATE 18 April 1970

RUN NO. 2

Ott Current Meter

q - cfs/ft

MANIFOLD DIAMETER 2 in.

ORIFICE SPACING 1/2 in.

 t_{H_2O} 19.6°C

GAGE READING AT SURFACE 4.10 ft.

LINE PRESSURE - psig.

 t_{air} - °F

GAGE READING (ft)	DISTANCE FROM SURFACE (ft)	REV/SEC	VELOCITY (fps)	REMARKS
.60	4.70	2.03	1.7	
.60	4.70	2.06	1.72	
.20	4.30	2.05	1.71	
.20	4.30	2.09	1.75	
.10	4.00	2.19	1.83	
.10	4.00	2.14	1.79	
.42	3.68	2.19	1.83	
.42	3.68	2.19	1.83	
.80	3.30	2.13	1.78	
.80	3.30	2.16	1.81	
1.35	2.75	2.08	1.74	
1.35	2.75	2.09	1.75	
1.35	2.75	2.10	1.76	
2.01	2.09	2.14	1.79	
2.01	2.09	2.16	1.81	
2.52	1.58	2.21	1.85	
2.52	1.58	2.16	1.81	
2.80	1.30	2.17	1.82	
2.80	1.30	2.20	1.84	
3.30	.80	2.32	1.94	
3.30	.80	2.26	1.89	
3.70	.40	2.29	1.91	
3.70	.40	2.31	1.93	
3.84	.26	2.31	1.93	

TEST NO. 7
RUN NO. 2

(continued)

DATE

q cfs/ft

MANIFOLD DIAMETER in.

ORIFICE SPACING 1/2 in.

t_{H_2O}

GAGE READING AT SURFACE ft.

LINE PRESSURE psig.

t_{air} °F

GAGE READING (ft)	DISTANCE FROM SURFACE (ft)	REV/SEC	VELOCITY (fps)	REMARKS
3.84	.26	2.33	1.95	
4.00	.10	2.30	1.92	
4.00	.10	2.32	1.94	

TEST NO. :

DATE 18 April 1970

RUN NO. 3

Ott Current Meter

q - cfs/ft

MANIFOLD DIAMETER 2 in.

ORIFICE SPACING in.

 t_{H_2O} 19.6 °C

GAGE READING AT SURFACE 2.43 ft.

LINE PRESSURE - psig.

 t_{air} - °F

GAGE READING (ft)	DISTANCE FROM SURFACE (ft)	DISTANCE OFF CL (ft)	REV/SEC	VELOCITY (fps)	REMARKS
2.35	.08	.52	1.91	1.60	Starting at south side
2.32	.11	.62	1.90	1.59	
2.32	.11	.52	2.00	1.67	
2.32	.11	.52	2.06	1.72	
2.32	.11	.43	2.22	1.86	
2.32	.11	.43	2.14	1.79	
2.32	.11	.45	2.17	1.82	
2.32	.11	.45	2.23	1.87	
2.32	.11	.35	2.33	1.95	
2.32	.11	.35	2.30	1.92	
2.32	.11	.15	2.30	1.92	
2.32	.11	.15	2.34	1.96	
2.32	.11	.05	2.33	1.95	
2.32	.11	.05	2.26	1.89	
2.32	.11	.0	2.32	1.94	
2.32	.11	.0	2.36	1.97	
2.32	.11	.10	2.31	1.93	
2.32	.11	.10	2.26	1.89	
2.32	.11	.20	2.28	1.91	
2.32	.11	.20	2.30	1.92	
2.32	.11	.30	2.23	1.87	
2.32	.11	.30	2.27	1.90	
2.32	.11	.40	2.06	1.72	

TEST NO. 7

DATE

RUN NO. 3 (continued)

q cfs/ft

MANIFOLD DIAMETER in.

ORIFICE SPACING in.

 t_{H_2O} °C

GAGE READING AT SURFACE ft.

LINE PRESSURE psig.

 t_{air} °F

GAGE READING (ft)	DISTANCE FROM SURFACE (ft)	DISTANCE OFF CL (ft)	REV/SEC	VELOCITY (fps)	REMARKS
2.32	.11	.40	2.09	1.75	
2.32	.11	.50	2.00	1.67	
2.32	.11	.50	2.00	1.67	
2.32	.11	.60	1.83	1.53	
2.32	.11	.60	1.87	1.57	

TEST NO. 8

DATE 21 April 1970

RUN NO. 1

Ott Meter

MANIFOLD DIAMETER 2 in.

ORIFICE SPACING 1/2 in.

 t_{H_2O} 19.6°C

GAGE READING AT SURFACE 2.30 ft.

LINE PRESSURE (psig)	t_{air} (°F)	GAGE READING (ft)	q ($\frac{cfs}{ft}$)	REV/SEC	VELOCITY (fps)	REMARKS
3.25	81	2.22	.0436	2.18	1.83	
3.25	81	2.22	.0436	2.10	1.76	
3.63	81	2.22	.0653	2.56	2.15	
3.63	81	2.22	.0653	2.56	2.15	
4.21	81	2.22	.0871	2.83	2.37	
4.21	81	2.22	.0871	2.83	2.37	
4.72	81	2.22	.109	3.06	2.56	
4.72	81	2.22	.109	3.12	2.61	
5.45	81	2.22	.131	3.48	2.91	
5.45	81	2.22	.131	3.34	2.79	
6.25	81	2.22	.152	3.66	3.06	
6.25	81	2.22	.152	3.67	3.07	
7.28	82	2.22	.174	3.82	3.19	
7.28	82	2.22	.174	3.71	3.10	
8.25	83	2.22	.196	3.91	3.27	
8.25	83	2.22	.196	3.93	3.29	
9.43	84	2.22	.218	3.86	3.23	
9.43	84	2.22	.218	3.86	3.23	
10.67	83	2.22	.240	4.03	3.37	
10.67	83	2.22	.240	3.94	3.29	
12.08	83	2.22	.261	4.09	3.42	
12.08	83	2.22	.261	4.15	3.47	
13.45	83	2.22	.283	4.23	3.54	
13.45	83	2.22	.283	4.19	3.50	
15.13	85	2.24	.305	4.40	3.68	
15.13	85	2.24	.305	4.51	3.77	
16.90	87	2.24	.327	4.34	3.63	

TEST NO.8

DATE

RUN NO. 1 (continued)

MANIFOLD DIAMETER in.

ORIFICE SPACING 1/2 in.

 t_{H_2O} °C

GAGE READING AT SURFACE ft.

LINE PRESSURE (psig)	t_{air} (°F)	GAGE READING (ft)	q ($\frac{cfs}{ft}$)	REV/SEC	VELOCITY (fps)	REMARKS
16.90	87	2.24	.327	4.50	3.76	
16.90	87	2.24	.327	4.36	3.64	
18.74	88	2.24	.348	4.43	3.70	
18.74	88	2.24	.348	4.59	3.83	
18.74	88	2.24	.348	4.34	3.63	
20.40	90	2.24	.370	4.57	3.82	
20.40	90	2.24	.370	4.60	3.84	
20.40	90	2.24	.370	4.60	3.84	
22.00	92	2.24	.392	4.74	3.96	
22.00	92	2.24	.392	4.75	3.97	
23.80	91	2.24	.414	4.83	4.03	
23.80	91	2.24	.414	4.98	4.16	
25.20	92	2.24	.436	4.80	4.01	
25.20	92	2.13	.436	4.82	4.03	
23.80	92	2.15	.413	4.47	3.74	
23.80	92	2.15	.413	4.62	3.86	
29.80	93	2.21	.496	4.99	4.17	
29.80	93	2.21	.496	4.60	3.84	

TEST NO. 9

DATE 23 April 1970

RUN NO. 1

Ott Meter

q - cfs/ft

MANIFOLD DIAMETER 2 in.

ORIFICE SPACING 1/2 in.

t_{H_2O} 19.6°C

GAGE READING AT SURFACE 4.26 ft.

LINE PRESSURE - psig.

t_{air} - °F

GAGE READING (ft)	DISTANCE FROM SURFACE (ft)	REV/SEC	VELOCITY (fps)	REMARKS
4.13	.13	2.15	1.80	
4.13	.13	1.96	1.64	
4.03	.23	2.19	1.83	
4.03	.23	2.09	1.75	
3.93	.33	2.12	1.77	
3.93	.33	2.05	1.72	
3.84	.42	2.53	2.11	
3.84	.42	2.18	1.82	
3.70	.56	2.09	1.75	
3.70	.56	2.10	1.76	
3.48	.78	2.26	1.89	
3.48	.78	2.21	1.85	
3.24	1.02	2.39	1.99	
3.24	1.02	2.27	1.90	
3.07	1.19	2.10	1.76	
3.07	1.19	2.53	2.11	
3.07	1.19	2.10	1.76	
2.89	1.37	2.10	1.76	
2.89	1.37	2.03	1.70	
2.71	1.55	2.16	1.80	
2.71	1.55	2.04	1.70	
2.56	1.70	2.31	1.70	
2.56	1.70	2.31	1.70	

ST NO. 9 (continued)
 RUN NO. 1

DATE

1 cfs/ft

MANIFOLD DIAMETER in.

ORIFICE SPACING 1/2 in.

t_{H_2O}

GAGE READING AT SURFACE ft.

LINE PRESSURE psig.

t_{air} °F

GAGE READING (ft)	DISTANCE FROM SURFACE (ft)	REV/SEC	VELOCITY (fps)	REMARKS
2.43	1.83	2.09	1.75	
2.43	1.83	2.06	1.72	
2.26	2.00	2.12	1.78	
2.26	2.00	2.11	1.76	
2.04	2.22	2.08	1.70	
2.04	2.22	2.09	1.75	
1.81	2.45	2.09	1.75	
1.81	2.45	2.08	1.74	
1.60	2.66	1.98	1.66	
1.60	2.66	2.03	1.70	
1.36	2.90	1.92	1.61	
1.36	2.90	1.88	1.50	
1.14	3.12	1.89	1.58	
1.14	3.12	1.95	1.64	
1.00	3.26	1.92	1.61	
1.00	3.26	1.90	1.60	
.85	3.41	1.99	1.66	
.85	3.41	1.97	1.65	
.71	3.55	1.96	1.64	
.71	3.55	1.97	1.65	
.49	3.77	1.99	1.66	
.49	3.77	2.00	1.67	
.25	4.01	1.99	1.66	
.25	4.01	2.03	1.70	
.12	4.14	2.02	1.70	

TEST NO. 9
RUN NO. 1

(continued)

DATE

q cfs/ft

MANIFOLD DIAMETER in.

ORIFICE SPACING 1/2 in.

t_{H_2O}

GAGE READING AT SURFACE ft.

LINE PRESSURE psig.

t_{air} °F

GAGE READING (ft)	DISTANCE FROM SURFACE (ft)	REV/SEC	VELOCITY (fps)	REMARKS
.12	4.14	2.03	1.70	
.04	4.22	1.96	1.64	
.04	4.22	2.01	1.68	
.04	4.22	2.03	1.70	

TEST NO. 9

DATE 24 April 1970

RUN NO. 2

Ott Current Meter

q .218 cfs/ft

MANIFOLD DIAMETER 2 in.

ORIFICE SPACING 1/2 in.

 t_{H_2O} 20°C

GAGE READING AT SURFACE 4.21 ft.

LINE PRESSURE 9.15psig.

 t_{air} 80 °F

GAGE READING (ft)	DISTANCE FROM BOTTOM (ft)	REV/SEC	VELOCITY (fps)	REMARKS
4.13	7.62	0	0	Ott Current Meter No. 18130
4.13	7.62	.735	.66	
4.13	7.62	.756	.68	
4.02	7.51	.69	.63	
4.02	7.51	.66	.59	
3.78	7.27	.467	.46	
3.78	7.27	.482	.46	
3.56	7.05	0	0	
4.11	7.60	1.57	1.31	
4.11	7.60	1.29	1.10	
3.99	7.48	1.265	1.06	
3.99	7.48	1.29	1.09	
3.85	7.33	.835	.75	
3.85	7.33	.73	.66	
3.85	7.33	.905	.80	
3.73	7.22	.332	.36	
3.73	7.22	.386	.40	
3.37	6.86	0	0	
4.05	7.54	2.08	1.74	
4.05	7.54	1.89	1.59	
3.17	7.63	1.56	1.56	New surface Rdg. 3.24 Now using Gurley Meter Ser. No. 660526
3.17	7.63	1.37	1.37	
3.05	7.51	.985	.985	Would be in air bubbles if moved farther.
3.05	7.51	1.03	1.03	
2.59	7.05	0	0	

TEST NO. 9

DATE

RUN NO. 3

Gurley Meter

q .436 cfs/ft

MANIFOLD DIAMETER 2 in.

ORIFICE SPACING 1/2 in.

 t_{H_2O} 22°C

GAGE READING AT SURFACE 3.26 ft.

LINE PRESSURE psig.

 t_{air} 90 °F

GAGE READING (ft)	DISTANCE FROM BOTTOM (ft)	REV/SEC	VELOCITY (fps)	REMARKS
3.21	7.65	1.6	1.6	
3.21	7.65	1.57	1.57	
3.08	7.52	1.47	1.47	
3.08	7.52	1.43	1.43	
2.44	6.88	.8	.8	
2.44	6.88	.87	.87	
2.34	6.78	-	-	
3.22	7.66	1.88	1.88	
3.22	7.66	1.78	1.78	
2.91	7.35	1.42	1.42	
2.91	7.35	1.33	1.33	
2.67	7.11	1.1	1.1	
2.67	7.11	.97	.97	
2.67	7.11	1.02	1.02	
2.44	6.88	.85	.85	
2.44	6.88	.83	.83	
2.04	6.48	.62	.62	
2.04	6.48	.53	.53	
2.04	6.48	.57	.57	
1.94	6.38	-	-	
3.12	7.56	1.9	1.9	
3.12	7.56	1.83	1.83	
2.88	7.32	1.35	1.35	
2.88	7.32	1.27	1.27	

TEST NO. 9 (continued)
 RUN NO. 3

DATE

q cfs/ft

MANIFOLD DIAMETER in.

ORIFICE SPACING 1/2 in.

t_{H_2O}

GAGE READING AT SURFACE ft.

LINE PRESSURE psig.

t_{air} °F

GAGE READING (ft)	DISTANCE FROM BOTTOM (ft)	REV/SEC	VELOCITY (fps)	REMARKS
2.88	7.32	1.37	1.37	
2.57	7.01	.80	.80	
2.57	7.01	.87	.87	
2.32	6.76	.60	.60	
2.32	6.76	.67	.67	
2.12	6.56	.53	.53	
2.12	6.56	.53	.53	
2.00	6.44	-	-	
3.11	7.55	2.07	2.07	
3.11	7.55	2.16	2.16	
3.11	7.55	2.10	2.10	
2.89	7.33	1.33	1.33	
2.89	7.33	1.23	1.23	
2.89	7.33	1.37	1.37	
2.63	7.07	.93	.93	
2.63	7.07	.83	.83	
2.63	7.07	.87	.87	
2.34	6.78	.75	.75	
2.34	6.78	.73	.73	
2.12	6.56	.70	.70	
2.12	6.56	.71	.71	
1.88	6.32	-	-	
3.08	7.52	2.25	2.25	
3.08	7.52	2.14	2.14	
3.08	7.52	2.20	2.20	

TEST NO. 9 (continued)
RUN NO. 3

DATE

q cfs/ft

MANIFOLD DIAMETER in.

ORIFICE SPACING 1/2 in.

t_{H_2O}

GAGE READING AT SURFACE ft.

LINE PRESSURE psig.

t_{air} °F

GAGE READING (ft)	DISTANCE FROM BOTTOM (ft)	REV/SEC	VELOCITY (fps)	REMARKS
2.86	7.30	1.50	1.50	
2.86	7.30	1.50	1.50	
2.58	7.04	1.00	1.00	
2.58	7.04	.97	.97	
2.22	6.66	.78	.78	
2.22	6.66	.73	.73	
2.22	6.66	.80	.80	
2.00	6.44	-	-	

TEST NO. 9

DATE 27 April 1970

RUN NO. 4

q .218 cfs/ft

MANIFOLD DIAMETER 2 in.

ORIFICE SPACING 1/2 in.

t_{H_2O} 22°C

GAGE READING AT SURFACE 3.34 ft.

LINE PRESSURE 9.25 psig.

t_{air} 81 °F

GAGE READING (ft)	DISTANCE FROM SURFACE (ft)	REV/SEC	VELOCITY (fps)	REMARKS
3.18	.16	2.73	2.73	
3.18	.16	2.8	2.80	
2.89	.45	2.08	2.08	
2.89	.45	2.06	2.06	
2.47	.87	.95	.95	
2.47	.87	.93	.93	
2.17	1.17	0	0	

TEST NO. 9

DATE 23 Feb. 1970

RUN NO. 5

Ott Meter

q .436 cfs/ft

MANIFOLD DIAMETER 2 in.

ORIFICE SPACING 1/2 in.

t_{H₂O} 20°C

GAGE READING AT SURFACE 3.34 ft.

LINE PRESSURE 25.25 psig.

t_{air} 93 °F

GAGE READING (ft)	DISTANCE FROM SURFACE (ft)	REV/SEC	VELOCITY (fps)	REMARKS
3.26	.08	3.78	3.78	
3.26	.08	3.67	3.67	
2.62	.72	1.77	1.77	
2.62	.72	1.80	1.80	
2.39	.95	1.15	1.15	
2.39	.95	1.10	1.10	
3.02	.42	2.81	2.81	
3.02	.42	2.93	2.93	
2.07	1.27	0	0	

APPENDIX IV

Table of Tests Performed

Flume Width	Test No.	Run No.	Test Type	Water Depth T	Orifice Size d	Manif. Depth H	SG Oil	Remarks
2.0'	5	1	Stag	2.0'	1/16"	23 1/4"	0.89	Determine of h at failure
"	"	2	"	"	"	"	"	" " "
"	"	3	"	"	"	"	"	" " "
"	"	4	"	"	"	"	"	" " "
"	"	5	"	"	"	"	"	" " "
2.0'	6	1	Stag	2.0'	1/16"	12"	0.85	Determine h at failure
"	"	2	"	"	"	"	"	" " "
"	"	3	"	"	"	"	"	" " "
"	"	4	"	"	"	"	"	" " "
"	"	5	"	"	"	"	"	" " "
2.0'	8	1	Stag	2.0'	1/16"	12"	0.89	Determine h at failure
"	"	2	"	"	"	"	"	" " "
"	"	3	"	"	"	"	"	" " "
"	"	4	"	"	"	"	"	" " "
2.0'	9	1	Waves	2.0'	1/16"	12"	0.89	Non-critical case
"	"	2	"	"	"	"	"	" " "
2.0'	13	1	Waves	2.0'	1/16"	12"	0.89	Waves from crit. dir.
"	"	2	"	"	"	"	"	" " "
"	"	3	"	"	"	"	"	" " "
"	"	4	"	"	"	"	"	" " "
"	"	5	"	"	"	"	"	" " "
18-inch	10	1	Stag	7.7'	1/16"	7.5'	0.85	Determine h at failure
"	"	2	"	"	"	"	"	" " "
"	"	3	"	"	"	"	"	" " "
18-inch	11	1	Current	7.7'	1/16"	7.5'	0.85	Check linear superposition
"	"	2	"	"	"	"	"	" " "

TEST NO. 5

DATE March 14, 1970

RUN NO. 1

MANIFOLD DIAMETER 1 in.

ORIFICE SPACING 1/2 in.

t_{H_2O} 19.6 °C

GAGE READING AT SURFACE ft.

U_{max} (fps)	h (ft)	$\sqrt{gh (1 - SG_o)}$	α	REMARKS
1.23	.1	.594	2.07	
1.23	.142	.709	1.73	
1.23	.208	.856	1.43	
1.23	.3	1.03	1.2	
1.23	.35	1.11	1.11	
1.23	.466	1.28	.96	
1.23	.525	1.36	.9	

TEST NO. 5

DATE March 15, 1970

RUN NO. 2

MANIFOLD DIAMETER 1 in.

ORIFICE SPACING 1/2 in.

t_{H_2O} 19.6 °C

GAGE READING AT SURFACE ft.

U_{max} (fps)	h (ft)	$\sqrt{gh} (1 - SG_o)$	α	REMARKS
.96	.102	.589	1.63	
.96	.125	.651	1.47	
.96	.157	.725	1.32	
.96	.176	.772	1.24	
.96	.205	.834	1.15	
.96	.231	.885	1.08	
.96	.262	.94	1.02	

TEST NO. 5

DATE March 17, 1970

RUN NO. 3

MANIFOLD DIAMETER 1 in.

ORIFICE SPACING 1/2 in.

t_{H_2O} 19.6 °C

GAGE READING AT SURFACE ft.

U_{max} (fps)	h (ft)	$\sqrt{gh (1 - SG_o)}$	α	REMARKS
1.55	.194	.81	1.92	
1.55	.236	.894	1.74	
1.55	.314	1.03	1.51	
1.55	.386	1.146	1.35	
1.55	.391	1.152	1.34	Near failure thru
1.55	.498	1.3	1.19	" " "
1.55	.557	1.4	1.1	Loss over

TEST NO. 5

DATE March 17.1970

RUN NO. 4

MANIFOLD DIAMETER 1 in.

ORIFICE SPACING 1/2 in.

t_{H_2O} 19.6 °C

GAGE READING AT SURFACE ft.

U_{max} (fps)	h (ft)	$\sqrt{gh (1 - SG_o)}$	α	REMARKS
1.99	.292	.99	2.0	
1.99	.353	1.09	1.83	
1.99	.421	1.19	1.67	Some thru losses
1.99	.746	1.37	1.45	Large thru losses
1.99	.782	1.44	1.38	" " "

TEST NO. 5
RUN NO. 5

DATE March 19, 1970

MANIFOLD DIAMETER 1 in.

ORIFICE SPACING 1/2 in.

t_{H_2O} 19.6 °C

GAGE READING AT SURFACE ft.

U_{max} (fps)	h (ft)	$\sqrt{gh (1 - SG_o)}$	α	REMARKS
1.41	.037	.36	3.92	
1.41	.079	.52	2.71	
1.41	.148	.71	1.98	
1.41	.21	.85	1.66	
1.41	.258	.94	1.5	
1.41	.397	1.16	1.22	
1.41	.419	1.19	1.18	
1.41	.485	1.28	1.1	
1.41	.609	1.44	.98	

TEST NO. 6

DATE March 20, 1970

RUN NO. 1

MANIFOLD DIAMETER 1 in.

ORIFICE SPACING 1/2 in.

t_{H2O} 19.6 °C

GAGE READING AT SURFACE ft.

U_{\max} (fps)	h (ft)	$\sqrt{gh (1 - SG_o)}$	α	REMARKS
1.18	.087	.637	1.85	
1.18	.111	.72	1.64	
1.18	.132	.79	1.5	
1.18	.166	.88	1.34	
1.18	.202	.97	1.22	
1.18	.24	1.06	1.12	
1.18	.286	1.16	1.02	
1.18	.341	1.26	.94	Large failure thru
1.18	.374	1.32	.9	" " "

TEST NO. 6

DATE March 21, 1970

RUN NO. 2

MANIFOLD DIAMETER 1 in.

ORIFICE SPACING 1/2 in.

t_{H_2O} 19.6 °C

GAGE READING AT SURFACE ft.

U_{max} (fps)	h (ft)	$\sqrt{gh} (1 - SG_o)$	α	REMARKS
1.07	.03	.38	2.8	
1.07	.066	.56	1.92	
1.07	.091	.66	1.62	
1.07	.11	.72	1.48	
1.07	.138	.81	1.32	
1.07	.172	.9	1.19	
1.07	.204	.98	1.09	
1.07	.249	1.07	1.0	
1.07	.263	1.11	.96	
1.07	.277	1.14	.94	
1.07	.273	1.13	.95	
1.07	.279	1.14	.94	
1.07	.289	1.16	.92	

TEST NO. 6

DATE March 21, 1970

RUN NO. 3

MANIFOLD DIAMETER 1 in.

ORIFICE SPACING 1/2 in.

t_{H_2O} 19.6 °C

GAGE READING AT SURFACE ft.

U_{max} (fps)	h (ft)	$\sqrt{gh} (1 - SG_0)$	α	REMARKS
.75	.021	.3067		
.75	.037	.4147		
.75	.047	.4687		
.75	.066	.5551		
.75	.087	.6372		
.75	.126	.7668		
.75	.162	.8705		
.75	.214	1.0		

TEST NO. 6

DATE March 24, 1970

RUN NO. 4

MANIFOLD DIAMETER 1 in.

ORIFICE SPACING 1/2 in.

WATER 19.6 °C

GAGE READING AT SURFACE 1 ft.

U_{max} (fps)	h (ft)	$\sqrt{gh} (1 - SG_s)$	α	REMARKS
1.44	.074	.5875		
1.44	.106	.702		
1.44	.14	.81		
1.44	.194	.9526		
1.44	.215	1.0022		
1.44	.247	1.0735		
1.44	.294	1.1707		
1.44	.338	1.2571		
1.44	.377	1.3262		
1.44	.403	1.3716		

TEST NO. 6

DATE March 24, 1970

RUN NO. 5

MANIFOLD DIAMETER 1 in.

ORIFICE SPACING 1/2 in.

t_{H_2O} 19.6 °C

GAGE READING AT SURFACE ft.

u_{max} (fps)	h (ft.)	$\sqrt{gh} (1 - SG_c)$	α	REMARKS
1.35	.078	.6084		
1.35	.143	.8165		
1.35	.167	.8834		
1.35	.221	1.0174		
1.35	.255	1.0908		
1.35	.297	1.1772		
1.35	.34	1.2593		
1.35	.358	1.2917		

TEST NO. 3

DATE 2 April 1970

RUN NO. 1

MANIFOLD DIAMETER 1 in.

ORIFICE SPACING 1/2 in.

t_{H2O} 19.4 °C

GAGE READING AT SURFACE ft.

U _{max} (ips)	h (ft)	$\sqrt{gh} (1 - SG_o)$	α	REMARKS
1.43	.115	.652		
1.43	.156	.76		
1.43	.211	.885		
1.43	.294	1.05		
1.43	.364	1.16		
1.43	.364	1.16		
1.43	.416	1.24		

TEST NO. 8

DATE 2 April 1970

RUN NO. 2

MANIFOLD DIAMETER 1 in.

ORIFICE SPACING 1/2 in.

WATER 19.4 °C

GAGE READING AT SURFACE ft.

U_{max} (fps)	h (ft)	$\sqrt{gh (1 - S_{G0})}$	a	REMARKS
.94	.080	.545		
.94	.139	.713		
.94	.171	.796		
.94	.224	.916		
.94	.265	.990		

TEST NO. 8

DATE 2 April 1970

RUN NO. 3

MANIFOLD DIAMETER 1 in.

ORIFICE SPACING 1/2 in.

t_{H_2O} 19.4 °C

GAGE READING AT SURFACE ft.

U_{max} (fps)	h (ft)	$\sqrt{gh (1 - SG_o)}$	α	REMARKS
1.26	.098	.602		
1.26	.175	.805		
1.26	.199	.857		
1.26	.231	.925		
1.26	.283	1.025		
1.26	.332	1.11		

TEST NO. 8

DATE 2 April 1970

RUN NO. 4

MANIFOLD DIAMETER 1 in.

ORIFICE SPACING 1/2 in.

H₂O 19.4 °C

GAGE READING AT SURFACE ft.

U_{max} (fps)	h (ft)	$\sqrt{gh} (1 - SG_o)$	α	REMARKS
.75	.076	.528		
.75	.105	.619		
.75	.161	.766		
.75	.174	.80		
.75	.207	.87		

TEST NO. 9

DATE 7 April 1970

RUN NO. 1

MANIFOLD DIAMETER 1 in.

ORIFICE SPACING 1/2 in.

t_{H_2O} 19.4 °C

GAGE READING AT SURFACE ft.

U_{max} (fps)	h (ft)	$\sqrt{gh} (1 - SC_D)$	α	REMARKS
1.43	.17	.79	1.81	
1.43	.21	.877	1.63	
1.43	.28	1.015	1.40	
1.43	.35	1.130	1.26	

TEST NO.9

DATE 4 April 1970

RUN NO. 2

MANIFOLD DIAMETER 1 in.

ORIFICE SPACING 1/2 in.

t_{H_2O} 19.4 °C

GAGE READING AT SURFACE ft.

U_{max} (fps)	h (ft)	$\sqrt{gh(1 - SG_o)}$	α	REMARKS
1.15	.047	.405	2.84	
1.15	.092	.568	2.02	
1.15	.146	.713	1.51	
1.15	.192	.820	1.40	
1.15	.273	.976	1.17	
1.15	.331	1.075	1.11	
1.15	.440	1.281	.90	

TEST NO. 13

DATE 2 May 1970

RUN NO. 1

MANIFOLD DIAMETER 1 in.

ORIFICE SPACING 1/2 in.

t_{H_2O} 19.6°C

GAGE READING AT SURFACE ft.

U_{max} (fps)	h (ft)	$\sqrt{gh} (1 - SG_o)$	α	REMARKS
1.03	.083	.546	1.89	
1.03	.129	.681	1.49	
1.03	.164	.770	1.34	
1.03	.193	.833	1.24	
1.03	.310	1.055	.98	
1.03	.425	1.250	.82	

TEST NO. 13

DATE 2 May 1970

RUN NO. 2

MANIFOLD DIAMETER 1 in.

ORIFICE SPACING 1/2 in.

ρ_{H_2O} 19.6 °C

GAGE READING AT SURFACE ft.

U_{max} (fps)	h (ft)	$\sqrt{gh(1 - SG_o)}$	α	REMARKS
.83	.080	.537	1.55	
.83	.169	.780	1.07	
.83	.245	.940	.88	
.83	.310	1.058	.79	

TEST NO. 13

DATE 2 May 1970

RUN NO. 3

MANIFOLD DIAMETER 1 in.

ORIFICE SPACING 1/2 in.

t_{H_2O} 19.6 °C

GAGE READING AT SURFACE ft.

U_{max} (fps)	h (ft)	$\sqrt{gh} (1 - SG_G)$	α	REMARKS
.67	.128	.679	.99	
.67	.176	.795	.84	
.67	.203	.855	.78	

TEST NO. 13

DATE 5 May 1970

RUN NO. 4

MANIFOLD DIAMETER 1 in.

ORIFICE SPACING 1/2 in.

T_{H_2O} 19.6 °C

GAGE READING AT SURFACE ft.

u_{max} (fps)	h (ft)	$\sqrt{gh} (1 - SG_o)$	α	REMARKS
1.26	.236	.925		
1.26	.333	1.10		
1.26	.362	1.17		
1.26	.393	1.19		
1.26	.437	1.26	1.00	

TEST NO. 13

DATE 5 May 1979

RUN NO. 5

MANIFOLD DIAMETER 1 in.

ORIFICE SPACING 1/2 in.

t_{p20} 19.6 °C

GAGE READING AT SURFACE ft.

U_{max} (fps)	h (ft)	$\sqrt{gh} (1 - SG_o)$	α	REMARKS
1.35	.313	1.06	1.30	
1.38	.346	1.12	1.23	
1.38	.392	1.19	1.16	
1.38	.478	1.31	1.05	

TEST NO. 10

DATE 14 May 1970

RUN NO. 1

HANFOLD DIAPHRAGM 2 in.

ORIFICE SPACING 1/2 in.

th₂O 19.6 °C

GAGE READING AT SURFACE ft.

U_{max} (fps)	h (ft)	$\sqrt{gh(1 - \phi_c)}$	u	REMARKS
2.0	.438	1.46	1.3	
2.0	.587	1.68	1.19	
2.0	.708	1.85	1.08	

TEST NO. 10

DATE 14 May 1970

RUN NO. 2

MANIFOLD DIAMETER 2 in.

ORIFICE SPACING 1/2 in.

t_{H_2O} 19.6 °C

GAGE READING AT SURFACE ft.

U_{max} (fps)	h (ft)	$\sqrt{gh} (1 - SG_o)$	α	REMARKS
3.0	.632	1.746	1.72	
3.0	.917	2.105	1.42	
3.0	1.111	2.32	1.29	

TEST NO.10

DATE 14 May 1970

RUN NO. 3

MANIFOLD DIAMETER 2 in.

ORIFICE SPACING 1/2 in.

t_{H_2O} 19.6 °C

GAGE READING AT SURFACE ft.

U_{max} (fps)	h (ft)	$\sqrt{gh} (1 - SG_o)$	α	REMARKS
2.58	.43	1.44	1.79	
2.58	.59	1.69	1.53	
2.58	.87	2.05	1.26	
2.58	.98	2.18	1.18	

TEST NO. 11

DATE 17 May 1970

RUN NO. 1

MANIFOLD DIAMETER 2 in.

ORIFICE SPACING 1/2 in.

t_{H_2O} 19.6 °C

GAGE READING AT SURFACE ft.

U_{max} (fps)	h (ft)	$\sqrt{gh(1 - SG_L)}$	α	REMARKS
.62	.06	.487		Leakage below

TEST NO. 11

DATE May 18, 1970

RUN NO. 2

MANIFOLD DIAMETER 2 in.

ORIFICE SPACING 1/2 in.

t_{H2O} °C

GAGE READING AT SURFACE ft.

U_{max} (fps)	h (ft)	$\sqrt{gh (1 - SG_o)}$	α	REMARKS
2.32	.076	.600		
2.17	.08	.616		
1.87	.07	.575		
1.42	.07	.575		
.97	.05	.487		
.82	.065	.555	1.48	
2.32	.125	.770		
2.17	.127	.776		
1.87	.123	.763		
1.42	.150	.842		
.97	.167	.889	1.1	
2.32	.173	.904		
2.17	.163	.879		
1.87	.15	.842		
1.42	.17	.897		
1.27	.26	1.104	1.15	

DATA CALCULATIONS APPENDIX

Run #	d_o (ft)	L (ft)	$d_o/L \times 10^3$	F°	Specific Gravity	Wind Speed U (fps)	$\sqrt{Lg(1-\rho_o/\rho_w)}$	$\sqrt{Lg(1-\rho_o/\rho_w)}$	U
1-1-1	0.223	29.42	7.55	64.6	.8906	29.44	10.17	10.17	2.89
1-1-2	0.216	35.17	6.12	66.5	.8913	26.84	11.14	11.14	2.41
1-1-3	0.201	40.33	4.98	66.9	.8915	23.81	11.92	11.92	2.00
1-1-4	0.190	45.92	4.16	68.0	.8919	21.47	12.71	12.71	1.09
1-1-5	0.176	48.25	3.65	68.0	.8919	18.16	13.06	13.06	1.39
1-1-6	0.159	56.83	2.80	67.3	.8916	15.56	14.12	14.12	1.10
1-1-7	0.149	61.77	2.41	66.4	.8913	13.20	13.20	13.20	.895
1-1-8	0.330	20.50	16.20	65.8	.8911	36.70	8.51	8.51	4.31
1-1-9	0.293	22.92	12.80	64.6	.8906	34.64	8.96	8.96	3.87
1-1-10	0.271	25.75	10.56	64.8	.8907	32.37	9.53	9.53	3.40

Run #	d_o (ft)	L (ft)	$d_o/L \times 10^3$	F°	Specific Gravity	Wind Speed U (fps)	$\sqrt{Lg(1-\rho_o/\rho_w)}$	$U \sqrt{Lg(1-\rho_o/\rho_w)}$
1-2-1	0.267	47.33	5.64	63.7	.8883	31.22	12.96	2.41
1-2-2	0.256	49.20	5.21	65.9	.8892	27.86	13.22	2.11
1-2-3	0.234	57.60	4.06	66.2	.8893	24.79	14.39	1.72
1-2-4a	0.219	63.69	3.43	66.5	.8894	20.81	15.04	1.38
1-2-4b	0.220	63.50	3.47	64.4	.8886	21.24	15.01	1.42
1-2-5	0.289	40.17	7.20	65.8	.8891	33.12	11.97	2.77
1-2-6	0.321	35.25	9.11	66.5	.8894	34.31	11.21	3.06
1-2-7	0.342	33.00	10.34	66.6	.8894	36.10	10.72	3.37

Run #	d _o (ft)	L(ft)	d _o /L x103	F°	Specific Gravity	Wind Speed U (fps)	$\sqrt{\text{Lg}(1-\rho_0/\rho_w)}$	$\sqrt{\text{Lg}(1-\rho_0/\rho_w)}$
1-3-1	0.270	66.17	4.07	65.1	.8908	26.03	15.26	1.71
1-3-2	0.274	64.58	4.24	65.5	.8910	27.01	15.05	1.80
1-3-3	0.283	62.25	4.55	66.5	.8914	28.48	14.81	1.92
1-3-4	0.284	60.17	4.73	66.9	.8915	30.25	14.58	2.08
1-3-5	0.296	58.92	5.00	66.9	.8915	31.95	14.35	2.23
1-3-6	0.307	56.42	5.45	66.5	.8914	33.58	14.08	2.39
1-3-7	0.312	49.92	6.25	66.5	.8914	35.04	13.04	2.69
1-3-8	0.334	49.33	6.78	67.0	.8915	36.75	13.19	2.79
1-3-9	0.405	35.67	11.32	66.9	.8815	37.76	11.20	3.37
1-3-10	0.485	30.50	15.90	66.7	.8914	39.09	10.37	3.77

Run #	d ₀ (ft)	L(ft)	d ₀ /L x10 ³	γ°	Specific Gravity	Wind Speed U (fps)	$\frac{Lg(1-\rho_0/\rho_w)}{\rho_w}$	$\frac{U}{Lg(1-\rho_0/\rho_w)}$
2-1-1	0.068	60.03	1.13	64.1	.8395	8.16	16.65	0.490
2-1-2	0.069	59.54	1.15	64.1	.8395	8.86	16.59	0.534
2-1-3	0.072	56.63	1.27	64.1	.8395	9.34	16.16	0.578
2-1-4	0.078	53.96	1.44	64.1	.8395	9.88	15.78	0.626
2-1-5	0.080	51.29	1.40	63.7	.8394	9.99	16.27	0.614
2-1-6	0.074	51.67	1.43	64.4	.8397	11.61	15.45	0.732
2-1-7	0.080	47.25	1.69	64.4	.8397	10.40	14.77	0.704
2-1-8	0.097	45.17	2.14	64.7	.8508	12.08	14.45	0.834
2-1-9	0.103	33.17	3.10	65.1	.8599	13.07	12.38	1.120
2-1-10	0.115	32.08	3.58	65.5	.8601	15.57	12.17	1.279

Run #	d_q (ft)	L (ft)	d_0/L x10 ³	V^*	Specific Gravity	Wind Speed U (fps)	$\frac{U}{\sqrt{g(L-d_0/96)}}$	$\frac{U}{\sqrt{g(L-d_0/96)}}$
2-2-1	0.169	60.67	2.45	66.2	.8603	16.06	16.74	9.958
2-2-2	0.166	56.23	2.91	65.8	.8602	17.29	16.11	1.073
2-2-3	0.181	54.83	3.30	65.8	.8602	18.05	15.81	1.142
2-2-4	0.186	49.58	3.71	65.5	.8601	19.03	15.16	1.257
2-2-5	0.206	47.00	4.36	65.5	.8601	20.31	14.74	1.391
2-2-6	0.208	43.83	4.56	65.7	.8601	20.60	14.56	1.417
2-2-7	0.215	43.00	5.00	65.8	.8602	23.45	14.29	1.664
2-2-8	0.223	41.50	5.37	65.0	.8602	23.68	13.85	1.710
2-2-9	0.238	38.50	6.18	66.0	.8603	26.32	13.34	1.972

Run #	ϕ_0 (ft)	L (ft)	$d_0/L \times 10^3$	θ°	Specific Gravity	Wind Speed U (fps)	$\sqrt{Lg(1-\rho_0/\rho_w)}$	$\frac{U}{\sqrt{Lg(1-\rho_0/\rho_w)}}$
2-3-1	0.320	61.67	3.37	65.5	.8596	21.39	16.88	1.267
2-3-2	0.237	58.17	4.00	65.5	.8596	22.23	16.41	1.355
2-3-3	0.256	56.50	4.55	64.9	.8594	23.60	16.15	1.461
2-3-4	0.275	54.50	5.04	64.9	.8586	23.22	15.86	1.464
2-3-5	0.277	52.75	5.25	64.7	.8583	23.35	15.60	1.625
2-3-6	0.275	52.50	5.24	64.7	.8581	25.55	15.59	1.639
2-3-7	0.283	51.67	5.48	64.7	.8583	26.40	15.45	1.709
2-3-8	0.306	49.25	6.21	64.7	.9593	25.40	15.08	1.690
2-3-9	0.313	48.17	6.50	64.7	.8583	27.78	14.92	1.862

Pit #	d_o (ft)	L (ft)	$d_o/L \times 10^3$	P^*	Specific Gravity	Wind Speed V (ft/min)	$\sqrt{g(L-d_o/\rho_w)}$	$\frac{V}{\sqrt{g(L-d_o/\rho_w)}}$
3-1-1	0.114	51.50	2.21	70.9	.9090	10.82	12.38	.874
3-1-2	0.129	46.10	2.80	74.5	.9075	12.07	11.72	1.030
3-1-3	0.132	39.17	3.37	74.8	.9075	13.82	10.80	1.280
3-1-4	0.155	30.50	5.08	74.8	.9075	17.30	9.58	1.806
3-1-5	0.165	28.17	5.86	75.2	.9075	18.55	9.16	2.025
3-1-6	0.182	25.27	7.23	74.8	.9075	20.44	8.65	2.360
3-1-7	0.205	21.83	9.39	74.8	.9075	22.91	8.06	2.842
3-1-8	0.333	19.25	12.10	74.5	.9075	26.02	7.57	3.437
3-1-9	0.269	17.50	15.37	74.5	.9075	26.76	7.22	3.706

Run #	$d_o(\text{ft})$	$L(\text{ft})$	$d_o/L \times 10^3$	F°	Specific Gravity	Wind Speed U (ips)	$\sqrt{\frac{Lg(1-p_0/\rho_w)}{U}}$	$\sqrt{\frac{Lg(1-p_0/\rho_w)}{U}}$
3-2-1	0.187	55.25	3.38	73.6	.9063	17.50	12.90	1.356
3-2-2	0.192	52.17	3.68	73.6	.9065	18.49	12.54	1.474
3-2-3	0.204	50.75	4.02	73.6	.9063	19.11	12.36	1.546
3-2-4	0.214	46.58	4.59	73.6	.9063	20.40	11.63	1.721
3-2-5	0.219	42.67	5.13	76.3	.9060	22.54	11.34	1.988
3-2-6	0.228	49.50	4.61	75.9	.9060	23.92	12.20	1.961
3-2-7	0.239	38.50	6.21	75.9	.9060	25.23	10.76	2.343
3-2-8	0.266	37.83	7.03	75.4	.9063	23.78	10.66	2.418
3-2-9	0.299	30.75	9.72	75.6	.9063	27.63	9.62	2.872
3-2-10	0.347	23.42	12.21	73.6	.9063	29.10	9.23	3.166

Run #	d_o (ft)	L (ft)	$d_o/L \times 10^3$	F°	Specific Gravity	Wind Speed U (fps)	$\sqrt{Lg(1-\rho_o/\rho_w)}$	$\frac{U}{\sqrt{Lg(1-\rho_o/\rho_w)}}$
3-3-1	0.239	64.08	3.73	75.2	.9065	21.58	13.66	1.557
3-3-2	0.245	60.50	4.05	76.5	.9065	22.85	13.47	1.696
3-3-3	0.246	63.58	3.87	74.8	.9070	22.66	13.81	1.641
3-3-4	0.253	60.33	4.19	76.6	.9065	23.72	13.45	1.764
3-3-5	0.264	57.24	4.61	76.6	.9065	23.95	13.10	1.828
3-3-6	0.279	54.67	5.10	74.8	.9070	25.64	12.81	2.002
3-3-7	0.301	50.50	5.96	76.3	.9067	26.67	12.31	2.166
3-3-8	0.327	45.92	7.12	76.4	.9065	27.82	11.74	2.370
3-3-9	0.344	44.25	7.77	76.4	.9065	28.44	11.52	2.469
3-3-10	0.378	39.00	9.69	76.6	.9065	29.49	10.81	2.728

APPENDIX

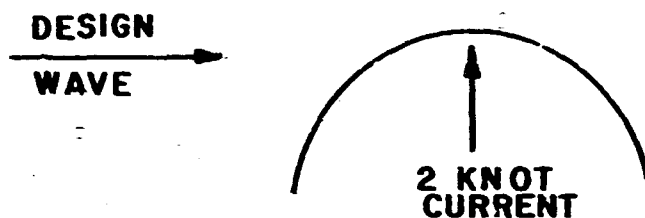
V. Miscellaneous

General comment

A number of questions were raised during the study regarding the gravity wave phenomenon and ocean environment. The questions raised and answers given are summarized on the following pages.

1. Questions

I. Is it possible to have the following situation?



II. If this can happen, could our barrier (on the surface) feel the full 2 knot current? If not, what what height cross wave would make the effects of the current negligible?

III. A.) If the situation in I. can happen, what % of time or under what conditions could it be expected?

B.) Is it true that most ocean currents (except Gulf stream, etc.) are wind driven?

IV. What are the forces on a submerged right circular 5 inch pipe due to water currents of 3 knots? 3 inch? 7 inch?

V. What vertical and horizontal water velocities will be found at depths from 16 to 32 feet due to waves of 20 to 30 feet in height?

VI. What are the approximate velocity profiles beneath large waves?

C.) What will be the effect on the curtain if the pipe is setting on the bottom?

2. Answers

I. Is it possible to have the following situation?



- A. Type of Current - Major ocean current such as Florida current (1.7-3.5 knots). Cromwell current (2.4 knots) and Gulf stream (>2.0 knots).

Definition of Major Ocean Currents - Currents classified as a part of the oceanic circulation.

Driving Force or Agent - Wind

- 1) Munk, W. H. and G. F. Carrier, The Wind -

Driven Circulation in Ocean Basins of Various Shapes, Themis, 2:158-167.

- 2) Munk, W. H., On the Wind Driven Ocean, Circulation. Jour. Meteor, 7:79-93.

Description - The currents are well defined major ocean currents which are a part of the oceanic circulation. It is possible to have a design wave approach these currents from any angle. The direction of approach depends on the location of the storm system which generated the design waves.

- B. Type of Current - Current caused by wind - drift (relative short duration).

Definition of Wind Drift Current -- Currents

resulting from winds blowing over a rather limited area for a limited time. (Although the area may be of the order of many square miles and the duration may be of the order of a day or so.)

Driving Force or Agent - Wind

Description - Wave particles have an appreciable net movement in the direction of wind travel.

The wind drift currents are normal \ll 2.0 knots and need not be considered. In this case the current and design wave is in the same direction.

C. Type of Current - Inertial

Description - The inertial currents are under the influence of inertia (after the driving force has stopped), fluid resistance at the boundaries, and coriolis force. The inertial currents are less than 2.0 knots and need not be considered.

D. Wave Induced Current.

E. Type of Current - Tidal Current

Definition of Tidal Currents - a) The rotary type (currents in the open ocean and along the sea coast), b) the rectilinear or reversing type

(currents in most inland bodies of water)

e) Hydraulic type (currents in straits connecting two independently tidal bodies of water).

Driving Force or Agent - Astronomical forces of the moon and sun.

Description - These currents are of tidal origin and are periodic. Tidal currents reach velocities up to 5 knots depending upon the character of the tide, the water depth, and the configuration of the coast.

In the open ocean, the tidal currents usually are rotating due to the effect of the coriolis force. (From hour to hour the currents change in both direction and speed). The rotary tidal currents are normally $\ll 2.0$ and need not be considered. The reversing tidal currents and hydraulic tidal currents may exceed 5 knots in certain locations. It is possible to have a design wave approach the rotary tidal current from any angle. The direction of approach depends on the location of the storm system which generated the wave.

It is not possible to have the design wave approach the reversing or hydraulic current from a 90° angle since the design wave is refracted as it approaches a shoreline at an angle. Consequently the waves "swing around" and tend to conform to the contours. The design wave therefore does not approach the reversing tidal current at an angle.

II. As discussed in Part I this situation would exist primarily in a major ocean current.

Ref. Page 58 - Stommel, H., The Gulf Stream, Univ. of California Press 1966.

Vertical velocity profiles in the gulf stream near Cape Hatteras indicate surface velocities up to 5 knots. Therefore a barrier in a major ocean current could experience a 2 knot surface current. With wave crests approaching at a 90° angle. A surface wave train (swells) would not be able to disturb a major ocean current although the particle velocities decay exponentially down to $L_0/2$.

With the 2 knot criteria we can assume that the condition stated in I will exist only in

a major current system such as Florida,
current etc.

3. Question

I. Is it true that most ocean currents are wind driven?

4. Answer

		Magnitude (Knots)
I. <u>Wind Driven Currents</u>		
A. Major ocean currents		up to 5.0
B. Currents caused by wind stress		< 0.5
II. <u>Inertial Currents</u>		
Inertial current		very small
III. <u>Wave Induced Current</u>		
Wave induced current		small
IV. <u>Tidal Current</u>		
Tidal current		up to 5.0 (depends on loca- tion)

V. 1.) What are the forces on a submerged right cylinder.

a.) 3 knot current 3" pipe = 0.25 ft. diameter

$$\text{Drag} = C_D A \frac{\rho U^2}{2}$$

Where C_D = Drag Coefficient

A = Projected Area of the Body on a Plane

Normal to the flow

ρ = Density of sea water

U = Velocity

$$B = \frac{UD}{\gamma} = \frac{(5.06)(0.25)}{1.2 \times 10^{-5}} = 1.05 \times 10^5$$

$$1 \text{ knot} = 1.6875 \text{ Ft/Sec}$$

$$3 \text{ knots} = 5.06 \text{ ft/Sec}$$

$$\gamma = 1.2 \times 10^{-5}$$

$$C_D = 1.2$$

Force of drag on a unit length

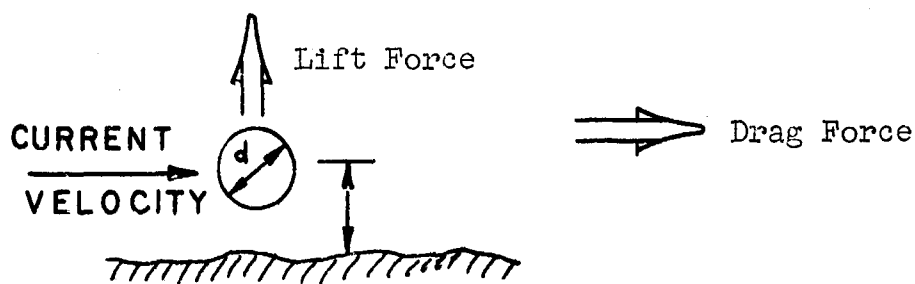
$$\text{Drag} = (1.2)(0.25)(1.99)(25.6)^2$$

$$F_{\text{Drag}} = 7.65 \text{ Lb/Unit Length}$$

$$\text{Lift} = C_L A \frac{\rho U^2}{2}$$

From Pg. 375 "Estuary and Coastline Hydrodynamics"

$$S/D = \frac{3.0}{0.51} = 60$$



Lift Force not critical

b.) 3 knot current

5" pipe = 0.417 ft

$$\text{Drag} = C_D A \frac{\rho U^2}{2}$$

$$\text{Drag} = (1.2) \left(\frac{5}{2}\right)^{0.417} (1.99)(25.6)^2$$

$$F_D = 12.8 \text{ lb./unit length}$$

c.) 3 knot current

$$7'' \text{ pipe} = 0.583 \text{ ft.}$$

$$\text{Drag} = C_D A \frac{\rho U^2}{2}$$

$$\text{Drag} = (1.2) \left(\frac{7}{12}\right)^{0.583} \frac{(1.99) (25.6)^2}{2}$$

$$F_D = 17.9 \text{ lb/unit length}$$

VI. What vertical and horizontal water velocities will be found at depths from 16 to 32 ft. due to waves of 20 to 30 ft in height

A. Answer. Orbital motions in a progressive wave

Horizontal component

$$U = \frac{agk}{\sigma} \frac{\cosh k (h - Z)}{\cosh kh} \sin (kx - \sigma t)$$

Vertical Component

$$W = - \frac{agk}{\sigma} \frac{\sinh k (h + Z)}{\cosh kh} \cos / kx - \sigma t$$

These equations can be used to determine particle velocity for any wave critier. Examples of use are enclosed.

From Criteria for deep water

$$L = 71 \text{ ft} , T = 4.6 \text{ Sec.}$$

From Plate D-1a TR-4

$$d \frac{Z}{E} 10 \text{ ft} \therefore \text{ N. G.}$$

$$\frac{d}{L} = \frac{10}{71} = 0.141$$

For deep water $d/L > \frac{1}{2}$

$$\therefore L_0 = 5.12T^2$$

$$L_0 = (5.12) (4.6)^2 = 109 \text{ ft}$$

$$d/L = \frac{1}{2} \quad \therefore 50' = \frac{32.2 (4.6)^2}{6.28} \tanh \frac{6.28(50)}{110}$$

check

$$L = \frac{32.2}{6.28} \tanh \frac{6.28}{L}$$

$$L = 110'$$

$$L = \frac{(32.2)(4.6)^2}{6.28} \tanh \frac{(6.28)(50)}{110}$$

$$L = 110'$$

Criteria

$$d = 50 \text{ ft}$$

Depth of submergence = 16 ft.

$$H = 20 \text{ ft.}$$

$$a = 10 \text{ ft.}$$

$$k = \frac{2\pi}{L} = \frac{6.28}{110} = 0.057$$

$$\sigma = \frac{2\pi}{T} = \frac{6.28}{4.6} = 1.366$$

34

$$U_{16} = \frac{(10)(32.2)(0.06)}{1.366} \frac{\cosh(0.057)(50-16)}{\cosh(0.057)(50)}$$

$$\sin \frac{2\pi x}{L} = \frac{R\pi}{T}$$

$$t = 0 \quad x = \frac{L}{4}$$

$$U_{16} = \frac{(10)(32.2)(0.06)}{1.366}$$

$$\sin \frac{2\pi}{L} \frac{L}{4} = \frac{2\pi}{T} (0)$$

$$U_{16} = \frac{(10)(32.2)(0.06)}{1.366} (4.1)$$

$$U_{16} = 5.45 \text{ ft/sec}$$

Check

$$U = \frac{a\pi}{c} \frac{\cosh k(h+z)}{\cosh kh} \sin(hx - ct)$$

$$U = \frac{(10)(32.2)}{\frac{2\pi}{4.6}} \frac{\cosh \frac{2\pi}{110} (3.55)}{\cosh \frac{2\pi}{110}} \sin(1 - \frac{2\pi}{T} t)$$

$$U = \frac{(10)(32.2)(4.6)(3.55)}{(110)(8.67)} = 5.5 \text{ ft/sec}$$

$$d = 50 \text{ ft}$$

$$U_s = 32 \text{ ft}$$

$$a = 10 \text{ ft}$$

$$k = 0.057$$

$$c = 1.366$$

$$u_{32} = \frac{(19)(32.2)(0.057)}{1.386} \frac{\cosh(0.57)(1.579)}{\cosh(8.67)(59)}$$

$$\sin\left(\frac{2\pi}{L} \frac{L}{2} - \frac{2\pi}{T} t_0\right)$$

$$u_{32} = \frac{(19)(32.2)(0.057)}{1.386} \frac{(0.181)}{(8.67)}$$

$$u_{32} = 2.44 \text{ ft/sec}$$

Summary Wave amplitude = $\frac{H}{2}$

Wave amplitude = $\frac{H}{2}$

Horizontal particle velocity = U

Wave angular frequency, $\frac{2\pi}{T} = \sigma$

Wave number = k

Distance below MWL to point of interest = Z

$$u = \frac{agk}{\sigma} \frac{\cosh k(h+Z)}{\cosh kh} \sin(\sigma t - kx)$$

To determine u_{\max}

W = Vertical velocity

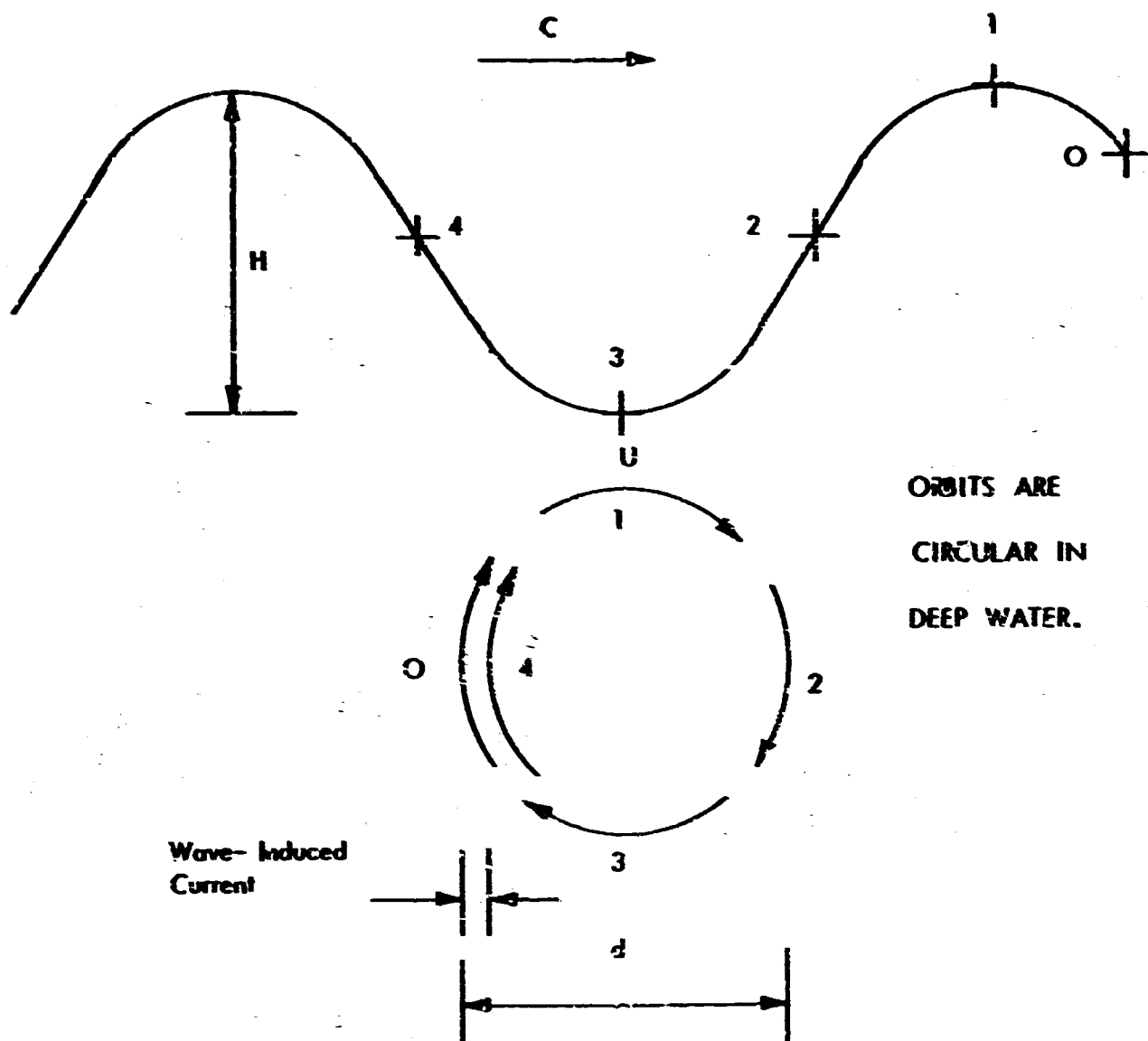
$$W = \frac{agk}{\sigma} \frac{\sinh k(h+Z)}{\cosh kh}$$

To determine W_{\max}

Set $X = \frac{L}{2}$ and $t = 0$.

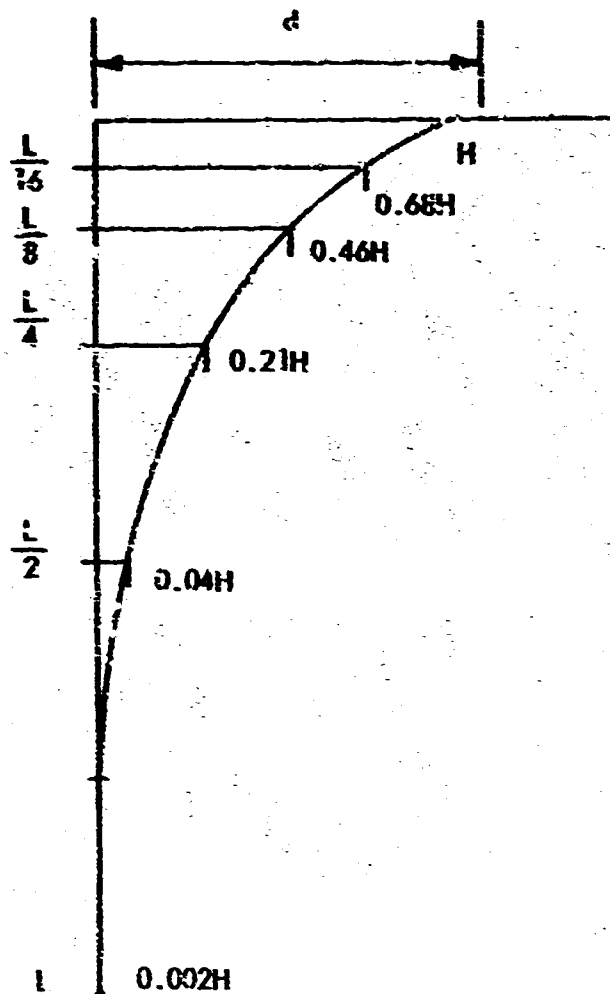
VII. What are the approximate velocity profiles beneath large waves?

DEEP WATER WAVE



Trajectory described by particle at surface as successive parts of wave travel past point O .

Decrease in orbital diameter with depth



Orbital Velocity

If one follows the floating barriers during the passage of a series of waves, it will be observed that it moves back and forth and up and down, undergoing an orbital motion that returns it to nearly the same position after each wave. The trajectory of the barrier will be a closed circle (in deep water) with a diameter equal to the wave height H. Since the barrier completes one revolution during each wave period, the orbital velocity is

$$U = \pi \frac{H}{T}$$

U = Vel.

where H = Wave Ht

T = Wave period

Reply to:

Suite 105
8561 Long Point Road
Houston, Texas 77055
468-7629



FAIRBANKS MORSE INC.

Fairbanks Morse Inc.
Turbo Compressor Operation

701 Lawton Avenue
Beloit, Wisconsin
Tel. 608/364-4411

In referring to this
Quotation please mention.

Quotation No. TRO-139

Date: May 18, 1970

Wilson Industries, Inc.
Marine Systems Division
1417 Conti Street
Post Office Box 1492
Houston, Texas 77001

Attn: Mr. Joe Nelson

Subject: Pollution Control Air Compressor Service
Estimating Proposal

Gentlemen:

We are pleased to offer the following estimating proposal covering an Air Compressor Package consisting of:

One (1) - Fairbanks Morse Model 250L Rotary Screw Compressor driven by an Avco Lycoming Gas Turbine Prime Mover.

We would propose to furnish the following equipment:

One (1) - Fairbanks Morse Model 250L Rotary, Positive Displacement, Axial Flow, Screw Compressor, driven by an Avco Lycoming Model TF35 Gas Turbine Engine. Please refer to Section 3 of the enclosed Gas Turbine Power Proposal Brochure for pertinent details and listing of equipment to be furnished as part of the Gas Turbine Package, as well as technical data. The Compressor Gas Turbine and associated equipment would be mounted on a common steel skid base. Reference to Page 3-2 and 5-8 of the Gas Turbine Package proposal mentions the use of inertial

CONDITIONS OF QUOTATION:

- 1—ESTIMATED SHIPMENT _____ WEEKS AFTER RECEIPT OF ORDER AND COMPLETE INFORMATION.
- 2—ONLY ITEMS QUOTED ABOVE TO BE FURNISHED BY FAIRBANKS MORSE INC. ANY OTHER COMPONENTS TO COMPLEMENT THIS EQUIPMENT TO BE FURNISHED BY CUSTOMER OR OTHERS.
- 3—WE WILL FURNISH ARRANGEMENTS, DRAWINGS AND FIELD WIRING DIAGRAMS FOR ORDER RESULTING FROM THIS QUOTATION COVERING _____
- 4—STANDARD TERMS AND CONDITIONS ARE SHOWN ON THE REVERSE SIDE. - 224a - OFFICE

type turbine air filter. In the case of operation in salt air conditions, this filter type would be changed to a panel type arrangement with no additional cost.

The air compressor intake and discharge silencers, intake filter, the gas turbine fuel supply tank and pump, fuel strainer, seawater strainer and auxiliary power unit will not be mounted on the turbine-compressor skid.

The estimated weight of the turbine-compressor package complete dry would be 60,000 lbs. This does not include the unmounted items mentioned in the previous paragraph.

Included with this proposal you will find Colt Industries' Drawing No. 12-062-847, which is a preliminary layout of the Model 250I. Compressor and the Gas Turbine Driver.

Performance:

Enclosed you will find Performance Data and Equipment Description sheet indicating the performance capability of this package. In abbreviated terms, we are offering a package which will deliver 18,675 CFM at inlet conditions at a pressure of 49.7 psia, requiring 2,255 BHP at the compressor shaft. Please refer to the Gas Turbine Proposal Brochure for technical data and performance information on the Gas Turbine Engine.

Price:

Our net estimated price, f.o.b. factories, would be..\$350,000.00

Adder for sea water coolers and pumps.....\$ 2,500.00

Acoustical enclosure for turbine and gear.....\$ 8,500.00

Delivery:

Delivery could be accomplished on this equipment in approximately 26 weeks from receipt of order and engineering approval.

We wish to point out that this package offers a heavy duty, light weight

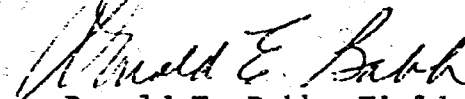
Letter 1, p.3

air compressor package which will offer continuous duty service reliability. Colt Industries is very much interested in this project and as it progresses will be willing to work with Wilson Industries in the possible development of lighter weight design compressors beyond the prototype units based on multiple equipment requirements. The writer will be available, as well as staff personnel from our Engineering Department, to discuss this application in detail as required.

We trust that this preliminary estimating information will be of interest and that we might look forward to working with Wilson Industries on this project in the future.

Yours very truly,

COLT INDUSTRIES, INC.
Gas Turbine-Compressor Operation


Donald E. Babb, Field Engineer

DEB:med
Enclosures

In referring to this
Quotation please mention:

Quotation No. TRO-139

Date: 5/18/70

PRELIMINARY ESTIMATE DATAROTARY, POSITIVE DISPLACEMENT COMPRESSORPerformance Data and Equipment DescriptionGeneral Arrangement Single Stage, Sole Plate Mounted, with H.S. CouplingCompressor Model 250L3PERFORMANCEGas Handled AirINLET CONDITIONSCapacity, CFM at Inlet Conditions 18675Absolute Inlet Pressure, PSIA 14.7Inlet Temperature, °F 90.Relative Humidity at Inlet, % 0Specific Heat Ratio ($\gamma = C_p/C_v$) 1.4Molecular Weight at Inlet 28.95Compressibility at Inlet, Z 1.DISCHARGE CONDITIONSAbsolute Discharge Pressure, PSIA 49.7Discharge Temperature, °F (Approx.) 362Compressor Speed, RPM 3330Driver Speed, RPM Power Req'd. @ Compressor Shaft, BHP 2255Power Req'd. @ Driver Shaft, BHP Interstage Conditions (for two-stage units only) (Cooling Water Temperature °F)Interstage Pressure, PSIA (Approx.) To Second StageGas Temperatures: To Intercooler °F, From Intercooler °F

Note: Compressor performance guarantees are subject to a variation of three percent (3%).

Compressor Division

Reference Number

Gas Turbine Power, Inc.

5205 Ashbrook, Houston, Texas 77036 Telephone (713) 666-6388

May 22, 1970

Professor E. I. Bailey, Ph. D.
P. O. Drawer FK
College Station, Texas 77840

Dear Professor Bailey:

In response to our recent visit to your office and our subsequent telephone conversation, we are pleased to advise the following information for your oil containment project.

We are enclosing a brochure on the Curtis Wright "Jet Air" compressor unit which we would employ in our system. If you refer to the drawing on the back page of this brochure, you will note that the physical size will not meet the optimum dimension which we discussed. By orienting the discharge pipe to a side discharge, redesign of the inlet plenum and providing a collapsible exhaust plenum, we can provide a unit approximately 20 feet long, 9 feet high and 9-1/2 feet wide so that two units can be shipped in a single C-130 aircraft.

By careful design of this system, we would expect to be able to supply a unit which would not exceed 21,000 pounds in weight, depending upon the amount of valving and piping required by the customer.

The units proposed are:

GTP-7150E employing a Curtis Wright
CW657E



GTP-7850E employing a Curtis Wright
CW657F



Letter 2, p. 2

Professor E. I. Bailey, Ph. D.
May 22, 1970

These prices are F.O.B. our plant, Houston, Texas and subject to our general terms and conditions attached.

The performance of these units for your service is as follows:

GTP-7150E - Inlet condition: 14.7 psia, 60°F,
22,000 scfm @ 40 psig and 400°F
fuel consumption 625 gph.

GTP-7850E - Inlet condition: 14.7 psia, 60°F,
24,400 scfm @ 50 psig and 400°F
fuel consumption 500 gph.

The GTP-7850E has the advantage of approximately 20% more flow with considerably less fuel consumption, but is a system that costs about \$100,000 more than the GTP-7150E.

The systems would be complete in an enclosure with the discharge pipe to the edge of the bedplate.

All controls for single pushbutton start and protective and alarm controls would be provided.

The fuel system would be complete with filter-separator and all controls and shutdown valves. It would not include a fuel transfer pump to supply fuel to our system.

The controls would be electric, designed to meet Class I, Group D, Division 2 explosion proof.

A CO₂ fire extinguishing system can be provided at additional cost.

Delivery of one unit would be 28 weeks from receipt of the order and settlement of details with one unit per week thereafter.



Letter 2, p. 3

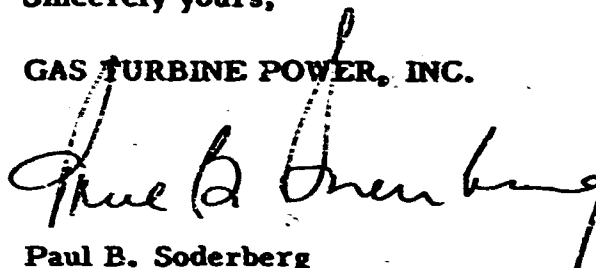
Professor E. I. Bailey, Ph.D.
May 22, 1970

Gas Turbine Power, Inc. would be pleased to discuss a lease-purchase arrangement with you for a prototype unit if you find this desirable.

We appreciate this opportunity to work with you and hope you are successful in getting approval to proceed with your system.

Sincerely yours,

GAS TURBINE POWER, INC.



Paul B. Soderberg
President

PBS:kd

Enclosures



WARRANTY

Gas Turbine Power, Inc., Houston, Texas, (hereinafter "Company") warrants the title of the equipment and also warrants the equipment to be of the kind and quality described in appropriate engine specification and free of defects in workmanship and material at the inception of the applicable period specified below. No other warranty shall be implied, and any statutory warranties shall be declared waived.

If within eighteen (18) months from date of shipment or twelve (12) months from start up, whichever occurs first, purchaser discovers that the equipment is not as warranted and promptly notifies Company of such failure, Company shall be obligated and shall have the right to remedy such failure by, at Company's option, adjustment, or repair, or replacement of the whole or any part of the equipment affected by such failure. Purchaser shall assume all responsibility and expense for removal, reinstallation and freight in connection with the foregoing remedies.

Company shall have the right of disposal of parts replaced by it hereunder. Company's liability by purchaser whether in contract or in tort, arising out of warranties, representations, instructions or defects from any cause, shall be limited exclusively to correcting the equipment and under the conditions as previously stated. No claim for warranty will be allowed if GTP's inspection reveals that, subsequent to shipment from our plant, the engine had been improperly adjusted, stored, or handled, or operated contrary to operating instructions, or subject to misuse, negligence or accident. GTP reserves the right to make such changes at any time which in its opinion will improve the quality of its products without incurring any additional responsibility as regards engines previously delivered.

This Warranty is expressly in lieu of all other warranties expressed or implied and all other obligations and liabilities direct or consequential on its part, and it neither assumes nor authorizes any other person or corporation to assume for it any other liability in connection with the sale of its engines and parts. GTP shall not be liable for consequential damages under any circumstances.



**GAS TURBINE POWER, INC.
STANDARD TERMS AND CONDITIONS
FOR COMMERCIAL SALES**

1. **Expiration:** Unless otherwise expressly stated, this proposal is limited to acceptance within 60 days from date and is subject to change upon notice until acceptance.
2. **Delivery:** All quotations are based on delivery F.O.B. our factory loading area within the time specified in the order. The Company shall in no event be liable for delays caused by fires, acts of God, strikes, labor difficulties, acts or restrictions of governmental or military authorities, delays in transportation or procuring materials, or cause of any kind beyond the Company's control.
3. **Prices:** All quotations submitted and all purchase orders and contracts are subject to acceptance by the Company. No alteration in this proposal, or specification attached hereto, may be made without our written consent. Any changes in the specification or terms and conditions of this offer, requested by purchaser after price quotation, will be subject to negotiation for price revision.
4. **Applicable Laws and Taxes:** This quotation and any subsequent order or contract with the purchaser are subject to the provisions of all municipal, state and federal statutes, directives or ordinances pertinent thereto. Unless specifically stated by the Company, this quotation is exclusive of tax, and all state, local and federal sales; use of similar taxes will be added to the quoted price upon invoicing and purchaser shall pay same to seller.
5. **Terms of Payment:** Standard terms of payment will be 10% with purchase order and progress payments as mutually agreed upon. In any event, 90% of the purchase order price shall be due on shipment of the equipment from GTP facilities and the final 10% of the purchase price due on satisfactory performance of the GTP supplied system. In the event acceptance tests are unable to be performed by the customer before 30 days after installation of the equipment or 60 days after shipment, the final 10% shall be due. In the event the purchaser's financial condition shall in our opinion become unsatisfactory, cash payments of satisfactory security may be demanded by us and in default of such payment or satisfactory security, deliveries hereunder may be discontinued.

If purchaser delays shipment, payments based on date of shipment shall become due as of the date when ready for shipment. Equipment held for purchaser shall be at purchaser's risk and expense.



STANDARD TERMS AND CONDITIONS

Page 2

6. **Title and Lien Rights:** Legal and equitable title to all equipment sold hereunder will pass to the Purchaser on the date of shipment as so defined. It is expressly understood and agreed however that the passage of title shall not be construed by the Company as an acceptance of the equipment by the Purchaser or a release from the Company's responsibility to fully carry out its obligations under this contract. The Company shall in event of the purchaser's default have the right to repossess such equipment.

7. **Patent Infringement:** The Company will indemnify the purchaser and the ultimate user of the equipment against liability for infringement of any United States patent by the equipment or any part thereof furnished pursuant hereto (other than parts of special design, construction or manufacture specified or originated by the purchaser). The foregoing indemnity shall not apply unless the Company has been promptly notified of any charge or infringement or any suit or action alleging such infringement, and the purchaser affords the Company full authority to negotiate settlement or defend such suit.

8. **Representations:** There are NO WARRANTIES, understandings or agreements either verbal or written relative to apparatus sold hereunder that are not fully expressed herein and no change shall be made unless reduced to writing and signed by both parties. The above statement is made (IN LIEU OF) any warranty hereunder either expressed or implied by law. No statement, recommendation or assistance made or offered by Company through its representatives in connection with the use of any product sold by us shall be or constitute a WAIVER by Company of any of the provisions hereof or change the purchaser's liability as herein defined.

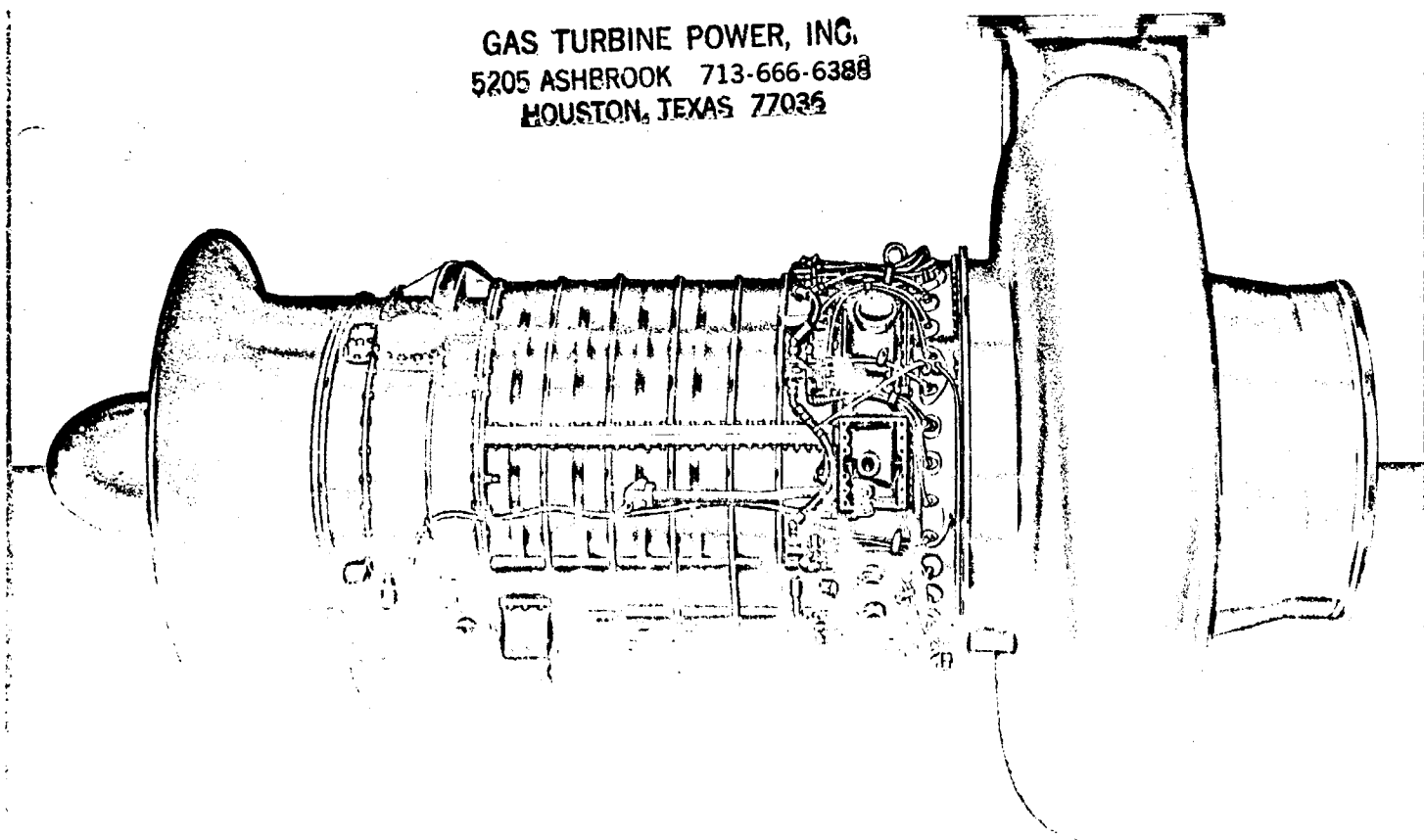
9. **LIMITATION OF LIABILITY:** THE SELLER'S LIABILITY FOR ANY LOSS OR DAMAGES ARISING OUT OF, CONNECTED WITH, OR RESULTING FROM THE MANUFACTURE, SALES, DELIVERY, RESALE, REPAIR, REPLACEMENT OR USE OF ANY PRODUCT SHALL IN NO CASE EXCEED THE PRICE OF THE PRODUCT, OR PART THEREOF, WHICH GAVE RISE TO CLAIM. IN NO EVENT SHALL THE SELLER BE LIABLE FOR SPECIAL OR CONSEQUENTIAL DAMAGES.



**CURTISS
WRIGHT**

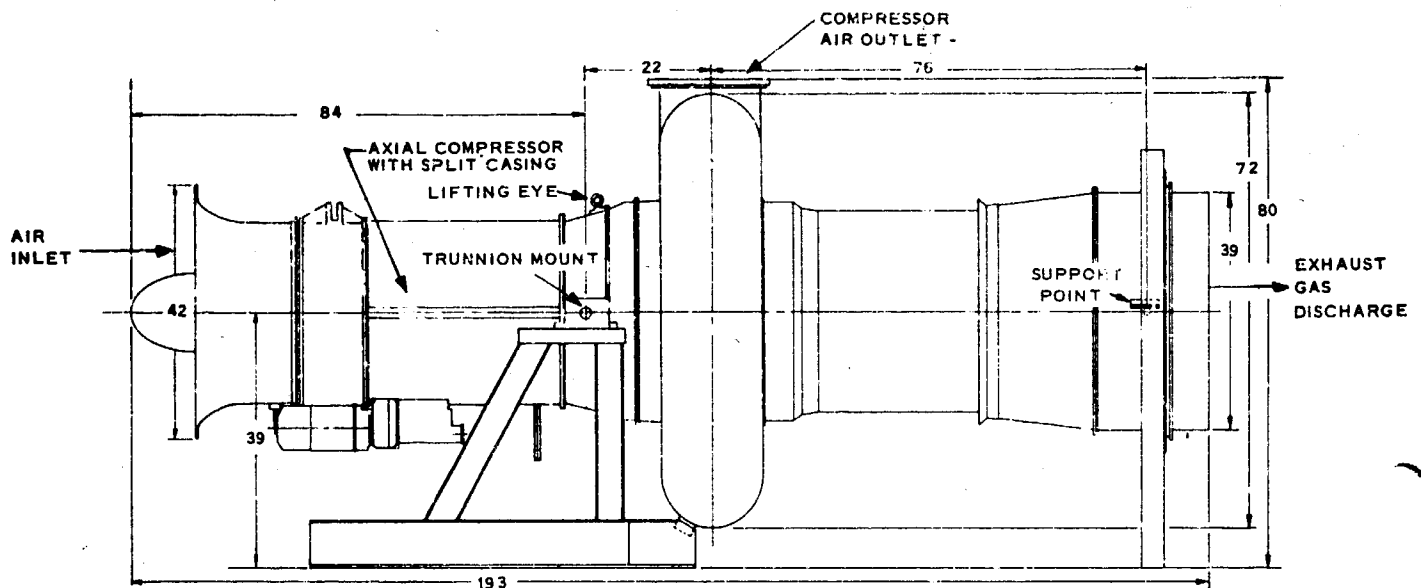
"JET AIR" COMPRESSOR

GAS TURBINE POWER, INC.
5205 ASHBROOK 713-666-6388
HOUSTON, TEXAS 77036



GAS TURBINE DRIVEN AIR COMPRESSOR

- 3 POINT INSTALLATION MOUNTING • 3 ANTI-FRICTION BEARINGS, 1 OIL SEAL
- SINGLE ROTATING SHAFT • SPLIT COMPRESSOR CASING • AXIAL FLOW COMPRESSOR
- PRECISION MACHINED AND BALANCED ROTATING PARTS



INSTALLATION ADVANTAGES

- Minimum Volume - Length 193 Inches - Width 72 Inches - Height 80 Inches
- Low Weight - 4500 Pounds
- No Cooling Water Required
- No External Oil Cooler Required
- Minimum Vibration
- Factory Packaged
- Indexing of Compressed Air Outlet Flange Optional
- Vertical Compressor Arrangement Optional

STANDARD EQUIPMENT

- Inlet Flare and Nose Cone
- Electric or Compressed Air Starter
- Ignition System Except Power Source
- Compressor Driven Fuel and Lube Oil Pumps
- Automatic Start and Safety Control
- Exhaust Diffuser
- Model CW657 F130 Includes Boost Compressor and Drive

OPTIONAL EQUIPMENT

- 85 and 130 PSIG Compressed Air Supply Systems
- Natural Gas Fuel System
- Dual Fuel System
- Compressor Mount and Base Plate

PERFORMANCE DATA

INLET CONDITIONS : 14.7 PSIA, 60° F

DISCHARGE AIR PRESSURE, PSIG	50	70	85	100	115	130
MODEL CW657E						
Compressor Air Flow, CFM Max	20,000	16,800	13,000			
Discharge Air Temperature, °F	420	470	507			
Fuel Flow-Liquid-GPH	645	740	805			
Gas-SCFM	1,340	1,535	1,665			
MODEL CW657F						
Compressor Air Flow, CFM Max	24,400	26,400	26,750			
Discharge Air Temperature, °F	402	462	507			
Fuel Flow-Liquid-GPH	500	590	660			
Gas-SCFM	1,030	1,223	1,360			
MODEL CW657F85						
Compressor Air Flow, CFM Max	24,500	26,550	26,650			
Discharge Air Temperature, °F	100	105	110			
Fuel Flow-Liquid-GPH	500	600	665			
Gas-SCFM	1,035	1,240	1,370			
MODEL CW657F130						
Compressor Air Flow, CFM Max				23,000	22,950	22,650
Discharge Air Temperature, °F				104	107	110
Fuel Flow-Liquid-GPH				650	670	690
Gas-SCFM				1,345	1,390	1,430

LIQUID FUEL LHV = 18,500 BTU/LB; NATURAL GAS LHV = 995 BTU/SCF

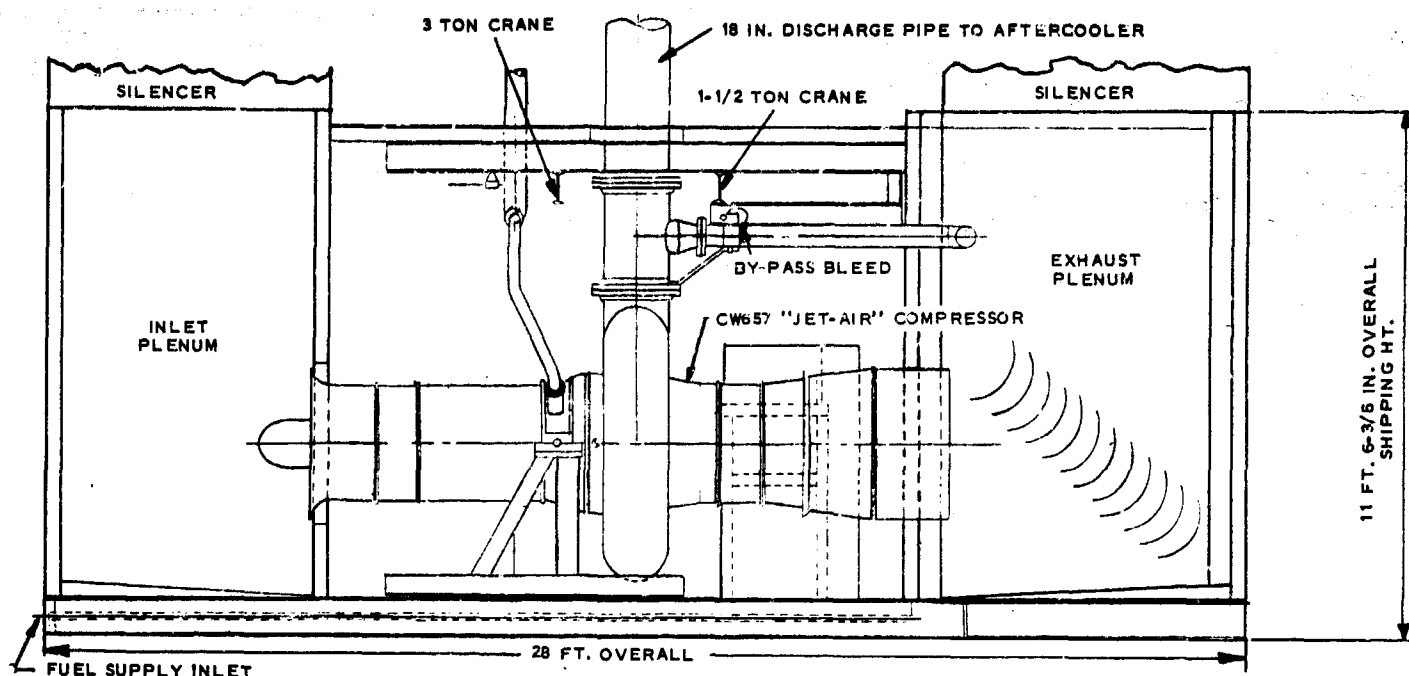
OPERATIONAL ADVANTAGES

Rapid Start to Maximum Compressed Air Flow in 75 Seconds
Oil-Free Air
Surge-Free Air at All Flows
Smoke-Free Exhaust
Multi-Fuel Capability
Continuous or Intermittent Duty
Unattended Operation
Exhaust Heat Available for Waste Heat Recovery Systems

APPLICATIONS

Manufacturing - Air Blasting, Drying, Spraying
Processing - Aeration, Combustion, Evaporation, Separation
Industrial - Pneumatic Actuation, Conveying, Pressurization

PACKAGED "JET-AIR" COMPRESSOR SYSTEMS



TYPICAL COMPRESSED AIR SUPPLY SYSTEM

INSTALLATION ADVANTAGES

- Compact Integrated Design – Minimum Site Preparation
- Factory Assembled and Tested – Minimum Field Installation
- Skid or Bedplate Mounted – Maximum Portability

STANDARD EQUIPMENT

- CW657E, CW657F or CW657F130 "Jet Air" Compressor
- Welded Steel Mount and Base Plate
- Inlet and Exhaust Plenum Chambers and Silencers
- Automatic Control System Suitable for Unattended Operation
- Associated Compressed Air Piping and Valves
- Enclosures for Compressor and Control System
- Aftercooler – Air Cooled

OPTIONAL EQUIPMENT

- Horizontal Discharge
- Compressed Air Supply Manifold
- Water Cooled Aftercooler
- Natural Gas or Dual Fuel System
- Trailer Mounting

GAS TURBINE POWER, INC.
5205 ASHBROOK 713-666-6388
HOUSTON, TEXAS 77036

REGIONAL OFFICES

BELLEVUE, WASHINGTON • DALLAS, TEXAS • DAYTON, OHIO • LOS ANGELES, CALIFORNIA
WARNER ROBBINS, GEORGIA • WASHINGTON, D.C. • DAUN/EIFEL, WEST GERMANY • ROME, ITALY

PRINTED IN U.S.A.

June 4, 1970

Wilson Industries, Inc.
Wilson Marine Systems Division
1301 Conti Street
Houston, Texas

Attention: Mr. Richard Hudson

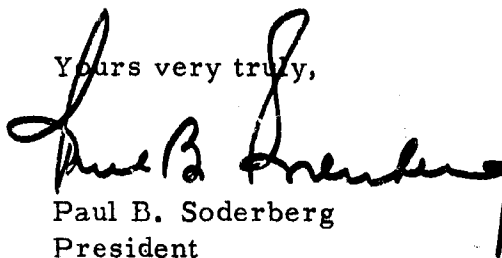
Gentlemen:

With reference to our letter quotation of May 22, 1970, to Professor E. I. Bailey, Ph.D., of Texas A & M University and our subsequent telephone conversation, we are pleased to advise as follows:

We believe that four (4) GTP-7150E units as proposed could be made available on a three-month lease arrangement for the sum of \$250,000.

Additional time will be required to make you a firm proposal on this basis; however, we assure you that we are most interested in supplying our equipment on your prototype system based on what we believe the potential market for this equipment will be.

Yours very truly,


Paul B. Soderberg
President

PBS:kd



Unclassified

DOCUMENT CONTROL DATA - R & D

1. CHRONOLOGICAL ACTIVITY (Company activity)

Wilson Industries, Inc.
1301 Conti Street, P. O. Box 1492
Houston, Texas 77002

20. REPORT SECURITY CLASSIFICATION

Unclassified

21. NUMBER

3. REPORT TITLE

Heavy Duty Oil Containment System
Pneumatic Barrier System

4. DOCUMENT TYPE (Type of report and inclusive dates)

Final Report

5. AUTHOR (Name, rank, position, institution)

John P. Hanser (editor)

6. REPORT DATE

January 1971

22. TOTAL NO. OF PAGES

596

23. NO. OF PAGES

89

7. CONTRACT OR GRANT NO.

DOT-CG-00,490-A

24. ORIGINATOR'S REPORT NUMBER

714102/A/004

8. PROJECT NO.

25. OTHER REPORT NUMBER (Any other number that may be used to identify this report)

10. DISTRIBUTION STATEMENT

Availability is unlimited. Document may be released to the Clearinghouse for Federal Scientific and Technical Information, Springfield, Virginia 22151 for sale to the public.

11. SUBJECT TERMS

Key Words:

Oil Spills; air barrier; Oil containment;
oil booms; oil barriers; oil pollution;
pneumatic barrier

12. SPONSORING MILITARY ACTIVITY

United States Coast Guard
Office of Research and Development
Washington, D. C. 20591

13. ABSTRACT

This report presents the results of studies and tests of a pneumatic heavy duty oil containment system. Deployment is accomplished using large Coast Guard vessels or navy salvage ships. The design is intended for long deployment periods.

The barrier design described uses a pneumatic curtain to contain the oil. The curtain air is provided by raft mounted compressors in juxtaposition to the submerged perforated pipe.